



Universidade de Aveiro
2021

**TÂNIA VANESSA DOS
SANTOS GAMEIRO**

**METODOLOGIAS SUSTENTÁVEIS BASEADAS NA
RECUPERAÇÃO DE RESÍDUOS PARA CONTROLO
DE pH NA DIGESTÃO ANAERÓBIA**

**SUSTAINABLE METHODOLOGIES BASED ON
RESIDUE RECOVERY FOR pH CONTROL IN
ANAEROBIC DIGESTION**



Universidade de Aveiro

2021

**TÂNIA VANESSA DOS
SANTOS GAMEIRO**

**METODOLOGIAS SUSTENTÁVEIS BASEADAS NA
RECUPERAÇÃO DE RESÍDUOS PARA CONTROLO
DE pH NA DIGESTÃO ANAERÓBIA**

Tese apresentada à Universidade de Aveiro para cumprimento dos requisitos necessários à obtenção do grau de Doutor em Ciências e Engenharia do Ambiente, realizada sob a orientação científica da Doutora Maria Isabel Aparício Paulo Fernandes Capela, Professora Associada do Departamento de Ambiente e Ordenamento da Universidade de Aveiro, e coorientação científica do Doutor Armando da Costa Duarte, Professor Catedrático (Aposentado) do Departamento de Química da Universidade de Aveiro

Dedico este trabalho ao meu companheiro de vida, ao meu filho e aos meus pais,
pelo incansável apoio e amor.

*“And however difficult life may seem, there is always something you can do, and
succeed at. It matters that you don’t just give up.”
Stephen Hawking (1942 – 2018)*

o júri

presidente

Prof. Doutora Ana Margarida Corujo Ferreira Lima Ramos
Professora Catedrática, Universidade de Aveiro

Prof. Doutor António José Guerreiro de Brito
Professor Associado com Agregação, Universidade de Lisboa

Prof. Doutora Maria Isabel Aparício Paulo Fernandes Capela (orientadora)
Professora Associada, Universidade de Aveiro

Prof. Doutora Leonor Miranda Monteiro do Amaral
Professora Associada, Universidade Nova de Lisboa

Prof. Doutor António João Carvalho de Albuquerque
Professor Auxiliar, Universidade da Beira Interior

Doutor Flávio Gonzaga Castro Santos Silva
Investigador Doutorado (nível 1), Universidade de Aveiro

agradecimentos

No final deste desafio, importa agradecer a quem tanto fez para que eu conseguisse aqui chegar.

Em primeiro lugar, agradeço à minha supervisora, Professora Isabel Capela, por todo o apoio ao longo de todos estes anos, todos os conselhos e orientações que permitiram que terminasse mais este passo da minha vida académica. Ao meu co-supervisor, Professor Armando Duarte, agradeço os sábios conselhos e dicas que sempre me incentivaram a melhorar.

Agradeço à Cátia Couras, todos os momentos bons (e menos bons!) passados no laboratório e fora dele, que nos fizeram crescer e ser melhores pessoas. Tem sido uma jornada e tanto, que vamos levar para a vida!

Agradeço a todos os colegas de laboratório, que sempre proporcionaram um bom ambiente de trabalho, que sempre tiveram uma palavra de apoio e um sorriso para partilhar. Agradeço aos “meus alunos” de mestrado, pelos bons momentos e aprendizagem que proporcionaram. Agradeço em especial à minha Catarina (Correia), que além da energia positiva, foi uma grande ajuda no laboratório, quando mais precisei. A tua “pedalada” salvou-me inúmeras vezes!

Agradeço ao Nuno Costa, todas as intervenções técnicas e ideias que ajudaram a melhorar o trabalho de laboratório. À Manuela Marques e à Diana Patoilo, que foram uma grande ajuda à realização dos trabalhos laboratoriais. Aos professores do DAO-UA, em especial ao Prof. Luis Tarelho, Prof. Isabel Nunes, Prof. Ana Paula Gomes e Prof. Arlindo Matos, por todas as positivas trocas de ideias.

À empresa Águas do Centro Litoral, na pessoa do Engenheiro Milton Fontes, agradeço a disponibilização da biomassa anaeróbia ao longo de todo o trabalho laboratorial.

À Ana Garrido, Rita Marinho, Cristiana, Andreia, Luís Melo e André Silva, o meu sincero agradecimento. Foram essenciais para que não desistisse nos momentos de crise, e estiveram comigo sempre. Sabem o quão importantes são para mim!

Aos meus pais, à minha tia Rosa e ao meu tio Daniel, agradeço o incondicional apoio e a oportunidade que me deram de concretizar os meus sonhos. Ao meu irmão, que em tempos de pandemia, e à sua maneira, foi uma inspiração preciosa na escrita!

Por último, e não menos importante, agradeço ao meu companheiro de vida, que além de me ter dado a oportunidade de ser mãe, sempre esteve do meu lado, sempre me apoiou e foi o verdadeiro ombro amigo nos momentos mais duros desta viagem alucinante! OBRIGADA!

Aqueles que passam por nós, não vão sós, não nos deixam sós. Deixam um pouco de si, levam um pouco de nós (Antoine de Saint-Exupéry).

palavras-chave

Digestão anaeróbia; esferas geopoliméricas; controlo de pH; metano; soro de leite; cinzas volantes; lamas vermelhas

resumo

O principal objetivo deste trabalho foi o estudo do efeito da adição de resíduos inorgânicos alcalinos (cinzas volantes e lama vermelha), incorporados em esferas geopoliméricas inorgânicas, para controlo de pH e melhoria de processos anaeróbios durante o tratamento de resíduos orgânicos complexos.

Numa primeira fase, foi estudada a adição de cinzas volantes a dois resíduos: efluente do primeiro estágio de branqueamento de uma fábrica de pasta e papel, com elevadas concentrações de compostos orgânicos pouco biodegradáveis (AOX) e pH muito baixo (≈ 2), e o subproduto da indústria de laticínios (soro de queijo), com elevada carga orgânica e rápida tendência para acidificação em condições anaeróbias. A adição de cinzas permitiu a redução de AOX em 62 % e remoção de 65 % de matéria orgânica do efluente de branqueamento. Por outro lado, a quantidade de cinzas volantes adicionadas ao processo de degradação anaeróbia de soro de queijo foi insuficiente para instigar a fase metanogénica, levando a elevadas concentrações de ácidos orgânicos voláteis e baixa produtividade de metano.

Na segunda fase, estudou-se a adição de esferas geopoliméricas, com cinzas volantes na sua constituição, a digestores anaeróbios descontínuos e semi-contínuos para o tratamento de soro de queijo, que possui um maior potencial de biodegradação. A adição de esferas com maior quantidade de cinzas (*FA-based*) na sua constituição obteve melhor produtividade em metano. Verificou-se também que o aumento da quantidade de esferas aumentava a produção de metano em cerca de 30 %. Além disso, a porosidade e quantidade das esferas influencia o desempenho anaeróbio. Maiores quantidades e maior porosidade das esferas melhoram a produção de metano em 82 %, mesmo após 2 adições consecutivas de substrato, comparativamente com a adição de alcalinidade química. Com 4 adições sequenciais de substrato, o sistema com esferas *FA-based* de alta porosidade também apresentou um desempenho muito bom a nível de estabilização de pH no digestor e uma melhoria de 8 % no rendimento de metano.

Na terceira fase, estudou-se a adição de esferas geopoliméricas, com lama vermelha na sua constituição (*RM-based*), a digestores anaeróbios semi-contínuos para o tratamento de soro de queijo. Com o aumento da carga orgânica, os sistemas anaeróbios foram temporariamente inibidos, tendo recuperado após um período mais longo. A diferença no desempenho entre os digestores com adição de alcalinidade química e com a adição de esferas geopoliméricas *RM-based* foi evidente após inibição por acumulação de substrato. As esferas promoveram uma lixiviação prolongada e lenta de alcalinidade, promovendo maior estabilidade do sistema e melhorando a produção de metano em 94 % e a remoção de matéria orgânica em 44 %. Após a utilização nos digestores anaeróbios, as esferas mantêm a sua integridade, podendo ser recuperadas e reutilizadas noutras aplicações, como adsorventes de poluentes ou integradas em cimentos e argamassas.

Com este estudo, pode-se concluir que a utilização de esferas geopoliméricas inorgânicas é uma estratégia inovadora e muito promissora para controlo de pH e para promover a estabilidade dos processos anaeróbios, contribuindo assim para o conceito de economia circular, utilizando resíduos (soro de leite, cinzas volantes e lama vermelha) em processos biológicos, para valorização em novos produtos (esferas geopoliméricas) e energia (metano).

keywords

Anaerobic digestion; geopolymer spheres; pH control; methane; cheese whey; fly ash; red mud waste

abstract

The main objective of this work was the study of the effect of the addition of alkaline inorganic residues (fly ash and red mud), incorporated in inorganic geopolymeric spheres, for pH control and improvement of anaerobic processes during the treatment of challenging organic wastes.

In the first phase, the addition of fly ash to two different effluents was studied. The effluent from the first bleaching stage of a pulp and paper industry was used, with high concentrations of low biodegradable organic compounds (AOX) and very low pH (≈ 2), as well as the by-product of a dairy industry (cheese whey), with high organic load and fast propensity to acidification under anaerobic conditions. The addition of fly ash allowed the reduction of AOX by 62 % and the removal of 65 % of organic matter from the bleaching effluent. On the other hand, the amount of fly ash added to cheese whey degradation process was insufficient to instigate the methanogenic phase, thus leading to high concentrations of volatile organic acids and low methane productivity.

In the second phase, it was studied the addition of geopolymeric spheres, with fly ash in their constitution, to discontinuous and semi-continuous anaerobic digesters for the treatment of cheese whey, which has a greater biodegradation potential. The addition of spheres with a greater amount of ash (FA-based) in its constitution obtained better productivity in terms of methane. It was also found that the increase in the number of spheres boost the production of methane by about 30 %. In addition, the porosity and concentration of the spheres influences anaerobic performance. Higher amounts and greater porosity of the spheres improve methane production by 82 %, even after 2 consecutive substrate additions, compared to the addition of chemical alkalinity. With 4 sequential additions of substrate, the system with FA-based spheres with high porosity achieved also a very good performance in terms of pH stabilization in the digester and achieved a methane yield improvement of 8 %.

In the third phase, it was studied the addition of geopolymeric spheres, with red mud in their constitution (RM-based), to semi-continuous anaerobic digesters for the treatment of cheese whey. With the increase of the organic load, the anaerobic systems were temporarily inhibited, recovering after a longer period. The difference in performance between digesters with the addition of chemical alkalinity and the addition of RM-based geopolymeric spheres was evident after inhibition by the substrate accumulation. The spheres promoted a prolonged and slow leaching of alkalis, promoting greater stability of the system and improving the production of methane by 94 % and the organic matter removal by 44 %. After being used in anaerobic digesters, the spheres keep their integrity and can be recovered and reused in other applications, such as pollutant adsorbents or integrated into cements and mortars.

With this study, it can be concluded that the use of inorganic geopolymeric spheres is an innovative and very promising strategy for pH control and to promote the stability of anaerobic processes, thus contributing to the concept of circular economy, using wastes (cheese whey, fly ash and red mud) in biological processes, for their valorization into new products (geopolymeric spheres) and energy (methane).

Table of Contents

1 	INTRODUCTION.....	3
1.1	MOTIVATION AND RELEVANCE	3
1.1.1	<i>From waste to energy: a sustainable approach.....</i>	3
1.1.2	<i>Sustainable Development Goals</i>	5
1.1.3	<i>Pulp and paper industry, dairy industry and alumina refining: How to connect them?</i>	6
1.2	OBJECTIVES	9
1.3	THESIS OUTLINE	10
2 	STATE-OF-ART	13
2.1	WASTE AND WASTEWATER PRODUCTION.....	13
2.1.1	<i>Bioenergy and the “European Green Deal”.....</i>	14
2.1.2	<i>Circular economy approach</i>	15
2.2	ANAEROBIC DIGESTION PROCESS FOR WASTEWATER TREATMENT.....	17
2.2.1	<i>History of the anaerobic digestion process.....</i>	17
2.2.2	<i>Definition and applicability of anaerobic digestion process</i>	19
2.2.3	<i>Biochemistry of the anaerobic digestion process.....</i>	21
2.2.3.1	Hydrolysis	24
2.2.3.2	Acidogenesis.....	25
2.2.3.3	Acetogenesis	25
2.2.3.4	Methanogenesis	27
2.2.3.5	Sulfate reduction	29
2.2.4	<i>Methane-rich biogas.....</i>	30
2.2.5	<i>Key parameters that affect the anaerobic digestion process</i>	31
2.2.5.1	pH and alkalinity	31
2.2.5.2	Temperature.....	32
2.2.5.3	Nutrients.....	34
2.2.5.4	Presence of toxicants	36
2.2.5.4.1	Volatile fatty acids	36
2.2.5.4.2	Organic compounds.....	36
2.2.5.4.3	Ammonia	37
2.2.5.4.4	Sulfide.....	37
2.2.5.4.5	Potentially toxic elements	38
2.2.5.4.6	Oxygen	38
2.2.5.4.7	Salinity	39
2.2.5.5	Hydraulic retention time	39
2.2.5.6	Organic load	40
2.2.6	<i>Configurations of anaerobic bioreactors</i>	40
2.3	PULP AND PAPER INDUSTRY	44
2.3.1	<i>Pulp making process</i>	45
2.3.1.1	Preparation of raw materials.....	45
2.3.1.2	Separation of the fibers.....	45
2.3.1.2.1	Mechanical and semi-chemical pulping.....	45
2.3.1.2.2	Chemical pulping	46
2.3.1.3	Bleaching process	48
2.3.1.4	Recovering of chemicals	49

2.3.2	<i>Waste and wastewater generation in Kraft pulping process</i>	50
2.3.2.1	Fly ashes from biomass burning	52
2.3.2.2	Dregs, grits and lime mud	54
2.3.2.3	Bleaching effluents	55
2.3.2.3.1	Adsorbable organic halides (AOX)	55
2.3.2.3.2	Treatment alternatives for bleaching effluents	56
2.3.2.3.3	Anaerobic digestion of bleaching effluents	58
2.4	DAIRY INDUSTRY	60
2.4.1	<i>Dairy products</i>	61
2.4.1.1	Milk	62
2.4.1.2	Cheese	62
2.4.1.3	Fat and fermented milk products	63
2.4.1.4	Other milk products	63
2.4.2	<i>Cheese whey generation and characteristics</i>	63
2.4.2.1	Cheese whey production from raw milk	63
2.4.2.2	Cheese whey characteristics	66
2.4.3	<i>Anaerobic treatment technologies for dairy effluents</i>	67
2.5	BAUXITE MINING AND ALUMINA REFINING	71
2.5.1	<i>Red mud generation during the alumina refining process</i>	72
2.5.1.1	Alumina refining process	72
2.5.1.2	Red mud characteristics	74
2.5.2	<i>Red mud applications</i>	75
2.5.2.1	Use of red mud in biological treatment processes	77
2.6	PH REGULATION IN ANAEROBIC DIGESTION PROCESSES	79
2.6.1	<i>Types of inorganic additives for anaerobic process enhancement</i>	79
2.6.2	<i>Geopolymer spheres as new pH buffering materials</i>	84
2.6.2.1	Definition and applicability of geopolymers	84
2.6.2.2	Fly ash-based geopolymers	86
2.6.2.3	Red mud-based geopolymers	87
2.6.2.4	Use of geopolymers as pH buffering materials in anaerobic digestion	88
3 	METHODOLOGY	91
3.1	INOCULUM	91
3.2	SUBSTRATES	92
3.2.1	<i>Bleaching effluent from pulp and paper industry (D₀ effluent)</i>	92
3.2.2	<i>By-product from cheese manufacturing (cheese whey)</i>	93
3.3	INORGANIC ADDITIVES FOR PH CONTROL	94
3.3.1	<i>Fly ash from biomass combustion</i>	94
3.3.2	<i>Waste-based geopolymer spheres</i>	95
3.3.2.1	Fly ash-based geopolymer spheres	95
3.3.2.2	Red mud-based geopolymer spheres	96
3.4	NUTRIENTS SUPPLEMENTATION	97
3.5	BIOREACTORS SET-UP AND OPERATIONAL CONDITIONS	98
3.5.1	<i>Oxitop System</i>	98
3.5.1.1	Experimental set-up	98
3.5.1.2	Operational conditions applied using oxitop system	99
3.5.2	<i>Batch and fed-batch bioreactors</i>	101
3.5.2.1	Bioreactors set-up	101

3.5.2.2	Operational conditions of batch and fed-batch bioreactors	102
3.6	METHODOLOGIES FOR MONITORING THE ANAEROBIC DIGESTION PROCESS	104
3.6.1	<i>pH, alkalinity and conductivity measurements</i>	105
3.6.2	<i>Chemical Oxygen Demand (COD)</i>	106
3.6.3	<i>Biochemical Oxygen Demand – 5 days (BOD₅)</i>	106
3.6.4	<i>Solids content</i>	108
3.6.4.1	Total Suspended Solids (TSS).....	108
3.6.4.2	Volatile Suspended Solids (VSS)	109
3.6.5	<i>Total phosphorous as orthophosphates</i>	109
3.6.6	<i>Adsorbable Organic Halides (AOX)</i>	110
3.6.7	<i>Volatile Fatty Acids (VFA)</i>	111
3.6.8	<i>Biogas composition (methane and carbon dioxide content)</i>	113
3.6.9	<i>Geopolymeric materials characterization</i>	113
3.6.10	<i>Metals (calcium, magnesium, iron, sodium and trace elements)</i>	114
3.7	ANAEROBIC PROCESS PERFORMANCE	115
3.7.1	<i>Organic matter removal</i>	115
3.7.2	<i>Acidification step</i>	115
3.7.2.1	Degree of acidification.....	115
3.7.2.2	Volatile fatty acids yield and fraction in the effluent	115
3.7.3	<i>Methanization step</i>	116
3.7.3.1	Methane volume	116
3.7.3.2	Methanization degree	117
3.7.3.3	Methane yield	117
3.7.3.4	Anaerobic biodegradability	117
3.7.3.5	Kinetic model for methane production	118
3.7.4	<i>Adsorbable organic halides removal</i>	118
4 	RESULTS AND DISCUSSION	121
4.1	PHASE 1: FLY ASH (POWDER) ADDITION TO ANAEROBIC DIGESTION ASSAYS	125
4.1.1	<i>Fly ash (powder) addition to anaerobic digestion of bleaching effluent from pulp and paper industry</i>	125
4.1.1.1	Inhibitory effect of adsorbable organic halides present in bleaching effluent	126
4.1.1.2	Anaerobic digestion of bleaching effluent with fly ash addition to control pH	130
4.1.1.3	Effect of fly ash addition in anaerobic digestion of bleaching effluent	136
4.1.2	<i>Fly ash (powder) addition to anaerobic digestion of cheese whey</i>	139
4.1.2.1	Anaerobic digestion of cheese whey with fly ash addition to control pH	139
4.1.2.2	Effect of fly ash addition in anaerobic digestion of cheese whey.....	143
4.1.3	<i>Comparison between bleaching effluent from pulp and paper industry and cheese whey from the dairy industry as substrates for methane production</i>	147
4.2	PHASE 2: FLY ASH-BASED GEOPOLYMERS ADDITION TO ANAEROBIC DIGESTION ASSAYS	151
4.2.1	<i>Fly ash-based versus metakaolin-based geopolymer spheres: anaerobic digestion assays with cheese whey</i>	152
4.2.1.1	Geopolymer spheres characterization before anaerobic digestion assays	152
4.2.1.2	Effect of geopolymer spheres addition on soluble chemical oxygen demand content	154
4.2.1.3	Oxitop batch assays with geopolymer spheres: effect of the binder composition	156
4.2.1.4	1-cycle batch assays: effect of spheres addition on the anaerobic digestion of cheese whey..	159
4.2.1.4.1	pH evolution	160
4.2.1.4.2	Volatile fatty acids production.....	161
4.2.1.4.3	Methane production.....	163

4.2.1.4.4	Anaerobic process performance	165
4.2.1.5	Geopolymer spheres characterization after anaerobic digestion assays	168
4.2.1.6	Cost comparison for replacing chemical alkalinity control by spheres addition	169
4.2.2	<i>Fly ash-based geopolymer spheres with low and high porosity: anaerobic digestion assays with cheese whey</i>	171
4.2.2.1	Geopolymer spheres characterization before anaerobic digestion assays	171
4.2.2.2	Oxitop batch assays with low and high porosity geopolymer spheres addition	173
4.2.2.3	2-cycle fed-batch assays: effect of the spheres porosity on the anaerobic digestion of cheese whey	176
4.2.2.3.1	pH evolution	176
4.2.2.3.2	Volatile fatty acids production	178
4.2.2.3.3	Methane production	180
4.2.2.3.4	Gompertz model for methane production	182
4.2.2.3.5	Anaerobic process performance	184
4.2.2.4	4-cycle fed-batch assays: effect of operation time on anaerobic digestion of cheese whey	187
4.2.2.4.1	pH evolution	188
4.2.2.4.2	Volatile fatty acids production	189
4.2.2.4.3	Methane production	191
4.2.2.4.4	Anaerobic process performance	193
4.2.2.5	Geopolymer spheres characterization after anaerobic digestion assays	196
4.2.3	<i>Comparison of fly ash-based geopolymer spheres assays for methane production</i>	199
4.3	PHASE 3: RED MUD-BASED GEOPOLYMERS ADDITION TO ANAEROBIC DIGESTION ASSAYS	205
4.3.1	<i>Red mud-based geopolymer spheres: anaerobic digestion assays with cheese whey</i>	206
4.3.1.1	Geopolymer spheres characterization before anaerobic digestion assays	206
4.3.1.2	Oxitop batch assays with the addition of red mud-based geopolymer spheres	207
4.3.1.3	Fed-batch assays with red mud-based geopolymer spheres addition	210
4.3.1.3.1	pH evolution	211
4.3.1.3.2	Volatile fatty acids production	213
4.3.1.3.3	Methane production	216
4.3.1.3.4	Anaerobic process performance	219
4.3.1.4	Geopolymer spheres characterization after anaerobic digestion assays	224
4.3.2	<i>Comparison of red mud-based geopolymer spheres assays for methane production</i>	226
4.3.3	<i>pH control of the anaerobic digestion process using geopolymer spheres based on fly ash versus based on red mud wastes</i>	228
5 	CONCLUSIONS AND PERSPECTIVES FOR FUTURE WORK	231
5.1	CONCLUSIONS	231
5.2	PERSPECTIVES FOR FUTURE WORK	235
6 	REFERENCES	239
7 	APPENDICES	259
7.1	EXAMPLE OF A CALIBRATION CURVE FOR TOTAL PHOSPHOROUS AS ORTHOPHOSPHATES DETERMINATION	259
7.2	DEVELOPMENT OF THE METHOD FOR DETERMINATION OF ADSORBABLE ORGANIC HALIDES	259
7.3	EXAMPLE OF CALIBRATION CURVES FOR VOLATILE FATTY ACIDS DETERMINATION	260
7.4	EXAMPLE OF CALIBRATION CURVES FOR INORGANIC COMPOUNDS DETERMINATION	262

List of Figures

FIGURE 1 WASTE(WATER)-TO-ENERGY PROCESS FLOW, ENCOMPASSING A PROCESS OF VALORIZATION THROUGH ANAEROBIC DIGESTION OF WASTE OR WASTEWATER STREAMS INTO ADDED-VALUE PRODUCTS, SUCH AS METHANE-RICH BIOGAS AND DIGESTATE.....	4
FIGURE 2 SUSTAINABLE DEVELOPMENT GOALS DEFINED BY THE UNITED NATIONS FOR 2030 (GRAPHICS FROM UN, 2020).	5
FIGURE 3 INTEGRATION OF DIFFERENT TYPES OF WASTES IN WASTE(WATER)-TO-ENERGY APPROACH, DIVIDED INTO THREE PHASES, ACCORDING TO THE TYPE OF INORGANIC WASTE ADDED. IN PHASE 1, THE ADDITION OF FLY ASH (FA) POWDER TO THE AD OF BOTH PULP AND PAPER (P&P) EFFLUENT AND CHEESE WHEY (CW); IN PHASE 2, THE ADDITION OF FLY ASH-BASED GS (FAGS) AND IN PHASE 3, THE ADDITION OF RED MUD-BASED GS (RMGS), BOTH TO THE AD OF CW FOR METHANE PRODUCTION.	7
FIGURE 4 NUMBER OF PUBLICATIONS FOR THE THREE MAIN WASTES UNDER STUDY: “RED MUD OR BAUXITE RESIDUE” FROM ALUMINA REFINING INDUSTRY, “FLY ASH” FROM BIOMASS COMBUSTION AND “CHEESE WHEY” FROM THE DAIRY INDUSTRY. DATA COLLECTED FROM THE SCOPUS DATABASE, IN MARCH 2020, AND INCLUDES ALL THE PUBLICATIONS UNTIL 2019. .	8
FIGURE 5 SCHEMATIC DIVISION OF THE WORK PRESENTED IN THIS THESIS.	10
FIGURE 6 MAIN TYPES OF WASTE GENERATED WORLDWIDE (A) AND THE ANNUALLY WASTE GENERATION BY REGION (B), BASED ON DATA PRESENTED BY KAZA ET AL. (2018).	13
FIGURE 7 LINEAR ECONOMY APPROACH FOR VIRGIN RESOURCES <i>VERSUS</i> THE CIRCULAR ECONOMY APPROACH FOR BIOLOGICAL NUTRIENTS (ADAPTED FROM PISCICELLI AND LUDDEN (2016)).	16
FIGURE 8 BIOCHEMISTRY OF ANAEROBIC DEGRADATION OF COMPLEX ORGANIC MATTER TO GENERATE METHANE-RICH BIOGAS. IN THE PRESENCE OF SULFATE, INTERMEDIATES SUCH AS VFA, ACETATE AND HYDROGEN, ARE DIVERTED FROM THE METHANE GENERATION AND USED FOR SULFATE REDUCTION WITH THE GENERATION OF HYDROGEN SULFITE.	22
FIGURE 9 USES OF BIOGAS PRODUCED IN AD PROCESS.....	30
FIGURE 10 GENERAL EFFECT OF THE CONCENTRATION OF THE ELEMENTS IN THE MEDIUM ON THE RATE OF BIOLOGICAL REACTIONS (BASED ON McCARTY (1964B)).	35
FIGURE 11 BIOREACTOR CONFIGURATIONS FOR ANAEROBIC TREATMENT OF HIGHLY POLLUTED INDUSTRIAL WASTEWATERS (GRAPHICS FROM (BACHMANN ET AL., 2008)): (A) ANAEROBIC CONTACT REACTOR; (B) ANAEROBIC FILTERS (AF) WITH DOWN-FLOW AND UP-FLOW; (C) ANAEROBIC FIXED FILM REACTOR (AFFR), WITH TWO DIFFERENT SUPPORTING STRUCTURES; (D) UP-FLOW ANAEROBIC SLUDGE BLANKET (UASB) REACTOR; (E) ANAEROBIC FLUIDIZED BED REACTOR (FBR).	41
FIGURE 12 FLOWCHART OF A P&P MILL, WITH KRAFT PULPING PROCESS AND BLEACHED PULP TO PRODUCE PAPER. IT IS HIGHLIGHTED TWO OF THE WASTES GENERATED IN THE P&P INDUSTRY: FLY ASHES FROM BIOMASS BURNING AND BLEACHING EFFLUENT FROM THE PULP BLEACHING PROCESS.	48
FIGURE 13 SIMPLIFIED FLOWSHEET FOR RAW MATERIALS USE AND FATE IN A TYPICAL P&P MILL (REPRODUCED FROM KAMALI ET AL. (2016) WITH AUTHORS AUTHORIZATION).....	51
FIGURE 14 MOST COMMON CHLORINATED ORGANIC COMPOUNDS IDENTIFIED IN P&P EFFLUENTS.....	56
FIGURE 15 CHEESE MANUFACTURING FROM RAW MILK WITH WHEY GENERATION, WITH THE INTEGRATION OF DIFFERENT TECHNOLOGIES FOR WHEY VALORIZATION.	64
FIGURE 16 LOCATION OF KARST AND LATERITE BAUXITE DEPOSITS WORLDWIDE (REPRODUCED FROM MEYER (2004)).	72
FIGURE 17 BAYER’S PROCESS FOR ALUMINA REFINING FROM BAUXITE, GENERATING A BY-PRODUCT (RED MUD).....	73
FIGURE 18 WWTP IN ILHAVO, WHERE THE ANAEROBIC INOCULUM WAS COLLECTED (PICTURE BY AdCL, 2019).	91
FIGURE 19 GEOPOLYMER SPHERES USED IN AD ASSAYS: (A) FA-BASED GEOPOLYMER SPHERES; (B) RM-BASED GEOPOLYMER SPHERES.....	95
FIGURE 20 OXITOP SYSTEM USED IN BATCH ANAEROBIC ASSAYS AND SAMPLE FLASKS. 1) MEASURING HEAD; 2) GLASS SAMPLE VESSEL; 3) NOZZLE AND SEPTUM SEAL.....	98
FIGURE 21 SCHEME OF BATCH AND FED-BATCH BIOREACTORS SET-UP, INCLUDING THE WATER DISPLACEMENT SYSTEM USED TO MEASURE THE BIOGAS VOLUME PRODUCED IN ANAEROBIC ASSAYS.	102
FIGURE 22 SUBSTRATE ADDITIONS PERFORMED (EXPRESSED AS GO ₂ /L) AND THEORETICAL F/M RATIO IN 5 L FED-BATCH AD REACTORS TREATING CHEESE WHEY, WITH RMGS AS BUFFER MATERIAL.	104
FIGURE 23 FLOWCHART FOR THE SAMPLING METHODOLOGY APPLIED TO BIOREACTORS’ SAMPLES.	105
FIGURE 24 RESPIROMETRIC BOD SYSTEM USED TO DETERMINE BOD ₅	107

FIGURE 25	EXAMPLE OF A CHROMATOGRAM OBTAINED IN VFA ANALYSIS (SAMPLE PRESENTED: STANDARD SOLUTION P#4).	112
FIGURE 26	ANAEROBIC PERFORMANCE OF <i>OXITOP</i> BIOREACTORS WITH DIFFERENT INITIAL D_0 CONCENTRATIONS: CUMULATIVE PRESSURE (A), CUMULATIVE METHANE VOLUME (B), MASS OF AOX REMOVED AND PERCENTAGE OF AOX REMOVAL (C) AND INITIAL AND FINAL PH (D).	126
FIGURE 27	ANAEROBIC PERFORMANCE OF <i>OXITOP</i> BIOREACTORS WITH DIFFERENT D_0 CONCENTRATIONS: INITIAL AND FINAL PH (A), CUMULATIVE METHANE VOLUME (B) AND AOX REMOVED AND PERCENTAGE OF AOX REMOVAL (C).	128
FIGURE 28	EFFECT OF INITIAL SCOD LOAD ON THE LAG PHASE (BLUE Δ), THE VOLUME OF METHANE PRODUCED IN THE FIRST 5 DAYS AFTER THE LAG PHASE (GREY \square) AND THE METHANE PRODUCTION RATE (ORANGE \circ).	129
FIGURE 29	AOX REMOVAL, METHANIZATION DEGREE, ANAEROBIC BIODEGRADABILITY (A) AND METHANE YIELD (B) FOR THE ANAEROBIC ASSAYS WITH AN INITIAL SCOD LOAD OF 0.9, 1.8, 2.0 AND 3.0 gO_2/L , USING D_0 AS SUBSTRATE.	130
FIGURE 30	PERFORMANCE OF <i>OXITOP</i> BATCH BIOREACTORS WITH DIFFERENT FA ADDITIONS REGARDING INITIAL AND FINAL PH AND ALKALINITY MEASURED (A) AND SCOD AND VFA (H-AC, H-PROP AND H-N-BUT) CONCENTRATIONS, EXPRESSED AS COD EQUIVALENTS (B).	132
FIGURE 31	MASS OF AOX REMOVED AND PERCENTAGE OF AOX REMOVAL (A), SCOD REMOVAL AND AOX REMOVAL (B) AND VFA YIELD (C), FOR THE ASSAYS WITH DIFFERENT ADDITIONS OF FA, USING D_0 AS SUBSTRATE.	133
FIGURE 32	METHANIZATION PERFORMANCE FOR THE ASSAYS WITH FA ADDITION, USING D_0 AS SUBSTRATE: CUMULATIVE METHANE VOLUME (A), METHANIZATION DEGREE AND ANAEROBIC BIODEGRADABILITY (B) AND METHANE YIELD (C).	134
FIGURE 33	METALS (CA, NA, MG, FE) CONCENTRATION AT THE BEGINNING AND AT THE END OF <i>OXITOP</i> BATCH ANAEROBIC ASSAYS WITH D_0 EFFLUENT AND FA ADDITION.	136
FIGURE 34	SBOD/SCOD RATIO BEFORE AND AFTER AD TESTS AND INCREASE ON CALCULATED RATIO AFTER THE ANAEROBIC TREATMENT.	136
FIGURE 35	REPRESENTATION OF THE THEORETICAL MASS OF EACH OXIDE/ELEMENT ADDED TO EACH BIOREACTOR, CONSIDERING THE TYPE OF ASHES USED (CA5 OR CTB).	138
FIGURE 36	PH VALUES (\pm STANDARD DEVIATION) MEASURED AT THE BEGINNING, ON THE 15 TH DAY AND AT THE END OF THE <i>OXITOP</i> BATCH ANAEROBIC ASSAYS WITH CHEESE WHEY AS SUBSTRATE AND FLY ASH FOR PH CONTROL.	140
FIGURE 37	RELATIONSHIP BETWEEN PH (INITIAL PH IN GREEN \square , AND FINAL PH IN BLUE Δ) AND FA CONCENTRATION ADDED, IN BATCH <i>OXITOP</i> OF CHEESE WHEY AD ASSAYS.	140
FIGURE 38	VFA COMPOSITION (H-AC, H-PROP AND H-N-BUT) OF THE INITIAL (A) AND FINAL (B) SAMPLES FOR THE AD OF CHEESE IN WITH DIFFERENT FA CONCENTRATIONS IN <i>OXITOP</i> BIOREACTORS.	142
FIGURE 39	ANAEROBIC PERFORMANCE FOR ANAEROBIC <i>OXITOP</i> ASSAYS WITH CHEESE WHEY AND DIFFERENT FA ADDITION FOR PH CONTROL: DEGREE OF ACIDIFICATION (DA), sCOD REMOVAL AND METHANE CONTENT IN BIOGAS (A) AND VFA YIELD (B) AT THE END OF THE EXPERIMENT.	144
FIGURE 40	METALS (CA, NA, MG, FE) CONCENTRATION AT THE BEGINNING AND AT THE END OF <i>OXITOP</i> BATCH ANAEROBIC ASSAYS WITH CHEESE WHEY AND FA ADDITION, AT DIFFERENT AMOUNTS.	145
FIGURE 41	REPRESENTATION OF THE THEORETICAL MASS OF EACH OXIDE/ELEMENT ADDED TO FOUR BIOREACTORS (CW_0.2, CW_3, CW_5 AND CW_9) WITH THE ADDITION OF CA5 FLY ASH POWDER.	146
FIGURE 42	OPTICAL (A AND E) AND SEM CHARACTERIZATION (B-D AND F-H) OF THE POROUS GEOPOLYMER SPHERES PREPARED WITH (A-D) 33 WT.% (MK-BASED SPHERES) AND (E-H) 75 WT.% FA (FA-BASED SPHERES). FIGURE (D) AND (H) CORRESPOND TO BINARY IMAGES (BLACK AND WHITE) OF THE SEM MICROGRAPHS.	152
FIGURE 43	CUMULATIVE AREA RATIO FOR THE DIFFERENT COMPOSITIONS, MK-BASED AND FA-BASED GS (MEASURED USING IMAGE ANALYSIS).	153
FIGURE 44	EDS SPECTRUM OF THE MK-BASED AND FA-BASED GEOPOLYMER SPHERES (LEFT); EDS MAPS (RIGHT) OF MK-BASED (A AND B) AND FA-BASED (C AND D) GEOPOLYMER SPHERES. THE FIRST COLUMN (A AND C) MAPS CORRESPOND TO THE SPHERES EXTERIOR SURFACE AND THE SECOND COLUMN (B AND D) TO THEIR INNER PART.	153
FIGURE 45	XRD PATTERNS OF MK-BASED AND FA-BASED GEOPOLYMERS SPHERES.	154
FIGURE 46	RESULTS FOR THE PRELIMINARY TESTS PERFORMED WITH THE ADDITION OF GS, REGARDING SCOD (A) AND PH (B) OVER TIME.	155
FIGURE 47	PH FLUCTUATION (AVERAGE VALUES \pm STANDARD DEVIATION) IN ANAEROBIC DIGESTERS AS A FUNCTION OF TIME WITH ALKALINE CHEMICALS (A), FA-BASED (B) AND MK-BASED (C) GEOPOLYMER SPHERES ADDITION.	158

FIGURE 48 METHANE CONTENT VS PH AT THE END OF OXITOP EXPERIMENTS CONTAINING DIFFERENT ALKALINE AGENTS AT DIFFERENT CONCENTRATIONS.	159
FIGURE 49 FLUCTUATION OF PH IN ANAEROBIC DIGESTERS TO OPTIMIZE METHANE PRODUCTION AS A FUNCTION OF TIME, WITH THE ADDITION OF DIFFERENT AMOUNTS OF FA-BASED GEOPOLYMER SPHERES.	160
FIGURE 50 TOTAL VFA CONCENTRATIONS, REPRESENTED AS ACETIC ACID EQUIVALENTS PER L, OVER TIME, FOR BATCH BIOREACTORS OPERATED, NAMELY FA1 (◊), FA2 (Δ) AND FA3 (□).	162
FIGURE 51 VFA COMPOSITION OVER TIME IN ANAEROBIC DIGESTERS FOR THE DIFFERENT SYSTEMS: (A) FA1 (WITHOUT CHEMICAL ALKALINITY OR SPHERES ADDITION); (B) FA2 (WITH 20 G/L OF FA-BASED SPHERES ADDITION); (C) FA3 (WITH 28 G/L OF FA-BASED SPHERES ADDITION).	162
FIGURE 52 CO ₂ /CH ₄ RATIO IN ANAEROBIC ASSAYS FA1 (◊), FA2 (Δ) AND FA3 (□) DURING THE INCUBATION TIME.	164
FIGURE 53 METHANE PRODUCTION IN THE BIOREACTORS FA1 (◊), FA2 (Δ) AND FA3 (□) DETERMINED OVER TIME IN ASSAYS WITH THE ADDITION OF DIFFERENT AMOUNTS OF FA-BASED GS (FA2 AND FA3) <i>VERSUS</i> THE ASSAY WITHOUT CHEMICAL ALKALINITY OF GS ADDITION (FA1): (A) METHANE PRODUCED, EXPRESSED AS COD EQUIVALENTS; (B) METHANE YIELD.	164
FIGURE 54 EVOLUTION OF CH ₄ (◊), TOTAL VFA CONCENTRATION (□), PH (Δ) AND SCOD CONTENT (○) WITH TIME FOR THE ASSAYS FA1, FA2 AND FA3.	166
FIGURE 55 PERFORMANCE PARAMETERS FOR BATCH ASSAYS FA1, FA2 AND FA3, DETERMINED AT THE END OF THE EXPERIMENTS: (A) DEGREE OF ACIDIFICATION (DA), SCOD REMOVAL AND METHANIZATION DEGREE AND (B) COD BALANCE CONSIDERING THE ACIDIFIED (AS G _{O2} /L) AND THE NON-ACIDIFIED FRACTION OF SCOD, THE GAS (METHANE) FORMED (AS G _{O2} /L) AND THE REMOVED SCOD.	168
FIGURE 56 SEM MICROGRAPHS AND EDS SPECTRUM OF THE FA-BASED GEOPOLYMER SPHERES AFTER THE 70 TH DAY OF BATCH TESTS INSIDE THE ANAEROBIC DIGESTER: (A) EXTERIOR SURFACE AND (B) INNER PART.	169
FIGURE 57 SEM MICROGRAPHS (A, B, D, E) AND EDS SPECTRA (C, F) OF THE GS PREPARED USING TWO DIFFERENT FOAMING AGENT AMOUNTS: (A, B AND C) LPGS AND (D, E AND F) HPGS.	172
FIGURE 58 XRD PATTERNS OF THE GEOPOLYMERIC SPHERES (LPGS AND HPGS) BEFORE AND AFTER AD TESTS.	173
FIGURE 59 PH FLUCTUATION (AVERAGE VALUES ± STANDARD DEVIATION) IN ANAEROBIC DIGESTERS AS A FUNCTION OF TIME WITH ALKALINE CHEMICALS ADDITION (A), LPGS ADDITION (B) AND HPGS ADDITION (C).	174
FIGURE 60 PH VALUES OVER TIME FOR 2-CYCLE FED-BATCH BIOREACTORS WITH LPGS AND HPGS. THE ADDITION OF SUBSTRATE IS MARKED BY THE DASHED LINE AND THE GREY BAR HIGHLIGHTS THE METHANOGENIC PH RANGE.	176
FIGURE 61 TVFA CONCENTRATIONS (REPRESENTED AS ACETIC ACID EQUIVALENTS PER L) OVER TIME, FOR THE FED-BATCH (2-CYCLE) BIOREACTORS OPERATED.	179
FIGURE 62 CONCENTRATION OF INDIVIDUAL VFA SPECIES, NAMELY ACETIC, PROPIONIC AND N-BUTYRIC ACIDS, WITH TIME, FOR FED-BATCH (2-CYCLE) BIOREACTORS OPERATED.	179
FIGURE 63 METHANE YIELD DETERMINED DURING THE 1 ST AD-CYCLE AND THE 2 ND AD-CYCLE, WITH THE ADDITION OF DIFFERENT AMOUNTS OF GS WITH DIFFERENT POROSITIES.	181
FIGURE 64 CO ₂ TO CH ₄ RATIO IN BIOGAS PRODUCED IN THE ASSAYS FA4 (○), FA5 (□), FA6 (Δ) AND FA7 (◊).	181
FIGURE 65 EVOLUTION OF CH ₄ PRODUCTION MEASURED (MARKERS) AND PREDICTED BY THE MODIFIED GOMPertz MODEL (LINES) IN THE ASSAYS FA4 (○), FA5 (□), FA6 (Δ) AND FA7 (◊).	183
FIGURE 66 EVOLUTION OF CH ₄ (◊), TOTAL VFA CONCENTRATION (□) AND PH (Δ) WITH TIME FOR ASSAYS FA4, FA5, FA6 AND FA7.	184
FIGURE 67 PERFORMANCE PARAMETERS FOR BIOREACTORS FA4 TO FA7, IN THE 1 ST AND THE 2 ND AD CYCLES, INCLUDING DEGREE OF ACIDIFICATION, SCOD REMOVAL AND DEGREE OF METHANIZATION.	185
FIGURE 68 COD BALANCE IN 1 ST AD CYCLE (A) AND 2 ND AD CYCLE (B), CONSIDERING THE ACIDIFIED (AS G _{O2} /L) AND NON-ACIDIFIED SCOD, THE GAS (METHANE) FORMED (AS G _{O2} /L) AND THE REMOVED SCOD.	187
FIGURE 69 PH VALUES OVER TIME FOR FED-BATCH ASSAYS WITH 4 AD CYCLES AND HPGS ADDITION. THE DASHED LINES MARK THE SUBSTRATE ADDITIONS AND THE GREY BAR IS HIGHLIGHTING THE OPTIMUM METHANOGENIC PH RANGE.	188
FIGURE 70 TOTAL VFA CONCENTRATION (REPRESENTED AS ACETIC ACID EQUIVALENTS PER L) OVER INCUBATION TIME OF 4-CYCLE FED-BATCH ASSAYS.	190
FIGURE 71 CONCENTRATION OF INDIVIDUAL VFA SPECIES, NAMELY ACETIC, PROPIONIC AND N-BUTYRIC ACIDS, OVER TIME, FOR FED-BATCH (4-CYCLE) OPERATED BIOREACTORS, NAMELY FA8, FA9 AND FA10.	190

FIGURE 72 METHANE YIELD DETERMINED OVER TIME IN ASSAYS WITH THE ADDITION OF DIFFERENT TYPES OF ALKALINE AGENTS (CHEMICAL COMPOUNDS VS HIGH POROSITY GEOPOLYMER SPHERES).....	192
FIGURE 73 CO ₂ TO CH ₄ RATIO IN BIOGAS PRODUCED IN ASSAYS FA8 (○), FA9 (◇) AND FA10 (Δ).....	193
FIGURE 74 EVOLUTION OF CH ₄ (◇), TOTAL VFA CONCENTRATION (□) AND PH (Δ) WITH TIME FOR THE ASSAYS FA8 AND FA9.	194
FIGURE 75 DEGREE OF ACIDIFICATION, SCOD REMOVAL AND METHANIZATION DEGREE FOR BIOREACTORS FA8 AND FA9, IN THE 1 ST , 2 ND , 3 RD AND 4 TH AD CYCLES.....	196
FIGURE 76 COD BALANCE AT THE END OF EACH AD CYCLE FOR FA8 AND FA9 BIOREACTORS, CONSIDERING THE ACIDIFIED (MEASURED AS GO ₂ /L) AND NON-ACIDIFIED sCOD, THE GAS (METHANE) FORMED (MEASURED AS GO ₂ /L) AND THE REMOVED SCOD.	196
FIGURE 77 SEM MICROGRAPHS (A, B, D, E) AND EDS SPECTRA (C, F) OF THE GS AFTER FED-BATCH TESTS INSIDE THE ANAEROBIC DIGESTER: (A, B, C) LPGS AND (D, E, F) HPGS.	197
FIGURE 78 PH RANGE IN STABILITY PHASE IN ASSAYS WITH FA-BASED GS (FA2, FA3, FA5, FA6, FA7, FA9 AND FA10) AND RESPECTIVE REFERENCE ASSAYS (FA4 AND FA8).....	199
FIGURE 79 OPTICAL MICROSCOPY PHOTOGRAPH (A) AND SEM CHARACTERIZATION (B) OF THE RED MUD-BASED INORGANIC POLYMER SPHERES, INCLUDING THE EDS SPECTRUM OF THE SPHERES SURFACE (C).	206
FIGURE 80 METHANE PRODUCTION (CUMULATIVE PRESSURE INSIDE OXITOP BIOREACTORS (A) AND CUMULATIVE METHANE VOLUME (B)) AND PH (C) AND CONDUCTIVITY VALUES AT 25 °C (D), MEASURED DURING THE INCUBATION TIME FOR OXITOP TESTS WITH RMGS ADDITION.	208
FIGURE 81 INITIAL AND FINAL VALUES FOR ALKALINITY AND SCOD IN THE OXITOP BIOREACTORS WITH RMGS ADDITION.....	209
FIGURE 82 METHANIZATION DEGREE, ANAEROBIC BIODEGRADABILITY, METHANE CONTENT AND SCOD REMOVAL PERCENTAGE OBTAINED AT THE END OF THE OXITOP BIOREACTORS TESTING THE ADDITION OF RMGS AS PH BUFFER MATERIAL.....	210
FIGURE 83 PH EVOLUTION WITH TIME FOR ASSAYS RM1 (○), RM2 (◇) AND RM3 (□). THE DASHED LINES MARK THE SUBSTRATE ADDITIONS AND THE GREY BAR IS HIGHLIGHTING THE OPTIMUM METHANOGENIC PH RANGE.	211
FIGURE 84 TOTAL VFA CONCENTRATION (REPRESENTED AS ACETIC ACID EQUIVALENTS PER L) DURING INCUBATION TIME OF RM1 (○), RM2 (◇) AND RM3 (□) ASSAYS.	214
FIGURE 85 CONCENTRATION OF INDIVIDUAL VFA SPECIES, NAMELY ACETIC, PROPIONIC AND N-BUTYRIC ACIDS, WITH TIME, FOR FED-BATCH BIOREACTORS OPERATED WITH THE ADDITION OF RMGS, NAMELY RM1, RM2 AND RM3.....	214
FIGURE 86 METHANE PRODUCED IN THE BIOREACTORS RM1 (○), RM2 (◇) AND RM3 (□), EXPRESSED AS COD EQUIVALENTS (A) AND METHANE YIELD (B) DETERMINED OVER TIME IN ASSAYS WITH THE ADDITION OF DIFFERENT TYPES OF ALKALINE AGENTS (CHEMICAL COMPOUNDS – RM2 – VS RED MUD-BASED GEOPOLYMER SPHERES – RM3).	217
FIGURE 87 CO ₂ TO CH ₄ RATIO IN THE BIOGAS PRODUCED IN THE ANAEROBIC ASSAYS RM2 (◇) AND RM3 (□).	218
FIGURE 88 EVOLUTION OF CH ₄ (◇), TOTAL VFA CONCENTRATION (□) AND PH (Δ) WITH TIME FOR THE ASSAYS RM1, RM2, AND RM3.	220
FIGURE 89 ANAEROBIC PERFORMANCE FOR EACH AD CYCLE IN BIOREACTORS RM2 AND RM3, INCLUDING DEGREE OF ACIDIFICATION (A), METHANIZATION DEGREE (B), SCOD REMOVAL (C), AND ANAEROBIC BIODEGRADABILITY (D).	222
FIGURE 90 COD BALANCE AT THE END OF EACH AD CYCLE FOR RM1, RM2, AND RM3 BIOREACTORS CONSIDERING THE ACIDIFIED (MEASURED AS GO ₂ /L) AND NON-ACIDIFIED sCOD, THE GAS (METHANE) FORMED (MEASURED AS GO ₂ /L), AND THE REMOVED SCOD.	223
FIGURE 91 OPTICAL MICROGRAPH (A), SEM MICROGRAPH (B), AND EDS SPECTRA (SPHERES SURFACE) (C) OF THE RED MUD-BASED GEOPOLYMER SPHERES AFTER AD ASSAYS.....	224
FIGURE 92 COMPARISON OF PH VALUES OVER TIME FOR ASSAYS WITH FA-BASED GS ADDITION (FA3 (□) AND FA7 (○)) AND RM-BASED GS ADDITION (RM2 (◇)).	228
FIGURE 93 EXAMPLE OF A CALIBRATION CURVE FOR THE DETERMINATION OF TOTAL PHOSPHOROUS AS ORTHOPHOSPHATES. .	259
FIGURE 94 EXAMPLE OF CALIBRATION LINES OBTAINED FOR INDIVIDUAL VFA DETERMINATION, NAMELY H-AC, H-PROP, H-I-BUT, H-N-BUT, H-I-VAL, H-N-VAL, AND H-N-CAP.....	261
FIGURE 95 EXAMPLE OF CALIBRATION LINES FOR METALS DETERMINATION.	263

List of Tables

TABLE 1 COMPARISON BETWEEN ANAEROBIC AND AEROBIC PROCESSES (FONSECA AND TEIXEIRA, 2006; HATTI-KAUL AND MATTIASSON, 2016).	20
TABLE 2 REPRESENTATION OF THE MOST COMMON MICROORGANISMS INVOLVED IN EACH AD METABOLIC STEP, NAMELY HYDROLYSIS, ACIDOGENESIS, ACETOGENESIS AND METHANOGENESIS. DESPITE ITS COMPETITIVE NATURE IN THE METHANE FORMATION, THE SULFATE REDUCTION WAS ALSO INCLUDED AS A METABOLIC STEP OF THE ANAEROBIC DEGRADATION OF ORGANIC MATTER.	23
TABLE 3 OPTIMUM PH RANGE FOR DIFFERENT STEPS OF ANAEROBIC CONVERSION OF ORGANIC MATTER INTO BIOGAS, CONSIDERED BY DIFFERENT AUTHORS.....	32
TABLE 4 TOXICITY LEVEL, THE IMPORTANCE FOR MICROORGANISMS AND THE BIOLOGICAL FUNCTION OF THE MOST REPRESENTATIVE MICRONUTRIENTS FOR ANAEROBIC SYSTEMS (MAO ET AL., 2015; PAULO ET AL., 2015; SHAH, 2014).	34
TABLE 5 CHEMICAL COMPOSITION OF DIFFERENT FLY ASH FROM PULP AND PAPER INDUSTRIES; MATERIALS COMPOSITIONS EXPRESSED AS OXIDES; LOI: LOSS ON IGNITION.	53
TABLE 6 SUMMARY OF BIOLOGICAL, ELECTROCHEMICAL AND CHEMICAL-PHYSICAL TECHNOLOGIES FOR THE TREATMENT OF AOX-RICH BLEACHING EFFLUENTS FROM P&P MILLS IN THE LAST 20 YEARS.....	57
TABLE 7 PHYSICO-CHEMICAL CHARACTERIZATION OF CHEESE WHEY STREAMS: SWEET WHEY AND ACID WHEY (CONSOLIDATED FROM DATA PRESENTED IN DRAGONE ET AL., 2011; DULLIUS ET AL., 2018; RAMA ET AL., 2019).	66
TABLE 8 SUMMARY OF PUBLISHED STUDIES REGARDING THE THEMATIC OF AD TREATMENT OF CHEESE WHEY FROM THE DAIRY INDUSTRY, IN THE LAST 20 YEARS.	70
TABLE 9 CHEMICAL COMPOSITION OF THE RED MUD RESULTING FROM THE BAYER PROCESS (CONSOLIDATED FROM DATA PRESENTED IN CENGELOGLU ET AL. (2003); PALMER ET AL. (2009); ZHANG ET AL. (2011).....	75
TABLE 10 RESUME OF BIOLOGICAL TECHNOLOGIES EMPLOYING RED MUD AS AN INORGANIC ADDITIVE.....	77
TABLE 11 EXAMPLES OF PUBLISHED WORKS REGARDING THE APPLICATION OF INORGANIC ADDITIVES TO THE AD PROCESS.	80
TABLE 12 COMPARISON BETWEEN GEOPOLYMERS AND ZEOLITES, REGARDING MAIN CHARACTERISTICS AND SYNTHESIS PROCESSES (HARDJITO ET AL., 2004; KOMNITSAS AND ZAHARAKI, 2007).	85
TABLE 13 PHYSICO-CHEMICAL CHARACTERIZATION OF THE ANAEROBIC BIOMASS USED AS AN INOCULUM IN THE AD ASSAYS (AVERAGE VALUE \pm STANDARD DEVIATION).	91
TABLE 14 PHYSICO-CHEMICAL CHARACTERISTICS OF D ₀ EFFLUENT (AVERAGE VALUE \pm STANDARD DEVIATION).	92
TABLE 15 PHYSICO-CHEMICAL CHARACTERISTICS AND ORGANOLEPTIC PARAMETERS OF CHEESE WHEY POWDER (PROVIDED BY THE CHEESE WHEY PRODUCER).	93
TABLE 16 CHARACTERIZATION OF CONCENTRATED CHEESE WHEY SOLUTION USED IN AD ASSAYS (AVERAGE VALUE \pm STANDARD DEVIATION).	93
TABLE 17 CHEMICAL COMPOSITION OF FA OBTAINED FROM DIFFERENT BIOMASS SOURCES (CA5 AND CTB), USED AS A POWDER ADDITIVE FOR AD EXPERIMENTS, FA USED AS A SOURCE OF ALUMINOSILICATES IN THE MANUFACTURE OF GEOPOLYMER SPHERES, IN ADDITION TO METAKAOLIN AND RED MUD RESIDUES. THE ELEMENTAL COMPOSITION OF THE MATERIALS WAS DETERMINED BY XRF AND IS EXPRESSED AS OXIDES. LOI WAS PERFORMED AT 1100 °C.	94
TABLE 18 MIXTURE COMPOSITION OF MK AND FA-BASED GEOPOLYMERS DURING THEIR PREPARATION.....	96
TABLE 19 MIXTURE COMPOSITION IN THE PREPARATION OF GEOPOLYMERS WITH LOW AND HIGH POROSITY.....	96
TABLE 20 MIXTURE COMPOSITION OF RED MUD-BASED GS CONTAINING 50 % OF RM WASTE.....	97
TABLE 21 COMPOSITION OF MICRO AND MACRONUTRIENTS SOLUTIONS ADDED TO ALL ANAEROBIC BIOREACTORS (COMPOSITION ADAPTED FROM VAN LIER ET AL., 1997).	97
TABLE 22 MAIN OPERATIONAL CONDITIONS FOR ANAEROBIC OXITOP BATCH ASSAYS WITH FLY ASH (POWDER) ADDITION, TESTING D ₀ AND CHEESE WHEY AS SUBSTRATES.....	99
TABLE 23 OPERATIONAL CONDITIONS FOR ANAEROBIC OXITOP BATCH ASSAYS WITH GEOPOLYMER SPHERES (FA-BASED, MK-BASED, LPGS, HPGS AND RMGS) ADDITION AND CHEESE WHEY AS SUBSTRATE.....	101
TABLE 24 OPERATIONAL CONDITIONS FOR ANAEROBIC BATCH/FED-BATCH ASSAYS WITH GEOPOLYMERS SPHERES ADDITION (FA-BASED, LPGS, HPGS AND RMGS).....	102

TABLE 25	THEORETICAL OXYGEN DEMAND (THOD) FOR THE ACIDIC SPECIES ANALYZED.	113
TABLE 26	WAVELENGTH AND FLAME TYPE USED FOR METALS DETERMINATION.	114
TABLE 27	PHYSICO-CHEMICAL CHARACTERISTICS (PH, AOX CONTENT AND ORGANIC MATTER CONTENT) OF D ₀ EFFLUENT AND THE MIXTURES: D ₀ +NAOH, D ₀ +CA5 AND D ₀ +CTB, USING FA FROM DIFFERENT TYPES OF BIOMASS BURNING (AVERAGE VALUE ± STANDARD DEVIATION).	131
TABLE 28	DURATION OF LAG PHASE, AD PERFORMANCE PARAMETERS AND AOX REMOVAL FOR D ₀ ASSAYS WITHOUT AND WITH FA ADDITION.	137
TABLE 29	PH VALUES ON DAYS 0 AND 21, METHANE CONTENT IN THE BIOGAS PRODUCED AND TOTAL VFA CONCENTRATION AT THE END OF THE EXPERIMENT, IN OXITOP BIOREACTORS CONTAINING DIFFERENT ALKALINE AGENTS (CaCO ₃ AND POWDER FA) IN DIFFERENT INITIAL CONCENTRATIONS.	141
TABLE 30	COMPARATIVE VALUES FOR THE PERFORMANCE OF AD OF D ₀ AND CHEESE WHEY WITH FA ADDITION.	147
TABLE 31	MIXTURES COMPOSITIONS FOR SCOD TESTING, WITH GS ADDITION.	155
TABLE 32	PH VALUES ON DAYS 0, 1 AND 21, IN OXITOP BIOREACTORS CONTAINING DIFFERENT ALKALINE AGENTS IN DIFFERENT CONCENTRATIONS.	157
TABLE 33	MAXIMUM VFA PRODUCTION RATE, SCOD CONSUMPTION RATE AND METHANE PRODUCTION RATE FOR BOTH FA2 AND FA3 ASSAYS.	166
TABLE 34	COST OF RAW MATERIALS USED IN THE PREPARATION OF THE COMMERCIAL BUFFER SOLUTION AND IN THE PRODUCTION OF FA-BASED GEOPOLYMER SPHERES PRODUCTION.	170
TABLE 35	PH VALUES AT DAY 0, 1 AND 21, IN OXITOP BIOREACTORS CONTAINING DIFFERENT ALKALINE AGENTS AND GS TYPES (LOW AND HIGH POROSITY) AT DIFFERENT CONCENTRATIONS.	174
TABLE 36	PARAMETERS OF THE MODIFIED GOMPertz MODEL FOR CH ₄ PRODUCTION	183
TABLE 37	MAXIMUM VFA PRODUCTION RATE, VFA CONSUMPTION RATE AND METHANE PRODUCTION RATE FOR FED-BATCH ASSAYS FA4, FA5, FA6 AND FA7 (VALUES AND RESPECTIVE DETERMINATION COEFFICIENT), DETERMINED INDEPENDENTLY FOR THE 1 ST AND 2 ND AD CYCLES.	186
TABLE 38	MAXIMUM VFA PRODUCTION RATE, VFA CONSUMPTION RATE AND METHANE PRODUCTION RATE FOR THE 1 ST AD CYCLE OF THE FED-BATCH ASSAYS FA8 AND FA9 (VALUES AND RESPECTIVE DETERMINATION COEFFICIENT), AND MAXIMUM METHANE PRODUCTION RATE IN THE 2 ND , 3 RD AND 4 TH AD CYCLES FOR BIOREACTORS FA8 AND FA9.	195
TABLE 39	CHEMICAL COMPOSITION OF THE GS WITH LOW AND HIGH POROSITY, BEFORE AND AFTER THE FED-BATCH AD TESTS; THE ELEMENTAL COMPOSITION OF THE MATERIAL AS DETERMINED BY XRF IS EXPRESSED AS OXIDES AND LOSS ON IGNITION (LOI) WAS DETERMINED AT 1100°C.	197
TABLE 40	COMPARATIVE VALUES FOR THE PERFORMANCE OF AD BIOREACTORS WITH CHEESE WHEY AS A SUBSTRATE, USING DIFFERENT TYPES OF GEOPOLYMER SPHERES, AS A pH CONTROL MATERIAL. FOR BIOREACTORS FA6, FA7 AND FA9, THE RESULTS ARE PRESENTED BY THE AD CYCLE.	200
TABLE 41	PH VALUES AT DAY 0, 1 AND 35, IN OXITOP BIOREACTORS CONTAINING DIFFERENT ALKALINE AGENTS AT DIFFERENT CONCENTRATIONS.	208
TABLE 42	MAXIMUM METHANE PRODUCTION RATE FOR ALL AD CYCLES PERFORMED WITH RM2 AND RM3 BIOREACTORS, EXPRESSED IN ML/D.	221
TABLE 43	COMPARATIVE VALUES FOR THE PERFORMANCE OF AD BIOREACTORS WITH CHEESE WHEY AS A SUBSTRATE, USING RM-BASED GS ADDITION, AS A pH CONTROL MATERIAL. FOR THE FED-BATCH BIOREACTOR, THE RESULTS OF THE 6 TH AD CYCLE ARE PRESENTED (EQUIVALENT TO THE SAME OPERATION TIME AND LOAD PERFORMED FOR THE BATCH BIOREACTOR R27).	226
TABLE 44	PREPARATION OF STOCK SOLUTIONS FOR TOTAL PHOSPHOROUS AS ORTHOPHOSPHATES DETERMINATION.	259
TABLE 45	CHECKING STANDARD SOLUTIONS FOR AOX DETERMINATION.	260
TABLE 46	CONCENTRATION OF ACIDIC SPECIES IN THE DILUTED STANDARD SOLUTIONS FOR VFA DETERMINATION.	261
TABLE 47	RETENTION TIME AND SLOP OF CALIBRATION LINES FOR EACH ACIDIC SPECIE.	261
TABLE 48	CONCENTRATIONS OF INTERMEDIATE STANDARD SOLUTIONS FOR METALS DETERMINATION.	262
TABLE 49	CONCENTRATION OF CALCIUM, MAGNESIUM, IRON, AND SODIUM IN THE DILUTED STANDARD SOLUTIONS FOR METALS DETERMINATION, AND AN INDICATION OF CHECK DILUTED STANDARD SOLUTION.	263

List of Abbreviations

AD – Anaerobic Digestion	LCFA – Long-chain Fatty Acids
AOX – Adsorbable Organic Halides	LOI – Loss on Ignition
Alk – Alkalinity	LPGS – Low Porosity Geopolymers Spheres (fly ash based)
A _r – Pore area ratio	MK – Metakaolin
BET – Brunauer, Emmett and Teller	nZVI – Nano zero-valent iron
BOD – Biochemical Oxygen Demand	OHPA – Obligate Hydrogen-producing Acetogens
CEPI – Confederation of European Paper Industries	PEG – Polyethylene Glycol
CHP – Combined Heat and Power	P&P – Pulp and Paper
CoA – Coenzyme A	RM – Red Mud
COD – Chemical Oxygen Demand	RMGS – Red Mud Geopolymer Spheres
CSTR - Continuous Stirred Tank Reactor	RMP – Refiner mechanical pulping
CTMP – Chemithermomechanical Pulping	sCOD – Soluble Chemical Oxygen Demand
DA – Degree of Acidification	SDG – Sustainable Development Goals
DIET – Direct Interspecies Electron Transfer	SEM – Scanning Electron Microscopy
ECF – Elemental Chlorine Free	SGWP – Stone Ground Wood Pulping
EDS – Energy Dispersion Spectroscopy	SRT – Sludge Retention Time
EGSB – Expanded Granular Sludge Bed	TCF – Total Chlorine Free
EU – European Union	TCOD – Total Chemical Oxygen Demand
FA – Fly Ash	thOD – Theoretical Oxygen Demand
FAGS – Fly Ash Geopolymer Spheres	TMP – Thermomechanical Pulping
GS – Geopolymer Spheres	TOC – Total Organic Carbon
GWP – Global Warming Potential	TSS – Total Suspended Solids
H-Ac – Acetic Acid	TVFA – Total Volatile Fatty Acids
H-i-But – iso-Butyric Acid	UASB – Up-flow Anaerobic Sludge Blanket
H-i-Val – iso-Valeric Acid	UN – United Nations
H-n-But – n-Butyric Acid	VFA – Volatile Fatty Acids
H-n-Cap – n-Caproic Acid	VS – Volatile Solids
H-n-Val – n-Valeric Acid	VSS – Volatile Suspended Solids
H-Prop – Propionic Acid	WW – Wastewater
HPGS – High Porosity Geopolymers Spheres (fly ash based)	WWTP – Wastewater Treatment Plant
HRT – Hydraulic Retention Time	XRD – X-ray powder diffraction
IET – Interspecies Electron Transfer	XRF – X-ray fluorescence

Introduction | 1

1 | Introduction

“In a world where demands for freshwater are continuously growing, and where limited water resources are increasingly stressed by over-abstraction, pollution and climate change, neglecting the opportunities arising from improved wastewater management is nothing less than unthinkable in the context of a circular economy.”

(United Nations World Water Assessment Programme, 2017)

1.1 Motivation and Relevance

1.1.1 From waste to energy: a sustainable approach

Worldwide, energy demand is increasing due to rapid population growth and the inevitable associated activities. Similarly, waste materials, including solid waste and wastewater, are constantly being generated and their accumulation or inadequate management can lead to significant environmental and health problems. All sectors of our environment are affected when poor waste management is the main practice (Kaza et al., 2018):

- oceans are contaminated due to dumped waste (organic and other, such as plastics) and wastewater discharges;
- natural disasters, such as floods, are more common every day due to clogging drains with several wastes;
- transmitted diseases and respiratory problems can be associated with the accumulation of untreated waste;
- animals may be at risk when consuming waste without knowing it;
- economic development is affected and does not benefit from untreated waste.

In this sense, it is urgent to develop new technologies in the field of waste and wastewater management that, at the same time, meet the population's requirements in terms of energy and preserve the maximum environmental resources. In parallel, there is a growing interest in the development of carbon-neutral fuels provided from biomass, thus taking advantage of natural resources. This change can help to reduce the impact of atmospheric carbon dioxide from the use of fossil fuels and, at the same time, contribute to the application of the circular economy concept (Mikheenko et al., 2019).

The possibility of recovering energy from waste and wastewater is growing in interest and several countries have already implemented waste(water)-to-energy systems, as the case of Mexico, Egypt, the USA, China, Brazil and India (Rodriguez et al., 2020). These integrated systems produce energy from waste or wastewaters in the form of electricity, to be used in transport and energy to heat homes, with the potential to replace the use of natural gas. These waste(water)-to-energy systems are inexpensive to implement, renewable and represent a solution for waste and wastewater, which are considered to be a form of energy readily available in cities around the world.

Anaerobic digestion (AD) process to convert the organic matter present in the waste or wastewater into methane-rich biogas (Figure 1) is a widely-used and well-established biological process, and it is very promising to be successfully integrated in the wastewater-to-energy treatment systems (Merlin Christy et al., 2014).

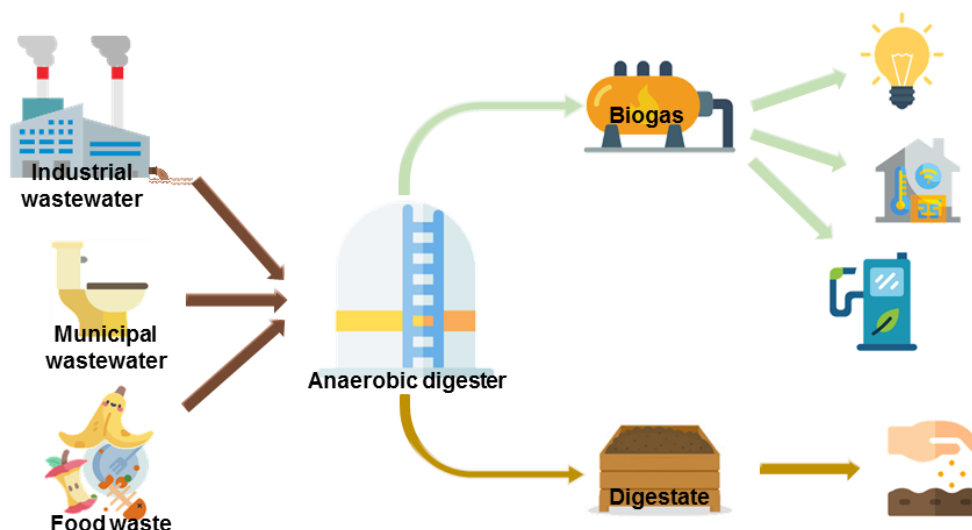


Figure 1| Waste(water)-to-energy process flow, encompassing a process of valorization through anaerobic digestion of waste or wastewater streams into added-value products, such as methane-rich biogas and digestate.

Several solid wastes such as food and garden waste, municipal wastewater (contaminated with human waste) and industrial wastewater (from industrial activities) can be effectively converted into methane by an AD process, reducing their pollution load. Methane formed during anaerobic processes (composting and AD) contributes to global greenhouse gas (GHG) emissions if released to the atmosphere, being 34 times more powerful than carbon dioxide in terms of the impact on the greenhouse effect (Ashrafi et al., 2015). However, in waste(water)-to-energy systems, methane is used as an energy source in several applications, preventing its natural release into the atmosphere, as occurs if waste or wastewater has not been properly managed or disposed of without treatment.

The energy vector (methane) produced in this cheaper approach can be used to replace costly and polluting energy sources, such as fossil fuels, to generate electricity, heat and fuel. In addition to this cost reduction during energy production, the digestate of the AD process can also be sold to be applied directly as a soil amendment, increasing the value of the generated products. The digestate can also be subjected to solid-liquid separation to obtain a compost (solid fraction) and a concentrated organic fertilizer (liquid fraction), both with the potential to be used in the agricultural sector as soil amendments.

With new approaches to wastes and wastewaters management, considering them as valuable resources instead of residues, it is possible to reduce the pollution load generated in several industrial, domestic and agricultural activities and create value in the form of energy vector and other secondary products with added value. Consequently, the AD process has the co-benefit of reducing GHG emissions, while preventing the formation of odors and the release of pollutants into the environment, and contributes to the maintenance of air, soil and water quality. In addition, other waste and wastewater treatment technologies, already fully implemented, also provide the mitigation of GHG emissions, improve health and environmental benefits and provide significant co-benefits for the adaptation and sustainable development of communities (Intergovernmental Panel on Climate Change, 2007).

1.1.2 Sustainable Development Goals

In 2015, all United Nations (UN) Member States adopted the 2030 Agenda for Sustainable Development. The 17 Sustainable Development Goals (SDG), as depicted in Figure 2, are a call for action and a list of guidelines for all the countries involved, and each SDG has several targets to be achieved until 2030 (United Nations, 2020).



Figure 2| Sustainable Development Goals defined by the United Nations for 2030 (graphics from UN, 2020).

The SDG defined that economic growth must be spurred and, at the same time, strategies must be adopted to end poverty, improve health and education and reduce inequality, with the ever-present problem of climate change, channeling efforts to preserve the oceans and the forests (United Nations, 2020). In line with the defined SDG, some of them can be framed in the work developed here:

- “SDG 6: Clean water and sanitation” is divided into eight main targets. One of the targets includes the reduction of pollution, elimination of dumping and minimizing the release of hazardous materials, with an increase in the amount of water to be treated, recycled and reused. Furthermore, the implementation of integrated water resources management is addressed in the SDG 6.
- As defined in “SDS 7: Affordable and clean energy”, it is important to increase energy efficiency and the share of renewable energies in the global energy mix. Biogas generation can be included as it is considered as renewable energy from renewable sources (wastes and wastewaters).
- “SDG 11: Sustainable cities and communities” highlights the importance of reducing the environmental impact of cities, paying special attention to air quality and the management of municipal and other waste.
- The “SDG 12: Responsible consumption and production” proposes the promotion of sustainable management and the efficient use of resources and energy, reducing the release of pollutants in water, air and soil to minimize their effects on human health and in the environment, and reduction of waste generated globally through prevention, reduction, recycling and reuse.

- “SDG 13: Climate action” refers to all modifications or solutions that promote the fight against climate change and its impacts. It includes the increase of renewable energy use and all measures to reduce GHG emissions, being this SDG transversal and interconnected to other goals.
- “SDG 14: Life below water” and “SDG 15: Life on land” are closely related and propose the conservation of oceans, water basins and forests, and the sustainable use of marine resources and terrestrial ecosystems.

The current waste and wastewater management measures applied in some countries already contribute to the achievement of the goals established for 2030 by UN, which focus on sustainability. However, with the increasing amounts of waste and wastewater generated every year, it is of high importance to improve and optimize the waste(water)-to-energy systems, creating solutions for effective reduction of pollution and wastewater treatment. The development of waste(water)-to-energy systems to manage both waste and wastewater, producing energy vectors like methane, is considered a renewable energy source. Potential applications for methane produced in the AD process can contribute to the reduction of fossil fuels consumption, replacing them in several applications. In addition, this integrated valorization process can reduce greenhouse gas emissions, avoiding inappropriate wastes deposition and the discharge of untreated wastewater. Thus, the proposed methodology for waste and wastewater valorization has the potential to contribute to the fight against climate change, the preservation of water and forest resources and the generation of clean and sustainable energy from materials that are discharged daily by human activities.

1.1.3 Pulp and paper industry, dairy industry and alumina refining: How to connect them?

Industrial activities generate a huge amount of solid and liquid waste. With the increase in environmental regulations, several sectors of the industry must adapt their practices to reduce the amount of waste generated in their production process and/or develop technologies to treat the waste and wastewater generated. In some industries, the complexity of waste hinders the success of technologies such as biological treatment.

In the case of the pulp and paper (P&P) industries, they are major consumers of freshwater and are a significant source of wastewater. Some wastewater streams generated in the process, mainly from pulp bleaching, can be potentially polluting and dangerous for the environment and human life (Ashrafi et al., 2015). In addition, the biomass combustion for energy generation in the P&P mill generates solid residues, namely bottom and fly ashes (FA), and they must be properly managed (Weiss-Hortala et al., 2020). In the integrated approach proposed here, the two types of waste (wastewater from pulp bleaching and fly ash from biomass combustion) can be combined through the implementation of an anaerobic biological process. On the one hand, in the anaerobic process the organic load and some complex compounds are removed from the pulp bleaching wastewater and, on the other hand, fly ash can be used as mineral additives to correct the pH in the treatment of highly acidic wastewater and improve the AD process in terms of methane production.

The dairy industries are considered the largest source of wastewater from food processing and use fresh water at all steps of the production process (Farizoglu and Uzuner, 2011). The high organic load and the high content of solids and fats in these wastewaters require specialized treatments to

minimize further environmental problems. Again, the development of anaerobic processes to treat this type of wastewaters has some advantages, such as energy formation, low sludge generation and low nutrient requirements, but it is important to strictly control the environmental conditions to avoid process failures. The use of fly ash (FA) from biomass combustion as an inorganic additive to control pH is a developing approach and is already used in a wide variety of substrates, such as biological sludge (Guerrero et al., 2019), sulfate-rich wastewaters (Montalvo et al., 2019), pulp and paper sludge (Huiliñir et al., 2015) or food waste (Huang et al., 2018). Thus, the use of FA as an inorganic additive in dairy effluents or by-products (such as cheese whey) can act as a process controller and enhancer regarding methane formation.

The recovering of fly ash after its use in anaerobic treatment can be a problem and have the aggravation that they can only be used once. An innovative approach to overcome these constraints is the manufacture of geopolymer spheres, to be used as a buffer material in anaerobic processes (Novais et al., 2017). The incorporation of fly ash in the geopolymer spheres structure is advantageous since the raw materials normally used (metakaolin) are replaced by a residue. Thus, FA-based geopolymer spheres (FAGS) can be used in a wide range of applications, as in the case of anaerobic processes (Novais et al., 2018c), as they also have the minerals from fly ashes in the structure, with the advantage of easy recovery.

The bauxite residue, also known as “red mud” is the largest industrial waste produced worldwide (Guevara et al., 2017). The huge amount of residue produced in the Bayer process for bauxite refining and its characteristics, such as extremely alkaline pH (> 10) and the presence of aluminum and iron in high concentrations, led to additional precautions regarding the treatment and disposal of bauxite residue. Several applications have already been explored to transform and valorize this residue, as reviewed by Klauber et al. (2011). An innovative application for bauxite residue is the incorporation of this residue in the geopolymer spheres (Novais et al., 2018a). The use of red mud-based geopolymer spheres (RMGS) to control the pH in the AD of complex substrates is an innovative alternative to the use of bauxite residue.

Thus, considering the three types of industries (chemical, food and mining) described, and some of the wastes generated in their production process, it is possible to integrate them as a new approach to the concept of waste(water)-to-energy, as depicted in Figure 3.



Figure 3| Integration of different types of wastes in waste(water)-to-energy approach, divided into three phases, according to the type of inorganic waste added. In phase 1, the addition of fly ash (FA) powder to the AD of both pulp and paper (P&P) effluent and cheese whey (CW); in phase 2, the addition of fly ash-based GS (FAGS) and in phase 3, the addition of red mud-based GS (RMGS), both to the AD of CW for methane production.

Solid wastes, such as FA and red mud (RM), can be used as inorganic additives in the powder form or in the form of geopolymer spheres (GS), in the AD treatment of liquid wastes, as effluents from pulp bleaching (P&P effluent) or by-products from dairy industry such as cheese whey (CW).

The use of different wastes in a treatment process, with the advantage of renewable energy formation as methane (CH₄), is a paradigm shift regarding waste and wastewater management.

Scientific interest in the application of these types of waste has increased in recent years, reflected in the number of publications by keywords, namely “red mud” or “bauxite residue”, “fly ash” and “cheese whey” (Figure 4).

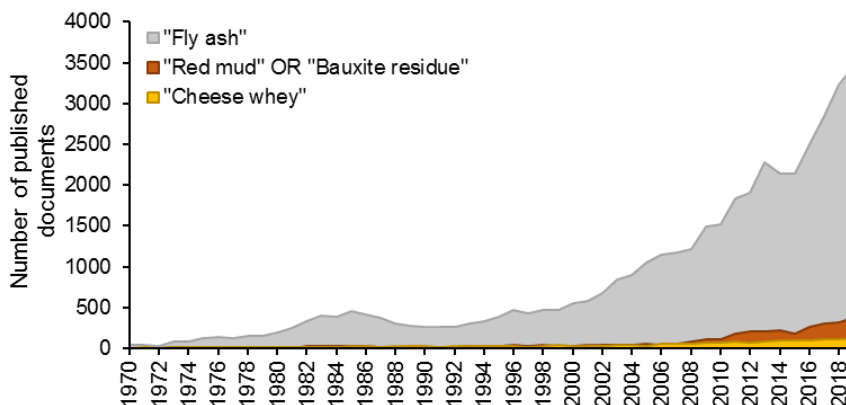


Figure 4| Number of publications for the three main wastes under study: “red mud or bauxite residue” from alumina refining industry, “fly ash” from biomass combustion and “cheese whey” from the dairy industry. Data collected from the SCOPUS database, in March 2020, and includes all the publications until 2019.

The generation, characterization and use of fly ash in different processes makes them the most studied waste. This is linked to the general keyword “fly ash” related to several thermochemical processes, in addition to the applications known as soil pH corrector or incorporated in types of cement or mortars. Red mud, due to its challenging characteristics, has increased interest, tripling the number of publications in the last 10 years, most of them related to the attention paid to this severely alkaline waste and its disposal in line with the challenges of sustainable practices, including waste management.

On the other hand, “cheese whey” has kept its number of publications in the last ten years, as it is considered a by-product and not a waste, and the technologies for its valorizations and production of added-value products are already implemented on an industrial scale. However, there is always room for the development of new technologies and the optimization of existing ones, justifying the growth in the number of publications.

Crossing these terms referring to the types of wastes with the term “anaerobic digestion”, the technology developed in this work, it is possible to observe that less than 0.5 % of the published documents with “red mud” or “fly ash” also consider the application of an anaerobic process. On the other hand, as anaerobic technology is already used to treat dairy effluents, 9 % of the published documents regarding the use of cheese whey also explore the application of the AD process. Again, this reinforces the innovation of the integrated process developed, using AD technology to treat complex streams, with the addition of inorganic materials.

1.2 Objectives

The main goal of this work was to provide new solutions for pH control in anaerobic digestion processes treating complex wastes, through the application of sustainable methodologies based on residue recovery. For this purpose, different streams, namely bleaching effluent from the pulp and paper industry and cheese whey, a byproduct from the dairy industry, were selected as a substrate for anaerobic digestion processes. Different solid wastes, such as fly ash from biomass combustion and red mud from bauxite refining, have been used as inorganic additives for anaerobic processes to promote pH stabilization, enhance the organic matter reduction and boost the energy formation in the form of methane.

The anaerobic biodegradability of a given stream is highly important for its valorization, whether energetic (methane) or material (volatile fatty acids or ethanol). Consequently, the anaerobic biodegradability of both selected streams was evaluated in the presence of powdered fly ash with different origins, to understand the effect of adding inorganic wastes on pH regulation and, ultimately, on the methane formation. In addition, with anaerobic biodegradability tests, it was possible to select a proper substrate to be studied in more detail, implementing new strategies for pH control in laboratory-scale reactors.

Usually, the addition of inorganic wastes to anaerobic processes focuses mainly on their effects on the process, neglecting the recovery and/or disposal of the inorganic materials used. For this reason, besides the addition of fly ash in the powder formulation, inorganic spheres incorporating residues (fly ash or a mixture of fly ash and red mud) in their composition were also used as new buffer materials for anaerobic degradation processes, with a material whose recovery is facilitated after its use in AD processes.

Therefore, this innovative approach used for pH control has been implemented to evaluate the performance of anaerobic systems concerning pH control and increased methane production. In addition, the performance of reactors with inorganic spheres was compared to the performance of reactors without pH control and with the performance of reactors with the addition of chemical compounds (such as NaOH or carbonates) as buffer materials, widely used in the laboratory and industrial-scale reactors. For this purpose, anaerobic batch reactors and anaerobic sequencing batch reactors have been operated for long periods. These different reactor configurations made it possible to understand the effect of the addition of inorganic spheres with different characteristics and in different concentrations on the main anaerobic operational parameters.

With this work, innovative buffer materials were produced from waste, with a huge potential to be used as inorganic additives in biological processes. The reduction or total replacement of virgin raw materials in different steps of the proposed approach, whether in the manufacture of inorganic spheres or in the replacement of chemicals used as buffer compounds for the anaerobic process, allowed the implementation of a more sustainable process, aligned with sustainable development goals.

1.3 Thesis Outline

This thesis is divided in seven chapters, including the introduction section, the reference list and the appendices section.

Chapter 2: “State-of-art” provides a general framework of the main issues relevant to this thesis, including the waste production from the pulp and paper industries, dairy industries and alumina industries, and the current solutions applied to several wastes. A review of relevant advances for pH control in anaerobic systems is also presented, including the use of new alkaline materials to replace the addition of the chemical compounds.

Chapter 3: “Methodology” details the substrates and inorganic additives for pH control, used in the operated bioreactors. The experimental set-up and the conditions applied in the anaerobic assays, and the methodologies for monitoring the developed anaerobic processes are detailed in this section. This chapter also explains the parameters calculated to evaluate the anaerobic performance of the bioreactors.

Chapter 4: “Results and discussion” is divided into three sections, as shown in Figure 5 for better understanding. The first and second sections are related to the use of fly ash as basic waste for pH control, and the third section is related to the use of red mud as the basic waste for pH control in the developed anaerobic digestion processes. In phase 1 (first section) the results and their discussion of anaerobic assays testing the addition of powder fly ash (from biomass combustion) to the anaerobic digestion of two types of substrates are presented: bleaching effluent from the pulp and paper industry and cheese whey by-product from the dairy industry. In phase 2 (second section) the results and their discussion for the anaerobic digestion tests are presented, using geopolymer spheres with fly ash in their constitution, as an additive for pH control in the anaerobic treatment of cheese whey. In phase 3 (third section) the results and their discussion are presented for the anaerobic digestion assays treating cheese whey and using geopolymer spheres with red mud wastes in their constitution.

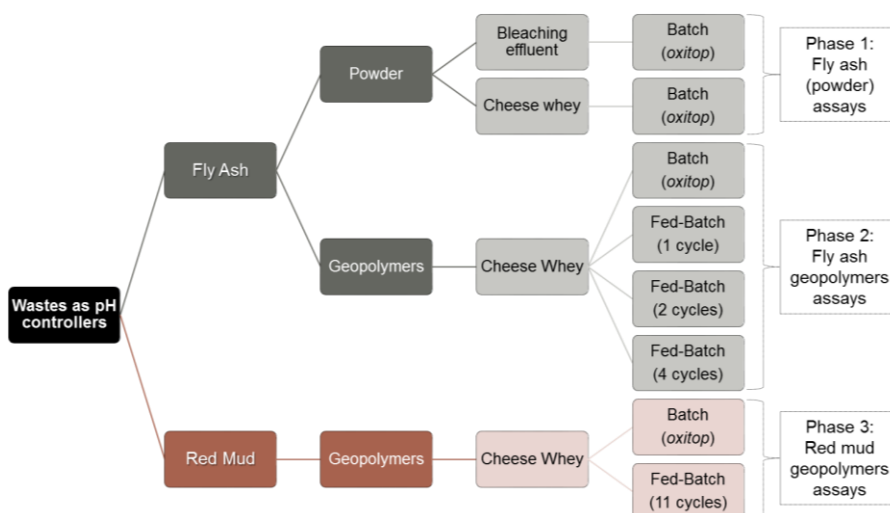


Figure 5] Schematic division of the work presented in this thesis.

Finally, Chapter 5: “Conclusions and perspectives for future work” presents the general conclusions of the biological processes developed and presented in this work, as well as suggestions for future research in this field of knowledge.

State-of-art | 2

2 | State-of-art

2.1 Waste and wastewater production

Driven by the increase in the world population in the last century, by the migration of populations to urban areas, by growing economies and by the change in lifestyle, the demand for energy and resources has increased exponentially. In addition, global water use has increased six-fold in the past 100 years and will continue to grow by 1 % per year, increasing pressures on limited natural resources and ecosystems. In addition, the production of waste and wastewater has also increased. The management strategies for these wastes and wastewaters depend on local management and can be recovered, treated, used directly, indirectly or discarded without value recovery (Mateo-Sagasta et al., 2015).

Currently, 2.01 billion tons of solid waste are generated worldwide, and the World Bank has estimated an increase of 70 % by 2050 unless measures are taken to reduce their generation (Kaza et al., 2018). Almost 45 % of the waste generated nowadays is organic, such as food and green waste (Figure 6 (a)), and metal, glass, plastic and paper and cardboard together represent 38 % of the total solid waste generated (data from 2018). Most waste is produced in developed (high-income) countries (Figure 6 (b)), thus showing a positive relationship with economic development. In low-income countries, at least 90 % of waste is disposed of without proper management, increasing the health risk and emissions, directly affecting the quality of life of the populations.

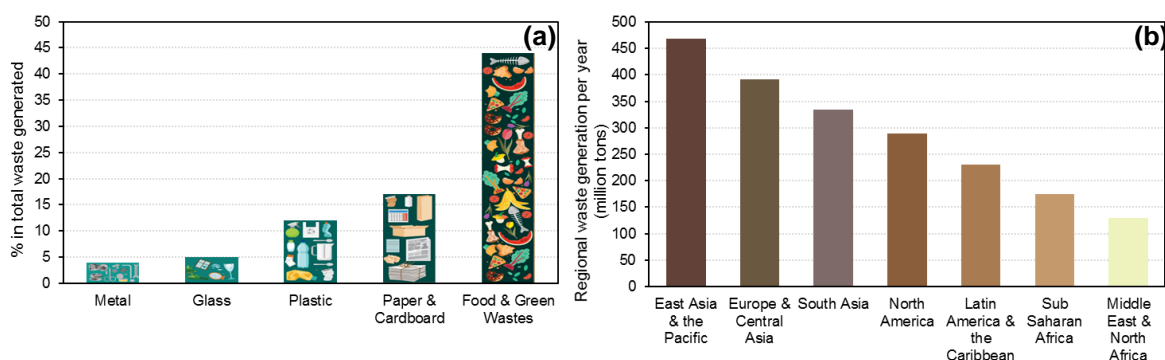


Figure 6| Main types of waste generated worldwide (a) and the annually waste generation by region (b), based on data presented by Kaza et al. (2018).

Wastewater is considered to be the combination of one or more sources of water discharge, including domestic wastewater, water from commercial establishments and institutions and hospitals, industrial effluents and agricultural runoff (Raschid-Sally and Jayakody, 2008). Considering the wastewater generation worldwide, most of this resource is discarded without treatment or collection. Every year, about 80 % of wastewater produced globally is released into the environment without proper treatment (Rodriguez et al., 2020).

With the change in consumption patterns and the increase in industrial activities, an increase in the demand for water resources was observed (Mateo-Sagasta et al., 2015). In addition, water quality directly influences public health, food security and several ecosystem services and functions. Untreated wastewater, in addition to environmental contamination, also contains pathogens, organics and other nutrients and can contain a variety of hazardous substances, including heavy

metals. Thus, water pollution limits opportunities for safe and productive use (or reuse) of water sources and this has become a problematic issue especially in regions that face water scarcity or where water-related infrastructure and services are inadequate.

To change this scenario, an alternative is the implementation of efficient measures for the management of waste and wastewater, emphasizing the recycling and valorization processes, applying a more circular and, therefore, more sustainable approach. In addition, it is necessary to implement appropriate technologies to exploit the energy potential of both domestic and industrial wastewaters generated, besides its use as an alternative source of clean water or nutrients, and as a support for sustainable agriculture. The collection and treatment of waste and wastewater management are costly and require significant amounts of energy, but the potential chemical, thermal and hydraulic energy contained in these streams can be recovered and generate value, and the initial investment cost is easily covered.

2.1.1 Bioenergy and the “European Green Deal”

Energy from bio-based sources (biomass or biological commodity), also called bioenergy, is considered a renewable source of energy. Currently, energy from bio-based sources has the largest renewable share and accounts for approximately 66 % of the total renewable energy mix. Regarding energy consumption, bioenergy represents about 14 % of total energy consumption, with oil (39 %), natural gas (21 %) and coal (20 %) being the main contributors (World Bioenergy Association, 2020).

Considering the period between 1990 and 2015, biogas is the third fastest growing renewable energy source worldwide, after solar photovoltaic and wind power. In Europe, 6 % of the total renewable electricity is generated from biogas and the currently produced methane represents about 4 % of the total natural gas consumed (European Biogas Association, 2019).

Although the high-energy potential of methane, it is one of the gases that causes global warming. The global warming potential (GWP) of methane, which measures the amount of energy that emissions of 1 ton of gas will absorb over a period of time, is 84 over a period of 20 years and 28 to 36 over a period of 100 years (Myhre et al., 2013). The CH₄ emitted today lasts about 10 years in the climate system, which is a shorter period than CO₂ (thousands of years). However, CH₄ also absorbs much more energy than CO₂, and the effect of CH₄ on global warming results from its high infrared absorbance and its role in the complex chemical reactions that occur in the stratosphere, also affecting ozone levels (Schaechter, 2004). Nonetheless, when captured instead of released into the atmosphere, methane is a clean source of energy and has the potential to replace natural gas of fossil origin, leading to a reduction in its environmental impact.

For many years, the trend observed worldwide has been the increase in waste disposal in landfills, driven by the increase in human activities. This behavior also tended to increase the amount of methane released into the atmosphere. Other sources of methane are agricultural activities, due to the increased use of ruminants for the production of meat and dairy products and the increased development of rice paddies (Schaechter, 2004). However, nowadays, the interest of the world population in the environment has led to a change in consumption patterns, reducing the use of products with a production cycle related to high pollution discharges in the environment, such as meat and dairy products. This change in mentalities has also led to a change in the way the world deals with the waste generated and the emissions of gases.

One approach to achieve the reduction of GHG is to implement the AD process to dispose of livestock and agricultural wastes (Aydin, 2017). In many European countries, the gas released in landfills (where the organic fraction of waste decomposes) is captured and used in a cost-effective way, mitigating GHG emissions. In addition, GHG savings of 240 % can be achieved by producing electricity from biogas, when compared to the use of fossil fuels (European Biogas Association, 2019). Besides the AD process to produce biogas from organic waste and wastewaters, the use of digestate also saves GHG emissions. Compared to the commonly used mineral fertilizer (fossil origin), the use of digestate allows the recovery of nutrients and contributes to the concept of circular economy applied to biological processes (European Biogas Association, 2019).

“European Green Deal” is a concept introduced by current Commissioners since October 2019. The idea of the new concept is to make Europe the world’s first climate-neutral continent by 2050 (European Commission, 2020). With the revision of legislation associated with climate change and GHG emissions, the new tight targets to be imposed in the coming years require the implementation of new sustainable technologies for the production of energy, with the potential to reduce GHG emissions. Consequently, the biogas industry will also be affected by tighter targets for the reduction of GHG compared to fossil fuels (European Biogas Association, 2020a).

The need to reduce our carbon footprint is dramatic. All industries, policy makers and individuals must implement measures to mitigate climate change. AD is a well-known technology, with the potential to generate renewable energy, reduce GHG emissions and recover nutrients. This technology has the potential to meet, at the same time, the climate change goals of the Paris Agreement, which aim to reduce of GHG from 2020, thus reducing global warming to temperatures below 2 °C (preferably below 1.5 °C) until 2100 (Jain, 2019). The implementation of biogas producing systems can reduce GHG emissions by 10 – 13 %, which corresponds to 3290 to 4360 million tons of CO₂ equivalents (European Biogas Association, 2020b). Biogas technology is also able to provide food security, correct waste management, protection of water bodies, soils and atmosphere, improved health and sanitation and job creation (Jain, 2019). The use of this alternative bioenergy source is one of the viable solutions to reduce the environmental footprint of producing more energy to meet the growing demands for water and services worldwide (United Nations World Water Assessment Programme, 2014).

2.1.2 Circular economy approach

The transition from the linear to the circular economy can be advantageous for both the economy and the environment. The linear economy approach is based on the production and consumption of products that are disposed of as wastes without further treatment. On the other hand, the concept of the circular economy is based on the premise that the economy can provide multiple mechanisms for creating value dissociated from the consumption of finite resources (Piscicelli and Ludden, 2016). Both linear and circular economy concepts are depicted in Figure 7. The concept of the circular economy is illustrated for biological nutrients.

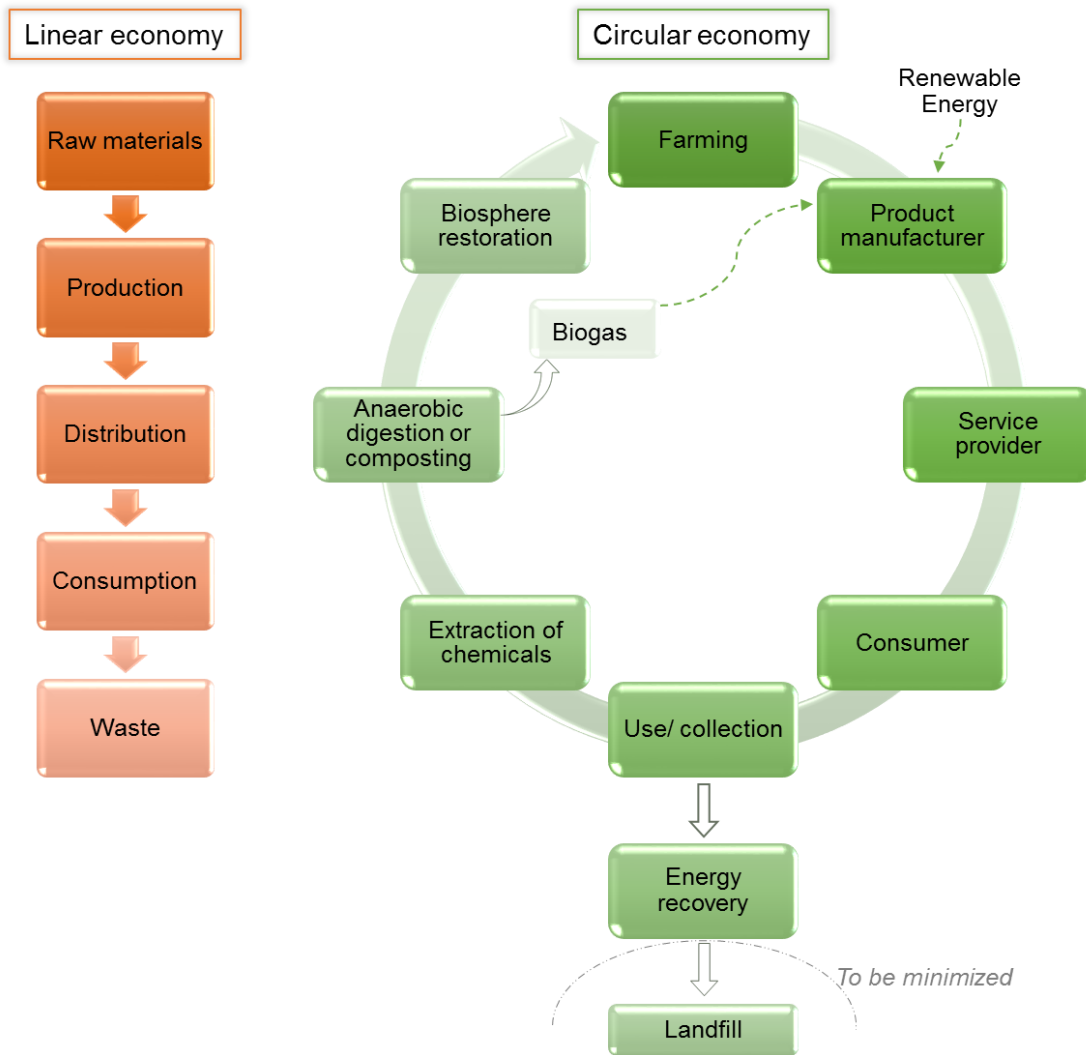


Figure 7| Linear economy approach for virgin resources *versus* the circular economy approach for biological nutrients (adapted from Piscicelli and Ludden (2016)).

In contrast to the linear economy concept, in the circular economy waste streams are treated and valorized. The implementation of biorefining processes can assist in the extraction of biochemical feedstock, such as high-quality materials and chemicals. AD or composting are processes suitable for producing energy and other byproducts, reducing the pollution load of a given stream. The main form of energy produced by AD or fermentation of biodegradable materials and contained in waste and wastewater is in the form of biogas, composed mainly of methane (CH₄) and carbon dioxide (CO₂). The energy produced is generally used in the plant or to the manufacturing process, and the byproducts, in the form of biofertilizer, returns to the soil, with the restoration of nutrients in the biosphere. This restoration helps to improve agriculture and closes the nutrient cycle, with the production of new feedstock.

2.2 Anaerobic digestion process for wastewater treatment

2.2.1 History of the anaerobic digestion process

The anaerobic digestion (AD) process is not new and has been widely studied since the early days of modern science. Ancient records report that biogas, the final product of anaerobic degradation of organic matter, has been used for heating water for baths since the 10th century BC in Assyria and the 6th century AD in Persia (Lusk, 1998). Some evidence indicates that biogas was used in China to heat brine during salt production, some 4000 years ago (Pullen, 2015). Additionally, Pliny reported the generation of combustible gas, presumably methane, during the Roman Empire (Schaechter, 2004).

In the 17th century AD, chemist Jan Baptista Van Helmont established that the degradation of organic matter could release flammable gases and the Italian physicist Count Alessandro Volta concluded, in 1776, that the degradation of organic matter from plant material (with cellulose) and the production of such flammable gases have a direct correlation (Buswell and Hatfield, 1936). Later, in 1808, sir Humphry Davy proved that methane was one of the gases produced during the anaerobic degradation of cattle manure (Ahammad and Sreekrishnan, 2016). At the end of the 19th century, it was found that the formation of methane was somehow connected to microbial activity (Lusk, 1998). In 1868, Antoine Bechamp, a student of Louis Pasteur, was the first to establish that methane formation was a microbial process (Schaechter, 2004), and discovered the microorganisms responsible for the methane production from ethanol. This biologist found that the products (intermediates) formed during the anaerobic process depend on the type of substrate used. In 1876, Herter, a collaborator of Hoppe-Seyler, reported the stoichiometric balance of acetate from sewage sludge converted to equal amounts of methane and carbon dioxide (Ahammad and Sreekrishnan, 2016).

Latter, in 1930, A. M. Buswell and other researchers identified some anaerobic microorganisms and the suitable conditions for methane formation (Ahammad and Sreekrishnan, 2016). The stoichiometric formula developed by Buswell and Hatfield (1936) is still used today to predict the methane formed by a complete conversion of biomass. The works from Buswell explored several issues regarding the AD process, such as the fate of nitrogen in the process, the stoichiometry of reactions or the production of energy from agricultural and industrial wastes through anaerobic processes (Adelekan, 2012).

During the 1950s, the concept of co-digestion (mixing two different substrates to achieve synergistic effects) was developed. In 1967, M. P. Bryant discovered two different bacterial species during the fermentation of ethanol: one breaks down ethanol into acetate and hydrogen, and the other converts CO₂ and hydrogen into methane (Pullen, 2015).

The first AD plant was built in 1859 to dispose of human waste from a leper colony in Matunga, near Bombay, India (Lusk, 1998). This pioneering construction was equipped with gas collectors and the gas produced in the tanks was used to drive gas engines (Buswell and Hatfield, 1936). In 1865, several researchers suggested the name “methane” for the gas called “marsh gas” or “carbonated hydrogen”, until then (Pullen, 2015). In Europe, this anaerobic technology was implemented in 1895 in England, for the recovery of gas from waste management, to be used as fuel for street lamps in Exeter, England (Lusk, 1998). As in India, in England, a system was installed with gas collectors to

recover the gas produced. Later, Dr. Travis constructed a two-phase digestion process in Hampton, England, and patented it in 1903. In Germany in 1906, Dr. Karl Imhoff implemented the well-known Imhoff tank, where the sedimentation and fermentation phases are separate (Buswell and Neave, 1930).

During the 20th century, several types of digesters were developed, designed according to the feedstock to be treated and the main goals of the treatment. The implementation of anaerobic digesters on farms has been widespread and many farmers have paid to implement this technology locally. However, anaerobic digesters are normally not fully integrated into the farming system, limiting the use of byproducts (digestate) as fertilizers (Adelekan, 2012). Since the '80s, the AD process for biogas generation has been widely applied in the treatment of industrial wastewaters and in the stabilization of municipal solid waste. However, it was only in the 90's that the energy potential of agricultural feedstock was recognized and led to a sharp increase in the development of the sector (European Biogas Association, 2019).

Interest in anaerobic technology is increasing all over the world and several plants have already been constructed to not only treat the organic waste and wastewaters but also to recover valuable products, such as biogas and digestate (Adelekan, 2012). In addition, the upgrade of biogas (removing carbon dioxide and trace gases present in biogas to increase the total methane share and obtaining a gas that meets the standards of natural gas) produces biomethane (European Biogas Association, 2019), which is more economically attractive than biogas and is highly applicable as a fuel and as a substitute of natural gas.

The biogas industry has been growing in recent years and, today, Europe is the largest producer of biogas. In 2017, the world production of biogas was 1.33 exajoules, representing an increase of more than 150 % in the last 10 years, and Europe accounted for more than half of that production (World Bioenergy Association, 2020). In 2018, 18,202 biogas plants and 610 biomethane plants are functioning in Europe, which represents three times more plants than in 2009. From 2017 to 2018, the number of biogas plants increased by 2 % and the number of biomethane plants increased 13 %, driven by the rapid evolution of the biomethane market, with a growing interest in renewable and alternative energies (European Biogas Association, 2020a). Currently, most European biogas production is converted to electricity and heat in combined heat and power (CHP) units, due to EU Directives on electricity and heating and cooling. The electricity produced is injected directly into the local electrical grid and heat is used in local applications (heating systems or outdoor swimming pools). As a comparison, the total installed electric capacity of European CHP units using biogas is greater than 10 GW, equivalent to 10 nuclear plants, with the huge advantage of the lack of nuclear risks (European Biogas Association, 2019).

In Portugal, in 2017, 64 biogas plants were accounted for, mainly landfill and sewage waste, which is equivalent to six biogas plants per 1 million inhabitants. The average installed electrical capacity of Portuguese biogas plants is 1.4 MW, slightly above the European average installed electrical capacity (close to 1 MW). Until now, no biomethane plants were operating in Portugal, with the biogas generated in Portugal being used directly for heating and power generation (European Biogas Association, 2018).

Although significant growth has been observed in the biogas industry in recent years, the modernization and industrialization of agriculture is not reflected in the intensification of the biogas

development, mainly due to the lack of optimization in the stability and operability of the process (Mao et al., 2015). The increase in the size of farms is expected to continue with increasing size in biogas plants, taking advantage of the potential of organic wastes and wastewaters for the energy and other byproducts formation.

2.2.2 Definition and applicability of anaerobic digestion process

The decomposition of organic material can take place as an abiotic process (degradation by chemical or physical processes) or a biotic process (metabolic breakdown by living organisms, such as bacteria, fungi and protozoa) (Merlin Christy et al., 2014). Decomposition by microorganisms can be either in aerobic or anaerobic conditions. Aerobic degradation converts organic matter into CO₂, water, nitrates and sulfates, and requires oxygen during the biological process. The inability to degrade some organic compounds and the formation of high amounts of sludge make aerobic degradation an unattractive treatment process for several wastes and wastewaters, compared to the anaerobic degradation process.

AD is an extremely efficient and diversified process that uses waste materials to produce energy, gas, heat, fertilizers and fuel. This technology is considered truly renewable, since it uses a biological process to degrade biomass from renewable origin, in comparison with natural gas, which is of fossil origin. In nature, this process occurs without human interaction in marshes, ponds, swamps, paddy fields, lakes, landfills, oceans, and also in the intestinal tract of animals and humans (Merlin Christy et al., 2014).

AD is a series of biological processes driven by a wide variety of microorganisms in sealed containers in the absence of oxygen, consisting of the degradation (reduction) of plants and/or animal materials in their mineral form (Merlin Christy et al., 2014). During the reduction of organic matter, it is produced biogas, composed mainly by methane ($\approx 60\%$) and carbon dioxide ($\approx 40\%$), with traces of other gases (water vapor and hydrogen sulfide). The remaining organic material is called "digestate" and is rich in organic matter and nutrients such as nitrogen, phosphorus and potassium (Koszel and Lorencowicz, 2015).

Organic materials of diverse origins are the "input" for a biogas producing system. Depending on the material's source and characteristics, some materials will be digested more easily than others will. The organic matter to be treated anaerobically may include animal manure, food scraps (including fats, oils and greases from restaurants), agricultural residues, wastewaters and wastewater solids, and byproducts of food and beverage production (Pullen, 2015). The plants can be implemented to produce energy on a small scale (for households and farms) or on a large scale (for part or entire cities) (Jain, 2019).

Within the digester, naturally occurring microorganisms, under controlled conditions regarding temperature and preferably in the oxygen absence, break down (also called "digestion") the organic material of the waste into intermediates for beneficial use or disposal, such as biogas and digestate. As long as the microorganisms inside the digester remain alive and fed, they will continuously produce biogas and digested material (Pullen, 2015). During the anaerobic process, organic matter is stabilized, pathogens and odors are reduced and the total solids from the organic material feed decrease through its partial conversion into biogas.

Biogas produced under anaerobic conditions is mainly composed of methane, which is the main component of natural gas, and represents the energy vector of biogas (Jain, 2019). It also contains carbon dioxide and small amounts of water vapor and trace compounds such as hydrogen sulfide. To replace natural gas in almost any application, biogas must be processed to remove non-methane compounds (biogas upgrading), forming the so-called “biomethane” or “renewable natural gas”. The level of purification that the biogas is subject to is highly dependent on the final application of the gas. Biomethane can be used in a wide range of applications, including to produce heat and electricity, as vehicle fuel or inject into natural gas pipelines and be used as the fossil-derived natural gas (Pullen, 2015).

The digested material, including liquid and solid material, has a high content of carbon and valuable nutrients, such as nitrogen, phosphorous and potassium (Koszel and Lorencowicz, 2015). In the digestate, solid and liquid fractions must be separated, according to the final application. Depending on the feedstock used for the anaerobic process, the digestate formed can be used directly or after processing, as fertilizer, compost, soil amendments, or as animal bedding (Pullen, 2015). The use of digestate as a fertilizer replaces the use of mineral fertilizers, since the elements N, P and K are readily available to be absorbed by plants (Koszel and Lorencowicz, 2015).

The final destination of biogas and digestate depends on local markets and needs (Pullen, 2015) and the scale of the biogas plant. The AD process applied to waste/wastewater management includes municipal and industrial wastewater treatment, septic tanks and sludge digesters for sludge treatment. It can also include agricultural waste management and hazardous waste management, inserted into a biogas plant.

AD technologies have some advantages compared to aerobic technologies, as listed in Table 1. The lower sludge generation in anaerobic processes results from lower biomass/substrate yields of anaerobic microorganisms compared to aerobic microorganisms. Anaerobic processes have fewer nutrient requirements and enable higher loading rates than aerobic processes, also allowing greater destruction of pathogens (Chen et al., 2014). Furthermore, anaerobic biomass can be preserved for several months and tolerate adverse environmental conditions, such as low temperatures and the presence of inhibitory substances. Nevertheless, anaerobic processes generally achieve less efficiency in organic matter removal, compared to aerobic processes. These differences are related to the lower affinity for the substrate (higher K_s values) in anaerobic processes, which can be overcome with efficient post-treatment (Fonseca and Teixeira, 2006).

Table 1| Comparison between anaerobic and aerobic processes (Fonseca and Teixeira, 2006; Hatti-Kaul and Mattiasson, 2016).

	Anaerobic process	Aerobic process
Capital and operational cost	Low	High
Energy consumption	Low	High
Sludge generation	Low	High
Process time	High	Low
Organic matter removal	80 – 90 %	90 – 98 %
Biomass growth	Low	High
Pathogens destruction	High	Low

Among the many benefits of AD already exposed, it is worth mentioning also some environmental and social advantages of this technology, which are closely related to the implementation and operation of biogas plants (Jain, 2019), namely:

- the low water input of the anaerobic process makes this bioprocess attractive, comparing it even with the generation of other biofuels;
- the generation of renewable energy, namely the biogas to be used by direct combustion and biomethane, after biogas upgrading, to be used as vehicle fuel or as a natural gas substitute in the grid;
- the mitigation of climate change, avoiding emissions of fossil fuels, when replaced by biomethane, and reducing direct methane emissions from landfills, capturing gas and using it in form of biogas (direct use or upgrade);
- the contribution towards a circular economy, using waste and wastewater as a source of energy, and returning nutrients to the soil in the form of fertilizers;
- the improvement of urban air quality, with the substitution of fossil fuels in vehicles by biomethane and avoiding the uncontrolled release of methane in landfills (mainly related to developing countries);
- the contribution to food security, with decreasing dependence on inorganic fertilizers (from fossil sources) and the use of organic nutrients and carbon from the digestate (from renewable sources);
- the improvement of health and sanitation achieved through better-quality waste management, reducing odors from the waste dumping (when waste is landfilled) and protecting water bodies, by reducing the carbon load in wastewaters;
- the economic development related to the infrastructure for the biogas generation and the revenues from digestate selling and biogas upgrading to biomethane and other valuable products.

Besides the use of anaerobic processes for the treatment of solid wastes and wastewaters in plants or for the remediation of contaminated soils and groundwater, anaerobic microorganisms can also be used in several biotechnological applications. Recent investigations focus on the use of extracellular enzymes from anaerobic microorganisms (bacteria and archaea) in the hydrolysis of polysaccharides for the chemical and pharmaceuticals manufacture. Some studies also focus on the genetic manipulation of anaerobic microorganisms to prevent the formation of byproducts or to help degrade new complex substrates, and on the use of anaerobic microorganisms in well-established industrial biotechnological processes, to improve the overall production processes (Hatti-Kaul and Mattiasson, 2016).

2.2.3 Biochemistry of the anaerobic digestion process

Cell growth generally involves a respiratory (electron transport phosphorylation) or fermentative (substrate-level phosphorylation) conversion of substrates into products, also called catabolism. This conversion releases energy in the form of adenosine-5-triphosphate – ATP. The energy that cells

obtain from catabolic reactions is used for the synthesis of new cells and for the maintenance of existing ones (anabolism). In metabolism, the production of ATP and the biomass formation are coupled (Gavala et al., 2003).

All biological metabolic processes require electron donors (a reducer) and electron acceptors (an oxidizer). In the case of aerobic microorganisms, they use oxygen as an electron acceptor, reducing it to CO_2 . When oxygen is absent in anaerobic environments, anaerobic microorganisms must find alternatives for electron acceptors, such as NO_3^- , Fe^{3+} , SO_4^{3+} or CO_2 . In the case of anaerobic fermentation, the organic compounds present in the wastes are the electron donors, and the internal cell products function as electron acceptors. Anaerobic metabolism generates less ATP yield than aerobic metabolism, due to the lack of an electron transport chain. In anaerobic metabolism, microorganisms (bacteria or fungi) can produce ethanol and organic acids, among other intermediate products (Hatti-Kaul and Mattiasson, 2016).

The anaerobic process to produce biogas is based on the synergistic relationships between different microbial consortia, mainly between acid-producing and consuming microorganisms. The metabolic activities of microorganisms in the AD process led to the definition of four distinct phases (Ahammad and Sreekrishnan, 2016). Figure 8 shows the metabolic steps of the anaerobic degradation process, highlighting the four main reactions: hydrolysis (complex organic matter is broken down into soluble organic molecules), acidogenesis (fermentation of soluble organic molecules into VFA and hydrogen), acetogenesis (formation of acetic acid and hydrogen) and methanogenesis (conversion of acetic acid and hydrogen into methane).

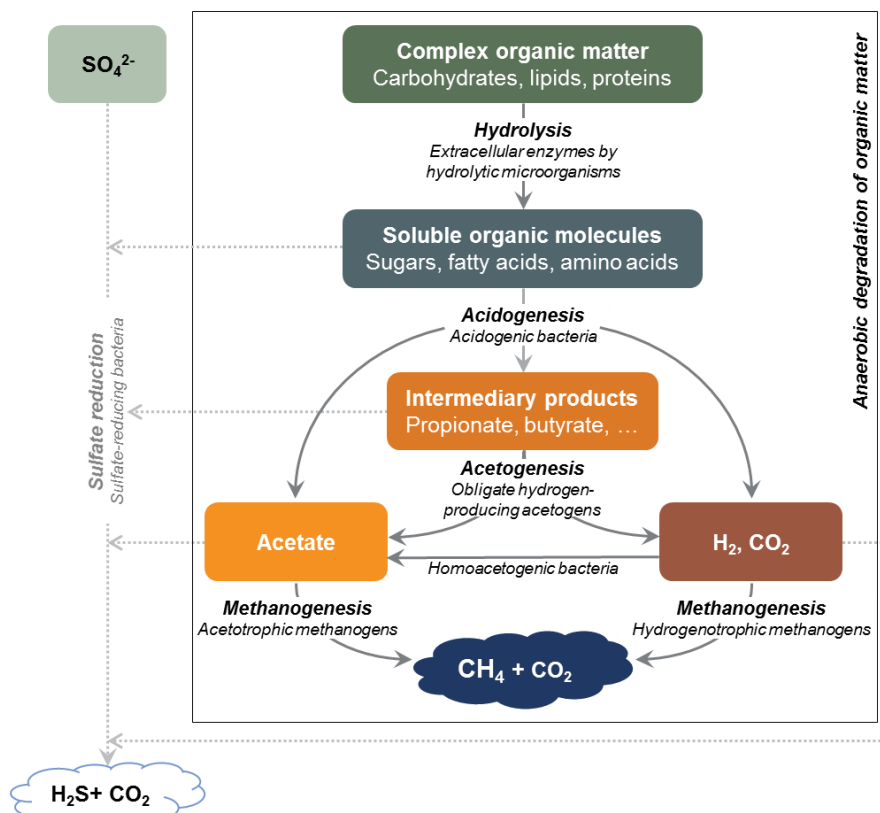


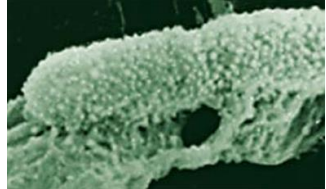
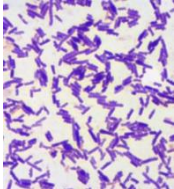


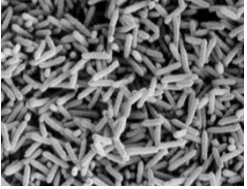

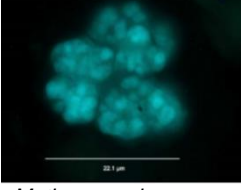
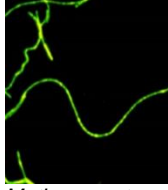
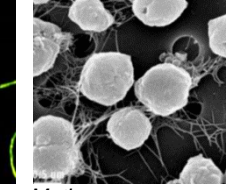



Figure 8| Biochemistry of anaerobic degradation of complex organic matter to generate methane-rich biogas. In the presence of sulfate, intermediates such as VFA, acetate and hydrogen, are diverted from the methane generation and used for sulfate reduction with the generation of hydrogen sulfite.

Some industries, such as pulp and paper and mining, use large amounts of sulfur compounds. These compounds generally increase the sulfate concentration in wastewaters and can cause disturbances during anaerobic treatment. In the presence of sulfate, competition for substrates (VFA, acetate and hydrogen) increases between methanogens and sulfate-reducing bacteria, decreasing the formation of CH₄ and increasing the amount of H₂S formed (Paulo et al., 2015). This alternative use of organic matter was included in Figure 8.

Several microorganisms from the Archaea and Bacteria domains are involved in the degradation of organic matter, presenting a synergistic relationship during anaerobic metabolism (Aydin, 2017). Some of the most representative microorganisms involved in each step of the AD process, including the sulfate reduction step, are shown in Table 2 and discussed in the subsequent sub-sections.

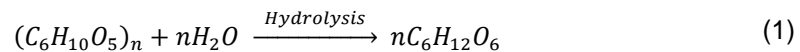
Table 2| Representation of the most common microorganisms involved in each AD metabolic step, namely hydrolysis, acidogenesis, acetogenesis and methanogenesis. Despite its competitive nature in the methane formation, the sulfate reduction was also included as a metabolic step of the anaerobic degradation of organic matter.

AD step	Most common microorganisms involved				
Hydrolysis	 <p data-bbox="507 1025 675 1048"><i>Pseudomonas</i> sp.</p>	 <p data-bbox="746 1025 866 1048"><i>Hartmannella</i> sp.</p>	 <p data-bbox="954 1025 1169 1048"><i>Acetivibrio cellulolyticus</i></p>	 <p data-bbox="1257 1025 1377 1048"><i>Clostridium</i> sp.</p>	
	Acidogenesis	 <p data-bbox="746 1247 866 1270"><i>Lactobacillus</i> sp.</p>	 <p data-bbox="954 1247 1137 1270"><i>Propionibacterium</i> sp.</p>		
		Acetogenesis	 <p data-bbox="738 1469 874 1491"><i>Acetobacter</i> sp.</p>	 <p data-bbox="978 1469 1161 1491"><i>Syntrophobacter</i> sp.</p>	
	Methanogenesis		 <p data-bbox="507 1691 691 1713"><i>Methanosarcina</i> sp.</p>	 <p data-bbox="778 1691 914 1713"><i>Methanosaeta</i> sp.</p>	 <p data-bbox="962 1691 1137 1713"><i>Methanococcus</i> sp.</p>
Sulfate reduction		 <p data-bbox="810 1912 1066 1935"><i>Desulfovibrio desulfuricans</i></p>			

The central microorganisms in the methane formation are methanogens, which generate CH₄ during growth. These microorganisms are members of *Archaea*, one of the three domains of life, which also includes *Bacteria* and *Eukarya*, as proposed by C. Woese, based on the 16S rRNA sequence. These microorganisms are unicellular, without a nuclear membrane or intracellular compartmentation, resembling *Bacteria*, but have some genetic features that resemble *Eukarya* (Schaechter, 2004). This group of microorganisms has the oldest evolutionary history of all prokaryotes, dating back to the geological ages of the Earth (Botheju, 2011). For this reason, these microorganisms have unique features, such as different cell membranes, enzymes and enzyme cofactors, and can thrive in extreme growth conditions such as environments with high temperature, high salinity or highly reduced O₂-free anoxic (Schaechter, 2004).

2.2.3.1 Hydrolysis

Hydrolysis (also called solubilization) is the first stage in the anaerobic organic matter degradation process. During hydrolysis, complex organic compounds, such as carbohydrates, lipids and proteins, are broken down into monomeric compounds, such as sugars, fatty acids and amino acids, due to the action of extracellular enzymes (Ahammad and Sreekrishnan, 2016), excreted by hydrolytic microorganisms to decompose the undissolved particulate material. This break down of organic matter is represented by reaction (1), with the generation of simpler sugar (glucose) from complex carbohydrates (Van et al., 2019). Examples of extracellular enzymes are cellulases (which break cellulose into glucose), amylases (which break starch into glucose), proteases (which break casein and other proteins into amino acids) and lipases (which break triglycerides into fatty acids and glycerol) (Seadi et al., 2008).

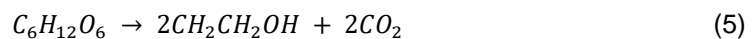
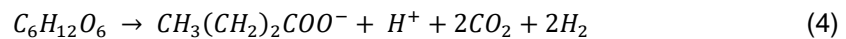
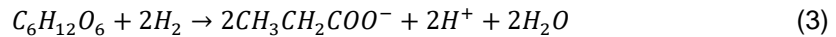
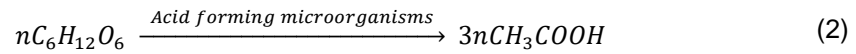


Hydrolysis can be considered as the rate-limiting step, depending on the type of substrate to be degraded (Ariunbaatar et al., 2014) and the amount of particulate organic matter (Botheju, 2011). When vegetable complex substrates with high cellulose, hemicellulose and lignin content are treated, hydrolysis is the speed determination step (Seadi et al., 2008). Hydrolysis allows for simpler assimilation of materials by microbial cells and facilitates the consumption of organic compounds by the acidogenic microorganisms (Meegoda et al., 2018). Hydrolysis products are used sequentially by microorganisms involved in the other steps of the AD process, for their own growth and metabolism.

Several types of microorganisms, such as Bacteria, Fungi and Protozoa, perform this step of anaerobic conversion, and the substrate composition has a determining role in the composition of the microbial population (Aydin, 2017). Usually, the same microorganisms capable of enzymatically degrading complex organic molecules also use the simplest molecules as a substrate for the acidogenesis step (Insam et al., 2010). *Clostridium* sp. can thrive in extreme environments and helps in the degradation of bio-waste (mainly cellulose), being the most common strains. Other species, including *Acetivibrio*, *Bacteroides* or *Ruminococcus*, are also common in anaerobic environments such as hydrolytic microorganisms (Insam et al., 2010). For the degradation of protein-rich materials, predominantly present in domestic wastewaters, *Clostridium* sp., *Bacillus* sp. and *Proteobacteria* are generally common (Aydin, 2017).

2.2.3.2 Acidogenesis

In the acidogenesis step (also called fermentation), the products of the hydrolysis step are converted into fatty acids, intermediate products of the anaerobic stabilization of organic matter. During this step, different types of fatty acids (long chain and short-chain fatty acids) are produced (Ahammad and Sreerishnan, 2016). The reactions for glucose conversion into acetic acid (Equation 2), propionate (Equation 3), butyrate (Equation 4) and ethanol (Equation 5) can be described as follows (Van et al., 2019):



When lipids are in large amounts in the waste, long-chain fatty acids (LCFA) (with more than twelve carbon atoms) are generally produced (Bruss, 2008). Volatile fatty acids (from 2 to 6 carbon atoms) are also generated from the fermentation of simple sugars such as glucose (from carbohydrates), the most common being acetic (C2), propionic (C3) and butyric (C4) acids (Akiba et al., 2018; Aydin, 2017). For amino acids, they can be degraded via two main ways: pairs of amino acids are degraded through the oxidation-reduction Stickland reaction, and single amino acids are degraded in the presence of H₂-utilizing bacteria (Kovács et al., 2013), through the specific fermentative pathway of each amino acid (Merlin Christy et al., 2014).

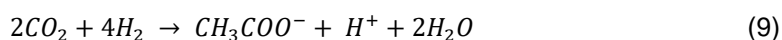
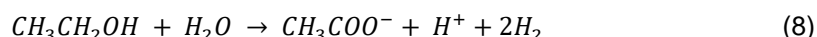
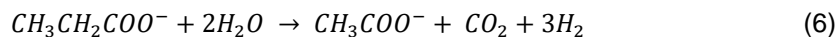
During acidogenesis, fermentative bacteria (acidogens) use organic matter to produce other intermediates, such as alcohols, ketones, hydrogen (H₂), carbon dioxide (CO₂), ammonia (NH₃) and hydrogen sulfide (H₂S) (Ahammad and Sreerishnan, 2016; Chen et al., 2014). The amounts of intermediates formed depend on the conditions inside the digester, with a focus on the pH variation and its correlation with the VFA content (Meegoda et al., 2018). The proportion of individual VFA species is important for the overall digester performance since both acetic and butyric acids are the preferred precursors for the methane formation (Merlin Christy et al., 2014). Generally, acidogenesis is the fastest step in the anaerobic process (Merlin Christy et al., 2014), and an unbalanced acidogenesis can lead to acidification of the medium, causing inhibition in several microorganisms, mainly in methanogens. The accumulation of electron sinks like propionate or butyrate are responsible for the increase of hydrogen concentration in the medium (Merlin Christy et al., 2014).

Among all the microorganisms present in a digester, such as bacteria, protozoa, fungi and yeasts, obligatory and facultative anaerobic bacteria (Table 2) carry out the fermentative conversion of simple molecules (sugars, amino acids and fatty acids) into products (VFA and alcohols) (Gavala et al., 2003). Hydrolytic and acetogenic microorganisms generally grow ten times faster than methanogens, which contributes to the rapid conversion of hydrolyzed organic matter (Merlin Christy et al., 2014).

2.2.3.3 Acetogenesis

The products from acidogenesis that cannot be used directly by methanogenic microorganisms (VFA species with more than two carbon atoms and alcohols with more than one carbon atom) are

converted by oxidation into methanogenic substrates, such as acetate, H₂ and CO₂, during the acetogenesis phase of AD (Seadi et al., 2008). Acetogenic reactions are not energetically favorable, with ΔG° values higher than 0 kJ/mol (Aydin, 2017), and the growth kinetics for acetogens is slower than for acidogens (Van et al., 2019). The conversion of propionate to acetate is only achievable with low hydrogen pressure (Merlin Christy et al., 2014). The conversion of propionate (Equation 6), butyrate (Equation 7) and ethanol (Equation 8) to acetate releases molecular hydrogen (H₂). The CO₂ and H₂ conversion to acetate releases water and can be described by the reaction presented in Equation 9.



In acetogenesis, microorganisms can use CO₂ as an electron acceptor and H₂ as the major electron donor during energy metabolism and autotrophic growth via acetyl Coenzyme A (CoA) pathway (Hatti-Kaul and Mattiasson, 2016). The degradation of lipids is performed via β-oxidation pathway, producing acetate from LCFA formed in the previous AD step. In this case, LCFA with an even amount of carbons can be degraded directly into acetate, while LCFA with an odd number of carbons is first degraded to propionate (Meegoda et al., 2018). These degradation reactions occur mostly in anoxic habitats since enzymes extremely sensitive to oxygen (O₂) are involved in this process (Merlin Christy et al., 2014).

The acetate production is a critical step for the success of the AD process since this acidic specie is the main precursor to the methane formation. Acetate can be formed by direct fermentation (mixed-acid fermentation) from soluble organic molecules during acidogenesis, but the major part is converted from intermediates (propionic or butyric acids, or others) by acetogenic bacteria (Ahammad and Sreekrishnan, 2016). Two groups of acetogens are commonly found in anaerobic environments, with two different types of acetogenic mechanisms:

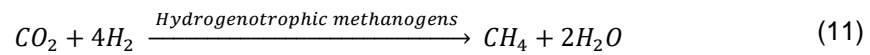
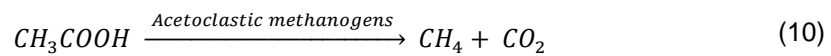
- Obligate hydrogen-producing acetogens (OHPA) or obligate proton-reducing bacteria: through acetogenic dehydrogenation, they produce acetate, carbon dioxide and hydrogen from VFA by anaerobic oxidation (Gavala et al., 2003). This is the dominant mechanism in the acetogenesis of AD and often the term “acetogenesis” refers to acetogenic dehydrogenations, specifically the anaerobic oxidation of long and short-chain fatty acids. The most common examples of OHPA are *Syntrophomonas* sp. and *Syntrophobacter* sp. (Merlin Christy et al., 2014).
- Homoacetogens: through acetogenic hydrogenation, they produce acetate as the only final product from carbon dioxide and hydrogen (Gavala et al., 2003), by anaerobic respiration; this mechanism is less dominant in acetogenic dehydrogenation.

The production of H₂ during acetogenesis (Equations 6, 7 and 8) led to an increase in the hydrogen partial pressure. This intermediate product inhibits the metabolism of acetogenic bacteria (mainly OHPA) and is converted into methane during methanogenesis by acetoclastic methanogens. Thus, both acetogenesis and methanogenesis steps occur in parallel, taking advantage of the

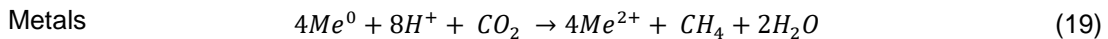
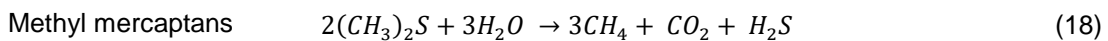
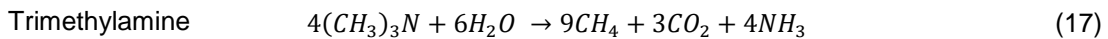
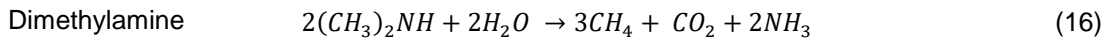
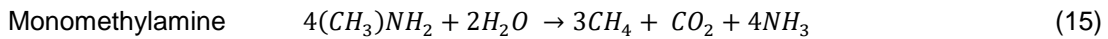
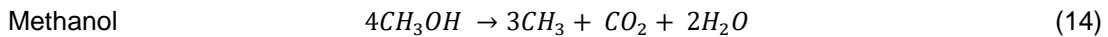
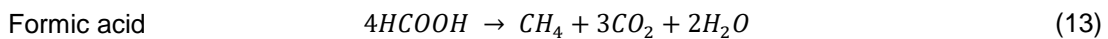
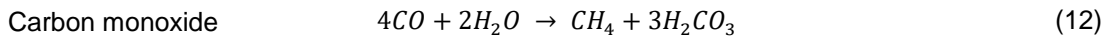
symbiosis of the two microorganisms groups (hydrogen interspecies transfer), avoiding inhibition by the product accumulation, and favoring the growth of both syntrophic microorganisms (Aydin, 2017).

2.2.3.4 Methanogenesis

Methanogenesis is the final stage of AD and is often the rate-limiting step when easily biodegradable substrates are treated (Ariunbaatar et al., 2014). The rate of methanogenesis also depends on the ratio of hydrolytic to methanogenic microorganisms (Meegoda et al., 2018). At this stage, methanogens convert acetate or carbon dioxide and hydrogen into methane (Ahammad and Sreekrishnan, 2016). In an AD system, about two thirds of methane is produced from acetate, while the remaining methane is produced from the conversion of H₂ and CO₂ (Seadi et al., 2008), as presented by the following Equations (Van et al., 2019):



Other organic compounds can also be used as a substrate for methanogenic microorganisms, such as carbon monoxide (Equation 12), formic acid (Equation 13), methanol (Equation 14), methylamines (Equations 15, 16, 17 and 18), dimethyl sulfide and metals (Equation 19), although to a lesser extent than the main substrates (acetate, H₂ and CO₂) (Gavala et al., 2003; Shah, 2017).



The conversion of VFA to methane is an endothermic process and does not occur naturally. To facilitate this conversion, a cooperative symbiosis occurs between fermentative bacteria and methanogenic archaea, with the interspecies electron transfer (IET) as the main driving force that contributes to the use of energy during the AD process (Ajay et al., 2020). IET can occur in three main modes, namely the interspecies hydrogen transfer (H₂ as electron carrier), the interspecies formate transfer (formate as electron carrier), and direct interspecies electron transfer (DIET), between oxidizing bacteria and methanogens (Zhang and Zang, 2019).

The predominant pathway for the exchange of electrons between fermentative bacteria and methanogenic archaea is the IET using H₂ and formate. However, DIET has several advantages, such as lower energy consumption, without the need for redox mediators to electron exchange or complex enzymatic steps, thus having clear thermodynamic advantages (Zhang and Zang, 2019). For the methane production, three different DIET mechanisms can occur, namely the DIET via

conductive pili (conductive nanowire in microorganisms), the DIET via membrane-bound electron transport proteins, and the DIET via abiotic conductive materials, which can build a bridge between fermentative bacteria and methanogenic archaea, thus enhancing the methanogenic activity (Ajay et al., 2020). Several researchers, to improve the AD process and the methane formation, have studied the addition of conductive materials, such as iron and carbon-based conductive materials. This issue will be further discussed, in section 2.6.

The microorganisms of the phylum *Euryarchaeota* from the *Archaea* domain are the main methane producers (Table 2) (Aydin, 2017). These microorganisms have many unique co-enzymes, such as F420, which are involved in one of the most chemically demanding redox reactions in biology, the single-carbon reactions of methanogenesis (Ney et al., 2017). Coenzyme F420 is a characteristic electron carrier associated with a pathway in which bicarbonates are reduced to methane via hydrogen (Dai et al., 2017).

Archaea microorganisms involved in the methanogenesis step belong to three different classes: Methanobacteria, which includes the genus *Methanobacterium*, Methanococci and Methanomicrobia, which includes the genus *Methanosarcina*, *Methanosaeta*, *Methanoculleus* and *Methanospirillum* (Tabatabaei et al., 2010). Parallel to this classification, methanogenic microorganisms can be divided into two main groups, according to their metabolic routes for the formation of methane:

- Acetotrophic (or Acetoclastic) methanogens: convert acetate to methane and produce CO₂ as a metabolic byproduct; are the dominant microorganisms. Includes *Methanosarcina* sp. (high concentration of VFA and low pH) and *Methanosaeta* sp. (low concentration of acetate). *Methanosarcina* sp. can perform methanogenesis through the acetoclastic or hydrogenotrophic pathway (Aydin, 2017) and can use a wide variety of substrates to produce methane, such as acetate, methanol, monomethylamine, dimethylamine, trimethylamine, H₂/CO₂ and CO (J. Zhang et al., 2020).
- Hydrogenotrophic methanogens: convert H₂ and CO₂ into methane; they are less dominant in the microbial community of the AD process than acetoclastic methanogens and mediate the syntrophic relationship between methanogens and acetogens. These methanogens play an important role in methanogenesis, maintaining low hydrogen partial pressure and supporting the growth of OHPA, to carry out the anaerobic oxidation of fatty acids. Hydrogenotrophic methanogens are more resistant to environmental changes than acetoclastic methanogens (Merlin Christy et al., 2014). *Methanobacterium*, *Methanoculleus* and *Methanospirillum* are the common hydrogenotrophic methanogens in mesophilic and thermophilic digesters.

The operational conditions applied to the digester are determinant for the methanogenic microorganism's activity. These microorganisms are strict anaerobes, thus the presence of oxygen inhibits the methane formation. Several authors claim that methanogenic microorganisms cannot synthesize the enzyme superoxide dismutase, used by aerobic microorganisms to neutralize oxygen and radicals such as O₂²⁻, O₂⁻ and OH[·] (Botheju, 2011). Thus, the activity of other important methanogenesis enzymes is also affected, contributing to the sensitivity to the oxygen presence of the methanogenic microorganisms.

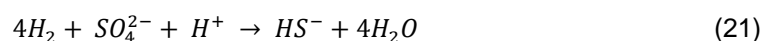
The neutral pH is favorable for the metabolic activity of methanogens and other parameters such as temperature, ammonia content, feedstock characteristics and feeding rate are also of high importance in the performance of these microorganisms (Schaechter, 2004; Van et al., 2019). Both OHPA and acetotrophic methanogens have slow growth rates (Schaechter, 2004), with acetotrophic methanogens having a much shorter doubling time than hydrogenotrophic methanogens (Van et al., 2019). For this reason, methanogenesis is often the rate-limiting factor in anaerobic degradation. To compensate for their slow metabolic activities, the reactors must be operated with high retention times of 14 days or greater (Schaechter, 2004).

The anaerobic system must have tight control, avoiding overloads of readily fermentable substrates, which can result in a rapid accumulation of H₂ and fatty acids, and avoiding the introduction of toxic compounds that disturb the microbial balance. The accumulation of fatty acids generally results in a pH drop and a possible inhibition of the entire process (Schaechter, 2004). Moreover, the decrease in the amount of methanogenic microorganisms, mainly acetoclastic methanogens (the most sensitive to pH and ammonia concentrations), may be indicative of instability in the microbial community (Aydin, 2017).

2.2.3.5 Sulfate reduction

Wastewaters with a high sulfate content present an additional problem in terms of anaerobic degradation performance (Liu et al., 2015). The AD process for the methane formation can be inhibited in the presence of sulfate, since sulfate-reducing microorganisms, obligate anaerobes that degrade simple organic compounds with sulfate as the final electron acceptor (Hatti-Kaul and Mattiasson, 2016), compete with methanogens for compounds like hydrogen. In addition, sulfate-reducing microorganisms will also compete with acetogens for compounds such as propionate and butyrate, and with hydrolytic and acidogenic microorganisms for other simple organic molecules (Dai et al., 2017). In anaerobic environments, sulfate-reducing microorganisms produce hydrogen sulfite (H₂S) as a metabolite from the sulfate. The degradation of sulfate is undesirable since the H₂S formed causes bad odors and reduces the methane yield, increasing toxicity and can induce the failure of the AD system (Liu et al., 2015).

The conversion of acetate and H₂ coupled with sulfate reduction (Equations 20 and 21, respectively) has a thermodynamic advantage over methanogenesis, with less Gibbs free energy, under standard temperature (293.15 K) and pressure (1 atm) conditions. For acetate, the conversion coupled to methanogenesis has $\Delta G^{\circ} = -31$ kJ, compared to the conversion coupled to sulfate reduction, with $\Delta G^{\circ} = -47.6$ kJ. Similarly, the conversion of H₂ coupled to methanogenesis has $\Delta G^{\circ} = -135.6$ kJ, compared to the conversion coupled to sulfate reduction, with $\Delta G^{\circ} = -151.9$ kJ (Paulo et al., 2015). In addition, sulfate-reducing microorganisms have a higher affinity for H₂ than methanogens.



2.2.4 Methane-rich biogas

The biogas composition is highly dependent on the feedstock used in the AD process, the digestion system and temperature, among other operational factors. The energy content of biogas from the AD process is in the form of methane (Seadi et al., 2008). Methane is an odorless, colorless and flammable hydrocarbon gas, which burns with a light blue flame, like natural gas. Methane is also a major component of natural gas (Merlin Christy et al., 2014). Considering an average methane content in biogas of 50 %, the heating value of this gas is 21 MJ/Nm³, the density is 1.22 kg/Nm³ and the mass is 1.29 kg/Nm³, similar to air (Seadi et al., 2008).

The main applications of biogas from the AD process are integrated in Figure 9. Biogas can be used in power stationary turbines, which, in turn, creates a source of bioenergy. In addition, biogas can be cleaned in a process known as biogas upgrading, to ensure that it is only pure methane (also called biomethane) and then used and piped into the main gas system (as a substitute for natural gas), or used as fuel in vehicles after gas compression. Carbon dioxide can also be recovered and then used as a feedstock in greenhouses or used for reconversion into new fuels. Biogas can also be processed into new high-value products such as bioplastics or biochemicals, such as methanol (Jain, 2019), through anaerobic oxidation of methane performed by archaea and sulfate-reducing bacteria (Thauer and Shima, 2008).

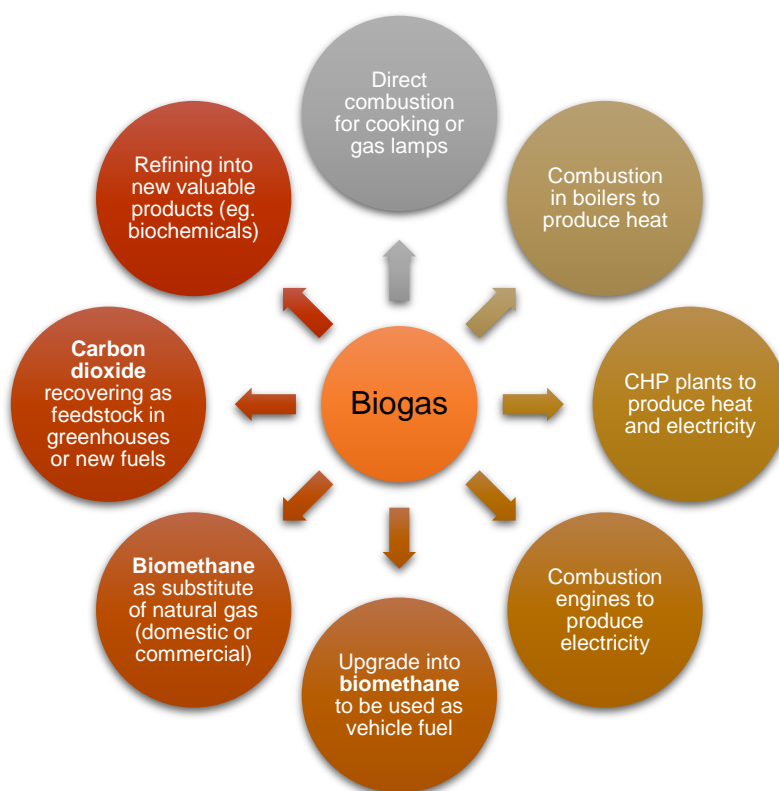


Figure 9| Uses of biogas produced in AD process.

Biomethane has several advantages over hydrogen, although both gases are needed for the success of the European energetic transition. The injection of biomethane into existing infrastructures does not damage them, while hydrogen can corrode the existing grid and cause damages. In

addition, the small size of the molecules and the energy density of hydrogen led to difficulties in storage when compared to methane (European Biogas Association, 2019).

One way to improve the anaerobic process and, consequently, achieve high methane productivity, is to implement a pre-treatment technique. This approach includes biological, chemical, mechanical and thermal pre-treatments (Liew et al., 2020). These are commonly applied to complex substrates with a high content of lignocellulosic material and help to increase the bioavailability of organics in waste, leading to easier hydrolysis and acidification (Meegoda et al., 2018). The pretreatment methods for waste can also be applied to obtain suitable by-products from the hydrolysis step and to improve the quality of the nitrogen and phosphorus components to be recycled (Ariunbaatar et al., 2014). Despite their advantages, physical and chemical pretreatments are considered expensive because they are highly energy demanded and generally have high operational costs (Liew et al., 2020).

2.2.5 Key parameters that affect the anaerobic digestion process

Several environmental or growth factors, such as pH and alkalinity, temperature and the presence of toxic compounds, such as VFA, oxygen or ammonia, and operational parameters, such as organic loading rate and hydraulic retention times affect the anaerobic process. In addition, the biogas potential of the feedstock, the design of the digester, the inoculum quality and the nature of the substrate also influence the biogas production. These parameters affect the activity of microbial anaerobic consortia (Van et al., 2019), particularly the most sensitive microorganisms such as methanogens.

In a biogas plant, several parameters are monitored to evaluate the performance of the process. Besides some economic parameters, essential from the point of view of economic viability, several operating parameters are considered in a biogas plant. The main operational parameters are temperature, operational pressure, reactor volume, gas quantity, HRT, organic load, methane concentration in biogas, specific biogas production and yield. It is also evaluated the gross energy and electricity production, output to the grid and efficiency of the CHP plant (Seadi et al., 2008; Van et al., 2019).

2.2.5.1 pH and alkalinity

The pH is a measure of the acidity or alkalinity level of a solution or substrate mixture (in the case of the AD process). Inside the digester, the pH depends on the partial pressure of CO₂ and the concentration of alkaline and acidic compounds in the liquid phase. The pH affects the growth of microorganisms, mainly methanogenic microorganisms. It also affects the dissociation of some important compounds for the anaerobic process, such as organic acids, ammonia, or sulfide (Seadi et al., 2008). Alkalinity is a measure of the amount of bases in the solution, capable of neutralizing hydrogen ions (H⁺) from acidic species. The most common buffering agents are bicarbonate (HCO₃⁻) and carbonate (CO₃²⁻) ions and are able of attenuating large pH variations in biological systems, which can occur during microbial activity (Mattson, 2014).

Usually, acidogenic microorganisms have a lower optimum pH value than methanogenic microorganisms (Table 3). Some authors report a wide pH range for the hydrolysis step, between 4

and 11, with values between 6 and 8 reported as the most favorable for the hydrolysis of organic material (Van et al., 2019). In the acidification step, the pH directly influences the composition of the VFA mixture formed by the microorganisms. Although highly tolerant to high VFA concentrations, acidogenic microorganisms are strongly inhibited by pH values below 4.0 (Van et al., 2019), with an optimum range between 5.5 and 6.5 (Mao et al., 2015). Other authors report a wider range for the action of acidogenic bacteria, between 4.0 and 8.5 (C. Zhang et al., 2014), being acidogenic microorganisms less sensitive to pH variations than other microorganisms within the AD process (Liew et al., 2020). Acetogenic microorganisms work better in environments with light-acidic conditions, with an optimum pH of around 6.0 (Van et al., 2019).

Table 3| Optimum pH range for different steps of anaerobic conversion of organic matter into biogas, considered by different authors.

AD step	Optimum pH range
Hydrolysis	5.0 – 7.0 (Meegoda et al., 2018)
	4.0 – 8.0 (Van et al., 2019)
Acidogenesis	4.0 – 8.5 (C. Zhang et al., 2014)
	4.0 – 6.5 (Speece, 1996)
	5.5 – 6.5 (Mao et al., 2015)
Acetogenesis	6.0 – 6.2 (Van et al., 2019)
	6.5 – 7.2 (C. Zhang et al., 2014)
Methanogenesis	7.0 – 8.0 (Seadi et al., 2008)
	6.5 – 8.2 (Mao et al., 2015)

Methanogenesis occurs at pH values between 6.5 and 8.2 and, generally, neutral pH (7.0) is considered as the optimum (Mao et al., 2015). An AD system with pH values below 6.6 is reported to have adverse conditions for the growth and activity of methanogenic microorganisms, as well as the release of free ammonia when pH values are higher than 7.8 (Van et al., 2019). Other authors report a restricted optimum pH for the methanogenic step, between 6.5 and 7.2, favoring the growth of methanogens (C. Zhang et al., 2014).

In a mesophilic AD process, a decrease in pH below 6.0 or an increase above 8.3 severely inhibits the process. In the mesophilic digesters, dissolved CO₂ forms carbonic acid when in contact with water, leading to a pH decrease; otherwise, in thermophilic digesters, the solubility of carbon dioxide in water decreases, due to the increase in temperature, and, consequently, the pH increases (Liew et al., 2020).

Additionally, the accumulation of VFA in the liquid phase leads to a decrease in pH values, and the effect of inhibition caused by VFA is higher in anaerobic systems with lower pH values. The accumulation of ammonia leads to an increase in pH, driven by the degradation of substrate proteins (Shah, 2014). To avoid these pH fluctuations, chemical alkalinity in the form of bicarbonates must be added to the digesters, to balance pH changes and avoid drastic pH variations.

2.2.5.2 Temperature

Temperature is among the most important operational factors in the AD process since it influences the activity of enzymes and co-enzymes and also the methane yield and the digestate quality (C. Zhang et al., 2014). In addition, temperature also influences the state of the substrate, regarding

solubility, metabolic rate and ionization equilibria (Van et al., 2019). The AD process can be conducted in a variety of temperature ranges, with different microbial stabilization (Aydin, 2017). Generally, the anaerobic degradation process can take place in three ranges (Seadi et al., 2008):

- Psychrophilic: < 20 °C
- Mesophilic: 30 – 40 °C
- Thermophilic: 43 – 55 °C

Despite this wide range of operation, a fluctuation in the temperature of the digester from that in which the culture has adapted can affect gas production, without directly affecting the production of VFA. Consequently, VFA can accumulate in the digester, leading to process failure (Buswell and Hatfield, 1936). In practice, the digestion temperature is applied according to the feedstock characteristics. Due to the sensitivity of anaerobic microorganisms, temperature variations inside the digesters should be minimized to less than 1 °C/d for thermophilic digestion and 2 – 3 °C/d for mesophilic digestion (Shah, 2014; Van et al., 2019).

The overall performance of an AD process increases with increasing temperature (C. Zhang et al., 2014). Both hydrolysis and acidogenesis steps can be enhanced by increasing the digestion temperature. However, the enhancement of hydrolysis and acidogenesis can have an adverse effect, with rapid VFA accumulation and the difficulty of slower acetogenic and methanogenic microorganisms to metabolize these intermediates can result in a pH decrease and, ultimately, in a process failure (Merlin Christy et al., 2014).

At psychrophilic conditions, methanogens have slower growth rates than in mesophilic or thermophilic conditions, and a previous acclimatization step of the inoculum is often required (Ware and Power, 2017), exposing anaerobic microorganisms to the lower temperatures they are used to, during a certain period of time. Only a few reactors at large scale are operated at psychrophilic temperature, being these systems highly dependent on geographic location, with generally lower ambient temperatures (Meegoda et al., 2018).

Mesophilic temperature is used in most biogas plants around the world, requiring less heating capacity than thermophilic plants (reduced operating costs), with the asset of more stability regarding methane production at mesophilic conditions. In addition, the mesophilic process is less sensitive to environmental changes than the thermophilic process, with a higher diversity of microorganisms (Merlin Christy et al., 2014). Furthermore, the rate of solubilization at mesophilic conditions is significantly lower, for food waste under thermophilic conditions (C. Zhang et al., 2014).

On the other side, thermophilic digesters are able to achieve higher biogas yields and accelerate the degradation rates, lowering the retention time and also reducing the amount of pathogens in the digestate (Seadi et al., 2008), with the disadvantage of the requirement of high energetic inputs and costs (Meegoda et al., 2018). Thermodynamically, a higher temperature in the digester is beneficial for endergonic reactions, such as the breakdown of propionate into acetate, CO₂ and H₂, but unfavorable to exergonic reactions, such as hydrogenotrophic and methanogenic conversions (C. Zhang et al., 2014). Therefore, a two-phase anaerobic system is considered ideal, with a thermophilic system for hydrolysis and acidogenesis steps and a mesophilic system for methanogenesis step (Merlin Christy et al., 2014).

2.2.5.3 Nutrients

The macronutrients that constitute microbial cells, namely carbon (C), nitrogen (N), phosphorus (P) and sulfur (S), are essential for the maintenance of living microbial organisms. In addition, the presence of micronutrients (or trace elements) such as iron, cobalt, nickel, selenium, molybdenum or tungsten are also very important for the growth and survival of microorganisms (Tabatabaei et al., 2018). These trace elements are of vital importance as a support for enzymatic activities and chemical reactions (Mao et al., 2015), as summarized in Table 4.

Table 4 Toxicity level, the importance for microorganisms and the biological function of the most representative micronutrients for anaerobic systems (Mao et al., 2015; Paulo et al., 2015; Shah, 2014).

Element	Toxicity	Importance for microorganisms	Stimulatory concentration (mg/L) Inhibitory concentration (mg/L) (Romero-Güiza et al., 2016)	Biological function	Stimulatory effect in AD
Fe	Low	High	Stimulatory: < 0.3 Inhibitory: --	Essential for cytochromes, ferredoxin and as a constituent of enzymes	Promotes organic degradation and help the hydrogenotrophic metabolism
Mo	Low	High	Stimulatory: < 0.05 Inhibitory: --	Present in formate dehydrogenase and formyl MF-dehydrogenase	Improves biogas production rate
Mn	Low	High	Stimulatory: < 0.027 Inhibitory: --	–	–
Mg	Low	High	Stimulatory: < 720 Inhibitory: --	–	–
Zn	Moderate	High to moderate	Stimulatory: 0.03 – 2 Inhibitory: 7.5 – 1500	Present in hydrogenases	Enhances methane content
Ni	Moderate	High to moderate	Stimulatory: 0.03 – 27 Inhibitory: 35 – 1600	Present in the synthesis of acetyl-CoA and needed for the synthesis of cofactor F430	Reduces ammonia and sulfide toxicity and stabilizes VFA levels
Cu	Moderate	High to moderate	Stimulatory: 0.03 – 2.4 Inhibitory: 12.5 – 350	Present in some superoxide dismutases	–
Co	Moderate	High to moderate	Stimulatory: 0.03 – 19 Inhibitory: 35 – 950	Required to build up the Co-containing corrinoid factor III and present in methyltransferase	–
Cr	Moderate	High to moderate	Stimulatory: 0.01 – 15 Inhibitory: 27 – 2500	–	Improves biogas production rate
W	Moderate	Moderate	Stimulatory: < 0.04 Inhibitory: --	–	Promotes process start-up and eliminates foam
Se	Moderate	Moderate	Stimulatory: < 0.04 Inhibitory: --	Needed for the synthesis of cofactor F430 and benzoyl-CoA	Improves process stability and enhances the growth of microorganisms
Cd	High	Low	Stimulatory: < 1.6 Inhibitory: 36 – 3400	Limited biological function	–
As, Ag, Sb, Hg, Pb, U	High	Low	–	Limited biological function	–

Macronutrients such as C, N, potassium (K), P and S are also essential for the activation and the functioning of microorganisms. Carbon is usually supplied by the substrate source and is required as energy and for the synthesis of cellular material. Nitrogen is essential for protein synthesis, potassium is required for maintaining the cell wall permeability, phosphorus is incorporated into the synthesis of nucleic acids and sulfur is used in numerous enzymes and is essential for the growth of methanogenic microorganisms (Mao et al., 2015). Na is also essential for the metabolism of methanogenic microorganisms, playing an important role in the formation of ATP and NADH oxidation (J. Zhang et al., 2020). The requirements for macronutrients depend on the microbial composition of the consortia and on the growth yields of microorganisms.

Depending on the concentrations, both macronutrients and micronutrients have a stimulating effect on the anaerobic production of biogas, as depicted in Figure 10. At low concentrations, the activity of microorganisms is usually stimulated. For some elements such as arsenic (As), silver (Ag), antimony (Sb), mercury (Hg), lead (Pb), or uranium (U), the toxicity is very high at very low concentrations and there are no clear stimulating effects or biological importance for the activity of microorganisms (Mao et al., 2015).

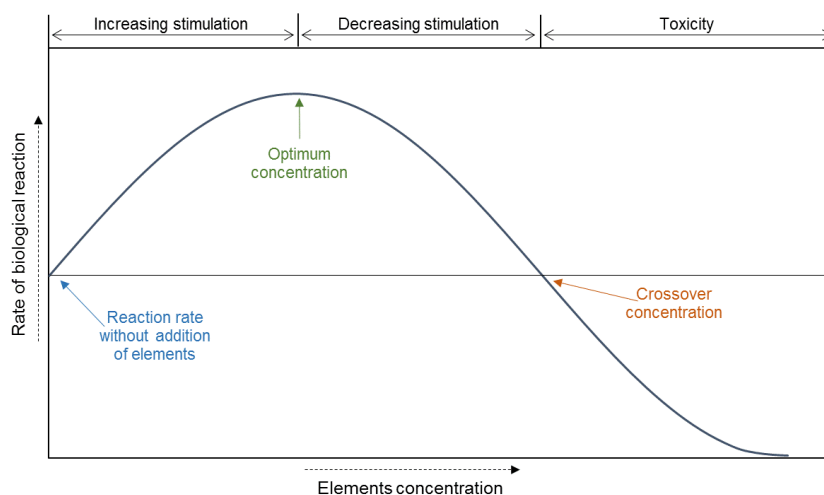


Figure 10| General effect of the concentration of the elements in the medium on the rate of biological reactions (based on McCarty (1964b)).

The extent of the stimulatory concentration range depends on the element, ranging from just a fraction of mg/L for some metals to more than one hundred mg/L for elements like sodium or calcium (McCarty, 1964a). Above the optimum concentration for biological activity, the rate of biological reactions begins to decrease and reaches the crossover concentration, initiating the inhibition of microorganisms, and less activity is observed than without the presence of the elements. At very high concentrations, the activity of microorganisms can be totally inhibited and can lead to failure of the anaerobic process. However, in most anaerobic processes, microorganisms have the ability to adapt to high concentrations of inhibitory compounds, thus increasing the optimum concentration for some elements, as depicted in Figure 10 (McCarty, 1964a).

The stimulating effect is more evident in the AD of solid wastes that do not have these elements, such as energy crops and crop residues, animal manure and organic fraction of municipal solid waste (Mao et al., 2015). The lack of macro or micronutrients can cause instability in the AD process (J.

Zhang et al., 2014). In anaerobic processes, the optimal ratio for macronutrients is considered 600:15:5:1 (C:N:P:S), corresponding to low amounts, because only a small amount of biomass is developed (Shah, 2014). The optimum C:N:P ratio for the enhancement of methane is reported as 200:5:1 (Mao et al., 2015).

2.2.5.4 Presence of toxicants

Anaerobic treatment is sensitive to the presence of toxicants. A wide variety of compounds, either organic (like VFA or other organic compounds) or inorganic (like ammonia, sulfide, or other potentially toxic elements) can inhibit the anaerobic process and, ultimately, cause failure. In addition, the presence of oxygen or high content of salts in the system can disturb the activity of anaerobic microorganisms and cause inhibition of the anaerobic process.

2.2.5.4.1 Volatile fatty acids

The stability of an anaerobic process is reflected by the amount of intermediate products accumulated. The main VFA species produced during AD of organic waste are acetic, propionic, butyric and valeric acids, and they are ultimately converted into CH₄ and CO₂ by syntrophic acetogens and methanogenic microorganisms. However, when high organic loads are applied, an excess of VFA in the medium can lead to drastic pH decreases, inhibiting methanogenesis. Nevertheless, when the AD system is properly buffered, the accumulation of intermediates does not reflect the pH values and the VFA accumulates beyond the maximum, causing inhibition. Buswell and Hatfield (1936) stated that the maximum VFA concentration inside a digester should not exceed 2 – 3 g/L (measured as acetic acid). In addition, for a stable methanogenesis step, the VFA concentration must remain below 0.2 g/L, and inhibition occurs frequently when acetic acid exceeds 3 g/L (Van et al., 2019).

The VFA composition in a digester is significantly influenced by pH (Mao et al., 2015). At low pH values, the main VFA species are acetic and butyric acids, while at slightly alkaline pH values (\approx 8), acetic and propionic acids are the main constituents of the mixture (Merlin Christy et al., 2014; C. Zhang et al., 2014). The concentrations of acetic acid and propionic acid can be used as an indicator of the AD performance and of possible imbalances in the digestion process. When the ratio between propionic and acetic acid is higher than 1.4, or the concentration of acetic acid exceeds 0.8 g/L, AD systems can fail due to acidic conditions (C. Zhang et al., 2014).

2.2.5.4.2 Organic compounds

The performance of anaerobic processes can be affected by the presence of organic compounds. Some of these compounds can accumulate inside the digester since they adsorb to the surface of the sludge and are poorly soluble in water. With the accumulation of such compounds in the cell membranes of microorganisms, the ion gradients are disrupted and can cause cell lysis (Chen et al., 2008).

Several organic compounds are reported to negatively influence the anaerobic digestion process. Some of them include phenols, chlorophenols, halogenated aliphatic compounds, acrylates,

aldehydes, ketones or pyridine. In addition, recalcitrant compounds commonly present in wastewaters can also inhibit the activity of methanogenic microorganisms.

LCFA have also been reported to have adverse effects on anaerobic digestion. LCFA are fats that have several carbons in their chain and include unsaturated and saturated fats. They can be found in oily/fatty wastes and wastewaters from the food processing industries, such as ice cream, dairy products, fish and slaughterhouses. These compounds are neither easy to treat by conventional treatment methods nor are suitable for biological decomposition (Chen et al., 2014). They promote a low release of gas bubbles by the granules, forming insoluble aggregates with LCFA adsorbed on the surface of the granular sludge. These aggregates tend to float on the surface of the wastewater and the presence of LCFA can hamper the supplementation of a substrate to the microorganisms present in the granules (Leitão et al., 2006).

2.2.5.4.3 Ammonia

Ammonia, formed with the biodegradation of proteins and other nitrogen-rich substrates, is an important compound for the anaerobic degradation process, existing mainly in the form of ammonium ion (NH_4^+) and free ammonia (NH_3) (C. Zhang et al., 2014). In the aqueous phase, the equilibrium between ammonium ions ($\text{NH}_{4(\text{aq})}^+$), free ammonia in solution ($\text{NH}_{3(\text{aq})}$), ammonia in the gas phase ($\text{NH}_{3(\text{g})}$), hydrogen ions (H^+) and hydroxyl ions (OH^-) is observed (Sung and Liu, 2003). Although its important role in the growth of microorganisms, NH_3 can act as an inhibitor in certain high concentrations (Chen et al., 2014), and this inhibition is particularly important when dealing with nitrogen-rich wastes (Dai et al., 2017).

The toxicity of NH_3 is highly influenced by temperature, increasing with increasing digestion temperature (Seadi et al., 2008). This toxicity can be caused by the facilitated diffusion through the cell membrane and, consequently, hindering the normal cell functioning, disrupting the potassium and proton balance in the cell, or by the direct inhibition of the methane synthesizing enzyme (Kayhanian, 1999). Among the diverse microbial populations in an anaerobic system, acetoclastic methanogens are more sensitive to high concentrations of NH_3 than hydrogenotrophic methanogens (C. Zhang et al., 2014).

In addition, the increase in pH leads to an increase in the NH_3 content (Seadi et al., 2008). NH_3 also enhances the buffer capacity of the AD system, whereas the VFA formed during acidogenesis can be neutralized by NH_3 . Ammonia can react with VFA, avoiding inhibition by low pH and providing enough VFA amount for the methane formation (C. Zhang et al., 2014). To avoid the inhibitory effect caused by the excess of NH_3 content, its concentration must be kept below 80 mg/L (Seadi et al., 2008). At higher concentrations (600 – 690 mg/L), the AD system has lost stability and methanogenic microorganisms are inhibited (Van et al., 2019).

2.2.5.4.4 Sulfide

Industries such as petrochemical plants, tanneries or pulp and paper plants, generate waste streams containing sulfides. When these streams are treated anaerobically, the sulfate-reducing microorganisms, besides to decreasing the rate of methanogenesis and the quantity of methane produced by competition for available carbon and/or hydrogen, also generate sulfide, which can have

an inhibitory or toxic effect on the methanogens and in sulfate-reducing microorganisms (Chen et al., 2014). Values for half of the maximum sulfide inhibitory concentration are commonly reported between 160 and 220 mg/L, with acetotrophic methanogens being more affected than hydrogenotrophic methanogens due to the presence of its undissociated form (H₂S) (Yamaguchi et al., 1999). For a satisfactory performance regarding organic matter removal, the sulfide content must be kept below 100 mg/L (Demirel and Yenigün, 2002).

Sulfide toxicity is often associated with interference with the assimilation of sulfur, affecting intracellular pH, and also with the facilitated passage of neutral molecules such as H₂S through cell membranes, reacting with intracellular components (Chen et al., 2014).

2.2.5.4.5 Potentially toxic elements

Some elements are vitally important for the synthesis of cells, such as carbon (C), hydrogen (H), oxygen (O) and nitrogen (N). Others, such as sodium (Na), potassium (K), magnesium (Mg), calcium (Ca), aluminum (Al), chromium (Cr), cobalt (Co), copper (Cu), zinc (Zn) and nickel (Ni) are also required by anaerobic microorganisms (Table 4), as these elements play an important role in the synthesis of enzymes and in the maintenance of microbial cells (C. Zhang et al., 2014). However, high concentrations of some elements such as Cr, Co, Zn, Fe, Cu, Cd and Ni, can be of particular concern for microorganisms (Chen et al., 2008).

Some compounds are considered toxic to microorganisms because they are not biodegradable and can accumulate in living organisms to potentially toxic concentrations (Paulo et al., 2015). For anaerobic microorganisms, these elements can cause inhibition due to their action on the function and structure of the enzymes (C. Zhang et al., 2014). They can enter the process with the feedstock or be generated along the digestion process. In most cases, if the toxicity levels are not very high, the microorganisms will be able to adapt and tolerate their presence. In some cases, anaerobic microorganisms are able to degrade the “new” compounds, depending on the environmental conditions inside the digester and the key parameters for their operation.

2.2.5.4.6 Oxygen

In an anaerobic system, small amounts of oxygen can be harmful to the methanogenic microorganisms and other anaerobic microorganisms involved (McCarty, 1964b). In the sludge granules formed within the anaerobic reactor, methanogenic microorganisms are well protected from oxygen, due to the different layers formed by different microorganisms (Botheju, 2011). In this group, the facultative oxygen-consuming microorganisms are essential to creating anaerobic conditions for methanogens, metabolizing part of the available substrate and removing oxygen. Thus, these specific microorganisms are able to create anaerobic microenvironments, rapidly consuming the oxygen dissolved in medium and allowing the survival of methanogenic microorganisms (Leitão et al., 2006), reducing oxygen stress in strict anaerobes (Botheju, 2011).

Some authors have improved methanogenesis and reduced oxygen-induced inhibition by immobilizing methanogenic microorganisms in a polymeric support (Lalov, 2001), thus protecting methanogenic microorganisms inside the support material. In large-scale plants, the discharge of effluents with high amounts of polluting compounds or oxygen can cause inhibition, depending on

the concentration. When an overload of oxygen occurs, the facultative oxygen-consuming microorganisms present in the granules can use this element before it affects methanogenic microorganisms. However, if the overload exceeds the maximum capacity of these microorganisms to consume oxygen, methanogens may be inhibited by the presence of this element (Leitão et al., 2006).

2.2.5.4.7 Salinity

The wastewater produced in several food industries has a saline content. The level of inhibition caused by salinity depends mainly on the concentration of sodium ions. This element is considered essential for the growth and activity of microorganisms, in low concentrations. Proper concentration of sodium enhances the methanogenic activity and can improve methane yield (J. Zhang et al., 2020). The salinity in the medium can affect methanogenic activity, thus reducing methane production (J. Zhang et al., 2020). The high concentration of sodium can cause an imbalance of cellular osmotic stress, which can lead to plasmolysis or cell death (S. Wang et al., 2017). It can also lead to an increase in the suspended solids content in the effluent, a reduction in the organic matter removal and the inhibition of overall bacterial metabolism (Chen et al., 2018).

Inhibitory concentrations of sodium depend on the type of waste under treatment (Chen et al., 2008). McCarty (1964b) referred that sodium concentrations between 100 and 200 mg/L have a stimulatory effect within an anaerobic system, whereas concentrations between 3500 and 5500 mg/L have a moderate inhibitory effect (McCarty, 1964a), and can result in a decrease in methane yield by approximately 35 – 40 % (S. Wang et al., 2017). Concentrations above 8000 mg/L are strongly inhibitory to anaerobic microorganisms and are considered toxic for biological reactions (McCarty, 1964a). As with other elements, the effect of sodium on the rate of biological reactions occurring in microorganisms is described by the pattern depicted in Figure 10.

Several microorganisms are able to adapt to high salt concentrations, such as microorganisms of the genus *Methanosarcina* sp., which grow in aggregates and form irregular cell clusters, increasing their tolerance to high concentrations of sodium and other toxic ionic elements (J. Zhang et al., 2020). It is also reported by several authors that the archaeal community is easily affected by high salinity (S. Wang et al., 2017), and acetoclastic methanogens show higher resistance to high salinity conditions than hydrogenotrophic methanogens (S. Wang et al., 2017; J. Zhang et al., 2020).

2.2.5.5 Hydraulic retention time

The hydraulic retention time (HRT) is denoted as the time that liquid remains in the digester and is determined by the ratio between the volume of the reactor and the flow rate. It determines the time in which the microorganisms and the substrate are in contact, enough to complete the transformation of organic matter (Van et al., 2019). This parameter is closely related to the organic load and has an inverse relationship with it (Meegoda et al., 2018). This operating parameter is associated with the microbial growth rate and also depends on the temperature and the substrate composition (Mao et al., 2015).

Normally, short HRT represents reduced operational costs, but it is associated with acidification of the digester and can cause inhibition of the anaerobic process (Meegoda et al., 2018), resulting

in insufficient utilization of the digester components (Mao et al., 2015). Long HRT implies high-volume digesters and increases investment and operating costs (Van et al., 2019). Nevertheless, long HRT (20 to 200 days) is required in conventional anaerobic digesters to ensure complete digestion of a given influent (Liew et al., 2020). To achieve constant and maximum methane yields, long HRT coupled with a low organic load is preferred (Mao et al., 2015).

2.2.5.6 Organic load

The organic load applied to a digester is related to the amount of organic matter fed per day, in continuous digesters (Meegoda et al., 2018). The organic loading rate (OLR) is given by the ratio between the organic concentration and the HRT. Both HRT and OLR are dependent on process parameters that influence microbial growth, such as temperature, pH and characteristics of the substrate (Van et al., 2019).

The robustness of the microbial population is very important in these types of systems, allowing the continuity of the anaerobic treatment and avoiding failures. The increase in OLR increases the biogas yield; however, the equilibrium and productivity of the AD can be disturbed, leading to the temporary inhibition of microbial activity (Mao et al., 2015). When high amounts of organic matter are added to an anaerobic system, accumulation of VFA can occur through rapid hydrolysis and acidification, and has the potential to inhibit methanogenesis and can lead to reactor failure. In specific cases, such as the treatment of oil and grease waste and glycerol, some authors reported the adaptation of the microbial population to the imposed organic shock, recovering from the inhibition of methanogenesis caused by the high VFA content (Ferguson et al., 2016). The increase in temperature to thermophilic conditions and the effluent recirculation have positive effects in relieving overload inhibition (Mao et al., 2015).

2.2.6 Configurations of anaerobic bioreactors

Many different configurations of anaerobic reactors have been developed over many years. Figure 11 shows the most common bioreactor configurations applied to the anaerobic treatment of highly polluted wastewaters (high-rate anaerobic process), such as dairy effluents (Bachmann et al., 2008). In addition to the configurations represented in the figure, the AD process can be performed in an anaerobic fermentation tank (similar to a continuous stirred reactor but without stirring), in an anaerobic rotating biological contact reactor (AnRBC) or in an anaerobic percolating filter (APF) (Bachmann et al., 2008).

Anaerobic digesters can vary in configuration, retention times, requirement of pre or post-treatment, operating temperature, among others, depending on the substrate (Jain, 2019). The operation of anaerobic digesters can be performed either as a batch or as a continuous reactor. In batch mode, the substrate is added to the reactor at the beginning of the operation, while in continuous mode the substrate is constantly added to the reactor (Merlin Christy et al., 2014). Considering physical separation, AD processes include single-stage, two-stage and three-stage systems (Van et al., 2019). Other reactor operation modes can be performed, according to the conditions to be imposed and the characteristics of the substrate to be treated. The solids content in the digester determines the designation of the systems, as "liquid" (Total solids (TS) between 4 and

10 %), “wet” (TS < 20 %) or “dry” (TS > 20 %). Dry digestion is typical of substrates such as energy crops (maize, miscanthus, among others) and silages.

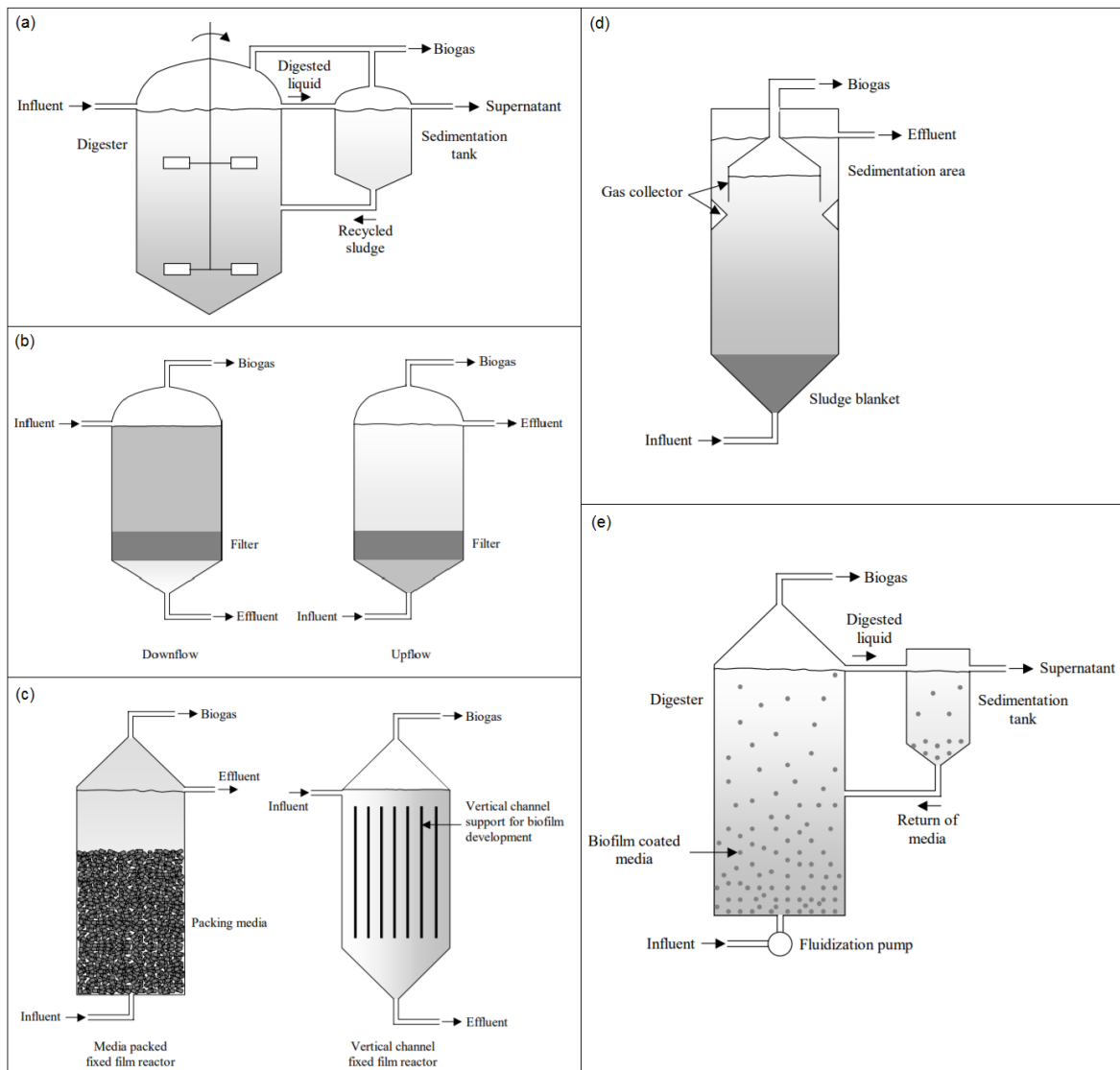


Figure 11 | Bioreactor configurations for anaerobic treatment of highly polluted industrial wastewaters (graphics from (Bachmann et al., 2008)): (a) Anaerobic contact reactor; (b) Anaerobic filters (AF) with down-flow and up-flow; (c) Anaerobic fixed film reactor (AFFR), with two different supporting structures; (d) Up-flow anaerobic sludge blanket (UASB) reactor; (e) Anaerobic fluidized bed reactor (FBR).

Batch reactors are very common in AD processes, mainly for the treatment of solid wastes. In batch reactors, the four main steps of AD occur sequentially, with the consumption of substrates by each type of microorganism and the production of their suitable product. The depletion of substrates had led to a decrease in the microorganism’s population, and the retention time of these types of reactors is often longer than other reactor types, with long start-up periods.

For fed-batch reactors, also called anaerobic sequential batch reactors (AnSBR), the same tank is used for treatment and fermentation steps. This single-tank fill-and-draw unit is considered a good option for the treatment of a wide range of wastewater strengths, allowing for good process control

and high process efficiency, with high biogas yield. The simplicity and flexibility of use, the cost-effectiveness, the final effluent quality and the lower process inputs, and the mechanical requirements that conventional reactors have are a significant advantage. However, high volumes are required, as well as some type of stirring, which is necessary to ensure the transfer of the substrate to the microorganisms in the granulated biomass (Mao et al., 2015).

Continuous systems are also very common, mainly for liquid wastes, with continuous loading of organic material and continuous organic matter removal and methane production. In continuous systems, contrary to what occurs in batch systems, the four main steps of AD occur at the same time. When a continuous system reaches a steady state, there is no VFA accumulation, because they are immediately converted into methane after formation (Meegoda et al., 2018). The continuous stirred tank reactor (CSTR) was the first high-rate anaerobic reactor and is known for its reliability and versatility, being widely used to treat streams with a high solids content (Mao et al., 2015). Coupled to the CSTR, a settling tank is commonly used, to settler sludge and recycle microorganisms into the main reactor (Figure 11 (a)).

High-rate anaerobic reactors, such as UASB (Figure 11 (d)), AF (Figure 11 (b)), FBR (Figure 11 (e)), AnSBR or expanded granular sludge bed (EGSB) can treat high organic loads per day with lower reactor volume, obtaining high efficiencies treating highly biodegradable substrates (Fonseca and Teixeira, 2006). These systems are characterized by high SRT due to biomass immobilization or granulation and are designed to operate at high HRT without the risk of biomass washout (Hatti-Kaul and Mattiasson, 2016). In addition, these bioreactors allow the recovery of the biogas produced to be reused (Liew et al., 2020). Almost all organic materials can be digested under anaerobic conditions, except for stable woody materials, since anaerobic microorganisms are unable to degrade lignin (Appels et al., 2008).

The UASB reactor is a simple, compact, inexpensive and common technology, widely used for the treatment of effluents (Mao et al., 2015). In the UASB reactor (Figure 11 (d)), biomass is immobilized by the aggregation of microorganisms into large granules, to form a biofilm at the bottom of the reactor (Aydin, 2017), ensuring good contact between biomass and wastewater (Mao et al., 2015). The efficiency of the treatment is highly dependent on the quality of the granules formed during the startup period. The granules can form different layers that include acetotrophic methanogens in the interior, OHPA in the middle layer and acidogenic (fermentative) microorganisms in the outermost layer. In the three-phase separator (gas-liquid-solid), anaerobic granules, treated water and gas are separated and the biogas is collected at the top of the reactor (Schaechter, 2004). The functioning of EGSB is similar to the UASB, but with a much higher upward flow velocity and with the recirculation of the effluent (Paulo et al., 2015). Generally, EGSB is used for the continuous treatment of low-strength soluble and complex substrates from small and medium-sized industries (Mao et al., 2015).

In fixed film reactors, such as AF, AFFR (Figure 11 (c)) and FBR (Figure 11 (e)), microorganisms grow attached to physical support, made of plastic, ceramic, glass, or sand, forming a biofilm (Schaechter, 2004). The immobilization technique allows the reduction of the microorganism's loss during an operation at high flow rates (Aydin, 2017). In AF, no mixing technology is employed and the organic material can flow through submerged support materials, being degraded by the microorganisms attached to the support material. These types of reactors can be operated under either an up-flow or down-flow (Figure 11 (b)), and recycling can be applied when very high-strength

wastewaters are treated (Mao et al., 2015). For the FBR, the immobilization supports are kept in suspension and mixed by the high upward velocity of the incoming wastewater (Paulo et al., 2015). FBR allows higher OLR values and greater resistance to inhibitors and the growth of a thin biofilm allows for a good mass transfer, compared to AF technology (Mao et al., 2015).

High-rate anaerobic reactors face some operational problems, despite their robustness, high removal of organic matter (> 80 %) and the possibility of high up-flow velocity at low HRT. AF and AFFR may face clogging of the fixed bed due to the high solids concentration. In UASB and EGSB, sludge floatation, foam and scum formation are common problems due to the high concentration of lipids in the wastewater (such as dairy effluents) (Liew et al., 2020).

Comparing the different configurations available for anaerobic treatment, EGSB seems to be the most advanced reactor configuration, being the most efficient for medium-strength wastewaters, with high resistance combined with high efficiency. The investment and operational costs associated with these technologies must be realized, considering the substrate under treatment. Thus, the development of the optimal cost to optimal input/output ratio for the digestion process ensures the overall sustainability of biogas technology (Mao et al., 2015).

2.3 Pulp and paper industry

The current digital world has led to a decrease in the demand for paper, either for writing, for newspapers or magazines. However, new markets and applications for pulp and paper products continue to increase, such as cardboard, tissue paper, textile applications, or pulp for personal care products (Cherian and Siddiqua, 2019). The need to replace plastic (produced from non-renewable sources) with paper in packaging applications is a sustainable alternative since the paper is derived from renewable feedstock (wood) and decomposes naturally. Thus, although the development of technology has led to changes in consumption patterns, the need for paper continues to grow, which makes the P&P industry one of the most important industries worldwide.

The P&P industry is considered one of the largest industries in the world (Bajpai, 2017), and the fifth largest energy consumer worldwide, behind industries such as chemical, iron and steel, and oil and gas refining (Energy Information Administration, 2019). The total consumption of primary energy in 2017 in the members of the Confederation of European Paper Industries (CEPI) reached 1.3 million TJ, and it includes the use of biomass (60 %), gas (33 %), coal (3 %), fuel oil (2 %) and other fuel sources. Electricity generated through a combined (on-site) heat and power plant accounts for 96 % of total electricity consumption (CEPI, 2019) and, for this reason, these industries are considered as energy-intensive manufactures (Energy Information Administration, 2019).

According to CEPI, the 500 pulp, paper and cardboard producing companies in 18 countries in Europe produced 38.3 million tons of pulp and 92.2 million tons of paper and cardboard in 2018 (CEPI, 2019). CEPI members account for 92 % of the European P&P industries and represent 21 % of the total world pulp production. Portugal is the third largest European pulp producer, behind Sweden and Finland. In terms of wood consumption for pulp manufacturing, 72 % are softwood (such as pine and spruce) and 28 % are hardwood (such as birch, eucalyptus, beech, ash, aspen, maple, acacia, oak, among others) (CEPI, 2019).

In addition to the high-energy demand, the P&P industries also generate solid waste, wastewater effluents and air emissions. Thus, these industries play an important role in the European climate change mitigation strategy. With direct CO₂ emissions of 32.22 megatons in 2017, a 44 % reduction in specific CO₂ emissions was observed in the last 16 years, reaching 0.30 kton_{CO2}/kton_{product} in 2017 (CEPI, 2019). Methane is also released in some steps of the paper life cycle, namely in fuels burning and decomposing of paper in landfills (EPN, 2018). For these reasons, the concern is focused at reducing CH₄ and CO₂ emissions to the atmosphere during the overall process of P&P manufacturing. An alternative is to increase the use of recycled paper; this measure not only reduces the impact by reducing the energy need in the manufacturing process but also avoids the landfill of waste paper, thus preventing the release of CH₄ from paper decomposition into the atmosphere.

In Portugal, P&P production is one of the most vital industrial activities. These industries have implemented, in recent years, measures to reduce GHG emissions and contribute to the concept of the circular economy. According to CELPA – Associação da Indústria Papeleira, the water used in the manufacturing process is normally recycled and reused or, alternatively, is treated and 79 % of the treated water returns to the process. For the energy generation in the CHP plants, 70 % of the fuel used is considered as biofuel, that is, biomass and lignin from wood. Every year are generated 3.44 TWh of electricity, 73 % of which is used directly at the P&P mill for the process and maintenance of the facilities. In addition, several wastes generated in the process are valorized as

energy or used as materials for the development of new products (by either P&P industries or other associated companies), and only a small fraction (24 %) of the waste is discharged without added value valorization (CELPA, 2018).

2.3.1 Pulp making process

Pulp derived from wood is the main raw material in the production of different types of paper. The pulp is also used as an absorbent material in diapers and other sanitary products (Cabrera, 2017). The process to produce pulp consists of several steps. Considering the use of new wood materials, which represent a large share of the pulp production, the process can be divided into three main steps: preparation of raw materials, separation of the fibers and bleaching process. The recovering of chemicals is also an important step that, although not directly in the pulp production line, contributes to its success and sustainability.

2.3.1.1 Preparation of raw materials

Before treatment, be it mechanical, semi-chemical, or chemical, the raw materials (softwoods, hardwoods and non-woody biomasses) are prepared, converting them into appropriate size and shape for the following processing. The logs are debarked and cleaned with water since the bark is a contaminant in the chemical pulping process. The clean logs are cut into identical small chips, thus maximizing the efficiency of the pulping process. Typically, very small or very large chips are separated and used for energy recovery (biomass burning) or are reprocessed for further treatment (Kramer et al., 2009).

2.3.1.2 Separation of the fibers

A resin called lignin binds the wood fibers tightly. In the pulp producing process, lignin must be eliminated and only fibers (cellulose) are extracted. Thus, the treatment process aims to separate the biomass components, namely, cellulose (40 – 50 %), hemicellulose (25 – 30 %) and lignin (25 – 30 %) (Naqvi et al., 2010), into individual components. After separation, the fibers are suspended in water in a slurry, to be used in the papermaking process. The treatment process is performed either by separation or by solubilization of the lignocellulosic components. Pulping processes can be divided into mechanical, semi-chemical and chemical pulping, according to the methodology and instruments used (Kumar et al., 2020).

2.3.1.2.1 Mechanical and semi-chemical pulping

In mechanical pulping processes, no chemicals are used in the process. In this process, the pulp fibers are separated from the raw materials by physical (mechanical) energy, such as grinding or shredding. In some mechanical processes, thermal and/or chemical energy is used for the raw materials pretreatment stage (Sandberg et al., 2020). The mechanical pulping process is used worldwide and grinding is the oldest mechanical pulping technology, developed in Germany in the 19th century (Lönnberg, 2009). The semi-chemical pulping process combines both mechanical and chemical methods, with the wood chips being initially softened or partially cooked with the addition of chemicals and then, mechanically pulped (Cabrera, 2017).

There are four main types of mechanical and semi-chemical pulping:

- *Stone ground wood pulping (SGWP)*: in this process, the small logs are ground against artificial bonded stones made of aluminum oxide or silicon carbide grits. This process has a high yield, but the fibers can be very short; in this case, the addition of expensive chemical fibers is needed to provide a strong pulp to withstand the pressure of the paper machine (Lönnberg, 2009).
- *Refiner mechanical pulping (RMP)*: in this pulping process, the wood feedstock (such as logs, wood scraps, or sawdust from lumber mills) is ground between two grooved discs. Combined with the high yield obtained, this process produces longer fibers with greater strength (Lönnberg, 2009).
- *Thermo-mechanical pulping (TMP)*: a pre-steaming step was introduced in the RMP process, to soften the lignin. This pre-treatment produces longer fibers and the highest quality mechanical pulp is obtained. This process is high energy-intensive and a further bleaching process is required to produce high-quality paper products (Takada et al., 2020).
- *Chemithermomechanical pulping (CTMP)*: for the CTMP, a chemical pre-treatment is performed, prior to the TMP treatment. The chemical addition allows a less destructive separation of the fibers, resulting in longer and more flexible fibers with a high fiber content in the pulp. Like the TMP process, CTMP is a high energy-intensive pulping process (Grötzner et al., 2018).

The mechanical pulping yields are higher than the typical yields obtained in chemical pulping processes (90 – 98 % versus 40 – 50 %, respectively). However, due to the short length of the fibers obtained by grinding, the fiber strength and the aging resistance of the pulp are low. In addition, the brightness and opacity of TMP pulps are lower than chemical pulps, due to the high lignin content (Takada et al., 2020). Thus, the applications of most mechanical pulps are limited to the production of lower quality papers, such as newsprint, magazines and cardboard.

The effluents generated in the mechanical pulping processes typically contain moderate to high organic matter contents, between 2 and 10 gO₂/L (expressed as chemical oxygen demand - COD), as well as high amounts of easily biodegradable compounds, such as carbohydrates and acetic acid (Meyer and Edwards, 2014).

2.3.1.2.2 Chemical pulping

Chemical pulping is the most common pulping process used worldwide. This type of pulping is preferred because the lignin removal is highly efficient (Takada et al., 2020). During the chemical pulping process, the majority of the lignin and hemicellulose contents are removed, resulting in low pulp yields (40 to 55 %), with a high degree of cellulose fibers (Meyer and Edwards, 2014). In this process, the lignin is separated from the remaining materials in a digester under pressure and using cooking chemicals. In the “cooking” of raw materials, such as wood chips, aqueous chemical solutions called “white liquor” are used, at high temperatures and pressure to extract the pulp fibers.

The three main chemical pulping processes are:

- *Soda pulping (alkaline)*: this pulping process is more effective when non-woody biomass is used (such as wheat straw, flax and bagasse). During chemical treatment, non-wood materials are treated with NaOH at temperatures below 160 °C (Kubes et al., 1980), to solubilize lignin by deprotonating the phenolic lignin subunits (Takada et al., 2020).
- *Sulfite pulping (acid)*: this process involves digestion of woody material at 140 – 170 °C using an aqueous solution of sulfite or bisulfite salt of Na, Mg or Ca, and delignification results from the cleavage of the lignin-carbohydrate bonds (Sangha et al., 2012) and sulfonation of lignin (Lora, 2008). This process has been displaced over the years by the Kraft pulping process due to the long cooking cycle and the complicated chemical recovery involved with sulfite pulping.
- *Kraft pulping or sulfate pulping (alkaline)*: this process is the main pulping process used worldwide, and although it presents relatively low yields ($\approx 45\%$), it is possible to obtain a pulp with better strength and brightness properties (Mesfun et al., 2014). In the Kraft process, the wood is digested with an alkaline mixture of NaOH and Na₂S, at around 150 – 170 °C (Naqvi et al., 2010), and the lignin is modified as it occurs in the soda pulping process (Takada et al., 2020).

2.3.1.2.2.1 KRAFT PULPING PROCESS

The Kraft process is the most used pulping process by P&P industries worldwide (Santos et al., 2013). The pulp produced by the Kraft process has superior strength, high resistance to aging and the bleaching process is simplified. Figure 12 shows a flowchart of the Kraft pulping process integrated into a P&P mill. It comprises the chemical recovery steps, including the energy production from chemicals and biomass burning, and the connection between the pulp manufacture, the bleaching process and the paper manufacture. Two types of effluents were highlighted in the figure: fly ash from biomass burning (solid waste) and effluent from the bleaching process (liquid waste), which are detailed below.

The Kraft process was developed with the main goal of removing lignin while preserving carbohydrates. The cooking of wood is performed with the addition of white liquor, an alkaline mixture of sodium hydroxide and sodium sulfite, to promote the lignin dissolution and the fiber release. The use of such chemicals is advantageous in terms of the final fiber strength but it leads to relatively low pulp yields, caused by the instability and degradation of carbohydrate during the alkaline reaction (Santos et al., 2013).

The cooking of the wood chips is performed at high temperatures (150 – 170 °C) and pressure. The lignin structure is modified and depolymerized by the action of the strong alkaline solution and the presence of hydrosulfide ions. In this digestion process, 90 – 95 % of the lignin is solubilized in the pulping liquor. A wide variety of wood species can be processed by the Kraft pulping process and the exact conditions of the process depend on the type of wood used (softwood or hardwood) (Gellerstedt, 2015). After cooking for 2 to 4 hours, the liquor and the pulp mixture are discharged from the digester. They are separated into a series of washers (Environmental Protection Agency, 2010). After washing, the pulp (fibers) is ready to be submitted to the bleaching process. The content

in lignin of softwood pulps is about 5 %, and this residual lignin is removed in the bleaching process, obtaining a brightening and high-quality pulp.

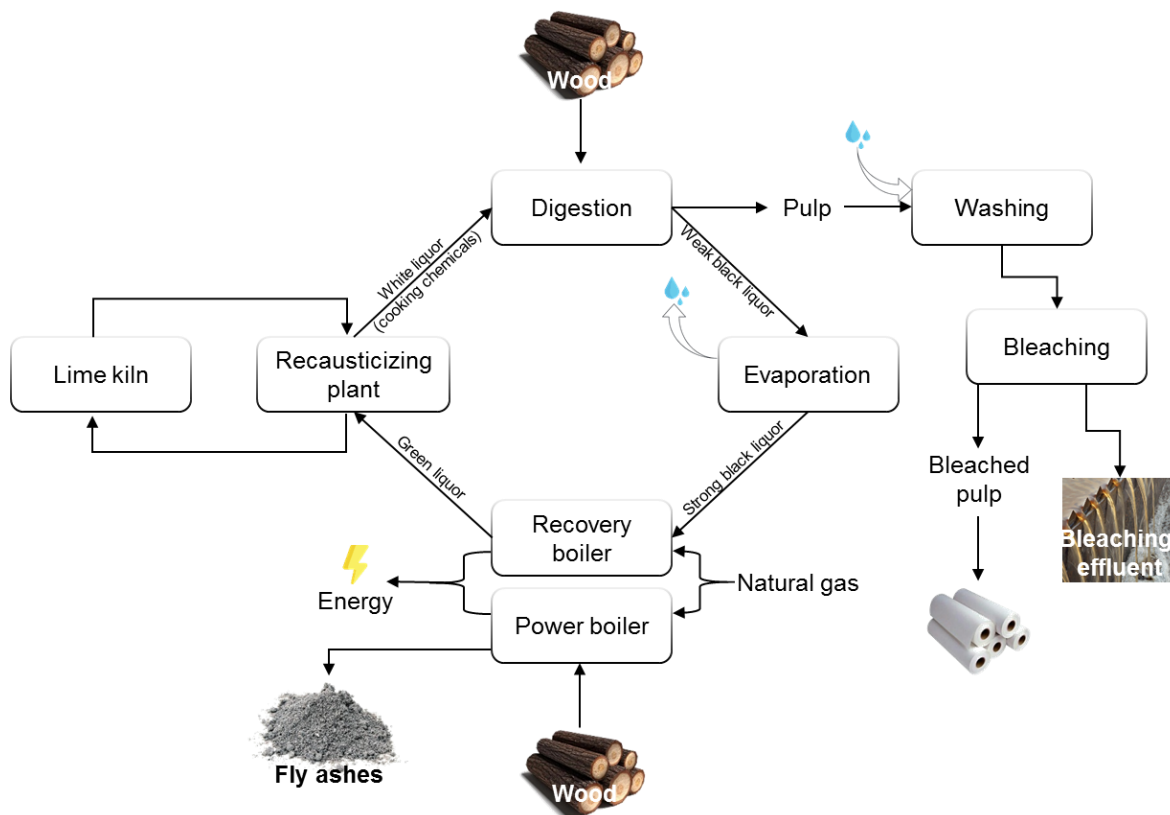


Figure 12| Flowchart of a P&P mill, with Kraft pulping process and bleached pulp to produce paper. It is highlighted two of the wastes generated in the P&P industry: fly ashes from biomass burning and bleaching effluent from the pulp bleaching process.

The Kraft process is the pulping process with maximum chemical recovery efficiency. The chemicals are collected after pulping and are set to the chemical recovery circuit. Figure 12 includes the three steps in the chemical recovery process, namely the black liquor concentration, the combustion of organic compounds and the causticizing and calcination. These steps are vital to the environmental and economic sustainability of the P&P industries and are detailed in the following sections.

2.3.1.3 Bleaching process

After chemical or mechanical pulping processes, the pulp obtained still contains high amounts of lignin and other colored compounds. To produce high-grade final products, the pulp must be bleached, to obtain a light-colored or white paper, preferred for many products and applications. The same bleaching process or sequence can be applied to any of the pulping processes (mechanical, semi-chemical, or chemical) (Environmental Protection Agency, 2010), detailed previously.

The bleaching process removes the pulp color caused by the presence of residual lignin. The addition of two or more chemicals and the sequence in which they are used depends on several factors, including costs, the type of pulp to be bleached and the requirement for the final product.

The addition of chemicals to the previously washed pulp is performed in stages in the bleaching towers. Between each stage, bleaching chemicals are removed in the washers. From these successive washes, the effluents generated are collected and sent to the wastewater treatment plant (Environmental Protection Agency, 2010).

The pulp fibers are delignified by the solubilization of additional lignin from the cellulose, in a process of chlorination and oxidation. Mechanical pulps are generally brightened with hydrogen peroxide and no chlorinated organic compounds are formed since no chlorine or chlorine-based chemicals are used. Chemical pulps are generally more complex to be brightened, and the processes normally comprise several stages. For many years, the most common bleaching agents (oxidants) used were elemental chlorine and sodium hypochlorite, due to their low cost and capacity to achieve high bright pulp. The use of such chemicals results in the formation of highly toxic and non-biodegradable pollutants, such as dioxins. Over the years, they have been replaced in almost all pulp mills by other bleaching agents, such as chlorine dioxide (ECF – elemental chlorine-free – bleaching), hydrogen peroxide, oxygen or ozone (TCF – total chlorine-free – bleaching) (Sharma et al., 2020).

ECF bleaching is the most used bleaching process by pulp mills all over the world. The addition of chlorine dioxide is beneficial because it is a selective bleaching agent, which preserves the quality of the pulp, in comparison to conventional bleaching with chlorine compounds (Sharma et al., 2020). During ECF bleaching, chlorine dioxide reacts with the pulp, forming chlorite, hypochlorous acid and molecular chlorine. Molecular chlorine is responsible for the formation of adsorbable organic halides (AOX), although in minimal amounts compared to the conventional bleaching process (Sangha et al., 2012).

Bleaching sequences are normally constituted by different bleaching methods. The most common methods involve bleaching with chlorine dioxide (D), oxygen bleaching (O), ozone bleaching (Z), extraction with sodium hydroxide (E), alkaline hydrogen peroxide (P), or sodium dithionite (sodium hydrosulfite) (Y). The D and EOP methods (a combination of three methods – E, O and P – in the same stage) are part of the ECF bleaching process and are often combined in the same sequence. The effluents from the D and EOP processes are often treated by anaerobic biological processes and both can contain high amounts of highly toxic chlorinated organic compounds (Meyer and Edwards, 2014).

2.3.1.4 Recovering of chemicals

In the chemical pulp mill industries, an additional step for the recovering of chemicals is performed, to recover the chemicals used in the wood cooking step. These recovery steps are considered essential in the chemical pulp industries, as they allow for the reduction of costs, reduction of the environmental impact of waste material (mainly black liquor), with the minimization of the raw materials use and with the recycling of chemical materials (Mesfun et al., 2014). In addition, the recovery of chemicals has the asset of co-generating steam and power, which is used as energy in the P&P mill.

In Kraft (and soda) pulp mills, the liquor from the cooking step is called “weak black liquor” and contains wood lignin, organic materials, oxidized inorganic compounds (such as Na_2SO_4 and Na_2CO_3) and white liquor (cooking chemicals such as NaOH – soda – or a mixture of NaOH and

Na₂S – Kraft). The “weak black liquor” comes from the pulp washers placed after the digesters (Naqvi et al., 2010).

The process for chemicals recovery includes three steps:

- *Black liquor concentration*: the concentration of weak black liquor is performed by a series of evaporators, to increase the solids content from 12 – 15 % to ≈ 65 %. It forms the so-called “strong black liquor”, capable of being combusted in the recovery furnace (Verma et al., 2019), in the next chemical recovery step. The condensate from the evaporators contains high concentrations of methanol and is sent to the treatment plant (Meyer and Edwards, 2014).
- *Combustion of organic compounds*: in the recovery furnace, “strong black liquor” is burned and the inorganic chemicals are reduced to a molten smelt, enriched with Na₂S and Na₂CO₃, after lignin decomposition. They are recovered from the bottom of the boiler and refined (Kramer et al., 2009). This combustion process generates energy in the form of electricity, which, in combination with the energy produced by the power boiler (wood burning), is used in the plant.
- *Causticizing and calcining*: the inorganic salts recovered in combustion are dissolved in the weak wash water and form the “green liquor” (Naqvi et al., 2010), which is filtered/clarified to remove the dregs. “Green liquor” is causticized with the addition of lime, to convert the Na₂CO₃ to NaOH (Santos et al., 2019). The calcium carbonate formed is removed as lime mud (He et al., 2009) and it is washed and the lime is regenerated in the lime kiln. The “white liquor” recovered is filtered and reused in the wood cooking process.

Typically, about 3.5 kg of steam is produced when 1 kg of black liquor solids are burned, depending on the efficiency of the recovery boiler. After the steam generation, it passes through a turbine to generate electricity and the amount generated depends on the turbine type and the quality of the steam. A mill, which produces 1000 ton/d of Kraft pulp, is capable of generating 25 to 35 MW of electricity by burning 1500 ton/d of black liquor dry solids in the recovery boiler (Tran and Vakkilainen, 2008).

2.3.2 Waste and wastewater generation in Kraft pulping process

Due to the large consumption of resources, including raw materials such as wood, water, and energy (such as fossil fuels, in some cases), the P&P industries are also considered an important source of environmental contaminants in both traditional and emerging P&P producers (Kamali et al., 2016). In a P&P industry, several wastes are produced at different steps of the process. When virgin fibers are used, the amount of waste generated depends on the pulping process implemented (Cherian and Siddiqua, 2019). The Kraft pulping process generates about 100 kg of waste per ton of air-dry pulp (kg/t_{AD}), whereas the semi-chemical and mechanical pulping process generates only about 60 kg/t_{AD} (Monte et al., 2009). With the new approaches considered in recent years for waste management, the use of different wastes generated in P&P mills as resources is a step towards green energy and environmental sustainability, moving from the conventional linear concept to the circular economy.

For the Kraft process, including the chemical recovery cycle, the main solid wastes generated are ashes from biomass burning (power boiler) and combustion of chemical products (recovery boiler), dregs (also called green liquor sludge) from clarification of green liquor, lime mud from the causticizing process, and grits from the regeneration of CaO after calcination in a lime kiln. Barks and other wood residues are burned for energy production, therefore, they are not considered waste (Simão et al., 2018). Of these wastes, the most abundant are dregs, grits and biomass ashes, with dregs currently being the most challenging residues, since, so far, there is no viable solution for their recycling (Novais et al., 2018b).

Industries highly water-dependent, such as P&P mills, are responsible for the suitable and sustainable management of water resources. Surface and groundwater are used in all the main stages of pulp and paper production (Figure 13). In addition to the process stages, water is also used in cleaning and cooling the machines and in the maintenance of the mill, being discharged as effluent to be treated in the mill's wastewater treatment plant (WWTP) (Kamali et al., 2016). In the overall process, only a small fraction is lost embedded in the products ($\approx 1\%$) or lost by conversion into water vapor during the manufacturing processes ($\approx 11\%$). The remaining $\approx 88\%$ are returning to surface waters after physical or biological treatment at the WWTP (Wiegand et al., 2011).

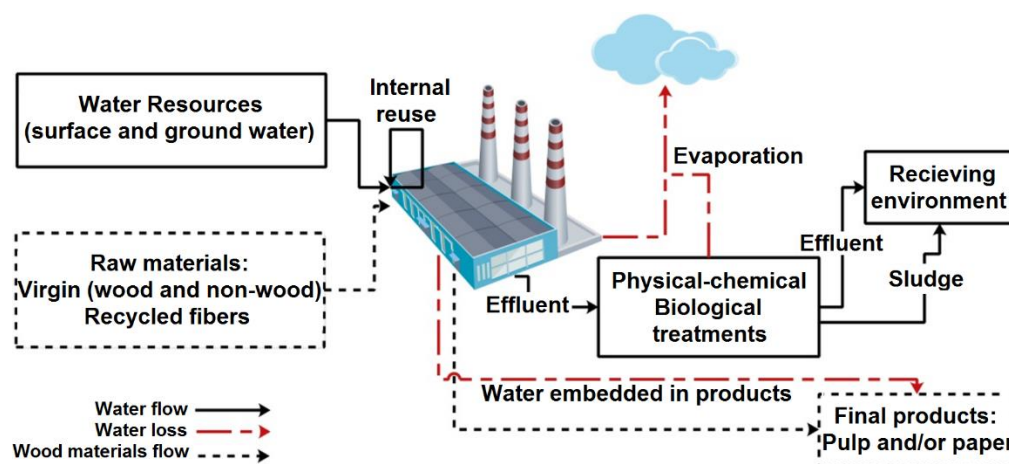


Figure 13| Simplified flowsheet for raw materials use and fate in a typical P&P mill (reproduced from Kamali et al. (2016) with authors authorization).

Of all the wastewater streams generated during the pulp and paper manufacturing processes, the most abundant are the bleaching effluents. The bleaching process generates up to 85 % of the total volume of effluent discharged in a P&P mill. These effluents formed in the pulp bleaching process have different characteristics and are highly toxic (EPN, 2018). The most problematic effluents are generated during the bleaching process with chlorine dioxide, due to the formation of organochlorine compounds (Meyer and Edwards, 2014). These effluents from the bleaching process are rich in dissolved lignin, carbohydrates, color, organic matter (measured as COD), AOX and inorganic chloride compounds (Sridhar et al., 2011).

The European Group for Integrated Pollution Prevention and Control prepared the reference document (BREF) with the description of the best available techniques for several industrial sectors, including the production of pulp, paper and cardboard (European Commission, 2015). In addition, the International Finance Corporation has defined some guidelines to be considered in the construction

of new P&P mills (International Finance Corporation, 2007). These guidelines and directives were defined to enhance and optimize industrial processes. Regarding the wastewater generation in the Kraft pulp process, the following measures from both commissions (European Commission, 2015; International Finance Corporation, 2007) must be considered (list adapted from Cabrera, 2017):

- Dry debarking of wood;
- Extended modified cooking to a low kappa number (batch or continuous);
- Collection and recycling systems for temporary and accidental discharges of process water spills;
- Closed screening;
- Efficient washing of the pulp before bleaching;
- Oxygen delignification before the bleaching plant;
- Elemental chlorine-free (ECF) or total chlorine-free (TCF) bleaching;
- Removal of hexenuronic acids by mild hydrolysis at the beginning of bleaching, for hardwood pulp, especially eucalyptus;
- Partial closure of the bleach plant combined with increased evaporation;
- Sufficient and balanced volumes of pulp storage, refuse storage and white water storage tanks to avoid or reduce process water discharges;
- Recycling of wastewater, with or without simultaneous recovery of fibers;
- Separation of contaminated and non-contaminated (clean) wastewaters;
- Biological secondary wastewater treatment.

2.3.2.1 Fly ashes from biomass burning

Due to the high amount of FA produced worldwide, it is considered the fifth largest material resource in the world (Zacco et al., 2014). Fly ash (FA) is considered a waste and is generated during the combustion of biomass at high-temperature in power boilers. In the combustion process, the fused particles of volatile matter and impurities are carried upwards with the flue gases and, as they approach the low-temperature zones, they solidify to form fly ash. These fine ashes are captured from the flue gases in the bag filters and electrostatic precipitators. The remaining residue is recovered at the bottom of the boiler and is called bottom ash. Fly ash consists mainly of precipitated volatiles and fine particles, typically with a high specific surface area (Cherian and Siddiqua, 2019).

The composition and quality of FA vary depending on the origin, and this defines the application of FA in different new products. In the recovery boiler of a P&P mill, the FA generated consists mainly of sodium sulfate ($\approx 85\%$) and sodium carbonate ($\approx 15\%$), and most of them return to the chemical cycle (Bajpai, 2015; Monte et al., 2009) because it contains important inorganics for the chemical recovery process. The FA from biomass/bark combustion consists mainly of calcium oxide, calcium carbonate and potassium salts (Bajpai, 2015). If fly ash from coal-burning is considered, the typical components are SiO_2 , Al_2O_3 , CaO and Fe_2O_3 , which exist in the form of amorphous and crystalline oxides or minerals (Zhuang et al., 2016).

The chemical analysis of five different fly ashes from biomass burning in the P&P industries reported in the literature can be found in Table 5. Different types of ashes sources, that is, the biomass burned (wood and non-wood materials), led to distinct fly ashes characteristics. The composition is largely dependent on the source, that is, the forest species, the part of the plant burned

(that is, bark, wood, leaves), the plant age, the climate or type of soil and the process of biomass combustion, as combustion conditions and technology (for example, fixed bed or fluidized bed) (Martins et al., 2007; Zacco et al., 2014).

Table 5| Chemical composition of different fly ash from pulp and paper industries; materials compositions expressed as oxides; LOI: loss on ignition.

Oxides (wt. %)	Novais et al., 2018b	Buruberri et al., 2015 ^a	Martins et al., 2007	Vichaphund et al., 2014	Mäkelä et al., 2012
SiO ₂	34.0	43.3	3.21	41.4	18.8
TiO ₂	0.65	0.67	0.07	0.6	--
Al ₂ O ₃	13.5	9.54	0.92	20.0	6.1
Fe ₂ O ₃	4.95	3.79	0.65	8.4	6.26 ^b
MgO	3.07	3.26	0.13	2.3	2.1
CaO	16.5	23.6	0.27	14.1	38.7
MnO	0.45	--	n.d.	--	--
Na ₂ O	1.52	1.51	n.d.	0.4	0.69
K ₂ O	5.49	4.30	0.27	2.0	0.09
SO ₃	2.77	3.64	0.07	4.9	1.0
P ₂ O ₅	1.11	1.44	n.d.	0.4	1.35
Cl	1.50	1.23	n.d.	--	0.05
LOI	14.3	3.90	78.9	4.8	--
P&P mill location	Portugal	Portugal	Brazil	Thailand	Finland

n.d. – not detected

^a Values presented as % mass of each element (not oxide); Oxygen content: 15.6 %.

^b Total Fe concentration

The volatile content is presented by LOI, that is, the unburned material for fresh and dry ashes from power combustion (Ribbing, 2007). The high LOI on FA analyzed by Martins et al. (2007) is indicative of an unfinished combustion process. The remaining FA presented a low volatile content, below 14 %. The main constituents of FA as oxides are silicon, calcium and aluminum, which account for 75 – 80 %, with different biomass sources. However, the presence of trace elements, such as chloride, can prevent some possibilities of reuse and recycling of wastes, due to the possible environmental impact associated with the residue application (Mäkelä et al., 2012).

Depending on the ashes quality, they can be landfilled without valorization and at a cost associated with this practice (Monte et al., 2009). Several studies have been carried out to use fly ashes from the P&P industry in agriculture, as a soil additive, and in the construction sector, incorporated in new materials. The land applications of fly ashes, the most common application, should preferably be performed in acidic soils, since the application of ash increases the soil pH, due to the calcium carbonate presence (Augusto et al., 2008).

Buruberri et al. (2015) used FA as a constituent of eco-Portland clinker, produced at lower temperatures than the conventional process employed in the industry, and in this case, the presence of chlorides did not affect the durability of the product, since a thermal treatment was applied. Vichaphund et al. (2014) used FA as a raw material for the zeolite catalyst to be applied in rapid pyrolysis processes, obtaining an enhanced process.

Other applications for FA include covering of mine tailings (Jia et al., 2014), demulsifier in crude oil emulsions (Adewunmi and Kamal, 2020), road building, waste stabilization (Zacco et al., 2014), surfaces for drying slime and be integrated in construction material for landfills (Ribbing, 2007). In addition, FA can act as a source of silica, alumina and iron, and for magnetite, cenospheres and carbon recovery (Zacco et al., 2014).

2.3.2.2 Dregs, grits and lime mud

During the clarification of the green liquor, an insoluble residue provided from the smelt solubilization is discarded and is called 'dregs'. Dregs are mainly composed of sodium and calcium carbonates, sodium sulfide, a low organic fraction that was not totally burned in the recovery boiler, and other salts from the pulp production process (Modolo et al., 2010). Grits are a mixture of calcium carbonate and lime that did not react in the slaker (where causticization takes place). During causticization, the reaction between Na_2CO_3 (in the green liquor) and lime (from the lime kiln) produces NaOH and calcium carbonate, which are the main contributors of the lime mud (Modolo et al., 2010). The pH of this waste is strongly alkaline (between 10.0 and 12.8) (Manskinen et al., 2011) due to the presence of alkaline oxides.

Dregs and grits are frequently landfilled, but this solution is environmentally unsustainable, not least because many landfills are reaching their limit and there is a need to reduce the quantity of wastes deposited. Several studies have been developed in recent years, to develop new products and applications for dregs, grits and lime mud, with a focus on applications for the construction sector.

The presence of chlorine prevents the application of dregs in common recycling applications, such as their incorporation into cement or concrete (Novais et al., 2018b). Recent studies have evaluated the feasibility of use dregs as a cement replacement in concretes and mortars (Martínez-Lage et al., 2016) or as an aggregate in the construction of road pavements (Pasandín et al., 2016), but the properties of developed materials were not suitable for the desired applications. The incorporation of dregs as a fine filler in the production of geopolymers, an eco-friendly alternative to Portland cement, has also been studied with promising results regarding the amount of waste incorporated in the final product, with good performance characteristics (Novais et al., 2018b).

Grits are exclusively applied in new materials for the construction sector. These wastes were tested by Modolo et al. (2010) as asphalt pavements, with very promising results, since this waste presents compatible characteristics with the aggregate already used for road pavements. Grits have also been successfully applied to cement mortars, bituminous mixtures (Santos et al., 2019) and cement clinker (Torres et al., 2020).

Depending on the treatment process, the lime mud may contain chlorine, which limits a wide range of applications for this highly alkaline waste. As the formation of cement occurs at high temperatures, the incorporation of this type of waste in the belite-based cement, incorporating 16 wt.% of lime mud in it was successful, and the characteristics of the final products are suitable for indoor and outdoor plasters (Buruberry et al., 2015). Moreover, the application of lime mud to stimulate the growth of specific botanical species has been successfully tested, increasing the acidic pH of the soil in degraded regions (He et al., 2009).

2.3.2.3 Bleaching effluents

The high demands for water in the pulp and paper processing led to the high amount of effluents generated. It is estimated that 230 – 380 m³ of water are required to produce 1 ton of paper, releasing 180 – 300 m³ of wastewater. This wastewater consists of residual lignin and several organic compounds, mainly from the bleaching process (Mandeep et al., 2020), which led to high levels of chemical oxygen demand (COD) and biochemical oxygen demand (BOD). The bleaching effluents also contain inorganics and suspended solid matter such as fibers and pieces of fibers, nutrients, color and toxic compounds (Catalkaya and Kargi, 2007).

Over the years, the substitution of chlorine as a bleaching agent (elemental chlorine process) by chlorine dioxide (ECF process) in the pulp bleaching step has led to a reduction of chlorinated compounds in the wastewater generated, as well as a reduction in the amount of dioxins, polychlorinated compounds and chloroform (Cabrera, 2017). The sum of the chlorinated compounds is measured as an adsorbable organic halogen (AOX) in an aquatic environment.

The characteristics of the wastewater generated depend on the type of wood, the degree of delignification of unbleached pulp, the bleaching sequence applied, the final brightness desired and the chemical and water consumption (Olli, 2008). Different types of wood (softwood vs hardwood) result in different levels of contaminants. Softwoods, such as pine, originate wastewater after the bleaching process with a higher amount of organic matter (measured as COD) and color than hardwoods, such as eucalyptus, due to the higher lignin content. Eucalyptus pulps generate more biodegradable effluents (Mealier et al., 2003) than softwood pulps, but the AOX levels in both softwoods and hardwoods are equivalent.

2.3.2.3.1 Adsorbable organic halides (AOX)

Comparing all streams generated in a P&P mill, bleaching effluents are the most toxic due to the presence of numerous chlorinated organic compounds generated in the bleaching process (Savant et al., 2006). Chlorination is, in many industries, the first stage of the bleaching step, and it is where the organochlorine compounds are formed (Bajpai, 2012). The reaction between the chlorine compounds of the bleaching agents, such as chlorine, chlorine dioxide and hypochlorite, and the organic matter present in the unbleached pulp, in the form of lignin and its derivatives, generates highly toxic and recalcitrant compounds (Singh et al., 2011). These chlorinated organic compounds are collectively measured as AOX – adsorbable organic halides. The “X” is related to halogens bonded to organic matter, including chlorine, bromine and iodine (Müller, 2003). For P&P wastewaters, AOX is a measure of chlorinated compounds content, since bromine and iodine compounds are absent.

More than 300 different organic compounds have been identified in P&P effluents and, among others, AOX include chlorinated hydrocarbons, chlorobenzenes, chlorophenols, chlorocatecols, chloroguaiacol, chloroform, dioxins and dibenzofurans (Gupta et al., 2010; Kumar et al., 2013) (Figure 14). AOX compounds can be classified as acidic, phenolic and neutral compounds. They are partly responsible for the oxygen demand (BOD and COD), color, toxicity, mutagenicity and carcinogenicity of the effluents from the bleaching process (Bajpai and Bajpai, 1997).

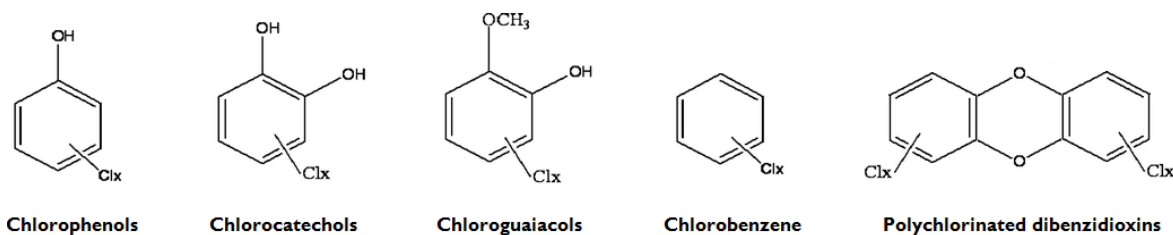


Figure 14| Most common chlorinated organic compounds identified in P&P effluents.

Organochlorine compounds tend to persist in nature due to their inherent recalcitrance (Bajpai, 2012). These complex compounds can be divided according to their molecular weight, into low molecular weight (LMW) and high molecular weight (HMW) compounds. The LMW compounds (< 1000 Da) are the main contributors to the mutagenicity and bioaccumulation of AOX in organisms since they are able to penetrate the cell membrane due to its hydrophobicity. These LMW compounds are genotoxic and are known to bioaccumulate in the aquatic food chain, mainly in the body fat of animals of higher trophic levels. HMW compounds (> 1000 Da) are, in most cases, biologically inactive and, thus, have a small contribution to toxicity and mutagenicity (Savant et al., 2006).

2.3.2.3.2 Treatment alternatives for bleaching effluents

To treat complex effluents from the bleaching process in a P&P mill, several chemical-physical, electrochemical and biological treatments have been developed over the years. Table 6 summarizes the most common technologies applied to treat AOX-rich bleaching effluents, published in the last 20 years, divided by biological, electrochemical, physical-chemical and combined treatments.

Many of the biological treatments and technologies to treat AOX-rich bleaching effluents were developed during the 1990s and were previously reviewed by Savant et al. (2006). In these biological treatments, the efficiency is mainly focused on the organic matter reduction and some persistent compounds (such as AOX) and the color of the lignin are kept during the treatment cycle (Taseli, 2008). Both aerobic and anaerobic processes are appropriate to treat effluents from the P&P industries, namely those from the bleaching stage, with a high content of AOX compounds and, generally, with very low biodegradability (Ashrafi et al., 2015).

Aerobic treatment as an activated sludge treatment is commonly used for P&P effluents, with the advantage of easy operation and relatively low capital and operation costs (Ashrafi et al., 2015). However, the high amounts of sludge produced and the uncertain removal efficiencies for recalcitrant compounds are disadvantageous (Tsang et al., 2007). A conventional approach is to implement post-treatment processes such as adsorption on granular activated carbon, to completely remove AOX from effluents. In addition, new reactor designs can be implemented, testing granular aerobic sludge to enhance the AOX removal, since microorganisms are able to tolerate high concentrations of toxics (Farooqi and Basheer, 2017).

Table 6| Summary of biological, electrochemical and chemical-physical technologies for the treatment of AOX-rich bleaching effluents from P&P mills in the last 20 years.

Type	Treatment system	Initial AOX concentration	Operational conditions	AOX reduction	Organic matter reduction	Reference
Biological	Aerobic granular sludge in SBR	15 – 20 mg _{Cl} /L	Incubation: 780 d OLR = 4.5 kg/m ³ /d HRT = 6 h	79 % < 5 mg _{Cl} /L	COD: 88 %	Farooqi and Basheer (2017)
	Up-flow anaerobic filter	1 st : 28 mg _{Cl} /L 2 nd : 42 mg _{Cl} /L	Incubation: 70 d HRT = 20 d	1 st : 88 % 2 nd : 28 %	COD: 20 % BOD: 70 %	Deshmukh et al. (2009)
	Anaerobic batch bioreactor	32.2 mg _{Cl} /L	Incubation: 70 d pH of effluent = 7	73 %	31 %	Ali and Sreekrishnan (2000)
	Horizontal packed-bed anaerobic reactor	16 – 22 mg _{Cl} /L	Incubation: 418 d HRT = 25 h	40 – 45 %	52 – 55 %	Chaparro and Pires (2011)
	Sequential anaerobic and aerobic reactors	--	Incubation: 7 d (anaerobic) + 7 d (aerobic with fungi or bacteria)	Anaerobic: 15 % Aerobic (fungi): 67 % Aerobic (bacteria): 82 % Combined: 82 %	Anaerobic: 42 % Aerobic (fungi): 88 % Aerobic (bacteria): 75 %	Singh and Thakur (2006)
	Biological removal with pure culture: <i>Pseudomonas aeruginosa</i>	8 mg _{Cl} /L	Incubation (after isolation): 24 h T = 37 °C; 150 rpm	78 %	--	Kumar et al. (2013)
Combined	Batch reactor with pure culture: <i>Penicillium camemberti</i>		Incubation: 10 d Acetate supplementation: 2.0 g/L	67 %	44 %	Taseli (2008)
	Coagulation + Anaerobic acidification + Aeration	57 mg _{Cl} /L	Incubation: 50 d HRT = 15 h pH = 7.2	98 % 0.92 mg _{Cl} /L	COD: 88 % BOD: 81 %	Chen et al. (2003)
	Horizontal-flow anaerobic immobilized biomass reactor + H ₂ O ₂ /UV	23.8 mg _{Cl} /L	Incubation: 112 d HRT = 19 h pH = 7-7.5	55 % 10.1 mg _{Cl} /L	COD: 61 % BOD: 90 %	(Ruas et al., 2012)
Chemical-physical	Fenton and Photo-Fenton reactor	124 mg _{Cl} /L	T = 60 °C; pH = 2 [H ₂ O ₂] = 177 mM; t = 10 min;	Fenton: 85 % Photo-Fenton: 95 %	--	Ribeiro et al. (2020)
	Fenton and Photo-Fenton reactor	1.94 mg _{Cl} /L	Fenton: pH = 5; [H ₂ O ₂] = 50 mM; t = 30 min Photo-Fenton: t = 5 min + UV	Fenton: 89 % Photo-Fenton: 93 %	--	Catalkaya and Kargi (2007)
	Catalytic wet oxidation	12 mg _{Cl} /L	CeO ₂ -based catalyst T = 186.85 °C; t = 1 h	90 %	80 %	Goi et al. (2006)
	Zerovalent iron nanoparticles (nZVI)	90 – 10 mg _{Cl} /L	nZVI 2 g/L; t = 60 min T = 60 °C pH = 2.0 – 4.0	> 70 %	--	Gameiro et al., 2019b
Electro-chemical	Electrochemical treatment	10 mg _{Cl} /L (synthetic)	t = 10 min; C.D. = 6 mA/cm ²	> 99 %	> 90 %	Patel and Suresh (2008)

The anaerobic treatment of bleaching effluents has also been widely studied, although its use in industrial P&P treatment plants is not as common as the use of aerobic processes (Ashrafi et al., 2015). These treatments have the advantages of less sludge produced and energy generation (biogas). Several bioreactor configurations are being studied, such as up-flow anaerobic sludge

blanket (UASB) reactor, anaerobic filter, expanded granular sludge bed (EGSB) reactor, continuous stirred tank reactor (CSTR), anaerobic contact process (Kumar et al., 2020) and anaerobic membrane reactors (Kamali et al., 2016). The UASB reactor is currently the dominant anaerobic technology implemented in full-scale facilities since these biological reactors have high levels of stability during operation and moderate efficiencies for organic matter removal, which is satisfactory in terms of wastewater treatment.

However, as with aerobic systems, most of anaerobic technologies do not have very high AOX or pollutants removal efficiency. The increase in hydraulic retention times (HRT) in anaerobic digesters, that is, the increase in the time that the effluent remains inside the bioreactor, helps to improve the process efficiency related to the pollutants removal since the pollutants and biomass remain in contact for longer periods. In both anaerobic and aerobic processes, the COD removal is satisfactory and in anaerobic systems, the removal of AOX and lignin is more successful than in aerobic systems (Ashrafi et al., 2015).

A wide variety of physico-chemical treatments can be applied to P&P effluents, such as sedimentation, flotation, screening, adsorption, coagulation, oxidation, ozonation, electrolysis, reverse osmosis, ultrafiltration and nanofiltration technologies (Pokhrel and Viraraghavan, 2004). These technologies are designed to remove suspended solids, colloidal particles, toxic compounds, floating matter and colors from wastewaters (Ashrafi et al., 2015). Physico-chemical treatments are expensive (Bajpai, 2012) and most of the time generate a high amount of sludge, which needs to be treated (Sridhar et al., 2011). These techniques are advantageous as they allow a high pollution reduction. As an example, Sridhar et al. (2011) used the electrocoagulation process to test the reduction of color and organic matter in the bleaching effluents, achieving a reduction of 87 % in the organic matter removal and 94 % in the color removal.

The insufficient treatment efficiency observed in some single technologies, such as the implementation of biological treatment alone) has led to the need for some authors to combine them to achieve considerable benefits. The economic and environmental aspects, as well as the potential synergistic effects of the studied combinations (called hybrid systems), led, in most cases, to higher pollution reductions and increases the performance of the treatment process (Kamali et al., 2019). Integrated systems can be a combination of two different chemical-physical treatments, one chemical-physical and one biological, or two biological processes, achieving a combined efficiency higher than individual efficiency.

2.3.2.3.3 Anaerobic digestion of bleaching effluents

Generally, effluents with a high content of chlorinated compounds are not suitable for anaerobic treatment without previous effluent dilution. Dilution may involve the co-digestion of bleaching effluents with less toxic streams or mix with the effluent from other biological treatments (Meyer and Edwards, 2014). In addition, the use of adapted microorganisms to the wastewater stream under treatment can dramatically improve anaerobic biodegradability.

The biodegradability of AOX-rich bleaching effluents is affected by several physical, chemical and nutritional factors. The anaerobic degradation of organochlorides occurs via dehalogenation with the release of an inorganic chlorine atom. The rate of the reductive dehalogenation process decreased with the increase of the chlorine amount removed (Katyal and Morrison, 2007). The degradation of

chlorinated compounds by anaerobic microorganisms occurs only if the compounds are biologically available, and microorganisms such as acetogens and methanogens reductively dechlorinate the chlorinated compounds in a co-metabolic reaction (Deshmukh et al., 2009; Holliger et al., 1998). The electrons needed for reductive dehalogenation came from the oxidation of an electron donor such as H₂, formed during the fermentation of organic compounds such as glucose or acetate (El-Hadj et al., 2007). Thus, supplementation of electron donors provides the most favorable conditions for the microbial dechlorination reaction to occur (Deshmukh et al., 2009).

The initial reaction time, called the “lag phase”, is very important for the adaptation of microorganisms to the pollutant compounds, for the growth of the active microbial population (Bajpai and Bajpai, 1997) or for the consumption of a preferential carbon source. Adequate exposure time allows methanogenic microorganisms to not only resist in biorecalcitrant and bioinhibitory environments but also to thrive in them (El-Hadj et al., 2007).

Nutritional factors such as the presence or absence of electron donors, sources of carbon, nitrogen, phosphate and micronutrients can also affect the biodegradability of chlorinated compounds (Savant et al., 2006). In addition, operational parameters such as type of reactor used, AOX concentration, hydraulic retention time, presence of co-substrate (such as glucose, methanol, ethanol or acetate), pH and temperature affect the efficiency of biodegradation.

2.4 Dairy industry

Milk from animals has been used for human consumption since all recorded history. The transformation of milk into food products like cheese and butter for family use has been known since 1000 B.C. Cheese whey generated by small farmers was usually applied as pharmaceutical and cosmetic medicine, but rarely used as food for humans. With the industrial revolution of the nineteenth century, the dairy industry began to expand and the volume of milk processed increased dramatically. In addition, whey generation has also increased and several environmental issues have been addressed, regarding the management of this highly polluted waste stream (Bachmann et al., 2008).

Nowadays, milk and other dairy products are an integral part of our daily lives and diets (Ganju and Gogate, 2017). Milk is the starting point in the dairy industries, where a wide variety of products such as yogurt, ice cream, butter, cheese and other milk products are manufactured through several different processes (Carvalho et al., 2013). Milk is largely produced worldwide and is one of the most valuable agricultural commodities, ranking third by a ton of production, contributing 27 % of the global added value of the feedstock (Food and Agriculture Organization, 2016). In the European Union, the dairy industry represents 4 % across the food industry and contributes 10 % to the creation of added value from feedstock (Naglova et al., 2017). In addition, the dairy industry is also a major contributor to the generation of industrial effluents in Europe (Carvalho et al., 2013).

In 2019, milk production worldwide increased by 1.4 %, compared to 2018, reaching 852 million tons. The main producers are the European Union, India, Pakistan, Brazil, the Russian Federation and the USA. Countries like Australia, Argentina, Turkey, Ukraine and Colombia are also major milk producers, but their production decreased last year. In Europe, milk production was estimated at 226 million tons. It represents the lowest annual growth rate since 2016 and is due to the reduction of dairy cattle members, driven by the poor quality of pastures, as a result of the heat and dry weather registered in the summer months in many European countries (Food and Agriculture Organization, 2020).

Dairy products exports increased in 2019 to 76.7 million tons, equivalent to an increase of 1 % compared to exports in 2018. Cheese, one of the dairy products, increased its share in exports by 5 % compared to 2018, reaching 2.6 million tons (Food and Agriculture Organization, 2020). The dairy products market is expected to grow more than 5 % from 2019 to 2025, and this increase is related to the population growth and urbanization, and, consequently, to the increasing demand for food (Food and Agriculture Organization, 2016).

Due to the large dimension of the dairy industry sector, the expected development can provide indirect assets in people's livelihoods, for the environment and public health. In fact, feeding dairy cows, sheep or goats requires 1 billion ha, corresponding to 7 % of the total land on earth, and consumes about 2.5 billion tons of dry feed annually (Food and Agriculture Organization, 2016). For these dimensions, labor is required to respond to market needs, thus increasing the employability of dairy-related regions. In addition, milk-processing technologies (such as cheese or yogurt manufacturing) also require a high number of employees, which highlights the importance of the dairy sector at the economic level (Fernández-Gutiérrez et al., 2017).

In Portugal, the average per capita consumption of dairy products, including milk, cheese and yogurts, was about 43 % higher than the average consumption in European Union, reaching 128.7 kg

per year in the last year (Eurostat, 2019). Although an increase in the dairy sector is expected, consumption patterns are changing worldwide and non-dairy milk substitutes, such as soybean and nut-based drinks, are gaining market share (Bórawski et al., 2020). The dairy industries are evolving and innovating, and the demand for new consumers is a challenge for industries to expand the range of products currently available.

Although the dairy industry has several cutting-edge technologies (Naglova et al., 2017), it also has some negative impact on the environment. Dairy activities led to the release of GHG, mainly methane and carbon dioxide, and other gases such as NO₂ and NO. In addition, the production of whey has the potential to discharge millions of cubic meters of polluted wastewater, which can lead to eutrophication of rivers and lakes, if discharged without treatment. Also, the production of tons of solids, from manure, can increase the pH and the concentration of NH₄⁺ and NO₃⁻ in soils, unbalancing their characteristics (Fernández-Gutiérrez et al., 2017). In dairy industries, washing processes can lead to pH peaks in the effluents generated, due to the nature of the chemical compounds used (Kasmi, 2018). Indirectly, the dairy industries also contribute to biodiversity loss and wildlife health, changing nutrients cycles (nitrogen and phosphorus) and land use (Clay et al., 2020).

Furthermore, the production and processing of milk require high amounts of energy and water, causing important environmental impacts (Clay et al., 2020). The effluents from the dairy industry are generated mainly during the processing and transformation of milk. The most pollutant milk transforming technology is cheese manufacturing, in which the production of 1 kg of cheese generates about 9 L of whey. Due to the high amounts generated, cheese whey is considered the main effluent of the dairy industry (Fernández-Gutiérrez et al., 2017).

2.4.1 Dairy products

Inserted daily in the Mediterranean diet, milk is a source of energy due to carbohydrates in the form of lactose, nitrogen (from proteins) and calcium (Ganju and Gogate, 2017). In addition to milk, other products are also processed by the dairy industries, using milk as raw material, mainly cheese, butter, fermented products (such as yogurt) and cream.

From a global perspective, milk is the major product of the dairy industry, accounting for 75 % of global consumption. Cheese (12 %) and butter (3 %) are also widely consumed. Other processed products from the dairy industry are also widely consumed, including fermented products such as yogurt or kefir, cream, dairy desserts, whey and casein (Food and Agriculture Organization, 2016). In the European Union, 156.8 million tons of whole milk were processed in 2018, resulting in 10.3 million tons of cheese and 2.4 million tons of butter and other fatty products, representing 67 % of the total whole milk available for processing. The remaining whole milk was processed for the production of cream (12 %), drinking milk (11 %), acidified milk (4 %), powdered products (3 %) and other products (3 %) (Eurostat, 2019).

To ensure food safety and stability, milk is treated before processing. The most common treatments include pasteurization and ultra-high temperature (UHT) processes, both of which must guarantee the reduction of deteriorating microorganisms and the destruction of all pathogenic bacteria. Pasteurization can be applied to all dairy products, while the UHT process is applicable to low-viscosity liquid products. The application of these types of heat treatment will stop the bacterial

and enzymatic activity and prevent the loss of quality, reducing the perishability of the food (Santonja et al., 2019). In pasteurization, the milk is heated to 72 – 75 °C for 15 to 20 seconds, while in the UHT process the milk is subjected to continuous heat flow at high temperature (> 135 °C) for a short period. Pasteurized milk has a shelf-life of about 8 to 10 days and must be preserved at 5 to 7 °C (Karlsson et al., 2019). UHT milk preserved in Tetra Pak® packaging has a shelf-life of up to six months, without the need for refrigeration or preservatives (Tetra Pak, 2015).

2.4.1.1 Milk

Milk is an animal product containing lactose, proteins, fats and water, being the dairy product most consumed and processed. It is collected from animals such as sheep, goats and buffalos, but cow's milk is the most important dairy product, accounting for around 81 % of the global milk production (Fernández-Gutiérrez et al., 2017). Milk can be divided into three categories, according to the fat content, namely whole milk, semi-skimmed milk and skimmed milk. It can be consumed raw or after processing, using technologies such as pasteurization, sterilization or ultra-high temperature to achieve a sterile and safe product (Carvalho et al., 2013).

Condensed milk is obtained when part of the water is removed from whole or skimmed milk, by heat-treatment and concentration. This product is sweetened mainly when sugar is added, but it can also be unsweetened (also called evaporated milk). In most countries, condensed milk is used for baking and cooking, as a substitute for jam. It can also be incorporated into other dairy products (Park and Drake, 2016).

Dry or powder milk is obtained by dehydration milk, in order to prevent or inhibit the growth and activity of microorganisms and to reduce the weight and volume of food, for cheaper transport and storage. Powdered milk has a wide range of applications, including incorporation into other dairy products, use in the bakery and chocolate industry, the production of baby food and use as animal feed.

2.4.1.2 Cheese

Cheese is one of the most consumed dairy products worldwide, with hundreds of varieties produced, and many of them are characteristic of a specific part of the globe (Fernández-Gutiérrez et al., 2017), with the majority of cheese varieties being produced in developed countries. In the European Union, Germany, France and Italy are the main cheese producers, achieving 53 % of all cheese manufactured in the EU. In Portugal, cheese production in 2018 reached 80 140 tons, corresponding to about 2 % of European production (Eurostat, 2019).

Cheese is produced from the coagulation of milk protein (casein), which is then separated from the whey (liquid fraction). There are several types of cheese, but they are normally grouped by their texture, such as soft fresh, soft cured, surface mold cured, semi-soft, hard and extra hard. Cheese processing technologies vary according to the type of cheese to be manufactured, as well as the type of milk and microorganisms used (Jalilzadeh et al., 2015).

2.4.1.3 Fat and fermented milk products

Butter is a fatty dairy product, obtained by whipping milk or cream. This dairy product can be divided into two main categories, namely sweet cream butter and cultured (or sour cream) butter, made from bacteriologically sour cream (Tetra Pak, 2015). Ghee is also a fatty dairy product, with more protein than butter, and is obtained by removing the water from the butter. This product is popular in countries from South Asia and has a very long shelf-life of up to two years (Alganesh and Yetenayet, 2017).

Fermented kinds of milk are commonly used to obtain other dairy products, such as yogurt (Aryana and Olson, 2017), kurut (Wang et al., 2020) and kefir (Rosa et al., 2017), among others. These products are obtained after fermentation of milk, using microorganisms to achieve the desired level of acidity in the product. Yogurt is obtained by lactic acid fermentation and kefir contains a mixture of lactic acid and yeast fermentation (Tetra Pak, 2015).

2.4.1.4 Other milk products

The cream is the part of the milk that is rich in milk fat and can be extracted from the milk by centrifugation or skimming (Alvarez, 2008). Cream-based products are sterilized and homogenized when processed. Despite their liquid texture, they are not normally consumed as drinks but are incorporated into several food products.

Other dairy products include proteins, namely whey and casein. Casein is the major phosphoprotein in milk, comprising about 20 % of the total protein content. The remaining 20 % includes whey and serum proteins (Han et al., 2019). This protein is extracted by enzymatic precipitation (rennet casein) or acidification of milk (acid casein), and is widely used in the food industry, including cheese and bakery products, and in the chemical industry, to be incorporated into paints and glues (Tetra Pak, 2015).

Whey is the liquid fraction that remains after casein precipitation in the cheese manufacturing process (Zotta et al., 2020). It is also generated during casein and yogurt manufacturing, being one of the biggest reservoirs of food protein available (Tetra Pak, 2015). Due to its unique composition, with about 55 % of the total milk nutrients (soluble proteins, lactose, vitamins and minerals), whey has gained importance in the market, mainly in sports, clinical and infant nutrition. In addition to the nutritional additive, this byproduct of the dairy industry is also used in animal feed, in the food and bakery industry, incorporated in other dairy products such as ice cream or cheese and in yeast products, and used in the pharmaceutical industry.

2.4.2 Cheese whey generation and characteristics

2.4.2.1 Cheese whey production from raw milk

Cheese is a food product present in many countries and cultures, since antiquity, being one of the oldest known types of manufactured foods (Yoon et al., 2016). Around the world, many varieties of cheese are produced, with different properties and characteristics. The manufacturing process of cheese from raw milk involves several procedures common to most types of cheese, as shown in Figure 15. The figure also highlights the whey formation in the process, as well as some technologies

used for whey transformation in a wide variety of products or their valorization in new materials or energy (based on information provided by Fernández-Gutiérrez et al. (2017); Ganju and Gogate (2017); Zotta et al. (2020)).

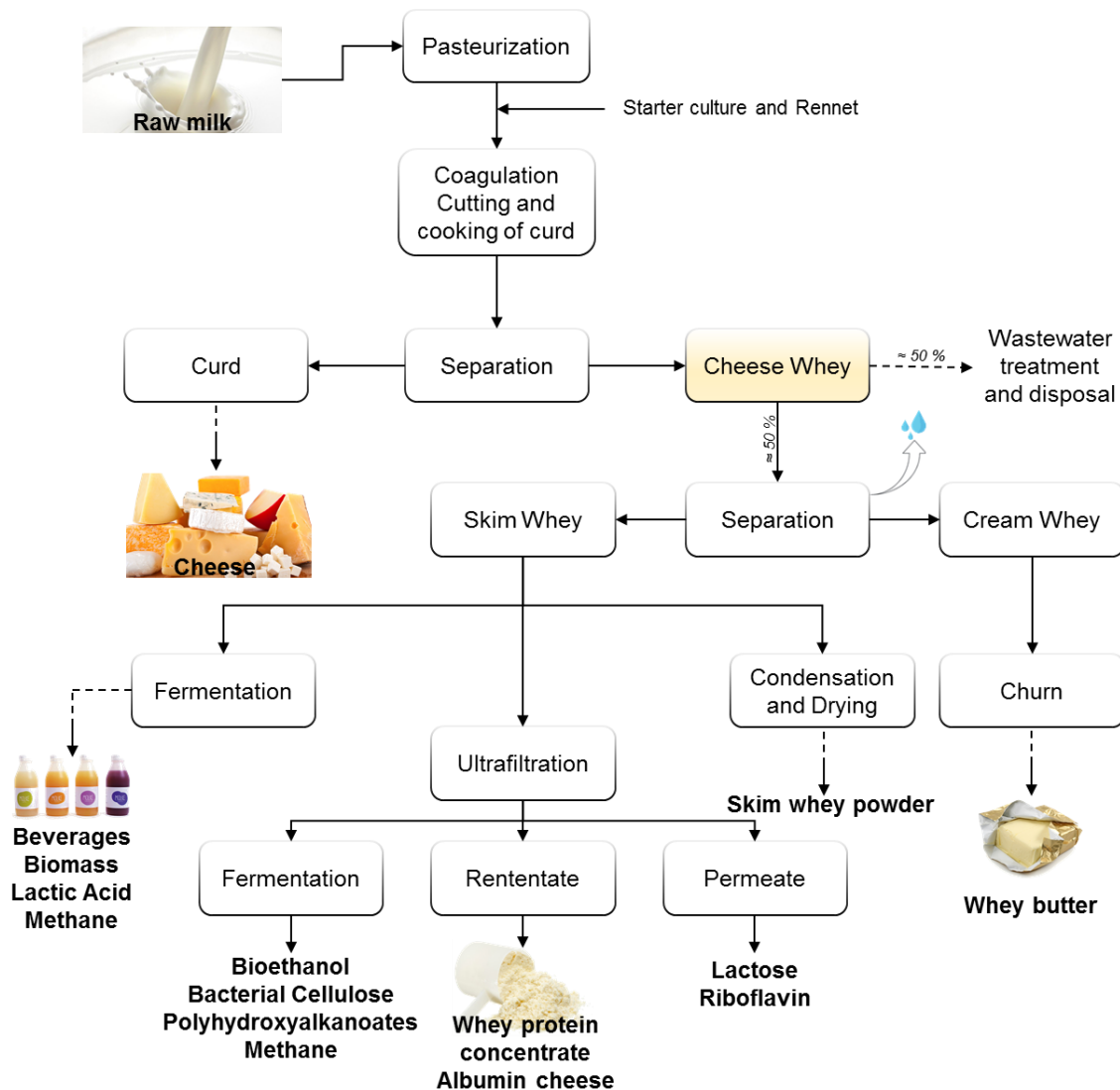


Figure 15| Cheese manufacturing from raw milk with whey generation, with the integration of different technologies for whey valorization.

Cheese manufacturing is a linear process, which involves many technological steps. Usually, raw milk is sterilized by pasteurization or UHT processes, prior to the production of coagulum. In alternative, raw milk can be used without pretreatment in the manufacturing of cheese, obtaining types of cheese with a more intense flavor, due to the presence of higher amounts of volatile compounds from the fermentation of milk components by natural microbial communities (Yoon et al., 2016). For the coagulation step, an initial culture of rennet and microorganism is added. The curd (solid part) formed is separated from the whey (liquid part) and is cut and processed to obtain the desired characteristics of the different types of cheese (Dragone et al., 2009). The structure and firmness of the curd and cheese yield are closely related to the casein content in milk. The cheese curd is mainly composed of insoluble caseins produced during the enzymatic conversion of κ -casein

into para- κ -casein (Han et al., 2019). During the production of cheese, the casein and fat present in the milk are concentrated. For hard and some semi-hard types of cheese, for example, the concentration is approximately 10 times (Tetra Pak, 2015).

In the past, cheese whey was considered a waste and was used only in animal feed, in dry form. With the development of technologies and increased interest in proteins and functional constituents of whey, it is now considered a byproduct of the dairy industry. The potential use of whey has reduced the channeling of the fraction of this liquid stream for the wastewater treatment. In addition, and due to strict environmental regulations, the discharge of whey into waterways or fields without proper treatment was prohibited (Smithers, 2015). However, in some developing countries, whey is still improperly managed and disposed of, representing an environmental threat for soils, waters and the atmosphere.

Currently, more than 200 million tons of whey are generated each year worldwide, including whey from yogurt and other milk products manufacturing (Smithers, 2015). According to Rama et al. (2019), about half of the whey generated worldwide is still discharged and treated as waste without valorization, mainly in developing countries. About 50 % of the whey is used as a raw material to produce ricotta and other whey-based products (25 %), cheese whey powder (15 %), lactose (8 %) and whey protein powder (3 %) (Rama et al., 2019). The high nutritional value of whey must not be overlooked and the processing of whey into new and valuable products contributes both to the reduction of environmental pollution commonly associated with dairy industries and to providing economic inputs from the sale of new products from whey (Ganju and Gogate, 2017).

One of the most popular cheese whey applications is its use to produce ricotta cheese. In this type of cheese manufacturing, a second cheese whey, also known as scotta or ricotta whey is generated, with about 60 % of the components of the cheese whey, mainly lactose (Carvalho et al., 2013), and high salinity, due to the addition of salts during the cheese production process (Rama et al., 2019). Both cheese whey and second cheese whey streams have very high organic loads and can represent an environmental source of pollution, if not properly managed or disposed of (Sansone et al., 2009).

During the transformation of the cheese whey, after removing about 80 % of the water from the skimmed whey, the concentrated whey is ultra-filtrated to obtain the whey permeate (the process where the lactose is concentrated) and the whey retained (the protein fraction, with lactose residues, to produce whey protein concentrate) (Ganju and Gogate, 2017). After ultrafiltration, skimmed cheese whey permeate can also be used in fermentation processes, to obtain high-value products such as bioethanol (Das et al., 2016), bacterial cellulose (Carreira et al., 2011), polyhydroxyalkanoates (Pais et al., 2010) or energy, in the form of methane (Novais et al., 2018c), or hydrogen (Venetsaneas et al., 2009). These valorization products are obtained mainly due to the presence of high lactose content, as well as other essential nutrients, which enhance microbial growth (Mollea et al., 2013). Other solid parts of the whey solution are still used as a fertilizer or animal feed supplement (El-Tanboly, 2017). Liquid cheese whey can be used directly in fermentation processes, as a culture medium for the growth of lactic bacteria, substituting commercial culture media (Rama et al., 2019).

Since the nutritional properties of cheese whey were widely explored in the 1990s, several alcoholic and non-alcoholic beverages have been developed since then, applying cheese whey

fermentation. Nowadays, market share and interest in whey-based beverages are increasing each year (Akai et al., 2019). The use of whey-based products has been gaining market share as these products improve texture, enhance the flavor and color of other products, emulsify and stabilize, helping to extend the shelf life, and, in addition, have a range of properties that increase the food quality of the product.

Several researchers have explored the use of cheese whey in recent years, as a precursor in the generation of several added-value products. This byproduct of the dairy industry can be used as a source of bioactive peptides normally used as ingredients in functional foods (Dullius et al., 2018) or protein hydrolysates (Mao and Kulozik, 2018). It can also act as a substrate for the synthesis of the enzymes (You et al., 2017) or lactic acid (Soriano-Perez et al., 2012), and be a precursor in the enzymatic synthesis of galato-oligosaccharides (Lisboa et al., 2012).

2.4.2.2 Cheese whey characteristics

Whey is the liquid part of milk obtained during the milk coagulation in the cheese or casein production (Fernández-Gutiérrez et al., 2017). Cheese whey represents 85 – 95 % of the milk volume processed in the dairy industry and retains about 55 % of the milk content (Rama et al., 2019), namely lactose, proteins and mineral salts. Depending on the casein precipitation method, the whey produced can be acidic (pH < 5.0) or sweet (pH ≈ 6.3) (González-Siso, 1996). Sweet whey is formed from the manufacture of pressed cheeses (cooked or uncooked), and acid whey is obtained from the manufacture of casein, fresh cheeses (Giroux et al., 2018) or Greek yogurt (Smithers, 2015). The acid whey is typically higher in salt content and lower in protein content than sweet whey, and its use in human and animal feeding is limited due to its sour flavor.

The composition of both sweet and acid cheese whey described by some authors can be found in Table 7 (Dragone et al., 2011; Dullius et al., 2018; Rama et al., 2019). The final composition and characteristics of the whey are closely related to the milk source (cow, sheep, other) and the feed of the milk-producing animal, the processing method and other environmental factors such as the time of year or the lactation stage of the animal (Ganju and Gogate, 2017).

Table 7 | Physico-chemical characterization of cheese whey streams: sweet whey and acid whey (consolidated from data presented in Dragone et al., 2011; Dullius et al., 2018; Rama et al., 2019).

Physico-chemical parameter	Sweet whey	Acid whey
Water	≈ 93 %	≈ 94 %
Lactose	4.5 – 5 %	3.8 – 4.3 %
Total proteins	0.8 – 1.0 %	0.8 – 1.0 %
Whey protein	≈ 0.65 %	≈ 0.65 %
Lipids	0.4 – 0.5 %	0.4 – 0.5 %
Mineral salts (NaCl, KCl and calcium salts)	0.5 – 0.7 %	0.5 – 0.7 %
Lactic acid	Trace	0.1 – 0.8 %
Citric acid	0.1 %	0.1 %
BOD	> 30 gO ₂ /L	> 35 gO ₂ /L
COD	> 60 gO ₂ /L	≈ 80 gO ₂ /L
pH	6.2 – 6.4	4.6 – 5.0

Besides the components presented in the table, whey also contains non-protein nitrogenous compounds, such as urea and uric acid, group B vitamins and other nutrients (González-Siso, 1996). Typically, cheese whey contains 99 % biodegradable organic matter, with very high BOD and COD values (Dullius et al., 2018). Compared to the pollution load of typical urban wastewater in developed countries, which presents COD and BOD values of approximately 0.6 gO₂/L and 0.3 gO₂/L respectively (Gallego-Schmid and Tarpani, 2019), the cheese whey has a pollution load about 150 times higher (Rama et al., 2019).

Due to its characteristics, acid whey is difficult to be used as a raw material in some biotechnological applications. With the growing interest in Greek-style yogurt products, the generation of acid whey is also growing (Smithers, 2015). The low pH of this stream limits its use and is normally mixed with silage for animal feed or used to produce energy through the AD process.

In addition, several other effluents are generated in dairy industries. The processing system and applied methods have a great influence on the characteristics of the effluents (Demirel et al., 2005), due to the wide variety of products generated in the dairy industries. These factors led to the complexity of dairy effluents and to the difficulties often observed in the application of efficient treatment processes. The use of physical-chemical treatment processes is a viable option in terms of efficiency, but the costs associated with chemical compounds make these processes too expensive to be applied on an industrial scale (Chatzipaschali and Stamatis, 2012). Thus, to overcome the high operational costs and low COD removal efficiencies observed in physical-chemical treatments, biological treatments are preferred for complex effluents from the dairy industry.

2.4.3 Anaerobic treatment technologies for dairy effluents

The treatment of dairy effluents dates back to the early 20th century when Bowles (1911) suggested a septic tank to treat pollution related to dairy waste. In 1932, Buswell et al. (1932) presented the results of their work, in which they tested the stabilization of milk waste under anaerobic conditions, achieving 95 % of pollution reduction. In addition, they stated that the anaerobic treatment of cheese whey coupled with the aerobic polishing step was more cost-effective than the aerobic process alone, with the advantage of less amount of sludge generated combined with the production of fuel biogas. This work is considered a milestone in the methanization of dairy industry wastes and also provides a scientific basis for future developments in the AD of these wastes (Bachmann et al., 2008).

Since the 1930s, several publications on the anaerobic treatment of cheese whey have been published. However, the application of biological treatment (mainly anaerobic) to cheese whey effluents can often be challenging. The low pH value (typically between 3.8 and 6.5 (Dullius et al., 2018)) and alkalinity, and high contents of sodium, free ammonia, potassium and volatile fatty acids (Prazeres et al., 2012), besides to a high amount of biodegradable organic matter in these effluents (see Table 7) can lead to failure of the biological process, if not properly controlled.

The application of AD to treat cheese whey and dairy wastewaters, as well as the use of cheese whey for the formation of other added-value products, has been extensively reviewed by several authors (Carvalho et al., 2013; Chatzipaschali and Stamatis, 2012; Demirel et al., 2005; Demirel and Yenigün, 2002; Kasmi, 2018; Liew et al., 2020; Prazeres et al., 2012; Rajeshwari et al., 2000). Several reactor configurations and operation modes can be applied, obtaining high efficiency for

COD removal with the benefit of methane formation, as an energetic vector. This technology can be a triple action process for complex wastewaters: pollution reduction, energy generation and nutrient recovery (Escalante et al., 2018). Table 8 lists the most relevant studies published in the last 20 years using cheese whey under anaerobic conditions (single digestion), to both treat and valorize this dairy stream.

The AD process applied to the treatment of cheese whey and other dairy effluents is an excellent solution related to energy saving and pollution control (Ergüder et al., 2001). The low implementation cost, the high-energy efficiency and the simplicity of the process compared to other wastewater treatment methods make anaerobic digestion advantageous to treat cheese whey (Saddoud et al., 2007). Several operational parameters influence the digestion process of cheese whey, namely pH and alkalinity, nutrients, temperature and reactor configuration, and, also, parameters related to the wastewater characteristics, such as the seasonality of milk production (Bachmann et al., 2008).

UASB reactors are particularly suitable to be applied in the treatment of high-organic strength wastewaters, such as cheese whey, due to their favorable features, such as low energy demand and operation under high organic loading rates (Diamantis et al., 2014). In addition, AD technology can achieve adequate organic matter (BOD and COD) removals from cheese whey, with the advantage of high methane production, close to the theoretical value (Chatzipaschali and Stamatis, 2012). However, the slow reaction time, which led to the operation in high hydraulic retention times, and the poor stability of the process, hindered the widespread implementation of AD technologies in the dairy industry, where the effluents are mainly constituted by rapidly acidifying compounds (Saddoud et al., 2007). In these systems, it is required a robust monitoring of operational parameters such as VFA concentration, pH and COD content to ensure the success of anaerobic processes.

Most studies carried out with AD technology for the treatment of cheese whey use a diluted effluent or whey with low protein content, which is much simpler to treat (Ergüder et al., 2001). With raw cheese whey, anaerobic digesters tend to become unstable due to high organic loads (high lactose contents) (Frigon et al., 2009), low bicarbonate alkalinity (50 mg/L as CaCO₃) and tendency to acidify rapidly (Saddoud et al., 2007), resulting in a sharp pH drop. When the pH reaches values close to 4, the concentration of non-dissociated VFA species in the liquid is very high, which inhibits the activity of the methanogenic microorganisms and led to the destabilization of the anaerobic digester (Yan et al., 1993). A strategy commonly used to overcome the rapidly pH decrease is the addition of buffer compounds (chemicals) to the digester. This alkalinity addition prevents acidification and, subsequently, the failure of the anaerobic process (Venetsaneas et al., 2009). The use of lime (Ca(OH)₂) is not recommended because it led to the formation of a calcium precipitate with the biomass (El-Mamouni et al., 1995). The use of bicarbonate or sodium hydroxide is recommended and widely used. In addition, the increase in retention times (over 5 days) tends to minimize the effect of the acidification step on the anaerobic degradation of cheese whey (Frigon et al., 2009).

Lipids are common in dairy effluents (and cheese whey wastewater), and can potentially be inhibitors in anaerobic systems, due to their low bioavailability (Demirel et al., 2005). Besides that, the tendency for lipids to accumulate on the surface of sludge can restrict the transport of soluble substrates to biomass and, thus, lead to decreased substrate conversion (Liew et al., 2020). During the anaerobic degradation process, lipids are first hydrolyzed to glycerol and LCFA, followed by β -oxidation, to generate acetate and hydrogen (Komatsu et al., 1991). Glycerol was found to be a non-

inhibitory compound, while LCFA can cause inhibition of methanogenic microorganisms (Demirel et al., 2005).

The two-phase anaerobic processes, separating the acidogenic from the methanogenic steps of the anaerobic degradation of organic matter, has the advantage of maximizing the different kinetic rates and achieving the highest process yield and may represent an alternative solution to the treatment of cheese whey (Venetsaneas et al., 2009). In fact, the separation of the acidogenic and methanogenic phases in two different reactors led to lower costs, improved efficiency with energy production and process stability (Saddoud et al., 2007).

The separation of anaerobic phases and the combination of different reactor configurations can improve the overall treatment process of cheese whey. Diamantis et al. (2014) tested a combination of CSTR and UASB reactors to treat diluted cheese whey, obtaining very promising results concerning methane formation (0.37 L_{CH₄}.gO₂ removed) without the need of chemical compounds supplementation to provide alkalinity to the anaerobic system. In this case, the enhancement of the acidification step led to an optimum operational and performance features, increasing the methane formation (Diamantis et al., 2014).

The implementation of aerobic processes to treat cheese whey usually leads to the formation of high sludge amounts and the cost associated with oxygen supplementation makes this type of treatment unfeasible (Gannoun et al., 2008). Several authors suggest the implementation of two-step treatment processes, with a first anaerobic treatment followed by an aerobic polishing step, which can be provided by aerated ponds, to lowering the final organic load of the effluent in order to meet the discharge requirements (Frigon et al., 2009).

From a different perspective, some authors also apply an AD process, but with the main objective of maximizing the production of intermediates, such as VFA. Jaroszynski et al. (2016) used whey wastewaters in an UASB reactor at low pH to achieve high amounts of caproic acid, an intermediate in the anaerobic conversion of organic matter. Yang et al. (2003) maximize the concentration of acetic and butyric acids in the cheese whey wastewater, separating the acidogenic from the methanogenic phase, in CSTR reactors. Lagoa-Costa et al. (2020) operated anaerobic sequential batch reactors to obtain a high concentration of VFA, testing different solids and hydraulic retention times, and achieving a high degree of acidification (more than 80 %).

A commonly used approach is to co-digest cheese whey with another substrate. The addition of different substrates in the digestion process can overcome some inhibition problems caused by the intrinsic characteristics of cheese whey. As an example, Ribera-Pi et al. (2020) used cattle manure (alkaline waste) to increase the pH of cheese whey (acidic waste) digestion, creating a synergistic effect on the substrates.

An alternative for green energy production is the use of cheese whey as a source of anaerobic microorganisms to generate and maximize the hydrogen production, in the acidogenic phase of anaerobic degradation. Under anaerobic conditions, microorganisms produce hydrogen as a by-product of the anaerobic degradation of organic matter into volatile fatty acids (acidogenic phase of AD), which are used to generate methane, in a process called dark-fermentative hydrogen production (Kapdan and Kargi, 2006).

Table 8| Summary of published studies regarding the thematic of AD treatment of cheese whey from the dairy industry, in the last 20 years.

Waste stream	Reactor type	Loading ^a	Operational conditions ^b	Methane yield (L _{CH₄} /gO ₂ removed)	Organic matter reduction	Reference
Synthetic whey wastewater	Moving anaerobic biofilm reactor	11.6 g _{COD} /L.d	T = 35 °C HRT = 1 d Alkalinity = 10 g/L as CaCO ₃	0.333 (CH ₄ = 63 %)	COD: 89 %	Rodgers et al. (2004)
Cheese whey	Up-flow anaerobic sludge-fixed film reactor	45.42 g _{COD} /L.d	T = 36 °C HRT = 48 h pH = 7.0 (NaOH)	-- (CH ₄ = 76 %)	COD: 97.5 %	Najafpour et al. (2008)
Cheese whey wastewater	2-phase CSTR	--	T = 55 °C HRT = 6 d pH = 7.0 (NaOH)	0.380 (CH ₄ = 68.3 %)	COD: 93.4 %	Yang et al. (2003)
Cheese whey	UASB	14.6 g _{COD} /L.d	T = 32 °C HRT = 4.95 d Alkalinity = 5-6 g/L as CaCO ₃	-- (CH ₄ = 77 %)	COD: 95.7 %	Ergüder et al. (2001)
Cheese whey	2-phase CSTR with membrane module	19.78 g _{COD} /L.d	T = 37 °C HRT = 4 d pH = 6.5	-- (CH ₄ = 70 %)	COD: 98.5 % BOD: 99 %	Saddoud et al. (2007)
Diluted cheese whey	SBR (aerobic + anaerobic)	1.55 g _{COD} /L.d	T = 20 °C Time/cycle = 2 d pH = 7.2-7.4 HRT = 23 d	--	COD: 88 %	Frigon et al. (2009)
Acidic cheese whey	2-phase CSTR	--	Alkalinity = 11 g/L as CaCO ₃	0.136 – 0.216 (CH ₄ = 65 %)	--	Jasko et al. (2011)
Diluted cheese whey	2-phase CSTR + UASB	≈ 11 g _{COD} /L.d (UASB)	T = 30 °C HRT = 10 h pH = 6.7	0.370 (CH ₄ = 58.6 %)	COD: 90 %	Diamantis et al. (2014)
Synthetic whey wastewater	Stirred SBR with immobilized biomass	5.7 g _{COD} /L.d	T = 30 °C Time/cycle = 8 h Alkalinity: 30 % of COD load	--	COD: 96 %	Ratusznei et al. (2003)
Filtered cheese whey	2-phase SBR	4.6 g _{COD} /L.d	T = 55 °C HRT = 8.3 d pH = 5.5	0.340 L _{CH₄} /gO ₂ feed	COD: 87.5 %	Fernández et al. (2015)
Cheese whey	2-phase CSTR + periodic anaerobic baffled reactor (PABR)	≈ 11 g _{COD} /L.d (PABR)	T = 35 °C HRT = 4.4 d pH = 7.1 Alkalinity = 5 g/L as CaCO ₃	0.310 L _{CH₄} /gO ₂ feed	COD: 94 %	Antonopoulou et al. (2008)
Synthetic whey wastewater	Submerged anaerobic membrane bioreactor (SAMBR)	≈ 7 g _{COD} /L.d	T = 35 °C HRT = 10 d	--	COD: 94 %	Casu et al. (2012)
Diluted cheese whey	UASB (+ electrochemical oxidation as post-treatment)	2 g _{COD} /L.d	T = 32 °C HRT = 3 d Alkalinity = 1-2 g/L as CaCO ₃	--	COD: 97 %	Katsoni et al. (2014)
Diluted cheese whey	Down-flow anaerobic filter (DAnF)	0.8 – 4.0 g _{COD} /L.d	T = 35 °C HRT = 5 d No pH control or alkalinity addition	0.280 – 0.340 (CH ₄ ≈ 60 %)	COD: ≈ 80%	Jo et al. (2016)
Filtered cheese whey	CSTR coupled to a cross-flow tubular ultrafiltration membrane	≈ 5 g _{COD} /L.d	T = 37 °C HRT = 6 d pH = 6.7 – 7.2	0.280	COD: ≈ 95%	Dereli et al. (2019)
Cheese whey wastewater	2-phase CSTR (H ₂ -CSTR + CH ₄ -CSTR)	1.7 – 2.2 g _{COD} /L.d (CH ₄ -CSTR)	T = 35 °C HRT = 20 d Alkalinity = 12.75 g/L as CaCO ₃ (from the effluent of H ₂ -CSTR)	6.7 L/L of influent	COD: 95.3 %	Venetsaneas et al. (2009)

^a The OLR indicated refers to the OLR applied at the stabilization phase to the methanogenic reactor

^b The HRT indicated refers to the final HRT tested or to the stabilization phase of the reactor; HRT, temperature and pH/alkalinity values refer to the methanogenic reactor

2.5 Bauxite mining and alumina refining

Although aluminum is the most abundant metal in the earth's crust, present in several minerals, it has a high affinity for oxygen and the stability of aluminum oxides and silicates has prevented its isolation for a long time (Rabinovich, 2013). In 1821, Pierre Berthier discovered bauxite in Les Beaux, France and French geologist Pierre Armand Dufrenoy named it "beauxite" (World Aluminium, 2020). In 1861 French chemist Henri Saint-Claire Deville renamed it "bauxite" and in 1856 he developed a method of preparing large amounts of aluminum from bauxite, but large-scale implementation was costly and several other chemists searched for economic alternatives (Quartz Business Media, 2008). In 1886, Charles Martin Hall (USA) and Paul L. T. Héroult (France) independently developed a method of producing aluminum from alumina. With the efficient method for alumina extraction from bauxite, developed by Karl Josef Bayer (Bayer process), the "Hall-Héroult" process has become economically viable and applicable on an industrial scale (Sushil and Batra, 2008).

Nowadays, the Bayer process applied to alumina refining is used worldwide and is the main process for transforming bauxite. Besides the Bayer process, alumina can be produced by the sintering process or by the combined Bayer-sintering process (Wang et al., 2019). Bauxite mining and alumina refining are the upstream operations of primary aluminum production. Thus, the production of metallic aluminum is performed via a two-stage process: first, the refining of bauxite into alumina employing the wet chemical caustic leaching process (Bayer process), and secondly, the electrolytic reduction of alumina in aluminum metal in a molten bath of natural or synthetic cryolite (Na_3AlF_6) (Hall-Héroult process) (Meyer, 2004). Aluminum is commonly used in packaging (beverage cans, aluminum foil), civil construction, transportation (trains, airplanes, cars and buses), technology (laptops and mobile phones) and energy sectors, among other applications (Ahn et al., 2015).

Bauxite is the main aluminum ore and is a mixture of related minerals. It is reddish-brown and appears in the form of a rock that occurs near the surface, normally with only 1 or 2 m of overburden (Donoghue et al., 2014) and may contain hydrated aluminum oxides in the form of gibbsite ($\gamma\text{-Al}(\text{OH})_3$), diaspore ($\alpha\text{-AlO}(\text{OH})$) or boehmite ($\gamma\text{-AlO}(\text{OH})$) (Palmer et al., 2009). Bauxite also contains other compounds, such as hematite (Fe_2O_3), goethite ($\text{FeO}(\text{OH})$), quartz (SiO_2), rutile/anatase (TiO_2), kaolinite ($\text{Al}_2\text{Si}_2\text{O}_5(\text{OH})_4$), ilmenite and other minor impurities (Donoghue et al., 2014; Liu et al., 2009). This heterogeneous sedimentary rock is extracted mainly for the formation of alumina (aluminum oxide), a white powder. Approximately 73 % of bauxite is refined to alumina used in the production of aluminum, and the remaining is used in non-metallurgical applications, such as the production of cement, chemicals, propping agents, refractories and abrasive materials (Bray, 2020). Alumina with the highest purity level is used predominantly to produce metallic aluminum by the Hall-Héroult process (Liu et al., 2009).

The worldwide development has led to an exponential use of aluminum in a wide range of applications in our daily lives. In the past few decades, alumina has grown in importance in the upstream value chain, which has led some aluminum producers to build their own bauxite refineries and expand existing aluminum-making infrastructures. Australia is currently the world leader in the bauxite refining to alumina, with 86.4 million dry tons of refined alumina per year, followed by China (79 million dry tons), Guinea (57 million dry tons), Brazil (29 million dry tons), India (23 million dry tons). Other countries like Indonesia, Jamaica, Russia, Vietnam and Saudi Arabia account for less than 11 million dry tons each year (Bray, 2020). Thus, China, Oceania and South America lead global

production with approximately 54, 15 and 8 %, respectively, of the total alumina production worldwide, accounting for the rest of the world by approximately 22 % (Wang et al., 2019).

Figure 16 depicts the location of bauxite deposits all over the world. Bauxite reserves are located mainly in Guinea, Australia, Vietnam, Jamaica, Indonesia and China (Bray, 2020). Of all the bauxite resources, 90 % of them are in tropical locations. Karst bauxite is predominant in Europe and Jamaica, whereas laterite bauxite appears in Australia, the Caribbean, Guyana and Brazilian shields in South America, as well as in the shield of Guinea and Cameroon (West Africa) (Meyer, 2004).

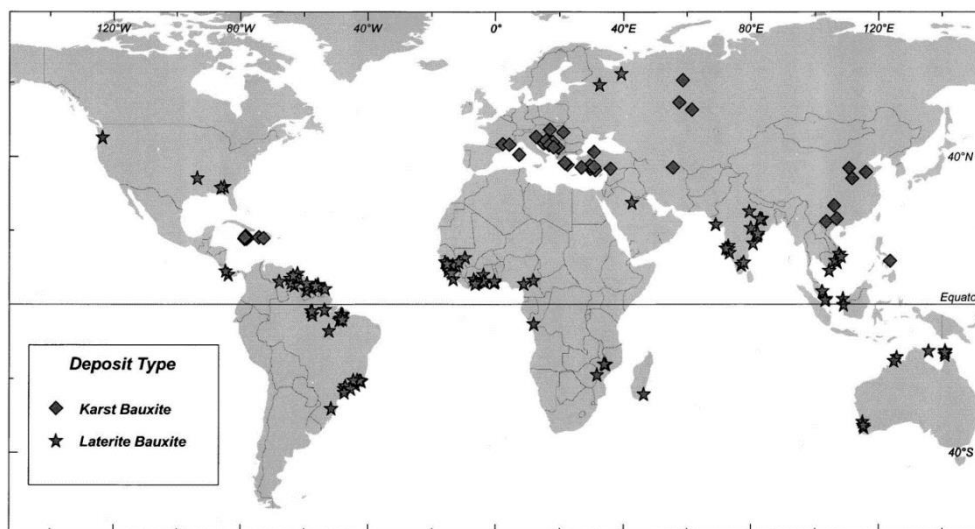


Figure 16] Location of karst and laterite bauxite deposits worldwide (reproduced from Meyer (2004)).

In aluminum-producing countries where bauxite reserves are insufficient, many alternatives for the alumina production are being studied. The use of different raw materials as clay resources is under study, but not yet implemented on a commercial scale, due to the high costs. Materials as alunite, anorthosite, coal wastes and oil shales are being considered as additional potential sources of alumina (Bray, 2020).

2.5.1 Red mud generation during the alumina refining process

Bauxite residue, also called red mud, is a hazardous solid clay-size waste derived from alumina refining, with an average particle size of $< 100 \mu\text{m}$ (Liu and Li, 2015), with 90 % of the particles below the size of $75 \mu\text{m}$ (Sushil and Batra, 2008). These particles have a high surface area (Sushil and Batra, 2008) and a BET (Brunauer, Emmett and Teller) specific surface area around $10 - 25 \text{ m}^2/\text{g}$ (Wang et al., 2008). This waste is generated during the alumina refining in the bauxite ore, primarily by the Bayer process, which uses caustic soda to dissolve the aluminum-bearing minerals in the bauxite (gibbsite, diasporite and boehmite) (Liu and Naidu, 2014), at elevated temperature and pressure (Palmer et al., 2009).

2.5.1.1 Alumina refining process

Most of the alumina produced commercially from bauxite is obtained via the Bayer process (R. Zhang et al., 2011), a process patented by Karl Josef Bayer in 1888 (Rabinovich, 2013). Bayer's

process for bauxite refining to produce alumina is shown in Figure 17, highlighting the red mud formation after washing insoluble components and presenting the four steps performed in a bauxite-refining mill: digestion, clarification, precipitation (for alumina production) and evaporation (for chemicals recovery).

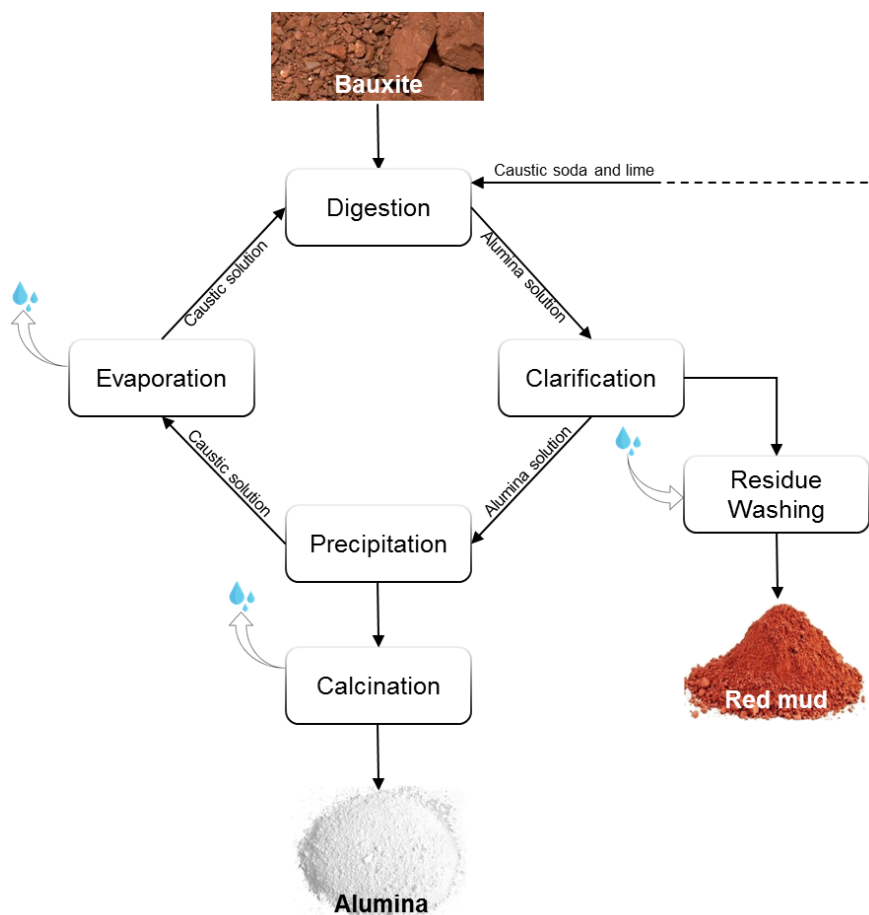


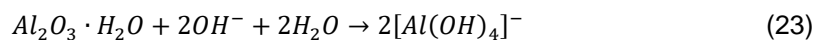
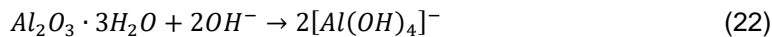
Figure 17 Bayer's process for alumina refining from bauxite, generating a by-product (red mud).

Prior to digestion, bauxite from mining is crushed into small particles, to form a fine slurry. The Bayer process involves the digestion of bauxite in a hot solution of sodium hydroxide, which leaches aluminum from bauxite (Hua et al., 2017), by a selective extraction of aluminum-bearing minerals (gibbsite, boehmite and diaspore) from the insoluble components (mostly oxide compounds). In this process, the caustic aluminate solution reacts with clay or quartz in the bauxite ore to form red mud (bauxite waste) and the aluminum-bearing minerals are dissolved as sodium aluminate (NaAlO_2) (Sushil and Batra, 2008), in a digestion step at a high temperature (normally between 145 and 265 °C) and pressure (Donoghue et al., 2014).

The caustic soda (called "spent liquor") is recycled back to the beginning of the refinery circuit (digestion process), after a series of separations and evaporation. This recycling step helps to reduce the production cost with raw chemicals and, at the same time, to reduce the alkalinity of the waste. The resulting sodium aluminate (NaAlO_2) is separated (clarification step) and selective precipitation of aluminum in the form of aluminum hydroxide ($\text{Al}(\text{OH})_3$) is performed (Liu et al., 2009). After

precipitation, aluminum hydroxide is subjected to calcination at approximately 1000 °C, forming anhydrous alumina (Al₂O₃), the final product of bauxite refining to alumina (Donoghue et al., 2014).

The chemical reactions for the selective precipitation of gibbsite (Equation 22) and both boehmite and diaspore (Equation 23) are as follows:



The processing conditions applied to operate the digester (caustic concentration, temperature and pressure) as well as operating costs, depend on the type of bauxite ore. The presence of gibbsite allows processing at about 140 °C, whereas the presence of boehmite requires higher temperatures (200 – 240 °C). The presence of diaspores, besides too high temperature and pressure, also requires a strong caustic solution (Liu et al., 2009). Thus, the production costs of processing bauxite ores with a high gibbsite content will be much lower than the costs required to process boehmite or diaspore.

2.5.1.2 Red mud characteristics

One of the major steps of this transformation process is the separation (clarification) of red mud solids from the caustic aluminate solution (liquor) (Chvedov et al., 2001). The washing step uses a large amount of water. In this process, some polymeric flocculants can be added to promote the sedimentation of solids in the washing and thickening stages (Liu et al., 2009). After washing, RM waste is normally disposed of in special facilities known as Bauxite Residue Disposal Areas (BRDA) or Residue Storage Areas (RSA). Soil rehabilitation in storage areas is difficult due to the alkaline characteristics of the waste. For soil treatment, the pH must be reduced, and several research projects are underway to develop new cost-effective technologies for the remediation of contaminated areas (World Aluminium, 2020).

RM can be stored in wet (less than 50 % of solid content), dry (about 50 % of solid content) or a mixture of both wet and dry forms, but dry stacking is the most current practice worldwide (Liu et al., 2009). Although widely applied, this disposal method uses a large land area, which is costly and intensifies the risk of environmental pollution, such as surface or groundwater pollution (Liu and Li, 2015). The land disposal of RM is also visually polluting and can be aesthetically harmful (Liu et al., 2009).

Annually, about 120 million tons of RM are produced, representing important disposal issues for the mining and metallurgy industries (Liu and Li, 2015). The production of 1 ton of alumina generates about 0.6 – 2.5 tons of red mud residue, depending on the bauxite mineralogy (Hua et al., 2017; Liu et al., 2009) and the efficiency of the alumina extraction process (R. Zhang et al., 2011). The huge amount of RM generated worldwide causes environmental impacts concerning its disposal, due to its high alkalinity and sodium compounds, such as sodium carbonate and sodium hydroxide (Brunori et al., 2005), and documented risks to sea life.

The data for the chemical composition (expressed as oxides %wt) of the red mud obtained as a byproduct of the Bayer process for the alumina production are found in Table 9. Generally, the chemical analysis of the red mud reveals the presence of Fe, Al, Si, Na, Ca and Ti, also in addition to minor constituents such as K, Cr, V, Ni, Mn, Cu, Zn and Pb. The most common mineral compounds in the red mud came from bauxite, such as crystalline hematite (Fe₂O₃), boehmite and goethite

(FeOOH), along with other aluminum hydroxides, calcium (in the form of calcite, CaCO_3 , whewellite, $\text{CaC}_2\text{O}_2 \cdot \text{H}_2\text{O}$, and gypsum, $\text{CaSO}_4 \cdot 2\text{H}_2\text{O}$) and titanium oxides and sodalite ($\text{Na}_4\text{Al}_3\text{Si}_3\text{O}_{12}\text{Cl}$) (Brunori et al., 2005; Wang et al., 2008). Trace amounts of undissolved alumina (2.12 – 33.1 %) (Liu and Li, 2015) are also found in RM, as well as a wide variety of organic compounds (Palmer et al., 2009). The RM generated in the Bayer process has a higher content of hematite than that produced by the combined process, whereas the RM produced by the sintering process has higher alumina content than that produced by the combined Bayer-sintering process (Wang et al., 2019). However, the silicon dioxide content in the RM produced by the combined Bayer-sintering process is normally less than the content of RM produced in the Bayer process (Wang et al., 2019).

Table 9 | Chemical composition of the red mud resulting from the Bayer process (consolidated from data presented in Cengeloglu et al. (2003); Palmer et al. (2009); Zhang et al. (2011)).

Oxide	%wt
Fe₂O₃	> 30 ^a
Al₂O₃	18 – 25
SiO₂	15 – 20
Na₂O	8 – 12
CaO	≈ 5 ^a
TiO₂	2 – 5
LOI	8.15 ^b
pH	> 10.6

^a The proportion varies greatly with the bauxite characteristics and leaching conditions

^b Value from Cengeloglu et al. (2003)

The oxidized form of iron (Fe^{3+}) present in high concentrations in the RM wastes is responsible for its characteristic red color. The pH of this waste is higher than 10.6, up to 13 or higher, depending on the concentration of the caustic solution in the digestion step (World Aluminium, 2020). The high pH value is due to the presence of large amounts of alkaline sodium compounds, such as sodium carbonate and sodium hydroxide (Brunori et al., 2005).

The presence of metals in wastewaters and wastes can pose an environmental problem, along with the loss of important resources. The red mud also contains valuable metals, such as titanium (TiO_2), which must be recovered to be reused in other industries. This circle use of resources reduces the cost of many raw materials and responds to difficult environmental pollutants such as red mud (Cengeloglu et al., 2003).

2.5.2 Red mud applications

Waste recycling is an integral part of the waste management system and represents the key usage alternative for energy reuse and recovery, in a waste-to-energy perspective. This approach is also applied to RM from alumina refining (Ahn et al., 2015). The amount of solid waste generated during the alumina production is attractive from the point of view of reusing RM in other applications and from the point-of-view of further industrial application. Nowadays, there are hundreds of patents under the scope of RM waste application, revealing the versatility nature of this type of residue (World Aluminium, 2020).

The use of different technologies for its activation, such as acidification and thermal treatment, makes RM suitable to be used as a sorbent, gas cleaner or as a catalyst. With these activation methods, RM's surface physico-chemical properties are improved, resulting in higher adsorption capacity and catalytic activity (Wang et al., 2008), as well as a higher surface area of RM particles (Sushil and Batra, 2008). The elements naturally found in RM wastes, such as titanium, scandium, gallium, sodium and iron, can be recovered and generate value (Liu et al., 2009). The worldwide scarcity of iron supply represents an opportunity for the development of new technologies for the use of RM as an iron source, with a focus on the development of both economically and environmentally desirable technologies (Liu and Naidu, 2014).

The physical properties and the high amounts available make RM a good candidate to be applied as a sorbent for the removal of several pollutants from water and wastewater. Other materials from various industries can also be applied as sorbents, namely fly ash, slag and different types of sludge. However, before application as a sorbent, the RM needs to be neutralized, to reduce the pH to values close to 8.0 (Bhatnagar et al., 2011). RM can be applied in water treatment, for removal of phenolic compounds (phenol, 2-chlorophenol, 4-chlorophenol, 2,4-dichlorophenol and 2,4-dinitrophenol), metals (arsenic, chromium, nickel, copper, cadmium, zinc and lead), inorganic anions (nitrate, phosphate and fluoride) and dye (Rhodamine B, fast green, methylene blue, Congo red, procion orange), as extensively reviewed by Bhatnagar et al. (2011). It can also be used as an agent for the decontamination of acidic leachates (Sushil and Batra, 2008). Several studies performed with the application of red mud concluded that this waste exhibits a low leaching behavior of its components. These findings imply that the reuse of this material after application in the wastewater treatment represents a low environmental impact, and can be incorporated into the brick production or disposed of as non-hazardous waste in landfills (Wang et al., 2008).

In addition, red mud has been successfully applied to building and structural materials, such as cement, ceramics and casting components. Several studies have focused on the production of construction materials based on RM obtained in the Bayer process. Tsakiridis et al. (2004) incorporated RM waste in Portland cement and, in low share, RM did not affect the processing of cement, having the potential to be incorporated as a raw material in cement production. In the same line and also with promising results, Sglavo et al. (2000) used almost 50 % of RM waste as a raw component in clay mixtures for the ceramic bodies production, not affecting the sample porosity and increasing density and flexural strength. Yang et al. (2008) used a combination of fly ash and red mud as a raw material in the successful production of glass-ceramics in the CaO-SiO₂-Al₂O₃ system. In all of these applications, the substitution of virgin raw materials by red mud wastes has the potential to reduce production costs, along with the environmental benefits of reuse, recycling and reduction of wastes.

RM can also be applied for soil and mine *in situ* remediation. Garau et al. (2007) studied the efficiency of RM as a material for metal immobilization, in polluted acidic soil. The increase in pH led to a decrease in the metals solubilization and, in addition, RM improved the microbial growth of bacteria naturally present in soils (Garau et al., 2007).

Other applications include the recovery of metals from RM, treatment of gold ores, a sorbent for gas cleaning (SO₂, H₂S) from hot exhaustion gases (Wang et al., 2008). The use of RM as catalysts has also been widely studied, due to the high iron oxide content, in hydrogenation, dechlorination and hydrodechlorination and catalytic oxidation of hydrocarbons. The application of RM as a catalyst

in several different reactions has been extensively reviewed by Sushil and Batra (2008). Amritphale et al. (2007) successfully applied RM and barium containing compounds for the production of X-ray shielding materials. The use of RM led to the formation of thickener shielding materials, with standard required properties (compressive strength and impact strength) (Amritphale et al., 2007).

Although this vast range of options for RM application, none of them have been economically applied on an industrial scale (Wang et al., 2008). An alternative for minimizing costs is the multiple recoveries of valuable products (metals). The integration of several techniques in the same physical space can reduce the costs of transportation and processing, also allowing the complete use of RM, for recovery of metals or activation by adsorbents and catalysts, and for their incorporation in other building materials, after metals leaching or usage (Liu and Naidu, 2014). Nonetheless, more detailed information about the RM characteristics (mainly concerning mineral characterization) is needed before the implementation of integrated valorization processes focusing on further maximization of such attractive characteristics (Wang et al., 2019).

2.5.2.1 Use of red mud in biological treatment processes

The use of red mud as an additive in biological treatments (anaerobic or aerobic processes), in its activated or non-activated form, is little reported in the literature, despite the promising results obtained so far. Table 10 lists the biological technologies described in the literature so far, and which have been developed using red mud as an inorganic additive.

Table 10| Resume of biological technologies employing red mud as an inorganic additive.

Treatment system	Substrate	Operational conditions ^a	Form and role of red mud	Performance	Reference
UASB	Palm oil mill effluent	$S_0 = 10 - 40$ (30) gO ₂ /L T = 35 °C HRT = 8 - 32 (16) h	Magnetic RM-Fe; Sludge granulation during effluent degradation	COD removal: 85%	Ahmad (2014)
Batch digester	Brewers' spent grain	Calcined RM: 10 g/L Organic rate: 10 gTS/L T = 55 °C	Calcined RM; Pretreatment of brewers' spent grain	Specific H ₂ production: 198.62 mL/gVS	Zhang and Zang (2016)
Batch digester	Waste activated sludge	RM: 20 g/L T = 35 °C $\Delta t = 28$ d	Powder RM; Methane improver	Methane production: 1.41 mmol/gVSS	Ye et al. (2018c)
Batch digester	Waste activated sludge	RM: 5, 10 and 20 g/L T = 35 °C $\Delta t = 28$ d	Powder RM; Conductive solid	COD removal: 52 %	Ye et al. (2018b)
Batch digester	Cow dung	T = 25 °C pH = 7.2-7.4	Powder RM; neutralize the alkaline pH of RM	--	Patel et al. (2018)
Batch digester	Waste activated sludge	RM: 20 g/L T = 15, 25 and 35 °C (35)	Powder RM; Conductive solid	Methane production: 1.39 mmol/gVSS	Ye et al. (2018a)

^a In parenthesis are the best conditions applied

Ahmad (2014) performed the activation and magnetization of red mud particles. The magnetic RM-Fe particles helped in the formation of biomass granules in the UASB reactor, and the addition of such particles at a concentration of 400 mg/L increased the average granule diameter by 82 %. The precipitation of ferrous sulfide (FeS) allowed the attachment of granules, with an enhanced production of extracellular polymeric substances, beneficial for the sludge aggregation. The

development of granules improved the development of methanogenic microorganisms and, thus, improving the overall yield of the treatment (Ahmad, 2014).

Zhang and Zang (2016) applied a pretreatment with calcined RM to their anaerobic system to produce hydrogen from the brewers' spent grains. The RM waste was dried at 100 °C for 12 h, and calcined at 850 °C for 5 h. After calcination, the RM was dissolved in an aqueous solution with brewers' spent grains and the mixture was feed to batch digesters to produce hydrogen, after 48h of mixing. In this case, the use of the RM waste helped in the alkaline hydrolysis of the substrate, depolymerizing the hemicellulose and solubilizing the lignin. This pretreatment increased the hydrogen formation by 68 % (Zhang and Zang, 2016).

Ye et al. (2018c) studied the addition of red mud to an anaerobic digester for methane production, focusing on hydrolytic and acidogenic steps for the intermediate generation (VFA). The addition of RM waste to the bioreactor promoted the hydrolysis and acidification of the sludge. The VFA content increased by 39 % with the addition of red mud, indicating a synergistic relationship between the inorganic additive (red mud) and the wasted activated sludge. Methane content also increased by 36 % compared to a control reactor, without the addition of RM powder (Ye et al., 2018c).

Ye et al. (2018b) studied the role of red mud during the AD of waste activated sludge, namely in the formation of aggregates that can influence the rapid direct electrons exchange during the direct interspecies electrons transfer. The use of RM promoted an increase in the methane formation (36 %) versus a control reactor without the RM addition, with the benefit of enhancing the solubilization of the organic matter suitable for the methanogenic step. The authors also found a positive correlation between extracellular polymeric substances and methane formation, increased by the addition of RM powder, forming large bio aggregates (Ye et al., 2018b).

Patel et al. (2018) studied the neutralization of RM wastes applying an AD process of cow dung, the neutralizing agent used in their study. Both the pH and the alkalinity of the RM decreased when 10 g of RM were mixed with 80 g of cow dung, after 40 days of anaerobic operation. This approach has the potential to be used to reduce the high pH of RM wastes, with the advantage of biogas formation during the anaerobic process (Patel et al., 2018).

Ye et al. (2018a) performed an additional study for the RM addition to the wasted activated sludge, at different temperatures, considering the previous results obtained by the authors (Ye et al., 2018b, 2018c). The authors found that temperature changes affect the key functional groups, which subsequently contribute to the CO₂ reduction into methane. In addition, the use of red mud stimulated methane accumulation, reaching 35 % more than the control reactor without the RM addition, due to the high content of alkaline compounds in the waste, inducing a high level of alkalinity, and resulting in increased substrate and enzyme activities (Ye et al., 2018a).

From a different point-of-view for biological treatments, RM wastes can be applied in the manufacture of anaerobic digesters instead of being added to the anaerobic process. A very popular digester in China during the 1990s is a plastic bag digester (Chen and Shyu, 1996). As an alternative to conventional plastic, some researchers have developed a red mud plastic digester, which is a mixture of PVC and red mud waste. These digesters are low cost, easy to maintain and transport and operate with short retention times (El-Haggag and Samaha, 2019).

2.6 pH regulation in anaerobic digestion processes

Nowadays, anaerobic technology for biogas production is well established and developed. However, several improvements to the optimization of key parameters must be made. The main factors affecting the efficiency of AD systems, including pH, must be tightly monitored and controlled, to create suitable environmental conditions for the development of sensitive methanogenic microorganisms. Regulation of pH on an industrial scale can be costly if the volume of wastewater to be treated is high. Thus, the technical solutions to be implemented should improve the process, ensuring very good performance and a low operating cost, to create attractive treatment processes.

An appropriate approach to improve the anaerobic process is the use of inorganic additives to promote an increase in the efficiency of the process. Several types of inorganic additives have been studied in recent years, including compounds to control pH, to reduce inhibitory effects, to improve anaerobic performance, or to provide physical support for attached microbial growth.

2.6.1 Types of inorganic additives for anaerobic process enhancement

The characteristics of the substrates commonly used in anaerobic degradation processes can result in low performance of the process if high loads or inadequate buffer capacity are provided. For easily biodegradable substrates, such as cheese whey or food wastes, the rapid accumulation of VFA can lead to an extra pH lowering and can cause inhibition of methanogenic microorganisms (D. Wang et al., 2017). Other wastes, such as manures, have a high ammonia content, often with concentrations greater than necessary for stable microbial growth, which can inhibit the AD process (Jiménez et al., 2015). Therefore, the addition of natural inorganic minerals or solid wastes can be beneficial for anaerobic processes treating complex waste streams. On the one hand, materials can release internal elements, and these elements can be incorporated as part of enzyme structures in microbial cells or have a significant effect on the degradation of organic matter and the methane formation (Jiménez et al., 2015). On the other hand, the materials can also act as a support material for microbial growth, allowing greater resistance and promoting, ultimately, methanogenic activity (Watanabe et al., 2013).

Table 11 lists some examples of works performed within the scope of anaerobic waste and wastewater treatment using organic additives to improve the overall AD process. The works listed are divided according to the main goal defined for the inorganic addition performed, namely, to overcome the ammonia inhibition caused by the substrate characteristics, avoid the sulfate inhibition, enhance the AD process and provide physical support for biomass growth. Other inorganic additives can also be used in anaerobic processes with the main goal of process improvements, such as nanoparticles (Ajay et al., 2020), membranes (Youngsukkasem et al., 2012), inorganic compounds such as magnesium chloride, nickel and cobalt compounds (Hijazi et al., 2020) or micro and macronutrients addition (N, P, S, Fe, Mo, among other trace elements) (Romero-Güiza et al., 2016).

Red mud wastes can also be used as inorganic additives for the anaerobic degradation process (Gameiro et al., 2020). The published works applying red mud wastes as inorganic additives for anaerobic processes enhancement (Ye et al., 2018b, 2018c, 2018a) were summarized in Table 10 and discussed previously.

Table 11| Examples of published works regarding the application of inorganic additives to the AD process.

	Inorganic additive	Waste stream under treatment	Effect of the inorganic additive in the AD process	Reference
Ammonia inhibition	Clay residue	Pig manure and rice straw (co-digestion)	<ul style="list-style-type: none"> - Reduced the inhibition of excess ammonia by adsorption at the surface of clay particles - Improved AD of pig manure 	Jiménez et al. (2015)
	Natural zeolite; modified zeolites	Pig manure (digestion)	<ul style="list-style-type: none"> - Increased cumulative methane production - Reduced the values of the TVF/Alk ratio, increasing the pH values in the medium - Enhanced microbial growth 	Milán et al. (2003, 2001)
	Natural mordenite	Sludge (digestion)	<ul style="list-style-type: none"> - Synergistic effect between the Ca²⁺ supply and the ammonia removal - Reduced the inhibition of ammonia 	Tada et al. (2005)
	nZVI	Sulfate-rich wastewater	<ul style="list-style-type: none"> - Enhanced the sulfate reduction and the COD removal when nZVI was added 	J. Zhang et al. (2011)
	Iron oxide-zeolite system	Cow manure and rice straw (co-digestion)	<ul style="list-style-type: none"> - Promoted stable pH operation and increased VFA concentration - Reduced ammonia inhibition - Enhanced attached microbial growth 	Lu et al. (2017)
AD enhancer	Iron scrap; iron scrap with rust	Sludge (digestion)	<ul style="list-style-type: none"> - Enhanced methane yield by 21 %, with better mass transfer efficiency of iron scrap than Fe⁰ powder - Iron scrap with rust induce microbial Fe(III) reduction and improve methane yield by 29 % 	Y. Zhang et al. (2014)
	Fly ash and bottom ash	Organic fraction of municipal solid waste	<ul style="list-style-type: none"> - The two types of ashes improved the biogas yield - Contributed to the immobilization of microorganisms - Leached compounds (alkalis, trace elements) improved the digestion performance 	Lo et al. (2012)
	Sludge incineration bottom ash	Sludge (digestion)	<ul style="list-style-type: none"> - Enhanced methane production by 27 % and decreased the methanization lag phase by 32 % 	Yin et al. (2018)
	Red mud powder	Waste activated sludge	<ul style="list-style-type: none"> - Enhanced methane production - Acted as a conductive solid to promote DIET 	Ye et al. (2018b, 2018c, 2018a)
	Waste-based geopolymers	Cheese whey	<ul style="list-style-type: none"> - Enhanced methane production - Increased methane content in the biogas - Promoted prolonged pH control in the AD of easily-acidifiable waste streams 	Gameiro et al. (2020, 2019a); Novais et al. (2018c)
Biomass support media	Cedar charcoal	Crude glycerol	<ul style="list-style-type: none"> - Improvement of methane production by 1.6 times - Enhancement of propionate degradation rate, decreasing its inhibitory effect 	Watanabe et al. (2013)
	Biochar	Sludge (digestion)	<ul style="list-style-type: none"> - Improvement of methane yield, biomethanation rate and maximum methane production rate by 7 to 28 % - The boosted in CH₄ content facilitated the CO₂ removal from the biogas - Reduced the inhibition of ammonia and increased alkalinity, creating a stable process 	Shen et al. (2015)

Jiménez et al. (2015) used clay residue to reduce the inhibition caused by pig manure in an anaerobic co-digestion process with rice straw. The high content of ammonia in this waste causes the inhibition of methanogenic microorganisms and, in this case, the added clay residue functioned as an ammonia adsorbent surface, leading to an improvement in the overall AD process, with a positive effect on the methane yield (Jiménez et al., 2015). In another study by the same authors, clay residue was added in an anaerobic system treating manure and rice straw, and an improvement in hydrolytic activity and methane production was observed. This process enhancement was due to

the mineral content and adsorbent properties of the inorganic additive used (clay residue from the oil clarification process) (Jiménez et al., 2014).

In their work, Milán et al. used natural zeolite (Milán et al., 2001) and modified zeolite (Milán et al., 2003) to improve the AD process of pig manure. These materials act as microbial support in the AD of different wastewaters due to the high immobilization capacity of microorganisms, the ability to reduce ammonia and ammonium ions in solution and, thus, improve the equilibrium of these ions (Milán et al., 2001). The modification of the natural zeolite surface with the deposition of metals such as nickel, cobalt, or magnesium had a positive effect on the two limiting steps of AD, hydrolysis and methanogenesis, increasing the microbial growth of microorganisms (Milán et al., 2003). These findings are also supported by the work of Fernández et al. (2007), who showed that microorganisms in an anaerobic FBR treating distillery wastewaters (vinasse) can grow attached to the surface and in the interior zones of natural zeolite, thus enhancing the anaerobic performance of the system (Fernández et al., 2007).

Tada and co-workers tested several inorganic materials as additives for the AD of ammonium-rich sludge (Tada et al., 2005). They tested, among others, inorganic adsorbent zeolites (mordenite, clinoptilolite, zeolite 3A, zeolite 4A), clay minerals (vermiculite), and manganese oxides (hollandite, birnessite). The natural mordenite was promising for leaching Ca^{2+} ions through $\text{Ca}^{2+}/\text{NH}_4^+$ exchange, which enhanced the methane production from ammonium-rich sludge. This material had a synergistic effect on calcium supply, as well as ammonia removal during the AD process, which prevented ammonia inhibition and promoted the methane formation (Tada et al., 2005).

Several authors have studied the use of nano zero-valent iron (nZVI) in anaerobic digesters, for the treatment of different wastes. J. Zhang et al. (2011) tested the use of nZVI, which, due to its reducibility, enhanced the anaerobic digestion of sulfate-containing wastewater. COD removal was enhanced when nZVI particles were added to the UASB reactor, increasing from 58 % in the control reactor to 87 % in the reactor with the particles. The addition of nZVI also improved the sulfate reduction, and the presence of nZVI can act as an additional electron donor and buffering agent, thus decreasing the concentration of un-dissociated H_2S and its negative impact on the anaerobic process (J. Zhang et al., 2011). The same authors also described the positive effect of nZVI addition to anaerobic digesters (UASB reactors), promoting the growth of methanogenic microorganisms and increasing the degradation rates at low temperatures (25 °C) and HRT (12 h) (Y. Zhang et al., 2011). Several other nanoparticles, containing silver, cerium, cobalt, copper, nickel, titanium or zinc, have been tested over the years as additives for anaerobic waste and wastewater degradation, as summarized in the review paper by Lee and Lee (2019).

Iron supplementation to an anaerobic system, in the form of a zeolite-iron oxide aggregate, can function as an electron flow medium and accelerate the syntrophic methanogenesis of acetate-oxidizing bacteria and methanogenic archaea. This solution showed its efficiency in the work of Lu et al. (2017), which obtained an improvement in the anaerobic performance of ≈ 370 % regarding the methane yield in the co-digestion of cow manure and rice straw. In addition, the authors observed a stable pH condition, higher total VFA concentration and lower ammonia content when using the iron oxide-zeolite system. This solution also presents physical support for the growth of biomass and, for this reason, the authors stated that the activity of methanogenic microorganisms was promoted in the presence of the system iron oxide-zeolite (Lu et al., 2017).

The addition of iron scrap to the sludge AD was studied by Y. Zhang et al. (2014), who compared the anaerobic performance with the addition of Fe⁰ powder to the AD system. The use of iron scrap, besides the practical and economic alternative, can accelerate the anaerobic performance of sludge digestion. The use of iron scrap with rust induced the microbial reduction of Fe(III), the hydrolysis and acidification of complex materials and the methane yield was improved by 30 % when compared to the addition of Fe⁰ powder to the sludge digestion. In addition, the authors observed the enrichment of the anaerobic consortium with iron-reducing microorganisms, which were responsible for the enhancement in the degradation of complex substrates such as sludge (Y. Zhang et al., 2014).

The incineration of municipal solid waste and other solid wastes, such as sludge from WWTP, is a widespread technology since it generates energy and reduces the volume of wastes by up to 90 %. However, this technology produces two types of solid wastes, namely bottom ash, classified as non-hazardous waste, and fly ash, classified as hazardous waste due to the high content of metals, soluble salts, chlorinated organic compounds and lime (Romero-Güiza et al., 2016). The addition of both bottom ash and fly ash to an anaerobic process can increase the metals content and the concentrations achieved can have beneficial or detrimental effects on the AD process.

Several authors have investigated the use of ashes from waste incineration as a source of alkalinity, due to the high content of CaO and high pH, in addition to trace elements for the AD process. Lo et al. (2012) used two different ashes in the AD of the organic fraction of municipal solid waste. The addition of ashes improved the biogas yield and the small size of the ash particles enhanced the anaerobic performance by providing an immobilization medium support for the microorganisms. The release of alkalis, such as calcium, potassium, sodium or magnesium, increased the pH control of the AD system. In addition, the release of other elements, such as iron, silicon, cobalt, molybdate, aluminum, or manganese, was also beneficial for the process performance (Lo et al., 2012). Sailer et al. (2020) tested the addition of wood ash to the AD process treating the organic fraction of municipal solid waste, as a source of trace elements. Ash supplementation led to an increase in the pH of the reactor and precipitation of CO₂ through metal oxides from ash increased largely the share of methane in biogas, reaching methane 98 % of the total biogas (Sailer et al., 2020).

Yin et al. (2018) studied the AD of waste activated sludge with the addition of bottom ash from sludge incineration. In their study, these authors obtained an increase in the performance of AD degradation steps, namely in hydrolysis (≈ 140 %), acidogenesis (≈ 87 %) and VFA degradation (≈ 100 %), with significant improvement in the methane formation. The bottom ash contributed to the increase of the calcium content inside the digester, promoting the carbonation of the anaerobic system and facilitating the CO₂ sequestration *in situ* (Yin et al., 2018). Similar results were obtained by Wei et al. (2020), who tested the addition of bottom ash from sludge incineration for the digestion of primary sludge. This anaerobic degradation process was enhanced and the presence of bottom ash led to an increase of 18 % in specific methane production and, in addition, the activity of hydrolytic and acidogenic microorganisms was accelerated (Wei et al., 2020).

Immobilization of anaerobic biomass, mainly methanogenic microorganisms, can be positive for the performance of the AD process. Immobilization avoids the washout of biomass and allows the operation of reactors with a low retention time and high organic load (Romero-Güiza et al., 2016). For this purpose, several materials have been tested over the years, such as natural zeolites

(Fernández et al., 2007; Jiménez et al., 2015), carbon filter, rock wool, loofah sponge, polyurethane foam (Yang et al., 2004) or charcoal (Watanabe et al., 2013).

The use of cedar charcoal in a CSTR-like digester for the digestion of glycerol was beneficial since the propionate inhibition was avoided. Watanabe et al. (2013) observed that the degradation rate of propionate was enhanced when charcoal was added to the anaerobic digester, avoiding the accumulation of this VFA specie, very common when glycerol is used as the substrate in an anaerobic degradation process. The presence of charcoal inside the reactor acted as a support for microbial attachment in the pores of the material, with higher methane productions being observed. In addition to these results, the authors also observed an increase in the hydrogenotrophic methanogens content in the microbial community, which led to an improvement in the glycerol conversion to methane (Watanabe et al., 2013).

Biochar is the porous carbonaceous solid residue obtained during the thermochemical treatment of raw biomass (Chiappero et al., 2020). The addition of biochar or carbon-based materials, such as activated carbon or carbon nanotubes, to the AD process, has several advantages since they promote the direct interspecies electron transfer (DIET), which is advantageous both for quality and for the quantity of biogas (Rasapoor et al., 2020). The biochar can act as an electron carrier or conductor to favor electron transfer and the conversion of ethanol or VFA to methane can be accelerated in the presence of biochar inside the digester (Chen et al., 2015). The properties of the biochar contribute to the mitigation of ammonia inhibition (D. Wang et al., 2017) and offer an immobilization matrix, which allows the improvement of the anaerobic process (Xu et al., 2015). In addition to these advantages, the biochar characteristics can be shaped according to the specific applications for this product (Chiappero et al., 2020), thus obtaining a highly efficient inorganic additive for the anaerobic degradation of complex wastes.

In the work by Shen et al. (2015), the advantages of the addition of biochar from corn stover to an anaerobic digester treating sludge were reported. The improvement in methane yield (by 7 %), in the biomethanation constant rate (by 8 %) and in the maximum methane production rate (by 28 %) demonstrates the potential of this material to improve the AD process. In addition, this material also presented characteristics that enable the increase in alkalinity and the reduction in the inhibition caused by high ammonia contents, providing a stable process for the degradation of organic matter (Shen et al., 2015).

To date, several other works have been published regarding the addition of inorganic materials to anaerobic treatment systems to improve their performance. The application of new materials, which can act as a support medium for microbial growth, as a buffer material for the control of pH inside the digester and, at the same time, can provide trace elements in stimulatory concentrations for the enhancement of the activity of microorganisms, is the most recent challenge for the control of anaerobic processes.

2.6.2 Geopolymer spheres as new pH buffering materials

2.6.2.1 Definition and applicability of geopolymers

During the 1950s, Victor Glukhovsky developed new alkali-activated systems containing calcium silicate hydrate and alumino-silicate phases, which were used in building construction in Russia, at the time of World War II. This scientist was the first to report that the geological transformations of some volcanic rocks into zeolites occur during the formation of sedimentary rocks at low pressure and temperature and that this approach can be applied to create new cement systems (Komnitsas and Zaharaki, 2007). Glukhovsky called these alkaline alumino-silicate cement systems “soil silicates” or “soil cements” (Krivenko and Kovalchuk, 2007). In these materials, alkalis act not only as activators of hydration, but also participate in the formation of durable products, very similar to natural zeolites (Dawczyński et al., 2016).

In 1972, French Professor Davidovits, who was inspired by Glukhovsky's investigations, named the tri-dimensional alumino-silicates structures that are formed in low-temperature conditions in a short time, as “geopolymers” (Komnitsas and Zaharaki, 2007). The term “geopolymerization” has also been suggested to describe the process of polycondensation of alkaline aluminosilicate cement systems in an artificial stone with a three-dimensional polymeric structure similar to that of natural zeolites (Krivenko and Kovalchuk, 2007). Davidovits based his research on the ability of the aluminum ion to induce crystallographic and chemical changes in a silica backbone, thus obtaining a mineral polymer from other natural mineral polymers (Davidovits, 1988).

Nowadays, several names are used to describe these alkaline materials, such as “alkali-bounded-ceramics”, “hydroceramics” and “alkali-activated-cements” (Komnitsas and Zaharaki, 2007). The most appropriate name describing these materials is “inorganic polymers” (Gameiro et al., 2020), and for these work, these alkaline materials are referred to only as “geopolymers”. In all cases, alkali-activation is an essential step for the development of these materials (Komnitsas and Zaharaki, 2007).

Geopolymers are inorganic aluminosilicate polymers synthesized by the alkaline activation of Si- and Al-rich materials at room temperature (Komnitsas and Zaharaki, 2007) or at temperatures below 100 °C, with very little CO₂ emissions (Zhuang et al., 2016). They are amorphous or quasi-crystalline gels with a three-dimensional network structure (Tang et al., 2015). The composition of raw materials and alkaline solutions used in the geopolymerization process, as well as curing conditions, determine the microstructure and mechanical properties of geopolymers (Singh, 2018; Zhuang et al., 2016).

The synthesis of geopolymers comprises three main sources, namely raw materials, inactive filler and geopolymer liquor. Raw materials are the main source of aluminosilicates and may be of natural mineral source or industrial waste materials such as fly ash or slag, rich in silicon and aluminum (Hardjito et al., 2004). The inactive filler is used in geopolymerization, as a source of aluminum; kaolinite or metakaolinite is generally used (Komnitsas and Zaharaki, 2007). Geopolymer liquor is the alkaline hydroxide solution required for the dissolution of raw materials. Sodium or potassium silicate solution act as a binder, alkali activator and dispersant in geopolymerization. The mixture of the aluminosilicate powder with the alkaline solution forms a paste that quickly turns into a hard geopolymer (Komnitsas and Zaharaki, 2007).

For synthesis, geopolymers do not require calcium-silicate-hydrate gel, but the polycondensation of silica and alumina precursors is used to achieve a higher level of resistance (Toniolo and Boccaccini, 2017). During the geopolymerization reaction, the following steps can be involved and can occur simultaneously (Singh, 2018):

- Si and Al atoms in fly ash can be dissolved by the action of hydroxide ions;
- Precursor ions can be converted into polymeric structures;
- Monomers can be polycondensed in polymeric structures.

Geopolymers are similar to zeolites in terms of chemical composition (Hardjito et al., 2004) and the chemical reactions involved, although the resulting products are different in structure (Komnitsas and Zaharaki, 2007). Table 12 lists the main differences between geopolymers and zeolites. To achieve optimum mechanical strength, an amorphous structure of a geopolymer is preferable. For special applications, a crystalline or semi-crystalline structure is suitable, since the crystals are more resistant to acid attack or thermal shock (Krivenko and Kovalchuk, 2007). The geopolymerization reaction with NaOH proved to be favorable for the formation of more crystalline and stable geopolymers, whereas the use of sodium silicate activator generates geopolymers with amorphous structures and less acidic stability (Singh, 2018).

Table 12| Comparison between geopolymers and zeolites, regarding main characteristics and synthesis processes (Hardjito et al., 2004; Komnitsas and Zaharaki, 2007).

Geopolymers	Zeolites
Tightly packed polycrystalline structure due to shorter setting and hardening time	Cage-like structure due to growth in a well-crystallized structure
Products without stoichiometric composition	Products with stoichiometric composition
Better mechanical properties	Lower density
Geopolymerization process: (1) leaching (2) diffusion (3) condensation (4) nanocrystalline and amorphous phase formation (5) hardening	Zeolite synthesis: (1) prenucleation (2) nucleation (3) crystal growth
Low-temperature requirements for geopolymerization process	High-temperature requirements for zeolite synthesis
Factors affecting the synthesis: pH, temperature, cations presence	Factors affecting the synthesis: pH, temperature, cations presence

The main factors affecting the synthesis of both geopolymers and zeolites are temperature, pH and the presence of cations (mainly calcium) (Komnitsas and Zaharaki, 2007). However, other factors also affect the geopolymerization process, namely the type and characteristics of the raw materials, the amount of aluminum and silicon, the presence of iron, calcium and other inert particles (mainly from fly ash), the curing conditions, type and concentration of the alkaline solution and water content (Singh, 2018).

In addition to the several advantages of geopolymers, compared to Portland cement, these inorganic polymeric types of cement have better mechanical, chemical, thermal and durability properties (Singh, 2018). The production process of geopolymers consumes 60 % less energy compared to the productive process of Portland cement, reducing emissions of CO₂ by more than three times. These materials are produced according to the principles of sustainable development (Komnitsas and Zaharaki, 2007), reducing the emissions of CO₂. Thus, geopolymers represent an eco-friendly innovative alternative to Portland cement, due to the low-cost materials and use of waste instead of large amounts of virgin resources such as limestone, clay and water needed for the Portland cement manufacturing process. Therefore, geopolymers have the potential to be used in widespread application fields, such as refractory filters, lightweight panels for thermal and acoustic insulation, low-cost ceramics and fire protection structures (Toniolo and Boccaccini, 2017).

In addition to substituting Portland cement in the construction sector, geopolymers can be used in several applications. Many studies have focused on the application of geopolymers as soil stabilizers (Abdullah et al., 2020), as photocatalysts in the degradation of pollutants (Zhang and Liu, 2013), as metal immobilization materials for catalytic reactions (Sazama et al., 2011), as catalysts in wastewater treatment (Ge et al., 2015) or as adsorbents in the removal of metals from industrial wastewater (Tang et al., 2015). New applications regarding the use of these innovative materials as enhancers of AD processes have been explored in recent years (Gameiro et al., 2020, 2019a; Novais et al., 2018c).

2.6.2.2 Fly ash-based geopolymers

The partial replacement of metakaolin as a source of aluminosilicate has been widely explored by several authors. The importance of geopolymeric binders is related to the use of waste materials, produced in large amounts in agriculture and industries (Singh, 2018). The use of fly ash as a source of aluminosilicates has a high potential for reducing costs associated with the geopolymers production, for incorporating wastes and reducing energy losses, and the materials can be incorporated additionally in the building construction (Novais et al., 2016a). In addition, the solidification of fly ash in geopolymers leads to the immobilization of potentially toxic metallic elements, simplifying the handling of this waste (Zhuang et al., 2016).

According to Novais et al. (2016a), the main advantages of geopolymers that incorporate fly ash in their composition are the use of low cost and green technology production practices, their non-flammable and high thermal stability, are safe for humans and demonstrate high resistance in freezing/thawing cycles, thus allowing a wide variety of applications and demonstrating a huge potential for the application of these innovative materials in the construction sector. The type and concentration of alkaline solutions, used in the geopolymerization process, influence directly the hydrolysis level of fly ash and the porosity of the geopolymeric structure. The porosity level influences the migration of alkali from the fly ash-based geopolymer into the solution. It also influences moisture and affects several properties of geopolymers, such as mechanical strength and durability (Zhuang et al., 2016).

The addition of a pore-forming agent (also called foaming agent or blowing agent) allows to control and increase the pore formation in geopolymers (Novais et al., 2016a). Due to the presence of a pore-forming agent, gases are developed and trapped in the structure of the materials before the gel

hardens (Singh, 2018). The increase in the amount of pore-forming agent (such as hydrogen peroxide, aluminum, silicon, limestone, among others), leads to an increase in the average area and the total area of the pores, also increasing the area proportion, leading to the formation of a highly porous material (porous geopolymer). The amount of pore-forming agent also determines the number of pores to be formed per mm², which decrease with the increase of the concentration of the pore-forming agent (Novais et al., 2016a). In addition, the water content, the binder nature or the curing temperature also determines the properties of porous geopolymers (Novais et al., 2020).

Several authors have studied the use of fly ash-based geopolymers as an eco-friendly alternative binder for soil stabilization. This solution replaces the need for Portland cement in the environmental and construction sectors, allowing the recycling of industrial wastes and, ultimately, reducing the carbon footprint associated with traditional soil chemical stabilization techniques (Abdullah et al., 2020). In addition, fly ash-based geopolymers are also used for the absorption and immobilization of potentially toxic elements, such as Ba, Cd, Co, Cr, Cu, Nb, Ni, Pb, Sn, and U (Zhuang et al., 2016).

2.6.2.3 Red mud-based geopolymers

In addition to fly ash as an aluminosilicate source in the production of geopolymers, other materials can be incorporated, such as clays, zeolite, silica fume (Singh, 2018), metallurgical slags (Novais et al., 2020), rice-husk ash, palm oil ash (Toniolo and Boccaccini, 2017) and also red mud wastes (Novais et al., 2019), to improve the reactivity of fly ash and the performance of geopolymers (Zhuang et al., 2016).

Red mud waste is an ideal precursor to produce geopolymers with a low carbon footprint, since its intrinsic alkalinity makes it difficult to incorporation into Portland cement mixtures (Novais et al., 2019), making alkali-activation advantageous (Gameiro et al., 2020). The use of red mud wastes as the only source of aluminosilicates in geopolymerization is difficult, due to the very low molar ratio of silicon to aluminum and the low amorphous phase of red mud (Toniolo and Boccaccini, 2017). The addition of red mud to the composition of fly ash-based geopolymers can adjust the SiO₂/Al₂O₃ molar ratio and reduce the amount of alkali activator needed for the geopolymerization process (Zhuang et al., 2016). This reduction of alkaline materials also reduces emissions of GHG, mainly CO₂.

The main challenge is to use waste materials both as a solid precursor and as an activator, which can contribute to cleaner production methodologies and towards the sustainability of wastewater treatment technologies and anaerobic digestion systems (Novais et al., 2020). Novais and co-workers, using fly ash from burning biomass and red mud from alumina refining as a source of aluminosilicates, developed a 100 % waste-based geopolymer. This innovative material has the potential to be used as a pH buffer material in biological systems and has the potential to promote prolonged pH control due to the continuous leaching of OH⁻ ions. A red mud content of up to 60 % has been used successfully, but the increase of red mud content above that value has negatively affected the spherical shape of the geopolymers. The very good performance regarding the alkalis leaching, only surpassed by geopolymers where a higher alkaline activators content of heat treatment was performed, ensures a more eco-friendly and cost-effective alternative for the geopolymers technology (Novais et al., 2018a).

2.6.2.4 Use of geopolymers as pH buffering materials in anaerobic digestion

Maintaining a narrow pH range in AD is a challenge, especially when using substrates with high organic loads due to rapid acidification, which hinders the methanogenesis step. To overcome the expected drop in systems efficiency, two approaches are commonly used: i) alkaline pre-treatment of wastes; or ii) addition of buffer materials to the AD reactor (Novais et al., 2018c). The most common approach to buffering the pH of AD systems is the addition of commercial alkaline powders, such as sodium hydroxide (NaOH) or calcium carbonate (CaCO₃). Nevertheless, this strategy can only ensure pH stabilization in the short-term and acidification can occur again when the alkaline materials are depleted (D. Wang et al., 2017). In addition, chemical additives cannot be recovered after exhaustion in the AD process.

In recent years, an innovative and greener alternative has been reported, which was the use of waste-containing geopolymer monoliths (Novais et al., 2016c) or spheres (Novais et al., 2017) that acted as pH regulators. When immersed in water, these materials leach significant amounts of hydroxide ions from their structure, which remained after the manufacturing. The presence of hydroxide ions provides a prolonged pH adjustment, which ensures a narrow pH fluctuation. Other investigations have shown that alkalis leaching from geopolymers can be controlled by the activator concentration (Z. Zhang et al., 2014), nature of the binder (Novais et al., 2017), solid-liquid ratio (Bumanis and Bajare, 2014) and porosity of geopolymers (Novais et al., 2016b).

However, all the studies mentioned have evaluated the ability of geopolymers to buffer the pH in an aqueous medium, which presents obvious differences when compared to a complex mixed liquor in an AD system. Thus, geopolymers have the potential to be applied as pH buffering materials in systems such as the anaerobic treatment systems. Despite the promising results obtained by Novais et al. (2016b) testing water, the report of the use of geopolymers in AD systems is very rare. Novais et al. (2016b) also suggested that the geometry of geopolymers has a major impact on their leaching behavior, and the use of spheres instead of discs or cubes favored the leaching of alkalis, due to the increase in the exposed area (Novais et al., 2016b). This pattern has been observed using both fly ash-based geopolymers and red mud-based geopolymers, demonstrating an advantage of using mm size spheres as pH buffering materials (Novais et al., 2020).

Ru gele and colleagues tested the addition of a composite alkaline material to an AD system treating cheese whey. This inorganic additive, with properties similar to geopolymers, acted as a buffer material and improved the methane formation during the digestion process (Ru gele et al., 2015a, 2014). In another work published by the same authors, the effect of the addition of alkaline-activated aluminosilicate material (cubic specimens) on the anaerobic degradation of cheese acid whey was described. A similar effect was achieved, with an improvement in anaerobic degradation by 22 % in comparison with reactors without the composite material, maintaining the pH values in an optimum range to favor methanogenesis, thus increasing the methane yield and the methane formation rate (Ru gele et al., 2015b).

The results reported here demonstrate the potential of using geopolymers in biological treatment processes, instead of commercial alkaline materials, to increase the efficiency and stability of processes such as anaerobic digestion. The potential of these materials (fly ash-based geopolymers and red mud-based geopolymers) was first reported in the present work, and the most relevant results have already been published (Gameiro et al., 2020, 2019a; Novais et al., 2018c).

Methodology | 3

3 | Methodology

To accomplish the goals proposed in this work, laboratory-scale anaerobic assays were operated in batch and fed-batch mode. The current section describes the main characteristics of the anaerobic inoculum, substrates and additives used. It also presents details of the bioreactors set-up and the experimental conditions studied, all the physico-chemical analysis carried out during the experimental work, as well as the calculations performed to evaluate the performance of the developed bioprocesses.

3.1 Inoculum

To be used as an inoculum in the operation of anaerobic bioreactors, the biomass was collected in an anaerobic mesophilic (38.2 °C) digester operating in a municipal WWTP in Ílhavo, Aveiro, Portugal. This WWTP (Figure 18) receives municipal and industrial effluents from Aveiro, Ílhavo, Mira and Vagos, and treats about 39000 m³ of effluent per day (Águas do Centro Litoral, 2019). The WWTP is equipped with two primary mesophilic digesters (3000 m³ each) and a secondary mesophilic digester (1370 m³).

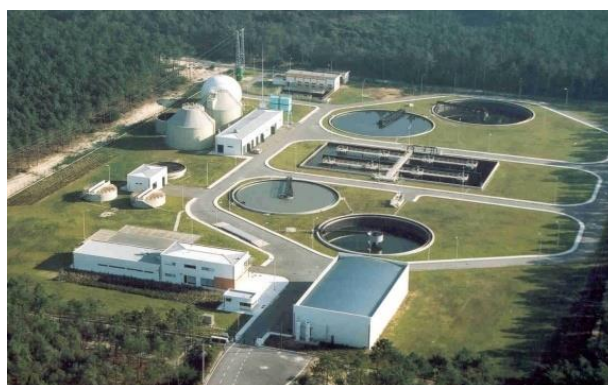


Figure 18| WWTP in Ílhavo, where the anaerobic inoculum was collected (picture by AdCL, 2019).

After collection, the anaerobic biomass was washed three times with water, to keep endogenous activity low. The excess water was removed by decanting and the sludge was preserved at 4 °C until use (no more than 1 month). Prior to use, anaerobic biomass was characterized in terms of total and volatile suspended solids, the content of soluble organic matter, pH and alkalinity. The physico-chemical characterization of the anaerobic biomass used as an inoculum in the anaerobic assays is found in Table 13.

Table 13| Physico-chemical characterization of the anaerobic biomass used as an inoculum in the AD assays (average value ± standard deviation).

TSS (g/L)	VSS (g/L)	% VSS	Moisture (%)	sCOD (gO₂/L)	pH	Alkalinity (mg/L as CaCO₃)
28.10 (± 0.28)	21.85 (± 0.18)	77.7 (± 0.21)	97.19 (± 0.22)	< 0.100	7.50 (± 0.01)	2350 (± 125)

3.2 Substrates

During the experimental work, two different substrates were tested: D₀, a bleaching effluent from a pulp and paper industry, and cheese whey, a by-product of a dairy industry. These two effluents are very different in terms of physico-chemical characteristics and the main compounds present, although both have a complex matrix, which can cause a problem in the implementation of a biological valorization process.

3.2.1 Bleaching effluent from pulp and paper industry (D₀ effluent)

The effluent from the first acidic stage of the bleaching process of Kraft pulp production, called D₀, was used in anaerobic batch assays. This effluent was collected in a large P&P mill industry in Portugal. This P&P mill operates with a 4-stage ECF bleaching process (bleaching sequence: D₀E_pD₁D₂, where D₀ is the chlorine dioxide stage, E_p is the alkali extraction with hydrogen peroxide, D₁ is the chlorine dioxide in stage 1 and D₂ is chlorine dioxide in stage 2). After collection, D₀ effluent was preserved at 4 °C and protected from light until use (no longer than 1 month). The physico-chemical characterization of D₀ effluent is shown in Table 14.

Table 14| Physico-chemical characteristics of D₀ effluent (average value ± standard deviation).

Parameter	Value	Parameter	Value	Parameter	Value
TSS (g/L)	0.27 (± 0.001)	TCOD (gO ₂ /L)	3.64 (± 0.68)	Ca (ppm)	448.4
VSS (g/L)	0.26 (± 0.007)	sCOD (gO ₂ /L)	3.43 (± 0.63)	Mg (ppm)	5.5
pH	2.21 (± 0.25)	BOD (mgO ₂ /L)	176.2 (± 10.0)	Fe (ppm)	1.1
AOX (mg/L)	86.6 (± 15.0)	Biodegradable fraction (%)	5.2	Na (ppm)	294.6
P (mg/L)	6.97 (± 0.38)				

Prior to use in AD experiments, D₀ effluent was diluted considering the theoretically defined organic load to be studied in each assay. For this calculation, the sCOD of the effluent was measured and the volume to be added to each bioreactor was determined as a function of the sCOD measured and the theoretically defined organic load. For example: taking into account the characteristics shown in Table 14, for a batch bioreactor with 200 mL of the working volume and considering 1.00 gO₂/L of applied organic load, the following volume of D₀ effluent was added to the mixture:

$$C_i \cdot V_i = C_f \cdot V_f \Rightarrow 3.43 \cdot V_i = 1.00 \cdot 200 \Rightarrow V_i = 58 \text{ mL} \quad (24)$$

In the first assays performed with D₀ effluent, to determine the anaerobic biodegradability of this effluent, the pH was adjusted to 7.0 with the addition of a 1 M NaOH solution. In the assays carried out to study the influence of the addition of fly ash, the pH was adjusted by adding a defined amount of ash, until it reached neutral pH values.

3.2.2 By-product from cheese manufacturing (cheese whey)

Cheese whey is the main by-product of the dairy industry, in the manufacture of cheese or casein from milk. For this work, a Portuguese company that produces cheese, located in Aveiro district, Portugal, supplied dehydrated cheese whey. In that company, cow's milk is the raw material for cheese production. From the manufacturing process of cheese, the resulting liquid fraction is called whey, which is concentrated and dehydrated prior to subsequent use. The company provided the main physico-chemical characteristics of the cheese whey, as well as the organoleptic parameters (color, odor and visual observation) and these characteristics are shown in Table 15.

Table 15| Physico-chemical characteristics and organoleptic parameters of cheese whey powder (provided by the cheese whey producer).

Physico-chemical parameter	Value	Organoleptic parameters	Description
Moisture	< 4 %	Color	White; yellowish
Ash	< 8.5 %	Odor	Weak
Total Proteins	11 %	Visual observation	Homogeneous; without impurities
Total Fat	< 1.5 %		
Titrateable Acidity	< 0.17 %		
Nitrites	Absent		
Lactose	> 70 %		
pH	6.2 – 6.7		

To perform the anaerobic experiments, a concentrated cheese whey solution was prepared by dissolving 150 g of powdered cheese whey in about 700 mL of distilled water. After 1 h of magnetic stirring at room temperature, the concentrated solution was diluted to 1000 mL and maintained at 4 °C until use (no more than five days). The physico-chemical parameters regarding pH and alkalinity, solids and organic matter content of the prepared concentrated whey solution were determined for all the prepared cheese whey solutions and the physico-chemical characterization is found in Table 16.

Table 16| Characterization of concentrated cheese whey solution used in AD assays (average value \pm standard deviation).

Parameter	Value	Parameter	Value	Parameter	Value
TSS (g/L)	30.9 (\pm 1.03)	TCOD (gO ₂ /L)	123.5 (\pm 2.21)	Ca (ppm)	73.8
VSS (g/L)	28.7 (\pm 0.90)	sCOD (gO ₂ /L)	106.8 (\pm 0.62)	Mg (ppm)	89.4
% VSS	92.7 (\pm 0.54)	BOD (gO ₂ /L)	72.9 (\pm 0.06)	Fe (ppm)	0.6
pH	5.69 (\pm 0.05)	Biodegradable fraction (%)	59.0 (\pm 0.42)	Na (ppm)	649.7
Alkalinity (mg/L as CaCO ₃)	1300 (pH _{final} = 4.49)	VFA (gO ₂ /L)	11.1 (\pm 1.14)	Mn (ppm)	0.2

For the AD assays, COD was the reference parameter and was measured for all prepared concentrated cheese whey solutions. The volume to be added to each AD bioreactor was determined in function of COD measured and the theoretically defined organic load (see the volume calculation as presented in Equation 24).

3.3 Inorganic Additives for pH control

The control of pH in an anaerobic process is vital for its stability. For this work, two types of additives were used with the main goal of buffering the culture media: powder, namely fly ash (FA) from biomass combustion and geopolymer spheres (GS), using fly ash or red mud residues as a basis for the manufacture of spherical materials.

Table 17 lists the chemical composition of inorganic additives used in anaerobic assays. It is shown the characterization of the FA obtained from different biomass sources used in this work as a powder additive, named CA5 and CTB fly ashes. These FA powders came from two different biomass boilers, which burn different wood and non-wood biomass. It is also shown the chemical composition of the FA, metakaolin (MK) and red mud (RM) used as raw materials in the preparation of different geopolymer spheres (FA-based and RM-based).

Table 17 | Chemical composition of FA obtained from different biomass sources (CA5 and CTB), used as a powder additive for AD experiments, FA used as a source of aluminosilicates in the manufacture of geopolymer spheres, in addition to metakaolin and red mud residues. The elemental composition of the materials was determined by XRF and is expressed as oxides. LOI was performed at 1100 °C.

Oxides (wt.%)	CA5 Ash	CTB Ash	Fly Ash ¹	Fly Ash ²	Metakaolin	Red mud ³
SiO ₂	3.93	34.38	25.34	33.1	54.4	5.67
TiO ₂	0.15	0.77	0.60	0.71	1.55	9.41
Al ₂ O ₃	1.50	10.53	6.05	13.3	39.4	14.63
Fe ₂ O ₃	1.41	5.19	4.15	5.32	1.75	52.25
MgO	1.66	3.20	3.61	3.35	0.14	0.08
CaO	22.73	26.11	36.72	22.2	0.10	1.88
MnO	0.70	0.55	0.42	0.57	0.01	0.06
Na ₂ O	26.15	1.38	0.95	1.68	-	4.82
K ₂ O	7.25	6.51	5.84	5.67	1.03	0.08
SO ₃	2.61	2.64	3.84	3.87	-	0.32
P ₂ O ₅	0.52	1.19	4.70	1.25	0.06	0.53
LOI	15.85	5.88	-	7.05	2.66	9.44

¹ FA used to produce geopolymer spheres used in 1-cycle batch assays

² FA used to produce geopolymer spheres used in 2-cycle and 4-cycle batch assays (low and high porosity)

³ Values from Novais et al. (2018a)

3.3.1 Fly ash from biomass combustion

Powder fly ash was used in this work as an inorganic additive, mainly to promote pH control in AD bioprocesses, using cheese whey or D₀ effluent as substrates. The FA (powder) used was collected from the residual biomass combustion equipment, in an industrial thermal power plant near Aveiro, Portugal.

For the f Phase 1 assays, two different ashes from different biomass sources were studied as an inorganic additive. CA5 FA powder came from a biomass-boiler that burns only Eucalyptus bark and CTB FA powder came from a boiler that burns several types of wood and non-wood biomass, such as olive and grape pomace, cuttings and sawdust, among other raw materials.

For the assays of Phase 2, the FA was collected from the biomass burning (mainly Eucalyptus forest residues), in a fluidized bed combustor located in a Portuguese thermal plant. These FA were

used as an aluminosilicate precursor in the preparation of geopolymeric spheres. In the preparation of FA-based geopolymers, metakaolin, whose chemical composition was included in Table 17, was also used in different proportions as a source of aluminosilicates, as explained below.

3.3.2 Waste-based geopolymer spheres

The geopolymer spheres were the material chosen to replace the use of chemical compounds (such as carbonates or sodium hydroxide) and to upgrade and optimize the use of fly ash powder as a source of alkalis in the AD process. They were selected since the agglomerates produced can be easily recovered and the release of minerals is controlled during the incubation time.

Figure 19 depicts the two types of GS used: FA-based (a) and RM-based (b) geopolymers. In the next sub-sections, the manufacturing process for both GS types is detailed. The CICECO group of “Biorefineries, biobased materials and recycling” from the Department of Materials and Ceramic Engineering at the University of Aveiro, prepared the buffer materials used in this experimental thesis work.

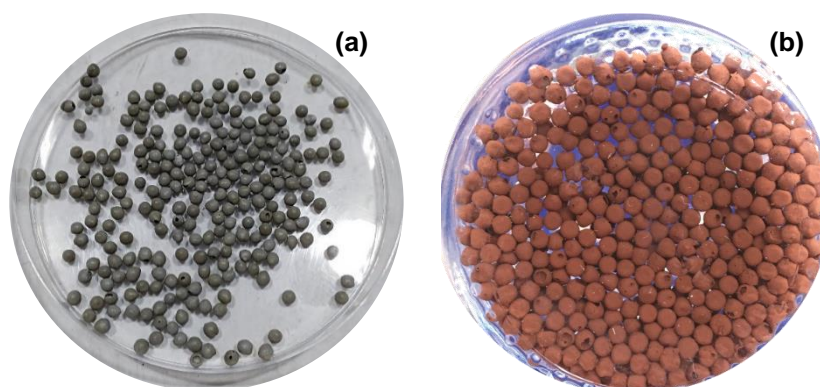


Figure 19 Geopolymer spheres used in AD assays: (a) FA-based geopolymer spheres; (b) RM-based geopolymer spheres.

3.3.2.1 Fly ash-based geopolymer spheres

FA from biomass combustion (see section 3.3.1) was used to produce the FA-based geopolymer spheres. The received FA contains a very broad particle size distribution that would hinder the geopolymer slurry injection to produce GS. For this reason, prior to mixing, the FA particles were sieved and then only the fraction with a particle size below 63 μm was used.

In the first phase, two different compositions were prepared, in which MK (Argical™ M1200S; Univar) was partially (33 and 75 wt.%) replaced by FA as a geopolymerization precursor. The compositions prepared and used in this work were selected considering the GS leaching behavior in water, reported by Novais et al. (2017). The alkaline activator was previously prepared by adding 13.22 g of NaOH to 100 g of sodium silicate solution with a ratio $\text{SiO}_2/\text{Na}_2\text{O}=3.09$. Then, the mixture of the alkaline solution, distilled water, MK and FA (quantity depending on the defined composition) was carried out in a planetary mixer. After that, the foaming agent (sodium dodecyl sulfate, $\text{CH}_3(\text{CH}_2)_{11}\text{OSO}_3\text{Na}$), was added to the blend and mixed to obtain a foamy slurry. The details of the mixture compositions prepared to be used in this study are shown in Table 18.

Table 18| Mixture composition of MK and FA-based geopolymers during their preparation.

GS type	FA content (wt. %)	Mixture proportion (g)				
		FA	MK	Alkaline activator	H ₂ O	Foaming agent
MK – based	33	5.0	10.0	24.4	4.15	0.59
FA – based	75	11.25	3.73	24.4	4.15	0.59

Finally, the slurry was injected in a polyethylene glycol (H(OCH₂CH₂)_nOH) (PEG) media under a bath temperature of 85 ± 5 °C, to induce curing in the specimens and produce geopolymeric spheres. The spheres were then collected and cured under controlled conditions, at 40 °C and 65 % relative humidity, for 24 h, using a climatic chamber. After this initial curing period, the spheres were placed at room temperature and cured, prior to being used in the AD batch experiments.

In the second phase, two different compositions were prepared with different levels of porosity. The GS were synthesized through suspension solidification, following the procedure described in detail by Novais et al. (2017). The activating solution, composed of a mixture of sodium hydroxide and sodium silicate, was added to the solid components used as aluminosilicates sources (FA and MK) and to a constant amount of water. The components were mixed thoroughly for 2 min. Then, the foaming agent, whose content depends on the formulation and the level of porosity (Table 19), was added to the slurry and blended for another 5 min, to produce a homogeneous paste. The geopolymeric slurry was injected into a PEG medium and the spheres were immediately collected, washed with distilled water, and cured for 24 h at 40 °C and at 65 % relative humidity. After this initial period, the spheres were cured under room conditions until the 28th day.

Table 19| Mixture composition in the preparation of geopolymers with low and high porosity.

GS type	Mixture proportion (g)				
	FA	MK	Alkaline activator	H ₂ O	Foaming agent
Low porosity GS	10.0	10.0	24.4	4.15	0.59
High porosity GS	10.0	10.0	24.4	4.15	0.75

The initial studies with GS to control pH in batch bioreactors (Novais et al., 2018c) addressed the influence of the chemical composition of the raw materials on the pH buffering capacity of the produced GS. Accordingly, for this second approach, the FA/MK ratio was kept constant across all compositions (Table 19). The amount of foaming agent in the GS composition was intentionally different to study the influence of the porosity of the spheres on the pH buffer capacity (Novais et al., 2016a).

3.3.2.2 Red mud-based geopolymer spheres

Red mud-based geopolymer spheres were prepared according to the methodology described by Gameiro et al. (2020). The red mud (RM) was supplied by a bauxite mining company and used as a source of alumina for the formation of geopolymers. Prior to use, the RM was dried, milled and sieved to obtain particles below 75 µm in size. FA from biomass combustion was collected as described previously (see section 3.3.1) and was used as a source of silica. Prior to alkaline activation, FA was sieved to obtain particle sizes below 63 µm. The solid precursors were activated using commercial sodium silicate and sodium hydroxide. Sodium dodecyl sulfate was used as a foaming agent and polyethylene glycol as the consolidation medium.

The RMGS were synthesized as the method reported by Novais et al. (2017), who report the injection of inorganic polymer slurry into a hot bath to ensure rapid consolidation. The composition of the spheres used to perform the anaerobic tests was selected considering previously published works that evaluated the performance of RMGS in aqueous media (Novais et al., 2018a). The composition of the mixture for RM-based GS synthesis is detailed in Table 20.

Table 20| Mixture composition of red mud-based GS containing 50 % of RM waste.

GS type	Mixture proportion (g)				
	FA	RM	Alkaline activator	H ₂ O	Foaming agent
RMGS	10.0	10.0	15.0	4.15	0.30

A blend of equal amounts of FA and RM wastes was alkali-activated using the mixture of alkaline activators and water. The mixing of solid components with the activator was performed in a planetary mixer for 2 min. The foaming agent was added to the slurry and mixed during 5 min. The foamed paste obtained was injected into a PEG medium to produce the porous spheres. After formation, the spheres were collected and cured for 24 h at 40 °C in a plastic container, to avoid rapid dehydration. The remaining 27 days of curing were at room temperature and in an open flask.

3.4 Nutrients supplementation

The composition of the mixtures prepared for both micro and macronutrients solutions are specified in Table 21.

Table 21| Composition of micro and macronutrients solutions added to all anaerobic bioreactors (composition adapted from Van Lier et al., 1997).

Micronutrients solution			Macronutrients solution		
Inorganic compound	Element	Concentration (µg/L)	Inorganic compound	Element	Concentration (mg/L)
FeCl ₂ .6H ₂ O	Fe	403	NH ₄ Cl	N	86.80
CoCl ₂ .6H ₂ O	Co	483	KH ₂ PO ₄	P	16.46
MnCl ₂ .4H ₂ O	Mn	135	CaCl ₂ .2H ₂ O	Ca	4.25
CuCl ₂ .2H ₂ O	Cu	11	MgSO ₄ .7H ₂ O	Mg	1.73
ZnCl ₂	Zn	23		S	2.28
H ₃ BO ₃	B	9			
(NH ₄) ₆ Mo ₇ O ₂₄ .4H ₂ O	Mo	48			
Na ₂ SeO ₃ .5H ₂ O	Se	29			
NiCl ₂ .6H ₂ O	Ni	12			
EDTA (C ₁₀ H ₁₆ N ₂ O ₈)	EDTA	976			

Micro and macronutrients solutions were added to the reaction medium of the AD assays, in order to avoid a lack of essential nutrients for microbial growth, which can affect the efficiency of the biological system (McCarty and Smith, 1986). The addition of nutrients is essential to stimulate the growth and the activity of methanogenic microorganisms (Bougrier et al., 2018; Guo et al., 2019), ensuring the success of the anaerobic treatment. For micronutrients, 1 mL of solution was added per 1 L of the reaction medium, while for macronutrients, 2 mL of solution was added per 1 L of the reaction medium.

3.5 Bioreactors set-up and operational conditions

To achieve the goals defined for this work, different types of bioreactors were assembled. To test several different conditions at the same time and choose the conditions to be applied later, 250 mL bioreactors (*oxitop*) were used and operated in batch mode. On a larger scale, 1 L glass bioreactors were used, operated in batch and fed-batch mode, to perform long-term operations using FA-based geopolymers. The 5 L glass bioreactors were used in sequential fed-batch mode, also to perform long-term operations with RM-based geopolymers.

3.5.1 *Oxitop* System

3.5.1.1 *Experimental set-up*

The *oxitop* system (WTW OxiTop®-C) used in AD batch experiments is depicted in Figure 20. The *oxitop* system consists of a glass vessel/reactor (number 2 in Figure 20) with a working volume of 200 mL and a total volume of 260 mL, with two side openings (number 3 in Figure 20) for biogas or liquid sampling, closed with rubber septum seals. A measuring head (number 1 in Figure 20), programmed to measure the pressure variation caused by the production of biogas, was attached to the top of the glass vessel. Also in the upper part, stuck between the measuring head and the glass vessel a small lid adapter with rack and seal containing KOH pellets, was inserted, for promoting the absorption of CO₂.



Figure 20| *Oxitop* system used in batch anaerobic assays and sample flasks. 1) Measuring head; 2) Glass sample vessel; 3) Nozzle and septum seal.

The values were recorded on a portable wireless controller (WTW OxiTop® OC 110 controller), which receives the infrared signal from the measuring heads. The bioreactors were incubated at a temperature of 36 ± 1 °C in an oven (WTC™ Binder E28) and were magnetically stirred on a shaking platform (WTW OxiTop® IS-12), during the entire experiment. To prevent exposure to air, an oxygen-free gas (100 % N₂) flushing was applied for at least 5 min in the sealing procedure for anaerobic bioreactors, prior to incubation.

3.5.1.2 Operational conditions applied using oxitop system

The *oxitop* system was used to test several different conditions at the same time. For this type of reactors, anaerobic sludge (see section 3.1) was used as an inoculum, with an initial VSS concentration of 2 ± 0.2 g/L, which is within the range of values reported in previous studies in batch AD of different wastewaters (Silva et al., 2013; Vergine et al., 2015). Micro and macronutrient solutions were added (see section 3.4) to each reactional mixture tested. The substrate (D_0 effluent or cheese whey) was added according to the defined concentration, as listed in Table 22 for the assays with fly ash (powder) addition, and in Table 23 for the assays with GS addition. The concentration of spheres is expressed as the mass of this material added per liter of bioreactor.

Table 22 | Main operational conditions for anaerobic *oxitop* batch assays with fly ash (powder) addition, testing D_0 and cheese whey as substrates.

	Bioreactor ID	Inorganic Additive	Inorganic additive concentration (g/L)	Substrate concentration (gO ₂ /L)	Chemical alkalinity concentration (mg/L as CaCO ₃)
D₀	D0_0.9	NaOH	(to pH=7.0)	0.9	-
	D0_1.2	NaOH	(to pH=7.0)	1.2	-
	D0_1.5	NaOH	(to pH=7.0)	1.5	-
	D0_1.8	NaOH	(to pH=7.0)	1.8	-
	D0_2.9	NaOH	(to pH=7.0)	2.9	-
	D0_2	NaOH	(to pH=7.0)	2.0	-
	D0_3	NaOH	(to pH=7.0)	3.0	-
	D0+CA5	FA (CA5)	4.97	2.0	-
	D0+CA5f	FA (CA5)	4.97	2.0	-
	D0+CTB	FA (CTB)	17.2	2.0	-
D0+CTBf	FA (CTB)	17.2	2.0	-	
Cheese Whey	CW_0	Blank	-	8.0	-
	CW_Alk2	Reference	-	8.0	2000
	CW_Alk4	Reference	-	8.0	4000
	CW_0.07	FA (CA5)	0.07	8.0	-
	CW_0.15	FA (CA5)	0.15	8.0	-
	CW_0.2	FA (CA5)	0.2	8.0	-
	CW_0.5	FA (CA5)	0.5	8.0	-
	CW_1.5	FA (CA5)	1.5	8.0	-
	CW_3	FA (CA5)	3.0	8.0	-
	CW_3.5	FA (CA5)	3.5	8.0	-
	CW_4	FA (CA5)	4.0	8.0	-
	CW_4.5	FA (CA5)	4.5	8.0	-
	CW_5	FA (CA5)	5.0	8.0	-
	CW_7	FA (CA5)	7.0	8.0	-
	CW_9	FA (CA5)	9.0	8.0	-

As shown in Table 22, the first seven assays with D_0 effluent used different concentrations of D_0 in the reactional mixture. This set of tests was carried out to study the inhibitory effect of AOX (present in high concentrations in this effluent) on methane production, COD removal and AOX removal. For such tests, 1 M NaOH solution was added directly to the D_0 effluent to neutralize its pH (± 7.0), and

no FA was used as an additive to adjust the pH of the effluent. The bioreactors were incubated for at least 21 days.

The second set of *oxitop* tests with D₀ effluent tested the addition of two fly ashes from different biomass sources, CA5 and CTB (see description on section 3.3.1), with the best substrate concentration of the previous assays. The comparison between the two different ashes made it possible to choose the type of ash to be used in cheese whey *oxitop* bioreactors. For these assays, since the pH of D₀ effluent was very low (approximately 2), the ashes were added directly to the effluent, until reaching neutral pH; after that, the - D₀ effluent neutralized with ash was used to make the incubation mixture, with anaerobic biomass as inoculum and micro and macronutrients (assays D0+CA5 and D0+CTB). A part of the mixture of D₀ effluent and fly ashes was filtered and the filtered fraction was used as a substrate in the assays D0+CA5f and D0+CTBf, studying the influence of the presence of fly ash during the AD process.

With cheese whey as a substrate, several *oxitop* bioreactors were performed, with different amounts of fly ash to promote pH buffering. In these assays, a blank assay was performed, without the addition of FA or chemical alkalinity (CW_0), and two different concentrations of chemical alkalinity were tested as reference assays (CW_Alk2 and CW_Alk4) for comparison with the assays with the addition of fly ash as pH regulator. Concerning the FA addition, concentrations between 0.07 and 9.0 g/L of FA powder were added to the bioreactors. The addition of FA was performed directly to the reactional mixture, composed by anaerobic biomass, concentrated cheese whey solution and micro and macronutrients solutions, and prior to the incubation.

As shown in Table 23, the *oxitop* bioreactors R0 – R14 were operated with the addition of GS as a pH buffer material. In these bioreactors, two types of spheres (MK-based or FA-based spheres) were added in different amounts (20, 40 and 80 g/L) to evaluate the influence of the binder characteristics (MK-based or FA-based) and quantity of spheres on the pH evolution of the AD system. These bioreactors were incubated for 21 days. This experiment was used to select the type and quantity of spheres for the study of methane production in larger assays (1 L working capacity, FA1 – FA3).

Oxitop bioreactors R15 – R24 were performed to test different porosities of FA-based geopolymer spheres: high porosity vs low porosity geopolymer spheres. For this test, different amounts of spheres (8 - 24 g/L of LPGS and 16 – 20 g/L of HPGS) were used, in order to obtain a pH control of the anaerobic system in the methanogenic range (6.5 to 7.2), promoting the formation of methane and evaluating the influence of the porosity of the spheres in the production of methane. A blank assay was also performed, without the addition of GS or chemical alkalinity (R15), and two different concentrations of chemical alkalinity were tested as reference assays (R16 and R17). The bioreactors were incubated for 21 days. These *oxitop* bioreactors were performed to select the conditions to be applied in larger volume assays (FA4 – FA7).

Oxitop bioreactors R25 – R28 (Table 23) were performed to test different concentrations of RMGS, namely 20 (R26), 30 (R27) and 40 g/L (R28) as buffer material in the cheese whey AD, to reach the suitable pH values of the methanogenic range. The bioreactor R25 was incubated as a reference, using the addition of chemical alkalinity (4 g/L). The bioreactors were incubated for 35 days. These *oxitop* bioreactors were performed to select the conditions to be applied in larger volume assays (RM1, RM2 and RM3).

Table 23 | Operational conditions for anaerobic *oxitop* batch assays with geopolymer spheres (FA-based, MK-based, LPGS, HPGS and RMGS) addition and cheese whey as substrate.

	Bioreactor ID	Inorganic Additive	Inorganic additive concentration (g/L)	Substrate concentration (gO ₂ /L)	Chemical alkalinity concentration (mg/L as CaCO ₃)
Cheese Whey	R0	Blank	-	8.0	-
	R1	Reference	-	8.0	2000
	R2	Reference	-	8.0	4000
	R3	FA-based	20	8.0	-
	R4	FA-based	20	8.0	-
	R5	FA-based	40	8.0	-
	R6	FA-based	40	8.0	-
	R7	FA-based	80	8.0	-
	R8	FA-based	80	8.0	-
	R9	MK-based	20	8.0	-
	R10	MK-based	20	8.0	-
	R11	MK-based	40	8.0	-
	R12	MK-based	40	8.0	-
	R13	MK-based	80	8.0	-
	R14	MK-based	80	8.0	-
	R15	Blank	-	8.0	-
	R16	Reference	-	8.0	2000
	R17	Reference	-	8.0	4000
	R18	LPGS	8	8.0	-
	R19	LPGS	12	8.0	-
	R20	LPGS	16	8.0	-
	R21	LPGS	20	8.0	-
	R22	LPGS	24	8.0	-
	R23	HPGS	16	8.0	-
	R24	HPGS	20	8.0	-
	R25	-	-	8.0	4000
	R26	RMGS	20	8.0	-
	R27	RMGS	30	8.0	-
R28	RMGS	40	8.0	-	

3.5.2 Batch and fed-batch bioreactors

3.5.2.1 Bioreactors set-up

Glass bioreactors with 1 L and 5 L of working volume were used to study a long-term operation, with GS (FA-based or RM-based) as a pH buffer material and comparing its efficiency with the addition of chemical alkalinity. The reactor set-up for these assays is shown in Figure 21.

The glass bioreactors (1), with 1 L or 5 L of working volume, had a sampling point (2), to collect liquid samples with a 20 mL syringe (3) during the incubation time. The addition of substrate, in fed-batch assays, was performed with a 50 mL syringe, inserted at the sampling point (2). The bioreactors were placed in a water bath (5), using a thermostat (4) to control the temperature at 36 ± 2 °C and were manually stirred once a day. The bioreactors also had a biogas outlet point (6), with a bypass rubber (7) to collect 2 mL of biogas samples. The biogas produced was washed (8) in

acidified water and the volume of gas produced was displaced in the separation funnel (9) and measured in the graduated cylinder (10).

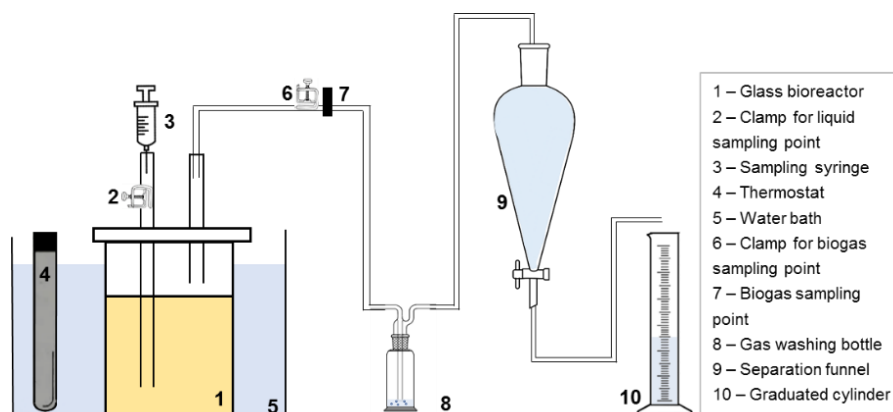


Figure 21| Scheme of batch and fed-batch bioreactors set-up, including the water displacement system used to measure the biogas volume produced in anaerobic assays.

3.5.2.2 Operational conditions of batch and fed-batch bioreactors

The batch (discontinuous) bioreactors were operated with only one addition of substrate, at the beginning of the experiment. Thus, for this type of reactor, only one operating cycle was performed. In sequential fed-batch mode, the substrate was added more than once, when the sCOD remaining in the liquid phase was <1 gO₂/L or until the total substrate depletion. The initial organic load applied to all batch/fed-batch bioreactors was 8 ± 0.5 gO₂/L, corresponding to a relatively high organic load, so that a rapid VFA accumulation could be achieved towards acidification, creating an unbalanced system. Micro and macronutrient solutions were added to all bioreactors operated in accordance with that described in section 3.4. During the sealing procedure, the anaerobic bioreactors were flushed with nitrogen gas to remove any residual O₂, during 15 to 20 min. The main operating conditions for these batch/sequential fed-batch bioreactors are detailed in Table 24.

Table 24| Operational conditions for anaerobic batch/fed-batch assays with geopolymers spheres addition (FA-based, LPGS, HPGS and RMGS).

	Bioreactor ID	Inorganic Additive	Inorganic additive concentration (g/L)	Chemical alkalinity concentration (mg/L as CaCO ₃)	Number of AD cycles
Cheese Whey	FA1	-	-	-	1
	FA2	FA-based	20	-	1
	FA3	FA-based	28	-	1
	FA4	-	-	4000	2
	FA5	LPGS	12	-	2
	FA6	LPGS	12	-	2
	FA7	HPGS	16	-	2
	FA8	-	-	4000	4
	FA9	HPGS	16	-	4
	FA10	HPGS	16	-	4
	RM1	-	-	-	11
	RM2	-	-	2000	11
	RM3	RMGS	15	-	11

The blank assays named FA1 and RM1 were performed without the addition of alkaline chemicals or spheres, while a buffer solution of NaHCO_3 and KHCO_3 was used to promote pH autoregulation in three other reference anaerobic fed-batch assays, to achieve 2 g/L (RM2) and 4 g/L (FA4 and FA8) of initial alkalinity measured as CaCO_3 . In the other eight assays, GS (FA-based, HPGS, LPGS or RMGS) were added in different amounts, as shown in Table 24.

The first assays (FA1 – FA3) were operated to evaluate the buffering capacity of FA-based geopolymers with two different GS concentrations and one AD cycle. In this 1 L batch bioreactors, operated during 70 days until the substrate is completely consumed, several physico-chemical parameters were monitored, focusing on methane production and pH buffering capacity. Anaerobic sludge was added to a VSS concentration of 2.7 ± 0.3 g/L.

The second assays (FA4 – FA7), performed after R15 – R25 *oxitop* bioreactors, were designed to access the performance of the GS as pH regulators in comparison to a reference (chemical addition of alkalis) in two successive AD cycles. After a period of 55 days (1st AD treatment cycle) and after reaching the reduction of almost all added sCOD (concentration below 1 gO_2/L), a similar amount (8 ± 0.5 gO_2/L) of concentrated cheese whey solution was added. This corresponds to the beginning of the 2nd AD treatment cycle. The bioreactors were then incubated until reaching again a concentration of sCOD below 1 gO_2/L , totaling 87 days of incubation. Following the preliminary studies, in which the concentration of spheres to be added to the bioreactors was evaluated, four different assays were carried out. GS were added to the other three assays (FA5 – FA7) to assess their potential as a pH buffer material. To study the influence of the porosity of the spheres on the pH evolution, two types of spheres were used in equal concentration (16 g/L). A fourth reactor containing a lower concentration (12 g/L) of the low porosity spheres (LPGS) was prepared to also evaluate the impact of the sphere's concentration on the AD process. Anaerobic sludge was added to a VSS concentration of 2.5 ± 0.3 g/L.

After the assays FA4 – FA7, to study a prolonged operation with high porosity GS, assays FA8, FA9 and FA10 were performed. During 128 days of operation, four substrate additions were made, each with 8 gO_2/L of the organic load of the concentrated cheese whey solution. The substrate was added to each bioreactor when sCOD concentration was less than 1 gO_2/L . The 1st AD cycle had the longest cycle in these assays, 47 days; the following AD cycles lasted for 30, 24 and 25 days. The GS used and its concentration are related to the best results obtained in the previous fed-batch assays FA4 – FA7: high porosity FA-based geopolymer spheres at 16 g/L of concentration. Anaerobic sludge was added as an inoculum, at a VSS concentration of 2.5 ± 0.3 g/L.

Following the preliminary studies performed in *oxitop* batch bioreactors (R26 – R29), in which the concentration of red mud spheres to be added to the bioreactors was evaluated, three different 5 L fed-batch bioreactors were assembled. Assays RM1, RM2, and RM3 were designed to test the capacity of RMGS to control the pH in a methanogenic pH range and keep the anaerobic system balanced, even with organic load shocks. In the RM2 reactor, 2 g/L measured as CaCO_3 were added to provide chemical alkalinity to the medium and, in the RM3 reactor, 15 g/L of RMGS were used to provide pH buffer for the anaerobic system.

The bioreactors were operated in fed-batch mode with eleven substrate additions in 110 days of incubation. Prior to incubation, the anaerobic sludge was acclimatized during 36 h at 36 ± 1 °C, in order to decrease the lag phase of the AD process and, thus, promote a faster accumulation of methane.

The amount of sCOD added at the beginning of each AD cycle had different values and the concentrations were chosen according to the behavior of the AD systems during their operation. Figure 22 depicts the different additions of the substrate, expressed as gO₂/L, during the time for the RM fed-batch assays. The theoretical variations of the food-to-microorganisms (F/M) ratio during the experiment are also inserted in the blue dashed line in Figure 22. The theoretical F/M ratio was determined considering the added organic matter (measured as gO₂/L) and the microorganism's concentration estimated by the VSS determination in anaerobic sludge used as an inoculum in digesters.

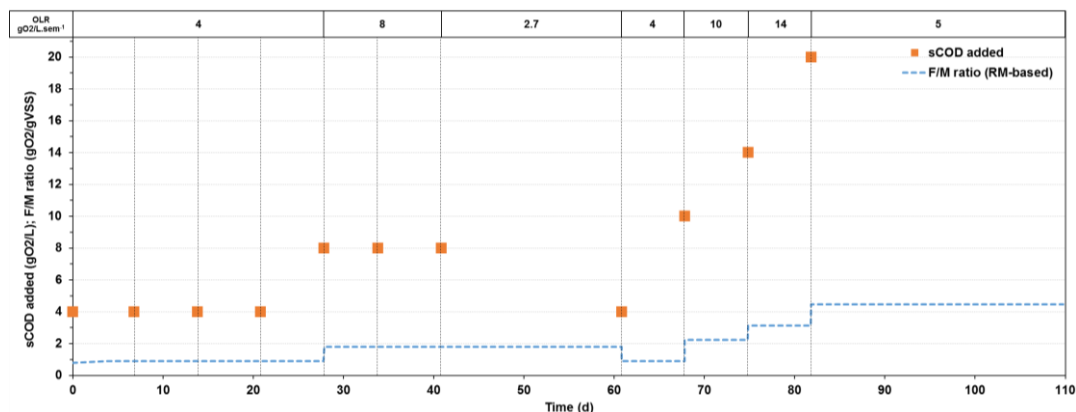


Figure 22 | Substrate additions performed (expressed as gO₂/L) and theoretical F/M ratio in 5 L fed-batch AD reactors treating cheese whey, with RMGS as buffer material.

The AD cycles had a duration of one week each, except for the 7th AD cycle (3 weeks) and the 11th AD cycle (4 weeks). These differences in the cycle's duration were due to the instability of the system observed by the low pH and without removal of sCOD, which was promoted by the high organic load from cheese whey addition. Anaerobic sludge was added at a VSS concentration of 4.5 ± 0.3 g/L, representing an initial F/M ratio of 0.9 gO₂/gVSS.

3.6 Methodologies for monitoring the anaerobic digestion process

During the experimental work, several physico-chemical parameters were determined, to monitor the evolution of the anaerobic processes performed. For all operated bioreactors, gas and liquid samples were collected periodically and the physico-chemical analysis followed the procedure outlined in Figure 23.

The gas samples were analyzed by gas chromatography to determine the content of methane (and carbon dioxide). The liquid sample was divided into three fractions:

- Total liquid fraction: this sample contains a replica of the content of the corresponding bioreactor, at a given time, and is formed by biomass, particulate and soluble organic matter and inorganics present in the reactional media. In this sample, pH and alkalinity, total chemical oxygen demand, total and volatile suspended solids were determined.
- Soluble liquid fraction (after filtration): this sample mainly contains the soluble fraction of the reactional medium, including soluble organic matter and inorganics. In this sample, it

was determined: soluble chemical oxygen demand, phosphorous, adsorbable organic halides, volatile fatty acids and metals, such as Ca, Mg, Na and Fe.

- Soluble liquid fraction (after centrifugation): in this sample, which mainly contains the soluble fraction of the reactional medium, it was determined the biochemical oxygen demand – 5 days.

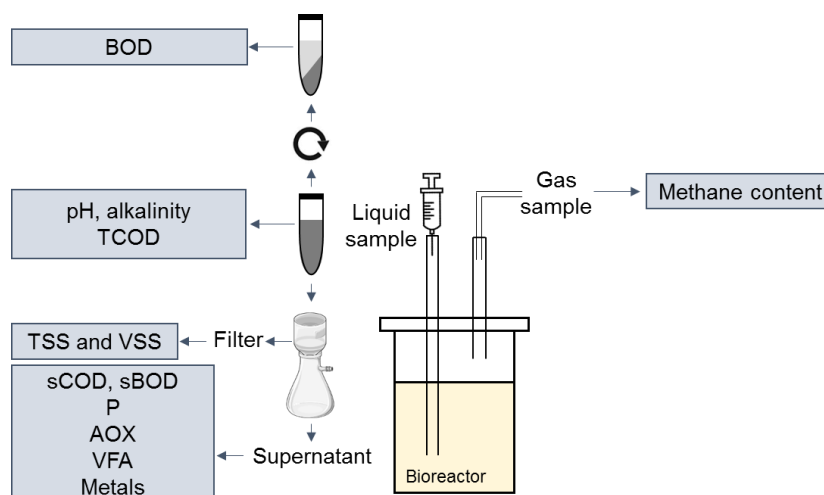


Figure 23| Flowchart for the sampling methodology applied to bioreactors' samples.

In the next sub-sections, the methodologies for the determination of physico-chemical parameters to evaluate the performance of anaerobic bioreactors are described, including also the methodology to characterize the materials used as inorganic additives, that is, FA powder or inorganic geopolymeric spheres.

3.6.1 pH, alkalinity and conductivity measurements

The pH of the samples was measured using a portable Consort™ P602 pH-meter equipped with a xerolite electrode (Consort™). The calibration of the pH-meter was performed periodically with commercial solutions at pH = 4.01 and pH = 7.00 (25 °C). The electrode was stored in a 3 M solution of KCl.

The alkalinity of a sample is its acid-neutralization capacity, that is, the sum of all the titratable bases (Mattson, 2014). It is considered an indicator of the concentration of carbonate, bicarbonate, and hydroxide since these compounds contribute a lot to the alkalinity of a sample. Typically, alkalinity in a stable anaerobic digester is in the range of 2000 to 4000 mg/L as calcium carbonate (CaCO₃) (Pohland and Bloodgood, 1963).

For the determination of alkalinity, the standard methodology (method 2320-B) was followed, applying the potentiometric titration method (APHA et al., 2017). 50 mL of the sample without dilution of the filtration was titrated with a standard solution of 0.1 M HCl. During the titration process, the sample was gently stirred magnetically. The pH was monitored during the titration and the chosen end-point was 4.5. To calculate the alkalinity of the samples, Equation 25 was used:

$$\text{Alkalinity} \left(\frac{\text{mg}}{\text{L}} \text{ as } \text{CaCO}_3 \right) = \frac{A \times N \times 50\,000}{V} \quad (25)$$

Where:

A = volume of standard acid used (mL),

N = normality of standard acid used in titration (N),

V = volume of sample tested (mL).

The conductivity of a given sample is a measure of the capacity to carry an electric current, being dependent on the presence of ions. Conductivity was measured in the samples using a conductivity meter (Hanna instruments EC215) and a potentiometric conductivity probe with an internal temperature sensor. The measurement was performed at 25 °C.

3.6.2 Chemical Oxygen Demand (COD)

The chemical oxygen demand (COD) is defined as the amount of a specific chemical oxidant that reacts with the organic fraction of the sample, susceptible to chemical oxidation under controlled conditions. This analysis is a good measure of organic pollution in a sample since organic matter “consumes” dissolved oxygen. The amount of chemical oxidant consumed is expressed in terms of oxygen equivalents.

For liquid samples, COD was determined by the closed reflux colorimetric method (method 5220-D) (APHA et al., 2017), using an adapted spectrophotometer (Aqualytic™ COD Vario PC compact). For total COD (TCOD), the samples were decanted and then diluted to be analyzed. For soluble COD (sCOD), the samples were filtered using 47 mm glass microfiber filters (Whatman Reeve Angel™ grade 403). Measurements were performed in triplicate for both TCOD and sCOD.

The COD range used for the analyzed samples was between 100 and 900 mgO₂/L, being necessary to dilute the concentrated samples. The samples were digested with an excess of chemical oxidant (dichromate) in acidic conditions, in sealed glass tubes (Aqualytic™ COD vario) for 2 h at 150 °C, using a thermoreactor Aqualytic AL125. The mixture contained the organic sample, chemical oxidant (potassium dichromate), sulfuric acid, silver sulfate to increase the oxidation of larger organic compounds, and mercury sulfate to reduce chlorine interference. The solutions used were prepared according to (APHA et al., 2017).

After cooling to room temperature, the tubes were shaken slightly and absorption was measured in a spectrophotometer ($\lambda = 620$ nm), using distilled water as blank. The readings were converted directly into mgO₂/L by the spectrophotometer and the calibration was performed periodically with standards of potassium hydrogen phthalate (KHP). After use, the tubes were washed in a 20 % nitric acid solution and distilled water and dried in an oven at room temperature.

3.6.3 Biochemical Oxygen Demand – 5 days (BOD₅)

The biochemical oxygen demand (BOD) test is widely used to measure the organic waste loading, mainly in WWTP. In this test, it is measured the molecular oxygen used during a specified incubation period for the biochemical degradation of organic material (carbonaceous demand) and the oxygen used to oxidize inorganic material such as sulfides and ferrous iron.

In this work, the measurement of oxygen consumed in a 5-day test period (BOD_5) was selected. For BOD_5 , the methodology was adapted from the method 5210-B of Standard Methods (APHA et al., 2017). Bacterial growth requires nutrients such as nitrogen, phosphorus, and trace metals and, for this reason, nutrient solutions have been added to the samples. The solutions added in the preparation step were described in detail in (APHA et al., 2017). Measurements for BOD_5 determination were performed in duplicate.

The apparatus used for the BOD respirometric determination (VELP Scientifica™ BOD sensor System 10), including the Ambar flasks and the pressure sensor, are shown in Figure 24.



Figure 24| Respirometric BOD system used to determine BOD_5 .

The BOD_5 range used was 0 – 600 mgO₂/L for samples with D₀ effluent as substrate and 0 – 1000 mgO₂/L for samples with cheese whey as substrate. If BOD_5 values are expected to be higher than the range limits, the samples were diluted in distilled water before incubation. For all samples, the pH was adjusted to 7.0 ± 0.3 using 1 M solutions of sulfuric acid and sodium hydroxide. To remove disinfectant agents from the samples, 2-3 drops of 0.025 N sodium sulfite solution were added to the neutralized sample. About 1 mL of aerobic seed was added to all samples before incubation. 1 mL of nutrients solutions, such as phosphate buffer solution, magnesium sulfate solution, calcium chloride solution and ferric chloride solution, were also added to the samples.

The Ambar color flask is used to prevent the growth of photosynthetic microorganisms and the blue head is a pressure transducer that converts the reading into oxygen consumed values, in mgO₂/L, after a defined time. On the top of the flask, a small rubber container (alkali holder) was inserted, where KOH pellets were inserted, to absorb the CO₂ fraction in the gas. The blue BOD sensor automatically saves five BOD values (measured in ppm or mg/L), with an interval of 24 h between them. The flasks were magnetically stirred in a 10-position stirring unit and kept at a controlled temperature of 20 ± 1 °C in an oven WTW TS 606/4-I, during the incubation period.

The calculation of the real BOD_5 is performed as showed in Equation 26, and considers the reading obtained in the sample and the blank (distilled water) flasks:

$$real\ BOD\ (mgO_2/L) = (sample\ BOD_5 - blank\ BOD_5) \times dilution \quad (26)$$

With the characterization of sCOD and soluble BOD (sBOD) of a sample, it is possible to define aerobic biodegradability, given by the ratio between the two parameters. The content of the biodegradable fraction of organic matter in a sample is described in Equation 27:

$$\text{Biodegradable fraction (\%)} = \frac{BOD}{sCOD} \quad (27)$$

3.6.4 Solids content

Solids refer to matter suspended or dissolved in water (or wastewater) and are a good indicator of the quality of water resources. "Total solids" is the term applied to the material residue left in the ceramic crucible after the evaporation of a sample and its subsequent drying in an oven at a defined temperature. Total solids include "total suspended solids", the portion of the total solids retained by a filter and "total dissolved solids", the portion that passes through the filter. In this work, only the total suspended solids (TSS) was determined. "Fixed solids" is the term applied to the residue of total, suspended, or dissolved solids after heating to dryness for a specified time, at a specified temperature. Weight loss on ignition is called "volatile solids". For this work, only volatile suspended solids (VSS) were determined.

3.6.4.1 Total Suspended Solids (TSS)

For TSS determination, a well-mixed sample is filtered through a weighed standard glass-fiber filter and the residue retained on the filter is dried to a constant weight at 103 to 105 °C. The increase in the weight of the filter represents the TSS. In all TSS determinations, three replicates were performed, based on method 2540-D of Standard Methods (APHA et al., 2017).

Firstly, the ceramic crucibles with 47 mm glass microfiber filters (Whatman Reeve Angel™ grade 403) were dried at 550 °C during 1 h in a furnace (Thermolab™ Fuji PXR-9); after that, the ceramic crucibles were cooled to room temperature in a desiccator and weighted in an analytical scale (Precisa™ XB 120A) (m_{crucible}).

The liquid samples were magnetically stirred and a known sample volume (V_{sample}) was vacuum filtered (Welch Ilmvac™ vacuum pump) using the weighted filters. After filtration, the filter was transferred to the ceramic crucible and dried at 104 °C (WTC™ Binder E28) during 24 h, to ensure a constant weight. The dried filter within the ceramic crucible was cooled to room temperature in a desiccator and weighted (m_{oven}).

To calculate the TSS of a sample, Equation 28 was used:

$$TSS \left(\frac{g}{L} \right) = \frac{m_{\text{oven}} - m_{\text{crucible}}}{V_{\text{sample}}} \quad (28)$$

Where:

m_{oven} = weight of filter within the crucible + dried residue at 104 °C (g),

m_{crucible} = weight of filter within the crucible (g),

V_{sample} = volume of sample filtered (L).

From the TSS calculation, it can be determined the moisture content of each sample, as presented in Equation 29:

$$\text{Moisture (\%)} = 100 - (TSS \times 100) \quad (29)$$

3.6.4.2 Volatile Suspended Solids (VSS)

The remaining solids resulting from the ignition of the residue from TSS determination represent the fixed total, dissolved, or suspended solids while the weight lost on ignition is the volatile solids. This determination is useful in controlling the WWTP operation because it offers a rough approximation of the amount of organic matter present in the solid fraction of wastewater, activated sludge, and industrial wastes. In all VSS determinations, three replicates were performed, based on method 2540-E of Standard Methods (APHA et al., 2017).

The crucible with the filter and the dried residue was ignited in a muffle furnace at 550 °C during 2 h, ensuring the constant weight. After the ignition, the ceramic crucibles were cooled to room temperature in a desiccator and weighted (m_{muffle}).

To calculate the VSS of a sample, Equation 30 was used:

$$VSS \text{ (g/L)} = \frac{m_{oven} - m_{muffle}}{V_{sample}} \quad (30)$$

Where:

m_{muffle} = weight of filter within the crucible after ignition at 550 °C (g).

From TSS and VSS calculations, it can be determined the volatile solids fraction in the samples, as presented by Equation 31:

$$\% VSS = \frac{VSS}{TSS} \times 100 \quad (31)$$

3.6.5 Total phosphorous as orthophosphates

Phosphorus occurs in natural waters and wastewaters almost exclusively as phosphates, classified as orthophosphates, condensed phosphates (pyro-, meta-, and other polyphosphates), and organically bound phosphates.

Of the various forms of phosphorous that can occur in a liquid mixture, only the total dissolved phosphorous determined as orthophosphates have been measured here, hereinafter called phosphorous (P). The methodology followed the standard method 4500-P-E – Ascorbic acid method (APHA et al., 2017). The methodology includes two steps: acid digestion, to convert the phosphorus form of interest into dissolved orthophosphate, and a colorimetric determination of dissolved orthophosphates.

The ascorbic acid method was chosen due to the range (0.01 to 6 mg/L). The samples were diluted prior to analysis. The determination of P was performed in the soluble fraction of the samples and the analysis was performed in duplicate. All glassware was washed with hot diluted HCl solution and then washed several times with distilled water prior to use.

For the digestion step, 100 mL of sample (or diluted sample) was transferred to an Erlenmeyer flask. While stirring, 21 mL of HCl and 7 mL of HNO₃ were added slowly to the sample, preventing foaming, and the mixture was left at rest until effervescence stopped, to react at room temperature. Some boiling regulators were added, and the mixture was digested in a sand bath (P Selecta™ Combiplac) until the volume was reduced to approximately 10 mL. After cooling, the edges of the flasks were washed with 20 mL of water and the mixture was heated again until it boiled. After 5 min,

the flasks were left at rest and cooled to room temperature. The digested mixture was filtered, transferred to a 100 mL volumetric flask and the volume was corrected to 100 mL.

For the colorimetric determination of P, 20 mL were transferred to a glass beaker and the pH was adjusted to 7.0 ± 0.2 . Then, in a 50 mL volumetric flask, the neutralized sample and 8 mL of combined reagent (mixture of sulfuric acid, potassium antimony tartrate solution, ammonium molybdate solution and ascorbic acid solution) were added, and the volume was corrected to 50 mL. After 10 minutes (and no more than 30 minutes), the samples were homogenized and the absorbance ($\lambda = 880$ nm) was read against the digestion blank (distilled water) in a PGTM T80+ UV-Vis spectrophotometer.

For standard solutions (preparation details in Appendix 7.1), 25 mL of each solution were transferred to a 50 mL volumetric flask, it was added 8 mL of combined reagent and the volume was corrected to 50 mL. The absorbance reading was performed as for the samples. For the calibration curve, the absorbance vs phosphate concentration was plotted to provide a straight line passing through the origin (see an example of a calibration line in Appendix 7.1).

For the calculation of P concentration in the samples analyzed, measured as orthophosphates, Equation 32 was applied:

$$P \text{ (mg/L)} = \frac{P_{\text{colorimetric}} \times 1000}{V_{\text{sample}}} \quad (32)$$

Where:

$P_{\text{colorimetric}}$ = mg of P calculated by the calibration curve,

V_{sample} = volume of sample that was digested (mL).

3.6.6 Adsorbable Organic Halides (AOX)

Adsorbable organic halides (AOX) are a measure used to estimate the total amount of halogen organic material dissolved in a liquid sample. The adsorption-pyrolysis-titrimetric method for AOX determination used measures only the total molar amount of organically bound dissolved halogen retained in the activated carbon adsorbent. With this methodology, no information about the structure or nature of the organic compounds to which the halogens are bound or about the individual halogens present is given. It is sensitive to organic chloride, bromide, and iodide, but does not detect fluorinated organics.

The AOX content, determined only for assays with D_0 effluent as a substrate, was determined based on ISO 9562 (2004). When collected, the samples were acidified with 1 M HNO_3 . The mass concentration of organic halides is reported as an equivalent concentration of organically bound chlorine in micrograms per liter. All solutions used for AOX determination were described in detail in Appendix 7.2.

The method for AOX determination consists of four processes, namely:

- adsorption of organic compounds on activated carbon by orbital stirring;
- substitution of inorganic halides attached to activated carbon using a solution of sodium nitrate acidified with nitric acid;

- incineration of activated carbon and organic material adsorbed with oxygen (carrier gas) at 1000 °C, forming CO₂ and bound halogens to hydrogen halide (HX);
- microcoulometric titration of absorbed HX formed in the incineration step, measuring the current produced by silver-ion precipitation of the halides.

Firstly, 100 mL of homogenized sample/diluted sample and 5 mL of nitrate stock solution were transferred to a 250 mL Erlenmeyer flask. About 50 mg of high-quality activated carbon (TraceElementalParts™) was added and the mixture was orbital stirred during 2 h at 150 rpm (SCIOLOGEX™ SCI-O330-Pro).

The sample was then vacuum filtered using the Whatman™ 25 mm Nuclepore™ polycarbonate track-etched membrane (0.4 μm of pore size) and the filtrate cake was washed with a maximum of 25 mL of nitrate washing solution.

The filtrate cake and the membrane were transferred to a quartz boat in equipment for AOX determination (AOX/TOC analyzer ECS 1220 by Thermo Fisher Scientific™). The sample was oxidized at 1000 °C using oxygen as a carrier gas. The flue gases carrying halide ions were conducted through a sulfuric acid scrubber to remove water. The dry and clean gases containing H-X species formed during combustion were determined in the microcoulometric cell in the presence of silver ions. The amount of current needed to regenerate the lost silver ions was directly related to the AOX content in the sample, and the values were expressed in Coulomb (C). For the blank, distilled water was used and the preparation procedure was similar to the sample procedure.

For AOX concentration calculation, Equation 33 was used:

$$AOX \left(\frac{mg}{L} \right) = \frac{(Q_s - Q_0) \times M \times 1000}{V \times F} \quad (33)$$

Where:

Q_s = value measured by the argentometric analyzer for the sample (μC),

Q_0 = value measured by the argentometric analyzer for the blank (μC),

M = atomic relative mass of chlorine (35.45x10³ mg/mol),

V = volume of original sample analyzed (mL),

F = Faraday constant (96485.33x10⁶ μC/mol).

3.6.7 Volatile Fatty Acids (VFA)

The measurement of volatile fatty acids (VFA) is considered as a control test for the AD process. VFA's are classified as water-soluble fatty acids that can be distilled at atmospheric pressure and can be removed from the aqueous solution by distillation, despite their high boiling points, due to co-distillation with water. This group includes water-soluble fatty acids with up to six carbon atoms, and the species determined individually were acetic, propionic, iso-butyric, n-butyric, iso-valeric, n-valeric and n-caproic acids.

The quantification of the mentioned acids was performed by gas chromatography. The samples for VFA analysis were filtered using glass microfiber filters (Whatman Reeve Angel™ grade 403), acidified with 10 v/v% of formic acid and preserved at 4 °C until chromatographic analysis. The

analysis was performed by manually injecting 0.5 µL of a sample (or blank, distilled water) with a Hamilton 7000.5N syringe.

The chromatographic analysis was performed on a gas chromatograph PerkinElmer™ Clarus 480, with an injector set to 300 °C. The flame ionization detector was adjusted to 240 °C and used hydrogen and constituted air. A 25 m × 0.53 mm SGE™ ID-BP1 5.0 µm column was assembled in an oven set to 70 °C of initial temperature. Helium was used as a carrier gas at 4.5 psi. The temperature program used was as follows: 1 min at 70 °C, a rise of 20 °C/min to 100 °C and then kept for 2 min; a rise of 10 °C/min to 140 °C and kept for 1 min; a rise of 35 °C/min to 235 °C and kept for 6 min (18.21 min of the total running time).

The TotalChrom Navigator™ (v.6.3.2.0646) acquisition software performed data acquisition and integration of the peak area results. An example of a real chromatogram is shown in Figure 25. The identification of each peak was made considering the retention time for each VFA specie analyzed. The retention times were determined by injecting different dilutions of a concentrated solution with a known composition of standard acids – mixed solution with seven compounds under analysis. The calculation of the concentration of each component was based on each standard linear regression (an example of calibration curves is included in Appendix 7.3).

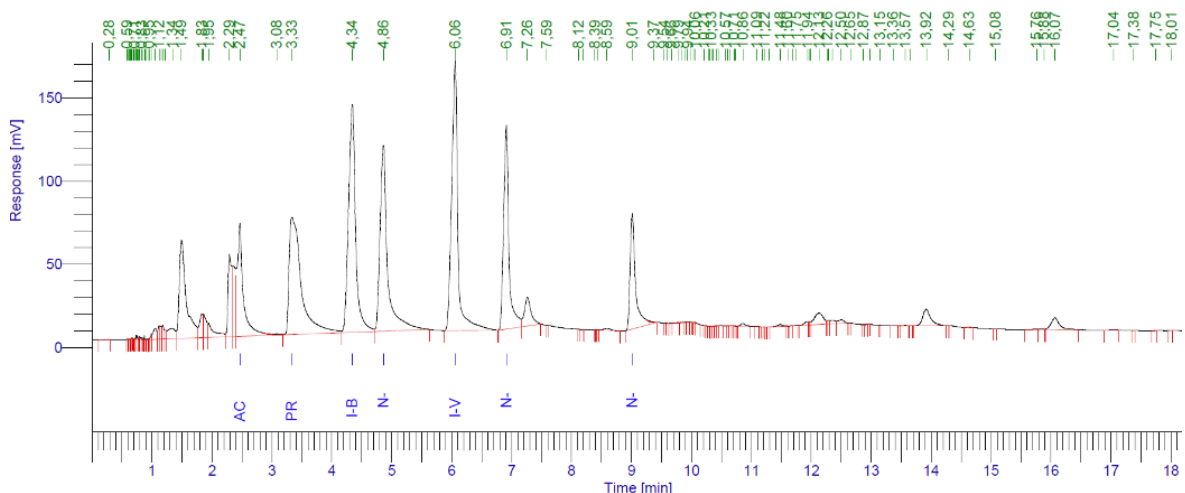
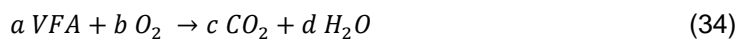


Figure 25] Example of a chromatogram obtained in VFA analysis (sample presented: standard solution P#4).

To standardize the results obtained, the VFA concentrations were expressed as COD equivalent. For that, the oxidation stoichiometry was used to convert the concentrations in g/L into COD equivalents, using theoretical oxygen demand (thOD). thOD was determined following Equations 34 and 35, and the values of thOD for each VFA specie analyzed are described in Table 25.



$$\text{thOD} \left(\frac{\text{gO}_2}{\text{gVFA}} \right) = \frac{b \times M_{\text{O}_2}}{a \times M_{\text{VFA}}} \quad (35)$$

Table 25| Theoretical oxygen demand (thOD) for the acidic species analyzed.

VFA specie	M (g/mol)	thOD (gO2/g)
H-Ac	60.05	1.066
H-Prop	74.08	1.512
H-i-But	88.11	1.816
H-n-But	88.11	1.816
H-i-Val	102.13	2.037
H-n-Val	102.13	2.037
H-n-Cap	116.16	2.204

3.6.8 Biogas composition (methane and carbon dioxide content)

During the AD process, biogas is produced mainly composed of methane (CH₄), carbon dioxide (CO₂) and a low amount of other gases including hydrogen (H₂) and hydrogen sulfide (H₂S). The gas-phase composition of the AD assays (CH₄ and CO₂ content) was performed by gas chromatography.

Samples from the bioreactors with a gas volume of 2 mL were analyzed in a SRI™ 8610C chromatograph, with a thermal conductivity detector set to 75 °C and a Haysep™ Q column (2.5 m x 2.1 mm) placed in an oven set to 61 °C. Helium was used as carrier gas at a flow of 10 mL/min. PeakSimple™ integration software (v.3.85) performed data acquisition and peak integration. The elution time for each sample was 5 min.

The calibration of the equipment was performed periodically using different volumes of pure CH₄ and CO₂ gases (Air Liquide™) and a molar mixture of 70:30 of the same gases. The remaining gases (N₂, H₂, H₂S) were not detected by the column used. The calculation for CH₄ and CO₂ content was performed according to the following equations:

$$CH_4 (\%) = 0.9896 \times \frac{A_{CH_4}}{A_{CH_4} + A_{CO_2}} \times 100 \quad (36)$$

$$CO_2 (\%) = 0.9924 \times \frac{A_{CO_2}}{A_{CH_4} + A_{CO_2}} \times 100 \quad (37)$$

Where:

A_{CH_4} = Area of the CH₄ peak,

A_{CO_2} = Area of the CO₂ peak.

3.6.9 Geopolymeric materials characterization

The characterization of geopolymeric materials was performed by the CICECO group of “Biorefineries, biobased materials and recycling” from the Materials and Ceramic Engineering Department at the University of Aveiro.

The morphology of the spheres was evaluated by optical microscopy (Leica EZ4HD microscope). Scanning electron microscopy (SEM - Hitachi S4100 equipped with energy dispersion spectroscopy, EDS – Rontec) was used, at 25 kV, to investigate the microstructure of the porous geopolymer spheres. *ImageJ* was used to measure the pore size and volume, providing the porous area distribution for each spheres composition, and the pore area ratio - A_r (sum of all pore areas divided

by the total sample area analyzed) (Novais et al., 2016a). The variation of the cumulative pore area ratio distribution with the agglomerate area provides a detailed statistical representation of the porous area distribution (described elsewhere (Novais et al., 2012)). For this analysis, eight spheres were evaluated and the average values were presented.

The mineralogical compositions of the geopolymer spheres were assessed by X-ray powder diffraction (XRD). The XRD was conducted on a Rigaku Geigerflex D/max-Series instrument (Cu-K α radiation, 10 – 80 °, 0.02 °, 2 θ step-scan and 10 s/step), and phase identification by PANalytical X'Pert HighScore Plus software. The raw materials chemical composition was determined by X-ray fluorescence technique (XRF, Philips X'Pert PRO MPD spectrometer) and the loss on ignition (LOI) was measured at 1100 °C, to estimate organic matter and carbonate content of the samples.

3.6.10 Metals (calcium, magnesium, iron, sodium and trace elements)

The determination of metals in liquid samples from anaerobic digesters, namely calcium (Ca), magnesium (Mg) and iron (Fe), was performed by flame atomic absorption spectrometry and was based on the methodology described by APHA et al. (2017), in the method 3111-B. The determination of sodium (Na) was performed by flame atomic emission spectrometry, based on the method 3500-Na B described in APHA et al. (2017). The determination of trace elements such as manganese (Mn), aluminum (Al), cobalt (Co), zinc (Zn), copper (Cu), molybdenum (Mo), nickel (Ni) and silicon (Si) was also performed by flame atomic absorption spectrometry, based on method 3111-B described by APHA et al. (2017).

Selected samples from anaerobic digesters were collected, filtered and the supernatant was used to determine the concentration of the dissolved metals. Until analysis, the filtered samples were preserved at 4 °C. Then, the samples were diluted prior to analysis, using the same acidified water used to prepare the standard solutions (see Appendix 7.4). The measurement was performed using a GBC™ 904 AA atomic absorption spectrophotometer equipped with hollow cathode lamps, specific for metals determination.

During the analysis, the samples were aspirated by a flow injection system, nebulized in a gas flame and analyzed. The standard calibration solutions were first analyzed to construct the calibration lines or curves and examples of those lines are presented in Appendix 7.4. After analyzing the sample, the concentration of each metal was determined using the calibration curve or lines. The wavelength and oxidant/fuel (gas) combination used for the determination of each element is detailed in Table 26.

Table 26| Wavelength and flame type used for metals determination.

Element	Wavelength (nm)	Flame type	Element	Wavelength (nm)	Flame type
Calcium (Ca)	422.7	Air-acetylene	Cobalt (Co)	240.7	Air-acetylene
Magnesium (Mg)	285.2	Air-acetylene	Zinc (Zn)	213.9	
Iron (Fe)	248.3	Air-acetylene	Copper (Cu)	324.8	Air-acetylene
Sodium (Na)	589.0	Air-acetylene	Molybdenum (Mo)	313.3	Nitrous oxide-acetylene
Manganese (Mn)	279.5	Air-acetylene	Nickel (Ni)	232.0	Air-acetylene
Aluminum (Al)	396.2	Nitrous oxide-acetylene	Silicon (Si)	251.6	Nitrous oxide-acetylene

3.7 Anaerobic process performance

The organic matter present in various types of waste can be decomposed under anaerobic conditions to form methane and carbon dioxide. The chemical reactions that take place in this transformation occur in two main steps: the complex organics are hydrolyzed and the VFA are formed (acidification step), and then, the acids are transformed into methane and carbon dioxide (methanization step).

In this subsection are presented the parameters determined to evaluate the AD process performance. These parameters were determined using one or more than one direct determination performed and described previously. It includes the organic matter and AOX content removal, process parameters associated with the acidification step, related to VFA production (degree of acidification, VFA yield and the fraction of VFA in the final effluent), and process parameters associated with the methanogenic step, focusing on methane production (methane volume, methanization degree, methane yield and anaerobic biodegradability), and on the kinetic model for methane production.

3.7.1 Organic matter removal

The organic matter removal was determined considering the initial sCOD measured and the final sCOD present at the end of the experiment, according to the following equation:

$$sCOD \text{ removal } (\%) = \frac{sCOD_{in} - sCOD_{final}}{sCOD_{in}} \times 100 \quad (38)$$

Where:

$sCOD_{in}$ = initial soluble chemical oxygen demand (gO₂/L),

$sCOD_{final}$ = final soluble chemical oxygen demand (gO₂/L).

3.7.2 Acidification step

3.7.2.1 Degree of acidification

The degree of acidification measures the performance of the acidogenic step of a given substrate by anaerobic degradation. This parameter represents the amount of solubilized organic matter that was converted into VFA, and was determined according to Equation 39 (Berhe and Leta, 2019). The TVFA represents the total VFA concentration expressed as theoretical equivalents of COD concentration as gO₂/L. The thOD values for each VFA specie were listed previously (Table 25).

$$\text{Degree of acidification } (\%) = \frac{TVFA}{sCOD_{in}} \times 100 \quad (39)$$

3.7.2.2 Volatile fatty acids yield and fraction in the effluent

The VFA yield was calculated as the amount of VFA produced during the acidogenic step, divided by the amount of substrate consumed in the process, as described by Gameiro et al. (2015), expressed as gO_{2VFA}/gO₂, as presented in Equation 40:

$$Y_{VFA/COD} = \frac{TVFA_{final} - TVFA_{in}}{(sCOD_{in} - TVFA_{in}) - (sCOD_{final} - TVFA_{final})} \quad (40)$$

Where:

$TVFA_{in}$ = initial total volatile fatty acids concentration (gO_{2VFA}/L),

$TVFA_{final}$ = final total volatile fatty acids concentration (gO_{2VFA}/L).

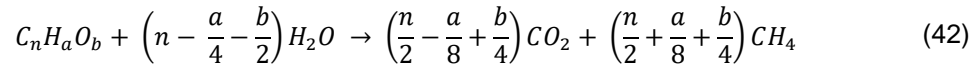
The VFA fraction of the effluent, that is, the composition in terms of VFA percentage of the net fraction of a sample, at time = n, is given by the following equation:

$$\% VFA = \frac{TVFA_{t=n}}{sCOD_{t=n}} \quad (41)$$

3.7.3 Methanization step

3.7.3.1 Methane volume

When the chemical composition of the waste is known, the theoretical methane yield potential can be determined in the oxidation-reduction reaction involving water, described by the stoichiometric formula developed by Buswell and Neave (1930) and represented in Equation 42. In this case, methane production is considered as the maximum stoichiometrically possible (Achinas and Euverink, 2016) and other metabolic routes for organic matter degradation are not considered.



Another approach to determine the theoretical methane volume is to use the COD values for the waste or wastewater to be treated anaerobically. Using Equation 43, derived from the equation presented by Tarvin and Buswell (1934), it is possible to determine the number of moles of methane produced:

$$n_{CH_4}(\text{mol}) = \frac{COD_{rem}}{64 \text{ g/mol}} \quad (43)$$

Where:

n_{CH_4} = amount of molecular methane (mol),

COD_{rem} = removed chemical oxygen demand (gO₂/L).

With n_{CH_4} , and using the ideal gas equation (Equation 44), the theoretical methane volume that can be produced by converting all the removed COD to methane, can be determined by applying Equation 45:

$$p \cdot V = n \cdot R \cdot T \quad (44)$$

$$V_{CH_4 \text{ theor}}(L) = \frac{n_{CH_4} \cdot R \cdot T}{p} \times 1000 \quad (45)$$

Where:

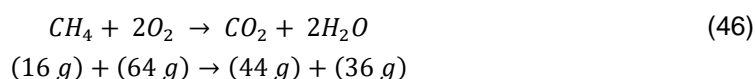
p = atmospheric pressure at laboratory conditions (pressure assumed: 101325 Pa),

$V_{CH_4 \text{ theor}}$ = theoretical methane volume (L),

R = gas constant: 8.3145 J.K⁻¹.mol⁻¹,

T = temperature of gas production (K).

To convert the volume of methane measured in L into COD equivalents, the stoichiometry of the complete oxidation of methane to carbon dioxide and water was used:



According to the previous stoichiometry, every 16 g of methane produced and lost in the atmosphere corresponds to the removal of 64 g of COD from the waste (Chernicharo, 2007). Thus, under normal conditions of temperature (0 °C) and pressure (1 atm), each 1 g of COD removed produces 0.350 L of methane. For this thesis, under the applied working conditions, that is, 309.15 K and 101325 Pa, the maximum theoretical methane volume is 0.396 L, per each gram of sCOD removed from the liquid medium.

3.7.3.2 Methanization degree

The methanization degree was determined to evaluate the methane produced (measured as COD equivalent) considering the organic matter added to each bioreactor, following the equation:

$$\% \text{Meth} = \frac{CH_4}{COD_{in}} \times 100 \quad (47)$$

Where:

CH₄ = Methane produced, expressed as COD equivalents,

COD_{in} = initial COD added.

3.7.3.3 Methane yield

From the removed COD, most of the organic matter is converted into methane, being a fraction used to cellular growth and maintenance. Methane yield was used to evaluate the performance of microorganisms, that is, their efficiency to convert sCOD into methane, and was determined using the following equation:

$$Y_{CH_4/COD_{rem}} = \frac{V_{CH_4}}{COD_{in} - COD_{final}} \quad (48)$$

Where:

V_{CH₄} = methane volume produced (L)

3.7.3.4 Anaerobic biodegradability

The anaerobic biodegradability of the substrates used, in several tests performed, was determined according to Baumann and Müller (1997), considering both produced and theoretical methane volumes (see Equation 45), as follows:

$$\text{Anaerobic Biodegradability (\%)} = \frac{V_{CH_4}}{V_{CH_4 \text{ theor}}} \times 100 \quad (49)$$

Where:

$V_{CH_4 \text{ theor}}$ = theoretical methane volume considering the sCOD removed (L).

3.7.3.5 Kinetic model for methane production

The modified Gompertz equation was used to adequately describe the cumulative methane production in anaerobic bioreactors operated. The equation can be presented as:

$$Y = Y_m \cdot \exp \left\{ -\exp \left[\frac{R_m \cdot e}{Y_m} (\lambda - t) + 1 \right] \right\} \quad (50)$$

Where:

Y = Cumulative methane volume produced (mL) at any time (t),

Y_m = Methane production potential (mL),

R_m = Maximum methane production rate (mL/d),

λ = Duration of lag phase (d),

t = Time (d),

e = Natural logarithm constant: 2.718.

The constants Y_m , R_m and λ were determined using the non-linear regression approach with the support of CurveExpert Professional software.

3.7.4 Adsorbable organic halides removal

The removal of AOX was determined considering the initial and the final AOX contents in the assays performed. The equation used to determine the AOX removal was:

$$\text{AOX removal (\%)} = \frac{AOX_{in} - AOX_{final}}{AOX_{in}} \times 100 \quad (51)$$

Where:

AOX_{in} = initial adsorbable organic halides concentration (mg_{Cl}/L),

AOX_{final} = final adsorbable organic halides concentration (mg_{Cl}/L).

Results and Discussion |4

4 | Results and Discussion

In this chapter, the results obtained during this thesis work are presented and discussed. The chapter is divided into three main sections, according to the type of inorganic additives used for pH control of the developed anaerobic processes. The sections are:

- 4.1 – Phase 1: Fly ash (powder) addition to AD assays

In this section, the results of assays in which inorganic additives in powder form, that is, fly ash from biomass combustion, have been added to anaerobic bioreactors treating two different types of substrates are presented. The treatment of the bleaching effluent from the pulp and paper industry and that of the cheese whey by-product from the dairy industry are compared, with the main goal of obtaining a higher methane production when the fly ashes were added to control the pH of the anaerobic processes.

- 4.2 – Phase 2: Fly ash-based geopolymers addition to AD assays

In this section, the results obtained in assays with the addition of fly-ash geopolymer spheres are presented. Different configurations of anaerobic digesters were studied, namely, *oxitop* bioreactors (250 mL batch bioreactors), batch and fed-batch bioreactors (1 L of working volume), with the objective of evaluating the extended performance of the digesters, mainly in terms of methane generation. In addition, all relevant parameters for assessing anaerobic performance are presented and discussed in this section.

- 4.3 – Phase 3: Red mud-based geopolymers addition to AD assays

In this section, the results obtained in assays with the addition of red mud geopolymer spheres are presented. To study the effect of this type of geopolymer spheres addition, two types of anaerobic bioreactors were used, *oxitop* bioreactors (250 mL batch bioreactors) and fed-batch bioreactors (5 L of working volume), in order to study the buffer efficiency of the spheres when organic loading shocks are applied in a prolonged operation time.

4.1 Phase 1: Fly ash (powder) addition to anaerobic digestion assays

4.1 Phase 1: Fly ash (powder) addition to anaerobic digestion assays

The results obtained in the study in which fly ash was used as an inorganic additive for pH control are presented below, in which the assays were performed in accordance with that described in section 3.5.1 and the applied conditions detailed in Table 22. Bleaching effluent (called D₀) from a pulp and paper industry (results presented in section 4.1.1) and concentrated cheese whey from a dairy industry (results presented in section 4.1.2) were used as a substrate in AD experiments, with the ultimate goal of energy (methane) valorization. For these assays, specific goals were defined, namely:

- I. Determination of the inhibitory effect of complex compounds present in D₀ effluent, namely adsorbable organic halides (AOX), in the production of methane and reduction of COD;
- II. Evaluation of the effect of fly-ash obtained from different biomass sources, as an inorganic additive in pH control in the production of methane and its effect in aerobic biodegradability of D₀ effluent;
- III. Definition of fly ash concentration to be used as an inorganic additive to control pH, in the AD of cheese whey to produce methane;
- IV. Comparison of the performance of two different substrates (D₀ effluent *versus* cheese whey) with inorganic additives (powdered fly ash), in the methane production and pH control of the AD process.

4.1.1 Fly ash (powder) addition to anaerobic digestion of bleaching effluent from pulp and paper industry

When chlorine compounds are used in the pulp production bleaching process, AOX compounds are formed. Taking into account environmental restrictions, in terms of AOX and COD discharge levels for treated effluents from the P&P industries, a common approach is to act directly in streams with a higher content of these concerning sources of pollution. The bleaching effluent (D₀) is the effluent generated during the pulp bleaching process with the highest AOX concentration, also presenting a high COD load.

Thus, in this work, D₀ effluent was used in AD assays to study the reduction of both COD and AOX contents and, at the same time, the valorization of this effluent in the form of an energy vector (methane). To accomplish this goal, two distinct steps were taken. First, the inhibitory effect of AOX compounds present in D₀ effluent was evaluated, studying different initial sCOD concentrations in anaerobic batch assays. As previously mentioned, the AOX compounds present in D₀ effluent have a potential inhibitory effect on microorganisms, including methanogenic microorganisms (Rintala et al., 1992). The inhibition of this type of microorganisms can lead to a decrease in methane formation and, ultimately, to the failure of the overall AD treatment process (Chen et al., 2008). Second, the use of two FA types from different biomass sources, produced by the combustion of residual biomass in an industrial thermoelectric plant, was evaluated. The addition of FA acts as an additive for pH control in the AD process, to produce methane and, ultimately, enhance the final biodegradability of the treated D₀ effluent.

4.1.1.1 Inhibitory effect of adsorbable organic halides present in bleaching effluent

To study the influence of AOX concentration in the AD process and in the methane formation, several *oxitop* bioreactors with different D_0 concentrations were performed. The initial concentration measured as sCOD varied between 0.9 and 2.9 gO₂/L. With these anaerobic biodegradation tests, the anaerobic biodegradability of the effluent under study is verified and the potential for its use in a full-scale anaerobic process is evaluated.

Figure 26 shows the main performance parameters of the mentioned *oxitop* bioreactors, namely: a) gas pressure measured periodically inside the bioreactors, by the *oxitop* measuring head; b) accumulated volume of methane; c) mass of AOX removed and percentage of AOX removal (compared to the initial AOX values); d) initial and final pH values of the reactional medium. In these assays, biogas was produced in the 27 days of incubation (Figure 26 (a)), as observed by the increase in pressure inside the bioreactors. However, the presence of methane was detected only from the 9th to 12th day of the incubation period and only for bioreactors with 0.9 and 1.8 gO₂/L (Figure 26 (b)). For these bioreactors, the pressure was measured only until 12th (0.9 gO₂/L) and 19th (1.8 gO₂/L) days, since the *oxitop* system has a major limitation on the pressure limit of the measuring head (\approx 333 hPa or 0.33 atm), which can cause restrictions in gas measurements (Pabón Pereira et al., 2012).

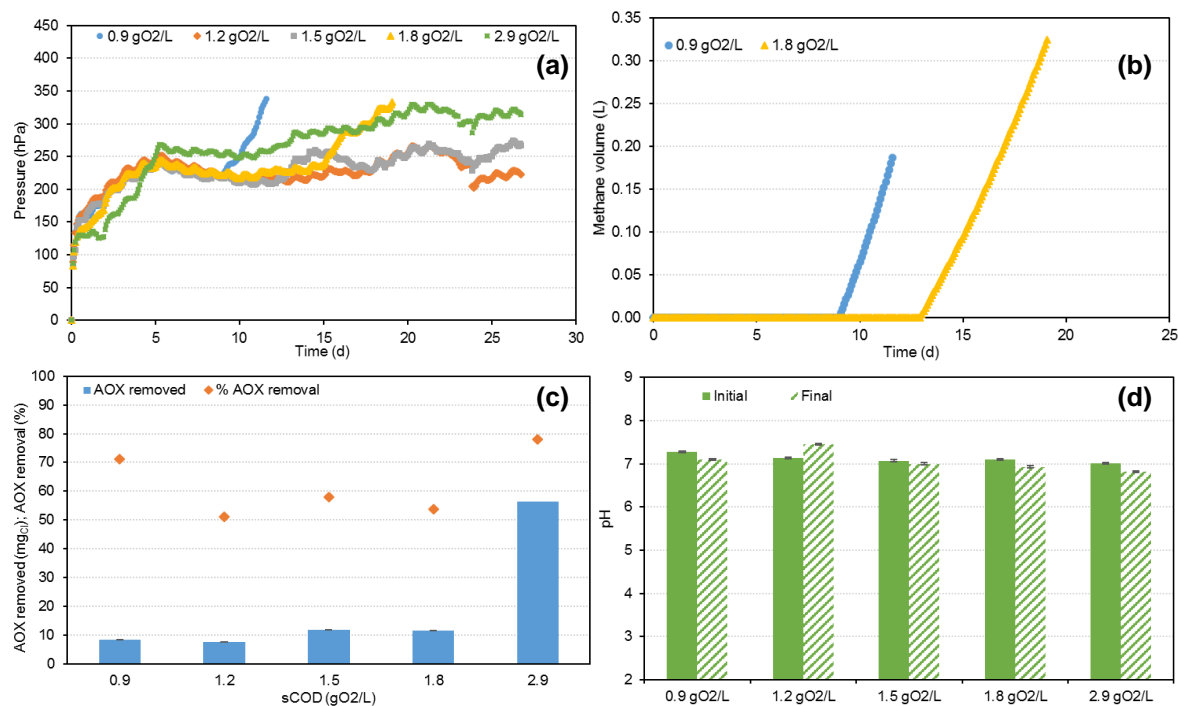


Figure 26 | Anaerobic performance of *oxitop* bioreactors with different initial D_0 concentrations: cumulative pressure (a), cumulative methane volume (b), mass of AOX removed and percentage of AOX removal (c) and initial and final pH (d).

In Figure 26 (b), it was also observed that the presence of AOX (increase with increasing concentrations of D_0 effluent) delayed the formation of biogas and, consequently, the formation of methane, leading to a slower anaerobic process than expected. In fact, it was expected that methanogenic microorganisms, after a suitable exposure time, would resist in environments with the presence of biorecalcitrant and bioinhibitory compounds (such as AOX), being able to survive and

thrive in these environments (El-Hadj et al., 2007). This adaptation period could explain the deceleration of the anaerobic process with D_0 effluent as a substrate.

At the end of the tests, a methane content corresponding to 63 % and 43 % of the biogas produced was obtained for the tests with the addition of 0.9 and 1.8 gO₂/L, respectively. In terms of methane volume, more than 157 mL to 324 mL were produced, considering only the initial days when the pressure was measured. The yield of methane considering the initial COD added decreased slightly when the organic load doubled: from 0.199 LCH₄/gO₂ added to 0.180 LCH₄/gO₂ added. The methanization degree, that is, the initial organic matter converted to methane (measured as COD), followed the same pattern, decreasing from 50 % to 46 % when the initial organic load doubled from 0.9 to 1.8 gO₂/L. It should be noted that the values obtained for the quantity and the yield in methane, or methanization degree, are not maximum values, given the practical restrictions in the measurement system of the produced biogas.

Although the bioreactor with 1.8 gO₂/L produced a higher methane volume, a lower yield was obtained than that obtained with the bioreactor with 0.9 gO₂/L, and this can be explained by the presence of higher amounts of inhibitory compounds, such as AOX. From these results, it can be said that anaerobic biomass (microorganisms) adapted to the presence of substrate (D_0 effluent) and, therefore, to AOX compounds, producing methane despite the long lag phase observed (about 13 days).

The initial AOX content varied according to the defined initial sCOD concentration, in the range of 12 to 72 mgCl/L. For AOX removal (see Figure 26 (c)), values higher than 51 % were obtained in all assays, despite the differences between initial concentrations. It was observed that the highest initial AOX concentration (72 mgCl/L) did not inhibit the AOX removal, reducing more than 77 % of AOX present in the liquid phase, which corresponds to a mass of 56 mg of AOX reduced. Despite this AOX reduction, no methane was detected in the gas phase of this bioreactor, even after 27 days of incubation.

Due to the strong acidic pH of D_0 effluent, it was neutralized with a concentrated solution of NaOH before being added into the bioreactors. As the effluent used in these studies is real (not simulated in the laboratory), it is subject to variations, some of which are imposed by the pulp manufacturing process. This leads to large differences in the amount of NaOH added to each lot of effluent. The volume of 1 M NaOH solution added varied between 46 and 48 mL, in order to neutralize the pH of the effluent (7.0 ± 0.1). The initial and final pH of the bioreactors is shown in Figure 26 (d). During anaerobic assays, the pH did not vary much, decreasing at most 0.30 points. The exception was for the bioreactor with 1.2 gO₂/L of the initial load, where the pH increased by 0.31 points. Both initial and final pH values are within the methanogenic range (6.5 – 7.2), promoting a favorable environment for methane formation.

Since the first assays with D_0 as a substrate for the anaerobic process did not show significant inhibition of microorganisms to produce methane in the presence of AOX, or to reduce these complex compounds, higher D_0 concentrations were tested: 2 gO₂/L and 3 gO₂/L. The assays were performed in *oxitop* bioreactors during 26 days. In Figure 27 are presented the main performance parameters of the mentioned *oxitop* bioreactors, namely, the initial and final pH values of the reactional medium (a), the cumulative methane volume (b), the mass of AOX removed and the percentage of AOX removal, compared to the initial AOX values (c).

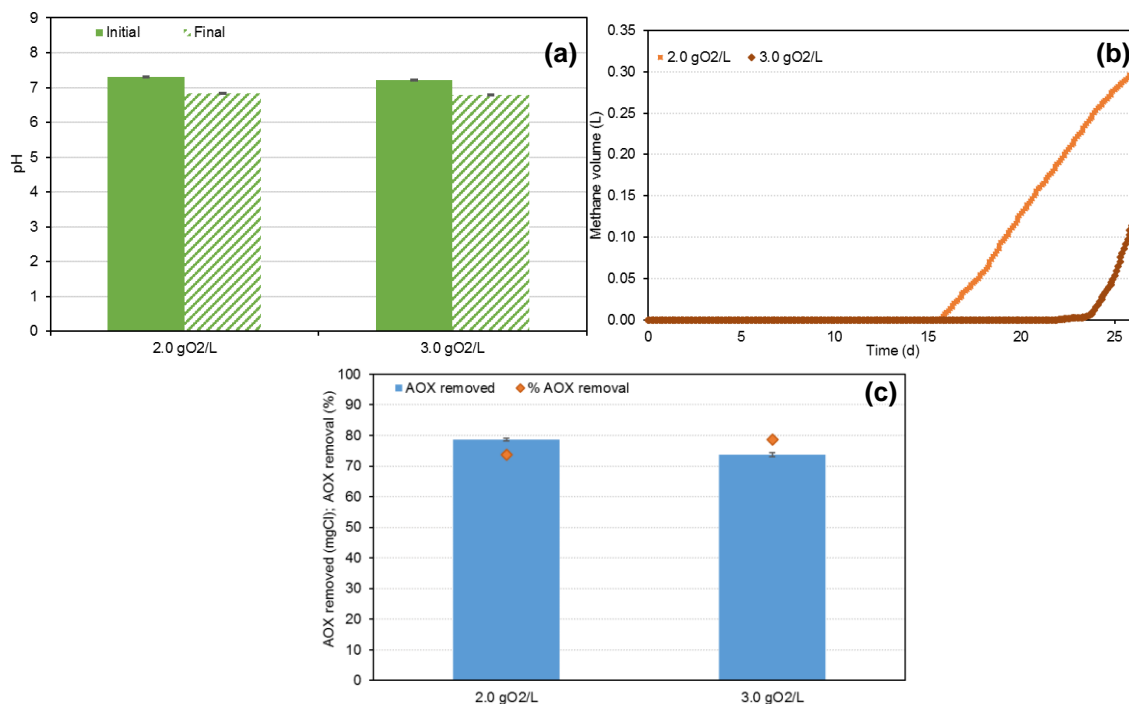


Figure 27 | Anaerobic performance of *oxitop* bioreactors with different D_0 concentrations: initial and final pH (a), cumulative methane volume (b) and AOX removed and percentage of AOX removal (c).

The pH values (Figure 27 (a)) decreased by about 0.45 points in both assays, from the beginning to the end of the incubation time. In addition, in both cases, the pH values are within the optimum pH range for methanogenic microorganisms (6.5 – 7.2), so an increase in methane production was expected. However, in both bioreactors, anaerobic biomass was slow to respond, increasing the lag phase and delaying the methane formation with the increase in the AOX concentration. Comparing these assays (Figure 27 (b)) with bioreactors with lower sCOD concentrations (see Figure 26 (b)), an increase in the initial sCOD load led to an increase in the lag phase from 9 to 13 days in assays with 0.9 – 1.8 gO₂/L and a delay of 15 to 22 days in assays with 2.0 – 3.0 gO₂/L, respectively. The presence of AOX in the effluent to be treated could have inhibited methanogenic microorganisms, which needed a longer time to adapt to higher pollutant concentrations, thus delaying the methane generation. After the lag phase, the methane volume increased rapidly, indicating the adaptation of biomass (microorganisms) to the substrate (D_0 effluent rich in AOX).

For AOX removal (Figure 27 (c)), percentages higher than 73 % were obtained in both conditions. With a higher initial sCOD load, a higher mass of AOX compounds removed from the liquid phase was observed. This may be partly related to the adsorption component of these compounds on the biomass surface, which will be higher with higher AOX concentrations. Adsorption is an important mechanism that influences the fate and the effect of organic compounds, namely in the AD process (Johnson and Young, 1983). When organic compounds with a high adsorption capacity, such as AOX compounds, are present in the media, they tend to adsorb and become unavailable for anaerobic degradation. This unavailability affects the determination of the methane potential of these types of compounds. In fact, the higher sCOD removal for the assay with higher initial sCOD load, that is, 48 % versus 26 % in the assay with 2.0 gO₂/L of the initial load, was not expressed in a higher methane production, after 27 days of incubation.

Figure 28 was plotted for a better understanding of the relationship between the initial sCOD load and the performance of the bioreactors in terms of methane volume and duration of the lag phase. As mentioned earlier, the lag phase increased with the increase in the initial sCOD load and may be related to the increase in the content of AOX compounds in the liquid phase. The direct relationship between the initial sCOD and the extension of the lag phase has a determination coefficient of 0.979, indicating that the linear model makes a good adjustment to the data obtained in the *oxitop* assays.

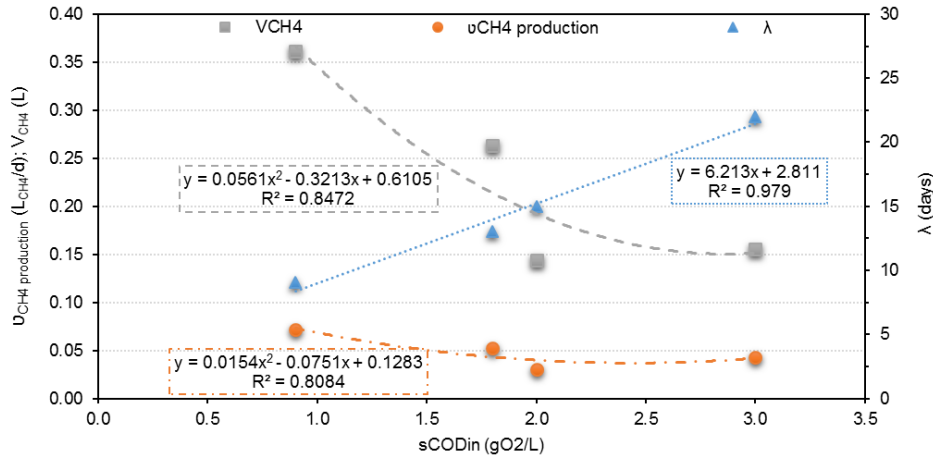


Figure 28 | Effect of initial sCOD load on the lag phase (blue Δ), the volume of methane produced in the first 5 days after the lag phase (grey \square) and the methane production rate (orange \circ).

An important issue to be careful about is the duration of these experiments. The extension of the lag phase (Figure 28) impaired the formation of methane, which led to the low volume of methane accounted for and the decrease in global performance parameters. For these experiments, the time of incubation was previously fixed (26 to 27 days) in order to compare the efficiency of the system under different conditions during a certain period. This digestion time, under mesophilic conditions, may not have been enough to, first, lead to the adaptation of the microorganisms to the presence of inhibitory compounds and, second, to the conversion of the sCOD of the substrate into methane by methanogenic microorganisms. For this reason, and so that these results can be comparable, a 5-day period was considered for the volume of methane produced, as shown in Figure 28, measured from the end of the lag phase. The volume of methane produced in 5-days for bioreactors with initial loads of 1.8 and 2.0 gO₂/L was taken directly from the data, and the values for bioreactors with initial loads of 0.9 and 3.0 gO₂/L were extrapolated from the methane production curve (Figure 26 (b) and Figure 27 (b), respectively).

On the other hand, neither the methane production rate nor the volume of methane has a linear relationship with the initial sCOD load. For the methane production rate, a second-order polynomial adjustment described 81 % of the variation of the data obtained. The trend was to decrease the methane production rate with an increase in the initial sCOD load. The methane volume follows a pattern similar to the methane production rate, decreasing when applying increasing sCOD concentrations. These parameters indicate that the presence of increasing AOX concentrations can inhibit methanogenic microorganisms and, consequently, drastically decrease the methane content in the biogas formed. The increase in the sCOD load from 2.0 to 3.0 gO₂/L, and consequently in the AOX content, showed no relevant inhibition in terms of the methane volume produced in the first 5 days after the lag phase.

Figure 29 shows the main parameters of anaerobic performance, namely: (a) methanization degree and anaerobic biodegradability of the total incubation time and (b) extrapolated methane yield for the initial methane production period (5 days). AOX removal is also included in Figure 29 (a) because this parameter is very important in the anaerobic degradation of the effluent under study. AOX removal (in percentage) does not seem to be related to the initial organic load, varying between 53 % and 78 %, with no linear trend. For the other parameters (methane efficiency parameters), they tend to decrease with the increase in the organic load applied at the beginning of the experiment, as shown previously.

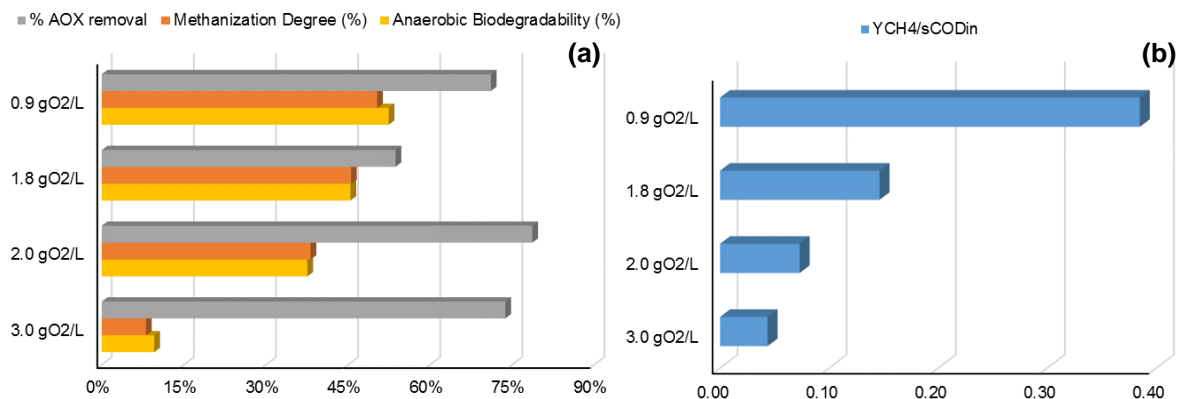


Figure 29 | AOX removal, methanization degree, anaerobic biodegradability (a) and methane yield (b) for the anaerobic assays with an initial sCOD load of 0.9, 1.8, 2.0 and 3.0 gO₂/L, using D₀ as substrate.

Anaerobic biodegradability represents the fraction of organic matter that can be converted into biogas composed mainly of methane and carbon dioxide, under controlled anaerobic conditions. In this study, anaerobic biodegradability was less than 52 % (0.9 gO₂/L), once again indicating the inhibitory nature of AOX compounds for methanogenic microorganisms and, possibly, for other types of microorganisms involved in different steps of organic matter degradation. The methane yield and the methanization degree trends corroborate this statement.

Taking into account the results obtained with the AOX-rich effluent in the anaerobic process of degradation to produce methane, it can be concluded that the low anaerobic biodegradability of the substrate is not ideal for energy recovery. In addition, the dilution of the substrate (that is, the study of lower sCOD initial concentrations) enhanced the anaerobic biodegradability and the methane yield obtained demonstrating an increasing potential for the application of anaerobic technologies to these complex effluents.

4.1.1.2 Anaerobic digestion of bleaching effluent with fly ash addition to control pH

To adjust the pH of D₀ effluent, instead of adding NaOH, two different types of fly ash (FA) were used. The FA used were collected as described in section 3.3.1 and the differences between them are also described in the referred section. For the assays with fly ash addition to control pH, the aerobic biodegradability of the D₀ effluent was determined before and after the AD processes. From these anaerobic processes, anaerobic biodegradability was also determined.

The main physico-chemical characteristics of D₀ effluent and mixtures D₀ + FA used in anaerobic assays are listed in Table 27. The increase in D₀ pH from acidic (≈ 2) to neutral (≈ 7) led to a reduction

in the AOX concentration of 18 % in the mixture with NaOH and of 33 - 35 % in the mixture with the addition of FA. This behavior was also reported by Dorica et al. (1992), who used liquid alkaline effluents from the pulp industry to increase the pH and, as a consequence, the AOX content decreased with the dilution factor and with the pH changes.

The AOX reduction observed was higher in mixtures with FA than in the mixture with NaOH. The FA added (CA5 and CTB) contained, among others, metallic elements such as Ca, Al, K, Fe and Mg in their oxidized forms, which accounted for 56 wt.% dry basis (Table 17). When mixed with water, they will be hydrolyzed and partially soluble (Duan and Gregory, 2003), and the soluble part of these ions will increase the pH of the media. The insoluble part of the FA can act as an adsorbent to compounds such as AOX (Gao and Fatehi, 2018; Han and Wei, 2012). Therefore, part of the AOX present in D₀ effluent can be adsorbed on the FA added, decreasing in a larger extent the AOX concentration measured in the liquid fraction. From the point of view of AOX removal, the use of FA as a neutralizing material has great potential and less environmental impact when compared to the use of chemical compounds (NaOH) to increase the pH.

Table 27| Physico-chemical characteristics (pH, AOX content and organic matter content) of D₀ effluent and the mixtures: D₀+NaOH, D₀+CA5 and D₀+CTB, using FA from different types of biomass burning (average value ± standard deviation).

	D ₀	D ₀ + NaOH	D ₀ + CA5	D ₀ + CTB
pH	2.21 (± 0.25)	7.01 (± 0.01)	7.04 (± 0.01)	7.34 (± 0.03)
AOX (mg_{Cl}/L)	69.5	57.0	46.0	44.9
sCOD (mgO₂/L)	2410 (± 54)	2620 (± 20)	2600 (± 50)	2720 (± 20)
sBOD (mgO₂/L)	-	234 (± 5)	309 (± 6)	176 (± 8)
sBOD/sCOD	-	0.089	0.119	0.065

The soluble COD of the mixtures did not vary with the addition of FA. The aerobic biodegradability of the effluent, given by the ratio between sBOD and sCOD, increased 33 % when CA5 fly ash was added to D₀; on the other hand, for CTB addition, the aerobic biodegradability decreased about 27 %, in comparison with the effluent with NaOH addition to neutralize the pH. In the three scenarios, aerobic biodegradability is very low (less than 12 %). The low biodegradability of this type of effluent is well documented and is mainly due to the presence of dissolved lignocelluloses and inhibitory substances (Gao and Fatehi, 2018; Rintala and Puhakka, 1994), such as AOX. Generally, an effluent with a sBOD/sCOD ratio higher than 0.40 is considered an effluent with a high biodegradable fraction; with a sBOD/sCOD ratio lower than 0.25 it is considered an effluent in which the inert fraction is high and the biodegradable fraction is low, making it difficult to implement a possible full-scale biological treatment process.

These mixtures, mentioned in Table 27, were used in anaerobic biodegradation tests to understand the role of FA addition in neutralizing pH and in improving the anaerobic process (methane production and AOX removal). For these tests, four different conditions were studied: two with CA5 addition and two with CTB addition. For both types of ash, the preparation of the substrate was performed in two different ways. In a first approach, the mixture of D₀ and FA was carried out (concentrations and details in section 3.5.1.2) and then added to the anaerobic sludge to be incubated; in this case, the FA was present in the anaerobic media during the process – assays D₀+CA5 and D₀+CTB. In a second approach, the mixture of D₀ effluent and FA was performed and

after a period of mixing, it was filtered and only the filtrate fraction was used in anaerobic tests – assays D₀+CA5f and D₀+CTBf.

Figure 30 and Figure 31 depicts the physico-chemical parameters determined in these experiments to evaluate the performance of the bioreactors operated using the *oxitop* system. Figure 30 includes the initial and final pH values and the alkalinity concentrations (measured as CaCO₃), and the initial and final sCOD concentrations and VFA concentrations for each bioreactor operated. In this figure, “others” refer to VFA species determined in much lower concentrations than acetic, propionic and butyric acids present in the samples, that is, i-butyric, i-valeric, n-valeric and n-caproic acids. Figure 31 includes the mass of AOX compounds removed from the liquid phase and the corresponding AOX removal (in percentage) (a), the VFA yield ($Y_{VFA/sCOD}$) (a) and the sCOD removal (b).

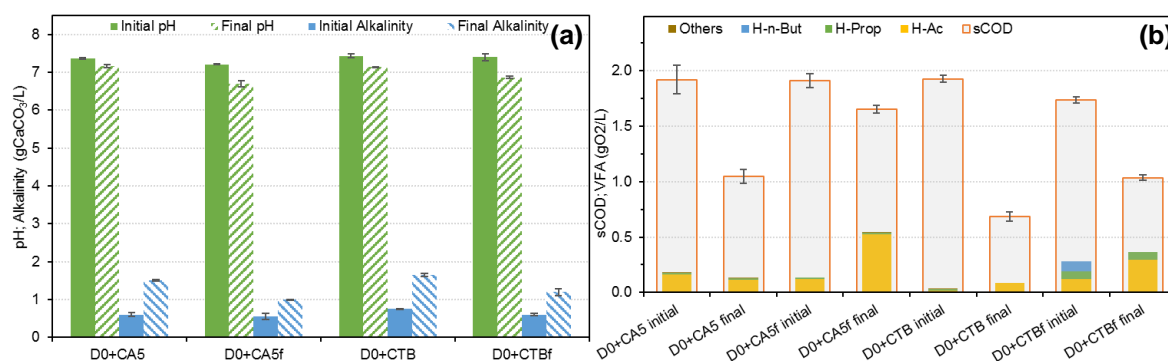


Figure 30] Performance of *oxitop* batch bioreactors with different FA additions regarding initial and final pH and alkalinity measured (a) and sCOD and VFA (H-Ac, H-Prop and H-n-But) concentrations, expressed as COD equivalents (b).

For the pH values (Figure 30 (a)), all conditions tested showed a decrease in pH at the end of the experiment, compared to the initial pH values. The difference between the initial and final pH is more pronounced (above 0.50 points) in assays with the filtered substrate, with final values below 6.90 in both cases (D₀ + CA5f and D₀ + CTBf). Although the variations observed in the pH, the values obtained are still in the optimum pH range of the methanogenic microorganisms, creating environmental conditions suitable for the production of methane.

Although these pH fluctuations are expected in anaerobic processes, the pronounced decrease may indicate an unstable process. In fact, in the bioreactors where the ash was kept during the anaerobic process, they tended to maintain a more stable pH, and this could be related to the presence of certain inorganic compounds, supplied from the added ash. According to Rajamma et al. (2009), FA typically contains large amounts of alkali metals, such as sodium and potassium, which are the main sources of alkaline properties of FA. pH stability is directly related to the increase in alkalinity, observed in all assays. The greatest difference between the initial and final alkalinities (0.9 g/L measured as CaCO₃) was observed in assays with FA during the process (D₀ + CA5 and D₀ + CTB), probably due to the progressive transfer of alkali metals from the ash to the liquid fraction, increasing its buffer capacity.

Analyzing the VFA content of the liquid phase (Figure 30 (b)), it can be observed that the assays with lower final pH values are the ones with higher VFA concentrations. For example, the assay D₀ + CA5f reached pH values at the end of the experiment of 6.70 (± 0.08), the lowest observed value,

and it is the assay in which the highest VFA concentration was measured, 542 mgO₂/L. In this case, acetic acid accounts for 96 % of the VFA content. In the case of the assay with D₀ + CTBf, at the end of the experiment, a VFA concentration of 364 mgO₂/L was measured, with acetic acid as the major constituent (82 %) and a pH value of 6.86 (± 0.03). For the initial points, very low VFA concentrations were measured. Generally, acetic acid (yellow bar in Figure 30 (b)) was the predominant VFA specie detected. Propionic (green bar) and n-butyric (blue bar) acids are present in some samples, but to a lesser extent than acetic acid. N-Butyric acid was detected only in the initial sample of the filtered mixture of D₀ and CTB and propionic acid was observed in both initial and final samples of the same studied condition. I-butyric, i-valeric, n-valeric and n-caproic acids were also analyzed, but in these assays, these acidic species were detected in very low concentrations (< 6 mgO₂/L).

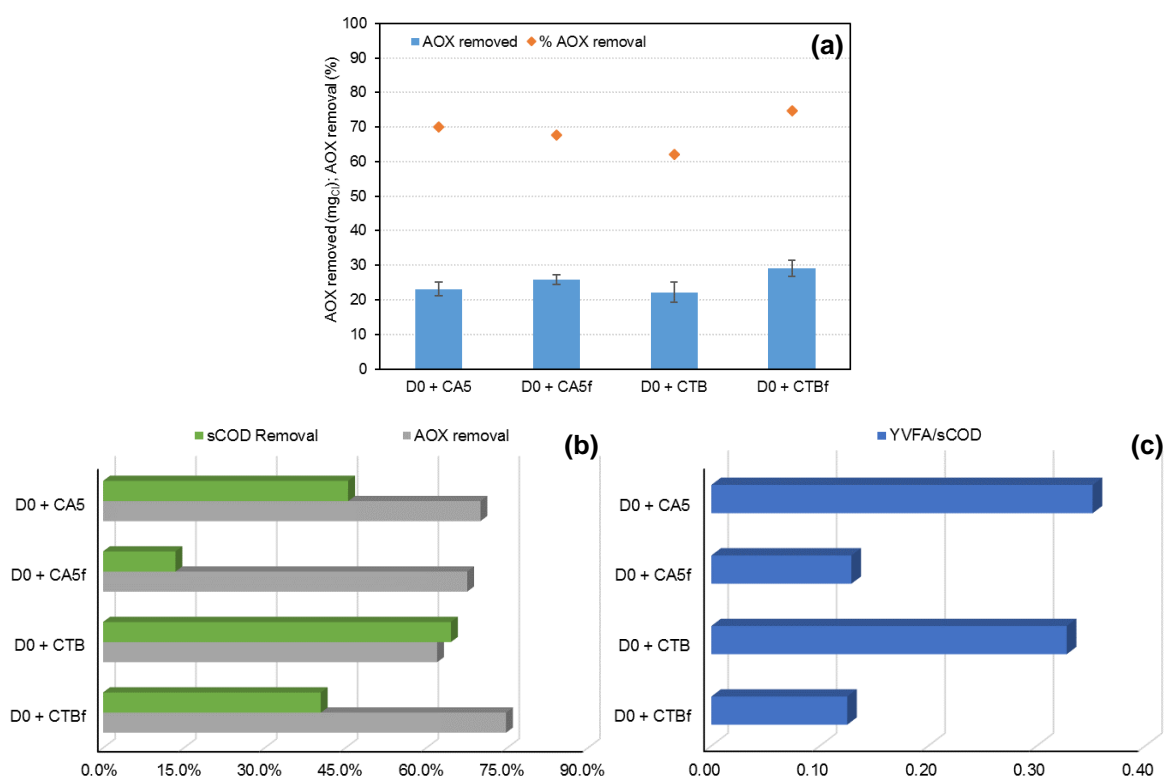


Figure 31 | Mass of AOX removed and percentage of AOX removal (a), sCOD removal and AOX removal (b) and VFA yield (c), for the assays with different additions of FA, using D₀ as substrate.

The ratio between VFA concentration and alkalinity can be an indicator of process stability (Castro et al., 2017). For this study, all four conditions presented VFA/alkalinity ratios below 0.6 mg_{Acetic acid}/mg_{CaCO₃}, which is considered the highest value for adequate process stability (Castro et al., 2017). Even though the values for the VFA/alkalinity ratio of the filtered mixture of D₀ and CA5 of the bioreactor are in the acceptable range referred to, they are the highest of the four tests (0.54 mg_{Acetic acid}/mg_{CaCO₃}), denoting some instability of the anaerobic process, concerning the methane production, due to the higher measured VFA concentration. The filtered mixture of D₀ and CTB also showed a significantly high VFA/alkalinity ratio (0.30 mg_{Acetic acid}/mg_{CaCO₃}), when compared to the unfiltered assays performed with CA5 (0.09 mg_{Acetic acid}/mg_{CaCO₃}) and CTB (0.05 mg_{Acetic acid}/mg_{CaCO₃}) ashes.

The initial sCOD measured for the conditions tested (on average 1.86 ± 0.12 gO₂/L) was very close to the theoretical value (2.0 gO₂/L). In all assays, a decrease in sCOD was observed from the beginning to the end of the experiment, with this organic matter being consumed mainly for cell growth or methane generation. The sCOD removal (Figure 31 (b)) tends to be higher in assays in which ash was present during the AD process. Thus, the removal of the solid fraction from the mixture was not beneficial for the sCOD removal or for the VFA generation. In the case of VFA yield, the use of the filtered mixture decreased the value obtained to less than half, obtaining in both cases 0.13 gVFA-O₂/gO₂. For assays with FA present, 33 to 35 % of the soluble fraction of the COD at the final sampling moment consists of VFA, mainly acetic acid.

The AOX removal observed in these assays (Figure 31 (a)) is in the same range as the removals obtained in previous assays: all conditions showed removals between 62 and 75 % of the initial AOX present in the liquid phase, with no apparent relationship between the conditions and the results obtained. For these assays, more than 22 mg_{Cl} of AOX compounds were removed and the remaining concentration does not exceed 13.6 mg_{Cl}/L of AOX. These low final AOX concentrations are promising, taking into account an industrial perspective. Prior to discharge into the receiving environment, the D₀ effluent is subjected to dilution (mixture with other effluents from P&P industry) and to biological treatment. Thus, a low AOX concentration in D₀ effluent led to a low AOX discharge level, avoiding several environmental problems.

Figure 32 depicts the parameters related to methane production, namely, methane volume produced during the tests (a), methanization degree (in percentage) and anaerobic biodegradability (b), and methane yield (c) calculated for each mixture performed, with CA5 and CTB ashes addition. Concerning the methane yield, the values in Figure 32 (c) were calculated by extrapolation the data to 5 days, taking into account the methane produced in the period presented in Figure 32 (a).

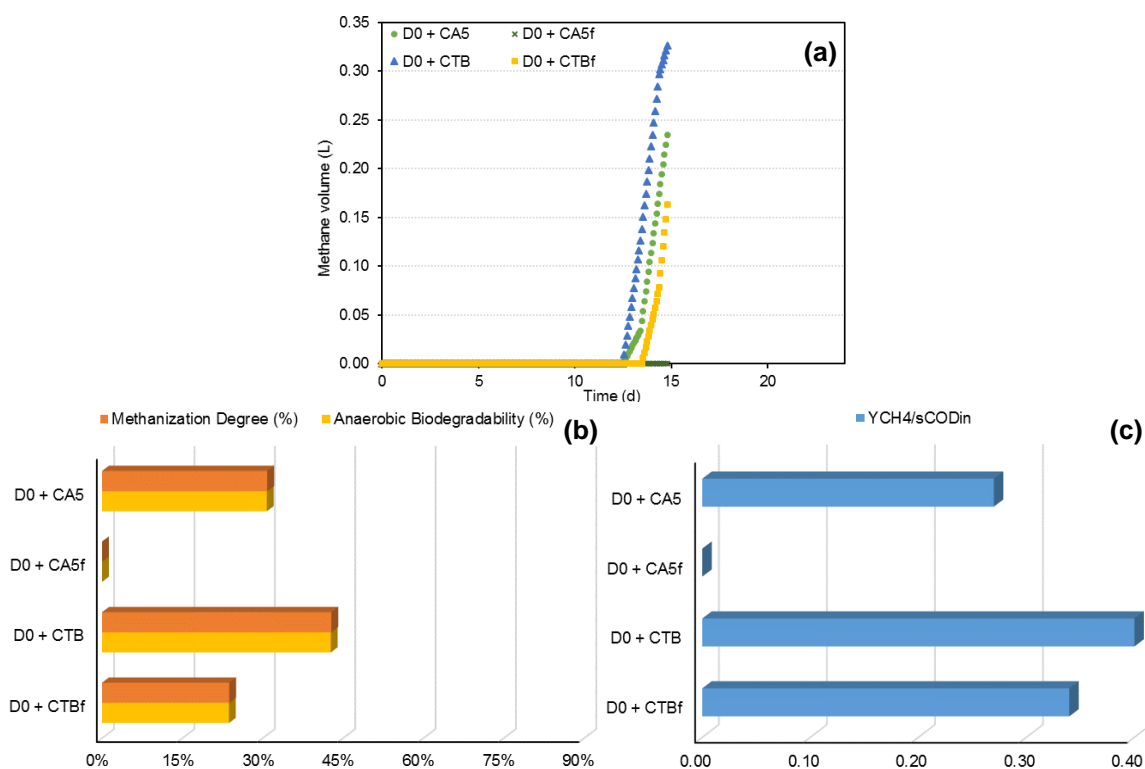


Figure 32 | Methanization performance for the assays with FA addition, using D₀ as substrate: cumulative methane volume (a), methanization degree and anaerobic biodegradability (b) and methane yield (c).

For the assay with a filtered mixture of D₀ and CA5, no methane formation was detected (Figure 32 (a)) during the experimental time. The assays with CA5 or CTB ashes inside bioreactors had a lag phase of 12 days, where no methane was detected and after that period, methane was detected until the *oxitop* heads reached the maximum pressure value. This caused some measurement restrictions for methane, as mentioned earlier, and it was not possible to determine the methane formation after the 15th day. For this reason, the results regarding methane formation presented here are only for the 15 days of incubation, in which it was possible to measure the pressure inside the bioreactors. For the assay with a filtered mixture of D₀ and CTB, the lag phase was slightly longer, 13 days. After the lag phase, methane increased rapidly, indicating the adaptation of the biomass to the substrate under study. In terms of methane volume produced, the mixture with D₀ and CTB ashes achieved a higher volume, 0.33 L, followed by the assay with the mixture of D₀ and CA5, 0.23 L. The reactor with a slower response (D₀ + CTBf) also produced less methane volume, 0.16 L. In all bioreactors where methane was detected, the methane content in biogas was higher than 40 %. In addition, assays in which the ashes were kept in the medium resulted in higher levels of methane in the biogas, reaching 60 to 65 % at the end of the experiment.

For the performance of the methanogenic phase, the mixtures where the ash was kept during the anaerobic process obtained better results than in the assays with filtered mixtures. Considering the methane volume extrapolated for a production period of 5 days and the initial sCOD added in each bioreactor, the yield of methane that represents the potential of each mixture for methanogenesis was determined, and these values are included in Figure 32 (c). The relationship between the volume of methane produced and the theoretical volume of methane (considering the maximum value for the initial sCOD added to each bioreactor) is given by the anaerobic biodegradability (in percentage) and is included in Figure 32 (b). Both the yield and the methanization degree follow the same pattern, decreasing with the filtration of the substrate. Anaerobic biodegradability also tends to decrease when ash is removed from the mixture.

The boost in the methane performance parameters, when ash is present in the mixture, may be related to the effect of ions from ashes that enhance the microorganism's activity, especially methanogenic microorganisms, increasing the methane production. The increased biodegradability of the mixture with CTB ash, compared to the mixture with CA5 ash, may be related to the amount of ash added. In the case of CA5, only 4.97 g/L was added, compared to a greater amount of CTB, 17.2 g/L, necessary to neutralize D₀ effluent. The higher concentration of CTB ash may have leached larger amounts of ions and led to a positive response from the microorganism's consortia.

Figure 33 shows the results obtained for the analysis of metals content, namely calcium, sodium, magnesium and iron, in the supernatant of initial and final samples of the bioreactors where different types of FA were added.

Although with only slight variations, the Ca content increased at the end of the experiments where ashes were kept during the anaerobic process, and the Na content only increased in the assays with CA5 ashes addition. The iron content decreased at the end of the experiments, for both types of FA added. The addition of CTB ashes did not increase the initial content of Na, Mg or Fe, although the amount of CTB ashes was much higher than the CA5 ash. Despite the difference in the amounts of ashes added, the concentration of minerals in the liquid phase did not increase but positively influenced the anaerobic process.

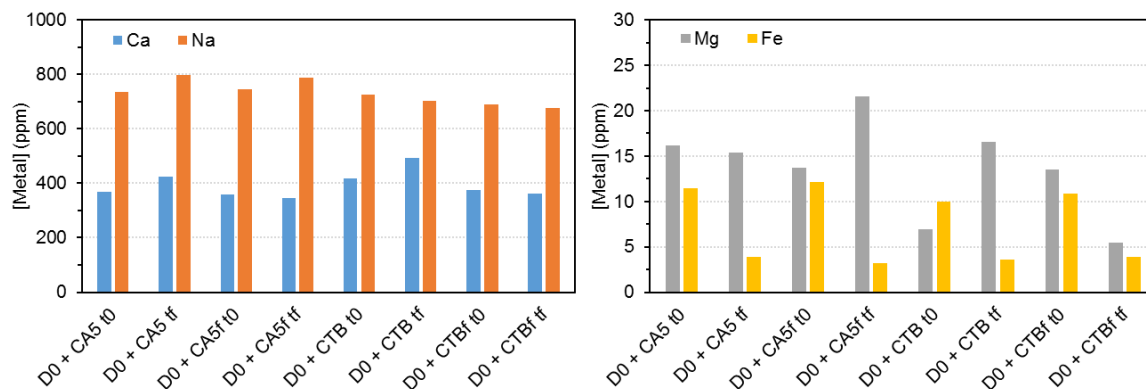


Figure 33| Metals (Ca, Na, Mg, Fe) concentration at the beginning and at the end of *oxitop* batch anaerobic assays with D₀ effluent and FA addition.

Figure 34 shows the aerobic biodegradability of the mixtures before and after the AD process and the values for the increase in aerobic biodegradability (in percentage). In all assays, aerobic biodegradability after the AD process increased by more than 150 %, which may indicate that an anaerobic treatment is suitable to increase the biodegradability of this type of effluent. The increase in sBOD was due to the anaerobic conversion of part of the organic matter into VFA (readily consumed substrates), the reduction of AOX in the liquid phase, which decreased the concentration of inhibitory compounds, and the transformation of complex compounds originally present in the D₀ effluent into others more simple and biodegradable.

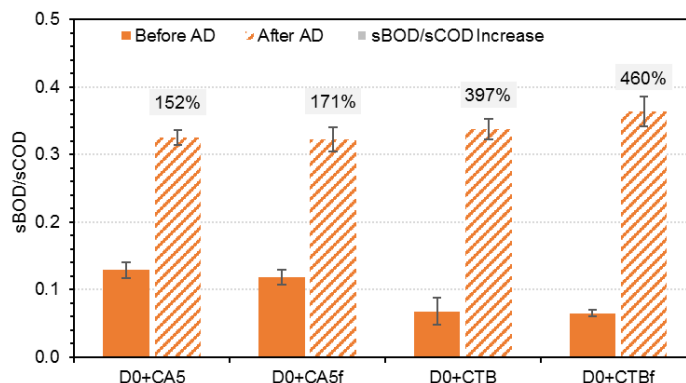


Figure 34| sBOD/sCOD ratio before and after AD tests and increase on calculated ratio after the anaerobic treatment.

The final aerobic biodegradability is higher than 0.32 in all assays, indicating that the treated effluents (the liquid fraction) of the assays performed are composed of a significant fraction of biodegradable organic matter. The range presented for the sBOD/sCOD ratio also indicates that the implementation of an anaerobic biological treatment process could be facilitated, after an anaerobic pre-treatment of D₀ effluent.

4.1.1.3 Effect of fly ash addition in anaerobic digestion of bleaching effluent

In order to compare the values obtained in the two assays, without FA addition and with two different types of FA addition, Table 28 summarizes the main performance parameters, namely sCOD removal, duration of the lag phase (λ), methane yield considering the initial sCOD addition,

methanization degree, anaerobic biodegradability and AOX removal. The assay with 2.0 gO₂/L of initial sCOD is presented in this table, as it had the same initial sCOD concentration used in the assays with FA addition and was the basic assay to understand the influence of FA addition to D₀ anaerobic treatment.

Table 28 | Duration of lag phase, AD performance parameters and AOX removal for D₀ assays without and with FA addition.

Assay	λ (d)	sCOD removal (%)	YCH ₄ /sCOD _{in} (mL/gO ₂)	Methanization (%)	Anaerobic biodegradability (%)	AOX removal (%)
2.0 gO₂/L	15.00	26.2	0.15	38.2	37.6	78.7
D₀ + CA5	12.57	45.5	0.12	30.8	30.7	70.0
D₀ + CA5f	-	13.4	-	-	-	67.6
D₀ + CTB	12.57	64.6	0.17	42.8	42.7	62.0
D₀ + CTBf	13.54	40.4	0.09	23.7	23.7	74.8

As can be seen, generally the addition of FA to neutralize the pH of D₀ effluent instead of NaOH (represented by the assay with 2.0 gO₂/L) had a positive effect on some AD performance parameters. With the exception for D₀ + CA5f, the sCOD removal increased by more than 15 % and the lag phase for the beginning of methane production decreased by at least 2 days, compared to the assay with 2.0 gO₂/L. For the AOX removal, the average value is 71 ± 6 % for the referred assays, which is a very promising removal, taking into account the complexity of the D₀ effluent.

With the addition of CA5 ash, the methane performance parameters (methane yield, methanization degree and anaerobic biodegradability) decreased slightly, compared to the assay with 2.0 gO₂/L. On the other hand, the addition of CTB ash slightly improved the methane performance parameters, with an increase in the methanization degree and anaerobic biodegradability of about 5 %. It is worth mentioning that the addition of CTB ash did not improve the sBOD/sCOD ratio (Table 27), as occurred with the mixture of D₀ and CA5 ash.

The improvement in methane production may be related to the release of metals from ash, at levels suitable for the improvement of the D₀ anaerobic process (Lo et al., 2012). For example, the presence of calcium is necessary for the formation of methanogenic microorganisms and microbial aggregates and can act as a driver for the methane formation (Liu et al., 2019). In this work, the amount of metals added in the different bioreactors varied according to the type of ash added, as can be seen from the theoretical values for oxides or element masses included in Figure 35. For the CA5 ash, 4.97 g was added to 1 L of D₀ effluent, in order to achieve pH values of 7.0 (neutral pH to enhance microbial growth and activity); for CTB ash, 17.2 g was added, to reach the same conditions.

The use of a larger amount of CTB ash made the (theoretical) concentration added of silicon (SiO₂), calcium (CaO), aluminum (Al₂O₃), iron (Fe₂O₃) and potassium (K₂O) to be much higher than the corresponding concentration with the CA5 ash. With CA5 ash, sodium (Na₂O) and chlorine (Cl) were added in higher amounts than with the addition of CTB ash. These differences may explain the results regarding pH control and methane formation. As mentioned earlier, the main sources of alkaline properties of FA are sodium and potassium (Rajamma et al., 2009), which present different amounts in the two scenarios. For CA5 ash, the amount used to neutralize the pH of D₀ effluent was less than that used for CTB and may be related to the presence of sodium, which contributed largely to the increase in pH, thus reducing the amount of ash added. Magnesium (MgO), calcium and iron

are vital metals for the enzymatic activities of methanogenic microorganisms (Takashima et al., 1990), and the increase in their concentration (as occurred with the addition of CTB ash) in the AD process could stimulate its activity, increasing methane production and overall anaerobic performance.

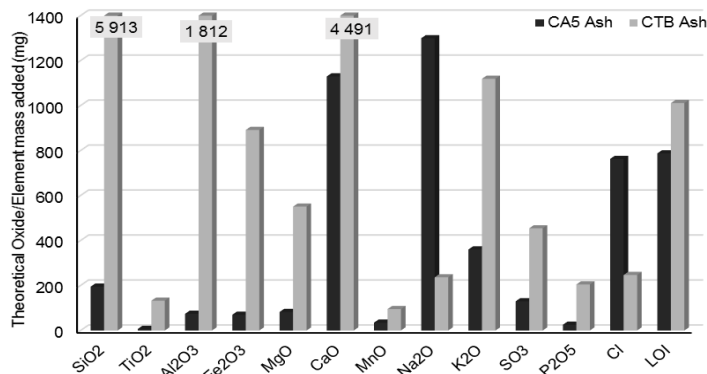


Figure 35| Representation of the theoretical mass of each oxide/element added to each bioreactor, considering the type of ashes used (CA5 or CTB).

The use of ash in the AD of several wastes and wastewaters is widely reported in the literature. Huiliñir et al. (2015) reported an increase in the methane volume produced and in the biodegradability of sewage sludge from the WW treatment of the paper industry by 135 % and 143 %, respectively, when FA was added to digesters as suppliers of trace metals. In this case, the increase in the volatile solids (VS) degradation was due to the higher microbial activity in the presence of ash, improving the methane production. Using fines from processing recovered paper, Steffen et al. (2016) observed that the presence of ash did not negatively influence the overall yield of the anaerobic conversion of organic material into methane. In their study, Montalvo et al. (2018) obtained an increase in the methane volume produced by 200 % compared to a reference assay, using a mixture of primary (60 %) and excess activated sludge (40 %) from a WWTP as a substrate. For this significant increase, these authors point out that the inclusion of solids could have contributed to the increase in the contact surface between microorganisms and substrate, enhancing the methane production. In addition, the FA used had several metals in its constitution, which leached and contributed to improve the anaerobic process and increase the methane production (Montalvo et al., 2018).

It is important to be aware of the different physico-chemical characteristics of the different types of wastes/wastewaters used in the AD process. For each type of waste, the AD process has different nutritional needs, making it necessary to adapt the process to the type of waste under study. In this case, a deep study focusing on the AD of D₀ with ash supplementation may be important to understand the influence of different types of ash on methane production and other important monitoring parameters.

Thus, with these results, it can be assumed that the use of CTB fly ash is beneficial for the AD process using D₀ as an effluent, as its presence during the digestion process enhances the sCOD removal with the benefit of methane formation. Besides that, the use of FA to neutralize acidic effluents from the P&P industry, such as D₀ effluent, can reduce operating costs with the acquisition of the chemical compounds (in this study NaOH was used to adjust pH). With this approach, it is possible to treat and value two different types of residues – solid residue as FA and liquid effluent like D₀ –, creating value from a sustainable process like AD with energy vector (methane) generation.

4.1.2 Fly ash (powder) addition to anaerobic digestion of cheese whey

Due to the high volume of effluent generated in the dairy industries, it is very important to treat those effluents efficiently. As mentioned earlier, dairy effluents, particularly those from cheese production, have a very high concentration of dissolved and particulate organic material, which can create several problems in the municipal WWTP (Carvalho et al., 2013). Cheese whey usually has a BOD/COD ratio above 0.5, being considered an easily biodegradable substrate, suitable for aerobic and anaerobic treatment (Prazeres et al., 2012).

The physico-chemical characteristics of this type of substrate led to an unstable operation in AD systems. The addition of alkalinity is essential for the stability of AD, in the start-up period or during the process (Gavala et al., 1999; Rodgers et al., 2004; Yang et al., 2003). The high organic loads present in the cheese whey effluents normally promote the production of VFA by acidogenic microorganisms, leading to the acidification of the system (Gutiérrez et al., 1991). In these cases, since the production of VFA is faster than its consumption by methanogenic microorganisms, they tend to accumulate in the reaction medium, causing a reduction in pH and suspending the COD removal from the liquid phase (Rodgers et al., 2004).

To overcome the pH inhibition caused by the accumulation of VFA in the medium, efficient methodologies for pH control can be applied. The use of fly ash in anaerobic systems is already documented, as a stimulant of the AD process as a source of micronutrients (Guerrero et al., 2019; Montalvo et al., 2019), and as a pH buffer material in the AD of municipal solid waste (Banks and Lo, 2003; Lo, 2005). However, to date, there are no studies presenting FA powder as a buffer material for an AD system treating cheese whey.

4.1.2.1 Anaerobic digestion of cheese whey with fly ash addition to control pH

The fly ash from an industrial thermal power plant (see section 3.3.1) was used mainly for pH buffering and stability control in the anaerobic system. The main objective of these small-scale bioreactors (*oxitop*) was to understand the effect of adding fly ash powder on the pH of the AD process in the treatment of cheese whey wastewater. The presented *oxitop* assays were performed according to the conditions described in section 3.5.1.2 (Table 22). The results presented here serve as a basis for the work developed and presented in the subsequent sections, namely, the application in AD processes of geopolymer spheres with fly ash in their constitution.

Figure 36 shows the pH values at the beginning, on the 15th day of incubation and at the end of the experiments, with different fly ash concentrations, ranging from 0.07 and 9 g/L. In Figure 36, the pH values are also shown for the reference assay (CW_0), without inorganic additives (fly ash or commercial chemical solution) for pH control, and for assays with the addition of commercial chemical solution (CW_Alk2 and CW_Alk4), with two different concentrations measured in alkalinity units (as CaCO₃). In all the different conditions tested, the pH dropped during the incubation period, with values approximately 50 % lower than the initial value at the end of the experiment. The only exception was the *oxitop* bioreactor where the highest FA amount was added (CW_9, with 9 g/L of fly ash), with a final pH value only 18 % lower than the initial pH value. After 15 days of incubation, the pH values were already low, close to those measured at the end of the experiment. *Oxitop* CW_7 was the exception, with an intermediate pH value (9.22) on day 15, in the mid-term between the initial and final pH values.

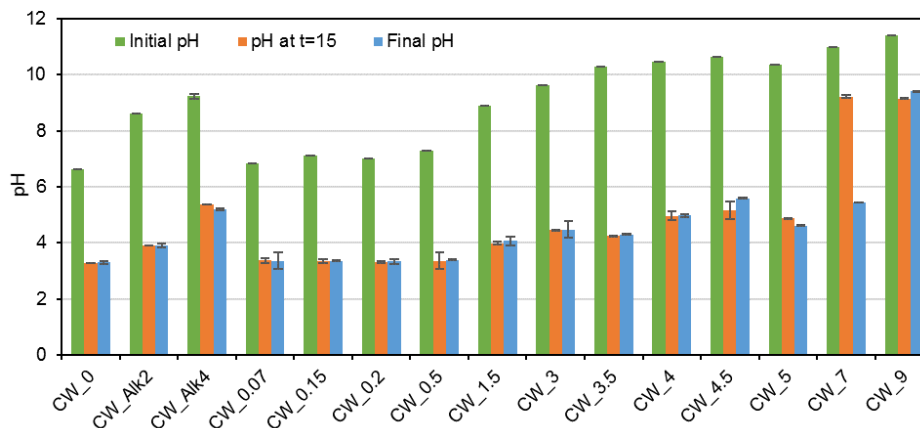


Figure 36] pH values (\pm standard deviation) measured at the beginning, on the 15th day and at the end of the *oxitop* batch anaerobic assays with cheese whey as substrate and fly ash for pH control.

Figure 37 illustrates the relationship between the pH values (initial and final) and the fly ash concentration added to each *oxitop* bioreactor. It was observed, as expected, that the initial pH value measured in each experiment increased with the increase in the FA amount added to act as an inorganic additive in pH control. This increase in the initial measured pH values followed a linear adjustment, with a determination coefficient of 0.852, indicating that the linear model described well the trend of the data presented. For the final measured pH values, the determination coefficient was slightly lower than the previous one (0.807), indicating that about 20 % of the data obtained do not follow the linear trend. For both initial and final pH values, the expected pH increase with the addition of FA (powder) was $0.539 (\pm 0.014)$ pH values per g/L of FA. This indicates that, even after 21 days of anaerobic incubation, the FA powder addition has a noteworthy influence on the pH values of the liquid fraction (digestate).

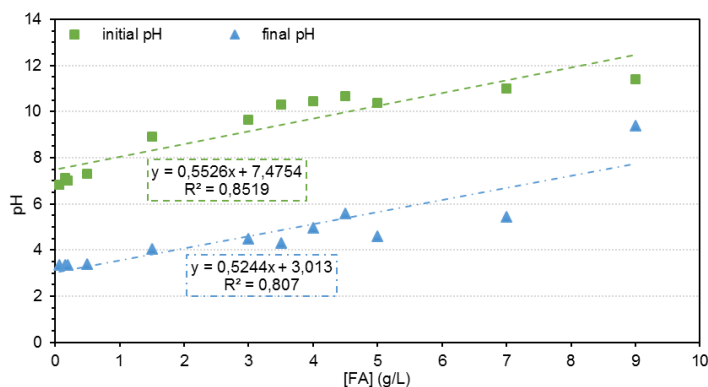


Figure 37] Relationship between pH (initial pH in green \square , and final pH in blue Δ) and FA concentration added, in batch *oxitop* of cheese whey AD assays.

The pH drop observed with the anaerobic process performed is indicative of microbial activity and the conversion of organic matter into intermediates such as volatile fatty acids (VFA). In fact, if VFA accumulation occurred during the acidogenesis step of AD, it results in a sharp drop in pH values and can inhibit the microbial community, especially methanogenic microorganisms (Wainaina et al., 2019). Acidogenic microorganisms are more tolerant to low pH values than methanogenic microorganisms and can tolerate slightly acidic conditions, being the optimal pH range for their

growth and activity often considered between 4.0 and 6.5 (Speece, 1996). These pH variations are normally counterbalanced by the formation of alkalinity through CO₂ production, promoting self-regulation of the system's pH.

Table 29 lists the measured initial and final pH values, the methane content in the formed biogas and the total VFA concentration at the end of the incubation time, presented as COD equivalents (gO_{2VFA}/L). Figure 38 shows the VFA composition of the initial and final samples for the conditions tested, regarding the VFA species present in large quantities, namely acetic, propionic and n-butyric acids. VFA species referred to as "others" refer to VFA species determined at much lower concentrations (i-butyric, i-valeric, n-valeric and n-caproic acids) than acetic, propionic and butyric acids.

Table 29| pH values on days 0 and 21, methane content in the biogas produced and total VFA concentration at the end of the experiment, in *oxitop* bioreactors containing different alkaline agents (CaCO₃ and powder FA) in different initial concentrations.

	Assay ID	Alkaline agent concentration (g/L)	pH at day 0	pH at 21 st day	CH ₄ content (21 st day) (%)	TVFA (21 st day) (gO _{2VFA} /L)
Reference	CW_0	-	6.62	3.31	0.0	0.42
Commercial solution	CW_Alk2	2	8.62	3.91	15.1	1.00
	CW_Alk4	4	9.23	5.19	27.6	6.05
Fly ash (powder)	CW_0.07	0.07	6.83	3.35	0.0	0.66
	CW_0.15	0.15	7.11	3.36	0.0	0.60
	CW_0.2	0.2	7.01	3.34	0.0	0.65
	CW_0.5	0.5	7.29	3.39	9.2	0.85
	CW_1.5	1.5	8.90	4.07	0.0	1.36
	CW_3	3.0	9.64	4.48	11.1	3.56
	CW_3.5	3.5	10.29	4.30	0.0	*
	CW_4	4.0	10.46	4.98	16.5	*
	CW_4.5	4.5	10.65	5.59	1.0	*
	CW_5	5.0	10.36	4.61	0.0	1.21
	CW_7	7.0	10.99	5.45	0.0	1.12
CW_9	9.0	11.41	9.41	0.0	0.68	

* not determined

At the beginning of the experiment, the total VFA concentration for all conditions tested with the addition of FA to control the pH varied between 0.31 and 0.58 gO_{2VFA}/L and tended to increase with the increase in the amount of FA added. The total VFA concentration at the end of the experiment increased by more than 50 % in all tested conditions, including in the tests with commercial alkalinity addition. For an intermediate FA addition (3 g/L), the total VFA concentration was greater than 3.5 g/L, confirming that the low pH value in the liquid phase was mainly due to the conversion of organic matter into VFA. For the test with 4 g/L as CaCO₃ addition of commercial alkalinity (CW_Alk4), a high VFA concentration of 6.05 gO_{2VFA}/L was obtained, which may be related to the more efficient buffering of the medium (higher initial alkalinity concentration), which created favorable acidogenic conditions within that bioreactor.

Acetic acid was the predominant acidic specie, accounting for over 60 % of the total VFA composition for all conditions at the beginning of the experiment and, in most conditions studied, it

is the predominant acidic specie at the end of the experiment (Figure 38). Propionic acid was also present in significant amounts at both sampling moments and butyric acid was formed mainly after AD of cheese whey. Butyric acid was present in larger concentrations when the conditions for the methane production were favorable, namely in the assays with 4 g/L of chemical alkalinity addition (CW_Alk4) and with 3 g/L of FA powder addition (CW_3). For these conditions, although the final pH values were not in the favorable methanogenic range (pH=5.19 for CW_Alk4 and pH=4.48 for CW_3), they did present methane in the biogas constitution. In fact, the presence of butyric acid and the production of methane are closely related, since this acidic specie, together with acetic acid, is the most favorable for methane production and a good indicator of the process performance (Lee et al., 2015).

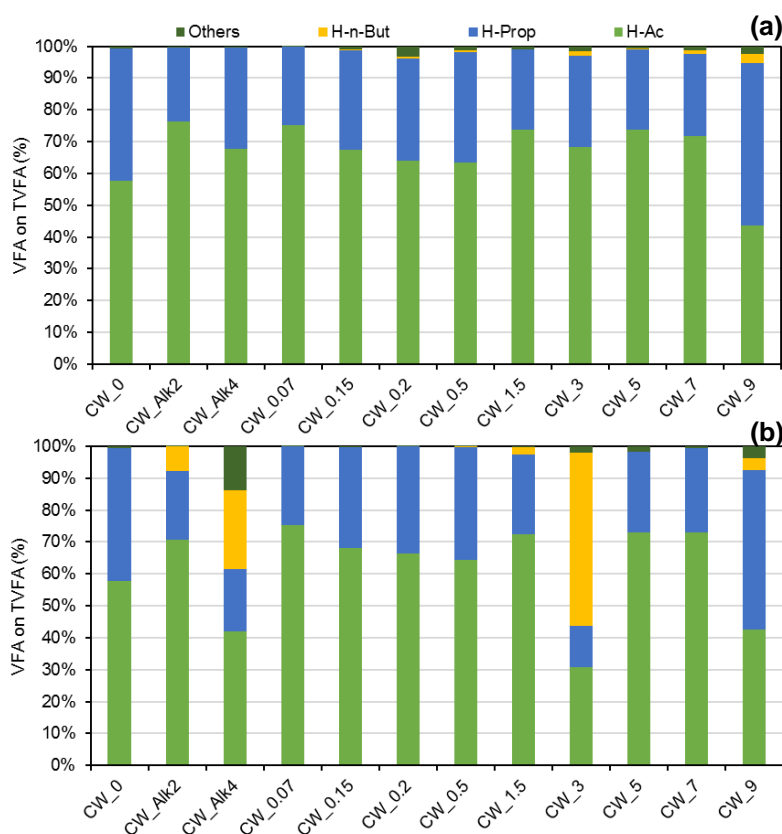


Figure 38 | VFA composition (H-Ac, H-Prop and H-n-But) of the initial (a) and final (b) samples for the AD of cheese in with different FA concentrations in *oxitop* bioreactors.

For these experiments, the methane content in the biogas obtained was very low, reaching a maximum of 28 % with chemical alkalinity addition and 17 % with FA addition. In this experiment, the methane content in the biogas and the pH values are not directly related, with the methane formation being observed in the bioreactors that presented final pH values below 5.2. The extreme conditions to which the microorganisms were subjected, initial pH above 9.0 (when more than 1.5 g/L of FA or 4 g/L as CaCO_3 of chemical alkalinity were added) or final pH below 4.5 (when less than 3.5 g/L of FA or 2 g/L as CaCO_3 of chemical alkalinity were added), they negatively influenced methane production. Very sensitive methanogenic microorganisms may have been partially inhibited with pH fluctuations and have resulted in a very low (or none) methane content in the biogas produced. This inhibition is related to lower growth rates of methanogens than other members of the anaerobic

microbial population (acidogens and acetogens), which require more time to survive and adapt to a new anaerobic system (Alkaya and Demirer, 2011) and, in this case, to extreme environmental conditions, such as pH.

Some authors have reported partial inhibition of methanogenic microorganisms in weak acidic conditions. Hwang et al. (2004) suggested that, at pH 4.5 – 5.0, not all methanogenic microorganisms are inhibited, in which the hydrogen utilizing (hydrogenotrophic) methanogens are active at low pH and, therefore, more tolerant than other methanogens under acidic conditions (Kim et al., 2004). Kim et al. (2004) also concluded that, if the reactor was operated for a sufficient time at pH 4.5, the growth of hydrogenotrophic methanogens was not completely inhibited and they presented some activity, while acetoclastic methanogens were completely inhibited.

4.1.2.2 Effect of fly ash addition in anaerobic digestion of cheese whey

For the experiments performed in the *oxitop* bioreactor, using cheese whey as a carbon source and adding FA powder to promote the pH regulation of the anaerobic system, some performance parameters were determined, mainly from the acidification step of AD. Figure 39 presents the performance parameters for the acidification step, such as the degree of acidification (DA) and the VFA yield (YVFA/COD), the organic matter (sCOD) removal and the methane content in the biogas. The parameters presented refer to the end of the experiment and the results for the assays with the addition of FA to control pH are shown and compared to the assay with the addition of 4 g/L as CaCO₃ of chemical alkalinity. Since the organic matter present in the medium was converted into VFA, and the time of incubation (21 days) was insufficient to achieve methane in the biogas (detectable for quantification) due to the adaptation of methanogenic microorganisms to extreme pH conditions, some tests showed zero sCOD removal and, for this reason, were excluded from Figure 39.

In these experiments, the sCOD removal was very low, obtaining values between 2 and 12 %. This indicates that only a small fraction of the solubilized organic matter (where VFA are included) has been removed from the liquid fraction, for methane and/or for microbial cell growth. The low methane content in the biogas (data in Table 29), together with the low sCOD removal is an indicator of the potential acidogenic behavior of the bioreactors.

The degree of acidification is the amount of solubilized organic matter that was converted into VFA and, in this case, was determined at the end of the experiment. For the assay with the addition of 4 g/L as CaCO₃ of chemical alkalinity, 58 % of sCOD was converted into VFA, presenting this bioreactor surely an acidogenic behavior. The assays with FA addition presented much lower DA than the assay with chemical alkalinity addition, with values between 6.8 and 13 %. The exception was the assay when 3 g/L of FA were added, which reached a maximum value of 40 %, due to the highest total VFA concentration obtained.

The VFA yield represents the amount of VFA produced from the substrate consumed by the microorganisms and provides an idea of the efficiency of the microorganism's metabolism. For this reason, both YVFA/COD and DA are closely related. When DA is high, such as the case of CW_Alk4 (58 %) and CW_3 (40 %), YVFA/COD is also high, with values above 0.78 gO_{2VFA}/gO₂. However, the value of sCOD removal is also related to the performance parameters of the acidogenic step. The sCOD removal in assay CW_Alk4 (15 %) is three times that obtained for assay CW_3 (5 %),

which makes the VFA yield of the CW_3 assay (0.87 gO_{2VFA}/gO₂) 11 % higher than the VFA yield of CW_Alk4 (0.78 gO_{2VFA}/gO₂). In this case, the microbial consortium was more efficient in the conversion of organic matter into VFA when 3 g/L of FA were used to control the pH of the anaerobic system. This slight improvement in the system when FA was added, may be related to the release of some metals present in FA, which enhanced the microbial anaerobic metabolism.

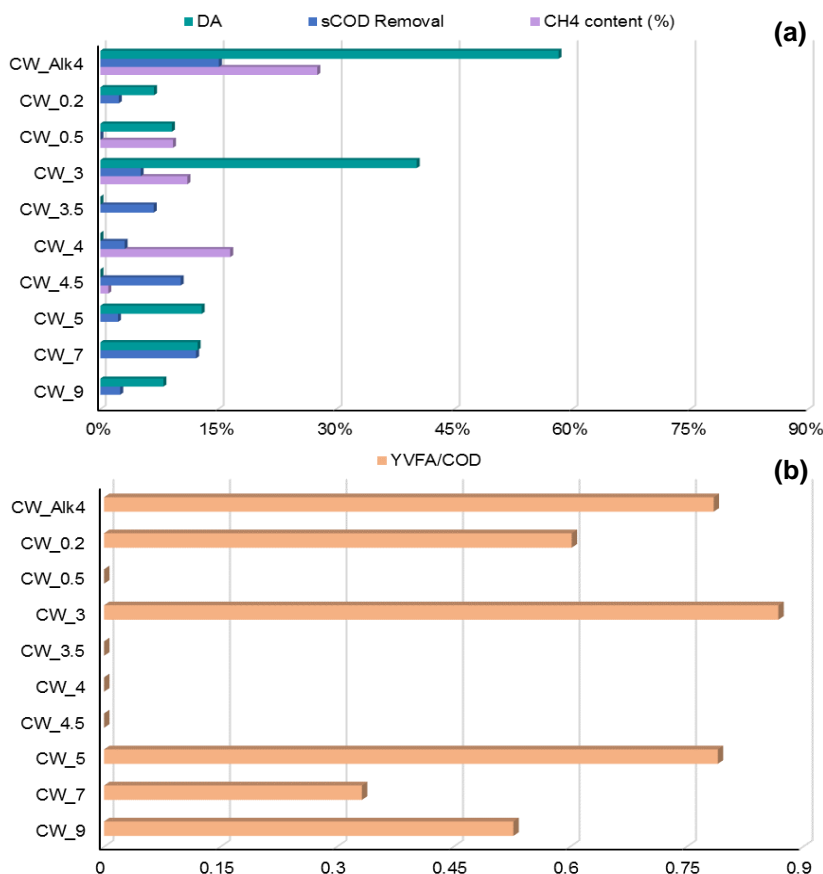


Figure 39 Anaerobic performance for anaerobic *oxitop* assays with cheese whey and different FA addition for pH control: degree of acidification (DA), sCOD removal and methane content in biogas (a) and VFA yield (b) at the end of the experiment.

Figure 40 shows the results obtained for the analysis of the content of the metals, specifically calcium, sodium, magnesium and iron, at the beginning and at the end of the batch experiments using different amounts of FA to control pH in the AD of cheese whey. The concentrations of metals were determined in the supernatant of each sample, thus representing the content of dissolved metals.

For the reference bioreactors, with chemical alkalinity addition, the sodium content is much higher than in test bioreactors, achieving more than 1200 ppm. In these bioreactors, the sodium content is provided by the addition of NaCO₃ to achieve the desired initial alkalinity concentration (4 g/L as CaCO₃). In test bioreactors, with the addition of FA powder to control pH, the calcium content is higher than the sodium content. With the incubation and anaerobic process, the calcium content increased in all conditions tested, at the end of the experiment. On the other hand, the sodium content remained almost constant with time in all bioreactors. This trend led to the conclusion that the calcium from fly ashes solubilized and was released during the time of the experiment. For magnesium and

iron, there is no trend in the content of the metals with the increase of fly ash added or with the time of the experiment. In the case of the reference bioreactors, the magnesium and iron contents are very low (< 25 ppm) and, in the test bioreactors, they remained below 138 ppm for magnesium and below 60 ppm for iron.

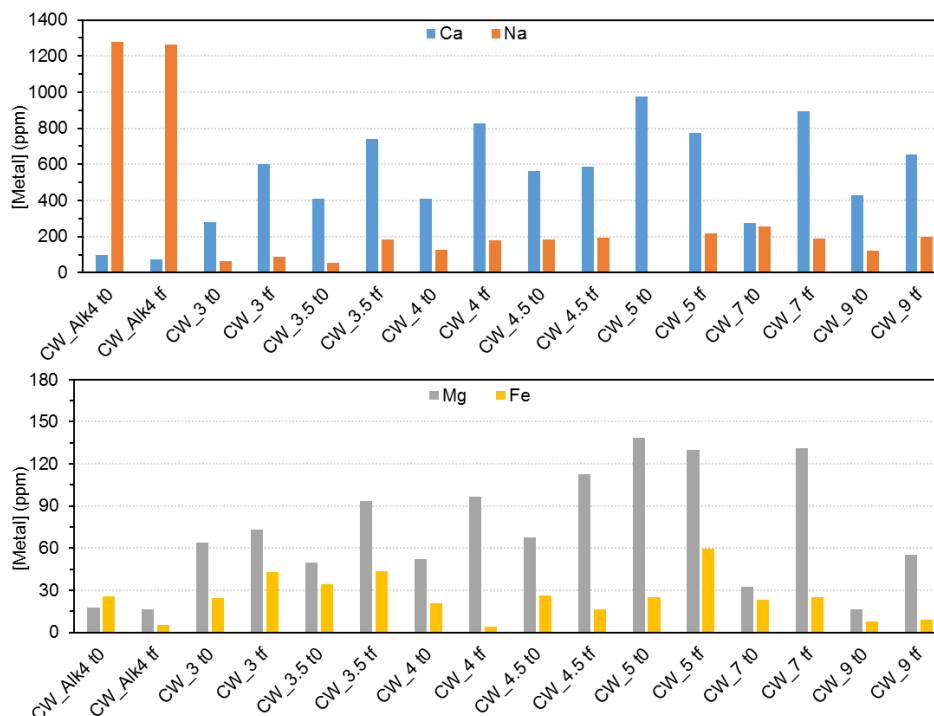


Figure 40 | Metals (Ca, Na, Mg, Fe) concentration at the beginning and at the end of oxitop batch anaerobic assays with cheese whey and FA addition, at different amounts.

As shown, the addition of FA to the medium led to an increase in the concentration of the metals leached from the ash. As shown previously (detailed characterization in Table 17), the CA5 ash used in this work has a high concentration on Na and Ca (both above 22 %), Cl (16 %) and K (7 %). With the increase in the amount of FA added, these elements (and other elements as Si, Mg, Al, Fe, Mn, P and Ti) potentially increased their concentration in the medium, since a part is solubilized and can be absorbed by the cells. The theoretical mass of each referred element added to four different bioreactors (CW_0.2, CW_3, CW_5, and CW_9) is included in Figure 41.

Elements as Ca, Na, K and Mg are considered essential for microbial growth, affecting the specific growth rate of microorganisms. However, its concentration must be moderate to stimulate growth, and excessive amounts of metals must be avoided since they can be severely inhibitory and toxic to microorganisms (Chen et al., 2008). The negative influence of metals in the AD process is determined not only by their concentration but also by their oxidation state, chemical form, pH of the medium and interactions with other compounds, which include antagonistic metals (Bożym et al., 2015).

The increase in buffer capacity when higher amounts of ash were added to the anaerobic system is related to the increase in the amount of Na and K, the main sources of alkaline properties of ash (Rajamma et al., 2009). Ca and Na increased widely with the increase in FA concentration but the inhibitory concentration for these elements was not achieved. For Ca, concentrations above

2400 mg/L can moderately inhibit the methane formation, while concentrations above 6000 mg/L of Na can cause total inhibition of the anaerobic system concerning methane production (Bożym et al., 2015)

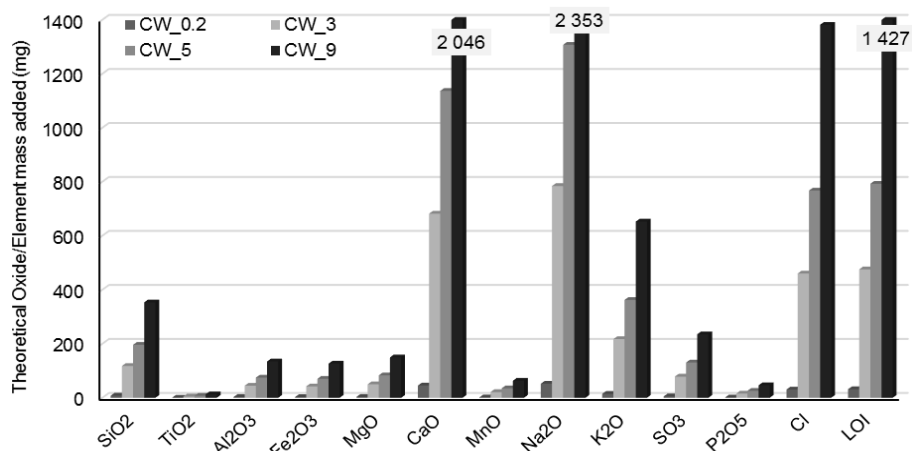


Figure 41| Representation of the theoretical mass of each oxide/element added to four bioreactors (CW_0.2, CW_3, CW_5 and CW_9) with the addition of CA5 fly ash powder.

Theoretically, other elements such as Si, Ti, Al, Fe, Mn, S and P were added in smaller amounts, not exceeding 200 mg/L of the element, even at the highest FA amount added. Chloride was present in the FA used in this work in high amounts (15 wt.% dry basis). In fact, FA has usually considered hazardous waste as it is mainly composed of metals, soluble salts and lime, with a high content of chloride (del Valle-Zermeño et al., 2014; Romero-Güiza et al., 2016). The increase in the chloride concentration in the liquid medium may have enhanced the inhibition observed in the methane formation for bioreactors with an addition higher than 4.5 g/L of FA.

With the results obtained, it can be assumed that the use of CA5 fly ash for the pH control of the AD process using cheese whey as a carbon source has some advantages. The methane formation was inhibited due to the low pH values achieved, however, the VFA production was favored and the microorganism's metabolism for the acidification step was slightly enhanced, compared to the use of the commercial alkalinity solution. As previously mentioned, the use of FA to control pH instead of commercial solutions can reduce operating costs and, at the same time, present solutions for waste management, with valorization potential (methane formation).

4.1.3 Comparison between bleaching effluent from pulp and paper industry and cheese whey from the dairy industry as substrates for methane production

Table 30 lists the main parameters used to evaluate the performance of the anaerobic assays performed with D₀ effluent and cheese whey as substrates, and with FA addition for pH regulation. The performance parameters include pH values, sCOD and AOX removals, and the parameters for evaluating acidogenic and methanogenic steps of AD.

Table 30 | Comparative values for the performance of AD of D₀ and cheese whey with FA addition.

	Parameter	D ₀ effluent *	Cheese whey **
pH	Initial pH	7.36	9.64
	Final pH	7.16	4.48
Organic matter	sCOD Removal (%)	64.6	5.1
Acidogenic step	[VFA] (mgO ₂ /L)	88	3563
	DA (%)	4.6	40.2
	YVFA/COD (gO ₂ VFA/gO ₂)	4.1	86.8
Methanogenic step	CH ₄ content (%)	21.5	11.1
	YCH ₄ /sCOD _{in} (mL/gO ₂)	0.26	***
	Methanization degree (%)	42.8	***
Adsorbable organic halides	AOX removal (%)	62.0	n.a.

* CTB fly ash addition (17.2 g/L), 2 gO₂/L of initial organic load from D₀ effluent

** CA5 fly ash addition (3 g/L), 8 gO₂/L of initial organic load from cheese whey

*** It was not possible to measure the pressure variation in *oxitop* vessel, making the determination unfeasible

n.a. – not applicable

The pH variation with cheese whey as a substrate indicates that the use of 3 g/L of FA (CA5) was not efficient to promote a methanogenic phase of the AD process. In fact, the addition of only 3 g/L of CA5 ashes to the AD process of cheese whey led to a low percentage of sCOD removal, high VFA concentration and low methane content in the biogas formed, evidencing a typical acidogenic behavior. On the other hand, the use of CTB ash in the anaerobic treatment process of D₀ effluent enhanced the methanogenic phase, with a low degree of acidification and a high methanization degree. In addition, in the AD process treating D₀ effluent, AOX removal from the liquid fraction was observed, reaching removal percentages above 60 %.

With the results obtained, it was observed that AOX has an inhibitory effect when the sCOD concentration of D₀ effluent added is greater than 2 gO₂/L, reducing the methane formed and the percentage of organic matter removal. In addition, in the AD of D₀ effluent with CTB fly ash (from a biomass-boiler that burns several types of wood and non-wood biomass) addition, a better methanogenic performance was obtained, compared to the addition of CA5 fly ash (from a biomass-boiler, which burns only Eucalyptus bark). CTB fly ash, in addition to increasing methane production, also increased the final aerobic biodegradability of the effluent.

The use of fly ash powder to promote pH control in the anaerobic treatment process of cheese whey was not effective, since the final pH and the performance parameters indicate that the systems presented acidogenic behavior. For this type of substrate, the use of a concentration higher than

5 g/L inhibited the formation of methane and a concentration of 3 – 4 g/L led to VFA accumulation, due to the poor alkalinity strength provided by the FA addition.

In the case of the bleaching effluent (D_0), its acidic nature can be problematic for the implementation of an anaerobic treatment, since the low pH can favor the VFA accumulation and the presence of compounds with low biodegradability requires a proper biomass adaptation (Jain and Mattiasson, 1998). On the other hand, the high organic matter content present in the cheese whey effluent can be converted into methane, if the environmental conditions inside the digesters favor methanogenesis, but it can also lead to the VFA accumulation, due to the low alkalinity of the effluent (Mockaitis et al., 2006) and rapid tendency to acidification (Escalante et al., 2018). Due to the characteristics of these two different effluents, mainly their organic load and biodegradability, cheese whey has a higher anaerobic treatment potential than D_0 effluent, with a high potential to be valorized into the energy vector (methane) (Escalante et al., 2018).

To ensure good methanogenic performance, pH and alkalinity must be controlled. The most common approach is the addition of chemical alkaline compounds, such as NaOH or NaHCO_3 , to increase the buffering capacity of the system, which makes the treatment more expensive (Charalambous et al., 2020) and sensitive to environmental changes. A good alternative is to explore the use of inorganic additives to promote pH control, such as fly ash, because they can release minerals, which act as micronutrients and neutralizing agents, ensuring good stabilization of pH (Shamurad et al., 2020). Some studies using fly ash in sludge (Guerrero et al., 2019) or municipal solid waste (Shamurad et al., 2019) digestion, have reported an improvement in methane production, showing the efficiency of this mineral supplementation in AD processes. Huang et al. (2018) also reported that the use of biomass FA in the two-step AD process treating food waste boosted the VFA accumulation in the acidogenic bioreactor and the methane formation in the methanogenic bioreactor.

However, the addition of fly ash (in powder formulation) to an anaerobic system does not allow the control of the alkalis' release, leading to a rapid increase in pH values, as was observed in *oxitop* bioreactors treating cheese whey, and poor long-term alkalinity control. For substrates with high acidogenic potential, as in the case of cheese whey, a controlled and prolonged pH regulation is crucial for the success of the AD treatment process.

The alternative developed and presented in the next sections to control the pH is the use of new materials that incorporate an alkalis source in their structure, as in the case of fly ash (or even red mud waste). New geopolymer spheres were developed to be tested in AD processes to improve the stability of the anaerobic system (in terms of pH) and increase the methane formation. To test their capacity and strength to control the system's pH, a substrate with high biodegradable potential and a tendency to acidify quickly, such as cheese whey, was studied.

4.2 Phase 2: Fly ash-based geopolymers addition to anaerobic digestion assays

Part of this chapter was published in:

“Gameiro, T., Novais, R., Correia, C., Carvalheiras, J., Seabra, M.P., Tarelho, L., Labrincha, J.A., Capela, I. (2021). Role of waste-based geopolymer spheres addition for pH control and efficiency enhancement of anaerobic digestion process”. *Bioprocess and Biosystems Engineering*. <https://doi.org/10.1007/s00449-021-02522-w> (IF=2.419)

“Novais, R.M., Gameiro, T., Carvalheiras, J., Seabra, M.P., Tarelho, L.A.C., Labrincha, J.A., Capela, I. (2018). High pH buffer capacity biomass fly ash-based geopolymer spheres to boost methane yield in anaerobic digestion. *J. Clean. Prod.* 178, 258–267. <https://doi.org/10.1016/j.jclepro.2018.01.033>” (IF=7.246)

Part of this chapter was presented in:

“Gameiro, T., Novais, R.M., Seabra, M.P., Tarelho, L.A.C., Labrincha, J.A., Capela, I. Geopolímeros para controlo de pH: aplicação em processos de digestão anaeróbia. *Environment International Conference in Portuguese*. 08 – 10 may 2018, Aveiro, Portugal. (Oral presentation)”

“Gameiro, T., Correia, C., Novais, R.M., Seabra, M.P., Labrincha, J.A., Capela, I. (2019). pH control in anaerobic bioreactors using fly-ash based geopolymers as buffer material. *International Conference on Green Energy and Environmental Technology*. 24 – 26 July 2019, Paris, France. (Oral presentation)”

4.2 Phase 2: Fly ash-based geopolymers addition to anaerobic digestion assays

In this section, the assays described in sections 3.5.1 and 3.5.2 were performed applying the operational conditions detailed in Table 23 and Table 24. The concentrated cheese whey solution was used as a substrate in anaerobic batch and fed-batch assays and geopolymer spheres used as a buffer material in the developed processes.

First, since the geopolymer spheres leach organic compounds into the liquid medium, a small test was performed to study the increase in sCOD caused by the GS addition. The composition of the GS binder based on fly ash was also evaluated, studying the difference in the pH control of the AD system using both metakaolin and fly ash as sources of aluminosilicates in the geopolymer spheres manufacture. Since fly ash-based geopolymers showed better anaerobic performance, they were used in long-term batch assays studying different GS concentrations.

The porosity of the spheres can also influence the anaerobic performance of the system. Thus, tests with low and high porosity geopolymer spheres were performed in batch and fed-batch scale. The HPGS showed an increase in methane formation and fed-batch assays with four AD cycles were performed to test the viability of using the spheres over a long period and organic load shocks.

For these assays, several goals were defined, namely:

- I. Determination of the influence of geopolymer spheres addition in liquid mixtures (with and without anaerobic biomass), in terms of soluble organic matter (measured in sCOD);
- II. Determination of the influence of the binder composition (metakaolin or fly ash, in different proportions) and concentration of geopolymer spheres in the pH control of the anaerobic degradation of cheese whey;
- III. Determination of the influence of fly ash-based geopolymer spheres concentration in the methane production from cheese whey anaerobic digestion batch process;
- IV. Evaluation of the anaerobic performance of batch bioreactors treating cheese whey and using fly ash-based geopolymers spheres as an inorganic additive to control pH;
- V. Study of the effect of porosity and geopolymer spheres concentration on methane production, operating a 2-cycle fed-batch anaerobic process treating cheese whey;
- VI. Evaluation of the anaerobic performance of 2-cycle fed-batch bioreactors treating cheese whey and using low and high porosity geopolymer spheres as an inorganic additive to control pH;
- VII. Study of the effect of the prolonged operation of multiple cycle fed-batch anaerobic system, using fly ash-based geopolymer spheres as buffer material and cheese whey as substrate;
- VIII. Comparison of different fly ash-based geopolymers spheres to promote pH control and methane boost in the anaerobic digestion process of cheese whey;
- IX. Definition of the type and concentration of the fly ash-based geopolymer spheres, suitable for use on in anaerobic digestion process treating cheese whey wastewater.

4.2.1 Fly ash-based versus metakaolin-based geopolymer spheres: anaerobic digestion assays with cheese whey

The use of waste-based GS with high buffer capacity can be an effective solution, in comparison with commercial alkaline materials, to promote prolonged pH control in AD of highly biodegradable waste streams. In addition, easier recovery and the possibility to reuse make these materials attractive compared to using FA (in powder form) to control the pH (see the results presented in section 4.1).

To determine the influence of the binder composition of GS, namely metakaolin or fly ash, several tests were performed, in *oxitop* batch bioreactors and in 1 L batch bioreactors. *Oxitop* bioreactors were performed to define the concentration of GS to be used on a larger scale (1 L batch bioreactors). The initial substrate concentration corresponding to sCOD of 8 gO₂/L and the initial biomass concentration of 2 gVSS/L were based on previous anaerobic tests with cheese whey as substrate performed by Silva et al. (2013).

4.2.1.1 Geopolymer spheres characterization before anaerobic digestion assays

After the GS synthesis, performed as described in section 3.3.2.1, the spheres to be used in the *oxitop* assays (results presented in section 4.2.1.2.2) and in the 1-cycle batch assays (results presented in section 4.2.1.3) were characterized as described in section 3.6.9 of the methodology chapter. Photographs of the produced geopolymer spheres (composition details in Table 18) containing 33 wt.% FA (MK-based GS) and 75 wt.% FA (FA-based GS) are shown in Figure 42 (a) and (e), respectively.

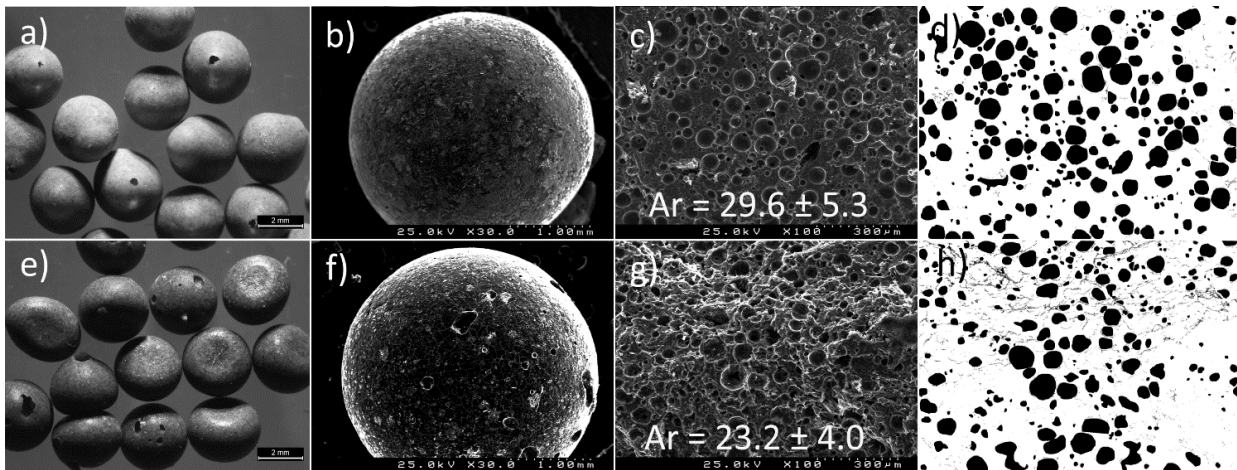


Figure 42| Optical (a and e) and SEM characterization (b-d and f-h) of the porous geopolymer spheres prepared with (a-d) 33 wt.% (MK-based spheres) and (e-h) 75 wt.% FA (FA-based spheres). Figure (d) and (h) correspond to binary images (black and white) of the SEM micrographs.

The spheres had a homogeneous particle size distribution with a diameter of about 3 mm. Figure 42 also includes SEM micrographs of the spheres' outer surface and their pore microstructure. Figure 42 (b) reveals a perfect and homogeneous surface for the MK-based spheres, while a more porous surface is observed for the FA-based spheres Figure 42 (f). Figure 42 (c) and (g) show that in both compositions a high number of closed pores is present. Nevertheless, to better assess the pore size and distribution, image analysis was performed on SEM micrographs of the spheres.

Average A_r was included in Figure 42 (c) and (g), while the cumulative area ratio is depicted in Figure 43. The results show a higher porosity ($\approx 6\%$ higher A_r) for MK-based spheres in comparison with FA-based ones. Moreover, the cumulative area ratio (see Figure 43) shows a broader pore size distribution for MK-based spheres. The differences observed in porosity and pore size distribution influence the particle surface area and, therefore, are expected to influence the leaching behavior of the spheres. It should be highlighted that, while providing useful information on pore size distribution image analysis, it can provide only a detailed two-dimensional image of the pores, while its connectivity, which will crucially affect leaching behavior, cannot be assessed using this technique.

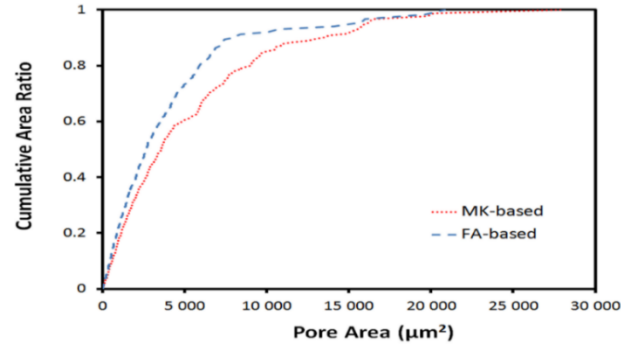


Figure 43| Cumulative area ratio for the different compositions, MK-based and FA-based GS (measured using image analysis).

Figure 44 shows the EDS spectrum of the surface and the inner part of the spheres for the two geopolymer compositions. Significant differences are perceived between the systems: the MK-based spheres have a higher sodium content on the surface and a lower content on the inside; while in FA-based spheres the opposite is observed.

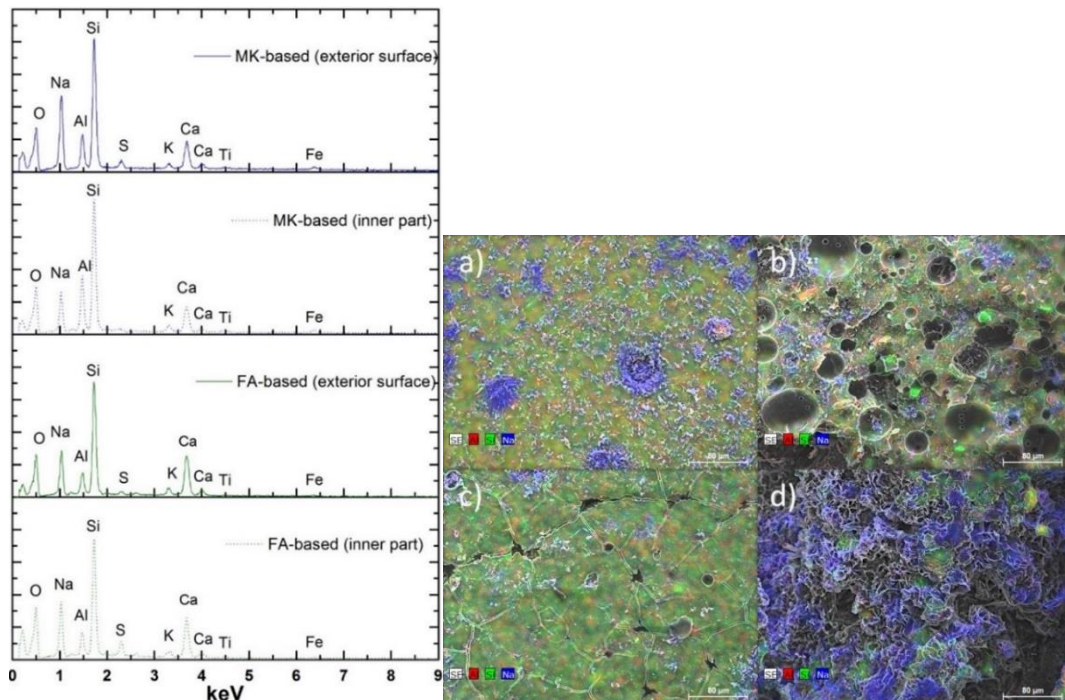


Figure 44| EDS spectrum of the MK-based and FA-based geopolymer spheres (left); EDS maps (right) of MK-based (a and b) and FA-based (c and d) geopolymer spheres. The first column (a and c) maps correspond to the spheres exterior surface and the second column (b and d) to their inner part.

The spectrum also shows that the aluminum content in MK-based spheres is greater than that observed in their FA-based counterparts. The latter observation is attributed to the different chemical composition of the precursors (see Table 17). In fact, the $\text{SiO}_2/\text{Al}_2\text{O}_3$ ratio is about 2.5 times higher in the FA (3.41) in comparison with MK (1.38). These differences are expected to affect the alkalis leaching from the geopolymers, and hence their ability to buffer the pH. A work performed by Novais et al. (2017) in water media showed that FA-based spheres leach higher alkalis amounts in comparison with their MK-based counterparts and, for this reason, a higher pH buffer capacity was obtained for this system.

To characterize the composition of individual spheres, EDS maps of their surface and inner part were collected and included in Figure 44. The maps clearly demonstrate the higher sodium content on the surface of the MK-based spheres in comparison with the FA-based specimens, in line with the EDS spectrum.

Figure 45 presents the XRD patterns of the different geopolymer spheres. The MK-based sphere pattern shows a broad hump at $2\theta = 20\text{-}40^\circ$, while a smaller hump is observed in the FA-based spheres, which is associated with a higher content of more crystalline FA and a smaller amount of highly amorphous MK, in this composition.

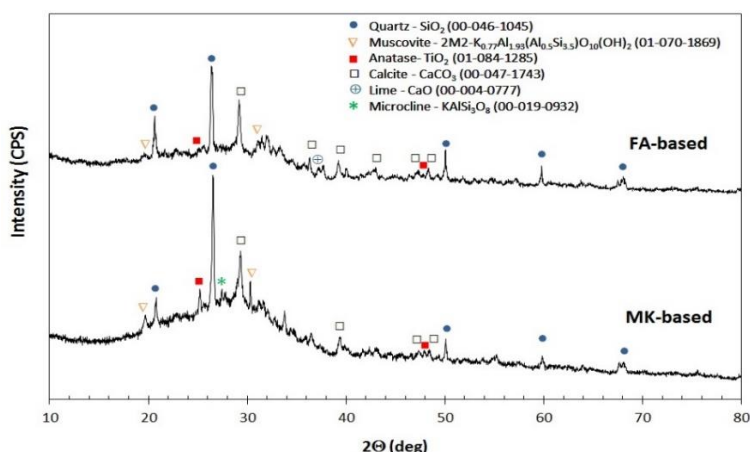


Figure 45| XRD patterns of MK-based and FA-based geopolymers spheres.

4.2.1.2 Effect of geopolymer spheres addition on soluble chemical oxygen demand content

During the manufacture of geopolymer spheres, they are immersed in a PEG solution (as described in section 3.3.2.1), and some molecules tend to be adsorbed on the GS surface. When immersed in an aqueous medium, these molecules tend to desorb and remain suspended in the aqueous medium, with the potential to be used by anaerobic microorganisms for growth and product formation.

To study the influence of GS addition on the increase in sCOD of mixtures with cheese whey, probably due to the leaching of PEG from GS, a small test was performed. Table 31 summarizes the conditions applied to the bioreactors. In these assays, the substrate and anaerobic biomass concentrations were the same as those tested in all *oxitop* bioreactors operated, implying the dilution of the concentrated cheese whey solution and the biomass collected in the WWTP. The assays were incubated for 20 days and the temperature was kept at $36 \pm 1^\circ\text{C}$ throughout the incubation time.

Table 31| Mixtures compositions for sCOD testing, with GS addition.

Assay	Cheese whey solution (CW) (8 gO ₂ /L)	Anaerobic biomass (2 gVSS/L)	Chemical alkalinity (Alk) (4 gCaCO ₃ /L)	FA geopolymers (GS) (4 g/L)	Water
COD1	✓	✓			✓
COD2	✓	✓	✓		✓
COD3	✓	✓		✓	✓
COD4				✓	✓
COD5		✓		✓	✓
COD6	✓			✓	✓

The results regarding the sCOD over time for the mixtures tested are shown in Figure 46 (a) and the corresponding pH values are presented in Figure 46 (b). The COD1 assay refers to the mixture of biomass and cheese whey (CW), without chemical alkalinity or GS addition to control the pH. In this mixture, the sCOD decreased by 27 % after 1 day of incubation and remained almost constant until the end of the experiment. The pH values for this bioreactor decreased to 3.5 on day 3 of incubation and remained strongly acidic until day 17. With this substrate, with a high organic load and biodegradable potential, it is expected that the absence of alkalinity (chemical or otherwise) leads to acidification of the bioreactor, which occurred in the COD1 assay.

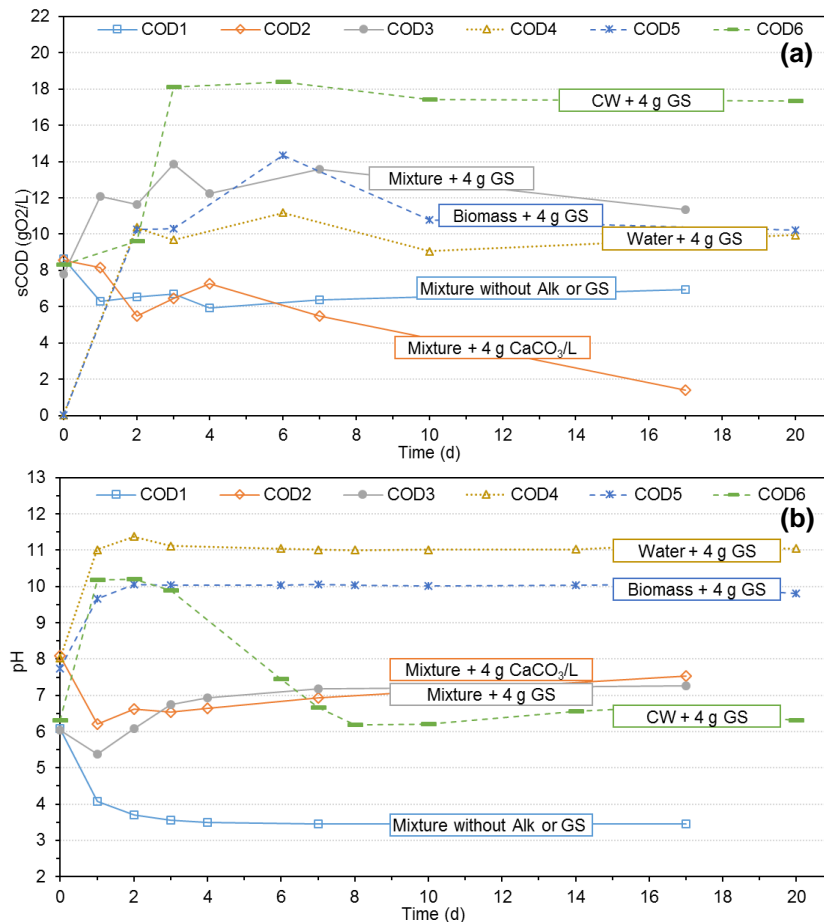


Figure 46| Results for the preliminary tests performed with the addition of GS, regarding sCOD (a) and pH (b) over time.

To confirm the need for alkalinity in this type of anaerobic system to be studied, the bioreactor COD2 was performed, with chemical alkalinity addition (4 g/L measured as CaCO₃). The sCOD tends to decrease with time, reaching 1.39 gO₂/L at the end of the experiment. The pH values confirm the potential of using chemical alkalinity to control the pH in anaerobic systems using cheese whey, with a high sCOD reduction (more than 80 % of sCOD removal) and pH values within the neutral range, suitable for methane production.

For the mixture represented by COD3, 4 g/L of FA-based GS were added to the mixture of biomass and cheese whey solution. The results show an increase in the sCOD from 7.81 to a maximum of 13.86 on day 3, which corresponds to an increase in the sCOD of 6.05 gO₂/L. This value is high, considering the sCOD added in the experiments (\approx 8 gO₂/L), and it corresponds to \approx 75 % of initial organic load added. The pH for the COD3 assay decreased slightly on the first day of incubation and, after a minimum value of 5.37, increased and remained in the neutral range after day 3 of incubation, similar to the pH profile of COD2.

To confirm the influence of the GS addition on the sCOD increment, three additional tests were performed, namely: COD4, with GS in water, COD5, with anaerobic biomass and GS, and COD6, with cheese whey (diluted) and GS. For the three tests, the increase in sCOD after the GS addition is very clear, obtaining values between 9.93 gO₂/L and 10.20 gO₂/L of the sCOD increment. In water and biomass, the pH was kept constant from day 2 to the end of the experiment, in values around 10 (COD5) and 11 (COD4). In these assays, the observed pH stability was expected, since the mixtures lack substrate, essential for anaerobic microbial activity. For the assay with cheese whey and GS, the pH increased to 10.2 on day 2 of incubation and started to decrease after that, stabilizing in the range 6.20 – 6.60 after day 7. The use of a non-sterile cheese whey solution and applied temperature (36 °C) boosted the development of microorganisms and promoted the organic matter degradation, which decreased the pH of the media, with the accumulation of volatile fatty acids and other biological intermediates.

From the assays performed, it is possible to conclude that the addition of GS to an aqueous medium increases the sCOD content by about 10 gO₂/L, probably due to the leaching of organic compounds (PEG) attached to the surface of the spheres. This organic compound can be degraded by the anaerobic microorganisms, as several authors have previously reported (Chen and Hu, 2015; Dosta et al., 2018; Huang et al., 2005; Otal and Lebrato, 2003). Thus, the determination of methane yields and sCOD removals in assays in which FA-based GS was used as a buffer material will take into account the increase in sCOD triggered by the leaching of organics from the GS addition.

4.2.1.3 *Oxitop batch assays with geopolymers spheres: effect of the binder composition*

It is recognized that the methanogenic digestion of highly biodegradable substrates is problematic. The proposed strategy can improve the stability and efficiency of the systems (e.g. methane yield) and simplicity (prevent the need for continuous pH adjustment). The influence of the binder composition (metakaolin (MK)-based or FA-based) and its content on the ability to control the pH in the AD of cheese whey (substrate with high acidogenic potential) was evaluated.

For this, 15 *oxitop* bioreactors were performed with different amounts of GS (MK and FA-based) additions (details in Table 23). In this experimental set-up, only the pH values were monitored during

the 21 days of incubation and the methane content was determined at four sampling moments during the incubation period. This preliminary pH assessment performed in *oxitop* bioreactors was used to select the optimal formulation and amount of GS for the study of methane production in larger-scale trials.

To evaluate the influence of the geopolymer composition on the pH evolution in the AD of cheese whey, several amounts added (20, 40 and 80 g/L) of the two types of spheres were studied over 21 days. Table 32 lists the initial pH (day zero) and pH on the 1st and 21st day and the methane content on the 21st day, for all bioreactors operated. Figure 47 shows the pH fluctuation inside the batch anaerobic digesters (total volume of 250 mL) as a function of time, representing the average values for the replicates performed, with standard deviation.

Table 32 | pH values on days 0, 1 and 21, in *oxitop* bioreactors containing different alkaline agents in different concentrations.

	Assay ID	Alkaline agent concentration (g/L)	pH at day 0	pH at 1 st day	pH at 21 st day	CH ₄ content (21 st day) (%)
Reference	R0	-	7.18	4.68	4.42	5.7
Commercial solution	R1	2	8.23	4.86	4.88	14.7
	R2	4	9.61	6.91	6.51	50.4
FA-based GS	R3 – R4	20	7.14	6.21	6.48	49.8
	R5 – R6	40	7.14	8.54	8.81	0.0
	R7 – R8	80	7.69	11.69	11.55	0.0
MK-based GS	R9 – R10	20	6.42	5.44	6.33	60.1
	R11 – R12	40	7.09	6.64	7.49	42.3
	R13 – R14	80	6.76	9.21	10.23	0.0

For bioreactors containing geopolymer spheres, the pH immediately after spheres addition (at day zero) was maintained at levels similar to those of the reference assay, showing a different behavior when compared to the alkali addition assay. In the following days, the pH was considered dependent on the spheres' content (20, 40 or 80 g/L) and composition (MK-based or FA-based). Higher amounts of spheres generally increase the pH, with higher values achieved for assays using FA-based spheres instead of MK-based spheres. In bioreactors containing MK-based spheres, the pH on the 1st day of incubation increased from 5.44 to 9.21 by increasing the amount of spheres from 20 to 80 g/L, while even higher pH values were observed when using larger quantities of FA-based spheres (ranging from 6.21 to 11.69 with the increasing amount of spheres). These results show that FA-based spheres leach higher amounts of alkali in the medium in comparison with the MK-based spheres, which may be associated with the lower geopolymerization degree achieved for the FA-based compositions, resulting in larger amounts of alkalis available for leaching (Novais et al., 2017).

To better understand the influence of the matrix (MK-based or FA-based) on the OH⁻ leaching behavior, without the contribution of the pore size and its connectivity, 1 g of spheres was milled and added to 50 mL of distilled water and magnetically stirred for 24 h. The leaching of OH⁻ ions was determined by the acid-base titration method (using 0.035 M HCl as the titrant and phenolphthalein as the acid-base indicator). The FA-based geopolymer leached 0.026 mol/dm³ OH⁻ ions, substantially higher than that observed for the MK-based one (0.016 mol/dm³). This result shows that the matrix composition crucially influences the leaching behavior of the spheres.

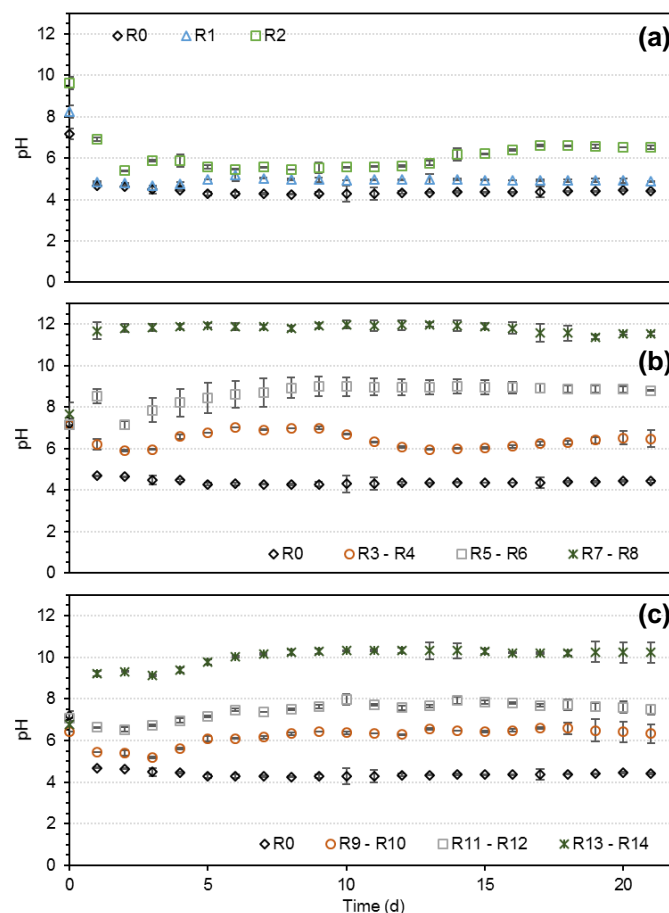


Figure 47 | pH fluctuation (average values \pm standard deviation) in anaerobic digesters as a function of time with alkaline chemicals (a), FA-based (b) and MK-based (c) geopolymer spheres addition.

The higher leaching behavior observed for FA-based spheres allows for an improved pH buffering ability. In fact, a narrower pH fluctuation was observed for FA-based geopolymer spheres. In these bioreactors, the pH gradient (pH difference between the 1st and the 21st day) was 0.27, 0.27 and 0.14, respectively, for bioreactors containing 20, 40 and 80 g/L of GS, being 0.89, 0.85 and 1.02 for those containing MK-based geopolymer spheres. This behavior clearly demonstrates the remarkable potential of this innovative material (FA-based geopolymer spheres) as a pH regulator in AD processes, due to its gradual and prolonged leaching behavior (narrower pH fluctuation). The results show that the pH level in the AD can be adjusted considering the desired application, for example, the generation of methane or hydrogen, through an energy valorization, or VFA recovery, through a material valorization. This versatility can be achieved using the appropriate combination of binder composition and amount of geopolymer spheres, which further demonstrates its interesting potential.

The results show that only for high concentrations of spheres (80 g/L of MK-based spheres and 40 and 80 g/L of FA-based spheres) the pH reached very high values for AD stability (9.21, 8.54 and 11.69, respectively, on the 1st day of the experiment), comparable with both assays with chemical alkali addition. The use of 20 g/L of FA-based spheres and 40 g/L of MK-based spheres maintained the pH between 5.90 and 7.14 and between 6.53 and 7.96, respectively, during the test period (21 days), which can be considered suitable for methane production in AD (C. Zhang et al., 2014). Hence, considering economic and environmental reasons (less amount of spheres and higher content in

FA), only FA-based spheres were selected for the next stage (evaluation of methane potential in larger batch bioreactors).

Regarding methane production, the results obtained for the methane content in biogas at the end of the *oxitop* experiments were also listed in Table 32. Figure 48 helps to understand the relationship between the final pH values measured in anaerobic bioreactors and the methane content in biogas at the end of the experiment.

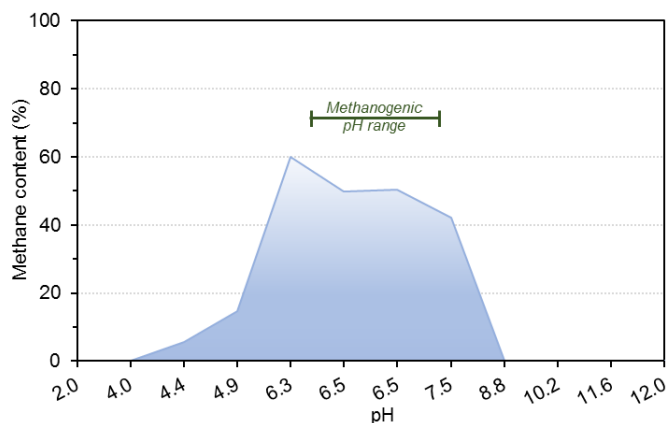


Figure 48 | Methane content vs pH at the end of *oxitop* experiments containing different alkaline agents at different concentrations.

As mentioned earlier, an acceptable pH range for the maximum methanogenic activity of methanogenic microorganisms is between 6.8 and 7.2. According to the results obtained (Table 32), the highest methane content (60 %) was obtained at a pH of 6.33 (R9 – R10). Although slightly below the optimum methanogenic pH range considered before (near-neutral pH range), the pH values measured in R9 – R10 bioreactors are perfectly acceptable for methane formation, as referred by many authors who have studied different types of substrates (Anderson et al., 2003; Ghaly et al., 2000). It is also stated that methane-producing microorganisms have an optimal growth in the pH range between 6.6 and 7.4, although the stability of the anaerobic system regarding methane formation can be achieved in a broader pH range, between 6.0 and 8.0. Below pH 6.0 and above pH 8.3, methane forming microorganisms can be inhibited, reducing methane formation and leading to process inhibition (Chernicharo, 2007).

4.2.1.4 1-cycle batch assays: effect of spheres addition on the anaerobic digestion of cheese whey

For batch tests on a larger scale, and to obtain a correct pH range for methane production, two different amounts of FA-based spheres were used: 20 (FA2) and 28 g/L (FA3), where the former was selected considering the results shown in the previous section, while the later was speculated from the tests presented previously (1st stage). In these 1-cycle batch assays, only geopolymer spheres were used as pH regulators. A blank test (FA1) was performed under the same conditions as the previously described bioreactors, but without the addition of chemical alkalinity or geopolymer spheres to promote pH control.

4.2.1.4.1 pH evolution

Figure 49 depicts the pH values measured during the incubation time in the performed bioreactors, namely FA1 (blank assay), FA2 (with 20 g/L of FA-based GS) and FA3 (with 28 g/L of FA-based GS). The experimental conditions applied to these anaerobic batch assays were summarized in Table 24 in the methodology section.

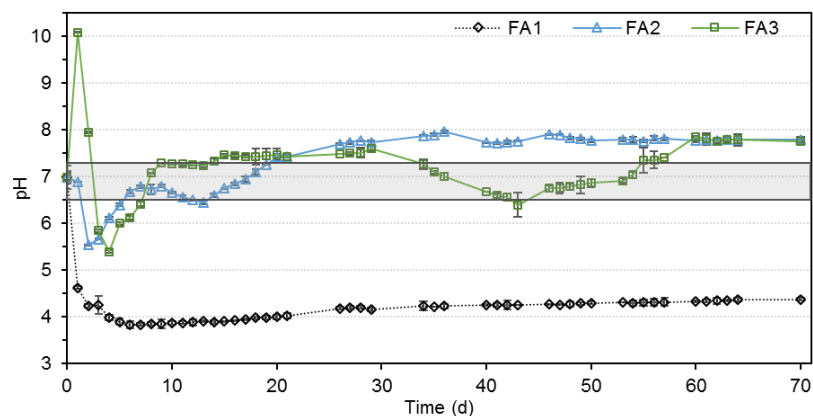


Figure 49| Fluctuation of pH in anaerobic digesters to optimize methane production as a function of time, with the addition of different amounts of FA-based geopolymer spheres.

The pH of the blank batch reactor (FA1) drops immediately on the 1st day of incubation, from 6.99 to 4.63, reaching values below 4.00 after the 4th day. After the 6th day of incubation and until the end of the experiment, the pH ranged between 3.84 and 4.38, and methane was not detected during the entire incubation period, confirming the acidification of this reactor, as expected due to the lack of alkalinity. Therefore, without alkalinity addition to the system, it was not possible to control the pH to values favorable to methane production (near neutral pH). This occurred mainly due to the nature of the substrate used, since the compounds present in cheese whey are highly biodegradable, containing lactose, proteins and fats (Prazeres et al., 2012).

The pH evolution in bioreactors containing GS was markedly different from the FA1 reactor. In the reactor containing 20 g/L of spheres (FA2), a smaller drop in pH (from 6.99 to 5.54) was observed in the first two days of incubation. In this reactor, after the fourth incubation day, the pH values remained above 6.10, mostly between 7.70 and 7.96 until the 70th day. A similar pH profile was obtained by Pagliano et al. (2019), with a decrease in pH to values close to 5.0, followed by a recovery of the system, stabilizing at values above 6.0 after 15 days of AD of cheese whey wastewater.

As for the reactor containing the highest concentration of spheres (28 g/L – FA3), the trend is close to that observed when using less concentration of GS, but with a much higher variation and a sharp increase in pH on the first day (up to 10.09). Hence, in bioreactors containing GS, the release of OH⁻ in the initial period (up to 10 days) allowed the pH to be maintained above 5.70, as opposed to the blank reactor, where the pH dropped to values below 4.00 and maintained at this value until the end of the experiment.

After this initial period, characterized by high pH fluctuations, it was possible to control the pH around 6.70 – 7.50 in both bioreactors containing GS, a favorable pH range for methane production, although under high volatile acids concentrations. This was possible due to the balance between carbon dioxide in the headspace (mostly between 20 – 50 vol.%) and the alkalinity provided by the

geopolymers leachate of OH^- (varying between 1000 and 6000 mg/L as CaCO_3). Although the values are in the favorable range for methane production, for the reactor FA2, the lowest pH values after the initial period (6.70 to 6.90) were obtained immediately after that period, when the carbon dioxide in the headspace was high (40 to 60 vol.%) and the alkalinity provided by the spheres leachate was lower. For the bioreactor FA3, the lowest pH values (6.70 to 6.90) were achieved in a later period (35 - 55 days), when carbon dioxide in the headspace was still high (40 to 50 vol.%). During this period, the alkalinity provided by the spheres was not enough to maintain high bicarbonate alkalinity, due to the volatile acids increase observed in that period (from 1600 to 2200 mg/L). These results (pH = 6.70 - 7.80) prove once again the high buffer capacity of the FA-based spheres when compared to those observed in the blank bioreactor (FA1).

4.2.1.4.2 Volatile fatty acids production

In the AD process, the two main steps (acidogenesis and methanogenesis) have different reaction rates, making the process naturally unbalanced (Hassan and Nelson, 2012), thus allowing the detection of VFA species present in the mixed liquor. The determination of the VFA composition of the soluble phase is very important since it provides some information on the metabolic pathways involved in the anaerobic degradation process (Parawira et al., 2004). Acetic, propionic and butyric acids are formed during the fermentation of carbohydrates and proteins and also during the anaerobic oxidation of lipids (Horiuchi et al., 2002).

Figure 50 shows the total VFA concentrations for all experiments, expressed as acetic acid equivalents. The amounts of acetic, propionic and n-butyric acids, which are the main constituents of the analyzed VFA mixtures, are shown in Figure 51 and the concentrations of each VFA specie were expressed as COD equivalents ($\text{mgO}_2\text{VFA/L}$). For the referred samples, i-butyric, i-valeric, n-valeric and n-caproic acids were also determined individually, but the concentrations were much lower when compared to the three main acids present in the liquid phase, and, therefore, were not represented in the figure.

In the blank bioreactor, a maximum VFA concentration of 2.99 gAC/L was obtained on day 9 of incubation. N-butyric acid was the main specie of the mixture, reaching 2.68 $\text{gO}_2\text{VFA/L}$ on day 3 (68 % of the total VFA), remaining constant until the end of the experiment. Over time, a decrease in the concentration of acetic acid was also observed, with a corresponding increase in the propionic acid concentration, without an increase in the total VFA concentration. The acidic pH of 4.63 was reached immediately on the first day of incubation (Figure 49), due to the lack of alkalinity addition (chemical compounds or buffer material as FA-based GS), and maintenance throughout the experiment seems to have not only inhibited the methane generation, but also the VFA formation, when compared to bioreactors with the GS addition. Hence, the maximum degree of acidification reached was only 49 % at the end of the experiment, and no methane production was detected throughout the entire experiment.

In the bioreactor FA2 (with 20 g/L of FA-based GS), the mixture of VFA was composed mainly of n-butyric and acetic acids, with n-butyric being the main acid formed after 6 days of incubation and acetic acid formed in similar amounts after 9 days of incubation. The maximum VFA concentration was reached on the 12th day (5.59 gAC/L), corresponding to 93 % acidification and without methane production. From that day on, fast methane production was observed, with VFA being rapidly

consumed, reaching 2.47 gAC/L on day 18 of incubation. This period, with the rapid decrease in VFA concentration, was characterized by a rapid increase in pH, from 6.45 to 7.70, stabilizing after the 30th day of incubation. On day 34, TVFA concentration was less than 0.66 gAC/L (corresponding to less than 1 gO_{2VFA}/L) and reached 0.02 gAC/L at the end of the experiment. This VFA profile confirms that, with the FA-based GS addition, suitable conditions have been achieved for methane generation within this bioreactor, with the conversion of VFA produced into methane-rich biogas.

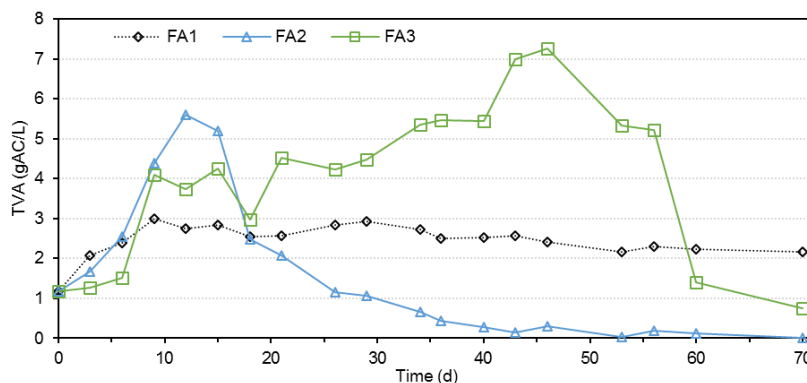


Figure 50] Total VFA concentrations, represented as acetic acid equivalents per L, over time, for batch bioreactors operated, namely FA1 (◇), FA2 (△) and FA3 (□).

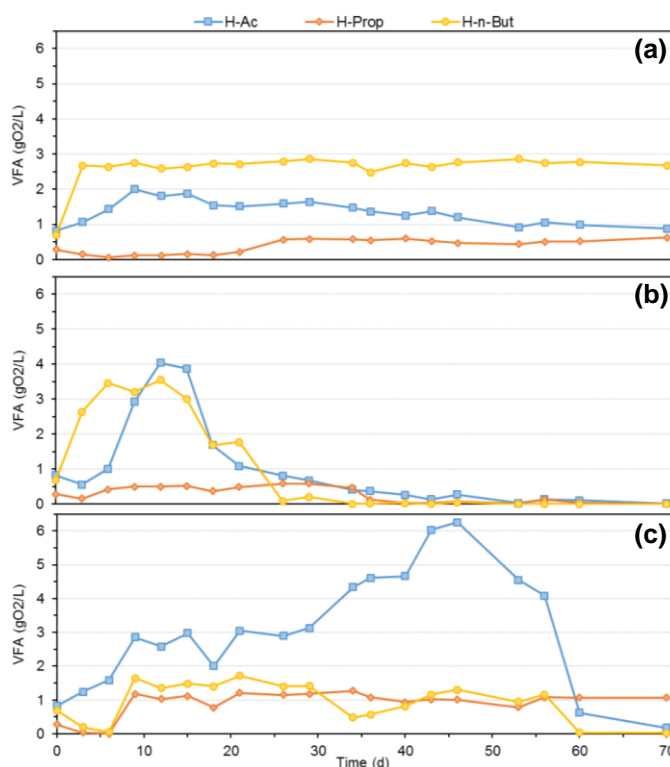


Figure 51] VFA composition over time in anaerobic digesters for the different systems: (a) FA1 (without chemical alkalinity or spheres addition); (b) FA2 (with 20 g/L of FA-based spheres addition); (c) FA3 (with 28 g/L of FA-based spheres addition).

Acetic acid is known as an important intermediate for the AD process, being directly related to the final product, biogas (a mixture of methane and carbon dioxide) (Lee et al., 2015). In the AD process,

the rapid methane formation is mainly attributed to the presence of acetic and butyric acids (Musa et al., 2018). During metabolism, n-butyric acid is converted to acetate (as with all VFA species). This conversion between acid species made n-butyric acid the first specie being depleted in the liquid medium, reaching concentrations below 0.10 gO_{2VFA}/L on day 26 of incubation, in the reactor FA2.

In the reactor with 28 g/L of FA-based spheres (FA3), and probably due to the initial pH increase to 10.09, the system delayed its response regarding the methane production, presenting a behavior similar to the blank reactor (FA1), with high VFA concentration. During the first half of the experiment, the FA3 bioreactor did not show methane production, although with a high degree of acidification (maximum of 90 %). The VFA concentration increased slowly over time, and the maximum value of 7.27 gAC/L was reached only at day 46 of the incubation, presenting a delay of around 35 days compared to the other bioreactor with GS addition (FA2). The slower response of this system improved the formation of acetic acid, which is the main constituent of the VFA mixture throughout the experiment. After day 9, propionic acid was also formed in quantities higher than those observed in the other bioreactors (FA1 and FA2), reaching a maximum concentration of 1.27 gO_{2VFA}/L on day 3, which remained practically constant (\approx 1.06 gO_{2VFA}/L) until the end of the experiment, accounting for 84 % of the total VFA content.

The presence of propionic acid in the AD process is important because this specie is the intermediate of 15 % of the electron flow, and its degradation is highly dependent on the H₂ formation and the acetic concentration (Gorris et al., 1989). However, the accumulation of propionic acid in the media can indicate a disturbance in the AD process balance (Lee et al., 2015). Although propionic acid plays an important role in the AD process, it is considered the most toxic VFA found in anaerobic digesters (Wijekoon et al., 2011). In fact, methanogenic microorganisms are inhibited at propionic acid concentrations above 1 – 2 g/L, while they can tolerate acetic and butyric acid concentrations up to 10 g/L (Inanç et al., 1999).

After day 46 of incubation, the FA3 bioreactor behaved similarly to FA2, where the VFA concentration decreased rapidly, in accordance with the fast pH increase. Due to the very high acetic acid concentration in the liquid fraction, the decrease in the total VFA concentration is parallel to the decrease in the acetic acid concentration, reaching this acid specie less than 0.2 gO_{2VFA}/L at the end of the experiment. Hence, these results confirm that the concentration of the added spheres is also an important factor for pH control, besides their binder composition (metakaolin or fly ash), as previously presented in *oxitop* batch assays.

4.2.1.4.3 Methane production

Figure 52 depicts the values obtained for the ratio of the carbon dioxide content to the methane content during the incubation time. This ratio helps to analyze the biogas composition over time, considering the proportions of CH₄ and CO₂. A CO₂/CH₄ ratio above 1 indicates a methane content of less than 50 % and, in the figure, this point is highlighted with a horizontal dashed line. In this representation, the null values indicate a zero methane content measured in the biogas. The methane content in the biogas produced by the bioreactor FA1 (blank assay) was zero during all the incubation time and is represented as zero in Figure 52. Figure 53 shows the methane concentration expressed as COD equivalents and the methane yield per removed sCOD and calculated during the incubation time for batch assays FA1, FA2 and FA3.

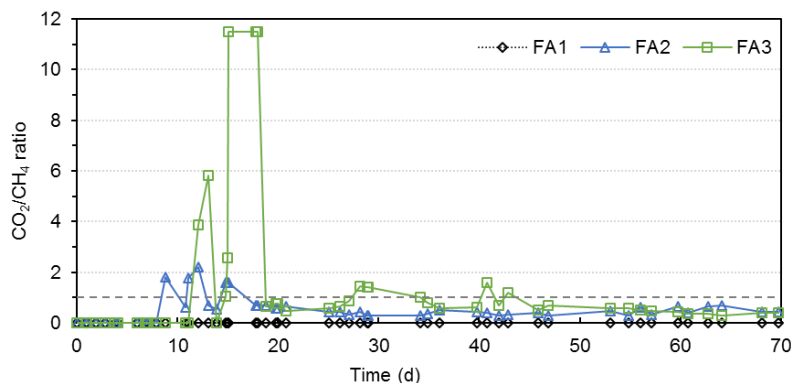


Figure 52| CO₂/CH₄ ratio in anaerobic assays FA1 (◇), FA2 (△) and FA3 (□) during the incubation time.

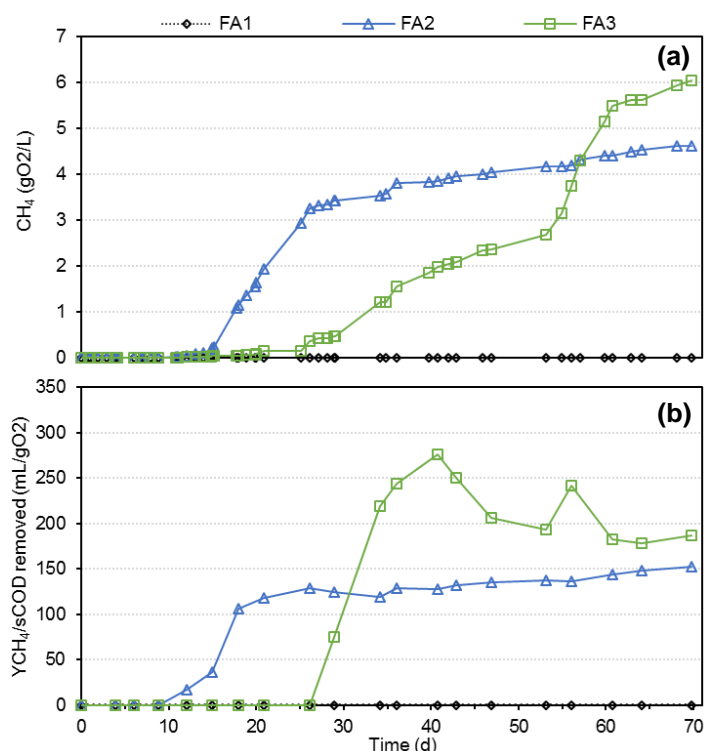


Figure 53| Methane production in the bioreactors FA1 (◇), FA2 (△) and FA3 (□) determined over time in assays with the addition of different amounts of FA-based GS (FA2 and FA3) versus the assay without chemical alkalinity of GS addition (FA1): (a) Methane produced, expressed as COD equivalents; (b) Methane yield.

In the initial incubation period, for approximately 10 days, methane was not detected in any of the bioreactors, leading to a zero CO₂/CH₄ ratio and methane yield. As no methane was detected in the bioreactor FA1, the null values for the CO₂/CH₄ ratio and methane yield were kept throughout the experiment. In the bioreactor FA2, with 20 g/L of FA-based GS addition, methane was formed after day 12 of incubation. As methane was being formed, the methane yield per sCOD increased, reaching a high value after 13 days of methane production. This value (128 mL_{CH₄}/gO₂ removed) was kept almost constant until the end of the incubation test, with a slight increase to ≈ 150 mL_{CH₄}/gO₂ removed on day 56. At that point, the system was stable and more than 94 % of the organic matter was removed from the liquid fraction.

In the bioreactor FA3, a delay in methane production was observed. This behavior may be related to the high pH value achieved on the 1st day of incubation (10.09), which may have led to the inhibition of some methanogenic microorganisms. Until the 10th day of incubation, methane was formed but accounts for low content in the biogas, leading to high CO₂/CH₄ ratios (Figure 52). These high CO₂/CH₄ ratios are characteristic of unstable anaerobic systems. After the initial period of instability, the microorganisms were able to recover and on the 26th day of incubation methane was detected in the biogas formed with the highest content. A fast methane formation from the removed sCOD led to a sharp increase in methane yield, up to 275 mL_{CH₄}/gO₂ removed. With the course of the reaction, the methane yield decreased slightly and stabilized at values close to \approx 180 mL_{CH₄}/gO₂ removed.

Although with some differences in reaction over time, already discussed, both bioreactors with FA-based GS addition achieved good methane performance. With a slightly more FA-based GS addition (FA3), and comparing it with the FA2 bioreactor (less amount of FA-based GS added), 30 % more methane volume (expressed as COD equivalents) was achieved and a methane yield 23 % higher, considering the sCOD removed from the liquid phase.

4.2.1.4.4 Anaerobic process performance

Figure 54 depicts the relationship between the methane volume produced (in mL), the measured pH values, the sCOD concentration and the total VFA concentration (expressed as COD equivalents) in all anaerobic batch assays performed (FA1, FA2 and FA3), during the incubation time. The increase in methane accumulation after day 15 (blue diamonds) is accompanied by a reduction in both sCOD (green circles) and the total VFA concentration (orange squares), with biogas reaching a maximum methane content of 77.6 vol.%, on day 41. Methane production was observed throughout the test until the 70th day, as shown by the cumulative methane curve.

The fast pH stabilization in the assay containing 20 g/L of FA-based spheres (FA2) promoted the early production of methane – after the 8th day of incubation. In addition, a rapid conversion of organic matter into VFA was observed, reaching more than 90 % of VFA in the soluble fraction on day 12, with acetic and butyric as the main acids, as already shown in Figure 51.

The initial sCOD increase was related to the solubilization of particulate organic matter and also to the leaching of PEG from geopolymeric spheres, as referred in section 4.2.1.1. The patterns of sCOD and total VFA concentration are similar, contributing VFA to the biggest fraction of soluble organic compounds. All soluble organic matter was consumed until day 34 (for FA2) and until the end of the experiment (for FA3), with sCOD presenting values below 1 gO₂/L at the end of the experiment. This stabilization was also observed in the cumulative methane volume, where the highest production rate was comprised between days 14 and 26 for bioreactor FA2, and between days 53 and 60 for bioreactor FA3, and after that increment, the methane formation stabilized in both bioreactors.

Table 33 lists the maximum production rate regarding VFA generation, maximum SCOD consumption rate and maximum methane generation rate. In both assays, the VFA consumption rate obtained the worst adjustment of values to the model, reflected by the low determination coefficient, and for this reason, the values were not listed in this table.

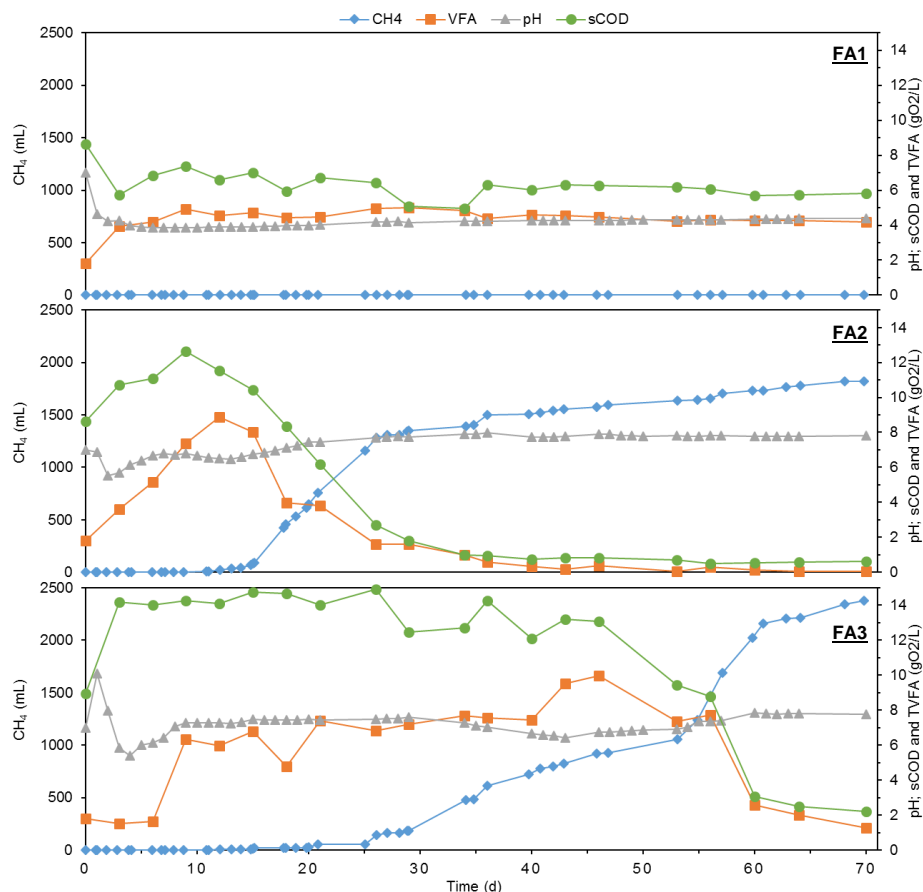


Figure 54| Evolution of CH₄ (◇), total VFA concentration (□), pH (Δ) and sCOD content (○) with time for the assays FA1, FA2 and FA3.

Table 33| Maximum VFA production rate, sCOD consumption rate and methane production rate for both FA2 and FA3 assays.

Parameter	FA2		FA3	
	Value	Det. Coeff.	Value	Det. Coeff.
VFA production rate (gO_{2VFA}/L/d)	0.598	0.997	0.154	0.766
sCOD consumption rate (gO₂/L/d)	0.581	0.987	0.632	0.931
Maximum CH₄ production rate (mL/d)	105.48 ¹	0.996	147.94 ²	0.991

¹ Determined considering the values obtained between days 14 and 26 of incubation.

² Determined considering the values obtained between days 53 and 60 of incubation; the values obtained until day 52 of incubation were discarded for the calculation of the maximum methane production rate.

For the FA2 assay, the models obtained had a good adjustment to the experimental values, with determination coefficients higher than 98 %. For FA3, only the methane formation rate and the sCOD consumption rate fit the model well, with determination coefficients higher than 93 %. VFA production, measured from the beginning of the experiments until the maximum value reached, was four times faster in the FA2 assay than in the FA3 assay. This could explain, along with other parameters, such as pH, the earlier methane formation, due to the faster microbial activity. Considering the sCOD consumption rate, directly related to the methane formation, the FA3 assay performed better, with the fastest sCOD being consumed by microbial consortia pools and also the methane formed at a higher rate (≈ 40 % faster) than in FA2 assay.

The addition of geopolymer spheres to anaerobic digesters, in addition to promoting pH regulation by prolonged OH⁻ leaching, can also affect methane production, acting as a support medium for microbial colonization, thus influencing the microbial community composition, which can be very important in extreme conditions, such as very high VFA concentrations. Poirier et al. (2017) referred that the presence of several types of support media had a beneficial effect on the anaerobic degradation process, under extreme concentrations of ammonia, due to its effect on the microbial composition.

As for the bioreactor containing 28 g/L of FA-based spheres (FA3), the initial destabilization of the system, due to an increase in pH to 10.09 on the 1st day, followed by a decrease to 5.40 on the 4th day, delayed methane production. In this bioreactor, the hydrolysis/acidogenesis steps lasted longer (up to more than 40 days), with the highest reduction in VFA concentration only after the 46th day of incubation, which was opposite to the FA2 bioreactor, where the highest VFA reduction occurred after the 12th day of incubation. Although the methane content in the biogas was observed after the 12th day, there was a significant increase in methane production only on the 50th day (35 days after the FA2 bioreactor), with the maximum methane content in the biogas (76.6 vol.%) achieved on the 64th day (also much later than FA2). Hence, the very high pH achieved in this bioreactor on the 1st day (10.09) and also the prolonged acidification phase with the corresponding pH fluctuation changed the kinetics of the anaerobic bioprocess performance.

At the end of the experiments, the methane yield, that is, the methane volume produced by the substrate consumption was slightly higher when 28 g/L of FA-based GS were added (FA3), reaching 0.352 L_{CH₄}/gO₂ removed, against the yield obtained in the batch bioreactor FA2 (0.228 L_{CH₄}/gO₂ removed), with 20 g/L of FA-based GS addition. Both methane yields were lower than the theoretical value of 0.396 L_{CH₄}/gO₂ removed, calculated under the same conditions as the methane-producing bioreactors, namely a temperature of 36 °C and normal pressure (1 atm) conditions. In the same way, the yield of methane produced by the initial biomass concentration reached 0.670 L_{CH₄}/gVSS_{in} in the bioreactor FA3, against the 0.514 L_{CH₄}/gVSS_{in} obtained in the bioreactor FA2. These results are in line with the higher stability found in the bioreactor with the lowest concentration of spheres (FA2), when part of the organic matter was channeled to biomass growth, in contrast to the findings of the reactor with the highest concentration of GS (FA3).

Other studies report similar values for the AD of cheese whey, very close to the theoretical value of 0.350 L_{CH₄}/gO₂ removed, measured at normal temperature (273.15 K) and pressure (1 atm) (Chatzipaschali and Stamatias, 2012). Yang et al. (2003) obtained, in a CSTR, methane yields up to 0.360 L_{CH₄}/gO₂ removed, when studying a single-phase anaerobic process with hydraulic retention times between 7.5 and 10 days. Gutiérrez et al. (1991) used a UASB reactor to treat a wastewater from non-acidified cheese whey with a low organic load and obtained a methane yield of 0.320 L_{CH₄}/gO₂ removed. Jung et al. (2016) obtained 0.270 L_{CH₄}/gO₂ fed in a CSTR with 5.0 gO₂/L as the initial substrate concentration, values close to those obtained for the batch bioreactor FA3 (0.266 L_{CH₄}/gO₂ initial) and higher than the values obtained in the batch bioreactor FA2 (0.211 L_{CH₄}/gO₂ initial). Kisiełowska et al. (2014) obtained 0.120 L_{CH₄}/gO₂ fed in a methanogenic UASB reactor with pH control, therefore, lower values for methane yield than those reported in FA2 and FA3 assays.

The addition of alkali-activated aluminosilicate material to the AD of acidic cheese whey improved the methane formation and achieved a stable and faster treatment system, as reported by Rugele et

al. (2015). Similar to the results presented in this work, Rugele and colleagues were able to achieve the process stability due to the addition of the alkaline materials, which contributed to the control of pH and for the reduction of adaptation time for the microorganisms (Rugele et al., 2015b).

Figure 55 depicts the performance parameters for batch assays FA1, FA2 and FA3. Figure 55 (a) shows the values for the degree of acidification (DA), soluble COD (sCOD) removal and methanization degree determined at the end of each AD batch experiment (values \pm standard deviation). Figure 55 (b) shows the COD composition at the beginning and at the end of the experiments, regarding the acidified sCOD (which is the VFA content expressed as $\text{gO}_2\text{VFA/L}$) and the non-acidified sCOD, gas production (expressed in the form of COD equivalents of methane) and sCOD removed from the liquid phase (for growth, for example).

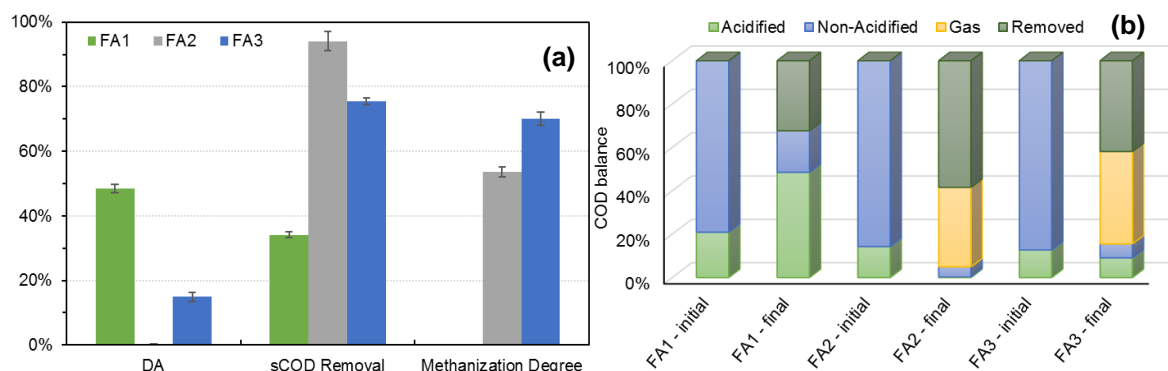


Figure 55 | Performance parameters for batch assays FA1, FA2 and FA3, determined at the end of the experiments: (a) Degree of acidification (DA), sCOD removal and methanization degree and (b) COD balance considering the acidified (as gO_2/L) and the non-acidified fraction of sCOD, the gas (methane) formed (as gO_2/L) and the removed sCOD.

The bioreactors with GS (FA2 and FA3) showed higher COD removals, reaching more than 75 % removal, confirming the potential of the spheres to promote the degradation of organic matter into methane, applying an anaerobic bioprocess. The bioreactor with the addition of 20 g/L of spheres (FA2) showed the highest performance in terms of COD removal (94 %), but a slightly lower methanization degree (54 %), when compared to the bioreactor with 28 g/L of spheres (FA3), which has 75 % sCOD removal and 70 % methanization degree. This difference may be related to the relevant biomass growth, as can be seen, expressed in the COD balance depicted in Figure 55 (b).

At the end of the experiment, for the degree of acidification (which represents the VFA formed from the available sCOD), bioreactors with the addition of FA-spheres exhibited lower values (below 15 %) than the FA1 bioreactor (49 %). Thus, the behavior of FA1 is typical of an acidogenic bioreactor, without methane production and high acidification at the end of the experiment, accounting the acidified portion as 49 % of the COD balance. The behavior of bioreactors with GS (FA2 and FA3) is typical of methanogenic bioreactors, as they present high methane production and low acidification at the end of the experiment.

4.2.1.5 Geopolymer spheres characterization after anaerobic digestion assays

At the end of the anaerobic incubation tests (day 70), the integrity of the spheres was assessed. Figure 56 shows the SEM micrographs and the EDS spectrum of the FA-based geopolymer spheres

used, after their recovery from the anaerobic digesters (FA2 and FA3). It was found that the GS maintained its integrity, as demonstrated by the SEM micrograph shown in Figure 56, although with a mass reduction of about 24 % for both bioreactors. This can be attributed to the alkalis leaching from the spheres during the experiments. The EDS spectrum of the spheres after 70 days of immersion in anaerobic batch assays showed a large decrease in sodium content, in comparison with the spectrum before this immersion (Figure 44).

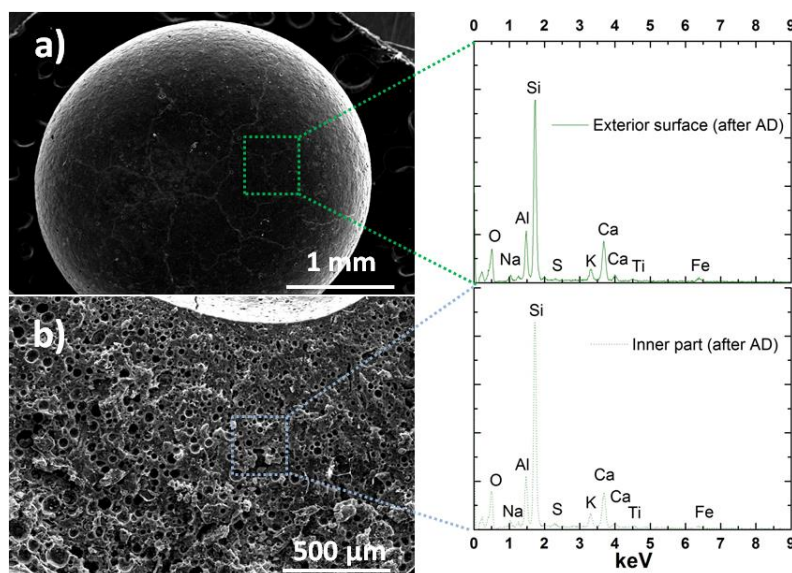


Figure 56 | SEM micrographs and EDS spectrum of the FA-based geopolymer spheres after the 70th day of batch tests inside the anaerobic digester: (a) exterior surface and (b) inner part.

The preservation of the spheres' integrity after their use as pH regulators in anaerobic digesters, as observed in batch assays, is very important, as it can allow their reuse, for example, as heavy metal adsorbents (Novais et al., 2016c), thus contributing towards a circular economy.

4.2.1.6 Cost comparison for replacing chemical alkalinity control by spheres addition

The cost of production GS (considering only the use of raw materials) and the cost of chemical alkalinity addition provided by a buffer solution of NaHCO_3 and KHCO_3 were estimated and compared, in order to assess the potential for GS to be used as pH regulators in the AD process. The raw material costs listed in Table 34 were collected from different sources: sodium bicarbonate, potassium bicarbonate, sodium hydroxide and sodium dodecyl sulfate are from commercial suppliers and FA, MK and sodium silicate from McLellan et al. (2011). Due to fluctuations in market prices, these values should only be considered as a rough estimate.

The addition of 4 g/L of commercial alkalinity to the bioreactors costs between 0.10 and 0.23 €, depending on the commercial supplier. The use of 28 g/L of geopolymer spheres, that is, the maximum amount of spheres used in the 1-cycle batch assays, costs around 0.15 € (spheres manufacture). Considering these values, it is demonstrated that the proposed methodology, namely the replacement of the addition of chemical alkalinity by the addition of FA-based geopolymer spheres to control the pH of anaerobic digesters, is cost-effective, which is crucial for its industrial application.

Table 34| Cost of raw materials used in the preparation of the commercial buffer solution and in the production of FA-based geopolymer spheres production.

	Material	Cost (€/kg)	Reference
Commercial buffer solution	Sodium bicarbonate	19.14	(FisherScientific, 2020)
		36.30	(Sigma-Aldrich, 2020)
	Potassium bicarbonate	28.40	(FisherScientific, 2020)
		76.90	(Sigma-Aldrich, 2020)
Geopolymer spheres production	Fly ash	0.03	
	Metakaolin	0.13	(McLellan et al., 2011)
	Sodium silicate	0.26	
	Sodium hydroxide	33.32	(FisherScientific, 2020)
		37.50	(Sigma-Aldrich, 2020)
	Sodium dodecyl sulfate	99.56	(FisherScientific, 2020)

It should be highlighted that, in the estimation of spheres' costs, the price of FA was considered to be that of coal fly ash (industrial by-product). However, biomass fly ash is still classified as a waste material, which has a significant cost for proper environmental management, e.g., mainly disposed of in landfills and, for this reason, the cost for the production of the spheres is overestimated here. The average landfill tax, which is 11 €/t in Portugal (Agência Portuguesa do Ambiente, 2020), should be considered as a cost-saving for a more realistic estimate of the benefits of using FA in the production of geopolymers.

Notwithstanding, this estimate clearly shows that the proposed approach using the GS for pH control is cost-effective, also presenting a good anaerobic performance with higher stability. Besides that, the use of GS has environmental benefits, such as the reduction of the natural raw materials consumption and mitigating disposal problems associated with some wastes, such as FA. The simplicity of the proposed methodology, which avoids the need for continuous pH adjustment, suggests that it can be easily transferred to an industrial context.

4.2.2 Fly ash-based geopolymer spheres with low and high porosity: anaerobic digestion assays with cheese whey

The results presented in the previous subsections act as a proof of concept, demonstrating the pH buffer potential of the FA-based GS over MK-based GS. The use of waste (fly ash) in the GS manufacture is a promising and sustainable approach, reducing costs and creating value from waste. At the same time, the use of this type of materials in AD is an asset, boosting methane production and also reducing operating costs with buffer chemicals. The manufacture of the GS is a wide field and the properties of the GS can be modified according to the specifications of the end-use. Regarding AD, an in-depth study is important to assess the feasibility of reusing the spheres in more than one AD treatment cycle (sequential fed-batch to simulate long-term use), and the influence of the spheres porosity on the ability to pH buffering in the long term AD operation.

To better understand the role of porosity and the spheres charge/concentration in the pH buffering capacity in AD processes, high organic loads of an easily-acidified substrate such as cheese whey were used. This condition was chosen to intentionally worsen the AD process, promoting strong acidifying conditions and, thus, testing the GS ability to control pH during organic loading shocks and prolonged anaerobic operation.

In a first phase, *oxitop* bioreactors were used to define the concentration of low porosity geopolymer spheres (LPGS) and high porosity geopolymer spheres (HPGS) to be used in fed-batch bioreactors (2-cycle and 4-cycle fed-batch bioreactors). In a second phase, with the concentrations defined for each type of GS (LPGS and HPGS), 2-cycle fed-batch bioreactors were performed, evaluating the prolonged pH control and the influence of the spheres concentration and porosity. In a third phase, using the GS with the best performance in the second phase, prolonged pH control was evaluated in a 4-cycle fed-batch bioreactor. For all fed-batch bioreactors, all performance parameters of the anaerobic process were monitored and the results are presented in the following sub-sections.

4.2.2.1 Geopolymer spheres characterization before anaerobic digestion assays

As performed in previous assays, after synthesis and before use in AD systems, GS (LPGS and HPGS) were characterized using the methodologies described in detail in section 3.6.9 of the methodology chapter. Figure 57 shows the SEM micrographs of the GS prepared with different contents of the foaming agent (preparation details in Table 19). Figures (a) and (b) are from LPGS and figures (d) and (e) are from HPGS, before being used in AD assays. The EDS spectra for both samples (LPGS and HPGs) are also included in Figure 57 ((c) and (f)).

Significant differences between the level of porosity of the spheres' external surface (Figure 57 (a) and (d)) are easily depicted from the micrographs. It is not surprising that a higher concentration of the foaming agent in the compositions has led to an increase in porosity on the surface of the spheres. The latter is expected to affect the leaching behavior of the spheres, with higher porosity promoting greater alkalis leaching from the specimens (Novais et al., 2016b). The microstructure of the inner part of the spheres shows the presence of a high number of closed pores in both specimens. However, the influence of the amount of foaming agent on the internal porosity of the spheres is not easily perceived from these micrographs. Anyway, it is expected that the higher surface porosity

observed in the HPGS allows higher water diffusion in the specimens, thus enhancing the leaching of hydroxyl ions.

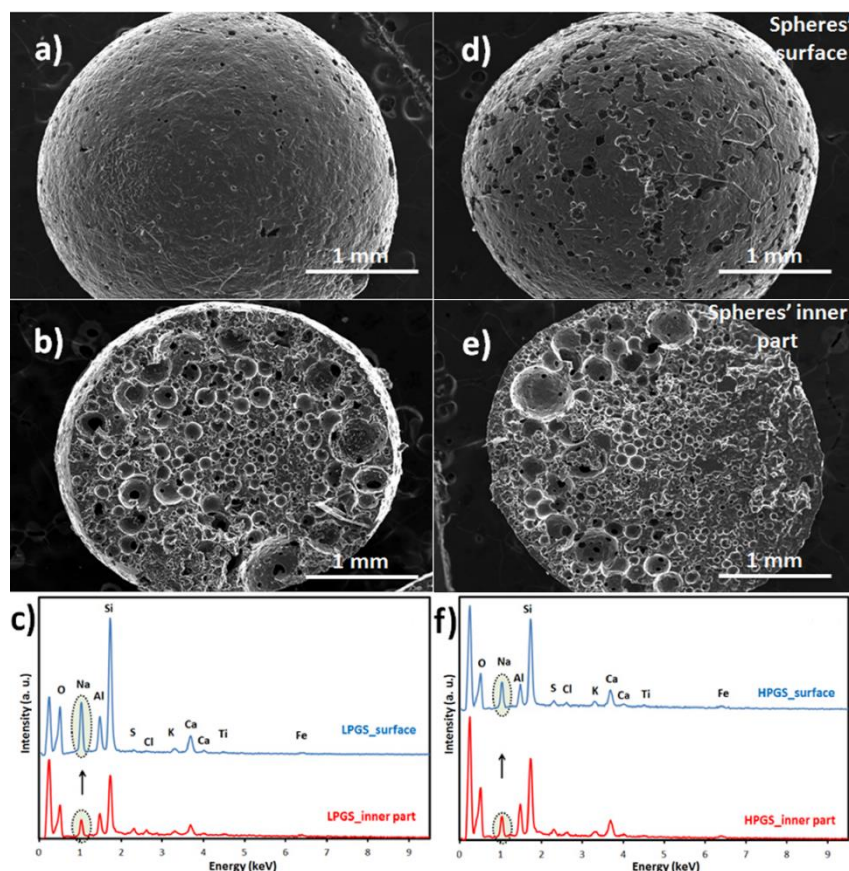


Figure 57 SEM micrographs (a, b, d, e) and EDS spectra (c, f) of the GS prepared using two different foaming agent amounts: (a, b and c) LPGS and (d, e and f) HPGS.

The EDS spectrum of the LPGS in Figure 57 (c) shows higher sodium content in the shell in comparison with their inner part. This feature suggests a migration of sodium from the interior to the surface of the GS, possibly induced by the washing step after their synthesis (section 3.3.2.1). It is expected that the unreacted alkalis (sodium hydroxide) present on the surface of the spheres will leach out rapidly when immersing the GS in the mixed liquor of the bioreactor. On the contrary, the alkalis in the interior will diffuse slowly towards the surface, promoting a prolonged pH regulation. A very similar spectrum was observed for HPGS (Figure 57 (f)), which was expected due to their similar composition (composition details in Table 19), except for the higher amount of foaming agent used.

Figure 58 shows the result obtained in the XRD pattern, with the inserted graph that corresponds to the XRD pattern of the LPGS before their use in anaerobic assays, highlighted in blue in the main graphic, further illustrating the broad amorphous hump at $2\theta = 20-40^\circ$. The XRD pattern is in line with the chemical composition of the spheres (Table 19). Similar elementary levels (expressed as wt. % oxides) were measured for both samples of geopolymer spheres. Nevertheless, a higher Na_2O content (14.3 versus 10.7 wt.%) and a lower loss on ignition (LOI) value (35.8 versus 41.2 wt.%) was observed for the HPGS in comparison with their low porosity counterparts (LPGS).

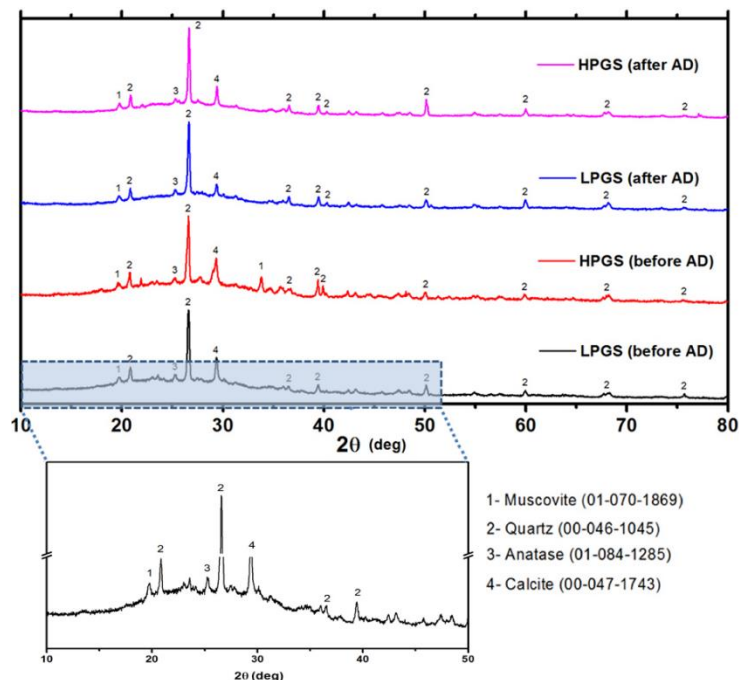


Figure 58 | XRD patterns of the geopolymeric spheres (LPGS and HPGS) before and after AD tests.

Before AD, no substantial differences were observed between the XRD patterns of the LPGS and the HPGS (Figure 58), in line with the similar EDS spectra (Figure 57) obtained for the two samples. Both XRD patterns show a broad amorphous hump, between $2\theta = 20\text{-}40^\circ$, characteristic of geopolymerization occurrence.

4.2.2.2 *Oxitop batch assays with low and high porosity geopolymer spheres addition*

In this first phase of the study using GS with different porosities, the *oxitop* bioreactors (R15 – R24) were used to define the concentration of low porosity geopolymer spheres (LPGS) and high porosity geopolymer spheres (HPGS), to be used in subsequent fed-batch bioreactors. In these bioreactors, two AD cycles (FA4, FA5, FA6 and FA7 assays) and four AD cycles (FA8, FA9 and FA10 assays) were tested with consecutive substrate additions.

For the initial batch assays, 10 *oxitop* bioreactors were performed with different amounts of low and high porosity GS additions (conditions detailed in Table 23). In this experimental set-up, only the pH values were monitored during all 21 days of incubation and the methane content was determined in eight sampling moments during the incubation period. This preliminary pH assessment performed in *oxitop* bioreactors was used to select the optimal formulation and amount of GS for the study of methane production in fed-batch bioreactors on a larger scale. The pH evaluation was chosen due to the importance of this regulation and control parameter in the growth and activity of methanogenic microorganisms.

To evaluate the influence of GS porosity on the pH control of an AD process, different amounts of GS were used, according to their porosity. With LPGS, 8, 12, 16, 20 and 24 g/L of spheres were added to the *oxitop* bioreactors; using HPGS, 16 and 20 g/L were tested. Figure 59 depicts the pH values inside batch *oxitop* bioreactors as a function of time, with standard deviation. Table 35 lists the initial pH (at day zero) and the pH at the 1st and 21st days of all bioreactors.

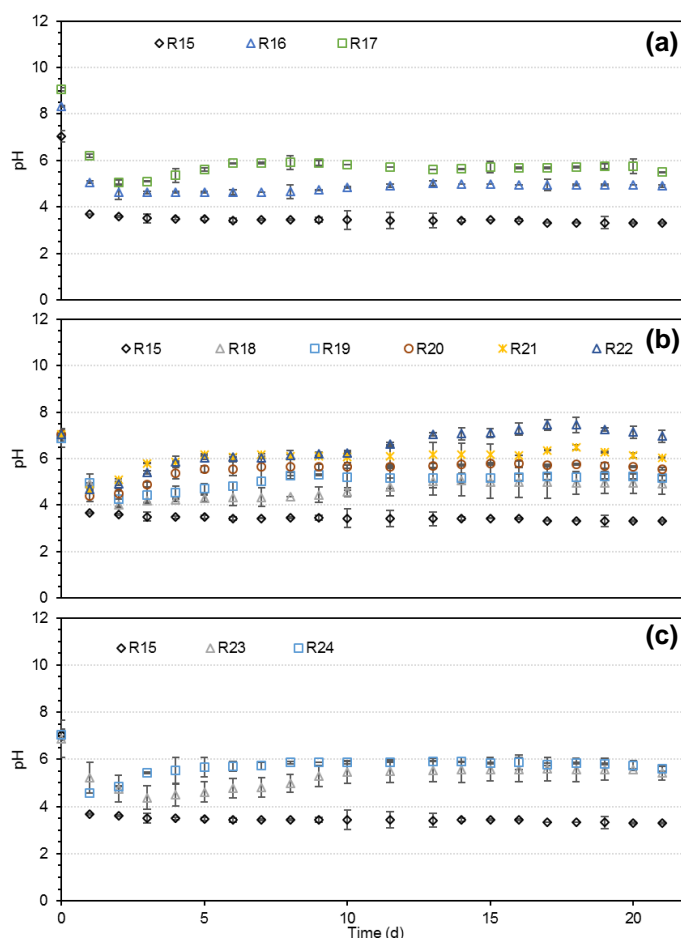


Figure 59 | pH fluctuation (average values \pm standard deviation) in anaerobic digesters as a function of time with alkaline chemicals addition (a), LPGS addition (b) and HPGS addition (c).

Table 35 | pH values at day 0, 1 and 21, in oxitop bioreactors containing different alkaline agents and GS types (low and high porosity) at different concentrations.

	Assay ID	Alkaline agent concentration (g/L)	pH at day 0	pH at 1 st day	pH at 21 st day	CH ₄ content at 21 st day (%)
Reference	R15	-	7.04	3.68	3.31	0.00
Commercial solution	R16	2	8.33	5.07	4.91	23.1
	R17	4	9.07	6.21	5.49	23.2
LPGS	R18	8	6.86	4.91	4.91	25.6
	R19	12	6.86	4.97	5.17	30.7
	R20	16	7.04	4.39	5.56	18.7
	R21	20	7.04	4.64	6.05	32.8
	R22	24	7.04	4.67	6.97	53.3
HPGS	R23	16	6.86	5.22	5.43	16.0
	R24	20	7.04	4.56	5.59	12.0

Without alkalinity addition (R15), the initial pH was neutral (7.04) and after 1 day of incubation, it decreased to less than 3.70 and remained constant (ranging between 3.68 and 3.31) until the end of the experiment. The strong acidifiable potential of cheese whey explained this behavior, being the

organic matter rapidly hydrolyzed and converted into volatile fatty acids, which accumulate in the liquid fraction and inhibit methanogenic microorganisms.

For the assays in which chemical compounds were added as a buffer (R16 and R17), the pH at the beginning tended to be higher with the increase in the initial alkalinity concentration and this trend was maintained throughout the experiment, with higher pH values in assays with higher alkalinity concentration. In these assays, the pH decreased rapidly, despite the presence of buffer chemicals and, on the 1st day, the pH reached acidic values (5.07 – 6.21), maintaining this pH range until the end of the experiment.

Comparing these pH values with those obtained in *oxitop* assays with FA and MK-based GS (Figure 47 (a) in section 4.2.1.3), it is clear that the assay with 2 g/L of alkalinity measured as CaCO₃ obtained the same pH values and profile. In this second set of tests, the pH values were 1 point lower than those obtained previously (R15 vs R0 without alkalinity addition and R17 vs R2 with 4 g/L of initial alkalinity measured as CaCO₃). However, despite the difference between the assays, the same trend in the pH profile was obtained. Without alkalinity addition, a fast pH drop was observed and the values were kept stable until the end of the experiment. With 4 g/L of initial alkalinity measured as CaCO₃, pH values fluctuated between 5 and 6 and stabilized after 17 days of incubation, for both assays (R17 and R2).

With LPGS addition, five concentrations were studied against the two conditions studied for HPGS. In this first approach, the use of LPGS was theoretically preferable, since the cost of manufacturing LPGS compared to HPGS is lower, due to the use of a lower amount of foaming agent (composition detailed in Table 19, where the amounts of each reagent are specified for both LPGS and HPGS types). Figure 59 (b) (LPGS) and (c) (HPGS) shows the pH values measured over time for the assays with the addition of the spheres, where the reference assay (R15) is also presented for comparison in both figures.

As expected, the increase in the initial GS concentration led to an increase in the final pH measured, as listed in Table 35. For the same GS amount, 16 g/L, the LPGS reached a slightly higher pH value (R20, pH = 5.56) than their higher porosity counterparts (R23, pH = 5.43). The same pattern occurred with 20 g/L, where the LPGS (R21, pH = 6.05) reached 0.46 points more in pH than HPGS (R24, pH = 5.59). These small differences are not clearly conclusive on the influence of GS porosity on the AD of cheese whey, and then, for fed-batch assays, the two formulations were studied. In all assays, the initial 10 to 15 days of incubation are characterized by instability of the system, in terms of pH. Once again, these variations are mainly related to the VFA production and accumulation in the liquid phase.

Comparing the assays with 20 g/L of GS, namely R21 with LPGS and R24 with HPGS, with R3 (using FA-based GS, results displayed in Figure 47 (b)), it can be observed that the small change in the GS composition allowed a more stable operation, without significant pH fluctuations, as observed in R3 bioreactor. For the bioreactor R3, the pH varied by more than 1 point, increasing and decreasing between days 3 and 12. For the other bioreactors, the variations did not exceed 0.6 points, after the initial destabilization. This is an important issue since the pH stability of the anaerobic system is very important to enhance microbial activity and, ultimately, methane production from the applied organic load.

For the biogas composition, presented in terms of methane content in Table 35, there is no apparent relationship between the spheres concentration added to each bioreactor and the methane content in the biogas produced. The increase in the LPGS amount added at the beginning of the experiment tends to promote an increase in the methane content, except for 16 g/L, where only 19 % of the biogas was methane.

4.2.2.3 2-cycle fed-batch assays: effect of the spheres porosity on the anaerobic digestion of cheese whey

After the assays presented in the previous subsection, performed in *oxitop* batch bioreactors, three experimental conditions were tested in fed-batch bioreactors: with LPGS, 12 g/L (FA5) and 16 g/L (FA6) were added to the bioreactors, while with HPGS, only the addition of 16 g/L (FA7) of spheres was tested. At the same time, a reference bioreactor was also performed with 4 g/L of initial added alkalinity measured as CaCO_3 (FA4), to compare the long-term operation under high organic load conditions. The amount of substrate (concentrated cheese whey solution) added in both additions performed was the same used in the previous batch assays (FA1 – FA3): 8 g/L measured as COD equivalents.

4.2.2.3.1 pH evolution

The pH values inside the bioreactors influence the performance of anaerobic systems, in terms of VFA accumulation (intermediates) and CH_4 generation (final AD product). Figure 60 displays the pH values measured over time in the fed-batch assays. There were two additions of substrate to the bioreactors: the first was performed at the beginning of the test (day 0), and the second was performed when almost all of the added COD was consumed (on the 55th incubation day). The two stages are divided in the figure for the sake of clarity by a vertical dashed line.

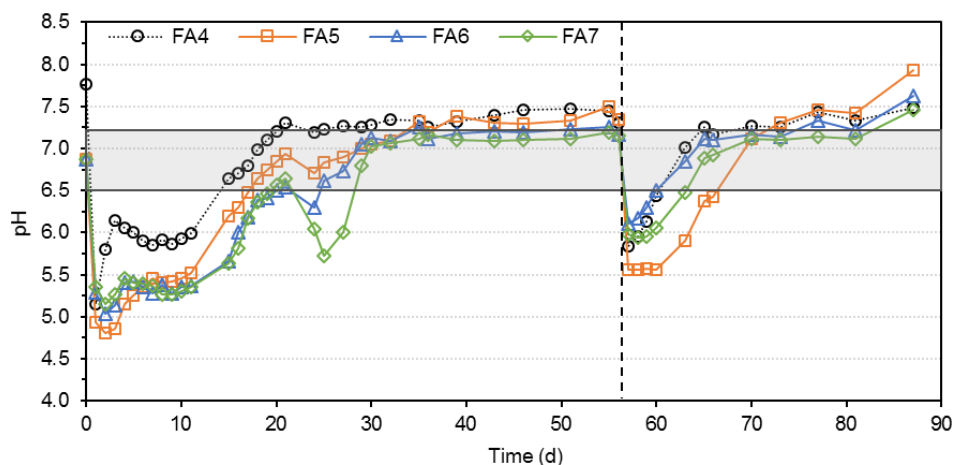


Figure 60 | pH values over time for 2-cycle fed-batch bioreactors with LPGS and HPGS. The addition of substrate is marked by the dashed line and the grey bar highlights the methanogenic pH range.

Before incubation, the pH value of the reference reactor FA4 (7.76) was significantly higher than the pH value of the remaining reactors FA5, FA6 and FA7 (6.87). After each substrate addition (on day 0 and day 55), the pH immediately falls to the acidic range in all reactors. However, the pH decay observed in both substrate additions, in terms of profile and absolute values, depends on the nature

and amount of the added alkalinity source, namely chemical alkalinity or GS, present in the mixed liquor.

For the first substrate addition, after the first incubation day, the lowest pH (4.93) was measured in the bioreactor FA5, containing the lowest concentration of LPGS (12 g/L). As expected, the reactor containing the highest concentration of this geopolymer type (16 g/L LPGS) showed a higher pH buffering capacity and a lower pH decay (pH of FA6 at 1st day = 5.29), when compared to FA5. This pH value was slightly higher than that observed when using commercial powdered alkaline agents (reference test FA4, pH at 1st day = 5.15), showing that, despite their millimeter size, geopolymeric spheres can leach out substantial amounts of hydroxyl ions. This behavior is in line with previous investigations, in which the geopolymers' potential to act as pH regulators in aqueous media was assessed (Novais et al., 2017, 2016). During this initial period, the behavior in the two assays containing equal amounts of GS, but with different porosities (LPGS and HPGS) was similar, although a slightly higher pH (pH at 1st day = 5.35) was measured in the case of HPGS. This result shows that an increase in the spheres porosity enhances the OH⁻ leaching from the specimens, enhancing their ability to regulate the pH.

In the initial incubation days, the pH evolution observed for the reference bioreactor (FA4) differs strongly from that observed when using GS. In fact, on the 3rd day of incubation, the pH of the assay FA4 reached 6.14, while in the remaining reactors the pH was still in the range of 4.86 to 5.27, probably due to the slower release of hydroxyl ions from the spheres. After this initial period, the pH stabilizes in all reactors, but in different ranges, until the 11th day. Moreover, the results also show that using a higher concentration of the same type of geopolymer spheres (LPGS) inside the bioreactor (16 g/L instead of 12 g/L) promotes slightly higher pH values in the initial days of incubation.

During the first 11 days of incubation, a high fluctuation in the pH values was observed, followed by a much more stable operation in terms of pH variation, after the 30th day. The initial instability is due to the rapid consumption of the carbon source, which led to a rapid accumulation of VFA, reflecting the easy biodegradability of the substrate used here (Mainardis et al., 2019).

After 30 days and until the 55th day, the pH stabilizes in all bioreactors, ranging from 7.02 to 7.25 in bioreactors FA6 and FA7 (containing 16 g/L of GS). After the 35th day of incubation, the bioreactor FA4 stabilized at higher pH values (7.35 – 7.47), slightly outside the optimum methanogenic pH range (between 6.5 and 7.2), while in the bioreactor containing 12 g/L of LPGS (FA5) the pH ranged from 7.32 to 7.50, being also slightly above the optimum methanogenic pH range.

At the beginning of the 2nd AD cycle (55th day of the test), the pH values dropped, reaching values between 5.56 (FA5) and 6.10 (FA6). Interestingly, the lower pH values achieved during the second AD cycle are generally higher than those observed in the 1st cycle, which can be attributed to the adaptation of the microorganisms' community to the added substrate (cheese whey). Except for the bioreactor having lower LPGS charge (FA5), all systems achieved the methanogenic pH range within the next four days of incubation. The pH in the bioreactor FA5 remained low (pH = 5.56) for 4 days but rapidly increased to values above 7.30 after 73 days of incubation, being outside the considered optimum methanogenic pH range. It is worth mentioning that the systems showed an enhanced capacity in the 2nd AD cycle to maintain high pH values that favor CH₄ production in detriment of VFA accumulation.

In opposition to what occurred in the 1st AD cycle, the use of 16 g/L LPGS (FA6) promoted a faster pH increase in comparison to higher porosity counterparts (HPGS; 16 g/L). The initial days of incubation are vital for the synthesis of intermediates (acetic, propionic and butyric acids) that will be essential for the subsequent CH₄ production step. Low pH values over long periods of time can inhibit the growth of methanogenic microorganisms, reducing the CH₄ volume generated and the COD being removed (Hassan and Nelson, 2012). Thus, the low initial pH values (1st AD cycle) and the prolonged period in acidic conditions after the 2nd AD cycle observed in the bioreactor FA5, compared to the other bioreactors, may have contributed negatively to the CH₄ production (see results in section 4.2.2.3.3).

Comparing the pH values of the reference bioreactor (FA4) with those obtained for bioreactors with 16 g/L of GS (FA6 and FA7), it is clear that in bioreactors with the GS addition to control the pH, the optimum pH range for methanogenic activity was kept for longer periods. For these bioreactors, a pH stabilization period was observed between days 30 to 55 – 1st AD cycle – and between days 65 to 80 – 2nd AD cycle. In these bioreactors, the slow hydroxyl ions leaching from the spheres promoted a prolonged pH regulation, preserving the pH in the optimum methanogenic pH range for a longer period.

4.2.2.3.2 Volatile fatty acids production

Figure 61 depicts the total VFA concentration (which is the sum of all individual VFA species) measured over all the entire incubation time and expressed as acetic acid equivalents (gAC/L). The individual VFA concentrations of acetic, propionic and n-butyric acids, expressed as COD equivalents (gO₂/L), as a function of time, are shown in Figure 62. The two AD cycles are divided in both figures for the sake of clarity by a vertical dashed line placed on day 55. For samples collected for VFA analysis, the levels of i-butyric, i-valeric, n-valeric and n-caproic acids were also determined individually, but the concentrations measured were very low when compared to the three main acids (acetic, butyric and propionic acids) present in the liquid phase. For this reason, the minor acidic species were not included in Figure 62 individually, but account for the TVFA calculation showed in Figure 61.

In the 1st AD cycle, the VFA presence was observed for all conditions studied since the 3rd day of incubation, reaching a maximum total VFA concentration between 2.97 (FA5) and 4.03 gAc/L (FA4) between days 9 and 11 (Figure 61). Afterward, until the 21st day, a significant increase in pH was observed in all assays, corresponding to a period in which VFAs were consumed by microorganisms, demonstrated by the slow decrease in TVFA concentration. The results also showed that the pH stabilization in the optimum methanogenic pH range occurred simultaneously with the decrease of the total VFA concentration in the liquid fraction, reaching very low values after the 30th day of incubation (less than 0.3 gAC/L), coinciding with higher values of measured pH (almost neutral range, Figure 60). This shift in the total VFA profile suggests that the biological system (microorganisms) had recovered from the initial pH decrease, thus corresponding to a balance between VFA generation from soluble organic matter and its accumulation in the liquid phase and the conversion of VFA into methane-rich biogas.

For the FA7 bioreactor, a peak in TVFA concentration was observed on day 25 of incubation, corresponding to 3.20 gAC/L. On that day, a higher acetic acid concentration than previous and next

samples was observed, indicating fast conversion of organic matter into VFA, mainly acetic acid, by acetogenic microorganisms. The accumulation of acetic acid in the liquid phase was detected prior to its consumption by methanogenic microorganisms.

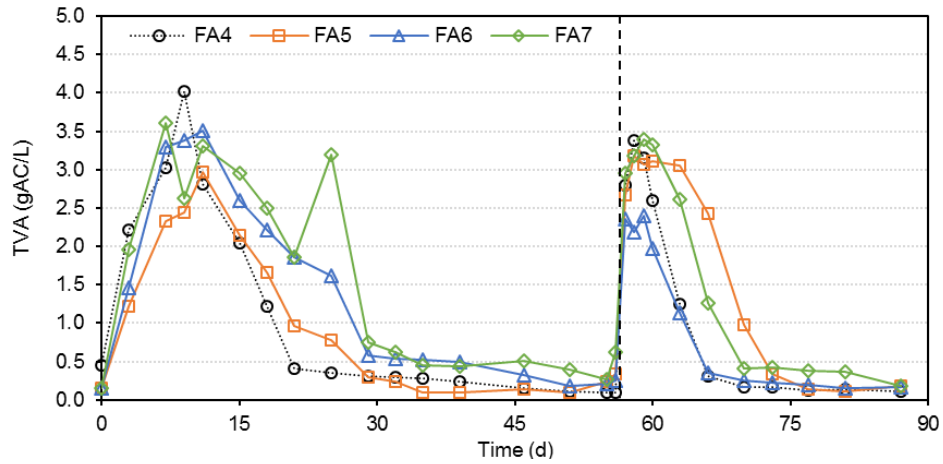


Figure 61 | TVFA concentrations (represented as acetic acid equivalents per L) over time, for the fed-batch (2-cycle) bioreactors operated.

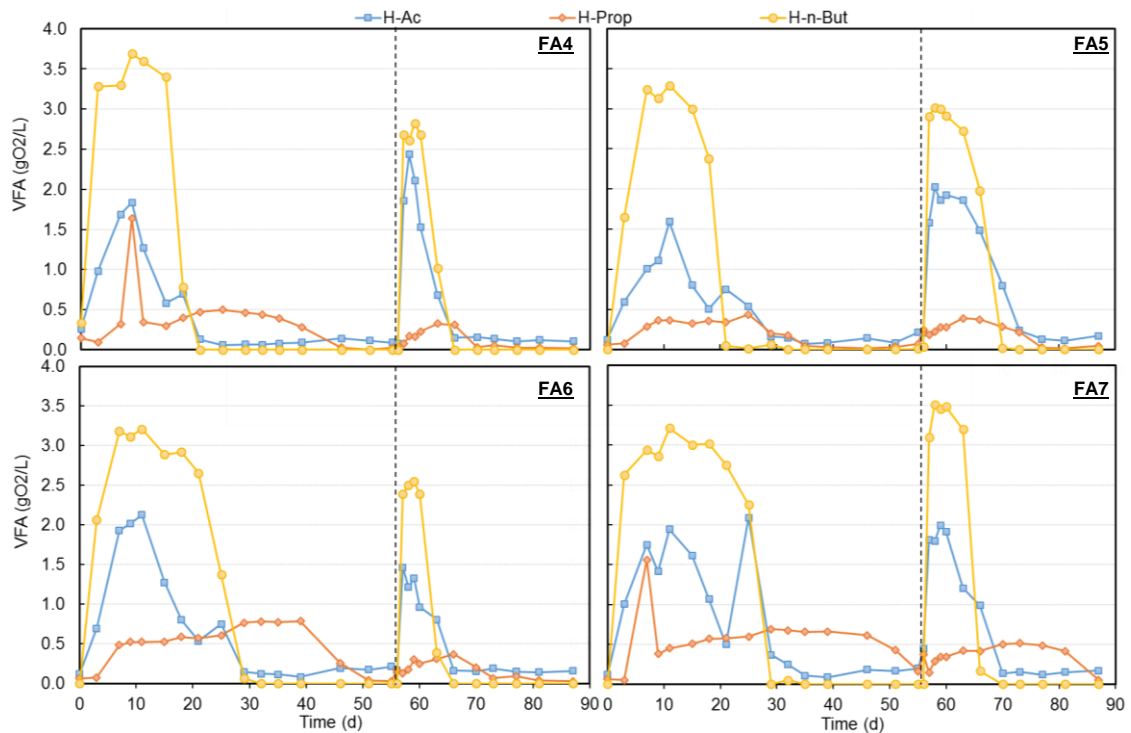


Figure 62 | Concentration of individual VFA species, namely acetic, propionic and n-butyric acids, with time, for fed-batch (2-cycle) bioreactors operated.

In the 2nd AD cycle, the total VFA concentration was slightly lower than that observed in the 1st AD cycle, reaching maximum concentrations 3 days after the substrate addition. Moreover, the acidification step in the 2nd AD cycle is much shorter than that observed in the 1st AD cycle. In fact, VFA was detected only in the liquid phase during the first 10 days after the substrate addition, whereas in the 1st AD cycle, VFA were measured for 30 days. This faster VFA metabolization in the

2nd AD cycle may be due to the adaptation of microorganisms to the carbon source used, also allowing for a faster methane formation and sCOD removal.

The predominant VFA specie detected in all assays was n-butyric acid, with concentrations higher than 3.2 gO_{2VFA}/L for all conditions. These maximum concentrations were obtained after 3 to 5 days of incubation in the 1st AD cycle (Figure 62). In the 2nd AD cycle, the measured n-butyric concentrations were slightly lower, reaching concentrations of up to 3.0 gO_{2VFA}/L, except for FA7, where this acidic specie was measured in higher concentration in the 2nd AD cycle (3.5 gO_{2VFA}/L), compared to the 1st AD cycle (3.2 gO_{2VFA}/L).

Acetic and propionic acids are also present, but in smaller amounts (up to 2 gO_{2VFA}/L), and other species such as i-butyric, i-valeric, n-valeric and n-caproic acids were also detected individually, but at much lower concentrations (< 0.2 gO_{2VFA}/L), and, for that reason, were not included in the Figure. Despite the high concentrations achieved, n-butyric acid was the first to be consumed by microorganisms, with propionic acid being the acidic specie that remained the longest in the liquid fraction. This trend was also observed in the assays with FA-based GS, presented in section 4.2.1.4.2, where butyric acid was also the predominant acidic specie and the first to be depleted.

4.2.2.3.3 Methane production

Figure 63 depicts the methane yield calculated over time for both 1st and 2nd AD cycles in FA4, FA5, FA6 and FA7 assays. The values were determined separately and are divided in the figure by a vertical dashed line, representing the two AD cycles performed. In both AD cycles, the methane production for each cycle was considered independent.

The bioreactor with the lowest concentration of LPGS (12 g/L, FA5) presented methane yield values below 50 mL_{CH₄}/gO₂ removed, during the entire experimental time (both AD cycles). This low performance may be related to the low recovery capacity of the system, after reaching pH values below 5.00 in the 1st AD cycle and 5.56 (for 4 days) in the 2nd AD cycle. The bioreactor FA6 (with 16 g/L LPGS) and the reference bioreactor (FA4) showed similar methane yields in the 2nd AD cycle, reaching the same value at the end of the experiment (187 – 189 mL_{CH₄}/gO₂ removed). In the 1st AD cycle, despite the close methane absolute volume produced, the FA6 bioreactor showed lower yield due to the higher organic matter removal, compared to the reference bioreactor (FA4).

The bioreactor FA7 (with 16 g/L HPGS) showed the highest methane yield in the 1st AD cycle, with 233 mL_{CH₄}/gO₂ removed. Remarkably, the methane yield for the bioreactor with 16 g/L HPGS was 1.3 times higher than that achieved in the reference bioreactor, in which alkalinity was ensured by the use of commercial powdered alkaline agents, which cannot be recovered or reused after the AD process. On the contrary, the millimeter size of GS promote easy recovery after AD, since it deposits rapidly, and, more importantly, can be reused in other applications after its exhaustion in an anaerobic process (e.g. incorporation as a lightweight aggregate in the production of mortars), since its stability is preserved.

In the 2nd AD cycle, the methane yield of the FA7 bioreactor was also higher than the yields in the other bioreactors, although slightly lower than at the end of the 1st AD cycle (203 mL_{CH₄}/gO₂ removed). The FA4 and FA6 bioreactors presented very similar values of methane yield and profile in the 2nd AD cycle, with slightly higher methane yield values for FA6 bioreactor after day 70 and until the end of the experiment. It is important to note that both FA4 and FA6 bioreactors increased their

methane yield performance by comparing the 2nd AD cycle with the 1st cycle, while the FA7 bioreactor kept similar methane yield performance.

Figure 64 depicts the values of the proportion of carbon dioxide in relation to the methane content during the incubation time. The AD cycles performed were divided in the figure by a vertical dashed line. This ratio is useful for analyzing the composition of biogas produced over time, in terms of methane and CO₂. A CO₂/CH₄ ratio above 1 indicates a methane content of less than 50 % and, in the figure, this point is highlighted with a horizontal dashed line. High values of the CO₂/CH₄ ratio (above 5) also indicate poor performance of the anaerobic process and may indicate a failure in terms of methane formation. In this representation, the null values indicate a zero methane content measured in the biogas.

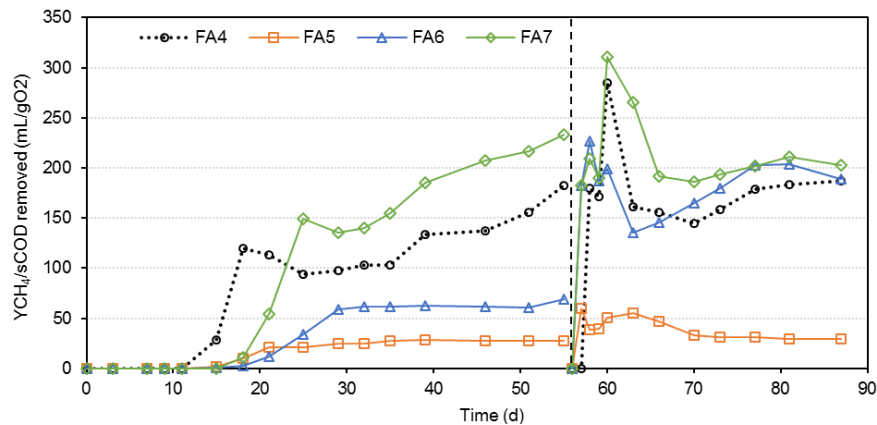


Figure 63 | Methane yield determined during the 1st AD-cycle and the 2nd AD-cycle, with the addition of different amounts of GS with different porosities.

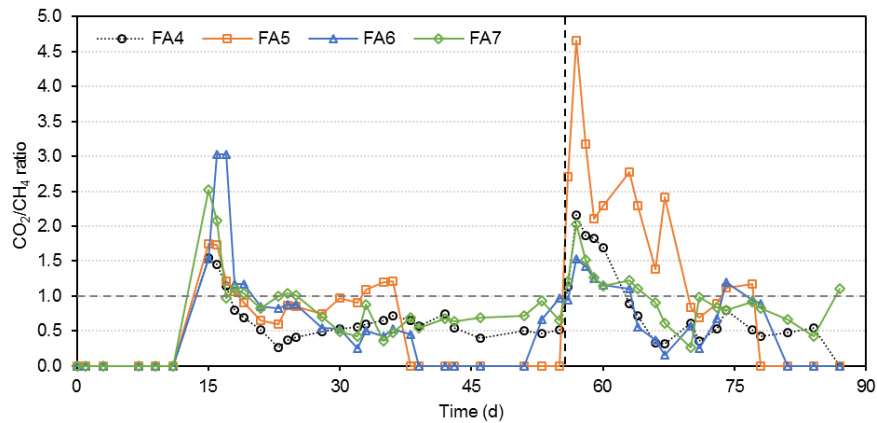


Figure 64 | CO₂ to CH₄ ratio in biogas produced in the assays FA4 (○), FA5 (□), FA6 (Δ) and FA7 (◇).

In the initial days of incubation, until approximately the 11th day, the methane yield was zero, since in the biogas analyzed, the presence of methane was not detected. In the first days of methane production (between the 11th day and the 18th day), instability in the CO₂/CH₄ ratio was observed, with the amount of CO₂ being higher than the amount of CH₄ in the biogas. After the 23rd day of incubation, the values calculated for the CO₂/CH₄ ratio tended to stabilize at values ranging between 0.25 (corresponding to 79 % of CH₄) and 0.90 (corresponding to 52 % of CH₄). After the substrate consumption, which occurred after the 29th day, methane production slowed down in the bioreactors

FA5 and FA6, reaching zero methane content from day 38 until the 2nd substrate addition on the 55th day, represented in Figure 64 as a null CO₂/CH₄ ratio.

For the 2nd AD cycle, after substrate addition, a similar initial destabilization was observed in the anaerobic systems, followed by a stabilization period. For the bioreactor FA5, the pH profile largely influenced the methane formation and, consequently, caused a higher destabilization of the CO₂/CH₄ ratio observed in the figure, compared to the other bioreactors. The maintenance of stable values of CO₂/CH₄ ratio was observed in bioreactors FA4 and FA7 from day 70 onwards, which also presented higher methane volume and yields. Although the FA4 and FA7 bioreactors presented a CO₂/CH₄ ratio less than one, in the 2nd AD cycle an increased instability regarding the biogas composition was observed during the incubation period. After substrate consumption, the bioreactors FA4 and FA5 presented again a null CO₂/CH₄ ratio due to the absence of methane in the biogas present in the bioreactor's headspace.

4.2.2.3.4 Gompertz model for methane production

The use of kinetic models to describe the evolution of methane production over time in AD processes is a practical way to understand the ultimate methane production in a short economic time. The modified Gompertz equation is the most commonly used model for determining the kinetics of methane production (Ware and Power, 2017). Figure 65 depicts both measured and predicted cumulative volumes of methane generated in all operated bioreactors, namely FA4, FA5, FA6 and FA7, with the indication of the second substrate addition with a dashed line on day 55 of incubation. Table 36 lists the relevant kinetic parameters obtained in the developed modified Gompertz model.

In the 1st AD cycle of the experiments, the methane production in the bioreactor FA4 (with chemical alkalinity) starts a little earlier than that of the other bioreactors. The use of higher GS loads delayed the starting of methane production, reflected in the values obtained for the lag period of the Gompertz model (λ). The methane production in bioreactors loaded with 16 g/L of GS (FA6 with LPGS and FA7 with HPGS) requires about 18 – 19 days to start, while the reference bioreactor requires 13.6 days.

Considering the cumulative volume of methane produced, the bioreactor loaded with 12 g/L LPGS (FA5) shows poor performance: only 583 mL after the two anaerobic cycles. This behavior is in line with greater difficulties in adjusting the pH values, as discussed in the previous sub-sections. However, the use of higher loads of this buffer material (LPGS) overcomes this difficulty and, as a result, methane production has been enhanced by a factor of 4.8 in the bioreactor FA6. The cumulative methane volume produced during the entire incubation time of the FA6 bioreactor (2797 mL) is only slightly less than that observed when using commercial alkaline reagents as a buffer solution (3123 mL produced in the FA4 bioreactor).

Remarkably, the use of HPGS (FA7) ensures much higher methane yields (Figure 63) and the absolute volume produced (Figure 65), reaches a stunning value of 5695 mL. This value is two times higher than that observed for the bioreactor containing the same amount of LPGS (FA6) and 1.8 times higher than the reference bioreactor (FA4), showing that, besides its concentration in the medium, the spheres' porosity has a crucial role in the process. The differences between the methane volumes attained in these bioreactors (FA4, FA5 and FA6) cannot be attributed only to the pH fluctuations shown in Figure 60. As mentioned above, HPGS are expected to leach higher

amounts of hydroxyl ions from their structure in comparison with their low porosity counterparts. Indeed, the pH value of 5.27 reached on the 3rd day of incubation when using 16 g/L of HPGS is slightly higher than that observed using an equal load of LPGS (pH = 5.14). This is attributed to the higher surface porosity of the HPGS, which facilitates the hydroxyl ions leaching and, therefore, to the pH regulation capacity.

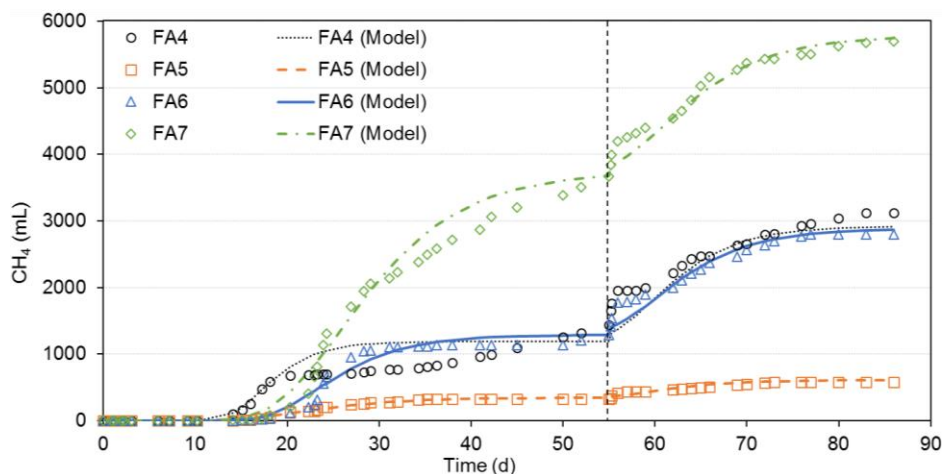


Figure 65] Evolution of CH₄ production measured (markers) and predicted by the modified Gompertz model (lines) in the assays FA4 (○), FA5 (□), FA6 (Δ) and FA7 (◇).

Table 36] Parameters of the modified Gompertz model for CH₄ production

			FA4	FA5	FA6	FA7
1st AD cycle	Modified Gompertz model parameters	Ym (mL)	1181	349	1292	3748
		Rm (mL/d)	128	19.9	88.5	188
		λ (d)	13.6	14.8	17.9	18.6
	Methane Volume	Measured (mL)	1438	322	1287	3674
		Predicted (mL)	1191	348	1288	3677
		Difference (%)	20.8	7.43	0.03	0.09
	Model adjustment to real data	%	88.1	98.9	97.1	98.9
2nd AD cycle	Modified Gompertz model parameters	Ym (mL)	1733	264	1597	2104
		Rm (mL/d)	78.3	48.1	107	126
		λ (d)	-	-	-	-
	Methane Volume	Measured (mL)	3123	583	2797	5695
		Predicted (mL)	2915	610	2870	5744
		Difference (%)	7.14	4.37	2.55	0.84
	Model adjustment to real data	%	95.1	93.8	97.2	98.2

Figure 65 also shows that the modified Gompertz model correctly describes the methane generation in all bioreactors, with small variations. The fitting of the experimental data obtained in the reference bioreactor FA4 is lower than for the other bioreactors, with differences in the methane volume produced (measured versus predicted) of 7 % for the 2nd AD cycle and 21 % for the 1st AD cycle. The differences in methane volume predicted and measured were less than 7 % for the

bioreactor FA5 and less than 3 % for the other bioreactors, considering both AD cycles. The model developed describes the data obtained well, with the bioreactor FA7 presenting the best fit of the model to the data. On the other hand, similarly to that as also for methane volume production, bioreactor FA4 presented the worst model fitting to the experimental data, in both AD cycles.

4.2.2.3.5 Anaerobic process performance

Figure 66 shows the values measured for the methane volume (absolute values), the total VFA concentration expressed as COD equivalents and the pH values measured during the incubation period, for bioreactors FA4, FA5, FA6 and FA7. The two AD cycles are divided in all figures for the sake of clarity by a vertical dashed line on day 55, corresponding to the beginning of the 2nd AD cycle with substrate addition.

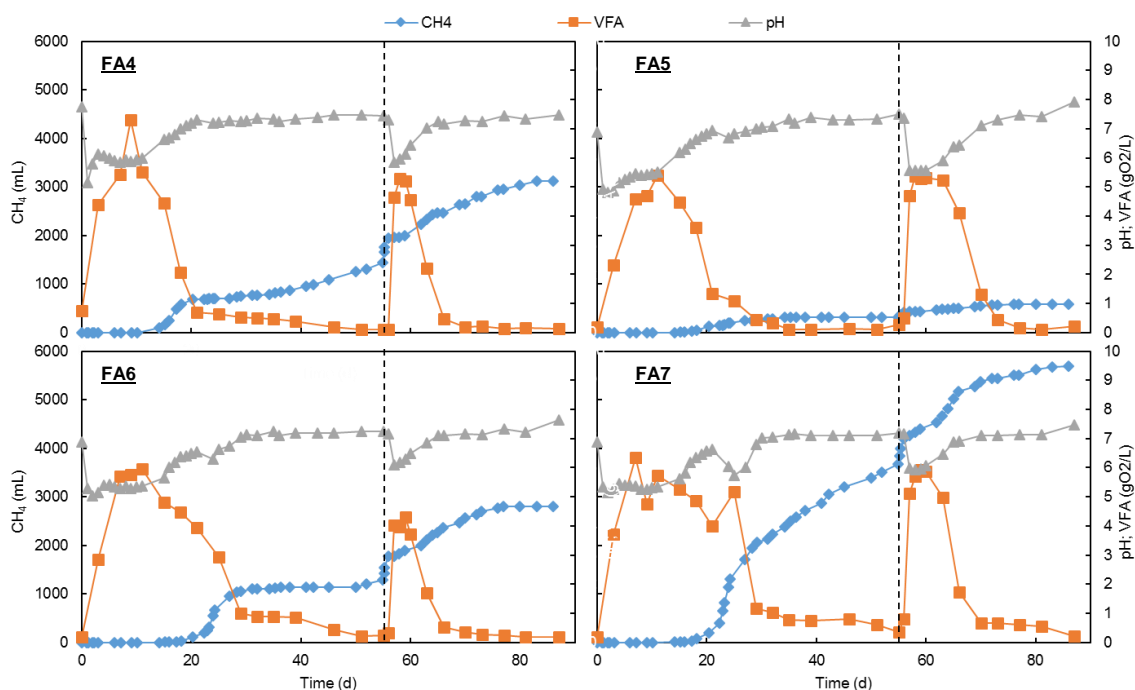


Figure 66] Evolution of CH₄ (◇), total VFA concentration (□) and pH (△) with time for assays FA4, FA5, FA6 and FA7.

Between days 21 and 25, all bioreactors showed a decrease in pH values, being more pronounced in the bioreactor containing 16 g/L of HPGS (FA7), where the pH dropped from 6.64 to 5.72. This decrease is explained by the accumulation of acetic acid in the liquid phase (Figure 62), reaching a peak at day 25, with a corresponding acetic acid concentration of 2.09 gO_{2VFA}/L in bioreactor FA7. During this period, methane production boosted, and the highest methane rate in the 1st AD cycle was achieved in bioreactor FA7, corresponding to 466.3 mL/d. The other GS-containing bioreactors showed similar behavior of methane production, but with lower rates (ranging from 20.59 to 252.29 mL/d) than those of FA7.

In the reference bioreactor without the addition of GS (FA4), methane formation started earlier and a slight increase in the acetic acid concentration was also observed, but earlier than in other reactors (on day 17th of incubation), coinciding with the period of greatest methane generation rate

of the 1st AD cycle for bioreactor FA4. Thus, it can be postulated that the methane formation in the referred periods is due to the conversion of acetate by acetoclastic methanogens.

Figure 67 shows the parameters determined to assess the anaerobic performance of bioreactors FA4 – FA7, regarding the degree of acidification, sCOD removal and methanization degree. The values of degree of acidification are very low for all bioreactors (< 5 %), determined at the end of each cycle. The very low VFA concentration led to the identification of the systems operated as methanogenic reactors.

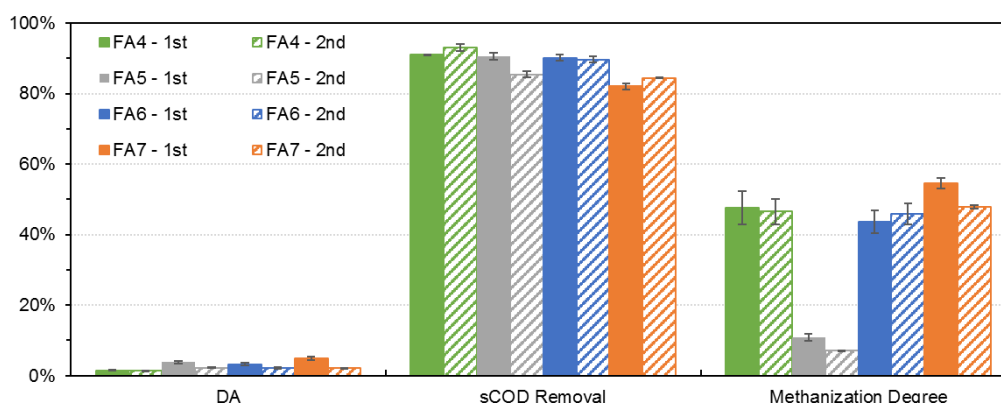


Figure 67 | Performance parameters for bioreactors FA4 to FA7, in the 1st and the 2nd AD cycles, including degree of acidification, sCOD removal and degree of methanization.

Considering the total VFA concentrations and the cumulative methane volume, the bioreactors loaded with 16 g/L of GS (FA6 and FA7) show typical methanogenic behavior, that is, high methane volume production and low acidification (total VFA concentration) at the end of the experiment or AD cycle. In addition, it was also observed that the pH values achieved in the stable phase of the AD cycles stimulate the methanogenic microbial population and enhanced the methane formation, instead of VFA accumulation in the liquid phase.

Regarding the percentage of sCOD removal, the values ranged from 82 to 91 % in the 1st AD cycle, and from 85 to 93 % in the 2nd AD cycle, for all assays. The adaptation of the microbial community to the substrate led to high values obtained for the sCOD removal in both AD cycles. The higher substrate consumption rate, led to values below 1 gO₂/L earlier (after 15 days of incubation) in the 2nd AD cycle, in comparison with the 25 days needed in the 1st AD cycle. These results suggest that suitable conditions have been achieved for the growth of methanogenic microorganisms and methane generation, that is, almost neutral pH and reduced VFA accumulation in the liquid fraction (Hassan and Nelson, 2012).

Table 37 lists the maximum consumption and production rates for total VFA and maximum methane generation rate, for both AD cycles performed. For all parameters presented, the corresponding determination coefficient is also presented in the table. It is concluded that the data present a good fit for the developed models, with determination coefficients higher than 93 % for the different calculated parameters. The exceptions are the VFA production rate of FA4 bioreactor, VFA consumption rate of FA5 bioreactor, the methane production rate of FA6 bioreactor and VFA consumption rate of the FA7 bioreactor, with determination coefficients ranging from 91 to 93 %.

Table 37 | Maximum VFA production rate, VFA consumption rate and methane production rate for fed-batch assays FA4, FA5, FA6 and FA7 (values and respective determination coefficient), determined independently for the 1st and 2nd AD cycles.

Parameter	FA4		FA5		FA6		FA7		
	Value	Det. Coeff.	Value	Det. Coeff.	Value	Det. Coeff.	Value	Det. Coeff.	
1 st AD Cycle	VFA production rate (gO _{2VFA} /L/d)	0.656	0.922	0.627	0.996	0.783	0.996	0.867	0.973
	VFA consumption rate (gO ₂ /L/d)	0.531	0.976	0.388	0.911	0.255	0.953	0.229	0.930
	CH ₄ production rate (mL/d)	128.25	0.966	20.59	0.965	252.29	0.925	466.3	0.996
2 nd AD Cycle	VFA consumption rate (gO ₂ /L/d)	0.687	0.995	0.508	0.976	0.552	0.985	0.565	0.929
	CH ₄ production rate (mL/d)	52.36	0.966	9.17	0.993	58.76	0.988	161.64	0.992

Considering the maximum VFA production rate, only the values of the 1st AD cycle were presented, since in the 2nd AD cycle, the maximum VFA concentration was achieved in the following day from the substrate addition, due to the rapid metabolization of organic matter into VFA. Although the values are quite similar, small differences can be noticed in the maximum values of the VFA production rate obtained. For bioreactor FA7 the VFA formation was faster (0.867 gO_{2VFA}/L/d) than for the other bioreactors (0.627 – 0.783 gO_{2VFA}/L/d), probably influenced by the type of buffer material used (HPGS) and the respective amount (16 g/L).

The maximum VFA consumption rate, which represents the rate of VFA depletion used mainly for the methane formation, increased significantly from the 1st to the 2nd AD cycles. For all assays, the VFA consumption rate increased between 30 % (FA4 and FA5) and 150 % (FA7), indicating, once again, an adaptation of the microbial population to the type of substrate, namely to the VFA present in the liquid phase. The FA7 bioreactor presented the lowest VFA consumption rate in the 1st AD cycle and this low value may be related to the small extension of the acidogenic phase, with VFA concentration higher than 4 gO_{2VFA}/L over a longer period of time (Figure 66), compared to the remaining bioreactors. In the 2nd AD cycle, all reactors presented similar VFA consumption rates, ranging from 0.508 to 0.687 gO_{2VFA}/L/d.

In contrast to the VFA consumption rate, the methane production rate in all bioreactors presented a better performance in the 1st AD cycle, decreasing globally by more than 55 % in the 2nd AD cycle. Despite this decreasing trend in values, the FA7 bioreactor is the one with the highest methane production rates, with values from 1.8 (FA6) to 22 (FA5) times higher than the other bioreactors. These differences can also be observed when the COD balance is performed, as shown in Figure 68. At the end of the 1st AD cycle, the FA7 bioreactor presented the highest COD fraction transformed into gas (methane production) and the highest methane yield (considering the removed sCOD), as previously showed in Figure 63.

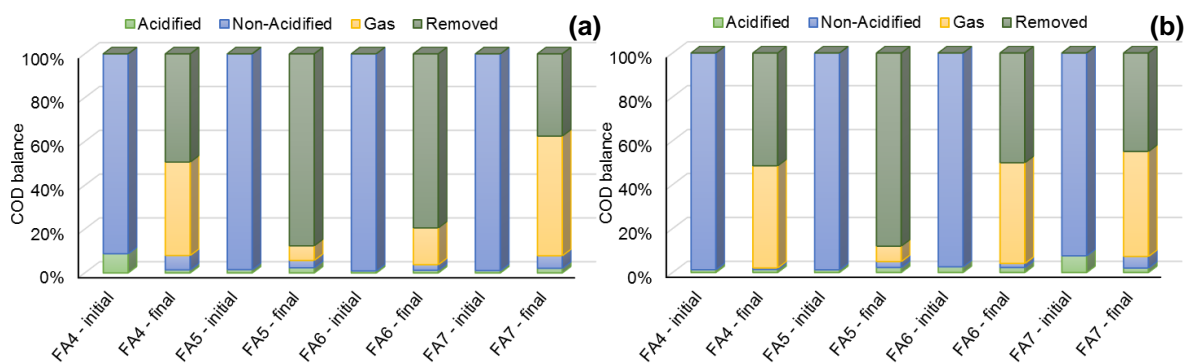


Figure 68 | COD balance in 1st AD cycle (a) and 2nd AD cycle (b), considering the acidified (as gO₂/L) and non-acidified sCOD, the gas (methane) formed (as gO₂/L) and the removed sCOD.

As already presented, the removed fraction of COD presented in the COD balance refers mainly to the sCOD used by microorganisms for growth and internal metabolism. At the end of the 1st AD cycle, the microorganisms present in FA5 and FA6 bioreactors did not use the removed sCOD for the final products (methane) generation (7 – 17 % of COD), but for growth (79 – 88 % of COD), with a very low amount of acidified COD (1 – 2 % of COD), which corresponds to intermediate products such as VFA. In bioreactors FA4 and FA7, the COD removed was mainly converted into methane (43 – 55 % of COD). At the end of the 2nd AD cycle, FA4, FA5 and FA6 bioreactors presented similar COD balance: about 46 – 48 % were converted into methane and 45 % were removed for microbial growth, with a very low fraction of COD transformed into intermediates (VFA).

In line with the previous results presented, it is possible to conclude that the FA5 bioreactor (12 g/L of LPGS) failed as a methanogenic system, producing a lower methane volume, with very low methane yields, regarding the removed organic matter. Comparing the bioreactors with the same amount (16 g/L) of different spheres (LPGS vs HPGS), it can be concluded that the increasing in the spheres' porosity enhanced the methane formation and led to a stable anaerobic process, with two additions of substrate and 87 days of operation.

4.2.2.4 4-cycle fed-batch assays: effect of operation time on anaerobic digestion of cheese whey

In the previous sub-section, the results of the comparison of anaerobic performance in bioreactors were presented with the addition of two types of geopolymeric spheres: low and high porosity geopolymer spheres. As the results presented showed, the HPGS addition promoted a better performance of the AD system for the treatment of cheese whey.

In order to evaluate the prolonged operation with the increase of substrate additions (from 2 to 4 substrate additions), three bioreactors were operated in fed-batch mode, following the main operational conditions listed in Table 24. The bioreactor FA8 was operated as a reference, with chemical alkalinity addition (4 g/L measured as CaCO₃) and bioreactors FA9 and FA10 act as replicates, with the same operating conditions and with the addition of 16 g/L of HPGS as buffer material. The four additions of about 8 gO₂/L of concentrated cheese whey solution were performed as described in detail on sub-section 3.5.2.2.

4.2.2.4.1 pH evolution

Figure 69 shows the pH evolution over time for bioreactors operated with four substrate additions, FA8, FA9 and FA10. Four substrate additions were made to the bioreactors: the first was done at the beginning of the test at day 0; the second was performed when almost all the added COD was consumed (on the 47th incubation day); the third was performed on day 78 of the incubation; the fourth was performed on day 103 of incubation. The four stages are divided in the figure, for clarity, by vertical dashed lines.

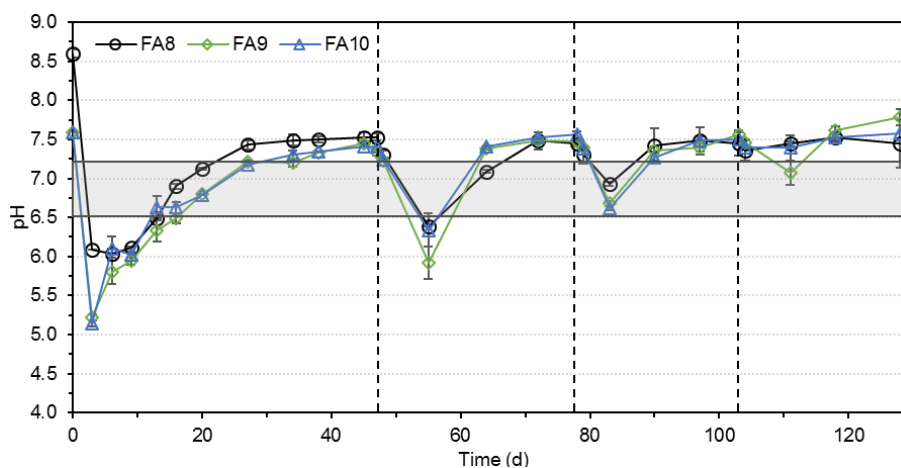


Figure 69 | pH values over time for fed-batch assays with 4 AD cycles and HPGS addition. The dashed lines mark the substrate additions and the grey bar is highlighting the optimum methanogenic pH range.

As before, after the first substrate addition, the pH dropped to acid values below 6.0 in all bioreactors. On the 3rd day of incubation, the pH values of the assays FA9 and FA10, with the addition of HPGS, were lower than the values of the reference assay, reaching a pH of around 5.14 – 5.22. After these low values, the systems recovered and reached almost neutral values around the 20th day. The pH profile of the reference bioreactor (FA8) is similar to the profiles of the FA9 and FA10 bioreactors, although a little higher in terms of pH values. The minimum pH value measured in the FA8 bioreactor was 6.0, on day 6 of incubation, and after 27 days of incubation, the reference system stabilized its pH at 7.5, which remained constant until the end of the 1st AD cycle.

On day 47 of the incubation, the 2nd substrate addition was performed and the 2nd AD cycle was started. The pH values dropped again to the slightly acidic range and the values measured after 4 days were, as previously observed, lower in the bioreactors with the addition of HPGS to control the pH. The minimum value of 6.38 was achieved in the reference bioreactor FA8, against 5.92 – 6.34 obtained in bioreactors FA9 and FA10, respectively. The recovery of the system, which is the establishment of an almost neutral pH in the AD system, was faster in the 2nd AD cycle than in the 1st AD cycle. For the 2nd AD cycle, the anaerobic systems took 16 days to reach the pH around 7, compared to the 20 days needed in the 1st AD cycle. This faster recovery may indicate an adaptation of the anaerobic microbial population to the substrate and a faster metabolization of the carbon source into VFA.

On day 78 of incubation, the 3rd AD cycle started with another substrate addition. This cycle did not show a pH drop as deep as previous AD cycles, with the lowest pH values remaining within the optimum methanogenic range, highlighted in Figure 69 by a grey bar. The lowest values were achieved, as expected, in bioreactors with the HPGS addition as buffer material, with pH values

averaging 6.65. After 12 days of the 3rd AD cycle, the pH values remained stable and slightly above the optimum methanogenic range until the end of the 3rd AD cycle.

On day 103 of incubation, the last cycle started with the fourth addition of substrate. In this last AD cycle, the pH did not decrease as in the previous cycles, except for bioreactor FA9, where the pH dropped from 7.46 to 7.07 in the first 7 days of the 4th AD cycle. After a slight variation in pH, the system recovers quickly and the pH values were maintained close to 7.5 in all bioreactors, until the end of the incubation time.

The difference between the initial pH values (beginning of the cycles) and the minimum pH values achieved after adding the substrate decreases with the course of the experiment, allowing for stable operation. For example, in the 1st AD cycle, the pH difference reached 2.44 ± 0.06 , while in the 3rd AD cycle, the difference between the initial and the minimum pH was only 0.61 ± 0.17 . The buffer capacity of the spheres was tested with four additions of substrate and, in all bioreactors, it is possible to observe that the anaerobic microorganisms present in the medium are able to adapt to adverse conditions, that is, an addition of easily biodegradable substrate, which promotes the development of the acidification step in an anaerobic process.

4.2.2.4.2 Volatile fatty acids production

Figure 70 shows the total VFA concentration measured during the entire incubation time and expressed as acetic acid equivalents (gAC/L) and Figure 71 shows the individual VFA concentrations of acetic, propionic and n-butyric acids, expressed as COD equivalents (gO₂/L), as a function of time. For the samples taken in these experiments, the levels of i-butyric, i-valeric, n-valeric and n-caproic acids were also determined individually, but the measured concentrations were lower when compared with the three main acids present in the liquid phase. For this reason, they were not included in Figure 71 but account for the TVFA calculation represented in Figure 70. The four AD cycles are divided in the figure for the sake of clarity by vertical dashed lines on days 47, 78 and 103 of incubation.

In all operated bioreactors, different VFA species accumulate in the liquid medium after the initial substrate (cheese whey) addition. In the 1st AD cycle, the total VFA concentration reached its maximum for the reference bioreactor (FA8), achieving a concentration of 3.73 gAC/L after 9 days of incubation. After day 9, the total VFA concentration decreased in bioreactor FA8 until day 27, reaching values below 1 gAC/L. For bioreactors FA9 and FA10, after an increase in VFA content up to ≈ 2.8 gAC/L on day 9, between days 9 and 20, the total VFA concentration remained almost constant, without significant VFA consumption or accumulation. After day 20 of incubation, a rapid VFA consumption was observed, which led to a rapid decrease in the total VFA concentration, reaching values below 1 gAC/L after day 34 of incubation. After the total VFA depletion, the values remained low and constant until the end of the first AD cycle.

In the 2nd AD cycle, a different profile was observed, compared to that observed in the 1st AD cycle. The total VFA concentration in the reference assay was lower than in the 1st AD cycle and then in the other bioreactors, reaching a maximum of just 2.02 gAC/L on day 64 of incubation. On the other hand, bioreactors FA9 and FA10 showed a fast increase in TVFA concentration, reaching approximately 3.8 gAC/L on day 55 of incubation. This maximum value was followed by a fast

consumption of the total VFA content, reaching values below 1 gAC/L after day 64 of incubation. After day 72, TVFA concentrations remained low and constant until the end of the 2nd AD cycle.

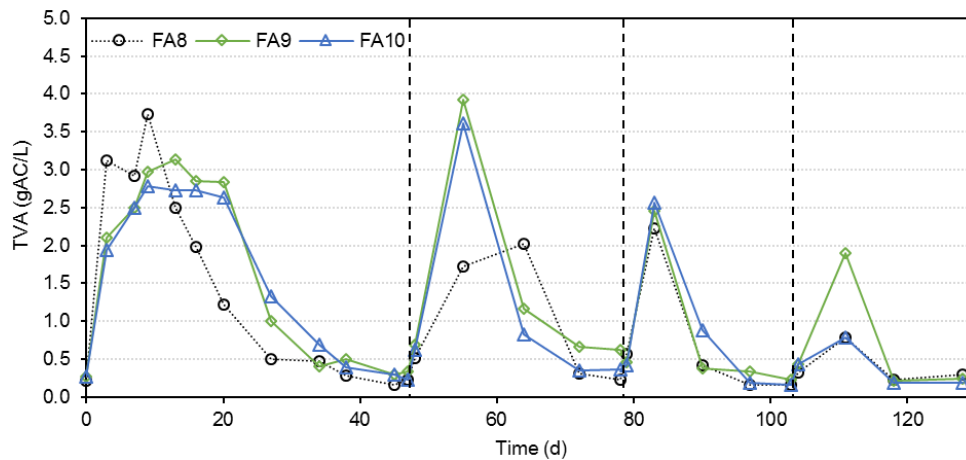


Figure 70 Total VFA concentration (represented as acetic acid equivalents per L) over incubation time of 4-cycle fed-batch assays.

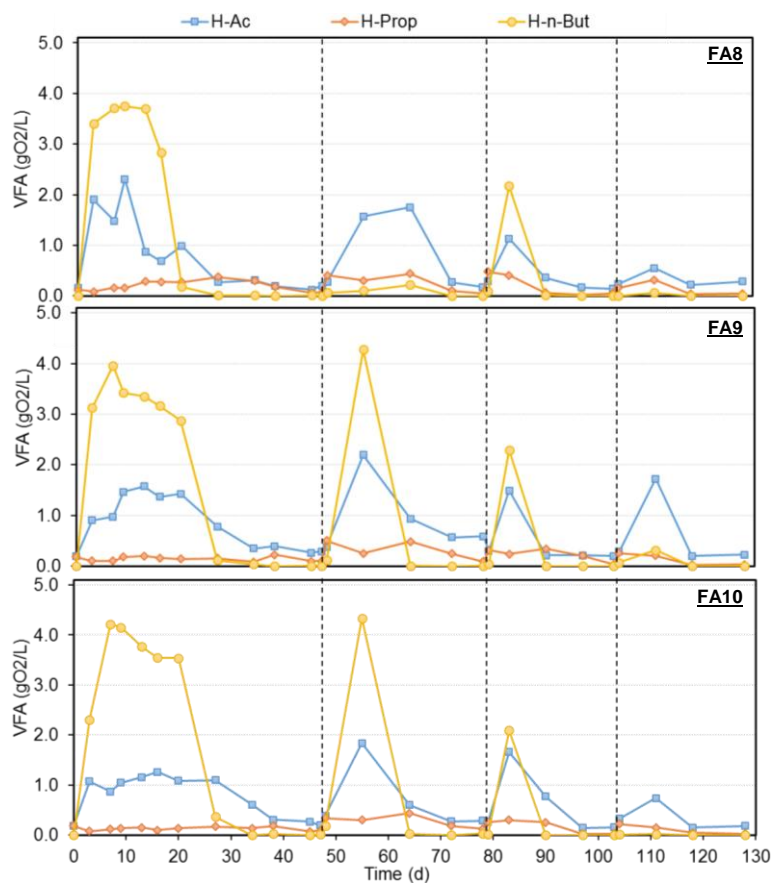


Figure 71 Concentration of individual VFA species, namely acetic, propionic and n-butyric acids, over time, for fed-batch (4-cycle) operated bioreactors, namely FA8, FA9 and FA10.

In the 3rd AD cycle, the three bioreactors had a similar total VFA profile, with a fast increase after the substrate addition, until reaching a maximum concentration of 2.2 – 2.5 gAC/L on day 83 of

incubation. The VFA decreasing profile was also similar in all bioreactors, obtaining concentrations below 1 gAC/L after 12 days of cycle (90 days of incubation). As verified in previous AD cycles, VFA production was not observed after reaching low values (< 1 gAC/L) and TVFA concentration remained constant until the end of the cycle, on day 103.

In the 4th AD cycle, the amount of VFA measured in the liquid phase was surprisingly less than in previous AD cycles, with the bioreactor FA9 reaching a maximum TVFA concentration of 1.9 gAC/L on day 111 of incubation. This maximum value corresponded to a peak in the acetic acid concentration measured at that point (Figure 71), resulting from the accumulation of this acidic specie in the liquid medium. The bioreactors FA8 and FA10 reached 0.79 gAC/L as a maximum value for the TVFA concentration measured in the 4th AD cycle and, after day 118 of incubation, TVFA concentrations were below 0.2 gAC/L and remained constant until the end of the cycle (in this case, also the end of the experiment).

The predominant VFA specie, in terms of maximum concentration, as occurred in the previous results presented, was n-butyric acid, as can be observed in Figure 71. It was formed immediately after the substrate additions, reaching its highest concentrations, and was the first acidic specie converted into methane or acetic acid. The exception was the 4th AD cycle, where n-butyric acid was not formed or was not detected in the liquid fraction due to its rapid consumption by the microorganisms' consortium. The gap between samples (from day 104 to day 111) could have contributed to the absence of n-butyric acid in the analysis. In fact, n-butyric acid was detected in the first 25 days of the 1st AD cycle, in the first 15 days of the 2nd AD cycle, in the first 10 days of the 3rd AD cycle and, in the 4th AD cycle, it should have been detected in the first 5 days, in which no samples were collected.

Acetic acid was also formed in large quantities and, although this acidic specie did not reach the highest individual VFA concentration (expressed in gO₂/L) as n-butyric acid, it remains longer in the liquid fraction in concentrations higher than 1 gO₂/L. On average, acetic acid accounts for about 50 % of the total VFA composition. As observed in previous assays, propionic acid was formed in inferior amounts, but microorganisms did not consume it, maintaining its concentration constant in the liquid until the depletion of other acidic species. In all assays, propionic acid did not exceed 0.5 gO₂/L, which corresponds, on average, to 18 % of the TVFA composition.

4.2.2.4.3 Methane production

Figure 72 depicts the values for methane yield determined over time for assays FA8, FA9 and FA10. In this figure, the AD cycles were divided for clarity, using vertical dashed lines. For the calculation of methane yields, the cycles were considered independent and it was considered that, at the beginning of each cycle, methane production was null, with $Y_{CH_4/sCOD} = 0$.

The 1st AD cycle showed the lowest methane yield values, less than 50 mL_{CH₄}/gO₂ removed, with the reference bioreactor (FA8) having the best performance. Although the environmental conditions applied were the best obtained in previous assays (FA4 to FA7), the anaerobic sludge used did not show an immediate adaptation response. The low methane volume produced in this cycle may be indicative of a low amount of methanogens in the mixed microbial population or low microbial activity, mainly regarding the methane production.

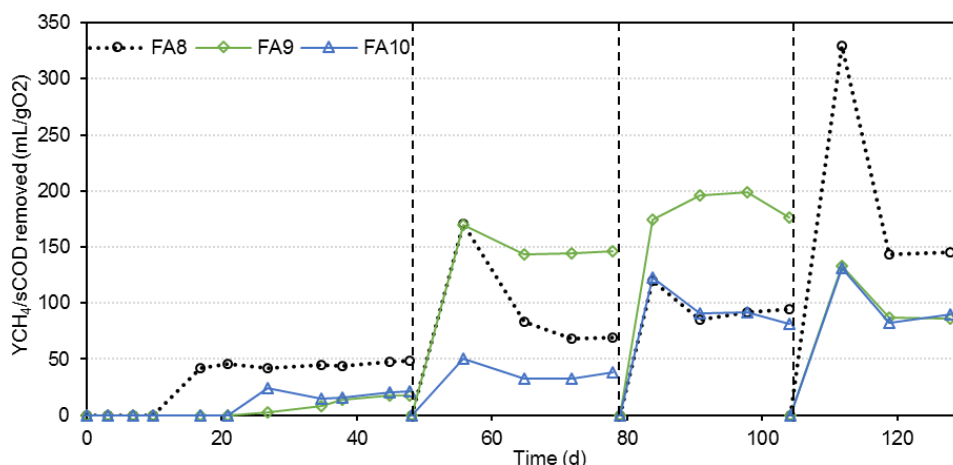


Figure 72] Methane yield determined over time in assays with the addition of different types of alkaline agents (chemical compounds vs high porosity geopolymer spheres).

With the second substrate addition, the anaerobic systems responded positively and part of the removed organic matter was converted into methane, which was reflected in the increase in the general methane yield values. In this 2nd AD cycle, FA8 showed a peak in methane yield, corresponding to a high conversion rate of organic matter into methane, achieving 170 mL_{CH₄}/gO₂ removed, after 56 days of incubation. After this peak, the values tended to stabilize at \approx 75 mL_{CH₄}/gO₂ removed. The values for FA9 and FA10 showed a very different behavior in this cycle, with very low methane yield values for the assay FA10 (\approx 40 mL_{CH₄}/gO₂ removed), and with higher methane yield values for FA9 (\approx 150 mL_{CH₄}/gO₂ removed).

The 3rd AD cycle followed the trend towards a slight increase in the average methane yield values per cycle. After an increase until 120 mL_{CH₄}/gO₂ removed on day 84 of incubation, both the reference bioreactor (FA8) and the bioreactor FA10 stabilized at values close to 90 mL_{CH₄}/gO₂ removed, until the end of the cycle. The bioreactor FA9 presented in this cycle the best methane performance, reaching values of methane yield close to 200 mL_{CH₄}/gO₂ removed during the entire cycle.

After the fourth substrate addition, both bioreactors FA9 and FA10 showed similar methane yield values and profile, with a peak on day 112 (\approx 130 mL_{CH₄}/gO₂ removed), followed by stabilization until the end of the experiment with values between 80 and 90 mL_{CH₄}/gO₂ removed. In this cycle, the reference bioreactor presented higher values in terms of methane yield, reaching a peak on day 112 (330 mL_{CH₄}/gO₂ removed) and stabilizing at 145 mL_{CH₄}/gO₂ removed until the end of the experiment. These instabilities observed in the methane yield values when the substrate was added to each bioreactor were due to the fast conversion of organic matter into methane. During the incubation time in each AD cycle, methane formation tends to slow down and the methane yield values tend to decrease and stabilize until the end of the cycles, as expected in batch tests with substrate depletion.

Although promising, these values obtained for the methane yield did not reach the maximum theoretical methane yield for the environmental conditions applied to each operated bioreactor, namely, 36 °C and an atmospheric pressure of 1 atm: 396 mL_{CH₄}/gO₂ removed. Considering the overall methane yield of these experiments (without the values of the first cycle due to biomass adaptation), the assay with the addition of HPGS as buffer material achieved values slightly higher than the reference assay (141 vs 98 mL_{CH₄}/gO₂ removed). This allows us to conclude that the use of geopolymer spheres is slightly beneficial for the methane formation, with the advantage of

recovering and reusing the buffer material, compared to the use of chemical compounds to control the pH in AD systems.

Figure 73 shows the values of the CO_2/CH_4 ratio, calculated over time for experiments FA8, FA9 and FA10. The four cycles performed in these experiments were divided in the figure by vertical dashed lines. A CO_2/CH_4 ratio above 1 indicates a methane content of less than 50 % and, in the figure, this point is highlighted with a horizontal dashed line. In this representation, the null values indicate a zero methane content measured in the biogas.

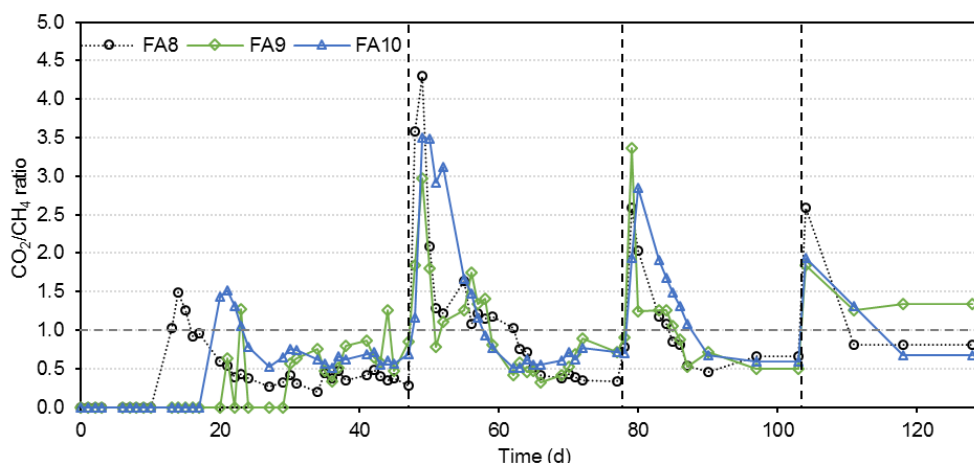


Figure 73| CO_2 to CH_4 ratio in biogas produced in assays FA8 (\circ), FA9 (\diamond) and FA10 (Δ).

After the first substrate addition, all bioreactors showed an initial period without methane content in the biogas. After day 13 of incubation, the presence of methane in the bioreactor FA8 was measured, corresponding to approximately 50 %. The reference system had almost constant methane content in the biogas until the end of the first cycle (65 – 70 %). The bioreactors FA9 and FA10 showed similar behavior, with a 7-day delay.

It was observed that in each substrate addition, on days 47, 78 and 103 of incubation, the CO_2/CH_4 ratio increased rapidly to values above 2.5, which corresponds to a methane content in the biogas less than 30 %. The systems recovered rapidly from the organic load shock and the methane content in the biogas increased with the substrate consumption, transforming the organic matter into methane-rich biogas. This shift in anaerobic metabolism led to a stabilization of the CO_2/CH_4 ratio at values below 1, corresponding to the methane content in the biogas above 50 %. Over time, there was a tendency to decrease the peak of the CO_2/CH_4 ratio measured after substrate addition, indicating good performance and adaptation of anaerobic microorganisms to the substrate, with a decrease in the microbial activity disturbance due to the organic shocks imposed on the anaerobic system with the substrate additions performed.

4.2.2.4.4 Anaerobic process performance

Figure 74 shows the measured values for the methane volume (absolute values), the total VFA concentration expressed as COD equivalents and the pH values measured during the incubation period, for bioreactors FA8 and FA9. As the results for FA10 are similar to those obtained in the FA9 bioreactor, only the performance of FA9 is presented and discussed, comparing it with the reference bioreactor FA8, with the addition of chemical alkalinity instead of highly porous geopolymers.

The four AD cycles are divided in the figure for clarity by vertical dashed lines on day 47, 78 and 103, corresponding to the beginning of the 2nd, 3rd, and 4th AD cycles, respectively, and to the new substrate additions.

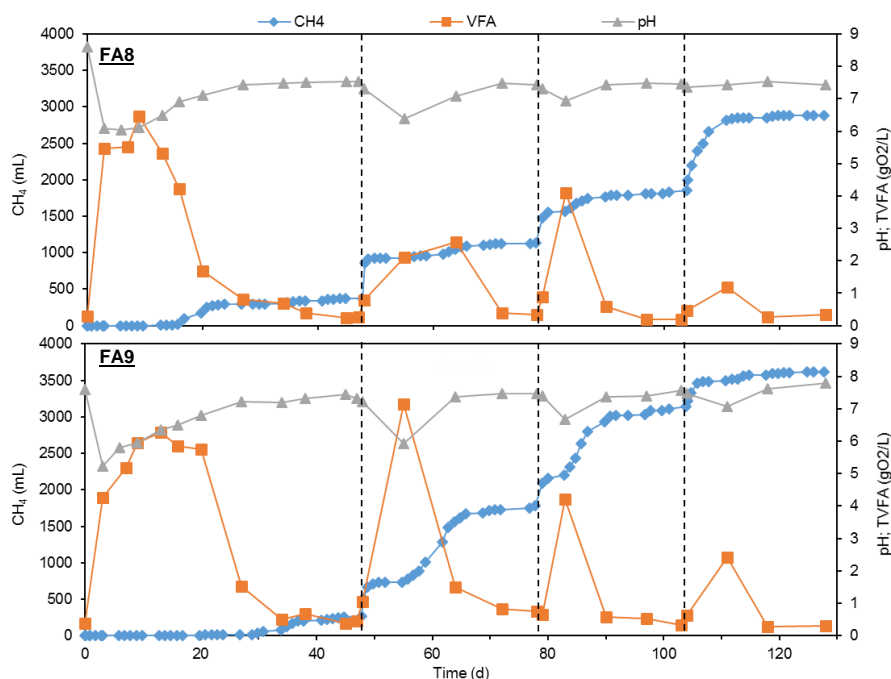


Figure 74| Evolution of CH₄ (◇), total VFA concentration (□) and pH (Δ) with time for the assays FA8 and FA9.

During the experiment, with successive substrate additions, a decrease in the disturbance of the systems was observed. The pH values tend to decrease after substrate additions, and the extent of the pH drop decreases with increasing incubation time. Similar behavior was observed in the VFA formation. The initial period, in which a high amount of VFA was measured in the liquid phase, is longer than the periods after subsequent substrate additions (2nd, 3rd and 4th AD cycles). As mentioned earlier, this behavior can be indicative of the good performance and adaptation of the systems to the imposed conditions.

Methane formation was also evaluated, in terms of the absolute methane volume produced. Until day 57 of incubation, the methane volume produced by the reference bioreactor (FA8) was higher than the volume accumulated by the bioreactor FA9. With the fast metabolization of VFA accumulated, mainly the n-butyric acid present in bioreactors with HPGS (Figure 71), and with the second substrate addition, methane production boosted after day 55, surpassing bioreactor FA8 in terms of absolute methane volume. The formation of n-butyric acid in bioreactors with HPGS was very important for the performance of the anaerobic digester in terms of methane formation. After the turning point during the 2nd AD cycle, in which n-butyric acid was formed at high concentrations, the methane volume formed in the bioreactors with HPGS was always higher than in the reference bioreactor, until the end of the experiment.

In terms of total VFA accumulation over time, the number of VFA species determined tended to decrease with successive substrate additions. A faster consumption of VFA species was observed, preventing its accumulation in the liquid fraction. The decrease in the total VFA concentration with

the increase in the number of cycles affected the pH, which, as previously discussed, tended to stabilize with the incubation time.

Table 38 lists the values and the respective determination coefficients calculated for the maximum rates of VFA production and VFA consumption in the 1st AD cycle, as well as the maximum methane production rate calculated in the 1st, 2nd, 3rd and 4th AD cycles. The VFA production and consumption rates were not evaluated for the 2nd, 3rd and 4th AD cycles due to the lack of experimental points (only two points in each cycle or variable).

Table 38| Maximum VFA production rate, VFA consumption rate and methane production rate for the 1st AD cycle of the fed-batch assays FA8 and FA9, and maximum methane production rate in the 2nd, 3rd and 4th AD cycles for bioreactors FA8 and FA9 (values and respective determination coefficient).

AD cycle	Parameter	FA8		FA9	
		Value	Det. Coeff.	Value	Det. Coeff.
1 st	VFA production rate (gO ₂ VFA/L/d)	0.594	0.730	0.569	0.857
	VFA consumption rate (gO ₂ /L/d)	0.337	0.941	0.375	0.889
	CH ₄ production rate (mL/d)	38.63	0.978	15.17	0.927
2 nd	CH ₄ production rate (mL/d)	28.92	0.987	104.3	0.990
3 rd	CH ₄ production rate (mL/d)	44.82	0.987	150.95	0.988
4 th	CH ₄ production rate (mL/d)	171.75	0.966	100.3	0.901

Regarding the acidogenic step of the AD process, both FA8 and FA9 bioreactors showed similar production and consumption rates. VFA species were produced faster than their consumption, and this is due to the fact that the methanogenic microorganisms, which metabolize VFA as a source of methane formation, have lower rates than acidogenic microorganisms (Anderson et al., 2003). For this reason, VFAs tend to accumulate in the liquid phase and, when readily biodegradable substrates are used, the total VFA amount is usually higher than 2 – 3 gO₂/L (Escalante et al., 2018).

For methane production rate, the values for both bioreactors tend to increase with the successive substrate additions. In the reference bioreactor FA8, methanogenic microorganisms improved their activity over time, increasing from 38.63 mL/d to 171.75 mL/d of methane produced. In the bioreactor FA9, with the addition of high porosity GS to control the pH, methane production in the 1st AD cycle was very low, but with the n-butyric production on day 55 of incubation (see the previous discussion), the methane production rate increased largely and achieved a maximum of 150.95 mL/d in the 3rd AD cycle. In the 4th AD cycle, the performance of the bioreactor FA9 decreased by 34 %.

Figure 75 shows the performance values for the assays with four AD cycles, considering the results for degree of acidification, organic matter removal and methanization degree in each of the four AD cycles performed, for both bioreactors (FA8 and FA9). Figure 76 shows the COD balances for bioreactors FA8 and FA9, at the end of each AD cycle. For the initial samples (beginning of AD cycles), it was considered that methane was not formed (0 % of COD as gas), no organic matter was removed for growth or activity of microorganisms (0 % of COD removed) and the non-acidified fraction of the COD accounts for 90 – 97 % of the COD present in each bioreactor.

Since the acidified fraction at the end of the experiments represents only a very small part of the initial sCOD present in the anaerobic digesters, the degree of acidification for both bioreactors in the different AD cycles was between 2 and 7 %. The methanization degree followed a trend similar to the maximum methane production rate, increasing with the successive substrate addition.

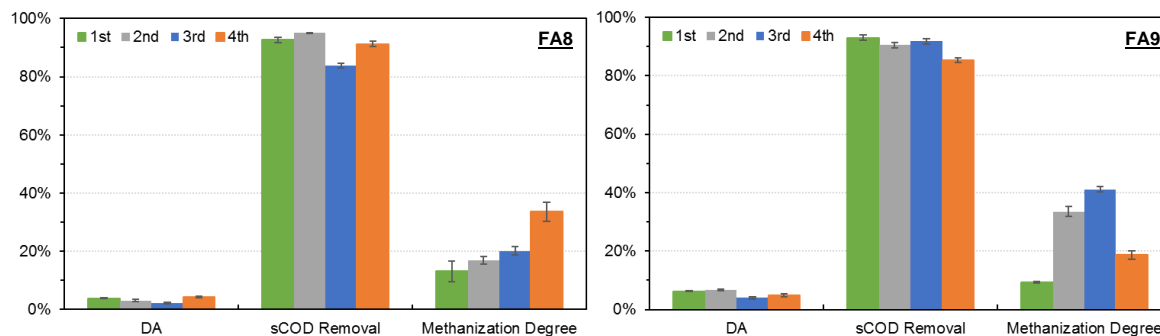


Figure 75| Degree of acidification, sCOD removal and methanization degree for bioreactors FA8 and FA9, in the 1st, 2nd, 3rd and 4th AD cycles.

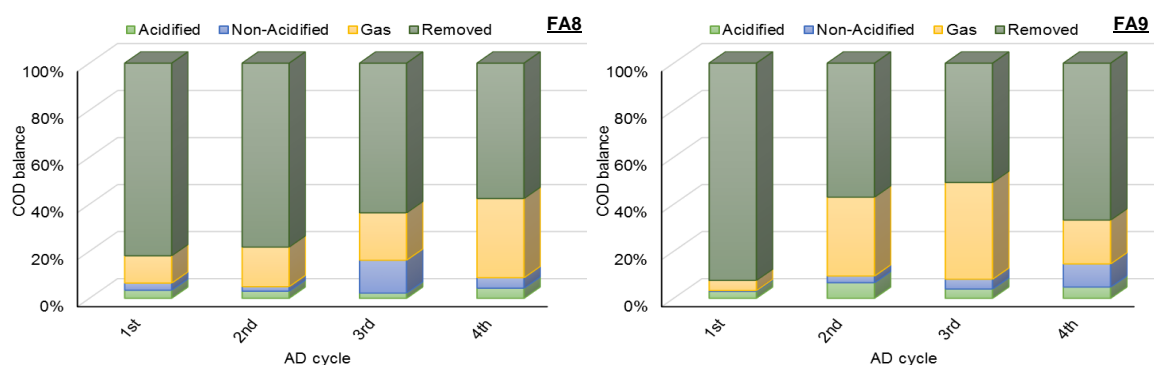


Figure 76| COD balance at the end of each AD cycle for FA8 and FA9 bioreactors, considering the acidified (measured as gO₂/L) and non-acidified sCOD, the gas (methane) formed (measured as gO₂/L) and the removed sCOD.

Regarding the sCOD removal, the values were higher than 84 %, with a slightly decreasing trend with the increase in the time of the experiment. Although these values are very promising, the presence of non-degraded organic material hindered sCOD removals above 95 %. These sCOD removal percentages are in line with those obtained for the previous assays presented (FA1 to FA7).

Thus, it is possible to conclude that the use of geopolymer spheres, namely those with higher superficial porosity (HPGS), is favorable to the increase in the volume of methane. These spheres allowed a stable process through the pH control, improved the VFA formation, specially the main acidic species for the methane formation (n-butyric and acetic acids), and boosted the methane volume produced in the bioreactors, compared to a reference assay in which chemical compounds were added to buffer the AD system. Besides that, the use of this type of materials has a sustainable advantage, as it can be recovered after AD tests. The integrity of the spheres was kept after use, and they can be recycled for other applications, meaning zero-waste generation.

4.2.2.5 Geopolymer spheres characterization after anaerobic digestion assays

In addition to the performance advantages, namely, the increase in methane production, in comparison to the use of commercial powdered alkaline chemicals, GS also show a crucial technical advantage, since it can be recovered after the AD process and then reused in other applications (e.g. lightweight aggregates in the production of mortars). Figure 77 shows SEM micrographs for geopolymer spheres samples before anaerobic fed-batch assays, namely LPGS (a and b) and HPGS

(d and e), and EDS spectra for the referred materials (c and f, respectively). The chemical composition of the spheres under study before and after the AD process is listed in Table 39.

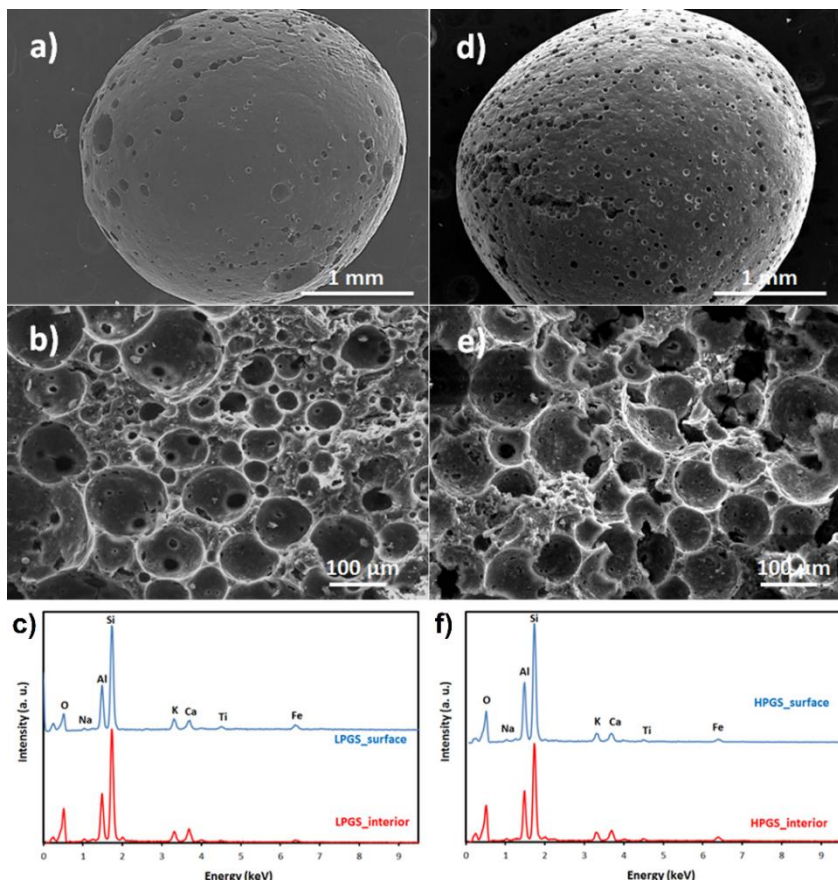


Figure 77 SEM micrographs (a, b, d, e) and EDS spectra (c, f) of the GS after fed-batch tests inside the anaerobic digester: (a, b, c) LPGS and (d, e, f) HPGS.

Table 39 Chemical composition of the GS with low and high porosity, before and after the fed-batch AD tests; the elemental composition of the material as determined by XRF is expressed as oxides and loss on ignition (LOI) was determined at 1100°C.

Oxides (wt.%)	Before AD tests		After AD tests	
	LPGS	HPGS	LPGS	HPGS
SiO ₂	28.0	27.9	52.1	56.4
TiO ₂	0.56	0.68	0.90	1.01
Al ₂ O ₃	10.2	9.75	19.8	20.9
Fe ₂ O ₃	1.45	1.85	2.49	2.71
MgO	0.41	0.42	0.82	0.80
CaO	4.06	4.85	5.14	5.71
MnO	0.11	0.14	0.14	0.15
Na ₂ O	10.7	14.3	1.25	1.17
K ₂ O	1.37	1.60	3.65	3.98
SO ₃	1.24	1.95	0.56	0.61
P ₂ O ₅	1.24	1.95	2.76	2.59
LOI	41.2	35.8	10.2	3.66

Figure 77 shows that, even after 87 days inside anaerobic digesters in adverse environmental conditions, the spheres preserve their integrity. Nevertheless, the SEM micrographs (Figure 77 (b) and (e)) show an increase in the porosity of both GS, certainly caused by alkalis leaching. Indeed, the EDS spectra shown in Figure 77 (c) and (f) show a massive reduction in sodium content in comparison with the results before use.

By the analysis of the main constituents of the spheres before and after AD tests, it is shown that sodium is almost depleted after AD process, decreasing 89 to 92 % at the end of the experiments, for both GS types. However, it also shows that $\text{SiO}_2/\text{Al}_2\text{O}_3$ remains almost unchanged (approximately 2.8), meaning that the composition of the aluminosilicate gel has not been seriously altered after use for such a long period of time and experiencing relatively low pH values at certain times.

4.2.3 Comparison of fly ash-based geopolymer spheres assays for methane production

In the previous sub-sections, the results obtained for the assays using fly ash-based geopolymer spheres as buffering material were presented. During the assays, several previously defined objectives were answered. It was observed that, although there was leaching of organic matter present in the spheres and detected when the spheres were added to the water, the anaerobic microbial population was able to convert this organic matter together with the added substrate into methane, thus achieving high methane yields.

Accordingly, with the results obtained in the anaerobic *oxitop* assays using both FA-based and MK-based geopolymer spheres, the addition of FA-based GS brings benefits for the AD of cheese whey, compared to the addition of MK-based GS. From an economic point of view, the use of FA-based geopolymers is preferential, since they contain a higher amount of waste (fly ash) in their composition. The use of FA-based GS instead of MK-based GS contributes to a more sustainable approach, giving a new life to waste through the creation of new products to be applied, for example, in the improvement of anaerobic processes.

After the *oxitop* assays performed, batch and fed-batch bioreactors were operated. The focus of these studies was the maintenance of the pH and the ability of the spheres to control pH within a naturally unbalanced anaerobic digester. For better understanding, the range of pH values achieved in the stability phase, which is after the initial period of instability due to the accumulation of VFA species, is shown in Figure 78. In the box plots presented, a horizontal line marks the median values (mid-point of the data), the middlebox (interquartile range) represents the middle 50 % of the scores for the data and the upper and lower whiskers represent the scores outside the middle 50 %. For this figure, only the values of the 1st AD cycle were considered. The grey band represents the optimum methanogenic pH range considered in this work (6.5 to 7.2). The pH range achieved in the FA1 bioreactor was much smaller than in the others, due to the lack of chemical alkalinity or GS addition to control the pH. The values ranged from 3.8 to 4.4 in the stability phase, without the formation of methane-rich biogas and, for this reason, were excluded from Figure 78.

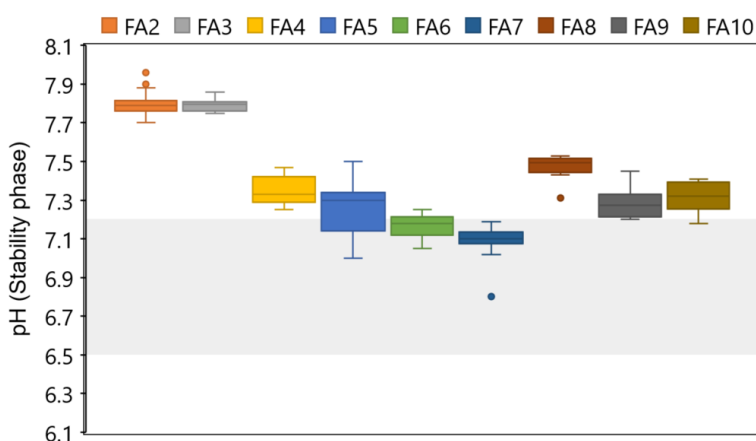


Figure 78 | pH range in stability phase in assays with FA-based GS (FA2, FA3, FA5, FA6, FA7, FA9 and FA10) and respective reference assays (FA4 and FA8).

The use of high amounts of spheres, as in FA2 and FA3 bioreactors, led to higher pH values, around 7.8, in the stability phase. These values are slightly higher than those considered as optimum

pH values for the methane formation. Comparing the reference assays (FA4 and FA8) with the corresponding tests (FA5, FA6 and FA7 for reference FA4, and FA9 and FA10 for reference FA8), it was observed that the addition of chemical alkaline solution led to generally higher pH values at the end of the 1st AD cycle than when using GS.

The conditions applied to the selected bioreactors compared here were summarized in Table 24. The bioreactors were selected according to the best performance obtained in terms of pH control/methane formation, in each set of assays, combined with different types of geopolymer spheres added. Table 40 summarizes the main parameters used to evaluate the performance of the different assays performed with the different types of spheres tested. The main parameters include the pH variation, the organic matter removal, the maximum total VFA concentration and the methane content, the methane yield, the final degree of acidification and the anaerobic biodegradability of each assay.

Table 40 Comparative values for the performance of AD bioreactors with cheese whey as a substrate, using different types of geopolymer spheres, as a pH control material. For bioreactors FA6, FA7 and FA9, the results are presented by the AD cycle.

	Parameter	FA3	FA6	FA7	FA9
Experimental conditions	Number of cycles	1	2	2	4
	GS type	FA-based	LPGS	HPGS	HPGS
	GS amount (g/L)	27	16	16	16
	Substrate added per AD cycle (gO ₂ /L)	8.0	8.0	8.0	8.0
pH	Initial pH	6.99	6.87 (1 st) 6.1 (2 nd)	6.87 (1 st) 5.98 (2 nd)	7.59 (1 st) 5.92 (2 nd) 6.68 (3 rd) 7.07 (4 th)
	Minimum pH	5.40	5.14	5.27	5.22
	Final pH	7.75	7.17 (1 st) 7.63 (2 nd)	7.15 (1 st) 7.46 (2 nd)	7.22 (1 st) 7.39 (2 nd) 7.46 (3 rd) 7.78 (4 th)
Organic matter removal	sCOD Removal (%)	75.5	90.1 (1 st) 89.7 (2 nd)	82.1 (1 st) 84.5 (2 nd)	93.0 (1 st) 90.5 (2 nd) 91.9 (3 rd) 85.4 (4 th)
	Acidogenic step	[VFA] _{max} (gO ₂ VFA/L)	9.96	5.97 (1 st) 4.31 (2 nd)	6.34 (1 st) 5.91 (2 nd)
Final DA (%)		14.9	2.26	2.06	4.77
Methanogenic step	Maximum CH ₄ content (%)	76.6	78.9 (1 st) 85.9 (2 nd)	73.1 (1 st) 78.4 (2 nd)	74.0 (1 st) 74.7 (2 nd) 65.9 (3 rd) 55.4 (4 th)
	Final YCH ₄ /sCOD (mLCH ₄ /gO ₂ removed)	187	68.6 (1 st) 188 (2 nd)	233 (1 st) 203 (2 nd)	17.7 (1 st) 145 (2 nd) 176 (3 rd) 90.2 (4 th)
	Global anaerobic Biodegradability (%)	88.8	47.8	89.2	30.0

With this summary, it is observed that the use of HPGS improved the methane formation. In fact, the highest methane yield of the removed sCOD was obtained in the bioreactor FA7, with a low degree of acidification and very good sCOD removal. The imposition of four AD cycles (bioreactor FA9) limited the methane production, with less anaerobic biodegradability and methane yield than in the bioreactor FA7. The reason for an anaerobic performance lower than the assays with two AD cycles may be related to the provenance and conditions of the anaerobic culture in the WWTP at the time of collection. In addition, maintaining an anaerobic culture for long periods can lead to a lower anaerobic performance, since microorganisms (especially methanogens) are very sensitive to temperature changes and the absence of sources of organic carbons.

The increase in porosity was an asset in the use of GS in the AD system. With the increase in the porosity of the spheres studied in the bioreactor FA7, the boosted anaerobic performance was obtained with a low amount of spheres (16 g/L), compared to the assay with FA-based GS using 27 g/L. Thus, a smaller amount is required to obtain similar results (comparison of FA7's first AD cycle with that of FA3 bioreactor).

Considering the variations in the pH values (Figure 78) and the anaerobic performance parameters (Table 40), it can be concluded that the use of 16 g/L of HPGS to control the pH in a 2-AD cycle process for cheese whey is appropriate for achieving proper environmental conditions to favor methane production. It is possible to achieve high methane yield, high anaerobic biodegradability and maintenance of pH values within the optimum methanogenic pH range when 16 g/L of HPGS were used.

4.3 Phase 3: Red mud-based geopolymers addition to anaerobic digestion assays

Part of this chapter was published in:

“Gameiro, T., Novais, R.M., Correia, C.L., Carvalheiras, J., Seabra, M.P., Labrincha, J.A., Duarte, A.C., Capela, I. (2020). Red mud-based inorganic polymer spheres: innovative and environmentally friendly anaerobic digestion enhancers. *Biores. Technol.* 316, 123904. <https://doi.org/10.1016/j.biortech.2020.123904>”
(IF=7.539)

Part of this chapter was presented in:

“Gameiro, T., Duarte, A.C., Capela, I.. pH control of anaerobic treatment systems using waste-based materials. Encontro de Ciência 2020. 03 – 04 November 2020, Lisbon, Portugal. (Poster presentation)”

4.3 Phase 3: Red mud-based geopolymers addition to anaerobic digestion assays

The results of the assays described in sections 3.5.1 and 3.5.2 were performed, applying the experimental conditions detailed in Table 23 and Table 24. Due to its methanogenic potential, cheese whey was used as a substrate in the AD assays. For these assays, red mud geopolymer spheres were used as buffer material. The main difference in the spheres used is the binder used in manufacture, which in this case is red mud (residue) instead of fly ash (residue) or metakaolin (commercial).

The first assays were performed in batch mode, using the *oxitop* system, to select the amount of spheres suitable to be used in prolonged anaerobic assays. The second assays were performed in fed-batch mode and were incubated for a long period, performing a total of eleven substrate additions. These substrate additions were performed to cause instability of the anaerobic system and enhance the prolonged pH control achieved by the addition of red mud spheres.

For these assays, several goals were defined, namely:

- I. Determination of the red mud-based geopolymer spheres concentration that promotes pH control in the optimum methanogenic pH range in the anaerobic digestion of cheese whey;
- II. Evaluation of the anaerobic performance of batch bioreactors treating cheese whey, with different amounts of red mud-based geopolymer spheres as buffer material;
- III. Study of the effect of organic shocks on the buffer capacity of red mud-based geopolymers spheres, in the anaerobic digestion process treating cheese whey;
- IV. Evaluation of the anaerobic performance of fed-batch bioreactors using red mud-based geopolymer spheres as a buffer material in the anaerobic digestion of cheese whey;
- V. Comparison of the performance of anaerobic fed-batch bioreactors using commercial alkalinity *versus* red mud geopolymer spheres in the treatment of cheese whey;
- VI. Evaluation of the potential of red mud-based geopolymer spheres as a buffer material in anaerobic systems.

4.3.1 Red mud-based geopolymer spheres: anaerobic digestion assays with cheese whey

4.3.1.1 Geopolymer spheres characterization before anaerobic digestion assays

Prior to use in anaerobic assays, the geopolymer spheres containing red mud wastes were analyzed. Figure 79 shows a representative optical micrograph of the red mud-based geopolymer spheres (a), a SEM micrograph (b)) and the EDS spectrum (c)) of the surface of the sphere. The optical micrograph shows a narrow particle size distribution of the spheres, with an average diameter of 2.36 ± 0.10 mm. The SEM micrograph reveals the presence of a significant amount of pores on the sphere's surface, which should enable the diffusion of alkalis from the interior and, as a result, regulate the pH inside the reactors. The EDS spectrum shows that iron, silicon, and calcium are the three most abundant elements in spheres, while other elements such as aluminum, titanium, sodium and potassium are present in smaller amounts. These elements are in line with the chemical composition of the precursors, namely red mud and fly ash wastes, as discussed by Novais et al. (2018a).

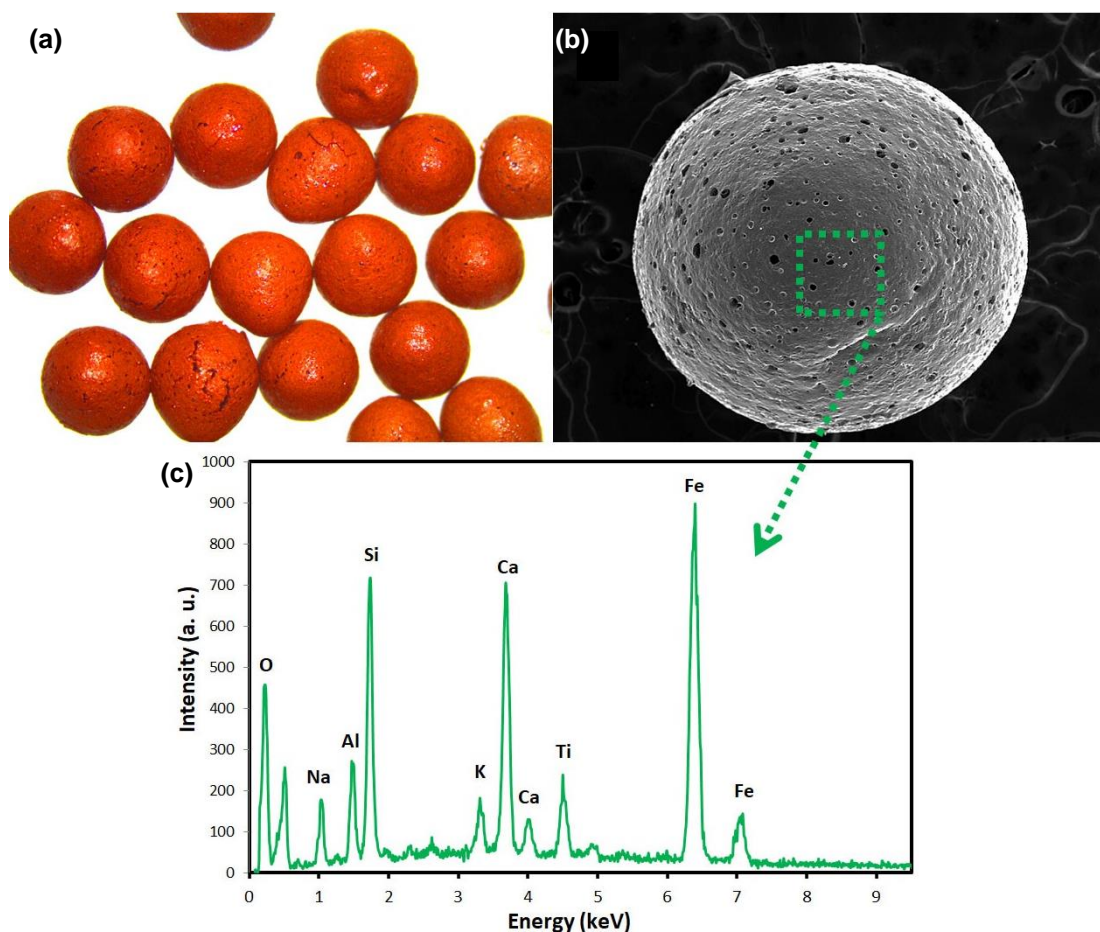


Figure 79 | Optical microscopy photograph (a) and SEM characterization (b) of the red mud-based inorganic polymer spheres, including the EDS spectrum of the spheres surface (c).

4.3.1.2 *Oxitop batch assays with the addition of red mud-based geopolymer spheres*

To evaluate the anaerobic performance of batch bioreactors treating cheese whey and using different amounts of red mud-based geopolymer spheres (RMGS) as a buffer material, the *oxitop* system was used, applying the conditions detailed in Table 23. In this experimental set-up, the pH values, conductivity values, and methane content were monitored during the 35 days of incubation. This preliminary pH evaluation performed in *oxitop* bioreactors was used to select the optimal concentration of RMGS to be used in fed-batch anaerobic digesters, performed in larger scale bioreactors.

The tested concentrations of RMGS (20, 30 and 40 g/L) were chosen due to previous work performed by Novais et al. (2018a). Comparing the leaching behavior of FA-based geopolymer spheres with RM-based geopolymer spheres, Novais et al. (2018a) concluded that the lower amount of alkaline activators present in RMGS led to less OH⁻ leaching capacity. In this way, the concentrations of RMGS tested were slightly higher than those used with FA-based spheres (27 g/L of FA-based GS and 16 g/L of HPGS), in order to theoretically obtain suitable pH values for energy valorization of cheese whey.

Figure 80 shows the values determined for the cumulative pressure inside the *oxitop* bioreactors (a), as well as the methane volume produced during the time (b). For the bioreactor R25, the pressure values were zero due to a failure of the *oxitop* system. For bioreactors R26, R27 and R28, the pressure was measured only until day 18 (R28) and 21 (R26 and R27), since the *oxitop* system has a major limitation on the pressure limit of the measuring head (≈ 333 hPa or 0.33 atm), which can cause restrictions on gas measurements (Pabón Pereira et al., 2012). With the biogas sampling, the pressure decreased each time a sample was taken, which allowed the continuity of measurements by the *oxitop* heads, until the referred days, where the methane formation continued and no pressure values were recorded.

The behavior of bioreactors with RM-based GS addition is similar, regarding the methane volume formed. The biological systems presented a lag phase of 10.6 days (R27 and R28) and 12.3 days (R26), which corresponds to small pressure variations. After the start of methane production, the pressure inside the bioreactors increased rapidly. After approximately 16 days of incubation, the pressure inside the bioreactors tended to slow down, which led to a stabilization in the methane volume formed. This stabilization in the pressure values is an indicator of the bioreactors stability during the anaerobic operation.

Figure 80 also shows the pH values (c) measured during the incubation time in all bioreactors with RM-based GS addition (R26, R27 and R28) and with chemical alkalinity addition (R25). Table 41 lists the pH values at the beginning, on the 1st day of incubation and at the end of the experiments, as well as the methane content at the end of the experiment.

After one day of incubation, the pH values decreased significantly, from 7.12 to 5.49 – 5.72. The reference bioreactor, with 4 g/L of alkalinity measured as CaCO₃, showed a similar pattern, decreasing largely from 8.09 to 5.56. This rapid decrease in pH values was due to the nature of the substrate (cheese whey), namely, its high biodegradability and capacity to form VFA from the organic matter present in the waste, under anaerobic conditions. It was observed that, with the increase in the amount of RM-based GS added to each bioreactor, the pH of the first incubation day tended to increase slightly, as expected. This trend was observed throughout the incubation time, as can be observed in Figure 80 (c), with the bioreactor R26 showing lower pH values than the other

bioreactors. At the end of the experiment, the final pH was higher in bioreactors with a higher amount of RM-based GS added. The final pH values were slightly above the optimum methanogenic pH range considered in this work (6.5 to 7.2) and, for this reason, the amount of RM-based GS added in fed-batch bioreactors, to be presented in the following sub-section, was slightly lower than that used in the *oxitop* bioreactor with the lower amount (R26, with 20 g/L). In addition, and comparing the *oxitop* assays with RM-based GS and with FA-based, the amount of spheres tested was similar, but the range of pH values was slightly different, coming close to 8 with RM-based GS and almost neutral (≈ 7) with FA-based GS. The composition of the spheres influences the leaching behavior of the spheres and, considering RM-based GS, the presence of a highly alkaline waste (red mud) led to an increase in pH values.

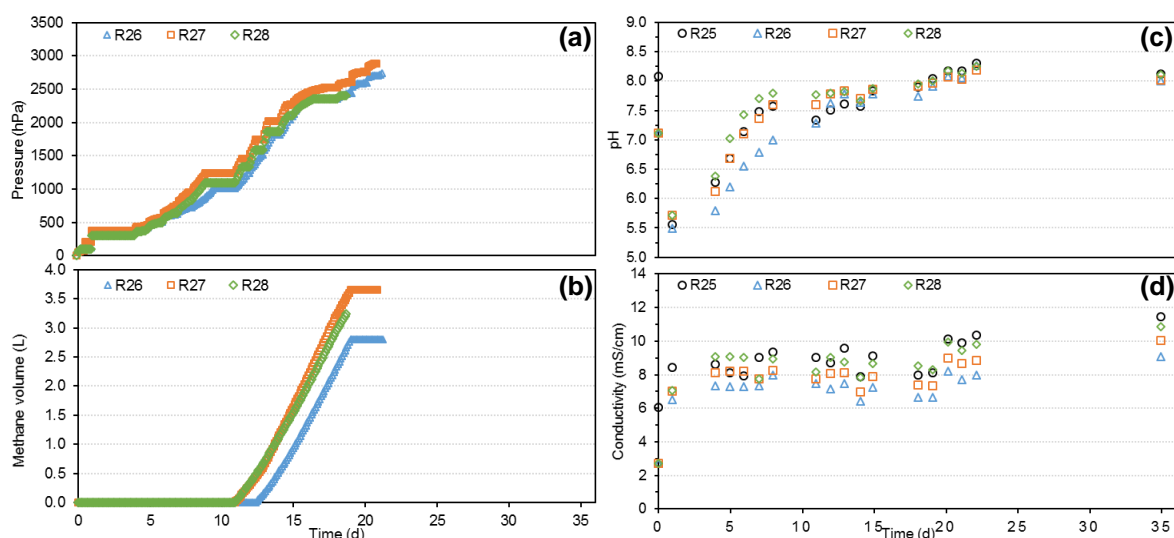


Figure 80 | Methane production (cumulative pressure inside *oxitop* bioreactors (a) and cumulative methane volume (b)) and pH (c) and conductivity values at 25 °C (d), measured during the incubation time for *oxitop* tests with RMGS addition.

Table 41 | pH values at day 0, 1 and 35, in *oxitop* bioreactors containing different alkaline agents at different concentrations.

	Assay ID	Alkaline agent concentration (g/L)	pH at day 0	pH at 1 st day	pH at 35 th day	CH ₄ content (35 th day) (%)
Chemical alkalinity	R25	4	8.09	5.56	8.12	60.9
Red mud-based GS	R26	20	7.12	5.49	8.00	56.9
	R27	30	7.12	5.72	8.02	59.7
	R28	40	7.12	5.72	8.11	63.4

After the initial pH drop observed on the first incubation day, corresponding to the minimum pH value reached for all four bioreactors, the pH increased until day 8 of incubation. No significant differences were observed in the bioreactors with 30 and 40 g/L of RMGS (R27 and R28, respectively), with pH values close to the reference reactor (R25), between days 3 and 8, where pH values of 7.6 – 7.8 have been achieved. The bioreactor R26, with the lowest amount of RMGS, showed values tending to be lower than the other bioreactors and, after 8 days of incubation, the pH measured was 7.0. For this bioreactor, the pH range of 7.6 – 7.8 was achieved only after 12 days of

incubation. This delay may be related to the lower pH value achieved on the 1st day of incubation (Table 41), which led the microorganisms to recover slowly from the acidic environmental conditions created by the addition of a readily biodegradable substrate.

From day 12 of incubation and until the end of the experiment, all four bioreactors showed pH values in the same range, tending to increase after day 18, to pH values above 7.9. Although VFA analysis was not performed in these bioreactors over time, the pH profile obtained is an indicator of VFA depletion of the liquid fraction. This depletion made it possible to stabilize the formation of methane-rich biogas, since the main precursors of methane have already been consumed and converted into the most reduced form of carbon.

Figure 80 (d) shows the conductivity values measured over time in the *oxitop* batch assays. The initial conductivity of the reference test, with the addition of chemical alkaline compounds to promote pH regulation, was more than twice the conductivity of the bioreactors R26, R27 and R28. The beginning of the experiment led to an increase in conductivity of 2.4 mS/cm for the reference assay and from 3.8 to 4.4 for bioreactors with RMGS addition. After the 1st incubation day, the increase in conductivity was less pronounced, with a variation of ± 1 mS/cm.

During the incubation time, the measured conductivity was higher with a higher amount of RM-based GS added, and these results suggested that the addition of RMGS improved the increase in the conductivity of the medium. This increase in conductivity is probably related to the leaching behavior of the spheres during the anaerobic incubation process. In their work, Ye et al. (2018) demonstrated that the addition of red mud to a sludge AD process increased the conductivity of the system, enhancing the electron transfer between different species of microorganisms, namely methanogens and syntrophic bacteria, with a beneficial effect in the methanogenesis step.

Figure 81 depicts the initial and final values of alkalinity and soluble organic matter. With the addition of RM-based geopolymer spheres, the final alkalinity increased to values above 2.6 g/L measured as CaCO₃, obtaining an even greater value the greater the amount of spheres added. For the reference bioreactor, a slight increase in final alkalinity was observed, mainly due to the depletion of VFA from the liquid medium, which increased the final measured pH values.

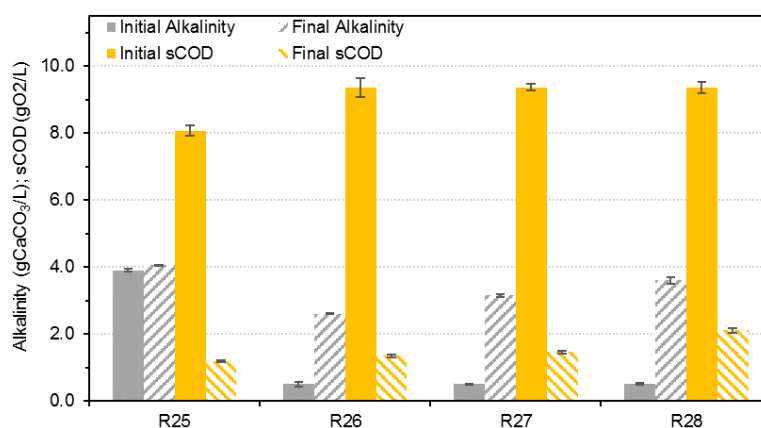


Figure 81 | Initial and final values for alkalinity and sCOD in the *oxitop* bioreactors with RMGS addition.

Figure 82 shows the parameters to evaluate the anaerobic performance of the operated *oxitop* bioreactors, namely, the methanization degree, the anaerobic biodegradability, the final methane content and the organic matter removal. For the bioreactor R25, the pressure values inside the flask

were not measured and, for that reason, the methanization degree and the anaerobic biodegradability were not determined for this bioreactor. The methane content was similar in all bioreactors, between 57 and 63 % at the end of the experiments.

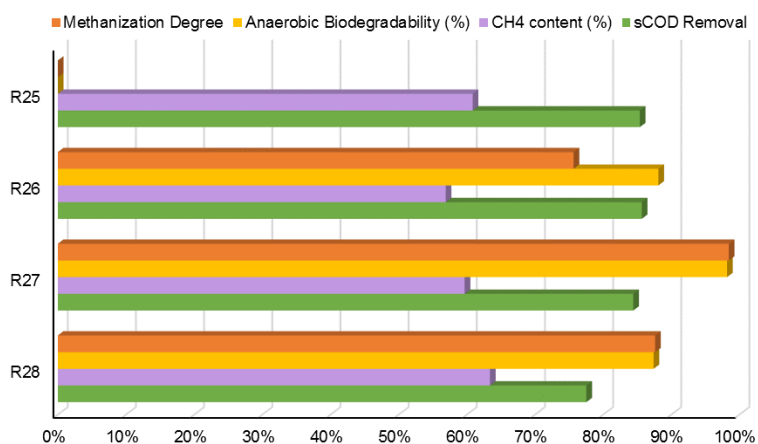


Figure 82| Methanization degree, anaerobic biodegradability, methane content and sCOD removal percentage obtained at the end of the *oxitop* bioreactors testing the addition of RMGS as pH buffer material.

In all bioreactors, the final soluble organic matter was highly reduced, reaching 77 – 85 % of the sCOD removal in bioreactors with the RM-based GS addition. The final sCOD values increased slightly with the increase in the spheres amount added, and from 1.34 gO₂/L to 2.10 gO₂/L remained in the liquid fraction of R26 and R28 bioreactors, respectively (Figure 81). This reduction in the sCOD removal with the increase in the spheres amount added may be related to the environmental conditions provided by the addition of increasing amounts of buffering material. With high pH values (above 8.1 in the bioreactor R28 at the end of the experiment), the conversion of VFA into methane can be impaired and the sCOD reduction is not as effective as, theoretically, at pH close to the neutral range.

Both the methanization degree and anaerobic biodegradability are directly related to the methane volume produced in each bioreactor. The higher methane volume produced by the bioreactor R27 led to the best methanogenic performance in this assay, although the final pH values achieved are slightly higher than 8.0. The 98 anaerobic biodegradability percentage indicates the potential of this system, using RM-based geopolymer spheres as a buffer material, to treat and valorize the cheese whey stream. For the other bioreactors, the values for the anaerobic biodegradability was ≈ 88 %, indicating that only about 12 % of the total removed sCOD was not converted into methane.

Considering the results presented for batch anaerobic assays, the use of RM-based GS is promising for pH control of the AD process treating cheese whey effluents. For fed-batch anaerobic assays operated to treat high-load cheese whey effluent, the amount of spheres used was slightly reduced, since the pH values at the end of the batch experiments were above the optimum methanogenic pH range, as discussed previously. On the other hand, the reduced amount of spheres was tested to evaluate the capacity of the spheres to buffer a naturally unbalanced anaerobic system.

4.3.1.3 Fed-batch assays with red mud-based geopolymer spheres addition

Fed-batch assays using RM-based geopolymer spheres were performed as described in section 3.5.2.2, applying the main operating conditions listed in Table 24. Three experimental conditions

were tested to compare the effect of RM-based geopolymer spheres addition, namely without chemical alkalinity or GS addition (RM1), with 2 g/L of initial added alkalinity measured as CaCO_3 (RM2), and with GS addition (RM3).

4.3.1.3.1 pH evolution

The pH evolution was monitored during all incubation time and the values are shown in Figure 83. In the figure, vertical dashed lines mark the substrate additions and the grey bar highlighted the optimum methanogenic pH range, for the sake of clarity. The substrate additions correspond to the starting point of a new AD cycle, totaling eleven AD cycles in this fed-batch experiment.

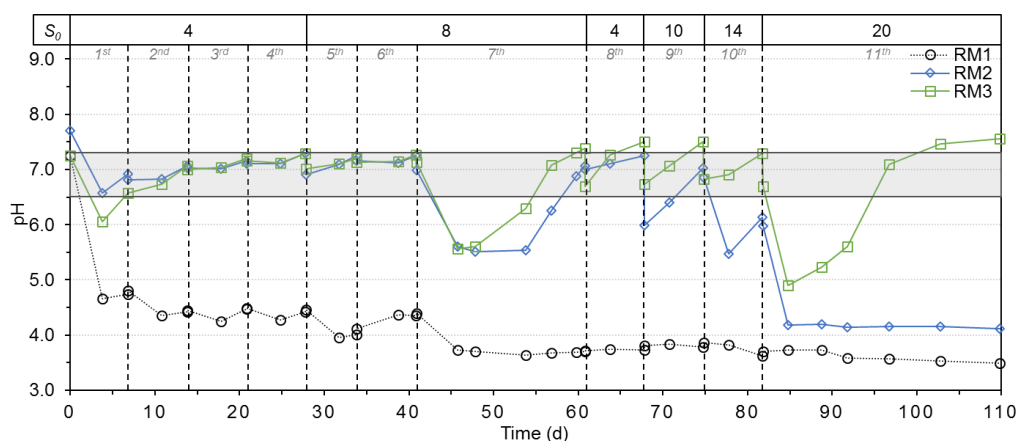


Figure 83 | pH evolution with time for assays RM1 (\circ), RM2 (\diamond) and RM3 (\square). The dashed lines mark the substrate additions and the grey bar is highlighting the optimum methanogenic pH range.

The addition of an easily biodegradable carbon source such as cheese whey to an anaerobic treatment system promotes a pH decrease in the medium, with the fast conversion of organic matter into volatile fatty acids, intermediate compounds of the AD process. As expected, the blank assay (RM1), without chemical alkalinity or GS addition, presented low pH values after substrate addition. After 3 days of incubation, the pH of the RM1 bioreactor decreased from almost neutral to values below 5.0. These acidic conditions are often associated with the decrease in the methane production and the increase in the acid accumulation, and this scenario can lead to a complete failure of the anaerobic system (Speece, 1996; Taconi et al., 2008). In this case, the anaerobic system was unable to recover from low pH values and the pH remained below 4.0 during all the incubation time. With successive substrate additions, the system tended to achieve pH values still low and, after 45 days of incubation, it stabilized at around 3.7 and no effect of substrate additions on the pH was verified after day 45 until the end of the experiment.

The reference bioreactor (RM2), with the chemical alkalinity addition, presented a pH profile similar to the test bioreactor (RM3), with the RM-based GS addition. The initial pH values are in the neutral range, with the bioreactor RM2 presenting slightly higher values, due to the type of alkalinity provided to the system. As chemical alkalinity was added in the form of a solution, the effect on pH was observed instantly, leading to a slightly higher pH value in the bioreactor RM2 (7.71) than that measured in the bioreactor RM3 (7.25), with RM-based GS addition. The slow release of OH^- ions was not perceived at the beginning of the experiment (sample at $t=0$), and the pH of the bioreactor RM3 remained unchanged, at values similar to those of the blank bioreactor (RM1).

As occurred in the RM1 bioreactor, the pH dropped after the substrate addition and, on the 3rd day of incubation, the anaerobic systems presented pH values above 6.0. Comparing these bioreactors with the previous anaerobic systems presented, with FA-based GS addition (see section 4.2), the reestablishment of almost neutral pH values was faster here (RM2 and RM3), with a less pronounced pH decrease. This behavior may be related to the experimental conditions applied in these bioreactors, with a lower initial organic load (4 gO₂/L instead of 8 gO₂/L of sCOD added at the beginning of the AD cycles), and a higher biomass concentration (4.5 gVSS/L instead of 2.5 gVSS/L), compared to assays using FA-based GS to control pH. Thus, the F/M ratio in these bioreactors was lower than in the bioreactors using FA-based GS as a buffer material, allowing for faster stabilization of the system in terms of pH values and prolonged operation using RM-based GS to control the pH.

The successive additions of 4 gO₂/L of substrate in the first 4 AD cycles did not significantly change the pH of the system, and the values remained in the favorable range for the methane formation. At the beginning of the 5th AD cycle, a slight decrease in pH values was observed, since the organic load doubled to 8 gO₂/L. The addition of increasing amounts of organic matter led to a decrease in pH values, due to the VFA formation, and an accumulation of organic matter in the bioreactors. At the beginning of the 7th AD cycle, the pH of the medium in both reference and test bioreactors severely decreased to values close to 5.5, due to the VFA accumulation. The accumulation of VFA reflects, in most cases, the imbalance between acid producer bacteria and acid consuming archaea (methanogens), and this imbalance is associated with a pH drop and a break in buffer capacity (Ahring, 1995; Franke-Whittle et al., 2014). Despite the VFA accumulation, anaerobic digesters were able to recover from low pH values and, after 13 days, the pH rose again to values close to neutrality in the bioreactor RM3. The bioreactor RM2 took 16 days to recover from the pH of 5.5, anticipating an increased difficulty in maintaining the buffer capacity of the system.

After the 20 days instability period in the 7th AD cycle, substrate additions had a clear effect on the pH of both systems. Immediately after substrate addition, the pH decreased at the beginning of the cycles in both bioreactors, the drop being more pronounced in the bioreactor RM3, with a decrease of at least 0.6 pH points. The bioreactor RM2 presented a more unstable operation in terms of pH variations from the eighth AD cycle, with the propensity to reach decreasing values over the incubation time. During the 10th AD cycle, the bioreactor RM2 was unable to recover from low pH values before the substrate addition on day 82 of incubation. At the beginning of the 11th AD cycle and after the substrate addition, the pH inside the reference reactor dropped to 4.15 and remained constant until the end of the experiment. In this case, it is clear that the anaerobic system failed, since the chemical alkalinity provided at the beginning of the experiment was not sufficient to provide adequate buffer capacity for the anaerobic system treating cheese whey, operated for long periods.

After the substrate addition and the consequent pH drop, the RM3 system recovered rapidly from the pH reduction in 8th, 9th and 10th AD cycles, with the pH, at the end of the cycles, above the optimum methanogenic pH range. With the addition of a high amount of organic matter (20 gO₂/L) at the beginning of 11th AD cycle, the pH dropped sharply to values close to 5.0. After 7 days of the AD cycle, the pH of the system begins to recover, reaching values close to neutrality after 13 days of instability. This second period of instability was caused by an organic loading shock, and the anaerobic culture took the same time to recover as in the first period of instability (7th AD cycle).

The recovery of the AD system of the RM3 bioreactor is an indication that the slow OH⁻ leaching from RM-based spheres is beneficial for pH control in a naturally unbalanced anaerobic system,

promoting a prolonged buffering capacity, contrary to the use of chemical compounds to provide alkali to the anaerobic process. The alkalinity of the RM3 bioreactor increased from 0.6 to 8 g/L measured as CaCO_3 at the end of the experiments, which indicates a great capacity of this system to withstand sudden pH changes. This value is above the value considered acceptable for most AD systems (up to 5 g/L measured as CaCO_3) and can cause problems related to foam and scum formation (Gerardi, 2003).

4.3.1.3.2 Volatile fatty acids production

Figure 84 shows the results for the VFA composition of each sample of the bioreactors RM1, RM2 and RM3, displayed as total VFA concentration as acetic acid equivalents (gAC/L). The individual concentration of VFA species, namely, acetic, propionic and n-butyric acids, was expressed as COD equivalents (gO₂/L) and is shown in Figure 85. The other VFA species (i-butyric, i-valeric, n-valeric and n-caproic acids) were also determined individually and presented a much lower concentration than the species in Figure 85, and for this reason were not presented individually, but as “others” in the figure, having been considered to calculate the TVA concentration over time presented in Figure 84.

In the blank bioreactor (RM1), the VFA concentration increased during almost the entire incubation time. The decrease in some individual VFA species concentration was not significant in the total VFA concentration expressed as acetic acid, presenting only small fluctuations. After the 7th substrate addition, the total VFA remained almost constant within the range of 3-4 gAC/L, until the beginning of the 10th AD cycle. The successive addition of organic matter from the cheese whey caused very low pH values and an accumulation of VFA. However, the very low pH measured in the blank test (Figure 83) led to the inhibition not only of methanogenic archaea, but also of hydrolytic and acidogenic bacteria. VFA species, at pH values below the acids' dissociation constant (4.86, at 25 °C), exist mainly as undissociated acids, which can easily diffuse into the cell's membrane and cause microbial inhibition (Wainaina et al., 2019). Thus, the very low pH did not favor either VFA accumulation or methane formation.

For bioreactors RM2 and RM3, the total VFA concentration remained mainly less than 1 gAC/L in the first six AD cycles. The increase in the organic matter concentration added in the fifth AD cycle led to a slight increase in the VFA concentrations detected in the liquid fraction. With the seventh substrate addition, in both RM2 and RM3 bioreactors there was a sharp increase in the total VFA concentration to values around 3 gAC/L, which corresponds to 5 to 6 gO₂/L of TVFA expressed as COD equivalents. This increase in VFA concentration was related to the addition of larger amounts of organic matter (an increase from 4 to 8 gO₂/L of sCOD concentration added). As mentioned earlier, the imbalance between the two main groups of microorganisms present in an anaerobic digester (acidogens and methanogens) led to the accumulation of VFA, since the methanogenic archaea consume the intermediates at a slower rate than the acidogenic bacteria produced them (Prazeres et al., 2012; Wainaina et al., 2019). With the increase in VFA concentration and its accumulation in the medium for long periods, methanogenic archaea tend to become markedly stressed and can cause the inhibition of methane formation (Treu et al., 2019).

Although this increase in VFA concentration, the buffer capacity of both anaerobic systems (RM2 and RM3) is sufficient to ensure the functioning of the processes and the feasibility of the anaerobic

treatment. After the 7th AD cycle, a shift in the behavior of the systems was observed, caused by the increase of the applied organic load. With a high amount of organic matter in the bioreactor, high concentrations of VFA were obtained and the VFA remaining in the medium at the end of each AD cycle was increasingly high, until the 11th AD cycle.

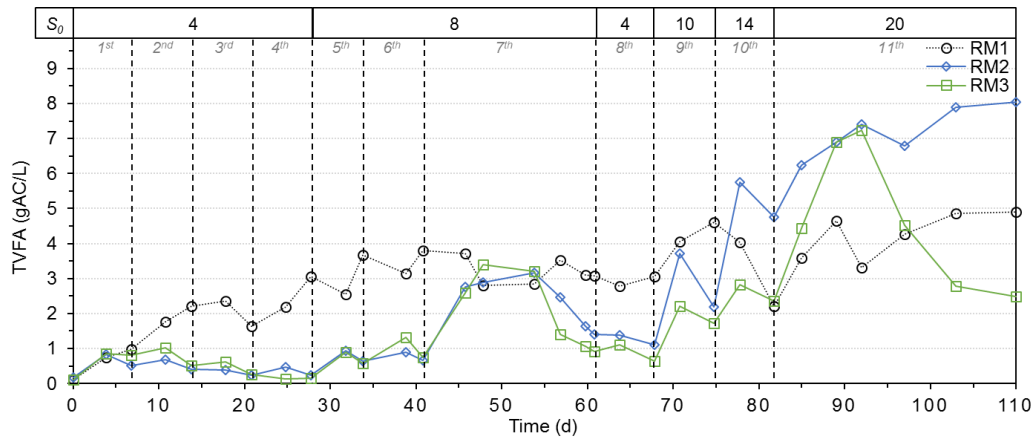


Figure 84 Total VFA concentration (represented as acetic acid equivalents per L) during incubation time of RM1 (○), RM2 (◇) and RM3 (□) assays.

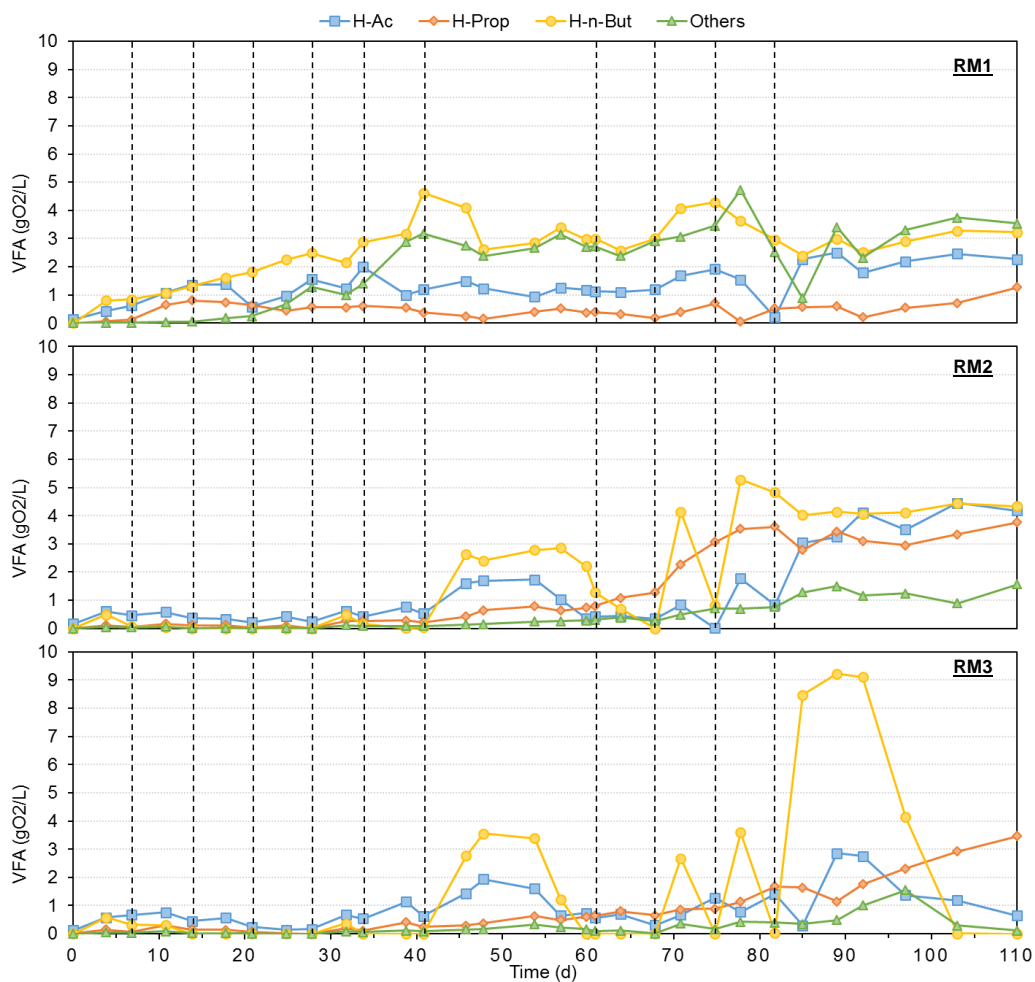


Figure 85 Concentration of individual VFA species, namely acetic, propionic and n-butyric acids, with time, for fed-batch bioreactors operated with the addition of RMGS, namely RM1, RM2 and RM3.

The last AD cycle was decisive for the success of the different types of buffer materials used. The high organic load applied caused a destabilization of the system, with a pronounced pH drop and an increase in VFA concentration, reaching about 7 gAC/L after 10 days of cycle. The buffer capacity of the RM2 bioreactor was unable to promote the recovery of the system, and the VFA concentration continued to increase until the end of the experiment, reaching a maximum TVFA concentration of 8.04 gAC/L. The bioreactor RM3 was able to recover from low pH and high VFA concentration, and methanogenic microorganisms converted the intermediates (VFA) into methane, removing them from the liquid phase. At the end of the experiment, the TVFA concentration reached 2.49 gAC/L, the lowest value of the three conditions tested.

In this experiment, the VFA profile shown in Figure 85 for the three conditions tested is very different. In the bioreactor RM1, without chemical alkalinity or RM-based GS, there was an accumulation of VFA in the liquid phase since the 1st substrate addition. The concentration of n-butyric acid increased over time, until the beginning of the 7th AD cycle. After the 7th substrate addition, the n-butyric acid concentration remained almost constant (3 to 4 gO₂/L) until the end of the experiment. Acetic acid was also formed after the 1st substrate addition, remaining between 1 and 2 gO₂/L until the beginning of the 11th AD cycle, where the concentration increased to values above 2 gO₂/L. Propionic acid remained constant after its formation on day 11 of incubation and at the end of the experiment the concentration was 1.28 gO₂/L. In this bioreactor, VFAs named “others” have a significant part of the total VFA mixture, accounting for more than 30 % of the total VFA after day 39 of incubation (during the 6th AD cycle). In this case, n-caproic acid was accumulated in a larger amount than iso-butyric, iso-valeric and n-valeric acids.

For the bioreactors RM2 and RM3, by the end of the 6th AD cycle, concentrations of the individual VFA are very low and acetic acid was the VFA predominant acidic specie. With the increase in organic load, n-butyric acid was produced and accumulated in the medium for 13 days of the 17th AD cycle. After that, and until the end of the cycle, VFA species were consumed, with acetic acid being the first depleted, followed by n-butyric acid. After the 7th AD cycle, the VFA profile changed and the amount of VFA measured increased, with peaks of n-butyric acid on the 3rd day of each AD cycle, being consumed thereafter.

The last AD cycle, as with the pH profile, led to the destabilization of anaerobic systems, with high VFA amounts accumulated. In the bioreactor RM2, n-butyric, acetic and propionic acids accumulated in the medium and remained until the end of the experiment. Considering the VFA profile, it is possible to conclude that methanogenic microorganisms were inhibited, reducing the conversion of VFA into methane, due to the low pH and unfavorable environmental conditions. With the ninth substrate addition, propionic acid was formed and its concentration reached more than 3 gO₂/L, corresponding to \approx 30 % of the TVFA concentration. At the end of the experiment, the propionic acid concentration was 3.77 gO₂/L.

In the last AD cycle of the bioreactor RM3, n-butyric acid accumulated in the medium, reaching more than 9 gO₂/L 8 days after the beginning of the 11th AD cycle. Despite the very high concentration achieved, this VFA specie was converted into methane and after 20 days of cycle the n-butyric concentration was only 0.01 gO₂/L. Acetic acid was also consumed, but at the end of the experiment 0.64 gO₂/L of acetic acid were still present in the liquid phase. This reduction in VFA content, accomplished by increasing pH values, reflects the capacity of RM-based GS to promote pH control in unbalanced systems and even in unfavorable conditions, such as high organic loads.

As observed in the bioreactor RM2, propionic acid started to accumulate in the ninth AD cycle and increased until the end of the experiment, reaching a final concentration of 3.46 gO₂/L. When all species were partially depleted, propionic acid accounts for 82 % of the TVFA at the end of the experiment for bioreactor RM3. Accumulation of propionic acid may be an indication of a disturbance of the anaerobic system. Several authors have reported the toxic effect of propionic acid in an anaerobic digester, with methanogenic microorganisms being vulnerable to propionic concentrations higher than 1.5 to 3.0 gO₂/L (Lee et al., 2015; Wijekoon et al., 2011). For some authors, the propionic concentration during the AD process must be monitored and the accumulation of this VFA specie can be understood as a warning sign and may suggest an imbalance in the anaerobic process (Ahring et al., 1995; Gourdon and Vermande, 1987).

Until the end of the 9th AD cycle, the blank bioreactor presented the highest TVFA concentration expressed as gO₂/L, compared to the reference (RM2) and test (RM3) bioreactors. With the inhibition of both methanogenic and acidogenic microorganisms in the bioreactor RM1 and with increased organic load in the bioreactors in which both groups of microorganisms are still active (RM2 and RM3), the TVFA concentration in the reference and in the test bioreactors exceeded the TVFA concentration in the blank assay. At the end of the experiment, the TVFA concentration of the reference assay (RM2) was 64 % higher than the blank assay (RM1) and more than three times the TVFA concentration in the test assay (RM3).

4.3.1.3.3 Methane production

Figure 86 depicts the volume of methane produced in the anaerobic fed-batch assays RM1, RM2 and RM3, expressed as gO₂/L, and the methane yield determined over time for the assays RM2 and RM3. In the figure, the AD cycles were divided for the sake of clarity, using vertical dashed lines. For the calculation of methane yields, the cycles were considered independent and it was considered that, at the beginning of each cycle, methane production was zero (YCH₄/sCOD removed = 0).

By the end of the fourth AD cycle, methane production in both the reference (RM2) and test (RM3) assays was very similar, with a slightly higher volume in the reference assay. With the 5th substrate addition, the bioreactor RM3, with the RM-based geopolymer spheres addition, increased its methane production and, at the end of the 5th AD cycle, the methane volume in RM3 was slightly higher than in RM2. In the 6th AD cycle, RM3 boosted its biogas production and obtained a higher methane volume than RM2, creating a significant difference between the two bioreactors' performance. From this AD cycle and until the end of the experiment, the RM3 bioreactor produced a higher accumulated methane volume than the RM2 bioreactor, reaching 16.1 L of methane (corresponding to a volume of 40.9 gO₂/L, expressed as COD equivalents), after 110 days of incubation. This final volume corresponds to almost twice the methane volume produced in the bioreactor RM2, which presented 8.3 L of methane (corresponding to a volume of 21.1 gO₂/L, expressed as COD equivalents).

As previously discussed, due to the strong inhibition of low pH and high VFA concentration, the blank bioreactor RM1 presented very low methane production throughout the incubation time. After six AD cycles, only 0.07 L of methane was produced, which corresponds to 0.17 gO₂/L (expressed as COD equivalents). For this reason, the methane yield for the blank bioreactor RM1 was not

included in Figure 86 (b), which presented very low yield values compared to the bioreactors with the addition of alkaline materials (RM2 and RM3).

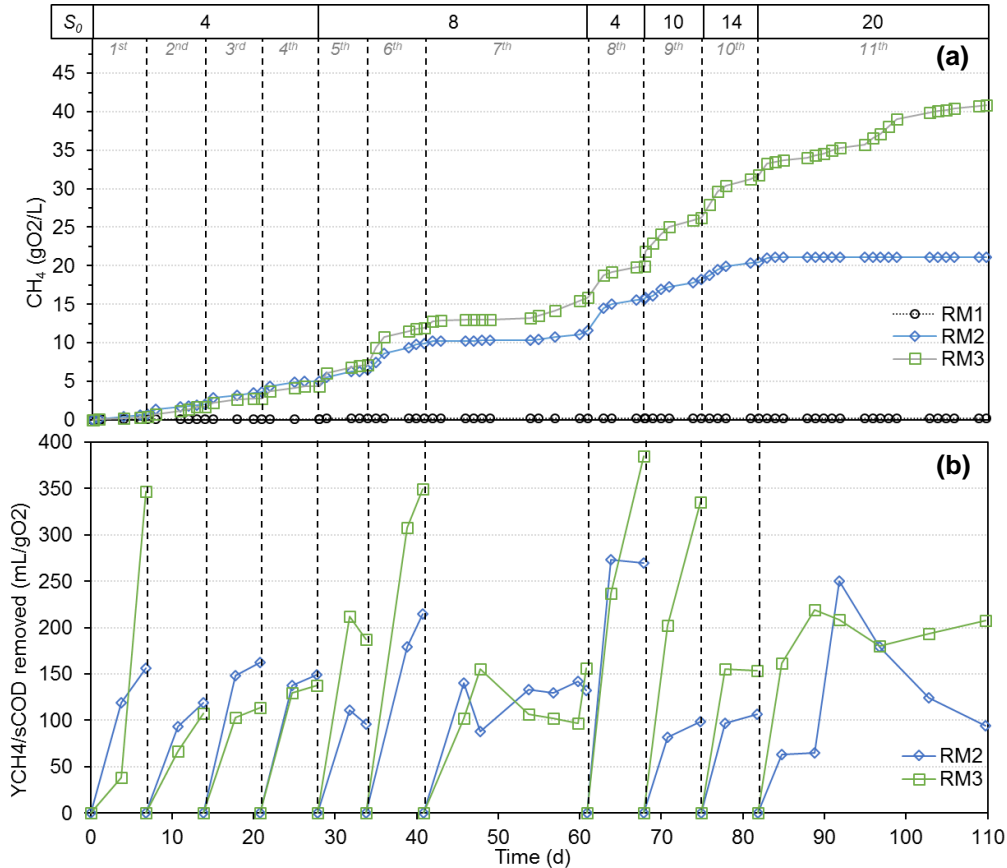


Figure 86| Methane produced in the bioreactors RM1 (○), RM2 (◇) and RM3 (□), expressed as COD equivalents (a) and methane yield (b) determined over time in assays with the addition of different types of alkaline agents (chemical compounds – RM2 – vs red mud-based geopolymer spheres – RM3).

Although the methane volume produced in the 1st AD cycle was similar in both RM2 and RM3, the differences in organic matter removed led to significant differences in the methane yield determined. Thus, in the bioreactor RM3, the microbial community converted a higher fraction of sCOD removed to methane instead of cell growth and maintenance. The methane yield determined for the bioreactors RM2 and RM3 was similar in several AD cycles, such as the 2nd, 3rd and 4th. In the 5th and 6th AD cycles, RM3 presented the highest methane yield, which corresponds to the methane volume boosted, as mentioned previously. The environmental conditions inside the bioreactor with the RM-based GS addition were more favorable for the methane production than inside the reference bioreactor with chemical alkalinity addition, that is, with similar organic loads, the methanogenic microorganisms converted a higher amount of sCOD into methane in the bioreactor RM3. A similar trend in methane yield was observed in the 8th, 9th and 10th AD cycles, with the RM3 bioreactor presenting better anaerobic performance, regarding the methane formation from the removed organic matter.

The instability observed in the 7th AD cycle, characterized by low pH values and organic matter and VFA accumulation, was also observed in the methane formation. The methane volume stagnated for 13 days and, when the systems recovered from low pH values, methane was formed.

The values achieved for the methane yield were similar to those obtained in previous AD cycles for the bioreactor RM2. However, in the bioreactor RM3, the values for the methane yield decreased compared to the 5th and 6th AD cycles, leading to the conclusion that the methanogenic microbial community was affected by low pH values, causing partial inhibition. After instability, anaerobic microorganisms were able to recover and achieve high methane yields, close to the maximum theoretical methane yield (0.396 L_{CH₄}/gO₂ removed).

With the increase of the organic load added in each AD cycle, the methane yield tended to decrease, making the conversion of sCOD to methane less efficient by methanogenic microorganisms. The 11th substrate addition caused the second period of instability due to the high content of organic matter added (20 gO₂/L), decreasing the pH inside the bioreactors and increasing the VFA concentration. The methane yield determined in this last AD cycle was almost constant at approximately 0.200 L_{CH₄}/gO₂ removed for the bioreactor RM3 and decreased to less than 0.100 L_{CH₄}/gO₂ removed in the bioreactor RM2, due to the stop in the methane formation with continuous removal of sCOD.

From the results obtained, an improvement in the methane volume accumulated was evident when RM-based GS were used to control the pH, instead of a chemical alkalinity solution. Similar results were obtained by Ye et al. (2018), who tested the addition of 20 g/L of red mud powder to an anaerobic digester, obtaining a 36 % increase in the methane volume accumulated. In the present study, the use of red mud geopolymer spheres increased the methane accumulation by 94 %, compared to the use of a chemical alkalinity solution. The use of GS led to a controlled release of alkalis, creating conditions more favorable to methanogenesis. Also, the presence of RM-based GS enhanced the hydrolysis and the acidification steps (Ye et al., 2018c), improving the overall AD treatment of cheese whey.

Figure 87 shows the values of the CO₂/CH₄ ratio determined over time. The vertical dashed lines indicate the AD cycles performed. A CO₂/CH₄ ratio above 1 indicates a methane content lower than 50 % and, in the figure, this point is highlighted with a horizontal grey line. In this representation, the null values indicate a zero methane content measured in the biogas. The values of the CO₂/CH₄ ratio for the blank bioreactor were not represented in the figure, as the methane content was very low, which generates very high values of the CO₂/CH₄ ratio. For the RM1 bioreactor, methane production was detected only in the initial days of incubation and its production was inhibited after four AD cycles.

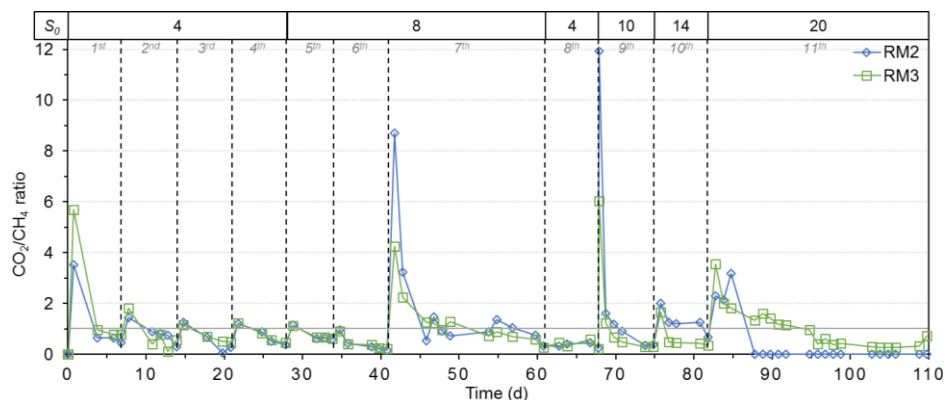


Figure 87| CO₂ to CH₄ ratio in the biogas produced in the anaerobic assays RM2 (◇) and RM3 (□).

For the fed-batch experiments RM2 and RM3, the CO₂/CH₄ ratio values were kept below 1 on most days when the biogas content was analyzed, which corresponds to a methane content higher than 50 %. Methane formation was observed after one day of incubation, with 20 % methane in biogas, with a rapid increase to 60 % methane in biogas on day 4. The lag phase in these experiments was drastically reduced when compared to assays using FA-based GS, due to the applied organic load, which did not lead to a sharp pH drop and enable to kept the system more stable, and due to the acclimatization of the anaerobic sludge at 36 °C, prior to incubation. The fact that the anaerobic sludge used as inoculum is already acclimatized to the mesophilic temperature caused an increase in the hydrolysis and acidogenesis rate, leading to a decrease in the lag phase related to the methane formation. Thus, the anaerobic treatment process is faster when the anaerobic sludge is already active and, considering a full-scale treatment, it is characterized by a lower operational HRT.

When substrate additions were performed, the CO₂/CH₄ ratio increased in all AD cycles, with a significant increase in the 7th and 9th AD cycles, meaning that the methane content decreased in the biogas formed. The increase in carbon dioxide formed in the acidogenesis and acetogenesis steps of the AD process, where organic matter is converted into VFA (and CO₂), causes these variations in the methane content. With the VFA accumulation in the digesters, an overflow of protons is induced, which decomposes the bicarbonates present in the liquid phase and produce CO₂, which increases the CO₂ content in the biogas and decreases the pH of the digester (Palacios-Ruiz et al., 2008).

With the fast conversion of VFA into methane, the methane content in the biogas increased, decreasing the CO₂/CH₄ ratio to values below 1. In the unstable AD cycles (7th and 11th), the methane content remained below 50 % by longer periods and, after about 13 days of cycle, increased to values above 60 %. In the last AD cycle, and due to the inhibition that occurred in the bioreactor RM2 due to VFA accumulation, the methane content was null from day 88 and until the end of the experiment. Similar behavior was observed by W. Zhang et al. (2020), who obtained a reduced methane content in the biogas, with the accumulation of VFA in the medium, when a high organic load was supplied to the digester.

4.3.1.3.4 Anaerobic process performance

Figure 88 depicts the values for the absolute methane volume (measured in mL), the total VFA concentration expressed as COD equivalents, and the pH values measured during the incubation period for the fed-batch bioreactors RM1, RM2, and RM3. The eleven AD cycles are divided in the figure for the sake of clarity by vertical dashed lines on days 7, 14, 21, 28, 34, 41, 61, 68, 75, and 82, corresponding to the beginning of each AD cycle with new substrate additions.

For these experiments with the addition of RM-based GS, the substrate was fed with an increase in load, starting at 4 gO₂/L and, after four substrate additions, the concentration increased to 8 gO₂/L. Compared to previous fed-batch bioreactors (see for example FA9 and FA10, with only four AD cycles), RM2 and RM3 bioreactors showed more variations in organic loads, which created a dynamic system. The initial F/M ratio applied to the bioreactors RM2 and RM3 was much lower (0.9 gO₂/gVSS) than the initial F/M ratio in the FA-based GS assays (approximately 3.5 gO₂/gVSS). These differences led to a faster metabolization of organic matter into VFA and a faster methane

formation from VFA (methane measured in biogas since the first day of incubation), leading to lower VFA concentrations and higher pH values. This faster metabolization may be related to the higher amount of microorganisms (twice as much as in FA-based GC assays), with half the concentration of organic matter, which is intended to avoid the inhibition of RM bioreactors caused by an excess of the substrate. This pattern was observed in the first six AD cycles of RM2 and RM3 bioreactors, with low VFA concentration (< 2 gO₂/L) and almost neutral pH values (≈ 7).

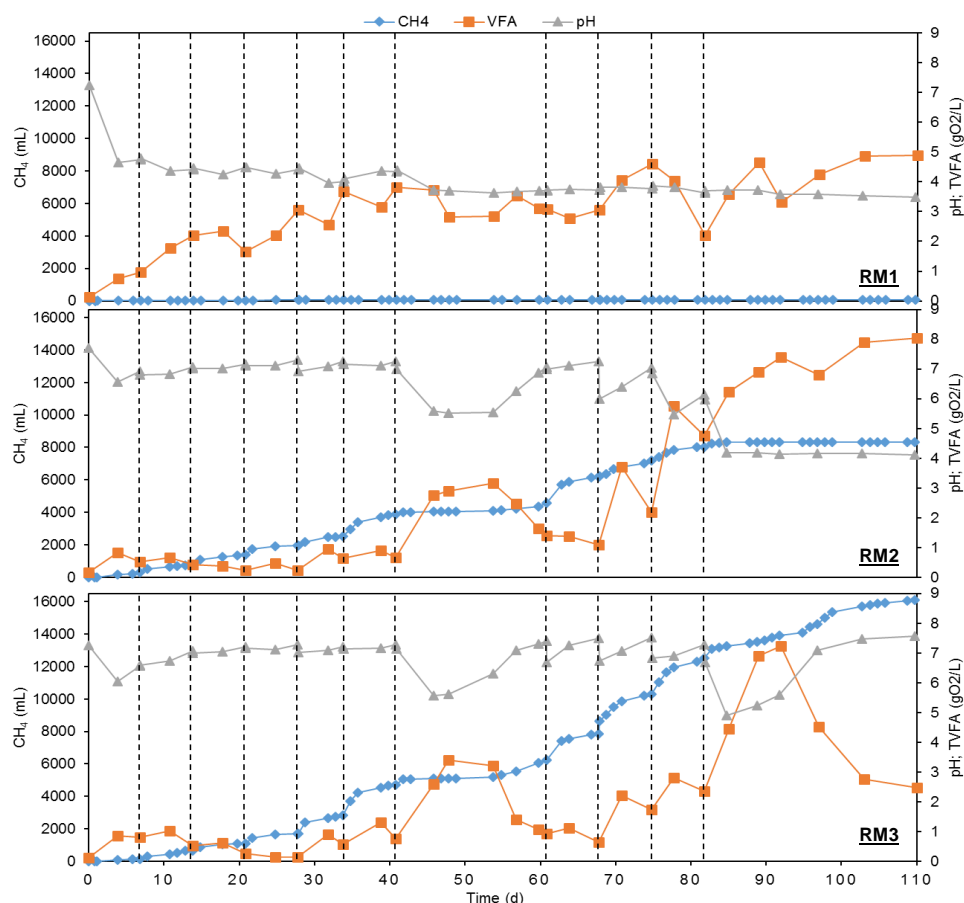


Figure 88] Evolution of CH₄ (◇), total VFA concentration (□) and pH (△) with time for the assays RM1, RM2, and RM3.

The destabilization of anaerobic bioreactors in the 7th and 11th AD cycles, characterized by a decrease in pH values and an increase in VFA concentration, can lead to changes in the metabolism of microorganisms, due to the organic overload observed inside the bioreactors. The use of RM-based geopolymer spheres clearly enhanced the formation of methane and allowed the implementation of a stable system in terms of the release of alkalis during the incubation time.

Table 42 lists the values and corresponding determination coefficients calculated for the maximum methane production rate calculated in all AD cycles, individually, for the bioreactors RM2 and RM3. The absence of methane in the biogas did not allow the calculation of the maximum methane production rate for the bioreactor RM1. The VFA production and consumption rates were not calculated for this experiment due to the lack of experimental points (only two sampling points were analyzed in each AD cycle). According to the determination coefficients obtained for these results, it can be concluded that the data has a good adjustment to the developed models, with

determination coefficients higher than 92 % for the methane production rates. The exception was the maximum methane production rate for the bioreactor RM2, in the 11th AD cycle, whose methane formation was unstable due to the substrate accumulation and consequent inhibition of the methanogenesis step, leading to the interruption of methane formation, three days after the beginning of the 11th AD cycle.

Table 42| Maximum methane production rate for all AD cycles performed with RM2 and RM3 bioreactors, expressed in mL/d.

AD cycle	RM2		RM3	
	Value	Det. Coeff.	Value	Det. Coeff.
1 st	48.67	0.996	23.96	0.987
2 nd	44.23	0.991	68.07	0.963
3 rd	49.64	0.996	39.71	0.917
4 th	37.31	0.914	39.58	0.936
5 th	70.50	0.949	88.57	0.993
6 th	144.66	0.915	150.21	0.885
7 th	49.90	0.997	145.95	0.992
8 th	464.54	0.955	466.97	0.952
9 th	200.26	0.951	429.80	0.998
10 th	218.92	0.983	474.64	0.959
11 th	127.86	0.868	323.07	0.977

For both assays, the four initial AD cycles presented methane production rates around 40 mL/d, both bioreactors being similar. With the fifth substrate addition and with an increase in the substrate concentration, both bioreactors presented a boost in the methane formation rate. With the seventh substrate addition, and due to the substrate overload, the methane formation decreased significantly and the maximum methane rate decreased to one third in the bioreactor RM2. In the bioreactor RM3, and despite the initial inhibition in the 7th AD cycle, the maximum methane rate was not widely affected. After the instability period in the 7th AD cycle, the bioreactor RM3 was able to produce large amounts of methane per day, reaching a maximum methane rate of 474.64 mL/d in the 10th AD cycle. In the bioreactor RM2, and despite a promising rate achieved in the 8th AD cycle (464.54 mL/d), the system was unable to keep high methane production rates, decreasing to less than a third in the 11th AD cycle, compared to the 8th AD cycle. These variations in the methane production rate are closely related to the substrate additions and the corresponding concentration of organic matter, leading to bacterial inhibition in the absence of adequate alkalinity addition.

Figure 89 shows the results for degree of acidification, methanization degree, organic matter removal, and anaerobic biodegradability, parameters determined in the eleven AD cycles operated in the bioreactors RM2 and RM3. The results for the bioreactor RM1 are not shown in Figure 89 because the methanization degree was close to zero (very low methane formation) and the sCOD removal was zero or very low, due to the VFA accumulation in the medium with successive addition of organic matter in each AD cycle operated. The VFA accumulation in the blank bioreactor (RM1) represents only about 30 % in terms of the degree of acidification, also indicating an inhibition of the acidogenic microbial population.

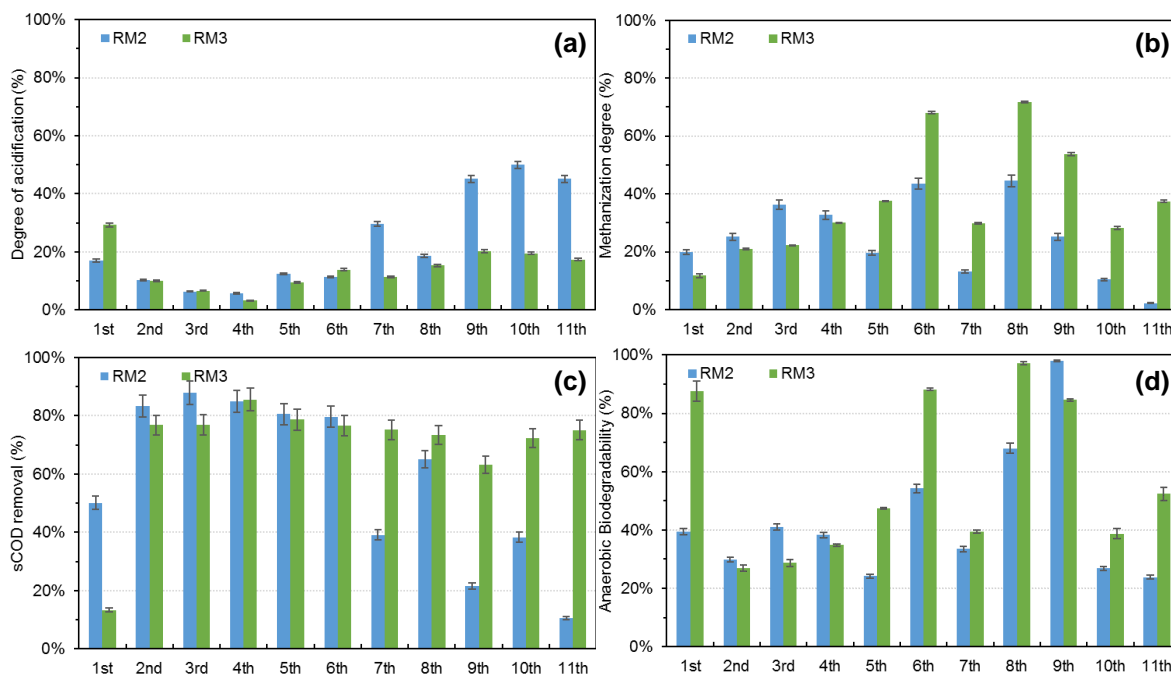


Figure 89] Anaerobic performance for each AD cycle in bioreactors RM2 and RM3, including degree of acidification (a), methanization degree (b), sCOD removal (c), and anaerobic biodegradability (d).

With the increase of substrate additions, the degree of acidification increased in the bioreactor RM2, with the VFA accumulation after the seventh substrate addition, reaching more than 40 % at the end of the experiment. With the inhibition of methane production, RM2 obtained a low methanization degree, mainly at the end of the experiment, where methane production was very low. Unlike the bioreactor with the addition of chemical alkalinity (RM2), the bioreactor with the addition of RM-based GS (RM3) obtained a high methanization degree and a low acidification degree (below 20 %), indicating a good anaerobic performance, even after the instability observed at the 7th AD cycle.

The sCOD removal between the 2nd and 6th AD cycles presented values above 75 % for the two reactors presented in Figure 89. The performance regarding the capacity to remove organic matter from the medium was affected by the instability observed in the 7th AD cycle, and the sCOD removal for the RM2 bioreactor decreased considerably to values below 50 %. For the bioreactor RM3, the sCOD removal was kept above 70 %, with sCOD being removed from the liquid to be converted into methane or new cellular material. This difference in behavior regarding sCOD removal for the bioreactors RM2 and RM3 after the 7th AD cycle is also an indicator of the viability of using the sphere's in detriment of chemical alkalinity, to control the pH in high load anaerobic systems.

For the bioreactor RM3, anaerobic biodegradability increased from the 2nd to the 6th AD cycle, indicating an improvement in the anaerobic performance by methanogenic microorganisms. Despite this trend, the bioreactor RM2 presented generally higher anaerobic biodegradability in the 2nd, 3rd, and 4th AD cycles. The instability in the 7th AD cycle led to a drop in anaerobic biodegradability of more than 38 % in RM2 and more than 55 % in RM3. The two bioreactors recovered, and the anaerobic biodegradability achieved its maximum value in the 8th and 9th AD cycles for RM3 and RM2, respectively. The increase in the organic matter content added to each bioreactor had a positive effect on methanogenic microorganisms, leading to an increase in the anaerobic

biodegradability of the substrate under study. For these bioreactors, the global anaerobic biodegradability was between 43 % (RM2) and 53 % (RM3), indicating that part of the total removed sCOD was not converted to methane, and this organic matter was removed for maintenance or cellular metabolism.

Figure 90 shows the COD balances performed for the blank (RM1), reference (RM2), and test (RM3) bioreactors at the end of each AD cycle performed. For the initial samples of each AD cycle, methane formation was considered zero (0 % of sCOD as “gas”) and no organic matter was removed for growth or microorganisms’ activity (0 % of sCOD as “removed”).

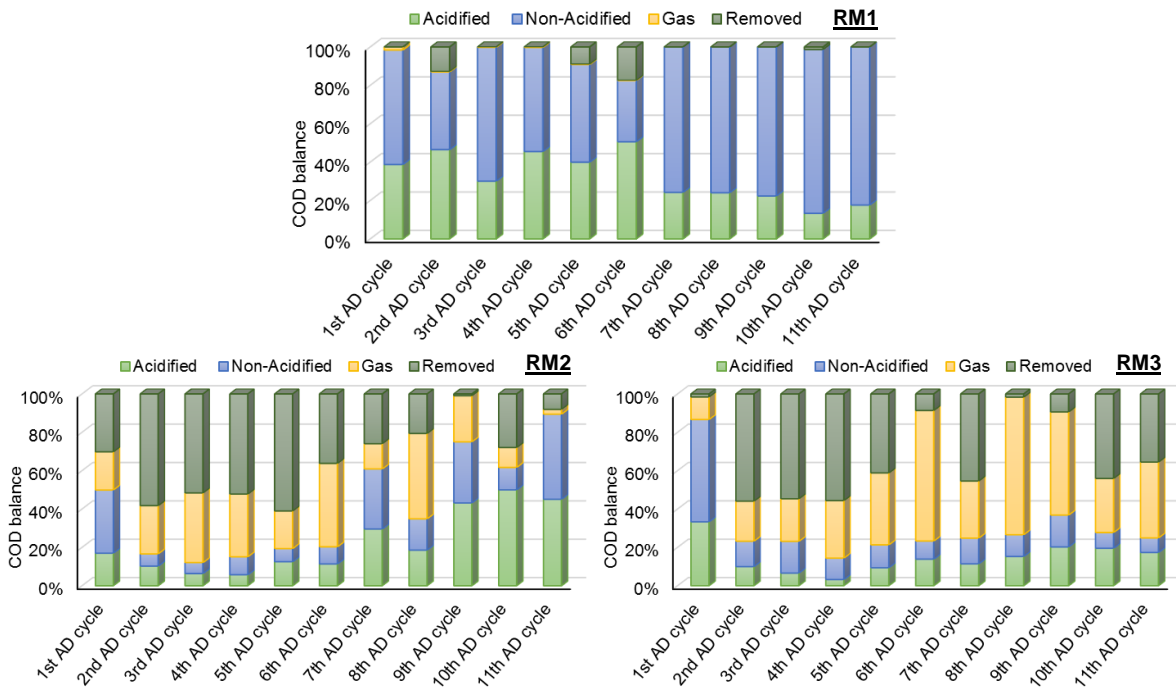


Figure 90 COD balance at the end of each AD cycle for RM1, RM2, and RM3 bioreactors considering the acidified (measured as gO₂/L) and non-acidified sCOD, the gas (methane) formed (measured as gO₂/L), and the removed sCOD.

According to the results presented, the blank bioreactor did not even show methanogenic behavior, as neither methane was formed during the experiment, nor acidogenic behavior, since the acidified COD fraction does not exceed 40 % until the 6th AD cycle and decreases to less than 20 % of the 7th AD cycle until the end of the experiment. This COD profile led to the conclusion that the blank bioreactor, without the addition of chemical alkalinity or RM-based GS to control the pH, was inhibited by the substrate accumulation. Thus, the treatment process of cheese whey that applies the environmental conditions studied in the bioreactor RM1 is not suitable to be implemented for valorization, since energy (methane) or material (VFA) recovery was not observed and, consequently, there was a poor anaerobic performance.

The RM2 and RM3 bioreactors presented a similar COD balance until the end of the 5th AD cycle. In the 6th AD cycle, with the increase in the sCOD concentration added to the bioreactors, the performance of the reference bioreactor decreased, accompanied by an increase in the VFA concentration and a decrease in methane production. The bioreactor RM3 presented a different

behavior, with an increase in the quantity of methane formed (expressed as gO₂/L) and maintenance of acidified and non-acidified fractions of soluble COD.

Comparing the two bioreactors with the addition of the alkaline materials (RM2 and RM3), it can be concluded that the addition of RM-based GS is preferable to the addition of chemical alkalinity solution, leading to a more stable system, with energy valorization assets. Due to its structure, which is kept almost intact during the anaerobic experiments presented here, the use of RM-based GS is also preferable due to the possibility of being recovered and reused in other applications, acting as an adsorbent for metals or dyes (Novais et al., 2018a) for example, thus contributing to the concept of the circular economy.

4.3.1.4 Geopolymer spheres characterization after anaerobic digestion assays

After the AD assays, the spheres were collected by settling and washed with water to remove residual biomass, prior to their microstructural characterization. Figure 91 (a) and (b) show optical and SEM micrographs representative of the spheres after their use in the 110 days of incubation, inside the bioreactors. Figure 91 (c) shows the EDS spectra of the spheres' surface after the AD assays. In these assays, the spheres kept their integrity, with a mass loss of 3 % (spheres from RM3 bioreactor), after 110 days of incubation within the anaerobic bioreactor.

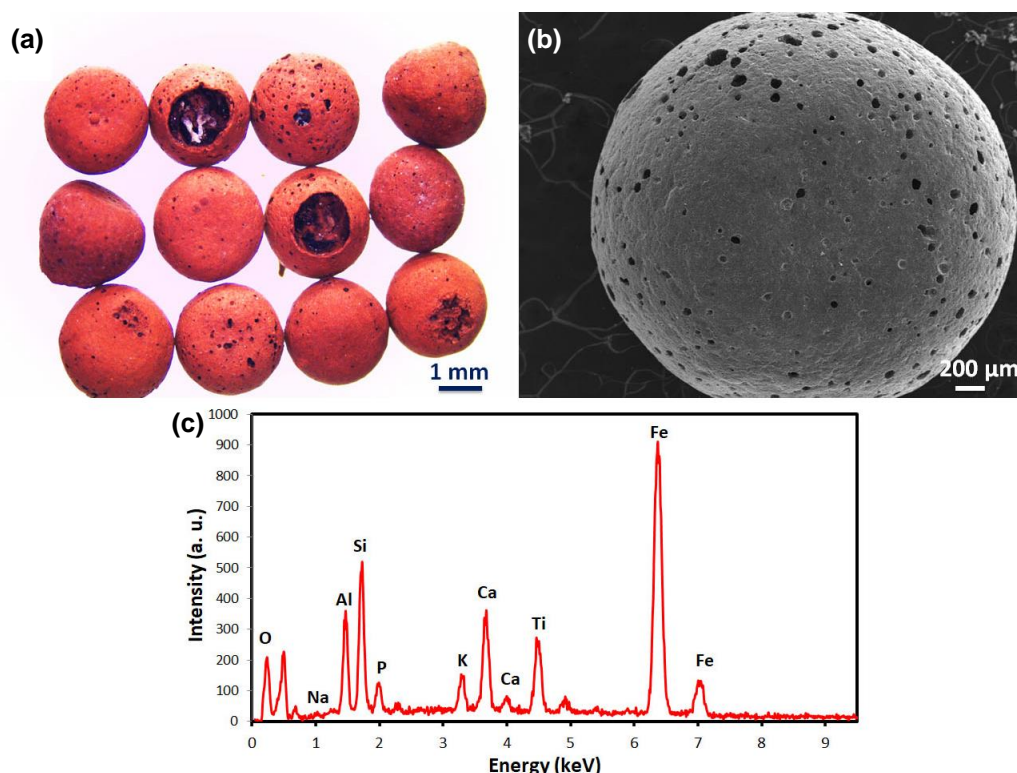


Figure 91 | Optical micrograph (a), SEM micrograph (b), and EDS spectra (spheres surface) (c) of the red mud-based geopolymer spheres after AD assays.

As can be observed, the spheres keep their integrity, even after the long immersion period inside the digesters, and this resistance, even after 110 days of the experiment, suggests that a strong

geopolymerization has occurred. This characteristic is very relevant, as it can allow the reuse of the spheres after their use in AD for a variety of applications, such as adsorbent of heavy metal.

The EDS spectra (Figure 91 (c)) shows that, as expected, the sodium content in the samples decreases sharply during the AD experiments (see Figure 79 (c) for the comparison of the EDS spectra of the spheres before the AD assays). This decrease in sodium content explains the high capacity of the spheres to regulate pH, as discussed in detail in the previous sections. Interestingly, after AD, the spheres show the presence of significant amounts of phosphorus on their surface and lesser amounts in their inner structure (results not shown), absent in the spheres' chemical composition before being used in AD. These differences in the phosphorous location suggest that the spheres may be acting as a support media for the growth of bacteria.

4.3.2 Comparison of red mud-based geopolymer spheres assays for methane production

With the RM-based GS addition, batch *oxitop* and fed-batch bioreactors were operated. Table 43 summarizes the main anaerobic performance parameters to compare these two types of bioreactors operated at similar conditions. The results for the bioreactor R27 consider the entire operation time (35 days) and the results for bioreactor RM3 consider only the 6th AD cycle (both reactors were operated under similar conditions of applied organic load). This cycle of the bioreactor RM3 is presented in Table 43, since it corresponds to the incubation time between days 34 and 41, where the initial load added (8 gO₂/L) is identical to that of bioreactor R27, thus enabling a comparison between the two different systems operated (batch vs fed-batch).

Table 43 Comparative values for the performance of AD bioreactors with cheese whey as a substrate, using RM-based GS addition, as a pH control material. For the fed-batch bioreactor, the results of the 6th AD cycle are presented (equivalent to the same operation time and load performed for the batch bioreactor R27).

	Parameter	R27	RM3
Experimental conditions	Total number of cycles	1	6 (11 in the entire experiment)
	GS type	RMGS	RMGS
	GS amount (g/L)	30	15
	Substrate added per AD cycle (gO ₂ /L)	8.0	Variable (sCOD _{6th AD cycle} = 8 gO ₂ /L)
pH	Initial pH	7.12	7.13 ^a
	Minimum pH	5.72	6.05
	Final pH	8.02	7.27 ^a
Organic matter removal	sCOD Removal (%)	84	77 ^a (94 ^b)
Acidogenic step	[VFA] _{max} (gO _{2VFA} /L)	n.d.	1.66 ^a
	Final DA (%)	n.d.	17 ^a
Methanogenic step	Maximum CH ₄ content (%)	82	81 ^a
	Y _{CH₄} /sCOD removed (mL _{CH₄} /gO ₂ removed)	389	349 ^a
	Anaerobic biodegradability (%)	98	88 ^a (53 ^b)

^a Values obtained considering the 6th AD cycle individually

^b Value obtained considering the first 6 AD cycles

n.d. – not determined

For batch *oxitop* assays, the bioreactor R27 is presented because the initial RMGS/substrate ratio is similar to that imposed at the beginning of the bioreactor RM3 operation (3.75 g_{spheres}/gO₂). For the bioreactor R27, 30 g/L of spheres were added to treat an initial organic load of 8 gO₂/L, whereas, for bioreactor RM3, half of the amount (15 g/L) of spheres was added to treat half of the initial organic load of reactor R27, i.e. 4 gO₂/L (value of the 1st AD cycle). On day 34, corresponding to the beginning of the 6th AD cycle, the organic load is similar to that applied to the bioreactor R27 (8 gO₂/L) and is the one considered in Table 43.

For the bioreactor R27, the reduction in the initial organic matter added did not exceed 84 %. However, from this removed organic matter, a high amount of methane was formed, achieving a high methane content in the biogas (82 %) and a high methane yield (389 mL_{CH₄}/gO₂ removed), with values closed to the theoretical methane yield, considering the experimental conditions performed (396 mL_{CH₄}/gO₂ removed). At the end of the experiment, the pH measured in bioreactor R27 was slightly above the optimum methanogenic pH range, with values close to 8. Comparatively, the bioreactor RM3 also presented good methanogenic performance, with high values for the methane yield of the 6th AD cycle (349 mL_{CH₄}/gO₂ removed) and the methane content in the biogas (81 %). The pH in fed-batch assays was kept in a pH range close to neutrality, with a final value of 7.27 at the end of the 6th AD cycle.

The use of a smaller amount of spheres in the fed-batch bioreactor RM3 was much more challenging regarding the stability of the reactors than in the case of the R27 reactor. In fact, in the reactor RM3, and until the 6th AD cycle, six substrate additions were made, totaling 32 gO₂/L added to the bioreactor, corresponding to 4 times more load than that applied to the batch bioreactor R27. In addition, the amount of spheres was lower in the bioreactor RM3 (15 g/L *versus* 30 g/L). Thus, and considering the first 6 AD cycles, lower amount of spheres had to control the pH in a more demanding environment with a higher total organic load. It was found that, even under these conditions, the spheres were able to maintain the ideal environment for achieving high biogas volumes, similar to those of the R27 reactor, and with a high methane content (81%). The pH was the main indicator of the buffer capacity of the spheres, achieving pH values at the end (7.27) lower than those observed in the batch bioreactor (8.0).

The time of consumption of the substrate by anaerobic microorganisms was also very important. Under batch conditions, the single addition of substrate for a long period (35 days) allowed complete substrate uptake, leaving a sCOD of less than 1.5 gO₂/L in the liquid phase. Regarding the reactor in which the feeding strategy was different (6 consecutive additions of the substrate), there was an increase in the rate of substrate consumption, which allowed, in the 6th AD cycle, the depletion of sCOD after 7 days of operation (approximately the duration of each AD cycle). This enhancement affected directly the global anaerobic biodegradability of the system. In the 6th AD cycle, the anaerobic biodegradability achieved was high (88 %), but considering the first 6 AD cycles, a lower anaerobic biodegradability of 53 % was obtained. This lower value was impaired by the initial adaptation period (1st and 2nd AD cycles) and conditioned by the high amount of total organic load added until the 6th AD cycle (32 gO₂/L).

Considering the results presented, the fed-batch (or even continuous) operation is preferable, since it can treat high amounts of effluents with a high load and, at the same time, achieve a very good methanogenic performance with high organic matter reduction. The red mud-based GS demonstrated its efficiency in buffering the pH in bioreactors with a high organic load.

4.3.3 pH control of the anaerobic digestion process using geopolymer spheres based on fly ash versus based on red mud wastes

The use of GS incorporating wastes from different sources, namely fly ash from biomass combustion and red mud wastes from alumina production, in the AD process to treat cheese whey from a dairy industry, led to differences in the performance of digesters. Figure 92 depicts a comparison of the pH values obtained during the entire incubation time for the most representative bioreactors, that is, the bioreactors that presented the best anaerobic performance in terms of methane production, and with the use of the two types of geopolymeric spheres tested in this work. In Figure 92, the results from the batch bioreactor FA3, with 28 g/L of FA-based GS, the fed-batch bioreactor FA7, with 16 g/L of high porosity FA-based GS, and the fed-batch bioreactor RM2, with 15 g/L of RM-based GS, were included, as well as a gray bar highlighting the suitable pH range for methanogenic activity.

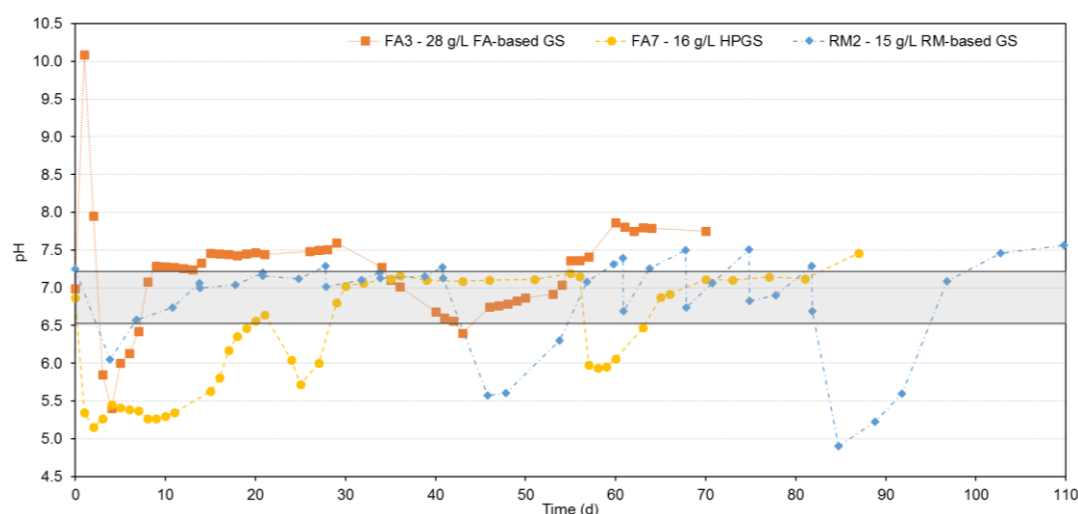


Figure 92 Comparison of pH values over time for assays with FA-based GS addition (FA3 (□) and FA7 (○)) and RM-based GS addition (RM2 (◇)).

All three bioreactors compared here presented very good anaerobic performance regarding methane formation, with methane yields higher than 200 mL_{CH₄}/gO₂ removed. The main monitoring parameter considered in this work (pH), over the entire incubation time, shows that all the solutions presented to replace the addition of chemical compounds to an anaerobic system treating cheese whey under demanding conditions are feasible. The three different types of spheres (FA-based GS, HPGS, and RM-based GS) allowed the continuous pH control, despite the organic shocks applied (high organic load) and the instability imposed on anaerobic systems, combined with an extended incubation time and several substrate additions.

In addition to the good results presented in terms of pH control (buffering capacity) and methane formation, these alkaline materials can contribute to a circular economy approach applied to biological processes. The use of these materials has led to a drastic reduction in chemicals (raw materials) to operate anaerobic systems, replacing the chemical addition to pH control and alkalinity supply. In addition, the incorporation of wastes in the creation of new products, and the valorization of wastes, either in new materials (fly ash and red mud in the geopolymer spheres) or in energy vectors (organic matter of the cheese whey into methane), contribute to increasing the sustainability of waste and wastewater treatment strategies.

Conclusions and perspectives for future

work | 5

5 | Conclusions and perspectives for future work

5.1 Conclusions

This work provided new sustainable solutions for the control of pH in complex anaerobic systems, throughout the recovery of different wastes. To accomplish this purpose, it was studied the valorization of a bleaching effluent from the pulp and paper industry and a by-product of the dairy industry, cheese whey, by anaerobic processes using anaerobic mixed cultures (microorganisms) to promote organic matter reduction and improve the energy (methane) formation. Both streams act as substrates in the AD process and, due to their characteristics, the anaerobic processes must be controlled, mainly in terms of pH. To control the pH, two types of approaches were used, to replace the addition of chemical compounds to the process, reducing costs and the environmental impact of the use of chemical raw materials. Firstly, the use of fly ash (powder) collected from the combustion of residual biomass was studied in the AD of bleaching effluents and cheese whey by-product. Second, the geopolymer spheres were manufactured using waste (fly ash or a mixture of fly ash and red mud waste) and added to the AD process by treating the cheese whey by-product.

Anaerobic biodegradability tests using fly ash (powder) addition to the AD of bleaching effluents from the pulp and paper industry show that the use of this inorganic additive promotes pH control and improves the methane formation when compared to the addition of chemical compounds for pH control. However, this type of effluent has a high concentration of complex adsorbable organic halides (AOX) and has an inhibitory effect on the methanogenic step of AD, when the sCOD concentration is higher than 2.0 gO₂/L. The use of CTB fly ash (from the biomass boiler that burns several types of woods) instead of CA5 fly ash (from the biomass boiler that burns only the Eucalyptus bark) in the AD of the bleaching effluent, led to a boosting in methane production and increased the final aerobic biodegradation of the effluent.

The addition of fly ash (powder) to the AD of cheese whey did not improve the methane formation, because it was insufficient to promote a good buffer performance of the anaerobic system. In these experiments, the use of more than 5 g/L of fly ash inhibited the methane formation due to high pH values, and the use of less than 3 – 4 g/L of fly ash led to the VFA accumulation and consequent inhibition of methanogenic microorganisms, due to the acidic conditions of the medium (low pH values). This highly biodegradable substrate requires a buffer material that promotes a prolonged alkalis release and, for this reason, geopolymer spheres were manufactured and tested in succeeding assays.

The geopolymer spheres were manufactured with fly ash wastes with a composition similar to those used in the tests with powder fly ash, described previously. The replacement of metakaolin (source of aluminosilicates) by fly ash in the geopolymers manufacture was studied, considering the influence of both types of spheres (FA-based and MK-based geopolymer spheres) in the AD treatment process of cheese whey. Of the batch operated *oxitop* bioreactors, the replacement of 75 % metakaolin (FA-based spheres) by fly ash in the geopolymer spheres composition led to an improvement in the methane volume formed and to a pH control within the range of values that favors the methanogenesis (6.5 to 7.2), comparing its performance with MK-based spheres (replacement of 33 % of metakaolin by fly ash).

On a larger scale, and considering the results of batch *oxitop* bioreactors, two different amounts of FA-based spheres were tested in order to understand the role of spheres concentration in the performance of cheese whey AD. This inorganic buffer material efficiency is highly dependent on the added concentration and the best performance results were obtained when a higher spheres amount was added (bioreactor FA3 with 27 g/L of FA-based geopolymer spheres). Using a higher number of spheres to control the pH in the batch anaerobic bioreactor treating cheese whey, an improvement in methane volume of 30 % and a boost in methane yield of 23 % were obtained. In addition, the increase in the spheres concentration added led to an improvement in methanogenic activity, since the methanogens converted a higher percentage of initial organic matter into methane (high methanization degree). These bioreactors presented a clear methanogenic behavior, with high methane production and low acidification at the end of the experiments. For this reason, it has been proven that the use of FA-based geopolymer spheres, in addition to the economic and eco-friendly approach, promotes an increase in the produced methane volume, thus improving the process of cheese whey valorization. The cost comparison between the manufacture of FA-based GS and the commercial buffer supplementation showed that the proposed methodology is cost-effective, which simplifies its possible industrial application.

In terms of the characteristics of the spheres, it is known that their porosity influences the leaching behavior of the hydroxide ions on the surface and inside the spheres. To study the influence of different porosity of the spheres in an anaerobic digester, a set of batch *oxitop* bioreactors was performed, studying different compositions and concentrations of spheres added. The increase in the number of spheres added led to higher final pH values, as expected. Besides that, the addition of LPGS reached pH values generally higher than the addition of HPGS, and this behavior may be due to the slower release of alkalis from this type of geopolymer spheres. From these tests, the concentrations and formulations applied in the subsequent fed-batch bioreactors were defined considering the results obtained.

Thus, 12 and 16 g/L of low porosity spheres (LPGS) and 16 g/L of high porosity spheres (HPGS) were tested in two-cycle anaerobic tests (with two substrate additions). Both LPGS and HPGS presented good pH control throughout the incubation time and high overall organic matter removal. The use of HPGS instead of LPGS represented an increment of 103 % in the methane volume and 87 % in the anaerobic biodegradability of the treatment system. The HPGS promoted a slower release of alkalis and, in both AD cycles, the methane yield obtained from the removed sCOD was improved compared to the LPGS addition (240 % higher in the 1st AD cycle and 8 % higher in the 2nd AD cycle). In addition, the modified Gompertz model was developed for these assays to predict the methane production potential and the duration of the lag phase and the models developed were adequate to obtain the kinetic constants and describe the methane volume produced, with correlation coefficients higher than 0.972 for both assays with 16 g/L of spheres (HPGS and LPGS).

In order to study a prolonged operation of an anaerobic digester treating cheese whey and using HPGS as an inorganic additive to control pH, bioreactors FA9 and FA10 were operated; for comparison, a reference bioreactor (FA8) was also operated, testing the addition of chemical alkaline compounds as buffer materials. The same conditions of the previous bioreactors were applied, that is, the addition of 16 g/L of HPGS to the fed-batch bioreactors, increasing the number of substrate additions to four. From these bioreactors, the anaerobic performance was lower than that obtained in the previous assays described, and these differences may be related to the higher organic load

applied in the assays FA8, FA9, and FA10. Compared with the reference test performed, although lower than the previous one, the bioreactor to which HPGS was added presented an 8 % higher methane yield from the sCOD removed and a 25 % higher methane volume produced.

From the assays using geopolymer spheres that incorporate fly ash in its composition, it can be concluded that the addition of HPGS promoted a better anaerobic performance than the other spheres tested. The addition of 16 g/L of HPGS, in addition to improving the methane volume formed, also increased the methane yield of the sCOD removed and the anaerobic biodegradability of the substrate. In the tested anaerobic systems treating cheese whey, the use of FA-based spheres achieved better results when a mesophilic 2-cycle fed-batch bioreactor was operated.

The incorporation of alkaline wastes to replace metakaolin in the geopolymer spheres manufacture was also studied, using red mud wastes. These wastes were used in RM-based GS and two types of bioreactors were operated: batch *oxitop* bioreactors and fed-batch bioreactors. The batch *oxitop* bioreactors were performed to choose the suitable conditions to be applied in the fed-batch bioreactors, as performed in assays with the FA-based GS addition.

In batch *oxitop* bioreactors, different RMGS concentrations were tested. The increase in the spheres concentration led to slightly increased final pH values, as expected. Regarding the anaerobic performance parameters, all conditions tested presented a clear methanogenic behavior, with high sCOD removals, high methane volume, high methane yield, and high anaerobic biodegradability. The use of a similar RMGS concentration than in previous assays with FA-based spheres also led to increased pH values (≈ 8). For this reason, and to minimize the amount of spheres to be added, for the fed-batch bioreactors, a slightly lower amount of spheres was used: 15 g/L of RMGS *versus* 16 g/L of HPGS *versus* 27 g/L of FA-based spheres.

The fed-batch bioreactors using RMGS were operated for a long period, performing eleven AD cycles, with different amounts of organic matter additions, performed according to the response of the system and with the increase of the added organic load. These differences in the operation mode were performed to destabilize the anaerobic system and demonstrate the robustness of using RMGS as alkaline materials to control the pH in the AD process treating cheese whey, against the use of chemical compounds as buffer material. For comparison, a blank fed-batch bioreactor without alkalinity addition or RMGS (RM1) and a reference fed-batch bioreactor with chemical alkalinity addition (RM2) were also performed under the same operating conditions.

Although the test bioreactor, with the RMGS addition (RM3), and the reference bioreactor presented similar anaerobic performance during the first six AD cycles, the RM3 bioreactor stood out and improved its performance compared to the bioreactor RM2 after the 8th AD cycle. The 7th AD cycle covered a period of instability and, due to the accumulation of organic matter (in the form of volatile fatty acids), the systems took almost three weeks to recover and restart to degrade the organic matter and convert it into methane. From this cycle until the end of the experiment, the test bioreactor presented better anaerobic performance than the reference bioreactor. At the end of the experiment, the bioreactor RM3 presented much better performance than the bioreactor RM2 in terms of organic matter removal (75 % *versus* 10 %), methanization degree (37 % *versus* 2 %), methane yield (94 *versus* 18 mL_{CH₄}/gO₂ removed) and anaerobic biodegradability (120 % higher), presenting a typical methanogenic behavior. The RM2 bioreactor presented an acidogenic behavior, with low-performance parameters and a high degree of acidification (45 % *versus* 17 % of RM3) and a VFA final concentration (13.9 gO₂/L).

This research work contributes to narrow the knowledge gap regarding the use of geopolymeric spheres as a buffer material in an anaerobic digestion process. It has been shown that this innovative approach can increase the process efficiency, mainly in terms of methane production, since the geopolymer spheres can release suitable alkali metals that improve digestion stability and performance. At the same time, due to its simplicity, the addition of geopolymer spheres to an anaerobic digestion process prevents the continuous need for alkalinity supply to adjust the pH, as often occurs in full-scale anaerobic digesters, thus reducing the process complexity. In addition, after being used in anaerobic processes with subsequent loss of pH control potential, the geopolymer spheres can be easily collected and reused in other applications, such as heavy metal adsorbents, which will increase the process sustainability (waste incorporation in geopolymers production and spheres reuse after exhaustion).

In conclusion, some alternatives were presented regarding the operation mode and the materials to be used in the control of anaerobic digestion processes. The wastes recovered and used in an anaerobic valorization process led to a shift in the waste treatment paradigm and contributed to the concept of the circular economy. This approach led to the creation of value from waste (bleaching effluent from the pulp and paper industry, cheese whey from the dairy industry, fly ash from biomass combustion, and red mud waste from alumina production), designing new added-value products (geopolymer spheres), and create energy (methane) by applying a natural biological system (anaerobic digestion). In addition, the proposed innovative strategy (use of geopolymer spheres to control pH in anaerobic systems) has environmental and performance advantages over the commercial use of powdered alkaline chemicals, produced from virgin raw materials.

This work was the basis of the publication in the form of three scientific articles (two of them published, one in 2018 and another in 2020, and a third article currently under review for publication). Two articles were also prepared for oral presentation at two international scientific conferences (one in Portugal, 2018, and another in France, 2019). Detailed information can be found at the beginning of each correspondent section in Chapter 4: Results and Discussion.

5.2 Perspectives for future work

Considering the work presented, some suggestions for future work are proposed:

- Test the continuous operation of anaerobic bioreactors

To operate a continuously fed stirred bioreactor to treat cheese whey by applying geopolymer spheres (FA-based GS or RM-based GS) as a pH buffer material, two approaches can be used, in terms of the GS location in the system setup. An alternative is to add the spheres to the bioreactor itself and another alternative is to add them to the feed stream. If the spheres are added to the bioreactor, they must be immobilized to allow the continuous leaching, without compromising the integrity of the spheres, due to the continuous stirring in this type of bioreactor. If the spheres are added to the feed stream, they will not come into contact with anaerobic microorganisms and the leachate compounds (alkalis and possibly some trace metals) enter the bioreactor within the substrate stream. The replacement of spheres in the feed stream, after a certain period or after exhaustion, can be evaluated according to the process conditions to be implemented.

- Evaluate the stability of the spheres in extreme environments

The durability of the spheres inside the anaerobic digesters can be evaluated under extreme environmental conditions, such as low pH, high temperature, high saline conditions, or the presence of potentially toxic compounds. The use of different substrates with complex characteristics can also demonstrate the effectiveness of the spheres and open the possibility of expanding this technical solution to treat a wide variety of effluents from the food or other high polluting industries. After use in anaerobic processes, the spheres can be recovered and reused in other applications, which may or may not include an additional biological anaerobic process. A wide variety of applications can be explored since these geopolymeric materials have a porous surface, which can be suitable for removing pollutants or nutrients by adsorption. These materials can also be used as photocatalysts, in the degradation of organic compounds with the application of UV radiation. In biological fixed-film bioreactors, geopolymer spheres can be used as a carrier medium, as leaching properties are not required in this type of bioprocesses. These approaches contribute to zero-waste generation processes, increasing their sustainability.

- Development of analytic methods suitable for a deeper understanding of the anaerobic systems with the addition of GS

The development of specific analytic methods appropriate for a deeper characterization of anaerobic processes in which GS is used as a buffer material can be an asset, helping to understand the evolution and behavior of anaerobic bioreactors that treat complex effluents. Furthermore, as the use of GS as buffer material in AD processes leads to the leaching of ions, metals, and organic compounds during the process, it would be interesting to identify and study the evolution of the content of such compounds in the liquid medium, which can directly or indirectly influence the AD process. Thus, analytical chemistry techniques can be very useful

in the optimization of complex biological processes and be highly important for a full-scale implementation of the anaerobic treatment process.

- Evaluate the microorganisms-buffer materials interaction

The interaction between microorganisms and buffer materials such as geopolymer spheres is unknown under anaerobic conditions. Thus, the study of the influence of microorganisms on the structure of the spheres and vice versa is very important to establish the interaction between the two components of an anaerobic system and to predict the performance of the system, as well as the need for GS supplementation during the process. For the characterization of specific groups of microorganisms, such as acidogens or methanogens, some molecular biology techniques can be used such as Fluorescence *in Situ* Hybridization (FISH) and Denaturing Gradient Gel Electrophoresis (DGGE). The deep characterization of the spheres can be performed, as well as the evaluation of the leaching profile before and after the AD process, namely the characterization of the leached compounds from the spheres and the characterization of the biofilms formed on the surface and pores of the spheres and how they affect the spheres' structures.

- Explore the potential of organic wastes to obtain added-value products, such as volatile fatty acids

An alternative to the valorization of complex organic waste into an energy vector (methane) is its valorization in added-value materials, such as VFA. The production of organic acids during the anaerobic digestion process is natural and, if the conditions are advantageous regarding the pH range, the accumulation of acids is enhanced, and they can be recovered and used in a wide range of applications. To channel the anaerobic digestion process to favor the acidogenic phase and avoid the methanogenic phase, appropriate quantities of spheres, different spheres' compositions, or different bioreactor operation modes can be tested. With this approach, the main challenge is to prevent the conversion of VFA into methane by methanogenic microorganisms, and to avoid the inhibition of acidogenic microorganisms due to high volatile fatty acids concentrations in the liquid phase, keeping the pH values in an acidic range (between 5 and 6, approximately).

References | 6

6 | References

- Abdullah, H.H., Shahin, M.A., Walske, M.L., 2020. Review of fly-ash-based geopolymers for soil stabilisation with special reference to clay. *Geosciences* 10, 249. <https://doi.org/10.3390/geosciences10070249>
- Achinas, S., Euverink, G.J.W., 2016. Theoretical analysis of biogas potential prediction from agricultural waste. *Resour. Technol.* 2, 143–147. <https://doi.org/10.1016/j.reffit.2016.08.001>
- Adelekan, B.A., 2012. Potentials of selected tropical crops and manure as sources of biofuels, in: Kumar, S. (Ed.), *Biogas*. InTech, Rijeka, Croatia, pp. 1–34.
- Adewunmi, A.A., Kamal, M.S., 2020. Evaluation of alkaline treated fly ash as a demulsifier for crude oil emulsions, in: *International Petroleum Technology Conference*. International Petroleum Technology Conference. <https://doi.org/10.2523/IPTC-20244-Abstract>
- Agência Portuguesa do Ambiente, 2020. Website of Agência Portuguesa do Ambiente [WWW Document]. URL <https://apambiente.pt/index.php> (accessed 3.4.20).
- Águas do Centro Litoral, 2019. Website of Águas do Centro Litoral [WWW Document]. URL <http://www.aguasdocentrolitoral.pt> (accessed 11.30.19).
- Ahammad, S.Z., Sreekrishnan, T.R., 2016. Biogas: An evolutionary perspective in the indian context, in: Soccol, C.R., Brar, S.K., Faulds, C., Ramos, L.P. (Eds.), *Green Fuels Technology*. Springer Switzerland, Switzerland, pp. 431–443. https://doi.org/10.1007/978-3-319-30205-8_17
- Ahmad, A., 2014. A novel application of red mud-iron on granulation and treatment of palm oil mill effluent using upflow anaerobic sludge blanket reactor. *Environ. Technol.* 35, 2718–2726. <https://doi.org/10.1080/09593330.2014.919034>
- Ahn, J.W., Thriveni, T., Nam, S.Y., 2015. Sustainable recycling technologies for bauxite residue (Red Mud) utilization, in: *Energy Technology 2015*. Springer International Publishing, Cham, pp. 173–179. https://doi.org/10.1007/978-3-319-48220-0_19
- Ahring, B.K., 1995. Methanogenesis in thermophilic biogas reactors. *Antonie Van Leeuwenhoek* 67, 91–102. <https://doi.org/10.1007/BF00872197>
- Ahring, B.K., Sandberg, M., Angelidaki, I., 1995. Volatile fatty acids as indicators of process imbalance in anaerobic digestors. *Appl. Microbiol. Biotechnol.* 43, 559–565. <https://doi.org/10.1007/BF00218466>
- Ajay, C.M., Mohan, S., Dinesha, P., Rosen, M.A., 2020. Review of impact of nanoparticle additives on anaerobic digestion and methane generation. *Fuel* 277, 118234. <https://doi.org/10.1016/j.fuel.2020.118234>
- Akal, C., Turkmen, N., Özer, B., 2019. Technology of dairy-based beverages, in: Grumezescu, A.M., Holban, A.M. (Eds.), *Milk-Based Beverages*, Volume 9. Elsevier, pp. 331–372. <https://doi.org/10.1016/B978-0-12-815504-2.00010-4>
- Akiba, Y., Said, H., Kaunitz, J.D., 2018. Luminal chemosensing and mucosal defenses in the upper gastrointestinal tract, in: *Physiology of the Gastrointestinal Tract*. Elsevier, pp. 709–719. <https://doi.org/10.1016/B978-0-12-809954-4.00030-X>
- Alganesh, T.G., Yetenayet, B.T., 2017. Traditional butter and ghee production, processing and handling in Ethiopia: A review. *African J. Food Sci.* 11, 95–105. <https://doi.org/10.5897/AJFS2016.1544>
- Ali, M., Sreekrishnan, T., 2000. Anaerobic treatment of agricultural residue based pulp and paper mill effluents for AOX and COD reduction. *Process Biochem.* 36, 25–29. [https://doi.org/10.1016/S0032-9592\(00\)00167-9](https://doi.org/10.1016/S0032-9592(00)00167-9)
- Alkaya, E., Demirer, G.N., 2011. Anaerobic acidification of sugar-beet processing wastes: Effect of operational parameters. *Biomass and Bioenergy* 35, 32–39. <https://doi.org/10.1016/j.biombioe.2010.08.002>
- Alvarez, V.B., 2008. Fluid milk and cream products, in: Clark, S., Costello, M., Drake, M., Bodyfelt, F. (Eds.), *The Sensory Evaluation of Dairy Products*. Springer US, New York, NY, pp. 73–133. https://doi.org/10.1007/978-0-387-77408-4_5
- Amritphale, S.S., Anshul, A., Chandra, N., Ramakrishnan, N., 2007. A novel process for making radiopaque materials using bauxite—Red mud. *J. Eur. Ceram. Soc.* 27, 1945–1951. <https://doi.org/10.1016/j.jeurceramsoc.2006.05.106>
- Anderson, K., Sallis, P., Uyanik, S., 2003. Anaerobic treatment processes, in: *Handbook of Water and Wastewater Microbiology*. Elsevier, pp. 391–426. <https://doi.org/10.1016/B978-012470100-7/50025-X>
- Antonopoulou, G., Stamatelatos, K., Venetsaneas, N., Kornaros, M., Lyberatos, G., 2008. Biohydrogen and methane production from cheese whey in a two-stage anaerobic process. *Ind. Eng. Chem. Res.* 47, 5227–5233. <https://doi.org/10.1021/ie071622x>
- APHA, A.P.H.A., AWWA, A.W.W.A., WEF, W.E.F., 2017. *Standard methods for the examination of water and wastewater*, 23rd ed. American Public Health Association. Washington, D.C. USA.
- Appels, L., Baeyens, J., Degreève, J., Dewil, R., 2008. Principles and potential of the anaerobic digestion of

- waste-activated sludge. *Prog. Energy Combust. Sci.* 34, 755–781. <https://doi.org/10.1016/j.pecs.2008.06.002>
- Ariunbaatar, J., Panico, A., Esposito, G., Pirozzi, F., Lens, P.N.L., 2014. Pretreatment methods to enhance anaerobic digestion of organic solid waste. *Appl. Energy* 123, 143–156. <https://doi.org/10.1016/j.apenergy.2014.02.035>
- Aryana, K.J., Olson, D.W., 2017. A 100-Year Review: Yogurt and other cultured dairy products. *J. Dairy Sci.* 100, 9987–10013. <https://doi.org/10.3168/jds.2017-12981>
- Ashrafi, O., Yerushalmi, L., Haghighat, F., 2015. Wastewater treatment in the pulp and paper industry: A review of treatment processes and the associated greenhouse gas emission. *J. Environ. Manage.* 158, 146–157. <https://doi.org/10.1016/j.jenvman.2015.05.010>
- Augusto, L., Bakker, M.R., Meredieu, C., 2008. Wood ash applications to temperate forest ecosystems - potential benefits and drawbacks. *Plant Soil* 306, 181–198. <https://doi.org/10.1007/s11104-008-9570-z>
- Aydin, S., 2017. Anaerobic Digestion, in: Singh, L., Kalia, V. (Eds.), *Waste Biomass Management – A Holistic Approach*. Springer International Publishing, Cham, pp. 1–14. https://doi.org/10.1007/978-3-319-49595-8_1
- Bachmann, R.T., Johnson, A.C., Hernandez, J.E., 2008. Biogas production from cheese whey: past, present and future, in: Cerdán, M.E., González-Siso, M.I., Becerra, M. (Eds.), *Advances in Cheese Whey Utilization*. Transworld Research Network, Kerala, India, pp. 35–80.
- Bajpai, P., 2017. *Anaerobic technology in pulp and paper industry*, 1st ed, SpringerBriefs in Applied Sciences and Technology. Springer Singapore, Singapore. <https://doi.org/10.1007/978-981-10-4130-3>
- Bajpai, P., 2015. *Management of pulp and paper mill waste*. Springer International Publishing, Cham. <https://doi.org/10.1007/978-3-319-11788-1>
- Bajpai, P., 2012. *Biological treatment of pulp and paper mill effluents*, in: *Biotechnology for Pulp and Paper Processing*. Springer US, Boston, MA, pp. 211–261. https://doi.org/10.1007/978-1-4614-1409-4_13
- Bajpai, P., Bajpai, P.K., 1997. Reduction of organochlorine compounds in bleach plant effluents, in: Eriksson, K.E. (Ed.), *Biotechnology in the Pulp and Paper Industry*. Advances in Biochemical Engineering/Biotechnology. Springer Berlin, Berlin, pp. 213–259. <https://doi.org/10.1007/BFb0102076>
- Banks, C.J., Lo, H.-M., 2003. Assessing the effects of municipal solid waste incinerator bottom ash on the decomposition of biodegradable waste using a completely mixed anaerobic reactor. *Waste Manag. Res.* 21, 225–234. <https://doi.org/10.1177/0734242X0302100306>
- Baumann, U., Müller, M.T., 1997. Determination of anaerobic biodegradability with a simple continuous fixed-bed reactor. *Water Res.* 31, 1513–1517. [https://doi.org/10.1016/S0043-1354\(96\)00406-X](https://doi.org/10.1016/S0043-1354(96)00406-X)
- Berhe, S., Leta, S., 2019. Anaerobic co-digestion of tannery wastes using two stage anaerobic sequencing batch reactor: focus on process performance of hydrolytic–acidogenic step. *J. Mater. Cycles Waste Manag.* 21, 666–677. <https://doi.org/10.1007/s10163-019-00837-1>
- Bhatnagar, A., Vilar, V.J.P., Botelho, C.M.S., Boaventura, R.A.R., 2011. A review of the use of red mud as adsorbent for the removal of toxic pollutants from water and wastewater. *Environ. Technol.* 32, 231–249. <https://doi.org/10.1080/09593330.2011.560615>
- Bórawski, P., Pawlewicz, A., Parzonko, A., Harper, Jayson, K., Holden, L., 2020. Factors shaping cow's milk production in the EU. *Sustainability* 12, 420. <https://doi.org/10.3390/su12010420>
- Botheju, D., 2011. Oxygen effects in anaerobic digestion – A review. *Open Waste Manag. J.* 4, 1–19. <https://doi.org/10.2174/1876400201104010001>
- Bougrier, C., Dognin, D., Laroche, C., Cacho Rivero, J.A., 2018. Use of trace elements addition for anaerobic digestion of brewer's spent grains. *J. Environ. Manage.* 223, 101–107. <https://doi.org/10.1016/j.jenvman.2018.06.014>
- Bowles, J.T.B., 1911. Treatment of creamery sewage by the septic tank process. *J. Ind. Eng. Chem.* 3, 400–403. <https://doi.org/10.1021/ie50030a011>
- Bożym, M., Florczak, I., Zdanowska, P., Wojdalski, J., Klimkiewicz, M., 2015. An analysis of metal concentrations in food wastes for biogas production. *Renew. Energy* 77, 467–472. <https://doi.org/10.1016/j.renene.2014.11.010>
- Bray, E.L., 2020. *Bauxite and Alumina*, in: *Mineral Commodity Summaries*. U.S. Geological Survey.
- Brunori, C., Cremisini, C., Massanisso, P., Pinto, V., Torricelli, L., 2005. Reuse of a treated red mud bauxite waste: studies on environmental compatibility. *J. Hazard. Mater.* 117, 55–63. <https://doi.org/10.1016/j.jhazmat.2004.09.010>
- Bruss, M.L., 2008. Lipids and Ketones, in: *Clinical Biochemistry of Domestic Animals*. Elsevier, pp. 81–115. <https://doi.org/10.1016/B978-0-12-370491-7.00004-0>
- Bumanis, G., Bajare, D., 2014. The Effect of Porous Alkali Activated Material Composition on Buffer Capacity in Bioreactors. *Int. J. Chem. Nucl. Metall. Mater. Eng.* 8, 1040–1046.

- Buruberri, L.H., Seabra, M.P., Labrincha, J.A., 2015. Preparation of clinker from paper pulp industry wastes. *J. Hazard. Mater.* 286, 252–260. <https://doi.org/10.1016/j.jhazmat.2014.12.053>
- Buswell, A.M., Boruff, C.S., Wiesman, C.K., 1932. Anaerobic Stabilization of Milk Waste. *Ind. Eng. Chem.* 24, 1423–1425. <https://doi.org/10.1021/ie50276a019>
- Buswell, A.M., Hatfield, W.D., 1936. Bulletin no. 32: Anaerobic Fermentations. Springfield, Illinois.
- Buswell, A.M., Neave, S.L., 1930. Bulletin no. 30: Laboratory studies of sludge digestion. Springfield, Illinois.
- Cabrera, M.N., 2017. Pulp mill wastewater: Characteristics and treatment, in: *Biological Wastewater Treatment and Resource Recovery*. InTech. <https://doi.org/10.5772/67537>
- Carreira, P., Mendes, J.A.S., Trovatti, E., Serafim, L.S., Freire, C.S.R., Silvestre, A.J.D., Neto, C.P., 2011. Utilization of residues from agro-forest industries in the production of high value bacterial cellulose. *Bioresour. Technol.* 102, 7354–7360. <https://doi.org/10.1016/j.biortech.2011.04.081>
- Carvalho, F., Prazeres, A.R., Rivas, J., 2013. Cheese whey wastewater: Characterization and treatment. *Sci. Total Environ.* 445–446, 385–396. <https://doi.org/10.1016/j.scitotenv.2012.12.038>
- Castro, L., Escalante, H., Jaimes-Estévez, J., Díaz, L.J., Vecino, K., Rojas, G., Mantilla, L., 2017. Low cost digester monitoring under realistic conditions: Rural use of biogas and digestate quality. *Bioresour. Technol.* 239, 311–317. <https://doi.org/10.1016/j.biortech.2017.05.035>
- Casu, S., Crispino, N.A., Farina, R., Mattioli, D., Ferraris, M., Spagni, A., 2012. Wastewater treatment in a submerged anaerobic membrane bioreactor. *J. Environ. Sci. Heal. Part A* 47, 204–209. <https://doi.org/10.1080/10934529.2012.640562>
- Catalkaya, E.C., Kargi, F., 2007. Color, TOC and AOX removals from pulp mill effluent by advanced oxidation processes: A comparative study. *J. Hazard. Mater.* 139, 244–253. <https://doi.org/10.1016/j.jhazmat.2006.06.023>
- CELPA, 2018. Boletim Estatístico - Indústria papeleira portuguesa. Lisboa.
- Cengeloglu, Y., Kir, E., Ersoz, M., Buyukerkek, T., Gezgin, S., 2003. Recovery and concentration of metals from red mud by Donnan dialysis. *Colloids Surfaces A Physicochem. Eng. Asp.* 223, 95–101. [https://doi.org/10.1016/S0927-7757\(03\)00198-5](https://doi.org/10.1016/S0927-7757(03)00198-5)
- CEPI, 2019. Key Statistics 2018: European Pulp & Paper Industry. Brussels.
- Chaparro, T.R., Pires, E.C., 2011. Anaerobic treatment of cellulose bleach plant wastewater: chlorinated organics and genotoxicity removal. *Brazilian J. Chem. Eng.* 28, 625–638. <https://doi.org/10.1590/S0104-66322011000400008>
- Charalambous, P., Shin, J., Shin, S.G., Vyrides, I., 2020. Anaerobic digestion of industrial dairy wastewater and cheese whey: Performance of internal circulation bioreactor and laboratory batch test at pH 5-6. *Renew. Energy* 147, 1–10. <https://doi.org/10.1016/j.renene.2019.08.091>
- Chatzipaschali, A.A., Stamatis, A.G., 2012. Biotechnological utilization with a focus on anaerobic treatment of cheese whey: Current status and prospects. *Energies* 5, 3492–3525. <https://doi.org/10.3390/en5093492>
- Chen, J.L., Ortiz, R., Steele, T.W.J., Stuckey, D.C., 2014. Toxicants inhibiting anaerobic digestion: A review. *Biotechnol. Adv.* 32, 1523–1534. <https://doi.org/10.1016/j.biotechadv.2014.10.005>
- Chen, S., Rotaru, A.-E., Shrestha, P.M., Malvankar, N.S., Liu, F., Fan, W., Nevin, K.P., Lovley, D.R., 2015. Promoting interspecies electron transfer with biochar. *Sci. Rep.* 4, 5019. <https://doi.org/10.1038/srep05019>
- Chen, T.-H., Shyu, W.-H., 1996. Performance of four types of anaerobic reactors in treating very dilute dairy wastewater. *Biomass and Bioenergy* 11, 431–440. [https://doi.org/10.1016/S0961-9534\(96\)00038-4](https://doi.org/10.1016/S0961-9534(96)00038-4)
- Chen, X., Hu, Y., 2015. Anaerobic degradation of polyethylene glycol 400, in: *Proceedings of the 2015 6th International Conference on Manufacturing Science and Engineering*. Atlantis Press, Paris, France. <https://doi.org/10.2991/icmse-15.2015.352>
- Chen, Y., Cheng, J.J., Creamer, K.S., 2008. Inhibition of anaerobic digestion process: A review. *Bioresour. Technol.* 99, 4044–4064. <https://doi.org/10.1016/j.biortech.2007.01.057>
- Chen, Y., He, H., Liu, H., Li, H., Zeng, G., Xia, X., Yang, C., 2018. Effect of salinity on removal performance and activated sludge characteristics in sequencing batch reactors. *Bioresour. Technol.* 249, 890–899. <https://doi.org/10.1016/j.biortech.2017.10.092>
- Chen, Y., Zhan, H., Chen, Z., Fu, S., 2003. Study on the treatment of the sulfite pulp CEH bleaching effluents with the coagulation-anaerobic acidification-aeration package reactor. *Water Res.* 37, 2106–2112. [https://doi.org/10.1016/S0043-1354\(02\)00599-7](https://doi.org/10.1016/S0043-1354(02)00599-7)
- Cherian, C., Siddiqua, S., 2019. Pulp and paper mill fly ash: A review. *Sustainability* 11, 4394. <https://doi.org/10.3390/su11164394>
- Chernicharo, C.A. de L., 2007. *Anaerobic reactors, Biological Wastewater Treatment Series*. IWA Publishing. <https://doi.org/10.2166/9781780402116>

- Chiappero, M., Norouzi, O., Hu, M., Demichelis, F., Berruti, F., Di Maria, F., Mašek, O., Fiore, S., 2020. Review of biochar role as additive in anaerobic digestion processes. *Renew. Sustain. Energy Rev.* 131, 110037. <https://doi.org/10.1016/j.rser.2020.110037>
- Chvedov, D., Ostap, S., Le, T., 2001. Surface properties of red mud particles from potentiometric titration. *Colloids Surfaces A Physicochem. Eng. Asp.* 182, 131–141. [https://doi.org/10.1016/S0927-7757\(00\)00814-1](https://doi.org/10.1016/S0927-7757(00)00814-1)
- Clay, N., Garnett, T., Lorimer, J., 2020. Dairy intensification: Drivers, impacts and alternatives. *Ambio* 49, 35–48. <https://doi.org/10.1007/s13280-019-01177-y>
- Dai, X., Hu, C., Zhang, D., Dai, L., Duan, N., 2017. Impact of a high ammonia-ammonium-pH system on methane-producing archaea and sulfate-reducing bacteria in mesophilic anaerobic digestion. *Bioresour. Technol.* 245, 598–605. <https://doi.org/10.1016/j.biortech.2017.08.208>
- Das, M., Raychaudhuri, A., Ghosh, S.K., 2016. Supply chain of bioethanol production from whey: A review. *Procedia Environ. Sci.* 35, 833–846. <https://doi.org/10.1016/j.proenv.2016.07.100>
- Davidovits, J., 1988. Geopolymers of the first generation: SILIFACE-Process. *Geopolymer* 88, 49–67.
- Dawczyński, S., Górski, M., Krzywoń, R., 2016. Geopolymers as an alternative ecological material for buildings, in: 14th International Conference on New Trends in Statics and Dynamics of Buildings. Faculty of Civil Engineering STU Bratislava, Bratislava, Slovakia.
- del Valle-Zermeño, R., Formosa, J., Prieto, M., Nadal, R., Niubó, M., Chimenos, J.M., 2014. Pilot-scale road subbase made with granular material formulated with MSWI bottom ash and stabilized APC fly ash: Environmental impact assessment. *J. Hazard. Mater.* 266, 132–140. <https://doi.org/10.1016/j.jhazmat.2013.12.020>
- Demirel, B., Yenigün, O., 2002. Two-phase anaerobic digestion processes: a review. *J. Chem. Technol. Biotechnol.* 77, 743–755. <https://doi.org/10.1002/jctb.630>
- Demirel, B., Yenigun, O., Onay, T.T., 2005. Anaerobic treatment of dairy wastewaters: a review. *Process Biochem.* 40, 2583–2595. <https://doi.org/10.1016/j.procbio.2004.12.015>
- Dereli, R.K., van der Zee, F.P., Ozturk, I., van Lier, J.B., 2019. Treatment of cheese whey by a cross-flow anaerobic membrane bioreactor: Biological and filtration performance. *Environ. Res.* 168, 109–117. <https://doi.org/10.1016/j.envres.2018.09.021>
- Deshmukh, N.S., Lapsiya, K.L., Savant, D.V., Chiplonkar, S.A., Yeole, T.Y., Dhakephalkar, P.K., Ranade, D.R., 2009. Upflow anaerobic filter for the degradation of adsorbable organic halides (AOX) from bleach composite wastewater of pulp and paper industry. *Chemosphere* 75, 1179–1185. <https://doi.org/10.1016/j.chemosphere.2009.02.042>
- Diamantis, V.I., Kapagiannidis, A.G., Ntougias, S., Tataki, V., Melidis, P., Aivasidis, A., 2014. Two-stage CSTR–UASB digestion enables superior and alkali addition-free cheese whey treatment. *Biochem. Eng. J.* 84, 45–52. <https://doi.org/10.1016/j.bej.2014.01.001>
- Donoghue, A.M., Frisch, N., Olney, D., 2014. Bauxite mining and alumina refining. *J. Occup. Environ. Med.* 56, S12–S17. <https://doi.org/10.1097/JOM.0000000000000001>
- Dorica, J.G., Sullivan, J., Douek, M., Hill, D.A., Milosevich, G.M., Morgan, J.P., 1992. Removal of AOX from bleach plant mill effluents by pH shift using the alkalinity/acidity sources available at the mill. Patent no. WO9205118 (A1).
- Dosta, J., Martin-Ryals, A., Garrigó, M., Ortiz-Roca, V., Fernández, I., Torres-Castillo, R., Mata-Álvarez, J., 2018. Acidogenic fermentation and anaerobic co-digestion of mechanically sorted OFMSW and polyethylene glycol. *Waste and Biomass Valorization* 9, 2319–2326. <https://doi.org/10.1007/s12649-018-0294-x>
- Dragone, G., Mussatto, S.I., Almeida e Silva, J.B., Teixeira, J.A., 2011. Optimal fermentation conditions for maximizing the ethanol production by *Kluyveromyces fragilis* from cheese whey powder. *Biomass and Bioenergy* 35, 1977–1982. <https://doi.org/10.1016/j.biombioe.2011.01.045>
- Dragone, G., Mussatto, S.I., Oliveira, J.M., Teixeira, J.A., 2009. Characterisation of volatile compounds in an alcoholic beverage produced by whey fermentation. *Food Chem.* 112, 929–935. <https://doi.org/10.1016/j.foodchem.2008.07.005>
- Duan, J., Gregory, J., 2003. Coagulation by hydrolysing metal salts. *Adv. Colloid Interface Sci.* 100–102, 475–502. [https://doi.org/10.1016/S0001-8686\(02\)00067-2](https://doi.org/10.1016/S0001-8686(02)00067-2)
- Dullius, A., Goettert, M.I., de Souza, C.F.V., 2018. Whey protein hydrolysates as a source of bioactive peptides for functional foods – Biotechnological facilitation of industrial scale-up. *J. Funct. Foods* 42, 58–74. <https://doi.org/10.1016/j.jff.2017.12.063>
- El-Hadj, T.B., Dosta, J., Torres, R., Mata-Álvarez, J., 2007. PCB and AOX removal in mesophilic and thermophilic sewage sludge digestion. *Biochem. Eng. J.* 36, 281–287. <https://doi.org/10.1016/j.bej.2007.03.001>

- El-Haggar, S., Samaha, A., 2019. Sustainable rural community, in: El-Haggar, S., Samaha, A. (Eds.), *Roadmap for Global Sustainability — Rise of the Green Communities*, Advances in Science, Technology & Innovation. Springer International Publishing, Switzerland, p. 112. <https://doi.org/10.1007/978-3-030-14584-2>
- El-Mamouni, R., Guiot, S.R., Mercier, P., Safi, B., Samson, R., 1995. Liming impact on granules activity of the multiplate anaerobic reactor (MPAR) treating whey permeate. *Bioprocess Eng.* 12, 47–53. <https://doi.org/10.1007/BF01112993>
- El-Tanboly, E., 2017. Recovery of cheese whey, a by-product from the dairy industry for use as an animal feed. *J. Nutr. Heal. Food Eng.* 6, 148–154. <https://doi.org/10.15406/jnhfe.2017.06.00215>
- Energy Information Administration, 2019. *International Energy Outlook 2019 with projections to 2050*. Washington DC.
- Environmental Protection Agency, 2010. *Available and emerging technologies for reducing greenhouse gas emissions from the pulp and paper manufacturing industry*. North Carolina, USA.
- EPN, 2018. *The state of the global paper industry*. North Carolina, USA.
- Ergüder, T., Tezel, U., Güven, E., Demirel, G., 2001. Anaerobic biotransformation and methane generation potential of cheese whey in batch and UASB reactors. *Waste Manag.* 21, 643–650. [https://doi.org/10.1016/S0956-053X\(00\)00114-8](https://doi.org/10.1016/S0956-053X(00)00114-8)
- Escalante, H., Castro, L., Amaya, M.P., Jaimes, L., Jaimes-Estévez, J., 2018. Anaerobic digestion of cheese whey: Energetic and nutritional potential for the dairy sector in developing countries. *Waste Manag.* 71, 711–718. <https://doi.org/10.1016/j.wasman.2017.09.026>
- European Biogas Association, 2020a. *Methane emission mitigation strategies - Information sheet for biogas industry*. Brussels, Belgium.
- European Biogas Association, 2020b. *The contribution of the biogas and biomethane industries to medium-term greenhouse gas reduction targets and climate-neutrality by 2050*. Brussels, Belgium.
- European Biogas Association, 2019. *Biogas basics*. Brussels, Belgium.
- European Biogas Association, 2018. *EBA Statistical Report 2018*. Brussels, Belgium.
- European Commission, 2020. *Circular Economy Action Plan: The European Green Deal*. <https://doi.org/10.2775/458852>
- European Commission, 2015. *Best Available Techniques (BAT) reference document for the production of pulp, paper and board*. European Commission, Luxembourg. <https://doi.org/10.2791/370629>
- Eurostat, 2019. *Agriculture, forestry and fishery statistics: 2019 edition*. European Union, Luxembourg. <https://doi.org/10.2786/798761>
- Farizoglu, B., Uzuner, S., 2011. The investigation of dairy industry wastewater treatment in a biological high performance membrane system. *Biochem. Eng. J.* 57, 46–54. <https://doi.org/10.1016/j.bej.2011.08.007>
- Farooqi, I.H., Basheer, F., 2017. Treatment of Adsorbable Organic Halide (AOX) from pulp and paper industry wastewater using aerobic granules in pilot scale SBR. *J. Water Process Eng.* 19, 60–66. <https://doi.org/10.1016/j.jwpe.2017.07.005>
- Ferguson, R.M.W., Coulon, F., Villa, R., 2016. Organic loading rate: A promising microbial management tool in anaerobic digestion. *Water Res.* 100, 348–356. <https://doi.org/10.1016/j.watres.2016.05.009>
- Fernández-Gutiérrez, D., Veillette, M., Giroir-Fendler, A., Ramirez, A.A., Fauchoux, N., Heitz, M., 2017. Biovalorization of saccharides derived from industrial wastes such as whey: a review. *Rev. Environ. Sci. Bio/Technology* 16, 147–174. <https://doi.org/10.1007/s11157-016-9417-7>
- Fernández, C., Cuetos, M.J., Martínez, E.J., Gómez, X., 2015. Thermophilic anaerobic digestion of cheese whey: Coupling H₂ and CH₄ production. *Biomass and Bioenergy* 81, 55–62. <https://doi.org/10.1016/j.biombioe.2015.05.024>
- Fernández, N., Montalvo, S., Fernández-Polanco, F., Guerrero, L., Cortés, I., Borja, R., Sánchez, E., Travieso, L., 2007. Real evidence about zeolite as microorganisms immobilizer in anaerobic fluidized bed reactors. *Process Biochem.* 42, 721–728. <https://doi.org/10.1016/j.procbio.2006.12.004>
- FisherScientific, 2020. *Website of Fisher Scientific [WWW Document]*. URL <https://www.fishersci.pt/pt/en/home.html> (accessed 3.4.20).
- Fonseca, M.M. da, Teixeira, J.A., 2006. *Reactores biológicos: Fundamentos e aplicações*. Lidel - Edições Técnicas Lda.
- Food and Agriculture Organization, 2020. *Overview of global dairy market developments in 2019*. Rome, Italy.
- Food and Agriculture Organization, 2016. *The global dairy sector: Facts*. Rome, Italy.
- Franke-Whittle, I.H., Walter, A., Ebner, C., Insam, H., 2014. Investigation into the effect of high concentrations of volatile fatty acids in anaerobic digestion on methanogenic communities. *Waste Manag.* 34, 2080–2089. <https://doi.org/10.1016/j.wasman.2014.07.020>

- Frigon, J.-C., Breton, J., Bruneau, T., Moletta, R., Guiot, S.R., 2009. The treatment of cheese whey wastewater by sequential anaerobic and aerobic steps in a single digester at pilot scale. *Bioresour. Technol.* 100, 4156–4163. <https://doi.org/10.1016/j.biortech.2009.03.077>
- Gallego-Schmid, A., Tarpani, R.R.Z., 2019. Life cycle assessment of wastewater treatment in developing countries: A review. *Water Res.* 153, 63–79. <https://doi.org/10.1016/j.watres.2019.01.010>
- Gameiro, T., Correia, C.L., Novais, R.M., Seabra, M.P., Labrincha, J.A., Capela, I., 2019a. pH control in anaerobic bioreactors using fly-ash based geopolymers as buffer material, in: *Green Energy and Environmental Technology*. Sciknowledge, Paris, France, p. 133.
- Gameiro, T., Kamali, M., Correia, C.L., Costa, M.E. V., Capela, I., 2019b. Magnetic zerovalent iron nanoparticles for adsorbable organic halides (AOX) removal from pulp and paper mill effluents, in: *Green Energy and Environmental Technology*. Sciknowledge, Paris, France, p. 84.
- Gameiro, T., Novais, R.M., Correia, C.L., Carvalheiras, J., Seabra, M.P., Labrincha, J.A., Duarte, A.C., Capela, I., 2020. Red mud-based inorganic polymer spheres: innovative and environmentally friendly anaerobic digestion enhancers. *Bioresour. Technol.* 123904. <https://doi.org/10.1016/j.biortech.2020.123904>
- Gameiro, T., Sousa, F., Silva, F.C., Couras, C., Lopes, M., Louros, V., Nadais, H., Capela, I., 2015. Olive oil mill wastewater to volatile fatty acids: Statistical study of the acidogenic process. *Water, Air, Soil Pollut.* 226, 115. <https://doi.org/10.1007/s11270-015-2311-z>
- Ganju, S., Gogate, P.R., 2017. A review on approaches for efficient recovery of whey proteins from dairy industry effluents. *J. Food Eng.* 215, 84–96. <https://doi.org/10.1016/j.jfoodeng.2017.07.021>
- Gannoun, H., Khelifi, E., Bouallagui, H., Touhami, Y., Hamdi, M., 2008. Ecological clarification of cheese whey prior to anaerobic digestion in upflow anaerobic filter. *Bioresour. Technol.* 99, 6105–6111. <https://doi.org/10.1016/j.biortech.2007.12.037>
- Gao, W., Fatehi, P., 2018. Fly ash based adsorbent for treating bleaching effluent of kraft pulping process. *Sep. Purif. Technol.* 195, 60–69. <https://doi.org/10.1016/j.seppur.2017.12.002>
- Garau, G., Castaldi, P., Santona, L., Deiana, P., Melis, P., 2007. Influence of red mud, zeolite and lime on heavy metal immobilization, culturable heterotrophic microbial populations and enzyme activities in a contaminated soil. *Geoderma* 142, 47–57. <https://doi.org/10.1016/j.geoderma.2007.07.011>
- Gavala, H.N., Angelidaki, I., Ahring, B.K., 2003. Kinetics and modeling of anaerobic digestion process., *Biomethanation I. Denmark*. <https://doi.org/10.1007/3-540-45838-7>
- Gavala, H.N., Kopsinis, H., Skiadas, I.V., Stamatelatos, K., Lyberatos, G., 1999. Treatment of dairy wastewater using an Upflow Anaerobic Sludge Blanket reactor. *J. Agric. Eng. Res.* 73, 59–63. <https://doi.org/10.1006/jaer.1998.0391>
- Ge, Y., Cui, X., Kong, Y., Li, Z., He, Y., Zhou, Q., 2015. Porous geopolymeric spheres for removal of Cu(II) from aqueous solution: Synthesis and evaluation. *J. Hazard. Mater.* 283, 244–251. <https://doi.org/10.1016/j.jhazmat.2014.09.038>
- Gellerstedt, G., 2015. Softwood kraft lignin: Raw material for the future. *Ind. Crops Prod.* 77, 845–854. <https://doi.org/10.1016/j.indcrop.2015.09.040>
- Gerardi, M.H., 2003. *The microbiology of anaerobic digesters*, Wastewater Microbiology Series. John Wiley & Sons, Inc., Hoboken, NJ, USA. <https://doi.org/10.1002/0471468967>
- Ghaly, A.E., Ramkumar, D.R., Sadaka, S.S., Rochon, J.D., 2000. Effect of reseeded and pH control on the performance of a two-stage mesophilic anaerobic digester operating on acid cheese whey. *Can. Agric. Eng.* 42, 173–183.
- Giroux, H.J., Veillette, N., Britten, M., 2018. Use of denatured whey protein in the production of artisanal cheeses from cow, goat and sheep milk. *Small Rumin. Res.* 161, 34–42. <https://doi.org/10.1016/j.smallrumres.2018.02.006>
- Goi, D., Leitenburg, C. de, Dolcetti, G., Trovarelli, A., 2006. COD and AOX abatement in catalytic wet oxidation of halogenated liquid wastes using CeO₂-based catalysts. *J. Alloys Compd.* 408–412, 1136–1140. <https://doi.org/10.1016/j.jallcom.2004.12.142>
- González-Siso, M.-I., 1996. The biotechnological utilization of cheese whey: A review. *Bioresour. Technol.* 57, 1–11. [https://doi.org/10.1016/0960-8524\(96\)00036-3](https://doi.org/10.1016/0960-8524(96)00036-3)
- Gorris, L.G.M., van Deursen, J.M.A., van der Drift, C., Vogels, G.D., 1989. Inhibition of propionate degradation by acetate in methanogenic fluidized bed reactors. *Biotechnol. Lett.* 11, 61–66. <https://doi.org/10.1007/BF01026788>
- Gourdon, R., Vermande, P., 1987. Effects of propionic acid concentration on anaerobic digestion of pig manure. *Biomass* 13, 1–12. [https://doi.org/10.1016/0144-4565\(87\)90067-9](https://doi.org/10.1016/0144-4565(87)90067-9)
- Grötzner, M., Melchior, E., Schroeder, L.H., dos Santos, A.R., Moscon, K.G., de Andrade, M.A., Martinelli, S.H.S., Xavier, C.R., 2018. Pulp and paper mill effluent treated by combining Coagulation-Flocculation-Sedimentation and Fenton processes. *Water, Air, Soil Pollut.* 229, 364. <https://doi.org/10.1007/s11270-018-1127-0>

018-4017-5

- Guerrero, L., Da Silva, C., Barahona, A., Montalvo, S., Huiliñir, C., Borja, R., Peirano, C., Toledo, M., Carvajal, A., 2019. Fly ash as stimulant for anaerobic digestion: effect over hydrolytic stage and methane generation rate. *Water Sci. Technol.* 80, 1384–1391. <https://doi.org/10.2166/wst.2019.391>
- Guevara, H.P.R., Ballesteros, F.C., Vilando, A.C., de Luna, M.D.G., Lu, M.-C., 2017. Recovery of oxalate from bauxite wastewater using fluidized-bed homogeneous granulation process. *J. Clean. Prod.* 154, 130–138. <https://doi.org/10.1016/j.jclepro.2017.03.172>
- Guo, Q., Majeed, S., Xu, R., Zhang, K., Kakade, A., Khan, A., Hafeez, F.Y., Mao, C., Liu, P., Li, X., 2019. Heavy metals interact with the microbial community and affect biogas production in anaerobic digestion: A review. *J. Environ. Manage.* 240, 266–272. <https://doi.org/10.1016/j.jenvman.2019.03.104>
- Gupta, S., Chakrabarti, S.K., Singh, S., 2010. Effect of ozonation on activated sludge from pulp and paper industry. *Water Sci. Technol.* 62, 1676–1681. <https://doi.org/10.2166/wst.2010.935>
- Gutiérrez, J.L.R., Encina, P.A.G., Fdz-Polanco, F., 1991. Anaerobic treatment of cheese-production wastewater using a UASB reactor. *Bioresour. Technol.* 37, 271–276. [https://doi.org/10.1016/0960-8524\(91\)90194-O](https://doi.org/10.1016/0960-8524(91)90194-O)
- Han, J., Chang, Y., Britten, M., St-Gelais, D., Champagne, C.P., Fustier, P., Lacroix, M., 2019. Interactions of phenolic compounds with milk proteins. *Eur. Food Res. Technol.* 245, 1881–1888. <https://doi.org/10.1007/s00217-019-03293-1>
- Han, L., Wei, Y., 2012. Low-temperature synthesis of Fe₃O₄ microroses and their application in water treatment. *Mater. Lett.* 70, 1–3. <https://doi.org/10.1016/j.matlet.2011.11.047>
- Hardjito, D., Wallah, S.E., Sumajouw, D.M.J., Rangan, B.V., 2004. On the development of fly ash-based geopolymer concrete. *ACI Mater. J.* 101, 467–472.
- Hassan, A.N., Nelson, B.K., 2012. Anaerobic fermentation of dairy food wastewater. *J. Dairy Sci.* 95, 6188–6203. <https://doi.org/10.3168/jds.2012-5732>
- Hatti-Kaul, R., Mattiasson, B., 2016. Anaerobes in industrial and environmental biotechnology, in: Hatti-Kaul, R., Mamo, G., Mattiasson, B. (Eds.), *Anaerobes in Biotechnology*. Springer, Cham, Switzerland, pp. 1–33. https://doi.org/10.1007/10_2016_10
- He, J., Lange, C.R., Dougherty, M., 2009. Laboratory study using paper mill lime mud for agronomic benefit. *Process Saf. Environ. Prot.* 87, 401–405. <https://doi.org/10.1016/j.psep.2009.08.001>
- Hijazi, O., Abdelsalam, E., Samer, M., Amer, B.M.A., Yacoub, I.H., Moselhy, M.A., Attia, Y.A., Bernhardt, H., 2020. Environmental impacts concerning the addition of trace metals in the process of biogas production from anaerobic digestion of slurry. *J. Clean. Prod.* 243, 118593. <https://doi.org/10.1016/j.jclepro.2019.118593>
- Holliger, C., Wohlfarth, G., Diekert, G., 1998. Reductive dechlorination in the energy metabolism of anaerobic bacteria. *FEMS Microbiol. Rev.* 22, 383–398. <https://doi.org/10.1111/j.1574-6976.1998.tb00377.x>
- Horiuchi, J.-I., Shimizu, T., Tada, K., Kanno, T., Kobayashi, M., 2002. Selective production of organic acids in anaerobic acid reactor by pH control. *Bioresour. Technol.* 82, 209–213. [https://doi.org/10.1016/S0960-8524\(01\)00195-X](https://doi.org/10.1016/S0960-8524(01)00195-X)
- Hua, Y., Heal, K. V., Friesl-Hanl, W., 2017. The use of red mud as an immobiliser for metal/metalloid-contaminated soil: A review. *J. Hazard. Mater.* 325, 17–30. <https://doi.org/10.1016/j.jhazmat.2016.11.073>
- Huang, H.-H., Wang, D.-H., Luo, Z.-F., Shang, W.-H., 2018. Effect of biomass fly ash addition on methane production in two-phase anaerobic digestion of food waste. *J. Agro-Environment Sci.* 37, 1277–1283. <https://doi.org/10.11654/jaes.2017-1518>
- Huang, Y.-L., Li, Q.-B., Deng, X., Lu, Y.-H., Liao, X.-K., Hong, M.-Y., Wang, Y., 2005. Aerobic and anaerobic biodegradation of polyethylene glycols using sludge microbes. *Process Biochem.* 40, 207–211. <https://doi.org/10.1016/j.procbio.2003.12.004>
- Huiliñir, C., Montalvo, S., Guerrero, L., 2015. Biodegradability and methane production from secondary paper and pulp sludge: effect of fly ash and modeling. *Water Sci. Technol.* 72, 230–237. <https://doi.org/10.2166/wst.2015.210>
- Hwang, M.H., Jang, N.J., Hyun, S.H., Kim, I.S., 2004. Anaerobic bio-hydrogen production from ethanol fermentation: the role of pH. *J. Biotechnol.* 111, 297–309. <https://doi.org/10.1016/j.jbiotec.2004.04.024>
- Inanç, B., Matsui, S., Ide, S., 1999. Propionic acid accumulation in anaerobic digestion of carbohydrates: an investigation on the role of hydrogen gas. *Water Sci. Technol.* 40, 93–100. [https://doi.org/10.1016/S0273-1223\(99\)00368-6](https://doi.org/10.1016/S0273-1223(99)00368-6)
- Insam, H., Franke-Whittle, I., Goberna, M., 2010. Microbes in aerobic and anaerobic waste treatment, in: Insam, H., Franke-Whittle, I., Goberna, M. (Eds.), *Microbes at Work*. Springer Berlin Heidelberg, Berlin, Heidelberg, pp. 1–34. https://doi.org/10.1007/978-3-642-04043-6_1
- Intergovernmental Panel on Climate Change, 2007. *Climate change 2007: Mitigation. Contribution of working group III to the fourth assessment report of the intergovernmental panel on climate change*. Cambridge

- University Press, Cambridge, United Kingdom and New York, USA.
<https://doi.org/10.1017/CBO9780511546013>
- International Finance Corporation, 2007. Environmental, health, and safety guidelines: Pulp and paper mills.
- ISO 9562, I., 2004. Water quality - Determination of adsorbable organically bound halogens (AOX). 3rd Ed.
- Jain, S., 2019. Global Potential of Biogas. London.
- Jain, S.R., Mattiasson, B., 1998. Acclimatization of methanogenic consortia for low pH biomethanation process. *Biotechnol. Lett.* 20, 771–775. <https://doi.org/10.1023/B:BILE.0000015920.45724.29>
- Jalilzadeh, A., Tuncturk, Y., Hesari, J., 2015. Extension shelf life of cheese: A review. *Int. J. Dairy Sci.* 10, 44–60. <https://doi.org/10.3923/ijds.2015.44.60>
- Jaroszynski, L., Duber, A., Chwialkowska, J., Oleskowicz-Popiel, P., 2016. Production of caproic acid from cheese whey wastewaters. *Proc. Water Environ. Fed.* 3, 2634–2637. <https://doi.org/10.2175/193864716819707175>
- Jasko, J., Skripsts, E., Dubrovskis, V., Zabarovskis, E., Kotelenecs, V., 2011. Biogas production from cheese whey in two phase anaerobic digestion. *Eng. Rural Dev.* 26, 373–376.
- Jia, Y., Maurice, C., Öhlander, B., 2014. Effect of the alkaline industrial residues fly ash, green liquor dregs, and lime mud on mine tailings oxidation when used as covering material. *Environ. Earth Sci.* 72, 319–334. <https://doi.org/10.1007/s12665-013-2953-3>
- Jiménez, J., Cisneros-Ortiz, M.E., Guardia-Puebla, Y., Morgan-Sagastume, J.M., Noyola, A., 2014. Optimization of the thermophilic anaerobic co-digestion of pig manure, agriculture waste and inorganic additive through specific methanogenic activity. *Water Sci. Technol.* 69, 2381–2388. <https://doi.org/10.2166/wst.2014.109>
- Jiménez, J., Guardia-Puebla, Y., Cisneros-Ortiz, M.E., Morgan-Sagastume, J.M., Guerra, G., Noyola, A., 2015. Optimization of the specific methanogenic activity during the anaerobic co-digestion of pig manure and rice straw, using industrial clay residues as inorganic additive. *Chem. Eng. J.* 259, 703–714. <https://doi.org/10.1016/j.cej.2014.08.031>
- Jo, Y., Kim, J., Lee, C., 2016. Continuous treatment of dairy effluent in a downflow anaerobic filter packed with slag grains: Reactor performance and kinetics. *J. Taiwan Inst. Chem. Eng.* 68, 147–152. <https://doi.org/10.1016/j.jtice.2016.08.021>
- Johnson, L.D., Young, J.C., 1983. Inhibition of anaerobic digestion by organic priority pollutants. *Water Pollut. Control Fed.* 55, 1441–1449.
- Jung, H., Kim, J., Lee, C., 2016. Continuous anaerobic co-digestion of Ulva biomass and cheese whey at varying substrate mixing ratios: Different responses in two reactors with different operating regimes. *Bioresour. Technol.* 221, 366–374. <https://doi.org/10.1016/j.biortech.2016.09.059>
- Kamali, M., Alavi-Borazjani, S.A., Khodaparast, Z., Khalaj, M., Jahanshahi, A., Costa, E., Capela, I., 2019. Additive and additive-free treatment technologies for pulp and paper mill effluents: Advances, challenges and opportunities. *Water Resour. Ind.* 21, 100109. <https://doi.org/10.1016/j.wri.2019.100109>
- Kamali, M., Gameiro, T., Costa, M.E. V., Capela, I., 2016. Anaerobic digestion of pulp and paper mill wastes - An overview of the developments and improvement opportunities. *Chem. Eng. J.* 298, 162–182. <https://doi.org/10.1016/j.cej.2016.03.119>
- Kapdan, I.K., Kargi, F., 2006. Bio-hydrogen production from waste materials. *Enzyme Microb. Technol.* 38, 569–582. <https://doi.org/10.1016/j.enzmictec.2005.09.015>
- Karlsson, M.A., Langton, M., Innings, F., Malmgren, B., Höjer, A., Wikström, M., Lundh, Å., 2019. Changes in stability and shelf-life of ultra-high temperature treated milk during long term storage at different temperatures. *Heliyon* 5, e02431. <https://doi.org/10.1016/j.heliyon.2019.e02431>
- Kasmi, M., 2018. Biological processes as promoting way for both treatment and valorization of dairy industry effluents. *Waste and Biomass Valorization* 9, 195–209. <https://doi.org/10.1007/s12649-016-9795-7>
- Katsoni, A., Mantzavinos, D., Diamadopoulos, E., 2014. Coupling digestion in a pilot-scale UASB reactor and electrochemical oxidation over BDD anode to treat diluted cheese whey. *Environ. Sci. Pollut. Res.* 21, 12170–12181. <https://doi.org/10.1007/s11356-014-2960-2>
- Katyal, A., Morrison, R.D., 2007. Introduction to environmental forensics, Second ed. ed. Elsevier, London. <https://doi.org/10.1016/B978-0-12-369522-2.X5000-3>
- Kayhanian, M., 1999. Ammonia inhibition in high-solids biogasification: An overview and practical solutions. *Environ. Technol.* 20, 355–365. <https://doi.org/10.1080/09593332008616828>
- Kaza, S., Yao, L., Bhada-Tata, P., van Woerden, F., 2018. What a waste 2.0: A global snapshot of solid waste management to 2050. World Bank, Washington, DC. <https://doi.org/10.1596/978-1-4648-1329-0>
- Kim, I.S., Hwang, M.H., Jang, N.J., Hyun, S.H., Lee, S., 2004. Effect of low pH on the activity of hydrogen utilizing methanogen in bio-hydrogen process. *Int. J. Hydrogen Energy* 29, 1133–1140. <https://doi.org/10.1016/j.ijhydene.2003.08.017>

- Kisielewska, M., Wysocka, I., Rynkiewicz, M.R., 2014. Continuous biohydrogen and biomethane production from whey permeate in a two-stage fermentation process. *Environ. Prog. Sustain. Energy* 33, 1411–1418. <https://doi.org/10.1002/ep.11890>
- Klauber, C., Gräfe, M., Power, G., 2011. Bauxite residue issues: II. Options for residue utilization. *Hydrometallurgy* 108, 11–32. <https://doi.org/10.1016/j.hydromet.2011.02.007>
- Komatsu, T., Hanaki, K., Matsuo, T., 1991. Prevention of lipid inhibition in anaerobic processes by introducing a two-phase system. *Water Sci. Technol.* 23, 1189–1200. <https://doi.org/10.2166/wst.1991.0570>
- Komnitsas, K., Zaharaki, D., 2007. Geopolymerisation: A review and prospects for the minerals industry. *Miner. Eng.* 20, 1261–1277. <https://doi.org/10.1016/j.mineng.2007.07.011>
- Koszel, M., Lorencowicz, E., 2015. Agricultural use of biogas digestate as a replacement fertilizers. *Agric. Agric. Sci. Procedia* 7, 119–124. <https://doi.org/10.1016/j.aaspro.2015.12.004>
- Kovács, E., Wirth, R., Maróti, G., Bagi, Z., Rákhely, G., Kovács, K.L., 2013. Biogas production from protein-rich biomass: fed-batch anaerobic fermentation of casein and of pig blood and associated changes in microbial community composition. *PLoS One* 8, e77265. <https://doi.org/10.1371/journal.pone.0077265>
- Kramer, K.J., Masanet, E., Xu, T., Worrell, E., 2009. Energy efficiency improvement and cost saving opportunities for the pulp and paper industry. Berkeley, CA.
- Krivenko, P. V., Kovalchuk, G.Y., 2007. Directed synthesis of alkaline aluminosilicate minerals in a geocement matrix. *J. Mater. Sci.* 42, 2944–2952. <https://doi.org/10.1007/s10853-006-0528-3>
- Kubes, G.J., Fleming, B.I., MacLeod, J.M., Bolker, H.I., 1980. Alkaline pulping with additives: A review. *Wood Sci. Technol.* 14, 207–228. <https://doi.org/10.1007/BF00350570>
- Kumar, A., Dhall, P., Kumar, R., 2013. Biological AOX removal of pulp mill plant effluent by pseudomonas aeruginosa - bench study. *J. Environmetal Eng. Landsc. Manag.* 21, 296–304. <https://doi.org/10.3846/16486897.2012.745413>
- Kumar, M., Morya, R., Gupta, A., Thakur, I.S., 2020. Anaerobic biovalorization of pulp and paper mill waste, in: *Biovalorisation of Wastes to Renewable Chemicals and Biofuels*. Elsevier, pp. 41–61. <https://doi.org/10.1016/B978-0-12-817951-2.00003-1>
- Lagoa-Costa, B., Kennes, C., Veiga, M.C., 2020. Cheese whey fermentation into volatile fatty acids in an anaerobic sequencing batch reactor. *Bioresour. Technol.* 308, 123226. <https://doi.org/10.1016/j.biortech.2020.123226>
- Lalov, I., 2001. Improvement of biogas production from vinasse via covalently immobilized methanogens. *Bioresour. Technol.* 79, 83–85. [https://doi.org/10.1016/S0960-8524\(01\)00045-1](https://doi.org/10.1016/S0960-8524(01)00045-1)
- Lee, D.-J., Lee, S.-Y., Bae, J.-S., Kang, J.-G., Kim, K.-H., Rhee, S.-S., Park, J.-H., Cho, J.-S., Chung, J., Seo, D.-C., 2015. Effect of volatile fatty acid concentration on anaerobic degradation rate from field anaerobic digestion facilities treating food waste leachate in South Korea. *J. Chem.* 2015, 1–9. <https://doi.org/10.1155/2015/640717>
- Lee, Y.-J., Lee, D.-J., 2019. Impact of adding metal nanoparticles on anaerobic digestion performance – A review. *Bioresour. Technol.* 292, 121926. <https://doi.org/10.1016/j.biortech.2019.121926>
- Leitão, R.C., Haadel, A.C. van, Zeeman, G., Lettinga, G., 2006. The effects of operational and environmental variations on anaerobic wastewater treatment systems: A review. *Bioresour. Technol.* 97, 1105–1118. <https://doi.org/10.1016/j.biortech.2004.12.007>
- Liew, Y.X., Chan, Y.J., Manickam, S., Chong, S., Tiong, T.J., Lim, J.W., Pan, G.-T., 2020. Enzymatic pretreatment to enhance anaerobic bioconversion of high strength wastewater to biogas: A review. *Sci. Total Environ.* 713, 136373. <https://doi.org/10.1016/j.scitotenv.2019.136373>
- Lisboa, C.R., de Simoni Martinez, L., Trindade, R.A., de Almeida Costa, F.A., de Medeiros Burkert, J.F., Burkert, C.A.V., 2012. Response surface methodology applied to the enzymatic synthesis of galacto-oligosaccharides from cheese whey. *Food Sci. Biotechnol.* 21, 1519–1524. <https://doi.org/10.1007/s10068-012-0202-2>
- Liu, C., Tong, Q., Li, Y., Wang, N., Liu, B., Zhang, X., 2019. Biogas production and metal passivation analysis during anaerobic digestion of pig manure: effects of a magnetic Fe₃O₄/FA composite supplement. *RSC Adv.* 9, 4488–4498. <https://doi.org/10.1039/C8RA09451A>
- Liu, W., Yang, J., Xiao, B., 2009. Review on treatment and utilization of bauxite residues in China. *Int. J. Miner. Process.* 93, 220–231. <https://doi.org/10.1016/j.minpro.2009.08.005>
- Liu, Y., Naidu, R., 2014. Hidden values in bauxite residue (red mud): Recovery of metals. *Waste Manag.* 34, 2662–2673. <https://doi.org/10.1016/j.wasman.2014.09.003>
- Liu, Y., Zhang, Y., Ni, B.-J., 2015. Evaluating enhanced sulfate reduction and optimized volatile fatty acids (VFA) composition in anaerobic reactor by Fe (III) addition. *Environ. Sci. Technol.* 49, 2123–2131. <https://doi.org/10.1021/es504200j>
- Liu, Z., Li, H., 2015. Metallurgical process for valuable elements recovery from red mud—A review.

- Hydrometallurgy 155, 29–43. <https://doi.org/10.1016/j.hydromet.2015.03.018>
- Lo, H.-M., 2005. Metals behaviors of MSWI bottom ash co-digested anaerobically with MSW. *Resour. Conserv. Recycl.* 43, 263–280. <https://doi.org/10.1016/j.resconrec.2004.06.004>
- Lo, H.M., Chiu, H.Y., Lo, S.W., Lo, F.C., 2012. Effects of micro-nano and non micro-nano MSWI ashes addition on MSW anaerobic digestion. *Bioresour. Technol.* 114, 90–94. <https://doi.org/10.1016/j.biortech.2012.03.002>
- Lönnberg, B., 2009. History of mechanical pulping, in: Lönnberg, B. (Ed.), *Mechanical Pulping*, 2nd Totally Updated Edition. Paper Engineers' Association, Helsinki, Finland, pp. 23–34.
- Lora, J., 2008. Industrial commercial lignins: Sources, properties and applications, in: *Monomers, Polymers and Composites from Renewable Resources*. Elsevier, Amsterdam, pp. 225–241. <https://doi.org/10.1016/B978-0-08-045316-3.00010-7>
- Lu, X., Wang, H., Ma, F., Zhao, G., Wang, S., 2017. Enhanced anaerobic digestion of cow manure and rice straw by the supplementation of an iron oxide–zeolite system. *Energy & Fuels* 31, 599–606. <https://doi.org/10.1021/acs.energyfuels.6b02244>
- Lusk, P., 1998. *Methane recovery from animal manures: A current opportunities casebook*, 3rd ed. Golden, CO: National Renewable Energy Laboratory, Washington, DC.
- Mainardis, M., Flaibani, S., Trigatti, M., Goi, D., 2019. Techno-economic feasibility of anaerobic digestion of cheese whey in small Italian dairies and effect of ultrasound pre-treatment on methane yield. *J. Environ. Manage.* 246, 557–563. <https://doi.org/10.1016/j.jenvman.2019.06.014>
- Mäkelä, M., Harju-Oksanen, M.-L., Watkins, G., Ekroos, A., Dahl, O., 2012. Feasibility assessment of inter-industry solid residue utilization for soil amendment - Trace element availability and legislative issues. *Resour. Conserv. Recycl.* 67, 1–8. <https://doi.org/j.resconrec.2012.06.012>
- Mandeep, Kumar Gupta, G., Shukla, P., 2020. Insights into the resources generation from pulp and paper industry wastes: Challenges, perspectives and innovations. *Bioresour. Technol.* 297, 122496. <https://doi.org/10.1016/j.biortech.2019.122496>
- Manskinen, K., Nurmiesniemi, H., Pöykiö, R., 2011. Total and extractable non-process elements in green liquor dregs from the chemical recovery circuit of a semi-chemical pulp mill. *Chem. Eng. J.* 166, 954–961. <https://doi.org/10.1016/j.cej.2010.11.082>
- Mao, C., Feng, Y., Wang, X., Ren, G., 2015. Review on research achievements of biogas from anaerobic digestion. *Renew. Sustain. Energy Rev.* 45, 540–555. <https://doi.org/10.1016/j.rser.2015.02.032>
- Mao, Y., Kulozik, U., 2018. Selective hydrolysis of whey proteins using a flow-through monolithic reactor with large pore size and immobilised trypsin. *Int. Dairy J.* 85, 96–104. <https://doi.org/10.1016/j.idairyj.2018.05.015>
- Martínez-Lage, I., Velay-Lizancos, M., Vázquez-Burgo, P., Rivas-Fernández, M., Vázquez-Herrero, C., Ramírez-Rodríguez, A., Martín-Cano, M., 2016. Concretes and mortars with waste paper industry: Biomass ash and dregs. *J. Environ. Manage.* 181, 863–873. <https://doi.org/10.1016/j.jenvman.2016.06.052>
- Martins, F., Martins, J., Ferracin, L., Dacunha, C., 2007. Mineral phases of green liquor dregs, slaker grits, lime mud and wood ash of a Kraft pulp and paper mill. *J. Hazard. Mater.* 147, 610–617. <https://doi.org/10.1016/j.jhazmat.2007.01.057>
- Mateo-Sagasta, J., Raschid-Sally, L., Thebo, A., 2015. Global wastewater and sludge production, treatment and use, in: *Wastewater*. Springer Netherlands, Dordrecht, pp. 15–38. https://doi.org/10.1007/978-94-017-9545-6_2
- Mattson, M.D., 2014. Alkalinity of freshwater, in: *Reference Module in Earth Systems and Environmental Sciences*. Elsevier. <https://doi.org/10.1016/B978-0-12-409548-9.09397-0>
- McCarty, P.L., 1964a. Anaerobic waste treatment fundamentals - Part three: Toxic materials and their control. *Public Work.* 95, 91–99.
- McCarty, P.L., 1964b. Anaerobic waste treatment fundamentals - Part two: Environmental requirements and control. *Public Work.* 95, 123–126.
- McCarty, P.L., Smith, D.P., 1986. Anaerobic wastewater treatment. *Environ. Sci. Technol.* 20, 1200–1206. <https://doi.org/10.1021/es00154a002>
- McLellan, B.C., Williams, R.P., Lay, J., van Riessen, A., Corder, G.D., 2011. Costs and carbon emissions for geopolymers in comparison to ordinary portland cement. *J. Clean. Prod.* 19, 1080–1090. <https://doi.org/10.1016/j.jclepro.2011.02.010>
- Mealier, L., Basta, J., Holtinger, L., Wäne, G., 2003. ECF bleaching of softwood and eucalyptus pulps - A comparative study. *JAPAN TAPPI J.* 57, 788–798. <https://doi.org/10.2524/jtappij.57.788>
- Meegoda, J., Li, B., Patel, K., Wang, L., 2018. A review of the processes, parameters, and optimization of anaerobic digestion. *Int. J. Environ. Res. Public Health* 15, 2224. <https://doi.org/10.3390/ijerph15102224>

- Merlin Christy, P., Gopinath, L.R., Divya, D., 2014. A review on anaerobic decomposition and enhancement of biogas production through enzymes and microorganisms. *Renew. Sustain. Energy Rev.* 34, 167–173. <https://doi.org/10.1016/j.rser.2014.03.010>
- Mesfun, S., Lundgren, J., Grip, C.-E., Toffolo, A., Nilsson, R.L.K., Rova, U., 2014. Black liquor fractionation for biofuels production – A techno-economic assessment. *Bioresour. Technol.* 166, 508–517. <https://doi.org/10.1016/j.biortech.2014.05.062>
- Meyer, F.M., 2004. Availability of bauxite reserves. *Nat. Resour. Res.* 13, 161–172. <https://doi.org/10.1023/B:NARR.0000046918.50121.2e>
- Meyer, T., Edwards, E.A., 2014. Anaerobic digestion of pulp and paper mill wastewater and sludge. *Water Res.* 65, 321–349. <https://doi.org/10.1016/j.watres.2014.07.022>
- Mikheenko, I.P., Gomez-Bolivar, J., Merroun, M.L., Macaskie, L.E., Sharma, S., Walker, M., Hand, R.A., Grail, B.M., Johnson, D.B., Orozco, R.L., 2019. Upconversion of cellulosic waste into a potential “Drop in Fuel” via novel catalyst generated using *Desulfovibrio desulfuricans* and a consortium of acidophilic sulfidogens. *Front. Microbiol.* 10. <https://doi.org/10.3389/fmicb.2019.00970>
- Milán, Z., Sánchez, E.P., Weiland, P., Borja, R., Martín, A., Ilangovan, K., 2001. Influence of different natural zeolite concentrations on the anaerobic digestion of piggery waste. *Bioresour. Technol.* 80, 37–43. [https://doi.org/10.1016/S0960-8524\(01\)00064-5](https://doi.org/10.1016/S0960-8524(01)00064-5)
- Milán, Z., Villa, P., Sánchez, E., Montalvo, S., Borja, R., Ilangovan, K., Briones, R., 2003. Effect of natural and modified zeolite addition on anaerobic digestion of piggery waste. *Water Sci. Technol.* 48, 263–269. <https://doi.org/10.2166/wst.2003.0411>
- Mockaitis, G., Ratusznei, S.M., Rodrigues, J.A.D., Zaiat, M., Foresti, E., 2006. Anaerobic whey treatment by a stirred sequencing batch reactor (ASBR): effects of organic loading and supplemented alkalinity. *J. Environ. Manage.* 79, 198–206. <https://doi.org/10.1016/j.jenvman.2005.07.001>
- Modolo, R., Benta, A., Ferreira, V.M., Machado, L.M., 2010. Pulp and paper plant wastes valorisation in bituminous mixes. *Waste Manag.* 30, 685–696. <https://doi.org/10.1016/j.wasman.2009.11.005>
- Mollea, C., Marmo, L., Bosco, F., 2013. Valorisation of cheese whey, a by-product from the dairy industry, in: Muzzalupo, I. (Ed.), *Food Industry. InTech*, pp. 549–588. <https://doi.org/10.5772/53159>
- Montalvo, S., Huiliñir, C., Borja, R., Castillo, A., Pereda, I., 2019. Anaerobic digestion of wastewater rich in sulfate and sulfide: effects of metallic waste addition and micro-aeration on process performance and methane production. *J. Environ. Sci. Heal. Part A* 54, 1035–1043. <https://doi.org/10.1080/10934529.2019.1623597>
- Montalvo, S., Vielma, S., Borja, R., Huiliñir, C., Guerrero, L., 2018. Increase in biogas production in anaerobic sludge digestion by combining aerobic hydrolysis and addition of metallic wastes. *Renew. Energy* 123, 541–548. <https://doi.org/10.1016/j.renene.2018.02.004>
- Monte, M.C., Fuente, E., Blanco, A., Negro, C., 2009. Waste management from pulp and paper production in the European Union. *Waste Manag.* 29, 293–308. <https://doi.org/10.1016/j.wasman.2008.02.002>
- Müller, G., 2003. Sense or no-sense of the sum parameter for water soluble “adsorbable organic halogens” (AOX) and “absorbed organic halogens” (AOX-S18) for the assessment of organohalogenes in sludges and sediments. *Chemosphere* 52, 371–379. [https://doi.org/10.1016/S0045-6535\(03\)00215-7](https://doi.org/10.1016/S0045-6535(03)00215-7)
- Musa, M., Idrus, S., Che Man, H., Nik Daud, N., 2018. Wastewater treatment and biogas recovery using anaerobic membrane bioreactors (AnMBRs): strategies and achievements. *Energies* 11, 1675. <https://doi.org/10.3390/en11071675>
- Myhre, G., Shindell, D., Bréon, F.-M., Collins, W., Fuglestedt, J., Huang, J., Koch, D., Lamarque, J.-F., Lee, D., Mendoza, B., Nakajima, T., Robock, A., Stephens, G., Takemura, T., Zhang, H., 2013. Anthropogenic and natural radiative forcing, in: Stocker, T.F., Qin, D., Plattner, G.-K., Tignor, M., Allen, S.K., Boschung, J., Nauels, A., Xia, Y., Bex, V., Midgley, P.M. (Eds.), *Climate Change 2013: The Physical Science Basis. Contribution of Working Group I to the Fifth Assessment Report of the Intergovernmental Panel on Climate Change*. Cambridge University Press, Cambridge, United Kingdom and New York, NY, USA, pp. 659–740.
- Naglova, Z., Boberova, B., Horakova, T., Smutka, L., 2017. Statistical analysis of factors influencing the results of enterprises in dairy industry. *Agric. Econ. - Czech* 63, 259–270. <https://doi.org/10.17221/353/2015-AGRICECON>
- Najafpour, G.D., Hashemiyeh, B.A., Asadi, M., Ghasemi, M.B., 2008. Biological treatment of dairy wastewater in an upflow anaerobic sludge-fixed film bioreactor. *Am. J. Agric. Environ. Sci.* 4, 251–257.
- Naqvi, M., Yan, J., Dahlquist, E., 2010. Black liquor gasification integrated in pulp and paper mills: A critical review. *Bioresour. Technol.* 101, 8001–8015. <https://doi.org/10.1016/j.biortech.2010.05.013>
- Ney, B., Ahmed, F.H., Carere, C.R., Biswas, A., Warden, A.C., Morales, S.E., Pandey, G., Watt, S.J., Oakeshott, J.G., Taylor, M.C., Stott, M.B., Jackson, C.J., Greening, C., 2017. The methanogenic redox cofactor F420 is widely synthesized by aerobic soil bacteria. *ISME J.* 11, 125–137.

<https://doi.org/10.1038/ismej.2016.100>

- Novais, R.M., Buruberry, L.H., Ascensão, G., Seabra, M.P., Labrincha, J.A., 2016a. Porous biomass fly ash-based geopolymers with tailored thermal conductivity. *J. Clean. Prod.* 119, 99–107. <https://doi.org/10.1016/j.jclepro.2016.01.083>
- Novais, R.M., Buruberry, L.H., Seabra, M.P., Bajare, D., Labrincha, J.A., 2016b. Novel porous fly ash-containing geopolymers for pH buffering applications. *J. Clean. Prod.* 124, 395–404. <https://doi.org/10.1016/j.jclepro.2016.02.114>
- Novais, R.M., Buruberry, L.H., Seabra, M.P., Labrincha, J.A., 2016c. Novel porous fly-ash containing geopolymer monoliths for lead adsorption from wastewaters. *J. Hazard. Mater.* 318, 631–640. <https://doi.org/10.1016/j.jhazmat.2016.07.059>
- Novais, R.M., Carvalheiras, J., Seabra, M.P., Pullar, R.C., Labrincha, J.A., 2019. Red mud-based inorganic polymer spheres bulk-type adsorbents and pH regulators. *Mater. Today* 23, 105–106. <https://doi.org/10.1016/j.mattod.2019.01.014>
- Novais, R.M., Carvalheiras, J., Seabra, M.P., Pullar, R.C., Labrincha, J.A., 2018a. Innovative application for bauxite residue: Red mud-based inorganic polymer spheres as pH regulators. *J. Hazard. Mater.* 358, 69–81. <https://doi.org/10.1016/j.jhazmat.2018.06.047>
- Novais, R.M., Carvalheiras, J., Senff, L., Labrincha, J.A., 2018b. Upcycling unexplored dregs and biomass fly ash from the paper and pulp industry in the production of eco-friendly geopolymer mortars: A preliminary assessment. *Constr. Build. Mater.* 184, 464–472. <https://doi.org/10.1016/j.conbuildmat.2018.07.017>
- Novais, R.M., Covas, J.A., Paiva, M.C., 2012. The effect of flow type and chemical functionalization on the dispersion of carbon nanofiber agglomerates in polypropylene. *Compos. Part A Appl. Sci. Manuf.* 43, 833–841. <https://doi.org/10.1016/j.compositesa.2012.01.017>
- Novais, R.M., Gameiro, T., Carvalheiras, J., Seabra, M.P., Tarelho, L.A.C., Labrincha, J.A., Capela, I., 2018c. High pH buffer capacity biomass fly ash-based geopolymer spheres to boost methane yield in anaerobic digestion. *J. Clean. Prod.* 178, 258–267. <https://doi.org/10.1016/j.jclepro.2018.01.033>
- Novais, R.M., Pullar, R.C., Labrincha, J.A., 2020. Geopolymer foams: An overview of recent advancements. *Prog. Mater. Sci.* <https://doi.org/10.1016/j.pmatsci.2019.100621>
- Novais, R.M., Seabra, M.P., Labrincha, J.A., 2017. Porous geopolymer spheres as novel pH buffering materials. *J. Clean. Prod.* 143, 1114–1122. <https://doi.org/10.1016/j.jclepro.2016.12.008>
- Olli, D., 2008. Volume 19 - Environmental Management and Control, in: Dahl, O. (Ed.), *Papermaking Science and Technology*. Finnish Paper Engineers' Association, Finland, pp. 70–84.
- Otal, E., Lebrato, J., 2003. Anaerobic degradation of polyethylene glycol mixtures. *J. Chem. Technol. Biotechnol.* 78, 1075–1081. <https://doi.org/10.1002/jctb.901>
- Pabón Pereira, C.P., Castañares, G., van Lier, J.B., 2012. An OxiTop® protocol for screening plant material for its biochemical methane potential (BMP). *Water Sci. Technol.* 66, 1416–1423. <https://doi.org/10.2166/wst.2012.305>
- Pagliano, G., Ventrino, V., Panico, A., Romano, I., Pirozzi, F., Pepe, O., 2019. Anaerobic process for bioenergy recovery from dairy waste: Meta-analysis and enumeration of microbial community related to intermediates production. *Front. Microbiol.* 9, 1–15. <https://doi.org/10.3389/fmicb.2018.03229>
- Pais, J., Gameiro, T., Farinha, I., Serafim, L.S., Reis, M.A.M., 2010. Sustainable conversion of whey into polyhydroxyalkanoates by *Haloferax mediterranei*. *J. Biotechnol.* 150, 575–576. <https://doi.org/10.1016/j.jbiotec.2010.10.064>
- Palacios-Ruiz, B., Méndez-Acosta, H.O., Alcaraz-González, V., González-Álvarez, V., Pelayo-Ortiz, C., 2008. Regulation of volatile fatty acids and total alkalinity in anaerobic digesters. *IFAC Proc. Vol.* 41, 13611–13616. <https://doi.org/10.3182/20080706-5-KR-1001.02305>
- Palmer, S.J., Reddy, B.J., Frost, R.L., 2009. Characterisation of red mud by UV–vis–NIR spectroscopy. *Spectrochim. Acta Part A Mol. Biomol. Spectrosc.* 71, 1814–1818. <https://doi.org/10.1016/j.saa.2008.06.038>
- Parawira, W., Murto, M., Read, J.S., Mattiasson, B., 2004. Volatile fatty acid production during anaerobic mesophilic digestion of solid potato waste. *J. Chem. Technol. Biotechnol.* 79, 673–677. <https://doi.org/10.1002/jctb.1012>
- Park, C.W., Drake, M., 2016. Condensed milk storage and evaporation affect the flavor of nonfat dry milk. *J. Dairy Sci.* 99, 9586–9597. <https://doi.org/10.3168/jds.2016-11530>
- Pasandín, A.R., Pérez, I., Ramírez, A., Cano, M.M., 2016. Moisture damage resistance of hot-mix asphalt made with paper industry wastes as filler. *J. Clean. Prod.* 112, 853–862. <https://doi.org/10.1016/j.jclepro.2015.06.016>
- Patel, S., Pal, B.K., Patel, R.K., 2018. A novel approach in red mud neutralization using cow dung. *Environ. Sci. Pollut. Res.* 25, 12841–12848. <https://doi.org/10.1007/s11356-018-1374-y>

- Patel, U., Suresh, S., 2008. Electrochemical treatment of pentachlorophenol in water and pulp bleaching effluent. *Sep. Purif. Technol.* 61, 115–122. <https://doi.org/10.1016/j.seppur.2007.10.004>
- Paulo, L.M., Stams, A.J.M., Sousa, D.Z., 2015. Methanogens, sulphate and heavy metals: a complex system. *Rev. Environ. Sci. Bio/Technology* 14, 537–553. <https://doi.org/10.1007/s11157-015-9387-1>
- Piscicelli, L., Ludden, G.D.S., 2016. The potential of design for behaviour change to foster the transition to a circular economy, in: *Design Research Society 50th Anniversary Conference*. Brighton, UK, pp. 1305–1321.
- Pohland, F.G., Bloodgood, D.E., 1963. Laboratory studies on mesophilic and thermophilic anaerobic sludge digestion. *J. (Water Pollut. Control Fed.* 35, 11–42.
- Poirier, S., Madigou, C., Bouchez, T., Chapleur, O., 2017. Improving anaerobic digestion with support media: Mitigation of ammonia inhibition and effect on microbial communities. *Bioresour. Technol.* 235, 229–239. <https://doi.org/10.1016/j.biortech.2017.03.099>
- Pokhrel, D., Viraraghavan, T., 2004. Treatment of pulp and paper mill wastewater - a review. *Sci. Total Environ.* 333, 37–58. <https://doi.org/10.1016/j.scitotenv.2004.05.017>
- Prazeres, A.R., Carvalho, F., Rivas, J., 2012. Cheese whey management: A review. *J. Environ. Manage.* 110, 48–68. <https://doi.org/10.1016/j.jenvman.2012.05.018>
- Pullen, T., 2015. *Anaerobic digestion: making biogas, making energy*. Taylor & Francis Group, New York, NY.
- Quartz Business Media, 2008. All about aluminium. *Alum. Int. Today* 20, 103.
- Rabinovich, D., 2013. The allure of aluminium. *Nat. Chem.* 76.
- Rajamma, R., Ball, R.J., Tarelho, L.A.C., Allen, G.C., Labrincha, J.A., Ferreira, V.M., 2009. Characterisation and use of biomass fly ash in cement-based materials. *J. Hazard. Mater.* 172, 1049–1060. <https://doi.org/10.1016/j.jhazmat.2009.07.109>
- Rajeshwari, K., Balakrishnan, M., Kansal, A., Lata, K., Kishore, V.V., 2000. State-of-the-art of anaerobic digestion technology for industrial wastewater treatment. *Renew. Sustain. Energy Rev.* 4, 135–156. [https://doi.org/10.1016/S1364-0321\(99\)00014-3](https://doi.org/10.1016/S1364-0321(99)00014-3)
- Rama, G.R., Kuhn, D., Beux, S., Maciel, M.J., Volken de Souza, C.F., 2019. Potential applications of dairy whey for the production of lactic acid bacteria cultures. *Int. Dairy J.* 98, 25–37. <https://doi.org/10.1016/j.idairyj.2019.06.012>
- Rasapoor, M., Young, B., Brar, R., Sarmah, A., Zhuang, W.-Q., Baroutian, S., 2020. Recognizing the challenges of anaerobic digestion: Critical steps toward improving biogas generation. *Fuel* 261, 116497. <https://doi.org/10.1016/j.fuel.2019.116497>
- Raschid-Sally, L., Jayakody, P., 2008. Drivers and characteristics of wastewater agriculture in developing countries: Results from a global assessment. Colombo, Sri Lanka.
- Ratusznei, S.M., Rodrigues, J.A.D., Zaiat, M., 2003. Operating feasibility of anaerobic whey treatment in a stirred sequencing batch reactor containing immobilized biomass. *Water Sci. Technol.* 48, 179–186. <https://doi.org/10.2166/wst.2003.0391>
- Ribbing, C., 2007. Environmentally friendly use of non-coal ashes in Sweden. *Waste Manag.* 27, 1428–1435. <https://doi.org/10.1016/j.wasman.2007.03.012>
- Ribeiro, J.P., Marques, C.C., Portugal, I., Nunes, M.I., 2020. AOX removal from pulp and paper wastewater by Fenton and photo-Fenton processes: A real case-study. *Energy Reports* 6, 770–775. <https://doi.org/10.1016/j.egy.2019.09.068>
- Ribera-Pi, J., Badia-Fabregat, M., Calderer, M., Polášková, M., Svojitka, J., Rovira, M., Jubany, I., Martínez-Lladó, X., 2020. Anaerobic Membrane Bioreactor (AnMBR) for the treatment of cheese whey for the potential recovery of water and energy. *Waste and Biomass Valorization* 11, 1821–1835. <https://doi.org/10.1007/s12649-018-0482-8>
- Rintala, J., Lepistö, R., Chand, S., 1992. Toxicity of kraft bleaching effluents on thermophilic and mesophilic VFA methanation. *Bioresour. Technol.* 42, 17–26. [https://doi.org/10.1016/0960-8524\(92\)90083-A](https://doi.org/10.1016/0960-8524(92)90083-A)
- Rintala, J., Puhakka, J.A., 1994. Anaerobic treatment in pul- and paper-mill waste management: A review. *Bioresour. Technol.* 47, 1–18. [https://doi.org/10.1016/0960-8524\(94\)90022-1](https://doi.org/10.1016/0960-8524(94)90022-1)
- Rodgers, M., Zhan, X.-M., Dolan, B., 2004. Mixing characteristics and whey wastewater treatment of a novel moving anaerobic biofilm reactor. *J. Environ. Sci. Heal. Part A* 39, 2183–2193. <https://doi.org/10.1081/ESE-120039383>
- Rodriguez, D.J., Serrano, H.A., Delgado, A., Nolasco, D., Saltiel, G., 2020. From Waste to Resource: Shifting paradigms for smarter wastewater interventions in Latin America and the Caribbean. World Bank, Washington, DC.
- Romero-Güiza, M.S., Vila, J., Mata-Alvarez, J., Chimenos, J.M., Astals, S., 2016. The role of additives on anaerobic digestion: A review. *Renew. Sustain. Energy Rev.* 58, 1486–1499. <https://doi.org/10.1016/j.rser.2015.12.094>

- Rosa, D.D., Dias, M.M.S., Grzeškowiak, Ł.M., Reis, S.A., Conceição, L.L., Peluzio, M. do C.G., 2017. Milk kefir: nutritional, microbiological and health benefits. *Nutr. Res. Rev.* 30, 82–96. <https://doi.org/10.1017/S0954422416000275>
- Ruas, D.B., Chaparro, T.R., Pires, E.C., 2012. Advanced oxidation process H₂O₂/UV combined with anaerobic digestion to remove chlorinated organics from bleached kraft pulp mill wastewater. *Rev. Fac. Ing. Univ. Antioquia* 63, 43–54.
- Ruģele, K., Bumanis, G., Eriņa, L., Erdmane, D., 2014. Composite Material for Effective Cheese Whey Anaerobic Digestion. *Key Eng. Mater.* 604, 236–239. <https://doi.org/10.4028/www.scientific.net/KEM.604.236>
- Ruģele, K., Bumanis, G., Mezule, L., Juhna, T., Bajare, D., 2015a. Application of industrial wastes in renewable energy production. *Agron. Res.* 13, 526–532.
- Ruģele, K., Skripsts, E., Mezule, L., Pitk, P., Bajare, D., Juhna, T., 2015b. Use of alkali-activated aluminosilicate material to enhance biogas production from acidic whey. *Open Biotechnol. J.* 9, 54–60. <https://doi.org/10.2174/1874070701509010054>
- Saddoud, A., Hassaïri, I., Sayadi, S., 2007. Anaerobic membrane reactor with phase separation for the treatment of cheese whey. *Bioresour. Technol.* 98, 2102–2108. <https://doi.org/10.1016/j.biortech.2006.08.013>
- Sailer, G., Eichermüller, J., Poetsch, J., Paczkowski, S., Pelz, S., Oechsner, H., Müller, J., 2020. Optimizing anaerobic digestion of organic fraction of municipal solid waste (OFMSW) by using biomass ashes as additives. *Waste Manag.* 109, 136–148. <https://doi.org/10.1016/j.wasman.2020.04.047>
- Sandberg, C., Hill, J., Jackson, M., 2020. On the development of the refiner mechanical pulping process – a review. *Nord. Pulp Pap. Res. J.* 35, 1–17. <https://doi.org/10.1515/npprj-2019-0083>
- Sangha, A.K., Petridis, L., Smith, J.C., Ziebell, A., Parks, J.M., 2012. Molecular simulation as a tool for studying lignin. *Environ. Prog. Sustain. Energy* 31, 47–54. <https://doi.org/10.1002/ep.10628>
- Sansonetti, S., Curcio, S., Calabrò, V., Iorio, G., 2009. Bio-ethanol production by fermentation of ricotta cheese whey as an effective alternative non-vegetable source. *Biomass and Bioenergy* 33, 1687–1692. <https://doi.org/10.1016/j.biombioe.2009.09.002>
- Santonja, G.G., Karlis, P., Stubdrup, K.R., Brinkmann, T., Roudier, S., 2019. Best Available Techniques (BAT) reference document for the food, drink and milk industries. European Commission, Luxembourg. <https://doi.org/10.2760/243911>
- Santos, V.R. dos, Cabrelon, M.D., Trichês, E. de S., Quinteiro, E., 2019. Green liquor dregs and slaker grits residues characterization of a pulp and paper mill for future application on ceramic products. *J. Clean. Prod.* 240, 118220. <https://doi.org/10.1016/j.jclepro.2019.118220>
- Santos, R.B., Hart, P., Jameel, H., Chang, H., 2013. Wood based lignin reactions important to the biorefinery and pulp and paper industries. *BioResources* 8. <https://doi.org/10.15376/biores.8.1.1456-1477>
- Savant, D.V., Abdul-Rahman, R., Ranade, D.R., 2006. Anaerobic degradation of adsorbable organic halides (AOX) from pulp and paper industry wastewater. *Bioresour. Technol.* 97, 1092–1104. <https://doi.org/10.1016/j.biortech.2004.12.013>
- Sazama, P., Bortnovsky, O., Dědeček, J., Tvarůžková, Z., Sobalík, Z., 2011. Geopolymer based catalysts—New group of catalytic materials. *Catal. Today* 164, 92–99. <https://doi.org/10.1016/j.cattod.2010.09.008>
- Schaechter, M., 2004. *The Desk Encyclopedia of Microbiology*. Elsevier Ltd, London.
- Seadi, T. Al, Rutz, D., Prassl, H., Köttner, M., Finsterwalder, T., Volk, S., Janssen, R., 2008. *Biogas Handbook*. University of Southern Denmark Esbjerg, Esbjerg, Denmark.
- Sglavo, V.M., Maurina, S., Conci, A., Salviati, A., Carturan, G., Cocco, G., 2000. Bauxite “red mud” in the ceramic industry. Part 2: production of clay-based ceramics. *J. Eur. Ceram. Soc.* 20, 245–252. [https://doi.org/10.1016/S0955-2219\(99\)00156-9](https://doi.org/10.1016/S0955-2219(99)00156-9)
- Shah, Y.T., 2017. Biogas and biohydrogen production by anaerobic digestion, in: Shah, Y.T. (Ed.), *Chemical Energy from Natural and Synthetic Gas*. CRC Press, New York, NY, pp. 219–275.
- Shah, Y.T., 2014. Anaerobic digestion of aqueous waste for methane and hydrogen, in: Shah, Y.T. (Ed.), *Water for Energy and Fuel Production*. CRC Press, New York, NY, pp. 205–225.
- Shamurad, B., Gray, N., Petropoulos, E., Tabraiz, S., Acharya, K., Quintela-Baluja, M., Sallis, P., 2019. Co-digestion of organic and mineral wastes for enhanced biogas production: Reactor performance and evolution of microbial community and function. *Waste Manag.* 87, 313–325. <https://doi.org/10.1016/j.wasman.2019.02.021>
- Shamurad, B., Gray, N., Petropoulos, E., Tabraiz, S., Membere, E., Sallis, P., 2020. Predicting the effects of integrating mineral wastes in anaerobic digestion of OFMSW using first-order and Gompertz models from biomethane potential assays. *Renew. Energy* 152, 308–319. <https://doi.org/10.1016/j.renene.2020.01.067>

- Sharma, N., Bhardwaj, N.K., Singh, R.B.P., 2020. Environmental issues of pulp bleaching and prospects of peracetic acid pulp bleaching: A review. *J. Clean. Prod.* 256, 120338. <https://doi.org/10.1016/j.jclepro.2020.120338>
- Shen, Y., Linville, J.L., Urgun-Demirtas, M., Schoene, R.P., Snyder, S.W., 2015. Producing pipeline-quality biomethane via anaerobic digestion of sludge amended with corn stover biochar with in-situ CO₂ removal. *Appl. Energy* 158, 300–309. <https://doi.org/10.1016/j.apenergy.2015.08.016>
- Sigma-Aldrich, 2020. Website of Sigma Aldrich [WWW Document]. URL <https://www.sigmaaldrich.com/portugal.html> (accessed 4.4.20).
- Silva, F.C., Serafim, L.S., Nadais, H., Arroja, L., Capela, I., 2013. Acidogenic fermentation towards valorisation of organic waste streams into volatile fatty acids. *Chem. Biochem. Eng. Q.* 27, 467–476.
- Simão, L., Hotza, D., Raupp-Pereira, F., Labrincha, J.A., Montedo, O.R.K., 2018. Wastes from pulp and paper mills - a review of generation and recycling alternatives. *Cerâmica* 64, 443–453. <https://doi.org/10.1590/0366-69132018643712414>
- Singh, N.B., 2018. Fly ash-based geopolymer binder: A future construction material. *Minerals* 8, 299. <https://doi.org/10.3390/min8070299>
- Singh, P., Katiyar, D., Gupta, M., Singh, A., 2011. Removal of pollutants from pulp and paper mill effluent by anaerobic and aerobic treatment in pilot-scale bioreactor. *Int. J. Environ. Waste Manag.* 7, 436–444. <https://doi.org/10.1504/IJEW.2011.039480>
- Singh, P., Thakur, I.S., 2006. Colour removal of anaerobically treated pulp and paper mill effluent by microorganisms in two steps bioreactor. *Bioresour. Technol.* 97, 218–223. <https://doi.org/10.1016/j.biortech.2005.02.022>
- Smithers, G.W., 2015. Whey-ing up the options – Yesterday, today and tomorrow. *Int. Dairy J.* 48, 2–14. <https://doi.org/10.1016/j.idairyj.2015.01.011>
- Soriano-Perez, S., Flores-Velez, L., Alonso-Davila, P., Cervantes-Cruz, G., Arriaga, S., 2012. Production of lactic acid from cheese whey by batch cultures of *Lactobacillus helveticus*. *Ann. Microbiol.* 62, 313–317. <https://doi.org/10.1007/s13213-011-0264-z>
- Speece, R.E., 1996. *Anaerobic biotechnology for industrial wastewaters*. Archae Press, Nashville, USA.
- Sridhar, R., Sivakumar, V., Prince Immanuel, V., Prakash Maran, J., 2011. Treatment of pulp and paper industry bleaching effluent by electrocoagulant process. *J. Hazard. Mater.* 186, 1495–1502. <https://doi.org/10.1016/j.jhazmat.2010.12.028>
- Steffen, F., Requejo, A., Ewald, C., Janzon, R., Saake, B., 2016. Anaerobic digestion of fines from recovered paper processing – Influence of fiber source, lignin and ash content on biogas potential. *Bioresour. Technol.* 200, 506–513. <https://doi.org/10.1016/j.biortech.2015.10.014>
- Sung, S., Liu, T., 2003. Ammonia inhibition on thermophilic anaerobic digestion. *Chemosphere* 53, 43–52. [https://doi.org/10.1016/S0045-6535\(03\)00434-X](https://doi.org/10.1016/S0045-6535(03)00434-X)
- Sushil, S., Batra, V.S., 2008. Catalytic applications of red mud, an aluminium industry waste: A review. *Appl. Catal. B Environ.* 81, 64–77. <https://doi.org/10.1016/j.apcatb.2007.12.002>
- Tabatabaei, M., Rahim, R.A., Abdullah, N., Wright, A.-D.G., Shirai, Y., Sakai, K., Sulaiman, A., Hassan, M.A., 2010. Importance of the methanogenic archaea populations in anaerobic wastewater treatments. *Process Biochem.* 45, 1214–1225. <https://doi.org/10.1016/j.procbio.2010.05.017>
- Tabatabaei, M., Valijanian, E., Aghbashlo, M., Ghanavati, H., Sulaiman, A., Wakisaka, M., 2018. Prominent parameters in biogas production systems, in: Tabatabaei, M., Ghanavati, H. (Eds.), *Biogas: Fundamentals, Process and Operation, Biofuel and Biorefinery Technologies*. Springer International Publishing, Cham, pp. 135–163. <https://doi.org/10.1007/978-3-319-77335-3>
- Taconi, K.A., Zappi, M.E., Todd French, W., Brown, L.R., 2008. Methanogenesis under acidic pH conditions in a semi-continuous reactor system. *Bioresour. Technol.* 99, 8075–8081. <https://doi.org/10.1016/j.biortech.2008.03.068>
- Tada, C., Yang, Y., Hanaoka, T., Sonoda, A., Ooi, K., Sawayama, S., 2005. Effect of natural zeolite on methane production for anaerobic digestion of ammonium rich organic sludge. *Bioresour. Technol.* 96, 459–464. <https://doi.org/10.1016/j.biortech.2004.05.025>
- Takada, M., Chandra, R., Wu, J., Saddler, J.N., 2020. The influence of lignin on the effectiveness of using a chemithermomechanical pulping based process to pretreat softwood chips and pellets prior to enzymatic hydrolysis. *Bioresour. Technol.* 302, 122895. <https://doi.org/10.1016/j.biortech.2020.122895>
- Takashima, M., Speece, R.E., Parkin, G.F., 1990. Mineral requirements for methane fermentation. *Crit. Rev. Environ. Control* 19, 465–479. <https://doi.org/10.1080/10643389009388378>
- Tang, Q., Ge, Y., Wang, K., He, Y., Cui, X., 2015. Preparation and characterization of porous metakaolin-based inorganic polymer spheres as an adsorbent. *Mater. Des.* 88, 1244–1249. <https://doi.org/10.1016/j.matdes.2015.09.126>

- Tarvin, D., Buswell, A.M., 1934. The methane fermentation of organic acids and carbohydrates. *J. Am. Chem. Soc.* 56, 1751–1755. <https://doi.org/10.1021/ja01323a030>
- Taseli, B.K., 2008. Fungal treatment of hemp-based pulp and paper mill wastes. *African J. Biotechnol.* 7, 286–289.
- Tetra Pak, 2015. Dairy processing handbook, 3rd ed. Tetra Pak International S.A., Sweden.
- Thauer, R.K., Shima, S., 2008. Methane as fuel for anaerobic microorganisms. *Ann. N. Y. Acad. Sci.* 1125, 158–170. <https://doi.org/10.1196/annals.1419.000>
- Toniolo, N., Boccaccini, A.R., 2017. Fly ash-based geopolymers containing added silicate waste. A review. *Ceram. Int.* 43, 14545–14551. <https://doi.org/10.1016/j.ceramint.2017.07.221>
- Torres, C.M.M.E., Silva, C.M., Pedroti, L.G., Fernandes, W.E.H., Ballotin, F.C., Zanuncio, A.J.V., 2020. Dregs and grits from kraft pulp mills incorporated to Portland cement clinker. *J. Mater. Cycles Waste Manag.* 22, 851–861. <https://doi.org/10.1007/s10163-020-00983-x>
- Tran, H., Vakkilainen, E.K., 2008. The Kraft chemical recovery process, in: *Proceedings of the Tappi Kraft Pulping Short Course*. St. Petersburg, FL, USA, pp. 1.1:1–1.1:8.
- Treu, L., Tsapekos, P., Peprah, M., Campanaro, S., Giacomini, A., Corich, V., Kougias, P.G., Angelidaki, I., 2019. Microbial profiling during anaerobic digestion of cheese whey in reactors operated at different conditions. *Bioresour. Technol.* 275, 375–385. <https://doi.org/10.1016/j.biortech.2018.12.084>
- Tsakiridis, P.E., Agatzini-Leonardou, S., Oustadakis, P., 2004. Red mud addition in the raw meal for the production of Portland cement clinker. *J. Hazard. Mater.* 116, 103–110. <https://doi.org/10.1016/j.jhazmat.2004.08.002>
- Tsang, Y.F., Hua, F.L., Chua, H., Sin, S.N., Wang, Y.J., 2007. Optimization of biological treatment of paper mill effluent in a sequencing batch reactor. *Biochem. Eng. J.* 34, 193–199. <https://doi.org/10.1016/j.bej.2006.12.004>
- United Nations, 2020. Website of United Nations [WWW Document]. URL <https://sustainabledevelopment.un.org/#> (accessed 4.3.20).
- United Nations World Water Assessment Programme, 2017. The United Nations world water development report 2017: wastewater the untapped resource. UNESCO, Paris, France.
- United Nations World Water Assessment Programme, 2014. The United Nations world water development report 2014: water and energy. UNESCO, Paris, France.
- Van, D.P., Fujiwara, T., Leu Tho, B., Song Toan, P.P., Hoang Minh, G., 2019. A review of anaerobic digestion systems for biodegradable waste: Configurations, operating parameters, and current trends. *Environ. Eng. Res.* 25, 1–17. <https://doi.org/10.4491/eer.2018.334>
- Van Lier, J.B., Rebac, S., Lens, P., van Bijnen, F., Oude Elferink, S.J.W.H., Stams, A.J.M., Lettinga, G., 1997. Anaerobic treatment of partly acidified wastewater in a two-stage expanded granular sludge bed (EGSB) system at 8°C. *Water Sci. Technol.* 36, 317–324. [https://doi.org/10.1016/S0273-1223\(97\)00538-6](https://doi.org/10.1016/S0273-1223(97)00538-6)
- Venetsaneas, N., Antonopoulou, G., Stamatelatou, K., Kornaros, M., Lyberatos, G., 2009. Using cheese whey for hydrogen and methane generation in a two-stage continuous process with alternative pH controlling approaches. *Bioresour. Technol.* 100, 3713–3717. <https://doi.org/10.1016/j.biortech.2009.01.025>
- Vergine, P., Sousa, F., Lopes, M., Silva, F., Gameiro, T., Nadais, H., Capela, I., 2015. Synthetic soft drink wastewater suitability for the production of volatile fatty acids. *Process Biochem.* 50, 1308–1312. <https://doi.org/10.1016/j.procbio.2015.04.007>
- Verma, O.P., Manik, G., Sethi, S.K., 2019. A comprehensive review of renewable energy source on energy optimization of black liquor in MSE using steady and dynamic state modeling, simulation and control. *Renew. Sustain. Energy Rev.* 100, 90–109. <https://doi.org/10.1016/j.rser.2018.10.002>
- Vichaphund, S., Aht-Ong, D., Sricharoenchaikul, V., Atong, D., 2014. Characteristic of fly ash derived-zeolite and its catalytic performance for fast pyrolysis of Jatropha waste. *Environ. Technol.* 35, 2254–2261. <https://doi.org/10.1080/09593330.2014.900118>
- Wainaina, S., Lukitawesa, Kumar Awasthi, M., Taherzadeh, M.J., 2019. Bioengineering of anaerobic digestion for volatile fatty acids, hydrogen or methane production: A critical review. *Bioengineered* 10, 437–458. <https://doi.org/10.1080/21655979.2019.1673937>
- Wang, B., Wang, J., Xu, L.Y., Zhang, J.H., Ai, N.S., Cao, Y.P., 2020. Characterization of the key odorants in kurut with aroma recombination and omission studies. *J. Dairy Sci.* 103, 4164–4173. <https://doi.org/10.3168/jds.2019-17521>
- Wang, D., Ai, J., Shen, F., Yang, G., Zhang, Y., Deng, S., Zhang, J., Zeng, Y., Song, C., 2017. Improving anaerobic digestion of easy-acidification substrates by promoting buffering capacity using biochar derived from vermicompost. *Bioresour. Technol.* 227, 286–296. <https://doi.org/10.1016/j.biortech.2016.12.060>
- Wang, L., Hu, G., Lyu, F., Yue, T., Tang, H., Han, H., Yang, Y., Liu, R., Sun, W., 2019. Application of red mud in wastewater treatment. *Minerals* 9, 281. <https://doi.org/10.3390/min9050281>

- Wang, S., Ang, H.M., Tadé, M.O., 2008. Novel applications of red mud as coagulant, adsorbent and catalyst for environmentally benign processes. *Chemosphere* 72, 1621–1635. <https://doi.org/10.1016/j.chemosphere.2008.05.013>
- Wang, S., Hou, X., Su, H., 2017. Exploration of the relationship between biogas production and microbial community under high salinity conditions. *Sci. Rep.* 7, 1149. <https://doi.org/10.1038/s41598-017-01298-y>
- Ware, A., Power, N., 2017. Modelling methane production kinetics of complex poultry slaughterhouse wastes using sigmoidal growth functions. *Renew. Energy* 104, 50–59. <https://doi.org/10.1016/j.renene.2016.11.045>
- Watanabe, R., Tada, C., Baba, Y., Fukuda, Y., Nakai, Y., 2013. Enhancing methane production during the anaerobic digestion of crude glycerol using Japanese cedar charcoal. *Bioresour. Technol.* 150, 387–392. <https://doi.org/10.1016/j.biortech.2013.10.030>
- Wei, W., Liu, X., Wu, L., Wang, D., Bao, T., Ni, B.-J., 2020. Sludge incineration bottom ash enhances anaerobic digestion of primary sludge toward highly efficient sludge anaerobic codigestion. *ACS Sustain. Chem. Eng.* 8, 3005–3012. <https://doi.org/10.1021/acssuschemeng.0c00015>
- Weiss-Hortala, E., Chesnaud, A., Haurie, L., Lyczko, N., Munirathinam, R., Nzihou, A., Patry, S., Pham Minh, D., White, C.E., 2020. Solid Residues (Biochar, Bottom Ash, Fly Ash, ...), in: *Handbook on Characterization of Biomass, Biowaste and Related By-Products*. Springer International Publishing, Cham, pp. 1307–1387. https://doi.org/10.1007/978-3-030-35020-8_15
- Wiegand, P.S., Flinders, C.A., Ice, G.G., Sleep, D.J.H., Malberg, B.J., Lama, I., 2011. Water profiles of the forest products industry and their utility in sustainability assessment. *TAPPI J.* 10, 19–27. <https://doi.org/10.32964/TJ10.7.19>
- Wijekoon, K.C., Visvanathan, C., Abeynayaka, A., 2011. Effect of organic loading rate on VFA production, organic matter removal and microbial activity of a two-stage thermophilic anaerobic membrane bioreactor. *Bioresour. Technol.* 102, 5353–5360. <https://doi.org/10.1016/j.biortech.2010.12.081>
- World Aluminium, 2020. Website of World Aluminium [WWW Document]. URL <http://bauxite.world-aluminium.org/home/> (accessed 5.26.20).
- World Bioenergy Association, 2020. Global Bioenergy Statistics 2019. Stockholm, Sweden.
- Xu, S., He, C., Luo, L., Lü, F., He, P., Cui, L., 2015. Comparing activated carbon of different particle sizes on enhancing methane generation in upflow anaerobic digester. *Bioresour. Technol.* 196, 606–612. <https://doi.org/10.1016/j.biortech.2015.08.018>
- Yamaguchi, T., Harada, H., Hisano, T., Yamazaki, S., Tseng, I.-C., 1999. Process behavior of UASB reactor treating a wastewater containing high strength sulfate. *Water Res.* 33, 3182–3190. [https://doi.org/10.1016/S0043-1354\(99\)00029-9](https://doi.org/10.1016/S0043-1354(99)00029-9)
- Yan, J.Q., Lo, K. V., Pinder, K.L., 1993. Instability caused by high strength of cheese whey in a UASB reactor. *Biotechnol. Bioeng.* 41, 700–706. <https://doi.org/10.1002/bit.260410704>
- Yang, J., Zhang, D., Hou, J., He, B., Xiao, B., 2008. Preparation of glass-ceramics from red mud in the aluminium industries. *Ceram. Int.* 34, 125–130. <https://doi.org/10.1016/j.ceramint.2006.08.013>
- Yang, K., Yu, Y., Hwang, S., 2003. Selective optimization in thermophilic acidogenesis of cheese-whey wastewater to acetic and butyric acids: partial acidification and methanation. *Water Res.* 37, 2467–2477. [https://doi.org/10.1016/S0043-1354\(03\)00006-X](https://doi.org/10.1016/S0043-1354(03)00006-X)
- Yang, Y., Tada, C., Miah, M.S., Tsukahara, K., Yagishita, T., Sawayama, S., 2004. Influence of bed materials on methanogenic characteristics and immobilized microbes in anaerobic digester. *Mater. Sci. Eng. C* 24, 413–419. <https://doi.org/10.1016/j.msec.2003.11.005>
- Ye, J., Hu, A., Cheng, X., Lin, W., Liu, X., Zhou, S., He, Z., 2018a. Response of enhanced sludge methanogenesis by red mud to temperature: Spectroscopic and electrochemical elucidation of endogenous redox mediators. *Water Res.* 143, 240–249. <https://doi.org/10.1016/j.watres.2018.06.061>
- Ye, J., Hu, A., Ren, G., Chen, M., Tang, J., Zhang, P., Zhou, S., He, Z., 2018b. Enhancing sludge methanogenesis with improved redox activity of extracellular polymeric substances by hematite in red mud. *Water Res.* 134, 54–62. <https://doi.org/10.1016/j.watres.2018.01.062>
- Ye, J., Hu, A., Ren, G., Zhou, T., Zhang, G., Zhou, S., 2018c. Red mud enhances methanogenesis with the simultaneous improvement of hydrolysis-acidification and electrical conductivity. *Bioresour. Technol.* 247, 131–137. <https://doi.org/10.1016/j.biortech.2017.08.063>
- Yin, C., Shen, Y., Zhu, N., Huang, Q., Lou, Z., Yuan, H., 2018. Anaerobic digestion of waste activated sludge with incineration bottom ash: Enhanced methane production and CO₂ sequestration. *Appl. Energy* 215, 503–511. <https://doi.org/10.1016/j.apenergy.2018.02.056>
- Yoon, Y., Lee, S., Choi, K.-H., 2016. Microbial benefits and risks of raw milk cheese. *Food Control* 63, 201–215. <https://doi.org/10.1016/j.foodcont.2015.11.013>
- You, S., Chang, H., Yin, Q., Qi, W., Wang, M., Su, R., He, Z., 2017. Utilization of whey powder as substrate for

- low-cost preparation of β -galactosidase as main product, and ethanol as by-product, by a litre-scale integrated process. *Bioresour. Technol.* 245, 1271–1276. <https://doi.org/10.1016/j.biortech.2017.08.092>
- Youngsukkasem, S., Rakshit, S.K., Taherzadeh, M.J., 2012. Biogas production by encapsulated methane-producing bacteria. *BioResources* 7, 56–65.
- Zacco, A., Borgese, L., Gianoncelli, A., Struis, R.P.W.J., Depero, L.E., Bontempi, E., 2014. Review of fly ash inertisation treatments and recycling. *Environ. Chem. Lett.* 12, 153–175. <https://doi.org/10.1007/s10311-014-0454-6>
- Zhang, C., Su, H., Baeyens, J., Tan, T., 2014. Reviewing the anaerobic digestion of food waste for biogas production. *Renew. Sustain. Energy Rev.* 38, 383–392. <https://doi.org/10.1016/j.rser.2014.05.038>
- Zhang, J., Wang, Q., Zheng, P., Wang, Y., 2014. Anaerobic digestion of food waste stabilized by lime mud from papermaking process. *Bioresour. Technol.* 170, 270–277. <https://doi.org/10.1016/j.biortech.2014.08.003>
- Zhang, J., Zang, L., 2016. Enhancement of biohydrogen production from brewers' spent grain by calcined-red mud pretreatment. *Bioresour. Technol.* 209, 73–79. <https://doi.org/10.1016/j.biortech.2016.02.110>
- Zhang, J., Zhang, R., He, Q., Ji, B., Wang, H., Yang, K., 2020. Adaptation to salinity: Response of biogas production and microbial communities in anaerobic digestion of kitchen waste to salinity stress. *J. Biosci. Bioeng.* 130, 173–178. <https://doi.org/10.1016/j.jbiosc.2019.11.011>
- Zhang, J., Zhang, Y., Quan, X., Liu, Y., An, X., Chen, S., Zhao, H., 2011. Bioaugmentation and functional partitioning in a zero valent iron-anaerobic reactor for sulfate-containing wastewater treatment. *Chem. Eng. J.* 174, 159–165. <https://doi.org/10.1016/j.cej.2011.08.069>
- Zhang, M., Zang, L., 2019. A review of interspecies electron transfer in anaerobic digestion. *IOP Conf. Ser. Earth Environ. Sci.* 310, 042026. <https://doi.org/10.1088/1755-1315/310/4/042026>
- Zhang, R., Zheng, S., Ma, S., Zhang, Y., 2011. Recovery of alumina and alkali in Bayer red mud by the formation of andradite-grossular hydrogarnet in hydrothermal process. *J. Hazard. Mater.* 189, 827–835. <https://doi.org/10.1016/j.jhazmat.2011.03.004>
- Zhang, W., Li, L., Wang, X., Xing, W., Li, R., Yang, T., Lv, D., 2020. Role of trace elements in anaerobic digestion of food waste: Process stability, recovery from volatile fatty acid inhibition and microbial community dynamics. *Bioresour. Technol.* 315, 123796. <https://doi.org/10.1016/j.biortech.2020.123796>
- Zhang, Y., Feng, Y., Yu, Q., Xu, Z., Quan, X., 2014. Enhanced high-solids anaerobic digestion of waste activated sludge by the addition of scrap iron. *Bioresour. Technol.* 159, 297–304. <https://doi.org/10.1016/j.biortech.2014.02.114>
- Zhang, Y., Jing, Y., Zhang, J., Sun, L., Quan, X., 2011. Performance of a ZVI-UASB reactor for azo dye wastewater treatment. *J. Chem. Technol. Biotechnol.* 86, 199–204. <https://doi.org/10.1002/jctb.2485>
- Zhang, Y., Liu, L., 2013. Fly ash-based geopolymer as a novel photocatalyst for degradation of dye from wastewater. *Particuology* 11, 353–358. <https://doi.org/10.1016/j.partic.2012.10.007>
- Zhang, Z., Provis, J.L., Reid, A., Wang, H., 2014. Fly ash-based geopolymers: The relationship between composition, pore structure and efflorescence. *Cem. Concr. Res.* 64, 30–41. <https://doi.org/10.1016/j.cemconres.2014.06.004>
- Zhuang, X.Y., Chen, L., Komarneni, S., Zhou, C.H., Tong, D.S., Yang, H.M., Yu, W.H., Wang, H., 2016. Fly ash-based geopolymer: clean production, properties and applications. *J. Clean. Prod.* 125, 253–267. <https://doi.org/10.1016/j.jclepro.2016.03.019>
- Zotta, T., Solieri, L., Iacumin, L., Picozzi, C., Gullo, M., 2020. Valorization of cheese whey using microbial fermentations. *Appl. Microbiol. Biotechnol.* 104, 2749–2764. <https://doi.org/10.1007/s00253-020-10408-2>

Appendices | 7

7 | Appendices

7.1 Example of a calibration curve for total phosphorous as orthophosphates determination

To perform the calibration curve for P determination, a stock solution was prepared. 0.1 g of KH_2PO_4 was weighed rigorously and dissolved in 500 mL of distilled water. In 100 mL volumetric flasks, the following six standards were prepared, with different concentrations:

Table 44| Preparation of stock solutions for total phosphorous as orthophosphates determination.

[P] (mg/L)	Volume of KH_2PO_4 stock solution (mL)
0.0	0.0
0.2	0.4
0.4	0.8
0.6	1.2
0.8	1.6
1.0	2.0

After spectrophotometric measurements at 880 nm of each standard, the calibration curve was prepared, plotting absorbance *versus* phosphate standard concentration. Figure 93 shows an example of the calibration curve for total phosphorous as orthophosphates determination.

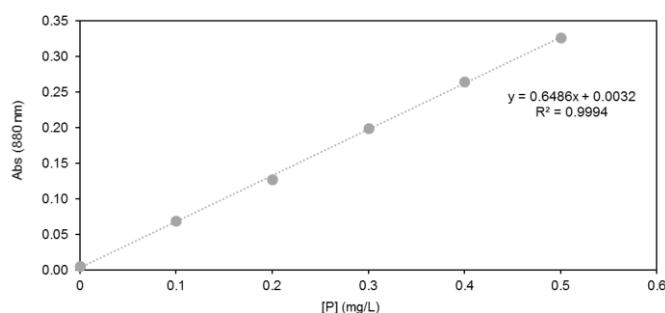


Figure 93| Example of a calibration curve for the determination of total phosphorous as orthophosphates.

7.2 Development of the method for determination of adsorbable organic halides

For adsorbable organic halides determination, the following solutions were used:

- Nitric acid (diluted): 0.02 M

In a 1000 mL volumetric flask, dilute 1.372 mL of concentrated nitric acid (65 %) in distilled water.

- Hydrochloric acid (diluted): 0.01 M

In a 1000 mL volumetric flask, dilute 0.821 mL of concentrated hydrochloric acid (37 %) in distilled water.

- Nitrate stock solution: 0.2 M

In a 1000 mL volumetric flask, dissolve 17 g of NaNO_3 in about 100 mL of distilled water; add 25 mL of concentrated nitric acid (65 %), and add distilled water until final volume.

- Nitrate washing solution: 0.01 M

Dilute 50 mL of nitrate stock solution in a 1000 mL volumetric flask and add distilled water until final volume.

- 4-chlorophenol (4-CF) standard stock solution: [AOX] = 200 mg_{Cl}/L

Dissolve 72.5 mg of 4-CF in distilled water using a 100 mL volumetric flask.

- 4-CF standard working solution: 1 mg_{Cl}/L

Dilute 5 mL of 4-CF standard stock solution in distilled water using a 1000 mL volumetric flask.

- Checking standard solutions:

Dilute the volumes indicated in Table 45 in distilled water using a 100 mL volumetric flask. On each analysis day, read at least one checking standard solution to confirm the signal of the equipment.

Table 45 | Checking standard solutions for AOX determination.

[AOX] (μg _{Cl} /L)	Volume of 4-CF standard working solution (mL)
10	1
50	5
100	10
200	20
250	25

- Electrolyte solution:

In a 1000 mL volumetric flask, add 1 g of sodium perchlorate to 750 mL of glacial acetic acid, and add distilled water until final volume.

7.3 Example of calibration curves for volatile fatty acids determination

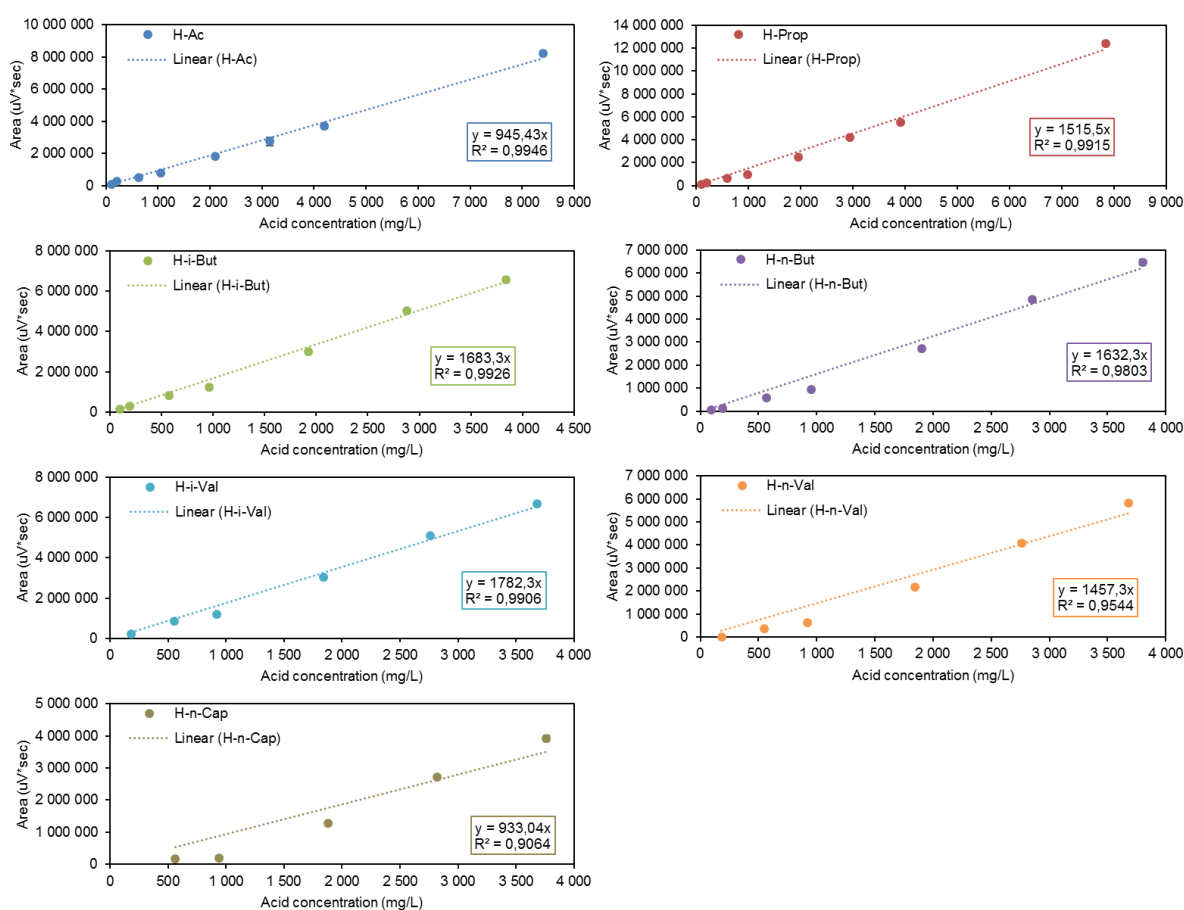
To perform the calibration curves for each acidic specie quantified, several standard solutions with different concentrations of VFA were analyzed under the same conditions as the samples from the digesters. The stock VFA solution contained a mixture of seven acid species, namely acetic, propionic, i-butyric, n-butyric, i-valeric, n-valeric, and n-caproic acids. It was prepared by adding 1 mL of commercial pure acids to a 100 mL volumetric flask. From the stock VFA solution, nine diluted standards were prepared in 25 mL volumetric flasks, with different VFA concentrations. The concentrations of each acidic specie in each standard are listed in Table 46.

The calibration curves were performed by plotting the area obtained by chromatographic analysis versus the concentration of each acidic specie. Figure 94 shows an example of the calibration curves for each quantified acidic specie. The figure shows the linear regression parameters for each calibration curve obtained by the ordinary least squares method.

Table 47 lists the retention time for each acidic specie and the slop obtained on the calibration lines. The slop was used to calculate the concentration of individual acidic species in the samples analyzed. This table also shows the determination coefficient for each calibration line.

Table 46| Concentration of acidic species in the diluted standard solutions for VFA determination.

ID	Volume of stock solution (mL)	H-Ac (mg/L)	H-Prop (mg/L)	H-i-But (mg/L)	H-n-But (mg/L)	H-i-Val (mg/L)	H-n-Val (mg/L)	H-n-Cap (mg/L)
P#1	0.125	52.5	49.0	48.0	47.5	46.0	46.0	47.0
P#2	0.25	105.0	98.0	96.0	95.0	92.1	92.1	94.1
P#3	0.5	210.0	196.0	192.1	190.1	184.1	184.1	188.1
P#4	1.5	630.0	588.1	576.2	570.2	552.4	552.4	564.3
P#5	2.5	1 050.0	980.1	960.3	950.4	920.7	920.7	940.5
P#6	5	2 100.0	1 960.2	1 920.6	1 900.8	1 841.4	1 841.4	1 881.0
P#7	7.5	3 150.0	2 940.3	2 880.9	2 851.2	2 762.1	2 762.1	2 821.5
P#8	10	4 200.0	3 920.4	3 841.2	3 801.6	3 682.8	3 682.8	3 762.0
P#9	20	8 400.0	7 840.8	7 682.4	7 603.2	7 365.6	7 365.6	7 524.0
P#10	25	10 500.0	9 801.0	9 603.0	9 504.0	9 207.0	9 207.0	9 405.0

**Figure 94|** Example of calibration lines obtained for individual VFA determination, namely H-Ac, H-Prop, H-i-But, H-n-But, H-i-Val, H-n-val, and H-n-Cap.**Table 47|** Retention time and slope of calibration lines for each acidic specie.

	H-Ac	H-Prop	H-i-But	H-n-But	H-i-Val	H-n-Val	H-n-Cap
Retention time (min)	2.571	3.502	4.461	5.037	6.199	7.098	9.160
m	945.4	1515.5	1683.3	1632.3	1782.3	1457.3	933.0
r²	0.9964	0.9960	0.9954	0.9917	0.9958	0.9875	0.9837

7.4 Example of calibration curves for inorganic compounds determination

The solutions used to construct the calibration curves for inorganic compounds determination were prepared using water containing 1.5 mL of concentrated HNO₃ per liter (hereinafter referred to acidified water). For the determination of Ca, Mg and Fe, the standards (as the samples) were diluted prior to analysis. For this reason, the calibration curves were plotted considering the original concentration of the standards before dilution with lanthanum (Ca and Mg) or calcium (Fe) solutions.

The stock solution for calcium determination was prepared by suspending 0.2497 g of CaCO₃ previously dried at 180 °C during 1 h, in acidified water. In a 100 mL volumetric flask, add 10 mL of concentrated HNO₃ and add acidified water to the final volume. The final concentration of this solution is 1000 µg_{Ca}/mL.

The stock solution for magnesium determination was prepared by dissolving 0.1658 g of MgO in a minimum amount of concentrated HNO₃. In a 100 mL volumetric flask, add 10 mL of concentrated HNO₃ and add acidified water to the final volume. The final concentration of this solution is 1000 µg_{Mg}/mL.

For Ca and Mg determination, prior to analysis, 10 mL of the samples or the standards prepared were mixed with 1 mL of lanthanum solution. The lanthanum solution was prepared by dissolving 58.65 g of lanthanum oxide (La₂O₃) in 250 mL of concentrated HCl, with slow addition of acid until complete dissolution. In a 1000 mL volumetric flask, add acidified water to the final volume.

The stock solution for iron determination was prepared by dissolving 0.10 g of iron wire in a mixture of 10 mL of HCl and 3 mL of concentrated HNO₃. In a 100 mL volumetric flask, add 5 mL of concentrated HNO₃ and add acidified water to the final volume. The final concentration of this solution is 1000 µg_{Fe}/mL. For Fe determination, prior to analysis, 10 mL of the samples or the standards prepared were mixed with 2,5 mL of calcium solution. The calcium solution was prepared by dissolving 630 mg of CaCO₃ in 50 mL of HCl 20 % (v/v). In a 1000 mL volumetric flask, add acidified water to the final volume.

The stock solution for sodium determination was prepared by dissolving 0.2542 g of NaCl previously dried at 140 °C during 1 h, in acidified water. In a 100 mL volumetric flask, add 10 mL of concentrated HNO₃ and add acidified water to the final volume. The final concentration of this solution is 1000 µg_{Na}/mL.

From the stock solutions (1000 ppm), intermediate solutions were prepared. Table 48 lists the concentrations used in the intermediate solutions. From the intermediate solutions, six diluted standards were prepared in 100 mL volumetric flasks, for each metal to be analyzed. Table 49 describes the concentrations of each metal per diluted stock solution, and the check solution is indicated (standard solution to adjust the operating conditions of the AA equipment).

Table 48| Concentrations of intermediate standard solutions for metals determination.

Metal	Volume of stock solution (mL)	[Metal] (ppm)
Ca	5	50
Mg	1	10
Fe	6	60
Na	10	100

Table 49] Concentration of calcium, magnesium, iron, and sodium in the diluted standard solutions for metals determination, and an indication of check diluted standard solution.

ID	Volume of stock solution (mL)	Calcium (ppm)	Magnesium (ppm)	Iron (ppm)	Sodium (ppm)
P1	1	0.5	0.1	0.6	1.0
P2	3	1.5	0.3	1.8	3.0
P3	4	2.0	0.4	2.4	4.0
P4	6	3.0	0.6	3.6	6.0
P5	8	4.0	0.8	4.8	8.0
P6	10	5.0	1.0	6.0	10.0
Check Solution	--	4 ppm	0.3 ppm	6 ppm	10 ppm

The calibration curves were performed by plotting the absorbance obtained by atomic absorption/emission spectroscopy analysis *versus* the concentration of each metal in the standard solutions. Figure 95 depicts an example of the calibration curves for each metal quantified. The figure shows the linear regression parameters for each calibration curve obtained by the ordinary least squares method.

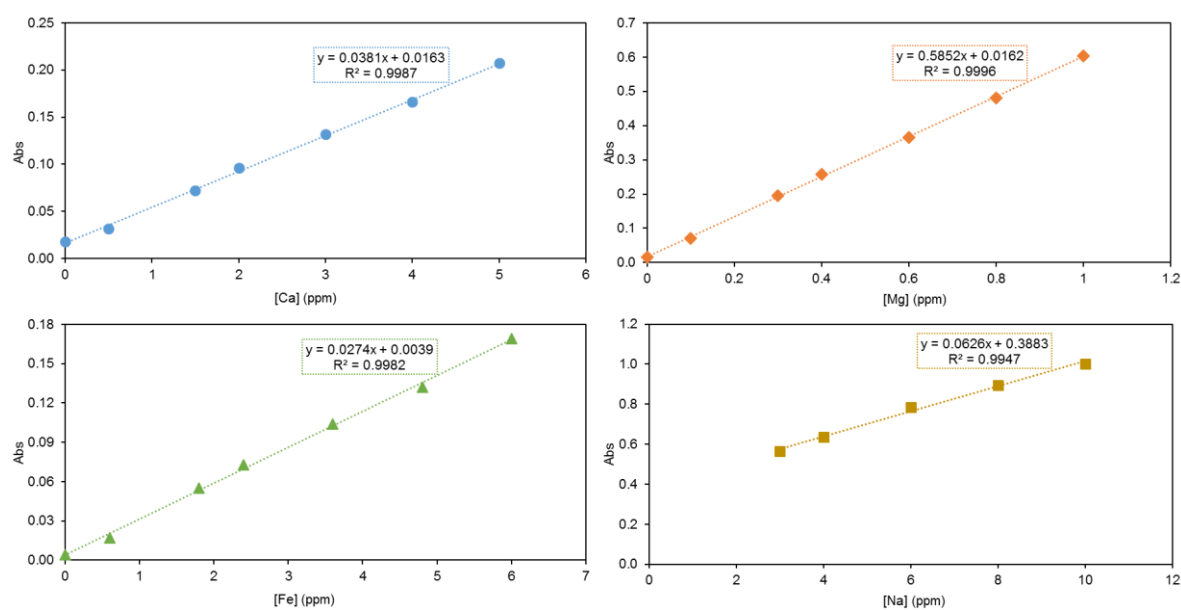


Figure 95] Example of calibration lines for metals determination.

